Strategies for Coagulation Pretreatment of Low-Pressure Membranes

Joseph D. Ladouceur

A thesis submitted to the University of Ottawa in partial fulfillment of the requirements for the degree of Doctor of Philosophy in Civil Engineering

Thesis Supervisors:

Dr. Roberto M. Narbaitz & Dr. Christopher Q. Lan



uOttawa

Department of Civil Engineering

Faculty of Engineering

University of Ottawa

© Joseph D. Ladouceur, Ottawa, Canada, 2026

Abstract

To mitigate natural organic matter (NOM)-induced fouling of low-pressure membranes (LPMs) in drinking water applications, coagulation pretreatment is widely applied. However, multiple process configurations exist and simulating full-scale performance at bench-scale remains a significant challenge. Accordingly, the main objectives of this dissertation were to compare the performance of alternative coagulation pretreatment strategies and to evaluate coagulation/flocculation mixing configurations for bench-scale LPM filtration studies. This research work was structured into four phases: (i) comparison of alternative coagulation pretreatment strategies across seasons and membrane types to identify optimal approaches; (ii) systematic investigation of the impact of helically coiled tube flocculator (HCTF) geometry on floc properties; (iii) evaluation of the influence of mixer configuration on bench-scale inline coagulation (C-IN) performance; and (iv) assessment of phased inline coagulation (C-IN-P), where coagulant is added for only a portion of the filtration cycle, as a more sustainable and cost-effective alternative to continuous C-IN.

Conventional coagulation-flocculation-sedimentation (CF-SED) has proven effective for LPM pretreatment, although, coagulation-flocculation-dissolved air flotation (CF-DAF) represents a promising high-rate alternative. C-IN, which omits particle separation prior to membrane filtration, has gained popularity due to its reduced footprint and operational simplicity. For two different membrane types, CF-DAF and CF-SED performed equally well, despite improved NOM removal by CF-DAF. In contrast, the performance of C-IN was membrane dependent as it yielded the lowest fouling rate amongst alternatives for an inside-out polyethersulfone (PES) membrane, but the highest fouling rate for an outside-in polyvinylidene fluoride (PVDF) membrane. This finding highlighted the importance of membrane material/configuration for the selection of optimal LPM pretreatment, even when using the same source water. Seasonal differences in C-IN performance appeared to be caused by changes in the organic matrix affecting the coagulated zeta potential (ZP), suggesting that real-time ZP monitoring may serve as a useful optimization tool for C-IN-LPM hybrid systems.

HCTFs represent a promising approach for improving continuous flow C-IN at bench-scale due to their strong secondary flow, which promotes effective mixing even for firmly laminar conditions. A replicated full-factorial design was used to evaluate the impact of the coil pitch, coil diameter, and pipe length on the properties of flocs. HCTF geometry was found to exert statistically significant impact on floc size and concentration, while floc structure (i.e., fractal dimension) remained relatively constant

across all studied geometries. The system flowrate (i.e., Reynolds number), however, exhibited the greatest impact on HCTF performance, likely the result of a trade-off between the hydrodynamic condition and the hydraulic residence time. Compared to a batch-reactor, the tested HCTF configurations produced smaller sized flocs in greater concentrations, while relative to a commercial inline static mixer (ISM), HCTFs yielded larger sized flocs in lower concentrations.

Bench-scale continuous-flow C-IN has proven difficult due to the low-flowrates involved. Accordingly, previous studies have used a wide variety of mixing configurations. The third phase of this study sought to elucidate the impact of mixer type/configuration on bench-scale C-IN performance by comparing three different continuous-flow flocculator types, namely, incidental flocculation in a straight pipe, an ISM, and two HCTFs, with and without the inclusion of rapid mixing. The performance of these continuous-flow approaches was additionally compared with a batch reactor, which have been extensively used in past studies due to their experimental simplicity. C-IN using a batch-reactor (with an extended contact time) yielded the lowest level of membrane fouling. Compared to rapid mixing or flocculation alone, combined rapid mixing and flocculation yielded reduced magnitude LPM fouling. Amongst alternative continuous-flow flocculator types, HCTFs had the lowest fouling rate, further supporting their suitability for bench-scale C-IN studies. These results indicate that LPM fouling is highly dependent on mixer type/configuration; direct comparison across studies using different C-IN approaches (including batch systems) may not be appropriate.

The final phase evaluated the performance of C-IN-P using three synthetic waters with varying hydrophobicity. Intermittent addition over 75% of the filtration cycle achieved comparable fouling mitigation and NOM removal to continuous dosing, with only marginal performance losses when the length of coagulant addition was further reduced to 50% of the cycle. The optimal membrane coating index (C-IDX), an operational control tool for C-IN-P defined as the mass of coagulant per unit membrane area, was higher than values reported in the literature, even for the same membrane type and low hydrophobicity water types. This suggests that the optimal C-IDX is uniquely defined for each membrane-water combination. For a given C-IDX value, optimal performance was achieved when the jar-test optimal dose was used rather than different dosing rates applied for extended or reduced durations.

Collectively, this work provides a comprehensive evaluation of alternative coagulation pretreatment strategies for LPMs and offers practical insights into the design, optimization, and bench-scale testing of these processes. The findings highlight the importance of membrane-specific optimization as well as the impact of mixer type/configuration on the outcome of bench-scale LPM studies.

Acknowledgements

First and foremost, I would like to express my deepest gratitude to my advisor, Roberto Narbaitz. Our journey together has been a long one, beginning when I first met you in my second year of undergraduate studies in 2016. You were the first person to encourage me to pursue graduate studies, and I have been incredibly fortunate to learn from and work alongside you ever since. Your constant support, thoughtful guidance, enthusiasm for research, and unwavering commitment to academic integrity have profoundly shaped me as both a researcher and an individual. Among the many lessons you taught me, the importance of "doing things the right way" is one that I will carry with me throughout my career and life. Even after your retirement, you generously agreed to remain my principal supervisor, allowing me to continue my doctoral studies at the University of Ottawa and pursue my academic aspirations. For this, I am deeply grateful.

I would also like to thank you for the many opportunities you provided to attend conferences and travel throughout my graduate studies. These experiences not only contributed significantly to my professional development but also allowed me to explore new places and build lasting connections within the water community. Finally, thank you for the many textbooks you entrusted to me over the years, particularly treasured volumes such as *Sontheimer*. They represent far more than reference materials; they are reminders of your mentorship, generosity, and passion for learning - I will cherish them as much as you did.

I would also like to sincerely thank Christopher Lan for taking me on as a student and enabling me to remain at the University of Ottawa for my doctoral studies. Your insightful comments, thoughtful discussions, and willingness to offer a different perspective consistently strengthened this work.

I have been fortunate to receive support from many members of the University of Ottawa community. I would like to thank Franco Ziroldo for the many enjoyable conversations and technical guidance with laboratory work, and Gerard Nina for assistance with LabVIEW programming. To Patrick D'Aoust, thank you for all the technical help and equipment assistance along the way. Richard Herard – thank you for helping me with the system wiring and for always being available to bounce ideas off of. I am also grateful to Luc Cloutier for always being willing to help with administrative matters, as well as to the professors and staff in the department who contributed to near decade-long journey at the University of Ottawa in countless ways. Special

thanks to Mr. Julian Fino, who spent two summers working with me as a research assistant — I hope I was able to teach you at least a fraction of what I learned myself along the way. I would also like to thank Onita Basu for allowing me to participate in training on the fluorescence spectrometer and for granting me access to her instrument.

To the friends I met throughout this journey — Pat, Tram, Richard, and Asma — thank you for the friendship and memorable moments along the way. I would especially like to acknowledge my lab mate, Kieran J. "J.D." Lobo. I valued our discussions immensely and always appreciated your helpful advice.

I gratefully acknowledge the financial support that made my doctoral studies possible. I would like to thank Natural Sciences and Engineering Research Council of Canada (NSERC) for supporting my supervisors through the NSERC Discovery Grant program and for supporting me through the Canada Graduate Scholarships program. To the Government of Ontario, thank you for providing financial support through the Ontario Graduate Scholarship program during my transition from maters to doctoral studies. I am also grateful to the American Membrane Technology Association for awarding me the Ian C. Watson Fellowship, and to the American Water Works Association and Dr. James K. Edzwald for awarding me the inaugural AWWA Dr. James K. Edzwald Scholarship, which was a tremendous honor. I am appreciative of the professional advice and guidance that Dr. Edzwald provided me during our chats and correspondence. Finally, I would like to thank the University of Ottawa for providing Excellence and Admission Scholarships, as well as support for attending international conferences.

Finally, to my family: thank you for your patience, encouragement, and unwavering support throughout this journey. None of this would have been possible without you.

Table of Contents

1. Introduction…….…. 1
1.1. General…….…….. 1
1.2. Research Objectives…… 5
1.3. Research Novelty and Contributions…….…….. 7
1.4. Thesis Outline…….… 9
1.5. References……..…….…… 13
2. Literature Review…….……. 23
2.1. Overview of Coagulation Configurations for Low-Pressure Membrane Pretreatment……... 25
2.1.1. Coagulation/Flocculation/Sedimentation (CF-SED) and Coagulation/Flocculation/Dissolved-Air-Flotation (CF-DAF)…… 25
2.1.2. Inline Coagulation (C-IN)…….. 27
2.1.2.1. Type I Configuration…….. 27
2.1.2.2. Type II Configuration……. 29
2.1.2.3. Type III Configuration…….….. 30
2.1.3. Phased-Inline Coagulation (C-IN-P)…….. 31
2.2. Membrane Fouling in the Hybrid Coagulation-LPM System……. 33
2.2.1. CF-SED……... 33
2.2.2. CF-DAF…….. 34
2.2.2.1. Comparison with C-IN……... 37
2.2.2.2. Comparison with CF-SED……. 38
2.2.2.3. Effects of Operating Parameters on Fouling of CF-DAF-LPM Systems……... 39
2.2.2.3.1. Water Quality…….… 39
2.2.2.3.2. Membrane Configuration…….…. 40
2.2.2.3.3. CF-DAF Parameters…….. 40
2.2.3. C-IN…… 41
2.2.3.1. Type I Configuration…….. 41
2.2.3.2. Type II Configuration……. 49

2.2.3.3. Type III Configuration…… 56
2.2.4. C-IN-P……. 68
2.2.4.1. Effects of the Coagulation Process…….. 71
2.2.4.2. Effects of the Cake Properties…… 72
2.2.4.3. Effects of Other Properties……. 74
2.2.4.4. The Coating Index for C-IN-P Operational Control……... 74
2.3. Treated Water Quality by the Hybrid Coagulation-LPM System…… 76
2.3.1. CF-SED……... 77
2.3.2. CF-DAF…….. 78
2.3.3. C-IN…… 81
2.3.4. C-IN-P……. 84
2.4. Conclusions of Literature Review…… 85
2.5. Research Needs……... 86
2.6. References…….…….. 89

3. Comparing Sedimentation, Flotation, and Inline Pretreatment for Low-Pressure Membrane Fouling Reduction……. 103
3.1 Abstract…… 105
3.2 Introduction…….. 106
3.3. Materials and Methods…… 108
3.3.1. Waters Tested……. 108
3.3.2. Filtration Apparatus and Membrane Module…….. 109
3.3.3. Inline Coagulation…….. 111
3.3.4. Multi-day Filtration Test Protocol…….. 112
3.3.5. Analytical Methods……. 112
3.3.6. Membrane Performance Indicators……. 113
3.3.6.1. Normalized TMP and Permeability Profiles……... 113
3.3.6.2. Fouling Index Modeling……. 114
3.3.6.3. Backwash Efficiency…….. 114
3.4. Results and Discussion…… 115
3.4.1. Challenge Water Quality…….… 115

3.4.2. Winter Backwash Efficiency Evaluation…… 117
3.4.3. Comparison of CF-DAF and CF-SED Pretreatment During Winter Season…….. 117
3.4.4. C-IN Pretreatment During winter Season……. 120
3.4.5. C-IN Seasonality Comparison and Relevant Correlations…….. 122
3.5. Practical Implications…….. 125
3.6. Conclusions……. 126
3.7. Acknowledgements……. 128
3.8. References……... 129

4. Reduced Low-Pressure Membrane Fouling by Inline Coagulation Pretreatment for a Colored River Water…… 133
4.1. Abstract……. 135
4.2. Introduction……. 136
4.3. Materials and Methods…… 139
4.3.1. Raw Water……. 139
4.3.2. Filtration Apparatus and Membrane Module……. 139
4.3.3. Pretreatment Methods……. 141
4.3.4. Multi-day Filtration Test Protocol……. 142
4.3.5. Membrane Performance Measures……. 144
4.3.5.1. Normalized TMP (nTMP) Profiles…… 144
4.3.5.2. Fouling Rates……. 144
4.3.6. Analytical Methods……. 145
4.4. Results……. 146
4.4.1. Water Quality……. 146
4.4.2. Comparison of CF-SED, CF-DAF, and C-IN Pretreatment During Winter Season…….. 148
4.4.3. C-IN Seasonality Assessment……. 150
4.5. Discussion……... 154
4.6. Conclusions……. 155
4.7. Acknowledgements……. 156

4.8. References……... 157

5. Characterizing the Impact of Geometry on the Performance of Inline-Coagulation Pretreatment Systems with Helical Flocculators 164

5.1. Abstract……... 168

5.2. Introduction……. 169

5.3. Materials and Methods…… 172

5.3.1. Synthetic Water…….. 172

5.3.2. Experimental Procedure……. 173

5.3.2.1. Full-Factorial Study……... 173

5.3.2.2. Bench-Scale Coagulation Systems……. 175

5.3.3. HCTF Geometrical Characterization…….. 176

5.3.4. Floc Characterization……. 177

5.3.4.1. Floc Sample Collection, Image Acquisition, and Processing……. 177

5.3.4.2. Floc Size, Concentration, and Fractal Dimension…….. 178

5.3.5. Statistical Analysis for FFD…… 180

5.4. Results and Discussion…… 180

5.4.1. Model Fitting and Adequacy Assessment…….. 180

5.4.1.1. Main and Interaction Effects…….……. 182

5.4.2. Impact of Torsion and Curvature on HCTF Performance…….. 186

5.4.3. Comparison with Alternative C-IN Mixer Types…….…….. 188

5.4.4. Effect of Reynolds Number on HCTF Performance…….. 191

5.4.5. Experimental Design Guidelines…… 193

5.5. Conclusions…….… 194

5.6. Acknowledgments…….…. 196

5.7. References……... 197

6. Impact of Flocculator Type on Continuous Inline Coagulation for Low-Pressure Membrane Pretreatment in Drinking Water Production……. 202

6.1. Abstract……. 205

6.2. Introduction…… 206

6.3. Materials and Methods…… 209
6.3.1. Synthetic Water…….. 209
6.3.2. Filtration Experiments…… 209
6.3.2.1. Bench-Scale Filtration Apparatus and Test Protocol……. 209
6.3.2.2. Small-Scale Rapid Mixer…… 212
6.3.2.3. Flocculator Types…….. 213
6.3.2.4. Mixer and HCTF Operational Properties…….. 214
6.3.3. Floc Characterization…….. 217
6.3.4. Membrane Fouling Assessment…….. 218
6.3.5. Analytical Methods and Statistical Analysis…….. 219
6.4. Results and Discussion…… 219
6.4.1. Validation of Continuous-Flow Bench-Scale Inline Rapid Mixer…….. 219
6.4.2. Comparison of LPM Fouling with Alternative Mixing Types…… 224
6.4.3. Impact of HCTF Properties on LPM Fouling in RM+FLOCC…….. 230
6.4.4. Treated Water Quality…… 234
6.4.5. Engineering Significance…… 235
6.5. Conclusions……. 237
6.6. Acknowledgements……. 239
6.7. References……... 240

7. Phased-Inline-Coagulation Pretreatment for Low-Pressure Membrane Fouling Reduction…… 246
7.1. Abstract……... 248
7.2. Introduction……. 249
7.3. Materials and Methods…… 252
7.3.1. Synthetic Water……... 252
7.3.2. Filtration Experiments……. 254
7.3.2.1. Coagulation/Flocculation……... 254
7.3.2.2. Continuous-Flow Bench-Scale System and Test Protocol……. 255
7.3.2.3. C-IN-P Pretreatment……... 256
7.3.2.4. Evaluation of C-IDX for C-IN-P Operational Control…… 257

7.3.3. Analytical Methods……. 257
7.3.3.1. Fouling Assessment…… 257
7.3.3.2. Water Quality Assessment…….. 258
7.3.3.3. Statistical Treatment……... 259
7.4. Results and Discussion…… 259
7.4.1. Evaluation of C-IN-P Performance……. 259
7.4.1.1. Fouling Mitigation…….. 259
7.4.1.2. Organics Removal by C-IN-P……. 264
7.4.1.3. FEEM Analysis……... 267
7.4.2. Sensitivity Analysis of C-IDX……. 271
7.4.2.1. Fouling Performance…….. 271
7.4.2.2. Organics Removals……. 273
7.5. Conclusions……. 277
7.6. Acknowledgements……. 278
7.7. References……... 279

8. General Conclusions and Directions for Future Research 284
8.1. General Conclusions and Engineering Significance…….. 284
8.2. Recommendations for Future Research…….. 287

Appendix A: Supplemental Information for Chapter 2 291
A.1. Fouling Data for Type III C-IN Studies……. 292
A.2. References…….. 302

Appendix B: Dissolved Air Flotation Pretreatment for Low-Pressure Membranes in Water Treatment: A Review of Fouling Mitigation and Product Water Quality…… 305
B.1. Abstract…….. 306
B.2. Introduction…… 307
B.3. Dissolved Air Flotation…… 310
B.3.1. A Brief Overview……... 310
B.3.2. Application of CF-DAF as LPM Pretreatment…….. 314

B.3.2.1. Drinking Water Treatment……. 314
B.3.2.2. Wastewater Treatment……... 316
B.4. Membrane fouling in the Integrated Flotation-LPM System…….. 318
B.4.1. Comparison with C-IN……... 320
B.4.2. Comparison with CF-SED……. 321
B.4.3. Effects of System Parameters on LPM Fouling……. 325
B.4.3.1. Water Quality……. 326
B.4.3.2. Membrane Properties……. 329
B.4.3.3. CF-DAF Properties…… 331
B.4.4. Summary of CF-DAF-LPM Studies and Fouling Mechanism…….. 332
B.5. Water Quality of Integrated DAF-LPM System……. 333
B.6. Economic Considerations……... 336
B.7. Conclusions and Future Research……... 341
B.8. Acknowledgements…… 342
B.9. References…….. 343

Appendix C: Phased-Inline Coagulation for Low-Pressure Membranes in Water and Wastewater Treatment: A Review of Fouling Mitigation, Process Control, and Water Quality…… 356
C.1. Abstract……. 357
C.2. Introduction…… 358
C.3. Phased-Inline Coagulation Process Configuration…… 362
C.4. Performance of Phased-Inline Coagulation as Pretreatment for LPMs……. 363
C.4.1. Fouling Mitigation……. 366
C.4.1.1. Effects of Coagulation Process……. 366
C.4.1.2. Effects of Cake Properties……. 367
C.4.1.3. Effects of Other Parameters…….. 370
C.4.2. Process Control: The Coating Index…….. 370
C.4.3. Removal of Natural Organic Matter…….. 374
C.5. Outlook and Future Direction……. 376
C.5.1. Research Needs for C-IN-P…… 376

C.5.2. Development of novel C-IN-P Strategies…….. 377
C.5.3. Regulatory Aspects Driving Technology Development…… 378
C.6. Conclusions…… 379
C.7. Acknowledgements…… 379
C.8. References……. 380

Appendix D: Supplemental Information for Chapter 3…… 391
D.1. Multi-Day Filtration Tests…….. 392
D.2. Molecular Weight Fractionation…… 393
D.2.1. Background…… 393
D.2.2. Procedures……. 393
D.3. Fouling Indices……... 395
D.4. Performance of Chemically Enhanced Backwash…….. 398
D.5. References……. 399

Appendix E: Supplemental Information for Chapter 4……. 400
E.1. Validation of Tubular Multichannel Membrane Potting Procedure…… 401
E.2. Preliminary Work…….. 402
E.3. Membrane Fouling Rate Calculation…….. 404
E.4. Supplemental Fouling Data……. 405
E.5. References…….. 406

Appendix F: Supplemental Information for Chapter 5……. 407
F.1. Additional Methodological Details…… 409
F.1.1. Preparation of Stock Model Organics…… 409
F.1.2. Preparation of Synthetic Water…….. 410
F.1.3. HRT Determination of Helically Coiled Tube Flocculators (HCTFs)….. 411
F.1.4. Jar Test Results for Challenge Water……. 411
F.2. Preliminary Screening Study…….. 415
F.2.1. Factorial Design and Alias Structure…….. 415
F.2.2. Experimental Factors for Screening Design……... 417

F.2.3. Results of Preliminary Screening Study…… 418
F.3. Estimation of Mean Velocity Gradient for Inline Static Mixer (ISM)……... 420
F.4. Additional Data for Full Factorial Design (FFD)……... 422
F.4.1. Randomized Run Order…… 422
F.4.2. FFD Model Fitting and Adequacy Check……... 422
F.4.3. Test for Model Curvature in FFD……... 423
F.4.4. Interaction Diagrams…… 424
F.5. Correlation Analysis……... 426
F.6. Batch Mixing Data…… 428
F.7. References…….. 429

Appendix G: Supplemental Information for Chapter 6……. 431
G.1. Additional Methodological Details……. 434
G.1.1. Critical Flux Test……... 434
G.1.2. Inline Rapid Mixer…… 435
G.1.3. Tracer Studies……. 436
G.1.4. Micro-Flow Imaging (MFI) Technologies…… 441
G.2. Supplemental Results……. 442
G.2.1. Evaluation of Small-Scale Inline Rapid Mixer……... 442
G.2.1.1. Floc Assessment and Imaging…… 442
G.2.1.2. Peclet Number for Hypothesized Mixing Mechanism…….. 446
G.2.1.3. Revised Rapid Mixer Design……. 446
G.2.2. Membrane Fouling Index……... 447
G.2.3. Evolution of LPM Fouling with Alternative Mixing Configurations…… 448
G.2.4. Carman-Kozeny Equation……. 451
G.2.5. Treated Water Quality Indicators……... 452
G.3. References……. 457

Appendix H: Supplemental Information for Chapter 7……. 459
H.1. Supplemental Methodological Details…… 462
H.1.1. Survey of Natural Water Quality…… 462

H.1.2. Preparation of Stock Model Organic Compounds and Synthetic Water…. 464
H.1.3. Standard Curved for Model Organic Compounds…….. 465
H.1.4. Preliminary Jar Testing…….. 467
H.1.5. Tracer Study for Hydraulic Residence Time Assessment……... 471
H.1.6. Critical Flux Assessment…… 473
H.1.7. Method of DOC Quantification…….. 476
H.2. Supplemental Results……. 477
H.2.1. Fouling Studies with C-IN-P…….. 477
H.2.2. Modeling FR_{hr}…… 482
H.2.3. Organics Removals by C-IN-P and Model Development…….. 483
H.2.4. FEEM Model Development……... 485
H.2.4.1. Background…… 485
H.2.4.2. Experimental Approach……...…….. 487
H.2.4.3. FEEM Model Validation…… 489
H.2.4.4. DOC Quantification from FEEM Data……... 495
H.2.5. Relationship Between FR_{hr} and Removal Rates of HA and SA……. 497
H.2.6. Fouling Data for Sensitivity Assessment of C-IDX for C-IN-P Operational Control…….. 499
H.2.6.1. Differences in FR_{hr}……..…… 499
H.2.6.2. Differences in FR_{hirr} and BWE…….. 500
H.2.7. Organic Removal Data for Sensitivity Assessment of C-IDX for C-IN-P Operational Control…….. 502
H.3. References……..... 504

List of Figures

Chapter 1

Fig. 1.1. Number of publications regarding coagulation pretreatment for LPMs in water treatment per 4-year period…….. 9

Chapter 2

Fig. 2.1. Low-pressure membrane system integrated with: (a) CF-SED pretreatment; (b) CF-DAF pretreatment…….. 26
Fig. 2.2. Schematic diagram of Type I C-IN pretreatment…….. 28
Fig. 2.3. Schematic diagram of Type II C-IN pretreatment……. 30
Fig. 2.4. Schematic of Type III C-IN batch test apparatus…….. 31
Fig. 2.5. Definition sketch of the system characteristics for: (a) continuous coagulant addition (C-IN); (b) phased coagulant addition (C-IN-P) ……... 32
Fig. 2.6. Schematic diagram of LPM system with C-IN-P pretreatment……. 33
Fig. 2.7. Relationship between fouling measures and coagulant dose for Type II C-IN……. 55
Fig. 2.8. Relationship between coagulant dose and rate of NSF decline for Type III C-IN… 58
Fig. 2.9. Relationship between 3-D fractal dimension ($D_{f,3}$) and coagulated ZP for Type III C-IN……. 61
Fig. 2.10. Relationship between rate of NSF decline and: (a) ZP; (b) $D_{f,3}$…….. 62
Fig. 2.11. Relationship between volume normalized rate of NSF decline and $D_{f,2}$……. 63
Fig. 2.12. Relationship between ZP and SCR for Type III C-IN……. 65
Fig. 2.13. Relationship between floc size and SCR……. 68
Fig. 2.14. Relationship between C-IDX and membrane permeability decline rate for: (a) C-IN-P; (b) C-IN…….. 75
Fig. 2.15. Removal of DOC, UV_{254}, and SUVA following CF-SED pretreatment and LPM filtration for select studies…… 78
Fig. 2.16. Relationship between applied coagulant dose and filtered removal of organics for pretreatment by Type I, Type II, and Type III C-IN…… 82

Chapter 3

Fig. 3.1. Outside-in membrane filtration system……. 110

Fig. 3.2. Schematic diagram of the outside-in lab-scale module……. 111

Fig. 3.3. ORW_w backwash evaluation: (a) Average BWEs; (b) Relationship between average BWE and SUVA……. 117

Fig. 3.4. Comparison of nTMP profiles for pre-treated ORW_w: (a) raw, CF-DAF, and CF-SED; (b) CF-DAF and CF-SED…….…….... 119

Fig. 3.5. Comparison of C-IN pre-treatment with CF-DAF and CF-SED during winter season……... 121

Fig. 3.6. Comparison of summer and winter C-IN pre-treatment: (a) 27 mg L^{-1} alum; (b) 34 mg L^{-1} alum. …… 122

Fig. 3.7. Relationship between average fouling indices and SUVA: (a) HIFI and SUVA; (b) CIFI and SUVA……..... 123

Fig. 3.8. Relationship between the 5-10 kDa organic fraction and: (a) HIFI; (b) CIFI…….. 124

Fig. 3.9. Relationships between Zeta Potential and: (a) HIFI; (b) CIFI…….. 125

Chapter 4

Fig. 4.1. Inside-out filtration apparatus……... 140

Fig. 4.2. Pressure-driven inside-out membrane: (a) module; (b) fiber cross-section…….. 141

Fig. 4.3. Comparison of ORWw filtration tests: (a) Raw ORW, CF-SED, CF-DAF nTMP profile; (b) Raw ORW and C-IN nTMP profile; (c) Three-day average total FR; (d) Three-day average hydraulically irreversible FR……... 149

Fig. 4.4. Comparison of summer and winter C-IN pretreatment at alum dose of: (a) 27 mg L^{-1}; (b) 34 mg L^{-1}……. 150

Fig. 4.5. Comparison of seasonal C-IN fouling rates: (a) hydraulically reversible; (b) hydraulically irreversible; (c) relationship between ZP and hydraulically irreversible…….. 152

Fig. 4.6. Relationships between zeta potential and chemically irreversible fouling: (a) following CEB; (b) following CIP…….. 154

Chapter 5

Fig. 5.1. Geometrical description of a helically coiled tube flocculator (HCTF)…… 171

Fig. 5.2. Schematic of bench-scale system…….. 176

Fig. 5.3. Microscopic analysis of floc ECD……. 179

Fig. 5.4. Response surface plots for ECD showing the interaction between: (a) d_c and p; (b) Length and p; (c) Length and d_c……..….. 183

Fig. 5.5. Response surface plots for D_p showing the interaction between: (a) d_c and p; (b) Length and p; (c) Length and d_c……. 184

Fig. 5.6. Response surface plots for floc concentration showing the interaction between: (a) d_c and p; (b) Length and p; (c) Length and d_c…….. 185

Fig. 5.7. Relationship between floc ECD and measures of torsion for HCTFs with high and low pipe length settings: (a) ECD vs. torsion parameter (β_0); (b) ECD vs. dimensionless pitch (γ)……... 187

Fig. 5.8. Relationship between floc concentration and measures of curvature for HCTFs with 1000 mm pipe length: (a) Concentration vs. curvature ratio (c) or dimensionless curvature (δ_{nd}); (b) Concentration vs. Dean number (De)…….. 188

Fig. 5.9. Comparison of HCTF floc properties with mixing by batch reactor or ISM: (a) ECD; (b) Floc concentration; (c) D_p…….. 191

Fig. 5.10. Effect of Reynolds number on ECD and floc concentration at FFD center point ($Length$ = 1500 mm; d_c = 67.5 mm; p = 30 mm)……. 192

Chapter 6

Fig. 6.1. Bench-scale filtration system…… 211

Fig. 6.2. HCTF geometry…… 214

Fig. 6.3. Comparison of floc properties for various flocculator types with and without inline rapid mixer: (a) ECD; (b) Floc concentration; (c) Perimeter-based fractal dimension (D_p)…….. 221

Fig. 6.4. Hypothesized coagulant dispersion mechanisms for: (a) FLOCC; (b) 222

RM+FLOCC……

Fig. 6.5. Impact of rapid mixing and flocculator type on: (a) FR_{hirr}; (b) FR_{hr} ……... 227

Fig. 6.6. Relationships between floc FR_{hr}, Floc ECD, and: (a) Floc circularity; (b) Floc concentration……... 229

Fig. 6.7. Relationships between FR_{hr} and: (a) ECD; (b) Floc circularity; (c) De for helical flocculators with varying length and pipe diameter. Note that ○→● and □→■ represent the impact of pipe length while ○→□ and ●→■ represent the impact of pipe diameter……. 231

Fig. 6.8. Impact of HCTF HRT on: (a) FR_{hr}; (b) Floc ECD; (c) Floc concentration; (d) Floc circularity…… 233

Chapter 7

Fig. 7.1. Schematic of bench-scale continuous-flow filtration system…… 255

Fig. 7.2. C-IN-P for LPM pretreatment: (a) Impact of water type and C-IDX on FR_{hr}; (b) Impact of water type and C-IDX on FR_{hirr}; (c) Relationship between FR_{hr} and C-IDX or coagulant dosing time…….. 260

Fig. 7.3. Percent removal of bulk measures of organics by C-IN-P across C-IDX values and water types: (a) True color; (b) DOC; (c) UV_{254}…… 265

Fig. 7.4. Trends in the removal of model organic compounds by C-IN-P with varying C-IDX and water type: (a) HA^*; (b) BSA^*; (c) SA^*…… 269

Fig. 7.5. Relationship between FR_{hr} and the removal of HA^*+SA^* for: (a) H-SUVA; (b) M-SUVA; (c) L-SUVA…… 271

Fig. 7.6. Impact of coagulant dose/dosing time and coagulant type on FR_{hr} for H-SUVA water and a C-IDX of 75 mg m^{-2}……. 272

Fig. 7.7. Impact of different combinations of coagulant dose/dosing time and coagulant type on the removal of water quality indices when treating H-SUVA water: (a) True color; (b) DOC; (c) UV_{254}; (d) SUVA; (e) HA^*; (f) BSA^*; (g) SA^*…… 274

Fig. 7.8. FEEM contour plot for C-IDX sensitivity analysis: (a) ALS-1.5 raw H-SUVA water; (b) PAX-45 raw H-SUVA water; (c) ALS-1.5 permeate; (d) ACH-45 permeate…… 276

Appendix A

Fig. A.1. Relationship between applied coagulant dose, pH, and filtered removal of organics for pretreatment by Type I, Type II, and Type III C-IN…….. 300
Fig. A.2. Relationship between applied coagulant dose, SUVA, and filtered removal of organics for pretreatment by Type I, Type II, and Type III C-IN…….. 301
Fig. A.3. Relationship between applied coagulant dose, coagulant type, and filtered removal of organics for pretreatment by Type I, Type II, and Type III C-IN……. 301

Appendix B

Fig. B.1. Number of publications regarding flotation pretreatment for LPMs…… 309
Fig. B.2. Schematic diagram of flotation basin…… 311
Fig. B.3. Low-pressure membrane system integrated with CF-DAF pretreatment……. 315
Fig. B.4. Factors influencing membrane fouling for LPMs in drinking water treatment…… 326
Fig. B.5. Relationships between fouling measures and source water quality parameters: (a) FR_{cirr} vs. CF-DAF UV_{254} Removal; (b) FR_{cirr} vs. CF-DAF Treated SUVA; (c) FR_{hirr} vs. Coagulated pH…… 328

Appendix C

Fig. C.1. Development and trends in coagulation pretreatment for LPMs…….. 360
Fig. C.2. Idealized permeability profiles for three filtration cycles with: (a) continuous coagulant addition (C-IN); (b) phased coagulant addition (C-IN-P)…….. 361
Fig. C.3. Schematic diagram of a LPM system with C-IN-P pretreatment……. 363
Fig. C.4. Visualization of the effect of cake layer properties on C-IN-P fouling: (a) incomplete coverage of membrane fiber by the cake layer; (b) complete coverage of membrane fiber by the cake layer; (c) uniform and smooth cake layer; (d) rough cake layer…….. 369
Fig. C.5. Rate of normalized flux decline with increasing coagulant dosage for C-IN-LPM system…….. 371
Fig. C.6. Relationship between C-IDX and membrane permeability decline rate for: (a) C-IN-P; (b) C-IN…… 372
Fig. C.7. Idealized permeability profiles for three filtration cycles with stepped coagulant addition (C-IN-S)…… 377

Appendix D

Fig. D.1. Serial filtration procedure…… 394

Fig. D.2. Visual description of fouling index cycles: (a) FI cycle classification; (b) Method of TFI analysis; (c) Method of HIFI analysis; (d) Method of CIFI analysis…….. 396

Fig. D.3. Surface cake removal at various stages of chemically enhanced backwash. View of white membrane fibers through translucent module casing. At time t = 0 min the CEB commences and a brown, gel-like cake layer is present on fiber surface. At time t = 20 min, the RO flush has visually removed the cake layer……. 398

Appendix E

Fig. E.1. Potted tubular multichannel membrane fiber: (a) Prior to sealing foam-like support structure; (b) After sealing support structure……. 402

Fig. E.2. Preliminary testing: (a) Critical flux determination; (b) Chemically enhanced backwash optimization…… 403

Fig. E.3. Fouling rate computation: (a) Individual filtration cycle reversible and irreversible fouling rate; (b) Chemically irreversible fouling rates…… 404

Fig. E.4. Relationship between FR_{hirr} and SUVA…… 405

Appendix F

Fig. F.1. Efficiency of alum compared to alternative coagulant types for synthetic challenge water…… 413

Fig. F.2. Removal of DOC by alum coagulant with varying: (a) Dose as aluminum; (b) Coagulated pH……. 414

Fig. F.3. QQ plots for model residuals: (a) ECD; (b) D_p; (c) Concentration……... 423

Fig. F.4. Interaction diagrams between pipe length and coil pitch for floc ECD: (a) Effect of pipe length at high and low factor setting of coil pitch; (b) Effect of coil pitch at high and low factor settings of pipe length…….. 424

Fig. F.5. Interaction diagrams between coil diameter and coil pitch for floc concentration: (a) Effect of coil diameter at high and low factor setting of coil pitch; (b) Effect of coil 425

pitch at high and low factor settings of coil diameter……..

Fig. F.6. Interaction diagrams between coil diameter and pipe length for floc concentration: (a) Effect of pipe length at high and low factor setting of coil diameter; (b) Effect of coil diameter at high and low settings of pipe length……... 426

Fig. F.7. Kinetic assessment of floc properties in batch reactor system with continuous-stirring at G=200 s^{-1}: (a) ECD; (b) Floc Concentration…….. 428

Appendix G

Fig. G.1. Flux-stepping test data and fitted models for critical flux determination……. 435

Fig. G.2. Schematic of inline rapid mixer…… 436

Fig. G.3. Cumulative distribution function curves derived from tracer studies for: (a) Rapid mixer; (b) HF-2000-⅛……. 438

Fig. G.4. Representative microscopic images of flocs produced by: (a) RM Only; (b) Batch; (c) RM+Control; (d) Control; (e) RM+ISM; (f) ISM; (g) RM+HF-1000-⅛; (h) HF-1000-⅛; (i) RM+HF-2000-⅛; (j) HF-2000-⅛……. 444

Fig. G.5. Relationship between percentage change in floc ECD and floc concentration for the addition of rapid mixing……. 445

Fig. G.6. Schematic of modified RM……... 447

Fig. G.7. Mean HIFI for direct filtration and C-IN pretreatment…… 448

Appendix H

Fig. H.1. Survey of WQIs from natural water sources reported in literature: (a) DOC; (b) Turbidity; (c) Alkalinity; (d) pH…….. 463

Fig. H.2. Standard curve relating mass concentration to DOC for: (a) HA; (b) BSA; (c) SA…… 466

Fig. H.3. Assessment of the reproducibility of mass-concentration:DOC relationships for HA, BSA, and SA…… 467

Fig. H.4. Preliminary jar test data for three synthetic challenge waters with alum: (a) DOC removal vs. alum dose; (b) DOC removal vs. coagulated pH; (c) Coagulated ZP vs. alum 470

dose……

Fig. H.5. Preliminary jar test data for three synthetic challenge waters with ACH: (a) DOC removal vs. alum dose; (b) DOC removal vs. coagulated pH; (c) Coagulated ZP vs. alum dose…… 471

Fig. H.6. Cumulative age distribution curves for preliminary tracer study tests conducted at 100 L m^{-2} h^{-1} equivalent flowrate: (a) Rapid mixer; (b) Helical flocculator…….. 473

Fig. H.7. Flux stepping data from critical flux testing for: (a) L-SUVA; (b) M-SUVA; (c) H-SUVA…….. 475

Fig. H.8. Variation in BWE across C-IDX values and water type…….. 479

Fig. H.9. Comparison of FR_{hr} before and after 4 h of operation at a C-IDX of 20 mg m^{-2} for: (a) H-SUVA; (b) M-SUVA; (c) L-SUVA…… 480

Fig. H.10. Core consistency graph for 2-Component model…….. 490

Fig. H.11. Split-half evaluation for: (a) 2-component model; (b) 3-component model……. 491

Fig. H.12. Comparison of PARAFAC model residuals for: (a) 2-component model; (b) 3-component model…… 492

Fig. H.13. FEEM PARAFAC model components: (a)-(c)-(e) 2-D Excitation-Emission spectra for component 1, 2, and 3, respectively; (b)-(d)-(f) 3-D Excitation-Emission spectra for component 1, 2, and 3, respectively…….. 494

Fig. H.14. (a) Emission; (b) Excitation loading diagrams for three component FEEM model…… 495

Fig. H.15. Linearity assessment of component scores for: (a) HA; (b) BSA…….. 496

Fig. H.16. Relationships between the removal of HA^{*} or SA^{*} and FR_{hr} for: (a) H-SUVA; (b) M-SUVA; (c) L-SUVA waters…….. 498

List of Tables

Chapter 2

Table 2.1. Summary of Pretreatment Parameters and Fouling Behavior for Selected CF-DAF-LPM Studies…….. 36

Table 2.2. Selected Bench-Scale Studies in Type I C-IN Pretreatment……. 42

Table 2.3. Selected Pilot-Scale Studies in Type I C-IN Pretreatment…… 44

Table 2.4. Selected Bench-Scale Studies in Type II C-IN Pretreatment…… 50

Table 2.5. Selected Pilot-Scale Studies in Type II C-IN Pretreatment…….. 51

Table 2.6. Summary of Fractal Dimension Impact on Membrane Fouling for Type III C-IN Studies…… 64

Table 2.7. C-IN-P Fouling Measures and Coagulation Characteristics……. 70

Table 2.8. Removals of Bulk Water Quality Parameters for Selected CF-DAF-LPM Studies……. 79

Chapter 3

Table 3.1. Water Quality Data for Raw ORW and Pre-treated ORW…… 116

Chapter 4

Table 4.1. Summary of Multi-day Testing Parameters…….. 143

Table 4.2. Water Quality Data for Raw and Pre-treated ORW…….. 147

Chapter 5

Table 5.1. Synthetic Water Quality…….……..…... 173

Table 5.2. Factor Level Settings for 2^3 FFD…….…….. 174

Table 5.3. ANOVA Analysis and Model Adequacy for 2^3 FFD…… 181

Chapter 6

Table 6.1. Summary of Mixer Hydrodynamic Properties…….. 216

Chapter 7

Table 7.1. Composition of Organic Matrix in Three Synthetic Waters……. 253

Table 7.2. Summary of Primary WQIs for Synthetic Challenge Waters…… 254

Appendix A

Table A-1. Results of Selected Type III C-IN Studies Using Synthetic Challenge Waters… 292

Table A-2. Results of Selected Type III C-IN Studies Using Natural Challenge Waters….. 297

Appendix B

Table B.1. Summary of Typical CF-DAF Parameters…… 312

Table B.2. Summary of Pretreatment Parameters and Fouling Behavior for Selected CF-DAF-LPM Studies…….. 319

Table B.3. Removals of Bulk Water Quality Parameters for Selected CF-DAF-LPM Studies……. 334

Table B.4. Survey of Operating Expenditure (OPEX) costs for Low-Pressure-Membrane and Dissolved Air Flotation Facilities……. 339

Appendix C

Table C.1. C-IN-P Fouling Measures and Coagulation Characteristics…….. 365

Appendix D

Table D.1. Summary of Multi-day Testing Parameters……. 392

Table D.2. Three-day Average Fouling Indices…….…… 397

Appendix E

Table E.1. Fitted Models from Critical Flux Testing……. 404

Table E.2. TMC Membrane Fouling Rates…… 405

Appendix F

Table F.1. HRT Values for Different HCTF Geometries…….……. 411

Table F.2. Coagulant Technical Data…… 412

Table F.3. Treatment Combinations for 2_{IV}^{6-2} Screening Design…….. 416

Table F.4. Alias Structure for Screening Design……... 417

Table F.5. Controlled Factor Level Settings for Preliminary Screening Design……... 418

Table F.6. Factor Screening Results for ECD……... 418

Table F.7. Factor Screening Results for D_p……...… 419

Table F.8. Factor Screening Results for Floc Concentration…… 420

Table F.9. Randomized Run Order for 2^3 Full-Factorial Design…….…. 422

Table F.10. Students t-Test for Assessment of Response Function Curvature……. 424

Table F.11. Multivariate Correlation Analysis Between Floc Response Variables and Measures of Torsion and Curvature for 1000 mm Pipe Length……. 427

Table F.12. Multivariate Correlation Analysis Between Floc Response Variables and Measures of Torsion and Curvature for 2000 mm Pipe Length……. 427

Appendix G

Table G.1. Fitted Models from Critical Flux Testing……. 435

Table G.2. Summary of Mixer Properties and Hydraulic Retention Times……... 440

Table G.3. Summary of Fitted Model Relating Percentage Change in Floc ECD and Concentration…….. 445

Table G.4. Summary of Hydraulically Reversible and Irreversible Fouling Rates Across Mixing Configurations…… 448

Table G.5. Results of Pooled *t*-test on Difference in Mean FR_{hr} Between Direct Filtration and Alternative C-IN Strategies…….. 450

Table G.6. Results of Pooled *t*-test on Difference in Mean FR_{hr} Between Batch Coagulation and Alternative Continuous-Flow Coagulation Strategies……. 450

Table G.7. Results of Pooled *t*-test on Difference in Mean FR_{hr} Between FLOCC and RM+FLOCC Across Four Flocculator Type…… 451

Table G.8. Results of Pooled *t*-test on Difference in Mean FR_{hr} Between RM and RM+FLOCC Across Four Flocculator Types…… 451

Table G.9. Removal of Key Water Quality Indicators by C-IN-LPM with Various Mixing Configurations…….….. 453

Table G.10. One-way ANOVA Test for Removal of WQIs by Direct Filtration and C-IN Pretreatment…… 454

Table G.11. One-way ANOVA Test for Removal of WQIs Across Different C-IN Mixing Configurations……. 455

Table G.12. One-way ANOVA Test for Removal of WQIs by HCTFs With Varying HRT……. 456

Appendix H

Table H.1. Regression Analysis of Standard Curves for Model Organics Measured by DOC Analyzer…….. 467

Table H.2. Summary of Technical Properties for Alum and ACH……. 468

Table H.3. Summary of Preliminary Tracer Study Data for Rapid Mixer and Helical Flocculator……... 473

Table H.4. Fitted Models from Critical Flux Testing…….. 475

Table H.5. Method Setup for DOC Analysis by Tekmar-Dohrmann Phoenix 8000…….. 477

Table H.6. Summary of Fouling Data for C-IN-P Pretreatment with Varying C-IDX and Water Type……. 478

Table H.7. Results of Pooled *t*-test on Difference in Mean FR_{hr} Between Water Types Across C-IDX Values of 30-150 mg m^{-2}……. 481

Table H.8. Fitted Model Adequacy Data for Relationship Between FR_{hr} and Coagulant Dosing Time…… 483

Table H.9. Summary of Organics Removals for C-IN-P Pretreatment with Varying C-IDX and Water Type……... 483

Table H.10. Fitted Model Adequacy Data for DOC Across Water Type…… 484

Table H.11. Fitted Model Adequacy Data for True Color Across Water Type……. 484

Table H.12. Fitted Model Adequacy Data for UV_{254} Across Water Type…….. 485

Table H.13. Summary of Reported FEEM Peaks and their Corresponding DOM Classification from Select Studies…….. 486

Table H.14. Synthetic Water Samples Tested for PARAFAC Model Calibration……. 487

Table H.15. Linearity Assessment of EEM Scores for Model Organics…… 496

Table H.16. Fitted Model Adequacy Data for Relationship Between FR_{hr} and Percent HA^{*} 498

or SA^* Removal……...
Table H.17. Fitted Model Adequacy Data for Relationship Between FR_{hr} and Percent HA^*+SA^* Removal…….. 499
Table H.18. Results of Pooled *t*-test on Sensitivity of FR_{hr} to Coagulant Dose/Dosing Time and Coagulant Type……. 500
Table H.19. One-way ANOVA Test for FR_{hirr} and BWE for Sensitivity Evaluation of C-IDX…….. 501
Table H.20. Removal of Organic WQIs for H-SUVA Water with C-IN-P Pretreatment at 75 mg m^{-2} During C-IDX Sensitivity Assessment…….. 502
Table H.21. One-way ANOVA Test for Removal of WQIs During C-IDX Sensitivity Analysis……... 503

List of Publications

Peer Reviewed Publications

1. **Ladouceur, J.D.**, Narbaitz, R.M., & Lan, C.Q. (2026). Impact of flocculator type on continuous inline coagulation for low-pressure membrane pretreatment in drinking water production. *Separation and Purification Technology (In Press).*
2. **Ladouceur, J.D.**, Narbaitz, R.M., & Lan, C.Q. (2026). Characterizing the impact of geometry on the performance of inline-coagulation pretreatment systems with helical flocculators. *Environmental Science: Water Research & Technology, 12(8), 2423-2438*
3. **Ladouceur, J.D.**, Narbaitz, R.M., & Lan, C.Q. (2024). Phased inline coagulation for low-pressure membranes in water and wastewater treatment: a review of fouling mitigation, process control, and water quality. *Environmental Technology Reviews, 13(1), 305-324.*
4. **Ladouceur, J.D.**, Narbaitz, R.M., & Lan, C.Q. (2023). Dissolved air flotation pretreatment for low-pressure membranes in water treatment: A review of fouling mitigation and product water quality. *Journal of Water Process Engineering, 56, 104391*.
5. **Ladouceur, J.D.**, & Narbaitz, R.M. (2023). Comparing sedimentation, flotation, and in-line pretreatment for low-pressure membrane fouling reduction. *Journal of Environmental Engineering (ASCE), 149(4), 04023002.*
6. **Ladouceur, J.D.**, & Narbaitz, R.M. (2022). Reduced low-pressure membrane fouling by inline coagulation pretreatment for a colored river water. *Membranes, 12, 1028*.

Magazine Articles

1. **Ladouceur, J.D.**, Narbaitz, R.M, & Lan, C.Q. (2024, June). Low-pressure membrane pretreatment by dissolved air flotation: Comparison with alternative coagulation strategies. American Membrane Technology Association (AMTA) *Solutions, 43(2),8-9*.
2. **Ladouceur, J.D.**, & Narbaitz, R.M. (2023, June). Comparing sedimentation, flotation, and inline pre-treatment for low-pressure membrane fouling reduction. American Membrane Technology Association (AMTA) *Solutions, 42(2), 8-9*.

Conference Presentations

1. **Ladouceur, J.D.**, Narbaitz, R.M., & Lan, C.Q. (2025). *State-of-the-art in drinking water treatment: Comparing alternative continuous-inline-coagulation mixing strategies for low-pressure membrane filtration pretreatment*. [Poster Presentation]. Presented at the University of Ottawa Research Celebration Day, Ottawa, ON, Canada, March 6, 2025.
2. **Ladouceur, J.D.**, Narbaitz, R.M, & Lan, C.Q. (2025). *Impact of helical flocculator configuration on continuous-inline-coagulation performance for low-pressure membrane pretreatment.* [Conference Presentation]. Presented at the AMTA/AWWA Membrane Technology Conference and Exposition, Long Beach, CA, USA, Feb. 24-27, 2025.
3. **Ladouceur, J.D.**, Narbaitz, R.M, & Lan, C.Q. (2024). *An overview of phased inline coagulation for low-pressure membranes.* [Conference Presentation]. Presented at the IWA World Water Congress & Exposition, Toronto, ON, Canada, Aug. 11-15, 2024.
4. **Ladouceur, J.D.**, Narbaitz, R.M, & Lan, C.Q. (2024). *Low-pressure membrane pretreatment by dissolved air flotation: Comparison with alternative coagulation strategies.* [Conference Paper]. Presented at the AMTA/AWWA Membrane Technology Conference and Exposition, West Palm Beach, FL, USA, March 4-7, 2024. **Best Student Paper Award.**
5. **Ladouceur, J.D.**, & Narbaitz, R.M. (2023). *Reduced low-pressure membrane fouling by inline coagulation pretreatment.* [Poster Presentation]. Presented at the IWA Membrane Technology Conference for Water and Wastewater Treatment and Reuse, St. Louis, MO, USA, July 23-26, 2023. **Outstanding Poster Presentation Award.**
6. **Ladouceur, J.D.**, & Narbaitz, R.M. (2023). *Evaluating flotation, sedimentation, and inline pretreatment of ultrafiltration fouling mitigation.* [Conference Paper]. Presented at the AMTA/AWWA Membrane Technology Conference and Exposition, Knoxville, TN, USA, Feb 20-23, 2023. **Best Student Paper Award.**

CHAPTER 1

Introduction

1.1. General

Ultrafiltration (UF) and microfiltration (MF) membranes have seen rapid growth in their installed capacity for drinking water treatment (DWT) applications over the past two decades (Alresheedi et al. 2022; Anis et al. 2019; Chang et al. 2017a; Lee et al. 2023; Li et al. 2019; Pearce 2018; Xu et al. 2022). The popularity of these low-pressure membrane technologies (LPM) may be attributed to several factors including: (1) modularity, which results in a compact process that can be operated with a high degree of automation (Peters et al. 2021; Schulz et al. 2016); (2) near complete or absolute removal of cellular microorganisms, including pathogenic bacteria, and protozoa (Huang et al. 2009; Li et al. 2019; Ren et al. 2021; Wray and Andrews 2014); (3) increasingly stringent treated water quality regulations (Bermea 1999; Obotey Ezugbe and Rathilal 2020; Pearce 2011); (4) decreasing membrane costs due to economies of scale and advances in membrane technology (Gao et al. 2011; Pearce 2011); (5) an increasing number of wastewater reuse applications (Aly et al. 2018; Delgado Diaz et al. 2012); and (6) the use of lower-quality freshwater sources in response to stress from climate change and population growth (Amjad et al. 2015). The growth in their application has been further aided by the fact that, when compared to deep bed filters, LPMs provide a reliable operation with a superior quality product water and are known to be less susceptible to raw water quality fluctuations (Crittenden et al. 2012; Kinser 2021; Suárez et al. 2015). As a result of these factors, the global cumulative installed capacity of LPMs surpassed 80,000 MLD in 2018, with an established long-term annual growth rate of 10,000 MLD based on data between 2011-2018 (Pearce 2018).

Although the number and size of LPM facilities continues to grow globally, membrane fouling persists as a major obstacle to a more widespread application of this technology (Hao et al. 2011; Kimura et al. 2004; Kimura and Kume 2020; Peiris et al. 2010; Yamamura et al. 2014; Zietzschmann et al. 2014). Fouling can be defined as the continual loss of performance (or productivity) of a membrane due to deposition on its surface or within its pores (AlSawaftah et al. 2021; Guo et al. 2012; Koros et al. 1996; Schäfer et al. 2021). For LPMs operated with a constant filtration flux, this productivity loss is manifested through greater transmembrane pressure (TMP) drops, which results in increased energy costs (Chang et al. 2017b; Souza and Basu 2013;

Tanudjaja et al. 2022). While physical cleaning methods, such as routine hydraulic backwashing and air sparging, can recover some degree of productivity loss (i.e., hydraulically reversible fouling), irreversible membrane fouling will develop over long periods of operation, leading to increased operating and maintenance costs as well as shortened membrane lifespan (Kimura and Kume 2020; Shi et al. 2014; Yamamura et al. 2007). Dissolved organics, particulate organic and inorganic materials, as well as microorganisms have all been recognized as important membrane foulants, with synergistic fouling between these components reported in the literature (Cui and Choo 2014; Gao et al. 2011; Guo et al. 2012; Hilal et al. 2005; Jermann et al. 2008b; a; Liu et al. 2019; Schulz et al. 2016; Tian et al. 2013a). For most LPM applications, however, natural organic matter (NOM) has been identified as the consensus principle foulant (Amy 2008; AWWA 2005; Cui and Choo 2014; Huang et al. 2007; Kim et al. 2006; Lee et al. 2008, 2004; Peters et al. 2021; Porcelli and Judd 2010; Zularisam et al. 2007, 2011).

NOM is ubiquitous in natural waters and is composed of a complex, heterogenous matrix of organic macromolecules with a wide range of functional groups (Matilainen et al. 2010, 2011; Sillanpaa 2015). Hydrophobic (HPO) acids constitute the major fraction (>50%) of aquatic NOM in typical surface waters, with humic substances (humic and fulvic acids) being the largest component (Aiken et al. 1985). The remaining NOM is described as non-humic and includes low molecular weight neutrals, proteins, and other hydrophilic (HPI) biopolymers (Sillanpaa 2015; Zularisam et al. 2011). The composition of aquatic NOM is known to be highly dependent on the biogeochemical cycles of the surrounding environment, and can even vary seasonally at the same location (Matilainen et al. 2011). Inconsistent findings have been reported by researchers regarding which fraction of NOM is primarily responsible for LPM fouling. Some studies have suggested that humic substances are responsible for severe membrane fouling (Peiris et al. 2013; Xu and Narbaitz 2016), while others, particularly more recent studies employing liquid chromatography organic carbon detection (LC-OCD) or fluorescence excitation-emission matrix (FEEM) analysis, have suggested that the HPI biopolymer fraction is the primary membrane foulant (Chen et al. 2014; Kimura et al. 2004; Kimura and Kume 2020; Tian et al. 2013b; Yamamura et al. 2019).

To control LPM fouling by NOM, strategies such as chemical cleaning (Arnal et al. 2009; Bogati et al. 2015; Ding et al. 2020; Gul et al. 2021; Park et al. 2018; Porcelli and Judd 2010; Shi et al. 2014; Zhu et al. 2024), feed water pretreatment (Cheng et al. 2016; Huang et al. 2019; Liang et al. 2008; Lin et al. 1999), membrane surface modification (Baghbanzadeh et al. 2016;

Mosqueda-Jimenez et al. 2004; Nguyen et al. 2007; Pezeshk and Narbaitz 2012; Rana and Matsuura 2010; Xie et al. 2016), and alteration of operating conditions (Alresheedi et al. 2022; Crozes et al. 1997; Kim et al. 2015; Li et al. 2014; Souza and Basu 2013) have all been investigated. Concerning feed water pretreatment, coagulation prior to LPM filtration has become the most common method for fouling reduction due to its simple implementation and relatively low cost, coupled with its familiarity to plant operators (Gao et al. 2011; Huang et al. 2009; Kamińska et al. 2020; Malkoske et al. 2020). Coagulation of LPM feed waters has been performed both with and without particle separation processes (Gao et al. 2011; Liang et al. 2008). For waters with elevated NOM concentrations or highly variable turbidity levels, a number of studies have reported conventional coagulation/flocculation/sedimentation (CF-SED) pretreatment to be successful at mitigating membrane fouling (Amjad et al. 2015; Ding et al. 2021a; Ma et al. 2020a; Minegishi et al. 2001; Moon et al. 2009; Yu et al. 2021, 2015a). The effectiveness of CF-SED pretreatment has largely been attributed to the reduced foulant load it imparts on the membrane surface, although cakes of low porosity are reportedly formed during filtration (Yu et al. 2015b). Compared to conventional CF-SED, coagulation/flocculation/dissolved-air-flotation (CF-DAF) is a high-rate process with a small footprint that compliments well the compactness of membrane installations. Furthermore, for highly colored or algal impacted waters, CF-DAF provides a superior performance compared to CF-SED due to the low densities of NOM and algae flocs, which makes them more amenable to removal by flotation than settling (Edzwald and Haarhoff 2012; Teixeira and Rosa 2006). As a result, several studies have reported the effectiveness of CF-DAF for LPM fouling mitigation (Goh et al. 2010; Hög et al. 2015; Kang et al. 2021; Lazaridis et al. 2004; Minhalma and de Pinho 2001; Shi et al. 2017).

For concentrations of particles and/or organics resulting in low to moderate fouling loads on the membrane surface, continuous inline-coagulation (C–IN) without particle separation (i.e., coagulated solids delivered directly to the membrane surface throughout the entire filtration cycle) can be employed prior to LPM filtration (Aly et al. 2021; Choi and Dempsey 2004; Ding et al. 2021b; Koyuncu et al. 2015; Ma et al. 2020b). A significant number of published studies have investigated C-IN pretreatment for LPM applications in recent years owing to its reduced process complexity and smaller footprint (resulting from shorter flocculation retention times) compared to conventional water treatment (Ding et al. 2016; Kamińska et al. 2020; Keucken et al. 2017; Lebeau et al. 1998; Sillanpaa 2015). More importantly, several authors have suggested that C-IN can be

successful at mitigating irreversible membrane fouling even at very low coagulant doses in the range of 0.3-1.0 mg L^{-1} as alum (Peleato et al. 2017; Tabatabai et al. 2009; Tang et al. 2019; Wray and Andrews 2014). Phased inline coagulation (C-IN-P) is a novel variation of C-IN pretreatment where, instead of continuous coagulant addition, the coagulant is dosed only for the initial portion (fraction) of the filtration cycle. Recently, several published studies have reported that C-IN-P pretreatment for LPM feed waters can not only successfully mitigate fouling by NOM, but also significantly reduce coagulant demand compared to C-IN (Buchta et al. 2017; Lok et al. 2017; Naim et al. 2014; Pronk et al. 2016). To achieve simultaneous reductions in operating costs and LPM fouling, several studies (Buchta et al. 2019; Schweiger et al. 2018a; b) introduced the membrane coating index (C-IDX), defined as the surface-area normalized mass of coagulant delivered to the membrane, as a simple process control tool. Successful implementation of C-IN-P has the potential to greatly reduce the cost associated with LPM pretreatment through lower chemical consumption and sludge processing/disposal costs when compared with C-IN (Lok et al. 2017).

To determine the relative performance of these various coagulation pretreatment strategies for specific combinations of source waters and membrane type (i.e., material and configuration), bench- and/or pilot-scale studies are necessary. However, due to the low flowrates that can be accommodated by the small-scale systems used in academic studies as well as industrial research and design, simulating continuous-flow coagulation remains a significant challenge. Consequently, previous studies have employed a wide array of coagulation mixing strategies including continuous mixing by a batch reactor (Cho et al. 2006; Neama et al. 2024; Peleato et al. 2017; Tang et al. 2019), straight pipe segments providing incidental flocculation (Kamińska et al. 2020), inline static mixers (Wang and Wang 2006), and modified jar-test apparatus (Malkoske et al. 2023a; b). Other researchers have attempted to simulate continuous-flow inline coagulation by transferring coagulated/flocculated suspensions from conventional jar test apparatus to batch membrane reactors for short duration tests (Choi et al. 2008; Ma et al. 2014; Yao et al. 2015). These C-IN approaches, however, are not fully representative of the expected hydrodynamic and mixing conditions encountered in continuous-flow full- or pilot-scale LPM systems.

Helically coiled tube flocculators (HCTFs), simply described as a helically coiled segment of pipe, represent a promising strategy to achieve efficient mixing/flocculation for C-IN at the low-Reynolds flow conditions typical of bench-scale coagulation systems. In addition to their highly

compact structure, HCTFs provide high mass transfer coefficients, an extended laminar flow regime, and elevated friction factors relative to straight pipes (Carissimi et al. 2018; Liou 1992). The primary reason for these advantages is the unique secondary flow pattern of HCTFs. For flow in curved pipes, it has been well established that fluid elements moving with different axial velocities induce a centrifugal force, generating a secondary flow which manifests itself as a pair of counter rotating vortices in the cross-section normal to the direction of flow (Carissimi et al. 2018; Dean 1928; Dean and Hurst 1959). For toroidal coils with no torsion, these vortices are symmetric and rotate towards the outer radius of curvature (Cioncolini and Santini 2006). For helicoidal tubes, however, the non-zero coil pitch introduces torsional effects and associated Coriolis forces, which further complicates the secondary flow field. It has been shown that the hydrodynamic nature of the secondary flow in helically coiled pipes is dependent on their geometrical characteristics, namely, the coil pitch, coil diameter, and pipe diameter. Several studies to date have evaluated the impact of geometry on HCTF performance (Cahyana et al. 2021; Carissimi and Rubio 2005; De Oliveira and Teixeira 2017), although, its effect has not been definitively elucidated due to the confounding effect of simultaneously changing multiple geometrical and system parameters. Thus, there is need to evaluate the suitability of HCTFs for continuous-flow coagulation in small-scale systems and to characterize the impact of geometry on their performance.

1.2. Research Objectives

The primary goal of this research was to evaluate and directly compare the performance of alternative coagulation pretreatment strategies for LPM systems, with emphasis on membrane fouling mitigation and organics removals. More specifically, the objectives of this research were to:

1. *Investigate the impact of membrane type on the performance of CF-SED, CF-DAF, and C-IN for a high organic feed water.*

   In the first phase of this research, which was originally anticipated as part of a master's thesis, the impact of membrane type on the relative performance of CF-SED and CF-DAF was evaluated by considering the same colored river water as previous members of our

research group (Walker and Narbaitz 2016; Xu and Narbaitz 2016), but membranes with different material type and configuration. For the first time, the performance of these two pretreatment strategies was directly compared with C-IN using identical membrane operating conditions. This assessment was made using water sampled across seasons, to evaluate the impact of intrannual variation in water quality, as well as using different coagulation chemistries corresponding to the jar-test optimal and 20% reduced dose conditions. Molecular weight fractionation and zeta potential analyses were used to identify key organic foulants and elucidate the coagulation conditions governing irreversible membrane fouling, a key driver of long-term LPM operating expenditures. Results of this work are presented in Chapter 3 and Chapter 4 of this thesis for an outside-in hollow-fiber polyvinylidene fluoride (PVDF) and an inside-out polyethersulfone (PES) tubular multichannel membrane, respectively. In Chapter 4 it is shown that, for a single membrane and water type, C-IN pretreatment yielded improved performance compared to more sophisticated coagulation-based treatment strategies including CF-DAF and CF-SED. This motivated further research on alternative C-IN dosing strategies, including C-IN-P, which is represented by Objective #4. Investigation of C-IN-P, however, required the development of a bench-scale continuous-flow coagulation system, the focus of Objective #2 and Objective #3.

2. *Evaluate the impact of key geometrical and hydrodynamic properties on the performance of HCTFs for small-scale continuous-flow coagulation systems.*

The primary objective of this phase of the research was to elucidate the impact of key geometrical and system variables on the performance of HCTFs for continuous-flow coagulation applications. This work used a designed experimental approach to screen the impact of a wide array of geometric and coagulation-related parameters on floc properties (size, fractal dimension, and concentration). A replicated full-factorial design was then used to determine the main and interaction effects of HCTF pipe length, coil diameter, and coil pitch (the most important geometrical parameters) on floc properties. Moreover, the properties of flocs generated by all tested configurations were directly compared with those formed by alternative coagulation/flocculation strategies commonly used in bench-scale studies including a commercial inline static mixer (ISM) and a batch reactor. The effect of

Reynolds number on HCTF performance was studied by varying the system flowrate. Results of the work in this chapter were used to develop HCTF design guidance for their application in different integrated system types (i.e., CF-SED vs. C-IN). Moreover, the results of the work presented in Chapter 5 were used to select HCTF geometries which formed flocs of disparate properties for use in the bench-scale filtration tests in Chapter 6.

3. *Examine the impact of bench-scale coagulant mixing configuration on the performance of C-IN pretreatment for LPMs.*

Over the past three plus decades, bench-scale membrane research studies have used a wide variety of strategies for coagulant mixing. Owing to their experimental simplicity, many studies have used batch coagulation approaches to simulate conditions of continuous-flow coagulation used in full-scale facilities. The primary objective of this phase of the research was to directly compare the performance of several alternative coagulant mixing strategies/devices for application in small-scale continuous-flow coagulation systems. A mini inline rapid mixer was developed in-house and its mixing efficiency was verified by tracer tests. The performance of a straight pipe control (i.e., incidental flocculation), two HCTFs (selected to yield disparate floc properties based on the results of Chapter 5), and a commercial ISM was compared in terms of floc properties, membrane fouling, and organics removals both with and without the rapid mixer. Results of this work are presented in Chapter 6.

4. *Compare the performance of C-IN-P and C-IN across a broad range of previously untested conditions including different water types and coagulant types.*

The final phase of this research focused on the evaluation of C-IN-P across a wide array of previously untested conditions. The impact of C-IDX and feed water type were evaluated by varying the length of coagulant dosing time and by considering three different challenge waters with varying organic matrices. LPM fouling and bulk organics removals were investigated across all these conditions and compared with direct filtration and C-IN. Fluorescence analysis was used to identify the key organic fractions governing C-IN-P performance for each water type. In addition, a set of experiments were conducted using different combinations of coagulant dose and dosing time, for a fixed C-IDX, to evaluate the

C-IDX as an operational control parameter. Results of this work are presented in Chapter 7.

1.3. Research Novelty and Contribution

This work provides several novel contributions. First, there exists a limited number of studies which evaluate the performance of CF-DAF as pretreatment for LPMs, with studies directly comparing the performance of CF-DAF and CF-SED or CF-DAF and C-IN being even fewer in number. In addition, this research was the first study to directly compare the performance of CF-SED, CF-DAF, and C-IN as LPM pretreatment using the same water. Furthermore, this comparison was more representative of full-scale operation compared to the approach followed by many published studies as it considered multi-day filtration tests with hollow-fiber membranes and numerous filtration cycles. In fact, continuous cyclical operation and realistic membrane modules were employed throughout all membrane tests in this research. This overcomes an important limitation of many studies in the literature that employ flat sheet membranes operated under a constant pressure and use only a small number of filtration cycles (often only one or two cycles), which does not inform on irreversible fouling development. Many membrane pretreatment studies to date have evaluated the fouling of a single membrane type and present their results generally, implying that they are universal. This work clearly showed that the optimal coagulation pretreatment strategy is membrane dependent.

This work advances the understanding of bench-scale continuous-flow C-IN systems. Although previous studies have employed a variety of coagulation configurations—including HCTFs, incidental pipe flocculation, commercial ISMs, and batch-mixing tanks—none have systematically investigated how the precoagulation method or hydrodynamic conditions influence pretreatment performance. For the first time, this research comprehensively characterized the effect of HCTF geometry on floc properties and subsequently demonstrated that differences in floc formation conditions can significantly impact LPM fouling behaviour. These findings highlight the importance of coagulation system design and operating conditions when conducting bench-scale LPM studies and provide guidance for future researchers conducting lab-scale investigations in selecting appropriate experimental configurations.

A second major contribution related to the work of Chapter 5 and Chapter 6 was the development and validation of a novel bench-scale continuous-flow coagulation system consisting of a syringe pump, mini-inline rapid mixer, and helical flocculator. By enabling direct coagulant

addition to the feed stream while maintaining realistic hydraulic retention times, this system more closely replicated full-scale C-IN processes than the batch-mixing approaches commonly used in previous studies. Collectively, these findings improve the understanding of bench-scale coagulation system design, provide a framework for more representative laboratory investigations, and may help to support the future development of more standardized testing methodologies for continuous-flow coagulation pretreatment.

Finally, this work represented the first comprehensive investigations of C-IN-P for LPM pretreatment. Despite increasing interest in coagulation pretreatment for LPMs (Fig. 1.1), including pretreatment by C-IN, there remains a dearth of studies regarding pretreatment by C-IN-P. To the authors' knowledge, no previous study had evaluated C-IN-P performance using different coagulant types or water types, especially those with elevated hydrophobicities. The findings from this research significantly improved understanding of the influence of water quality, coagulant type, and operating conditions (i.e., C-IDX) on C-IN-P performance. This work also established the C-IDX as a useful framework for C-IN-P optimization, while highlighting its practical limitations.

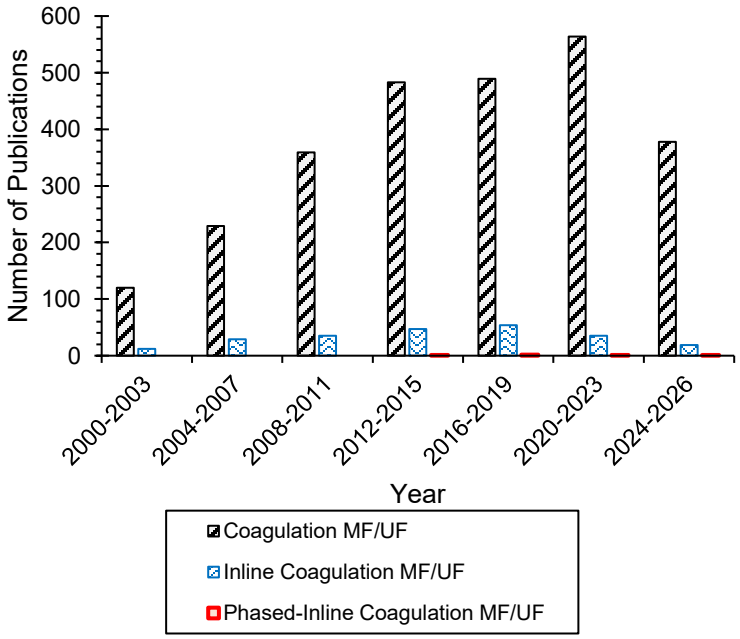


Fig. 1.1. Number of publications regarding coagulation pretreatment for LPMs in water treatment per 4-year period. Note: Data retrieved from SCOPUS 24 May 2026. Note: Boolean search queue for coagulation MF/UF was (coagulation AND (ultrafiltration OR microfiltration) AND water);

for inline coagulation MF/UF was (precoagulation OR "inline coagulation" OR pre-coagulation OR "in-line coagulation") AND (ultrafiltration OR microfiltration))); and for phased inline coagulation MF/UF was (("phased coagulation" OR "phased inline coagulation" OR "phased in-line coagulation" OR "intermittent coagulation" OR "intermittent in-line coagulation" OR "intermittent inline coagulation") AND (ultrafiltration OR microfiltration)))

1.4. Thesis Outline

This doctoral thesis is structured as a thesis-by-articles and comprises eight distinct chapters. As this thesis was part of a fast-tracked PhD program, chapters three and four present the articles related to work originally conducted for the master's research, while chapters five, six, and seven present the articles related to the doctoral research. The structure of the thesis is as follows:

- Chapter 1, *General Introduction*, presents a general background on alternative coagulation pretreatment strategies for LPMs as well as an overview of the challenges associated with small-scale testing for continuous-flow coagulation systems. The chapter also presents the research objectives, discusses the novelty of the proposed research, and outlines the organization of the thesis.

- Chapter 2, *Literature Review*, presents a current and comprehensive overview of the alternative coagulation pretreatment strategies for LPM fouling mitigation including CF-SED, CF-DAF, C-IN, and C-IN-P. This chapter resulted in two review articles, presented in Appendices B and C, which were published as:

    - Ladouceur, J.D., Narbaitz, R.M., & Lan, C.Q. (2023). Dissolved air flotation pretreatment for low-pressure membranes in water treatment: A review of fouling mitigation and product water quality. *Journal of Water Process Engineering*, 56, 104391.

    - Ladouceur, J.D., Narbaitz, R.M., & Lan, C.Q. (2024). Phased-inline coagulation for low-pressure membranes in water and wastewater treatment: a review of fouling mitigation, process control, and water quality. *Environmental Technology Reviews*, 13:1, 305-324.

- Chapter 3, *Comparing Sedimentation, Flotation, and Inline Pretreatment for Low-Pressure Membrane Fouling Reduction*, directly compares the performance of CF-SED, CF-DAF, and C-IN for pretreatment of a PVDF hollow-fiber membrane. A version of this chapter was published as:

  - Ladouceur, J.D., & Narbaitz, R.M. (2023). Comparing sedimentation, flotation, and in-line pretreatment for low-pressure membrane fouling reduction. *Journal of Environmental Engineering (ASCE)*, 149 (4), 04023002.

- Chapter 4, *Reduced Low-Pressure Membrane Fouling by Inline coagulation Pretreatment for a Colored River Water*, expands on the work of Chapter 3 by using an alternative membrane, namely, a PES tubular multichannel (TMC) membrane to study the impact of membrane type/configuration on the relative performance of CF-SED, CF-DAF, and C-IN. A version of this chapter was published as:

  - Ladouceur, J.D., & Narbaitz, R.M. (2022). Reduced low-pressure membrane fouling by inline coagulation pretreatment for a colored river water. *Membranes*, 12(11), 1028.

  The remaining work of this thesis is related to the investigation of C-IN-P as a novel coagulation-based LPM pretreatment strategy, including the development of a bench-scale continuous-flow coagulation system in Chapter 5 and Chapter 6.

- Chapter 5, *Characterizing the Impact of Geometry on the Performance of Inline-Coagulation Pretreatment Systems with Helical Flocculators*. To expand the work of Chapter 4 to novel coagulation-based pretreatment strategies, including C-IN-P, a bench-scale continuous-flow coagulation system needed to be developed. This was the focus of Chapter 5 and Chapter 6. In Chapter 5, HCTFs are evaluated as a tool for effectively implementing continuous-flow coagulation under low Reynolds conditions used at bench-scale. A designed experimental approach was used to systematically characterize the impact of helical coil geometry on the properties of flocs using a single coagulant and water type. The impact of Reynolds number on floc properties was also considered. A version of this chapter was published as:

  - Ladouceur, J.D., Narbaitz, R.M., & Lan, C.Q. (2026). Characterizing the impact of

geometry on the performance of inline-coagulation pretreatment systems with helical flocculators. *Environmental Science: Water Research & Technology, 12(8), 2423-2438.*

- Chapter 6, *Impact of Flocculator Type on Continuous Inline Coagulation for Low-Pressure Membrane Pretreatment in Drinking Water Production*. This chapter develops a small-scale inline rapid mixer for use in low Reynolds number continuous-flow coagulation applications. Floc properties were assessed following rapid mixing only, as well as for rapid mixing+flocculation for four different flocculators, namely, a control (incidental flocculation via straight pipe), an inline static mixer, and two HCTFs developed in Chapter 5. Using an automated bench-scale filtration system, the impact of the coagulant mixing conditions on LPM fouling development was studied for a single water, membrane, and coagulant type. A version of this chapter was published as:

    - Ladouceur, J.D**.**, Narbaitz, R.M., & Lan, C.Q. (2026). Impact of flocculator type on continuous inline coagulation for low-pressure membrane pretreatment in drinking water production. *Separation and Purification Technology (In Press).*

- Chapter 7, *Phased-Inline Coagulation Pretreatment for Low-Pressure Membrane Fouling Reduction*. In this chapter, the performance of C-IN-P is evaluated across a range of C-IDX values as well as for three water types with organic matrices of varying hydrophobicity. The performance of C-IN-P in terms of both fouling mitigation and organics removals is compared against direct filtration and C-IN for each water type. Moreover, the impact of coagulant dosing strategy and coagulant type on the suitability of the C-IDX as a process control tool for C-IN-P is evaluated.

- Chapter 8, *General Conclusions*. This chapter synthesizes the findings and conclusions presented in the five research articles and uses these to highlight directions for future research.

1.5 References

Aiken, G. R., D. M. McKnight, R. L. Wershaw, and P. MacCarthy. 1985. *Humic Substances in Soil, Sediment, and Water: Geochemistry, Isolation, and Characterization*. 1st ed. Toronto: John Wiley & Sons.

Alresheedi, M. T., S. L. D. Kenari, B. Barbeau, and O. D. Basu. 2022. "Flux modulation: A novel approach for ultrafiltration fouling control." *Journal of Water Process Engineering*, 46: 102551. https://doi.org/10.1016/j.jwpe.2021.102551.

AlSawaftah, N., W. Abuwatfa, N. Darwish, and G. Husseini. 2021. "A comprehensive review on membrane fouling: Mathematical modelling, prediction, diagnosis, and mitigation." *Water*, 13 (9): 1327. https://doi.org/10.3390/w13091327.

Aly, S. A., W. B. Anderson, and P. M. Huck. 2018. "Biological filtration with and without prior in-line coagulation to reduce uf fouling by secondary effluent." *Journal of Water Reuse and Desalination*, 8 (2): 176–191. https://doi.org/10.2166/wrd.2017.154.

Aly, S. A., W. B. Anderson, and P. M. Huck. 2021. "In-line coagulation assessment for ultrafiltration fouling reduction to treat secondary effluent for water reuse." *Water Science and Technology*, 83 (2): 284–296. https://doi.org/10.2166/wst.2020.571.

Amjad, H., Z. Khan, and V. V. Tarabara. 2015. "Fractal structure and permeability of membrane cake layers: Effect of coagulation–flocculation and settling as pretreatment steps." *Separation and Purification Technology*, 143: 40–51. https://doi.org/10.1016/j.seppur.2015.01.020.

Amy, G. 2008. "Fundamental understanding of organic matter fouling of membranes." *Desalination*, 231 (1–3): 44–51. https://doi.org/10.1016/j.desal.2007.11.037.

Anis, S. F., R. Hashaikeh, and N. Hilal. 2019. "Microfiltration membrane processes: A review of research trends over the past decade." *Journal of Water Process Engineering*, 32: 100941. https://doi.org/10.1016/j.jwpe.2019.100941.

Arnal, J. M., B. Garcia-Fayos, M. Sancho, and G. Verdu. 2009. "Ultrafiltration membrane cleaning with different chemical solutions after treating surface water." *Desalination and Water Treatment*, 7 (1–3): 198–205. https://doi.org/10.5004/dwt.2009.709.

AWWA. 2005. "Committee Report: Recent advances and research needs in membrane fouling." *Journal AWWA*, 97 (8): 79–89. https://doi.org/10.1002/j.1551-8833.2005.tb07452.x.

Baghbanzadeh, M., D. Rana, C. Q. Lan, and T. Matsuura. 2016. "Effects of inorganic nano-additives on properties and performance of polymeric membranes in water treatment." *Separation & Purification Reviews*, 45 (2): 141–167. https://doi.org/10.1080/15422119.2015.1068806.

Bermea, E. A. 1999. "Dual-membrane treatment of the Rio Grande: Meeting El Paso's future water demands." M.Sc, University of Texas at El Paso.

Bogati, R., C. Goodwin, K. Marshall, K. T. Leung, and B. Q. Liao. 2015. "Optimization of chemical cleaning for improvement of membrane performance and fouling control in drinking water treatment." *Separation Science and Technology (Philadelphia)*, 50 (12): 1835–1845. Taylor & Francis. https://doi.org/10.1080/01496395.2015.1009116.

Buchta, P., P. Berg, A. Schweiger, and D. Vial. 2019. "In-line coagulation upstream ultrafiltration - comparison of continuous vs. intermittent addition." 8. New Orleans, LA: American Water Works Association.

Buchta, P., A. Kripahle, D. Vial, R. Winkler, and P. Berg. 2017. "In-out ultrafiltration in tertiary wastewater applications- Comparison of different operational strategies." *Desalination and Water Treatment*, 73: 145–154.

Cahyana, G. H., P. Suwandhi, and T. Mulyani. 2021. "Novel helical or coiled flocculator for turbidity reduction in drinking water treatment: a performance study." *IOP Conference Series: Earth and Environmental Science*, 623 (1): 012009. https://doi.org/10.1088/1755-1315/623/1/012009.

Carissimi, E., and J. Rubio. 2005. "The flocs generator reactor-FGR: a new basis for flocculation and solid–liquid separation." *International Journal of Mineral Processing*, 75 (3–4): 237–247. https://doi.org/10.1016/j.minpro.2004.08.021.

Carissimi, E., D. G. Sanagiotto, E. B. C. Schettini, and J. Rubio. 2018. "Revisiting coiled flocculator performance for particle aggregation." *Water Environment Research*, 90 (4): 322–328. https://doi.org/10.2175/106143017X14902968254935.

Chang, H., H. Liang, F. Qu, B. Liu, H. Yu, X. Du, G. Li, and S. A. Snyder. 2017a. "Hydraulic backwashing for low-pressure membranes in drinking water treatment: A review." *Journal of Membrane Science*, 540 (May): 362–380. Elsevier B.V. https://doi.org/10.1016/j.memsci.2017.06.077.

Chang, H., B. Liu, H. Liang, H. Yu, S. Shao, and G. Li. 2017b. "Effect of filtration mode and backwash water on hydraulically irreversible fouling of ultrafiltration membrane." *Chemosphere*, 179 (2): 254–264. https://doi.org/10.1016/j.chemosphere.2017.03.122.

Chen, F., S. Peldszus, R. H. Peiris, A. S. Ruhl, R. Mehrez, M. Jekel, R. L. Legge, and P. M. Huck. 2014. "Pilot-scale investigation of drinking water ultrafiltration membrane fouling rates using advanced data analysis techniques." *Water Research*, 48 (1): 508–518. https://doi.org/10.1016/j.watres.2013.10.007.

Cheng, X., H. Liang, A. Ding, F. Qu, S. Shao, B. Liu, H. Wang, D. Wu, and G. Li. 2016. "Effects of pre-ozonation on the ultrafiltration of different natural organic matter (NOM) fractions: Membrane fouling mitigation, prediction and mechanism." *Journal of Membrane Science*, 505: 15–25. Elsevier. https://doi.org/10.1016/j.memsci.2016.01.022.

Cho, M. H., C. H. Lee, and S. Lee. 2006. "Effect of flocculation conditions on membrane permeability in coagulation-microfiltration." *Desalination*, 191 (1–3): 386–396. https://doi.org/10.1016/j.desal.2005.08.017.

Choi, K. Y. J., and B. A. Dempsey. 2004. "In-line coagulation with low-pressure membrane filtration." *Water Research*, 38 (19): 4271–4281. https://doi.org/10.1016/j.watres.2004.08.006.

Choi, Y. H., H. S. Kim, and J. H. Kweon. 2008. "Role of hydrophobic natural organic matter flocs on the fouling in coagulation-membrane processes." *Separation and Purification Technology*, 62 (3): 529–534. https://doi.org/10.1016/j.seppur.2008.03.001.

Cioncolini, A., and L. Santini. 2006. "An experimental investigation regarding the laminar to turbulent flow transition in helically coiled pipes." *Experimental Thermal and Fluid Science*, 30 (4): 367–380. https://doi.org/10.1016/j.expthermflusci.2005.08.005.

Crittenden, J. C., R. R. Trussell, D. W. Hand, K. J. Howe, and G. Tchobanoglous. 2012. *Water Treatment: Principles and Design*. 3rd ed. New York, NY: McGraw-Hill.

Crozes, G. F., J. G. Jacangelo, C. Anselme, and J. M. Laîné. 1997. "Impact of ultrafiltration operating conditions on membrane irreversible fouling." *Journal of Membrane Science*, 124 (1): 63–76. https://doi.org/10.1016/S0376-7388(96)00244-X.

Cui, X., and K. H. Choo. 2014. "Natural organic matter removal and fouling control in low-pressure membrane filtration for water treatment." *Environmental Engineering Research*, 19 (1): 1–8. https://doi.org/10.4491/eer.2014.19.1.001.

De Oliveira, D. S., and E. C. Teixeira. 2017. "Experimental evaluation of helically coiled tube flocculators for turbidity removal in drinking water treatment units." *Water SA*, 43 (3): 378. https://doi.org/10.4314/wsa.v43i3.02.

Dean, W. R. 1928. "The stream-line motion of fluid in a curved pipe." *The London, Edinburgh, and Dublin Philosophical Magazine and Journal of Science*, 5 (30): 673–695. https://doi.org/10.1080/14786440408564513.

Dean, W. R., and J. M. Hurst. 1959. "Note on the motion of fluid in a curved pipe." *Mathematika*, 6 (1): 77–85. https://doi.org/10.1112/S0025579300001947.

Delgado Diaz, S., L. Vera Peña, E. González Cabrera, M. Martínez Soto, L. M. Vera Cabezas, and L. R. Bravo Sánchez. 2012. "Effect of previous coagulation in direct ultrafiltration of primary settled municipal wastewater." *Desalination*, 304: 41–48. https://doi.org/10.1016/j.desal.2012.08.005.

Ding, Q., K. Ochiai, and H. Yamamura. 2020. "In situ and online monitoring of the chemical cleaning efficiency by solid-phase fluorescence excitation–emission matrix spectroscopy (SPF-EEM)." *Journal of Membrane Science*, 611: 118296. https://doi.org/10.1016/j.memsci.2020.118296.

Ding, Q., H. Yamamura, N. Murata, N. Aoki, H. Yonekawa, A. Hafuka, and Y. Watanabe. 2016. "Characteristics of meso-particles formed in coagulation process causing irreversible membrane fouling in the coagulation-microfiltration water treatment." *Water Research*, 101: 127–136. https://doi.org/10.1016/j.watres.2016.05.076.

Ding, Y., T. Li, K. Qiu, B. Ma, and R. Wu. 2021a. "Membrane fouling performance of Fe-based coagulation-ultrafiltration process: Effect of sedimentation time." *Environmental Research*, 195: 110756. https://doi.org/10.1016/j.envres.2021.110756.

Ding, Y., T. Li, K. Qiu, B. Ma, and R. Wu. 2021b. "Membrane fouling performance of Fe-based coagulation-ultrafiltration process: Effect of sedimentation time." *Environmental Research*, 195: 110756. https://doi.org/10.1016/j.envres.2021.110756.

Edzwald, J. K., and J. Haarhoff. 2012. *Dissolved Air Flotation for Water Clarification*. New York, NY: McGraw-Hill.

Gao, W., H. Liang, J. Ma, M. Han, Z. Chen, Z. Han, and G. Li. 2011. "Membrane fouling control in ultrafiltration technology for drinking water production: A review." *Desalination*, 272 (1–3): 1–8. Elsevier B.V. https://doi.org/10.1016/j.desal.2011.01.051.

Goh, Y. T., J. L. Harris, and F. A. Roddick. 2010. "Reducing the effect of cyanobacteria in the microfiltration of secondary effluent." *Water Science and Technology*, 62 (7): 1682–1688. https://doi.org/10.2166/wst.2010.482.

Gul, A., J. Hruza, and F. Yalcinkaya. 2021. "Fouling and chemical cleaning of microfiltration membranes: A mini-review." *Polymers*, 13 (6): 846. https://doi.org/10.3390/polym13060846.

Guo, W., H.-H. Ngo, and J. Li. 2012. "A mini-review on membrane fouling." *Bioresource Technology*, 122: 27–34. https://doi.org/10.1016/j.biortech.2012.04.089.

Hao, Y., A. Moriya, T. Maruyama, Y. Ohmukai, and H. Matsuyama. 2011. "Effect of metal ions on humic acid fouling of hollow fiber ultrafiltration membrane." *Journal of Membrane Science*, 376 (1–2): 247–253. https://doi.org/10.1016/j.memsci.2011.04.035.

Hilal, N., O. O. Ogunbiyi, N. J. Miles, and R. Nigmatullin. 2005. "Methods employed for control of fouling in MF and UF membranes: A comprehensive review." *Separation Science and Technology*, 40 (10): 1957–2005. https://doi.org/10.1081/SS-200068409.

Hög, A., J. Ludwig, and M. Beery. 2015. "The use of integrated flotation and ceramic membrane filtration for surface water treatment with high loads of suspended and dissolved organic matter." *Journal of Water Process Engineering*, 6: 129–135. Elsevier Ltd. https://doi.org/10.1016/j.jwpe.2015.03.010.

Huang, H., N. H. Lee, T. Young, A. Gary, J. C. Lozier, and J. G. Jacangelo. 2007. "Natural organic matter fouling of low-pressure, hollow-fiber membranes: Effects of NOM source and hydrodynamic conditions." *Water Research*, 41 (17): 3823–3832. https://doi.org/10.1016/j.watres.2007.05.036.

Huang, H., K. Schwab, and J. G. Jacangelo. 2009. "Pretreatment for low pressure membranes in water treatment: A review." *Environmental Science and Technology*, 43 (9): 3011–3019. https://doi.org/10.1021/es802473r.

Huang, W., W. Lv, W. Zhou, M. Hu, and B. Dong. 2019. "Investigation of the fouling behaviors correlating to water characteristics during the ultrafiltration with ozone treatment." *Science of the Total Environment*, 676: 53–61. Elsevier B.V. https://doi.org/10.1016/j.scitotenv.2019.04.271.

Jermann, D., W. Pronk, and M. Boller. 2008a. "Mutual influences between natural organic matter and inorganic particles and their combined effect on ultrafiltration membrane fouling." *Environmental Science & Technology*, 42 (24): 9129–9136. https://doi.org/10.1021/es800654p.

Jermann, D., W. Pronk, R. Ka, M. Halbeisen, and M. Boller. 2008b. "Influence of interactions between NOM and particles on UF fouling mechanisms." *Water Research*, 42: 3870–3878. https://doi.org/10.1016/j.watres.2008.05.013.

Kamińska, G., W. Pronk, and J. Traber. 2020. "Effect of coagulant dose and backflush pressure on NOM membrane fouling in inline coagulation-ultrafiltration." *Desalination and Water Treatment*, 199: 188–197. https://doi.org/10.5004/dwt.2020.25657.

Kang, J., J. Seong, J. Yoo, P. Kim, K. Park, J. Lee, J. Cheon, H. Kim, and S. Lee. 2021. "Applicability of a combined DAF-MF process to respond to changes in reservoir water quality through a two-year pilot plant operation." *Membranes*, 11 (12): 964. https://doi.org/10.3390/membranes11120964.

Keucken, A., G. Heinicke, K. M. Persson, and S. J. Köhler. 2017. "Combined coagulation and ultrafiltration process to counteract increasing NOM in brown surface water." *Water*, 9 (9): 697. Multidisciplinary Digital Publishing Institute. https://doi.org/10.3390/w9090697.

Kim, H.-C., J.-H. Hong, and S. Lee. 2006. "Fouling of microfiltration membranes by natural organic matter after coagulation treatment: A comparison of different initial mixing conditions." *Journal of Membrane Science*, 283 (1–2): 266–272. https://doi.org/10.1016/j.memsci.2006.06.041.

Kim, Y.-J., J.-W. Jung, and S. Lee. 2015. "Comparison of fouling rates for pressurized and submerged ultrafiltration membranes." *Desalination and Water Treatment*, 54 (13): 3610–3615. https://doi.org/10.1080/19443994.2014.923208.

Kimura, K., Y. Hane, Y. Watanabe, G. Amy, and N. Ohkuma. 2004. "Irreversible membrane fouling during ultrafiltration of surface water." *Water Research*, 38 (14–15): 3431–3441. https://doi.org/10.1016/j.watres.2004.05.007.

Kimura, K., and K. Kume. 2020. "Irreversible fouling in hollow-fiber PVDF MF / UF membranes filtering surface water: Effects of precoagulation and identification of the foulant." *Journal of Membrane Science*, 602 (February): 117975–117975. Elsevier B.V. https://doi.org/10.1016/j.memsci.2020.117975.

Kinser, K. 2021. "Membrane Filtration: Past, Present, and Future." *Journal AWWA*, 113 (8): 72–75. https://doi.org/10.1002/awwa.1791.

Koros, W. J., Y. H. Ma, and T. Shimidzu. 1996. "Terminology for membranes and membrane processes (IUPAC Recommendations 1996)." *Pure and Applied Chemistry*, 68 (7): 1479–1489. https://doi.org/10.1351/pac199668071479.

Koyuncu, I., R. Sengur, T. Turken, S. Guclu, and M. E. Pasaoglu. 2015. "Advances in water treatment by microfiltration, ultrafiltration, and nanofiltration." *Advances in Membrane Technologies for Water Treatment*, 83–128. Elsevier.

Lazaridis, N. K., C. Blöcher, J. Dorda, and K. A. Matis. 2004. "A hybrid MF process based on flotation." *Journal of Membrane Science*, 228 (1): 83–88. https://doi.org/10.1016/j.memsci.2003.07.024.

Lebeau, T., C. Lelièvre, H. Buisson, D. Cléret, L. W. Van de Venter, and P. Côté. 1998. "Immersed membrane filtration for the production of drinking water: combination with PAC for NOM and SOCs removal." *Desalination*, 117 (1–3): 219–231. https://doi.org/10.1016/S0011-9164(98)00101-5.

Lee, E. K., V. Chen, and A. G. Fane. 2008. "Natural organic matter (NOM) fouling in low pressure membrane filtration — effect of membranes and operation modes." *Desalination*, 218 (September 2006): 257–270. https://doi.org/10.1016/j.desal.2007.02.021.

Lee, N., G. Amy, J.-P. Croué, and H. Buisson. 2004. "Identification and understanding of fouling in low-pressure membrane (MF/UF) filtration by natural organic matter (NOM)." *Water Research*, 38 (20): 4511–4523. https://doi.org/10.1016/j.watres.2004.08.013.

Lee, Y.-G., J. Shin, S. J. Kim, K. H. Cho, P. Westerhoff, H. Rho, and K. Chon. 2023. "An autopsy study of hollow fiber and multibore ultrafiltration membranes from a pilot-scale ultra high-recovery filtration system for surface water treatment." *Science of The Total Environment*, 866: 161311. https://doi.org/10.1016/j.scitotenv.2022.161311.

Li, K., G. Wen, S. Li, H. Chang, S. Shao, T. Huang, G. Li, and H. Liang. 2019. "Effect of pre-oxidation on low pressure membrane (LPM) for water and wastewater treatment: A review." *Chemosphere*, 231: 287–300. https://doi.org/10.1016/j.chemosphere.2019.05.081.

Li, L., H. E. Wray, R. C. Andrews, P. R. Bérubé, L. Li, H. E. Wray, R. C. Andrews, P. R. Bérubé, L. Li, H. E. Wray, R. C. Andrews, and P. R. Bérubé. 2014. "Ultrafiltration fouling: Impact of backwash frequency and air sparging." *Separation Science and Technology*, 49 (18): 2814–2823. Taylor & Francis. https://doi.org/10.1080/01496395.2014.948964.

Liang, H., W. Gong, and G. Li. 2008. "Performance evaluation of water treatment ultrafiltration pilot plants treating algae-rich reservoir water." *Desalination*, 221 (1–3): 345–350. https://doi.org/10.1016/j.desal.2007.01.093.

Lin, C. F., Y. J. Huang, and O. J. Hao. 1999. "Ultrafiltration processes for removing humic substances: Effect of molecular weight fractions and PAC treatment." *Water Research*, 33 (5): 1252–1264. https://doi.org/10.1016/S0043-1354(98)00322-4.

Liou, T. M. 1992. "Flow visualization and LDV measurement of fully developed laminar flow in helically coiled tubes." *Experiments in Fluids*, 13 (5): 332–338. https://doi.org/10.1007/BF00209507.

Liu, L., X.-B. Luo, L. Ding, and S.-L. Luo. 2019. "Application of nanotechnology in the removal of heavy metals from water." *Nanomaterials for the Removal of Pollutants and Resource Reutilization*, 83–147. Elsevier.

Lok, A., H. Wray, P. Bérubé, and R. C. Andrews. 2017. "Optimization of air sparging and in-line coagulation for ultrafiltration fouling control." *Separation and Purification Technology*, 188: 60–66. https://doi.org/10.1016/j.seppur.2017.06.064.

Ma, B., Y. Ding, B. Wang, Z. Qi, Y. Bai, R. Liu, H. Liu, and J. Qu. 2020a. "Influence of sedimentation with pre-coagulation on ultrafiltration membrane fouling performance." *Science of the Total Environment*, 708: 134671–134671. Elsevier B.V. https://doi.org/10.1016/j.scitotenv.2019.134671.

Ma, B., Y. Ding, B. Wang, Z. Qi, Y. Bai, R. Liu, H. Liu, and J. Qu. 2020b. "Influence of sedimentation with pre-coagulation on ultrafiltration membrane fouling performance." *Science of The Total Environment*, 708: 134671. https://doi.org/10.1016/j.scitotenv.2019.134671.

Ma, B., W. Yu, H. Liu, and J. Qu. 2014. "Effect of low dosage of coagulant on the ultrafiltration membrane performance in feedwater treatment." *Water Research*, 51: 277–283. https://doi.org/10.1016/j.watres.2013.10.069.

Malkoske, T. A., P. R. Bérubé, and R. C. Andrews. 2020. "Coagulation/flocculation prior to low pressure membranes in drinking water treatment: A review." *Environmental Science: Water Research and Technology*, 6 (11): 2993–3023. Royal Society of Chemistry. https://doi.org/10.1039/d0ew00461h.

Malkoske, T. A., P. R. Bérubé, and R. C. Andrews. 2023a. "Impact of extended versus typical rapid mixing HRTs on continuous-flow coagulation-ultrafiltration." *Separation and Purification Technology*, 319: 124041. https://doi.org/10.1016/j.seppur.2023.124041.

Malkoske, T. A., P. R. Bérubé, and R. C. Andrews. 2023b. "Leveraging coagulation mechanisms to reduce fouling and increase natural organic matter removal during coagulation/flocculation-ultrafiltration treatment." *Separation and Purification Technology*, 327: 124877. https://doi.org/10.1016/j.seppur.2023.124877.

Matilainen, A., E. T. Gjessing, T. Lahtinen, L. Hed, A. Bhatnagar, and M. Sillanpää. 2011. "An overview of the methods used in the characterisation of natural organic matter (NOM) in relation to drinking water treatment." *Chemosphere*, 83 (11): 1431–1442. https://doi.org/10.1016/j.chemosphere.2011.01.018.

Matilainen, A., M. Vepsäläinen, and M. Sillanpää. 2010. "Natural organic matter removal by coagulation during drinking water treatment: A review." *Advances in Colloid and Interface Science*, 159 (2): 189–197. https://doi.org/10.1016/j.cis.2010.06.007.

Minegishi, S., N.-Y. Jang, Y. Watanabe, S. Hirata, and G. Ozawa. 2001. "Fouling mechanism of hollow fiber ultrafiltration membrane with pretreatment by coagulation/sedimentation process." *Water Supply*, 1 (4): 49–56. https://doi.org/10.2166/ws.2001.0066.

Minhalma, M., and M. N. de Pinho. 2001. "Flocculation/Flotation/Ultrafiltration Integrated Process for the Treatment of Cork Processing Wastewaters." *Environmental Science & Technology*, 35 (24): 4916–4921. https://doi.org/10.1021/es010119n.

Moon, J., M.-S. Kang, J.-L. Lim, C.-H. Kim, and H.-D. Park. 2009. "Evaluation of a low-pressure membrane filtration for drinking water treatment: pretreatment by coagulation/sedimentation for the MF membrane." *Desalination*, 247 (1–3): 271–284. https://doi.org/10.1016/j.desal.2008.12.030.

Mosqueda-Jimenez, D. B., R. M. Narbaitz, and T. Matsuura. 2004. "Manufacturing conditions of surface-modified membranes: Effects on ultrafiltration performance." *Separation and Purification Technology*, 37 (1): 51–67. https://doi.org/10.1016/j.seppur.2003.07.003.

Naim, R., R. Epsztein, A. Felder, M. Heyer, M. Heijnen, and V. Gitis. 2014. "Rethinking the role of in-line coagulation in tertiary membrane filtration of municipal effluents." *Separation and Purification Technology*, 125: 11–20. Elsevier B.V. https://doi.org/10.1016/j.seppur.2014.01.036.

Neama, M.-A. A. M., W. A. Elbarki, M. Fayed, and S. Aly. 2024. "Upgrading the eastern wastewater treatment plant effluent quality in Egypt for reuse by means of in-line coagulation followed by ultrafiltration." *Water Practice & Technology*, 19 (12): 4754–4772. London, UK: IWA Publishing. https://doi.org/10.2166/wpt.2024.285.

Nguyen, A. H., R. M. Narbaitz, and T. Matsuura. 2007. "Impacts of hydrophilic membrane additives on the ultrafiltration of river water." *Journal of Environmental Engineering*, 133 (5): 515–522. https://doi.org/10.1061/(asce)0733-9372(2007)133:5(515).

Obotey Ezugbe, E., and S. Rathilal. 2020. "Membrane technologies in wastewater treatment: A review." *Membranes*, 10 (5): 89. https://doi.org/10.3390/membranes10050089.

Park, S., J.-S. Kang, J. J. Lee, T.-K.-Q. Vo, and H.-S. Kim. 2018. "Application of physical and chemical enhanced backwashing to reduce membrane fouling in the water treatment process using ceramic membranes." *Membranes*, 8 (4): 110. https://doi.org/10.3390/membranes8040110.

Pearce, G. K. 2011. *UF/MF Membrane Water Treatment: Principles and Design*. 387. 1st ed. Bangkok: Water Treatment Academy.

Pearce, G. K. 2018. "Is the Water Membrane Market in a State of Flux?" *Water World*.

Peiris, R. H., H. Budman, C. Moresoli, and R. L. Legge. 2010. "Understanding fouling behaviour of ultrafiltration membrane processes and natural water using principal component analysis of fluorescence excitation-emission matrices." *Journal of Membrane Science*, 357 (1–2): 62–72. Elsevier B.V. https://doi.org/10.1016/j.memsci.2010.03.047.

Peiris, R. H., M. Jaklewicz, H. Budman, R. L. Legge, and C. Moresoli. 2013. "Assessing the role of feed water constituents in irreversible membrane fouling of pilot-scale ultrafiltration drinking water treatment systems." *Water Research*, 47 (10): 3364–3374. Elsevier Ltd. https://doi.org/10.1016/j.watres.2013.03.015.

Peleato, N. M., R. L. Legge, and R. C. Andrews. 2017. "Characterization of UF foulants and fouling mechanisms when applying low in-line coagulant pre-treatment." *Water Research*, 126: 1–11. Elsevier Ltd. https://doi.org/10.1016/j.watres.2017.08.064.

Peters, C. D., T. Rantissi, V. Gitis, and N. P. Hankins. 2021. "Retention of natural organic matter by ultrafiltration and the mitigation of membrane fouling through pre-treatment, membrane enhancement, and cleaning - A review." *Journal of Water Process Engineering*, 44: 102374. https://doi.org/10.1016/j.jwpe.2021.102374.

Pezeshk, N., and R. M. Narbaitz. 2012. "More fouling resistant modified PVDF ultrafiltration membranes for water treatment." *Desalination*, 287: 247–254. https://doi.org/10.1016/j.desal.2011.11.048.

Porcelli, N., and S. Judd. 2010. "Chemical cleaning of potable water membranes: A review." *Separation and Purification Technology*, 71 (2): 137–143. https://doi.org/10.1016/j.seppur.2009.12.007.

Pronk, W., J. Traber, and G. Kamińska. 2016. "Optimization of process parameters of the coagulation/ultrafiltration process for the reduction of membrane fouling." In: *Advances in Particle Science and Separation: Meeting Tomorrow's Challenges*, 198–205. Oslo, Norway: International Water Association.

Rana, D., and T. Matsuura. 2010. "Surface modifications for antifouling membranes." *Chemical Reviews*, 110 (4): 2448–2471. https://doi.org/10.1021/cr800208y.

Ren, L., C. Liu, T. Meng, and Y. Sun. 2021. "Effects of micro-flocculation pretreatment on the ultrafiltration membrane fouling caused by different dissolved organic matters in treated wastewater." *Journal of Water Reuse and Desalination*, 11 (4): 597–609. https://doi.org/10.2166/wrd.2021.051.

Schäfer, A. I., N. Andritsos, A. J. Karabelas, E. M. V. Hoek, R. Schneider, and M. Nyström. 2021. "Fouling in nanofiltration." *Nanofiltration: Principles, applications, and new materials*, edited by A. I. Schäefer and A. G. Fane, 273–379. 2nd ed. Wiley-VCH GmbH.

Schulz, M., A. Soltani, X. Zheng, and M. Ernst. 2016. "Effect of inorganic colloidal water constituents on combined low-pressure membrane fouling with natural organic matter (NOM)." *Journal of Membrane Science*, 507: 154–164. Elsevier. https://doi.org/10.1016/j.memsci.2016.02.008.

Schweiger, A., P. Buchta, D. Vial, and P. Berg. 2018a. "Coating of ultrafiltration membranes - the solution to improve the efficiency of the pre-treatment." In: *Desalination for the Environment - Clean Water and Energy*. Athens.

Schweiger, A., C. Starke, D. Vial, P. Buchta, and P. Berg. 2018b. "Coating - a dramatic change in ultrafiltration treatment of secondary effluent." Valencia, Spain.

Shi, X., G. Tal, N. P. Hankins, and V. Gitis. 2014. "Fouling and cleaning of ultrafiltration membranes: A review." *Journal of Water Process Engineering*, 1: 121–138. Elsevier Ltd. https://doi.org/10.1016/j.jwpe.2014.04.003.

Shi, Y., J. Ma, D. Wu, and Q. Pan. 2017. "Dessolved air flotation in combination with ultrafiltration membrane modules in surface water treatment." *Journal of Harbin Institute of Technology*, 24 (3).

Sillanpaa, M. 2015. *Natural Organic Matter in Water*. 1st ed. Oxford, UK: Butterworth-Heinemann.

Souza, N. P. D., and O. D. Basu. 2013. "Comparative analysis of physical cleaning operations for fouling control of hollow fiber membranes in drinking water treatment." *Journal of Membrane Science*, 436: 28–35. Elsevier. https://doi.org/10.1016/j.memsci.2013.02.014.

Suárez, J., B. Salgado, A. Casañas, J. C. González, and J. Pordomingo. 2015. "One-year operational experience with ultrafiltration as pretreatment of seawater reverse osmosis desalination system (Maspalomas-I Plant)." *Desalination and Water Treatment*, 55 (10): 2813–2821. https://doi.org/10.1080/19443994.2014.959742.

Tabatabai, S. A. A., M. D. Kennedy, G. L. Amy, and J. C. Schippers. 2009. "Optimizing inline coagulation to reduce chemical consumption in MF/UF systems." *Desalination and Water Treatment*, 6 (1–3): 94–101. https://doi.org/10.5004/dwt.2009.653.

Tang, C. K., N. M. Peleato, P. R. Bérubé, and R. C. Andrews. 2019. "Impact of low coagulant dosages on protein fouling of ultrafiltration membranes." *Journal of Water Process Engineering*, 31: 100801. https://doi.org/10.1016/j.jwpe.2019.100801.

Tanudjaja, H. J., A. Anantharaman, A. Q. Q. Ng, Y. Ma, M. B. Tanis-Kanbur, A. L. Zydney, and J. W. Chew. 2022. "A review of membrane fouling by proteins in ultrafiltration and microfiltration." *Journal of Water Process Engineering*, 50: 103294. https://doi.org/10.1016/j.jwpe.2022.103294.

Teixeira, M. R., and M. J. Rosa. 2006. "Comparing dissolved air flotation and conventional sedimentation to remove cyanobacterial cells of Microcystis aeruginosa. Part I: The key

operating conditions." *Separation and Purification Technology*, 52 (1): 84–94. https://doi.org/10.1016/j.seppur.2006.03.017.

Tian, J., M. Ernst, F. Cui, and M. Jekel. 2013a. "Effect of particle size and concentration on the synergistic UF membrane fouling by particles and NOM fractions." *Journal of Membrane Science*, 446: 1–9. https://doi.org/10.1016/j.memsci.2013.06.016.

Tian, J. yu, M. Ernst, F. Cui, and M. Jekel. 2013b. "Correlations of relevant membrane foulants with UF membrane fouling in different waters." *Water Research*, 47 (3): 1218–1228. Elsevier Ltd. https://doi.org/10.1016/j.watres.2012.11.043.

Walker, S., and R. M. Narbaitz. 2016. "Hollow fiber ultrafiltration of Ottawa River water: Floatation versus sedimentation pre-treatment." *Chemical Engineering Journal*, 288: 228–237. Elsevier B.V. https://doi.org/10.1016/j.cej.2015.11.064.

Wang, J., and X. C. Wang. 2006. "Ultrafiltration with in-line coagulation for the removal of natural humic acid and membrane fouling mechanism." *Journal of Environmental Sciences (China)*, 18 (5): 880–884. https://doi.org/10.1016/S1001-0742(06)60008-9.

Wray, H. E., and R. C. Andrews. 2014. "Optimization of coagulant dose for biopolymer removal: Impact on ultrafiltration fouling and retention of organic micropollutants." *Journal of Water Process Engineering*, 1: 74–83. https://doi.org/10.1016/j.jwpe.2014.03.007.

Xie, Y., B. Ma, X. Zhang, H. Liu, and J. Qu. 2016. "Modification of ultrafiltration membrane with iron/aluminum mixed hydrolyzed precipitate layer for humic acid fouling reduction." *Desalination and Water Treatment*, 57 (54): 26022–26030. https://doi.org/10.1080/19443994.2016.1159991.

Xu, B., and R. M. Narbaitz. 2016. "Improved membrane pretreatment of high hydrophobic natural organic matter (NOM) waters by floatation." *Journal of Membrane Science*, 518: 120–130. Elsevier. https://doi.org/10.1016/j.memsci.2016.02.056.

Xu, X., Y. Yang, T. Liu, and B. Chu. 2022. "Cost-effective polymer-based membranes for drinking water purification." *Giant*, 10: 100099. https://doi.org/10.1016/j.giant.2022.100099.

Yamamura, H., Q. Ding, and Y. Watanabe. 2019. "Solid-phase fluorescence excitation emission matrix for in-situ monitoring of membrane fouling during microfiltration using a polyvinylidene fluoride hollow fiber membrane." *Water Research*, 164: 114928. https://doi.org/10.1016/j.watres.2019.114928.

Yamamura, H., K. Kimura, and Y. Watanabe. 2007. "Mechanism involved in the evolution of physically irreversible fouling in microfiltration and ultrafiltration membranes used for drinking water treatment." *Environmental Science and Technology*, 41 (19): 6789–6794. https://doi.org/10.1021/es0629054.

Yamamura, H., K. Okimoto, K. Kimura, and Y. Watanabe. 2014. "Hydrophilic fraction of natural organic matter causing irreversible fouling of microfiltration and ultrafiltration membranes." *Water Research*, 54: 123–136. Elsevier Ltd. https://doi.org/10.1016/j.watres.2014.01.024.

Yao, M., J. Nan, Q. Li, D. Zhan, T. Chen, Z. Wang, and H. Li. 2015. "Effect of under-dosing coagulant on coagulation–ultrafiltration process for treatment of humic-rich water with divalent calcium ion." *Journal of Membrane Science*, 495: 37–47. https://doi.org/10.1016/j.memsci.2015.08.001.

Yu, H., H. Chang, X. Li, Z. Zhou, W. Song, H. Ji, and H. Liang. 2021. "Long-term fouling evolution of polyvinyl chloride ultrafiltration membranes in a hybrid short-length sedimentation/ ultrafiltration process for drinking water production." *Journal of Membrane Science*, 630: 119320. https://doi.org/10.1016/j.memsci.2021.119320.

Yu, W., J. Qu, and J. Gregory. 2015a. "Pre-coagulation on the submerged membrane fouling in nano-scale: Effect of sedimentation process." *Chemical Engineering Journal*, 262: 676–682. https://doi.org/10.1016/j.cej.2014.09.102.

Yu, W., J. Qu, and J. Gregory. 2015b. "Pre-coagulation on the submerged membrane fouling in nano-scale: Effect of sedimentation process." *Chemical Engineering Journal*, 262: 676–682. https://doi.org/10.1016/j.cej.2014.09.102.

Zhu, X., C. Fan, Y. Fang, W. Yu, Y. Xie, and H. Liu. 2024. "Fouling and chemical cleaning strategies for submerged ultrafiltration membrane: Synchronized bench-Scale, full-scale, and engineering tests." *Membranes*, 14 (12): 251. https://doi.org/10.3390/membranes14120251.

Zietzschmann, F., M. Ernst, M. Godehardt, H. Paar, X. Zheng, and M. Jekel. 2014. "Linking UF reversible and irreversible fouling to the water quality of surface water and treated municipal wastewater." *Desalination and Water Treatment*, 52 (40–42): 7598–7608. https://doi.org/10.1080/19443994.2013.834271.

Zularisam, A. W., A. Ahmad, M. Sakinah, A. F. Ismail, and T. Matsuura. 2011. "Role of natural organic matter (NOM), colloidal particles, and solution chemistry on ultrafiltration performance." *Separation and Purification Technology*, 78 (2): 189–200. Elsevier B.V. https://doi.org/10.1016/j.seppur.2011.02.001.

Zularisam, A. W., A. F. Ismail, M. R. Salim, M. Sakinah, and H. Ozaki. 2007. "The effects of natural organic matter (NOM) fractions on fouling characteristics and flux recovery of ultrafiltration membranes." *Desalination*, 212 (1–3): 191–208. https://doi.org/10.1016/j.desal.2006.10.010.

CHAPTER 2

Literature Review

Context: In this study, alternative coagulation pretreatment strategies for low-pressure membranes (LPMs) will be investigated as a means to achieve integrated drinking water treatment (DWT) goals of fouling mitigation and natural organic matter (NOM) removal (for disinfection byproduct (DBP) formation potential reduction). To this end, the literature review will first provide an overview of the alternative coagulation strategies to be investigated, followed by a more detailed analysis of the factors which influence LPM fouling and organics removals for each configuration.

The contents of this literature review contributed to the publication of two review articles:

1. Ladouceur, J.D., Narbaitz, R.M., & Lan, C.Q. (2023). Dissolved air flotation pretreatment for low-pressure membranes in water treatment: A review of fouling mitigation and product water quality. *Journal of Water Process Engineering, 56, 104391*.
2. Ladouceur, J.D., Narbaitz, R.M., & Lan, C.Q. (2024). Phased-inline coagulation for low-pressure membranes in water and wastewater treatment: a review of fouling mitigation, process control, and water quality. *Environmental Technology Reviews, 13:1, 305-324.*

As the contents of these articles extend beyond the scope of the material covered in this chapter of the thesis, they are additionally provided in Appendix B and Appendix C.

List of Abbreviations

BSA	Bovine serum albumin
CF-DAF	Coagulation/flocculation/dissolved air flotation
CF-SED	Coagulation/flocculation/sedimentation
C-IN	Inline coagulation
C-IN-P	Phased-inline coagulation
COD	Chemical oxygen demand
DAF	Dissolved air flotation
DBP	Disinfection by-product
D_f	Fractal dimension
$D_{f,2}$	2-D fractal dimension (area-based)
$D_{f,3}$	3-D fractal dimension (volume-based)
DOC	Dissolved organic carbon
DWT	Drinking water treatment
G	Mean velocity gradient
HCTF	Helically coiled tube flocculator
HIFI	Hydraulically irreversible fouling index
HRT	Hydraulic retention time
LC-OCD	Liquid chromatography organic carbon detection
LPM	Low-pressure membrane
MF	Microfiltration
MWCO	Molecular weight cut-off
PES	Polyethersulfone
PVDF	Polyvinylidene fluoride
SCR	Specific cake resistance
SE	Secondary effluent
SEM	Scanning electron microscope
SUVA	Specific ultraviolet absorbance at 254nm
SWRO	Seawater reverse osmosis
TFI	Total fouling index

TMP	Transmembrane pressure
TOC	Total organic carbon
UF	Ultrafiltration
WTP	Water treatment plant
ZP	Zeta potential

List of Variables

Variable	Description
α_{CR}	Specific cake resistance (m kg^{-1})
Δt	Represents the difference in time between times t_i and t_f (where $t_f > t_i$) (h)
ε_c	Cake layer porosity (dimensionless)
ρ_{pp}	Density of primary particles that form the cake (kg m^{-3})
$C - IDX$	Membrane coating index (mg m^{-2})
d_{pp}	Primary particle diameter (m)
J	Membrane gross flux (L m^{-2} h^{-1})
J_0	Initial clean water flux (L m^{-2} h^{-1})
J_{t_i}	Membrane flux at time t_i (L m^{-2} h^{-1})
J_{t_f}	Membrane flux at time t_f (L m^{-2} h^{-1})
Q	Coagulant dose (as metal) (mg L^{-1})
$RNFD$	Rate of normalized flux decline (h^{-1})
T	Duration of coagulant addition (min)

2.1. Overview of Coagulation Configurations for Low-Pressure Membrane Pretreatment

2.1.1. Coagulation/Flocculation/Sedimentation (CF-SED) and Coagulation/Flocculation/Dissolved-Air-Flotation (CF-DAF)

The schematic overview of the low-pressure membrane (LPM) system with CF-SED and CF-DAF pretreatment is presented in Fig. 2.1a and Fig. 2.1b, respectively. In both cases, the pretreatment process includes coagulation/flocculation, while for CF-SED clarification occurs by sedimentation and for CF-DAF clarification is by dissolved-air-flotation (DAF). The integration of either CF-SED or CF-DAF as pretreatment for LPMs is often necessary due to the low rejection of natural

organic matter (NOM) afforded by LPMs (<10-20%) (Pearce 2011) and are promising techniques to simultaneously mitigate membrane fouling as well as minimize the formation potential of disinfection by-products (DBPs). The high-quality product water (reduced turbidity and dissolved organic carbon (DOC)) collected following clarification is used as influent to the LPM system, delivering a greatly reduced foulant loading compared to direct filtration. Concerning CF-DAF, it is anticipated that its use as LPM pretreatment for drinking water production will continue to grow in the coming years. Increased demand for seawater reverse osmosis (SWRO) facilities (for which CF-DAF-LPM is used as pretreatment) (Deka et al. 2020; Khanzada et al. 2017), as well as increasing frequency of algae blooms and decreased quality of natural waters are driving designers to implement the hybrid CF-DAF-LPM system, which has been proven as an effective treatment (or pretreatment for SWRO) technology for these water types (Edzwald and Haarhoff 2012; Guastalli et al. 2013; Harvey et al. 2020).

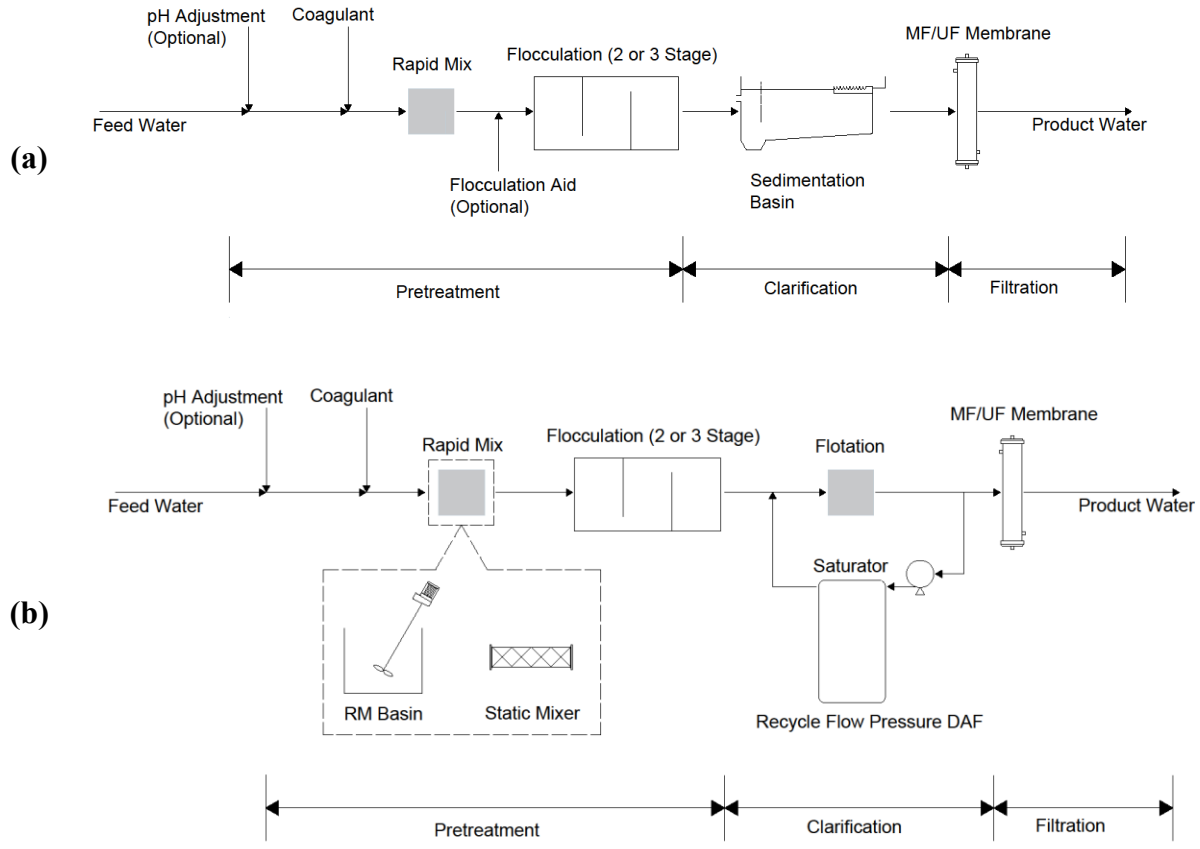


Fig. 2.1. Low-pressure membrane system integrated with: **(a)** CF-SED pretreatment; **(b)** CF-DAF pretreatment (not to scale).

2.1.2. Inline Coagulation (C-IN)

Continuous C-IN pretreatment for LPMs involves the direct addition of coagulant (as well as any acid/base or flocculants) to the feed stream (for the entire filtration cycle) prior to LPM filtration without any pre-clarification process. Recent interest regarding C-IN pretreatment is largely due to its significantly reduced footprint compared to conventional treatment by CF-SED, which can lead to considerable savings in capital costs (Sillanpaa 2015). Moreover, the operation of C-IN has a reduced complexity compared (Kamińska et al. 2020) to CF-SED or CF-DAF and may also achieve savings in energy consumption (e.g., no saturator, no flocculation basin). In addition, it is reported that C-IN can effectively mitigate LPM fouling with ultra-low coagulant dosages (unsuitable for CF-SED or CF-DAF), which can further reduce operating costs (Hu et al. 2021; Ma et al. 2014; Peleato et al. 2017; Tabatabai et al. 2009; Tang et al. 2019; Wray and Andrews 2014), although, this is at the expense of reduced NOM removals, which may create the need for additional treatment to minimize the formation of harmful DBPs. C-IN pretreatment in this review will be categorized according to its three principal configurations: (1) Type I, which includes a dedicated flocculation stage prior to LPM filtration; (2) Type II, in which flocculation is incidental; and (3) Type III, where the coagulated water is produced in batches for lab-scale studies prior to LPM filtration. This section will present an overview of these three most common configurations used for C-IN pretreatment of LPMs.

2.1.2.1. Type I Configuration

The Type I configuration includes coagulation and flocculation prior to LPM filtration (Fig. 2.2) and in many regards is similar to the treatment scheme employed at the majority of North American conventional multi-media filtration DWT facilities (except multi-media filtration is replaced by LPM filtration). For this reason, Type I configuration has been the method of choice for designers retrofitting existing facilities who are looking to capitalize on the existing media filtration basins (Lebeau et al. 1998; Moon et al. 2009). Successful implementation of submerged LPMs or modular (compact) ceramic flat sheet LPMs within the existing media filtration basin has been reported (Poje 2023). The use of a Type I configuration is expected to increase in coming years and extend to larger facilities as existing water treatment plants (WTPs) reach the end of their life cycle and water purveyors seek a technology capable of increasing capacity (but not footprint), while meeting current and future water quality regulations (AWWA Membrane Process Committee 2008;

Kinser 2021). From the literature surveyed, rapid mixing in Type I configuration has been performed using either mechanical mix basins (Arhin et al. 2018; Jang et al. 2010; Kim et al. 2006; Lee et al. 2000; Zularisam et al. 2009) or an inline static mixer (Citulski et al. 2008; Hillis 2006; Ratajczak et al. 2012; Schimmoller et al. 2000). For mechanically mixed systems, the duration of rapid mix ranges between 30 s and 300 s (Barbot et al. 2008; Kim et al. 2006; Kimura et al. 2008; Zularisam et al. 2009), while for inline static mixers authors report near instantaneous and complete blending of the coagulant and feed water streams (Ratajczak et al. 2012). The most common flocculation technologies reported were variable speed turbine flocculators (Arhin et al. 2018; Dixon et al. 2013; Lee et al. 2000; Malkoske et al. 2023b; c, 2025; Tao et al. 2024), hydraulic flocculators (Best et al. 2001; Hillis 2006; Jang et al. 2010; Zularisam et al. 2009), and pipe flocculation (Meyn et al. 2012; Meyn and Leiknes 2010). For studies considering turbine and hydraulic flocculators, flocculation times were between 10 min and 30 min, while for studies with pipe flocculation a much shorter flocculation time of 10 s to 240 s is reported. It should be noted that flocculation conditions producing small sized floc aggregates, which could potentially be unsuitable for sedimentation, may be successful for C-IN pretreatment as the flocs need only to be larger than the membrane pore, and not necessarily settleable (Jung and Kang 2003; Keucken et al. 2017; Naim et al. 2014). For pilot-scale studies, the flocculation tended to be performed more commonly using hydraulic flocculation basins, whereas at bench-scale, batch turbine flocculators were the most commonly employed method.

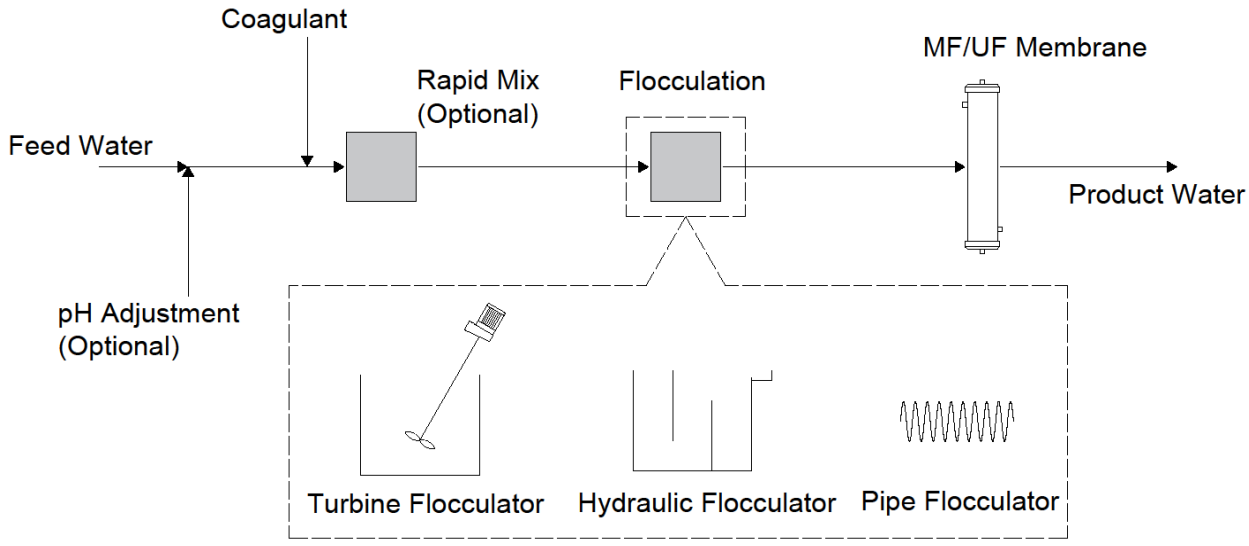


Fig. 2.2. Schematic diagram of Type I C-IN pretreatment (not to scale),

2.1.2.2. Type II Configuration

Type II C-IN only considers rapid mixing of coagulant prior to LPM filtration (Fig. 2.3) and does not have a dedicated flocculation stage. Most studies surveyed from the literature considering Type II C-IN were performed at pilot-scale (Farahbakhsh and Smith 2002; Galjaard et al. 2001; Judd and Hillis 2001; Lerch et al. 2003; Wang and Wang 2006; Xiangli et al. 2008), although several bench-scale studies have also been reported (Kamińska et al. 2020; Neama et al. 2024; Oh and Lee 2005; Paar et al. 2011). In terms of coagulant mixing equipment, conventional rapid mix basins (Farahbakhsh and Smith 2002; Oh and Lee 2005), static mixers (Farahbakhsh and Smith 2002; Judd and Hillis 2001; Wang and Wang 2006) and pipe turbulence or helically coiled tube flocculators (HCTFs) (Galjaard et al. 2001; Kamińska et al. 2020; Lerch et al. 2003; Paar et al. 2011; Xiangli et al. 2008) have all been employed. Reported residence times within static mixers range from instantaneous mixing (Judd and Hillis 2001) to 60 s (Galjaard et al. 2001; Wang and Wang 2006). For HCTFs, residence times less than 60 s are reported (Paar et al. 2011).

HCTFs offer a promising approach for promoting efficient floc generation under the low-flow conditions typical of laboratory-scale investigations. Consisting of a helically wound segment of pipe, HCTFs require considerably lower HRTs than conventional flocculators, resulting in a markedly reduced footprint (De Oliveira and Teixeira 2017; García-Ávila et al. 2023). Their performance is attributed to the strong secondary flows generated by the curved flow path, which induces centrifugal forces that drive fluid towards the outer radius of curvature. This flow subsequently bifurcates, generating a pair of recirculating vortices that promote effective mixing, even under firmly laminar conditions (Huttl and Friedrich 2000; Mansour et al. 2017, 2020a). The helical coil geometry (coil pitch, coil diameter, pipe diameter), however, have all been shown to alter the hydrodynamic flow pattern within the flocculator (Sartori et al. 2015; Tang et al. 2016; Yamamoto et al. 2002), which is expected to influence the properties of the formed floc aggregates. Despite the well-established relationship between coil geometry and flow behavior (Mansour et al. 2020b), the influence of controlled geometry on floc properties during continuous-flow coagulation has not been systematically investigated. Consequently, further research is needed to establish design guidelines for selecting HCTF geometries that promote effective floc formation in continuous-flow coagulation systems.

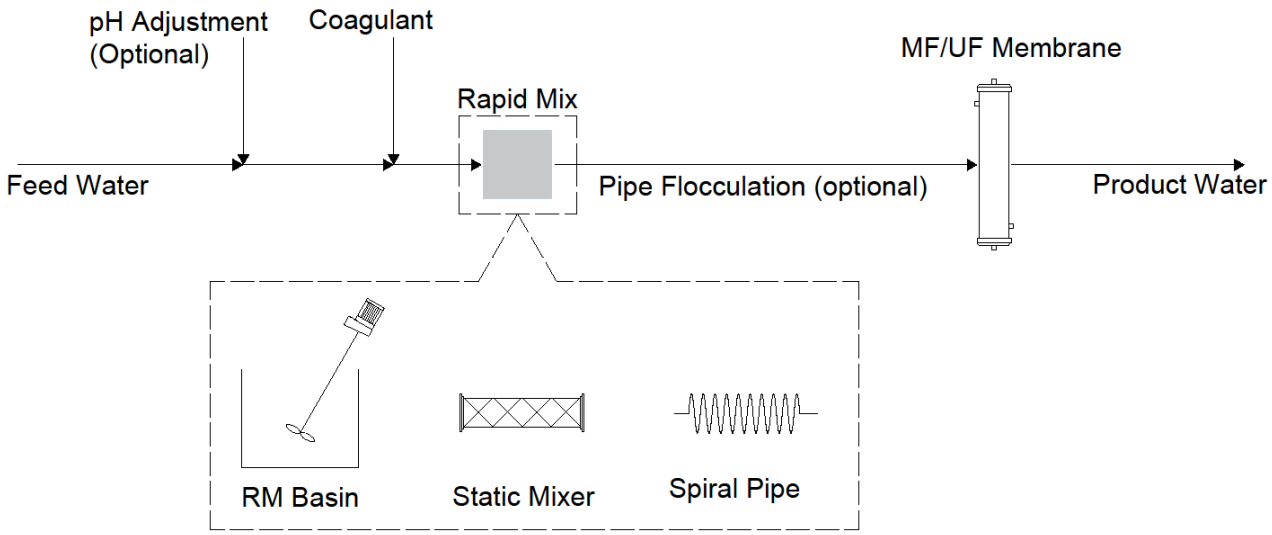


Fig. 2.3. Schematic diagram of Type II C-IN pretreatment (not to scale).

2.1.2.3. Type III Configuration

For simplicity, a great deal of LPM research has been conducted at lab-scale using batch coagulation and/or batch-stirred cell reactors. The batch-stirred cell reactors used in these tests (e.g., Amicon Cells) are typically operated at a constant transmembrane pressure (TMP) and use flat sheet membrane discs. Common TMPs used for Type III C-IN tests are reported to range from 0.1 MPa to 0.35 MPa (Amjad et al. 2015; Carroll et al. 2000; Pikkarainen et al. 2004; Yao et al. 2015). Most tests are short duration (<1.5 h) (Cho et al. 2006; Jung and Kang 2003; Kim et al. 2001; Wu et al. 2023; Xie et al. 2016) and used small water volumes (<1,500 mL) (Ma et al. 2014; Wang et al. 2010, 2013). Feed water for the batch cell tests is commonly prepared using conventional jar test apparatus, after which the coagulated suspension is gently transferred to the batch cell or an optional feed reservoir (Fig. 2.4). These batch tests are not considered representative of the C-IN conditions expected at full-scale LPM facilities (i.e., flat sheet membrane with a constant TMP vs. hollow-fiber membranes operated using a constant permeate flux) (Kimura et al. 2008, 2014), however, many authors still consider them for mechanistic studies as they are easier to implement experimentally. Given these significant differences in operation, it would be of interest to directly compare the performance of a LPM system with C-IN pretreatment by batch coagulant mixing to that of a system with C-IN pretreatment by continuous flow inline coagulation (direct addition of coagulant to the feed stream).

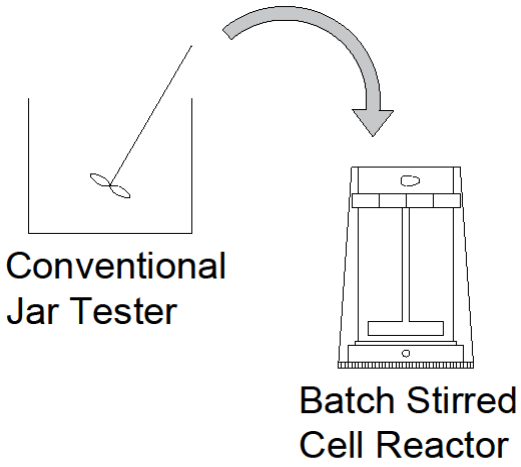


Fig. 2.4. Schematic of Type III C-IN batch test apparatus.

2.1.3. Phased-Inline Coagulation (C-IN-P)

Phased-inline coagulation (C-IN-P) is a variation of C-IN pretreatment where, instead of continuous coagulant addition, the coagulant dose is set to zero after the initial portion (fraction) of the filtration cycle. The concept of C-IN-P is best exemplified in Fig. 2.5, where an idealized permeability profile for three filtration cycles (with hydraulic backwash) is shown. For comparative purposes, the schematic shown in Fig. 2.5a presents the operation of C-IN pretreatment. For each of the three filtration cycles the coagulant is added continuously to the feed at a prescribed dosage for the entire filtration cycle. In Fig. 2.5b the operation of C-IN-P pretreatment is presented where, unlike conventional C-IN, the coagulant is dosed only for a pre-determined portion of the filtration cycle immediately following the hydraulic backwash. Once the coagulant has been added for the prescribed duration to produce a filter cake, the addition is ceased, and filtration proceeds for the remainder of the filtration cycle with untreated (raw) water.

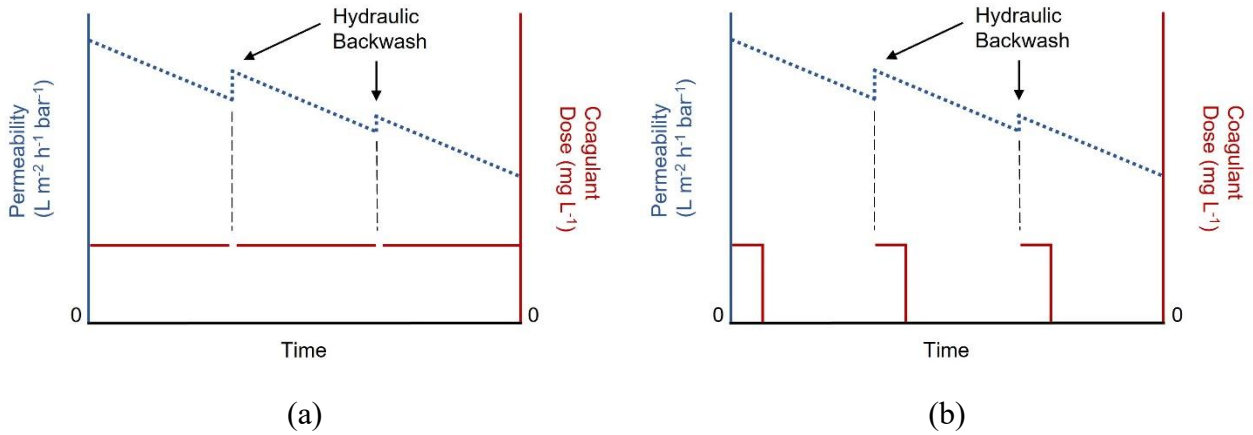


Fig. 2.5. Definition sketch of the system characteristics for: **(a)** continuous coagulant addition (C-IN); **(b)** phased coagulant addition (C-IN-P)

Studies investigating C-IN-P have most commonly been performed at pilot-scale without a dedicated flocculation stage (i.e., no flocculation basin is used) (Buchta et al. 2017, 2019; Lok et al. 2017; Naim et al. 2014; Schweiger et al. 2018b; a). For example, in the pilot-scale study by Naim et al. (2014), a rapid mix basin with a retention time between 10 s and 21 s was used for coagulant mixing, while for the bench-scale investigation by Park et al. (2002) the velocity gradients that exist in the peristaltic feed pump (Formato et al. 2019; Palmada et al. 2022) were used to provide the necessary turbulence for blending of coagulant (added to the suction side) with the feed water. Buchta et al. (2019) and Lok et al. (2017) reported injecting the coagulant directly inline in their pilot-scale investigations such that the coagulant was blended using only the turbulence of the system. Commercial inline static mixers (ISMs) are a third possible option for blending of coagulant/pH adjustment chemicals with the feed water, although their use has not been specifically investigated in C-IN-P studies. It is recommended that future C-IN-P studies investigate the effect that different mixing types (i.e., mechanical vs. incidental) have on the formed coating layer and the subsequent impact this has on membrane fouling. No C-IN-P studies available in the literature systematically evaluate the impact of the coagulation setup (i.e., static mixer, rapid mix tank, etc.) or their operating conditions (i.e., mean velocity gradient and contact time) on pretreatment performance. This is despite the fact that C-IN studies have demonstrated altered floc and cake structure (and hence membrane fouling) resulting from differing mixing conditions (Amjad et al. 2015; Cho et al. 2006; Malkoske et al. 2023b; Nan et al. 2016). Fig. 2.6 below presents a schematic diagram of the C-IN-P LPM system.

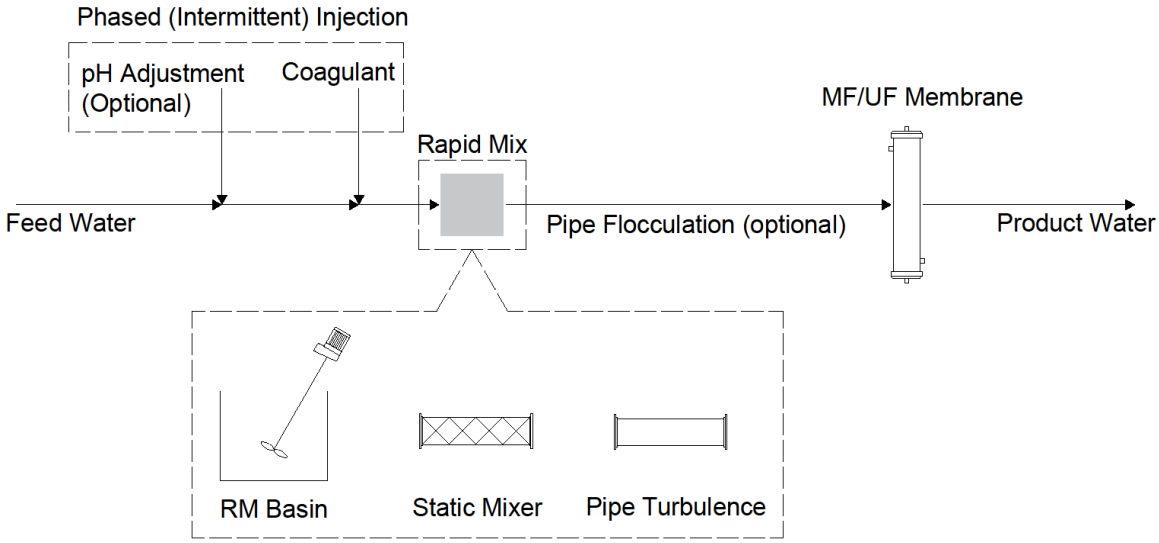


Fig. 2.6. Schematic diagram of LPM system with C-IN-P pretreatment (not to scale).

2.2. Membrane Fouling in the Hybrid Coagulation-LPM System

2.2.1. CF-SED

Conventional CF-SED pretreatment has been reported to be successful at mitigating membrane fouling in a number of studies (Jang et al. 2005; Liang et al. 2008; Minegishi et al. 2001; Moon et al. 2009). The performance of CF-SED pretreatment appears to be largely dependent on an interaction between the floc morphology and structure (i.e., size, fractal dimension (D_f)) as well as the foulant mass loading (i.e., the cake thickness). Amjad et al. (2015) reported a trade-off between floc morphology/structure and mass loading when comparing the performance of C-IN and CF-SED as pretreatment for a flat sheet ultrafiltration (UF) membrane using different flocculation mixing intensities (measured by the product of the mean velocity gradient and the mixing time or Gt). For CF-SED pretreatment, reduced magnitude flux decline was observed compared to pretreatment by C-IN. Despite having the highest magnitude specific cake resistances, pre-settling by CF-SED greatly reduced the mass loading delivered to the membrane surface (by up to 85%) resulting in the thinnest cakes. Therefore, although the non-settleable flocs packed into a low porosity surface cake with a high resistance to filtration, the reduced cake thickness compared to C-IN resulted in lower levels of total fouling.

Ding et al. (2021) evaluated the effect of sedimentation time, water temperature, and pH on the performance of the hybrid CF-SED ultrafiltration (UF) system for a relatively low DOC surface water (2.5 mg L^{-1}). Tests were performed both at room temperature as well as at low temperatures (typical of winter season operation) using ferric chloride as coagulant and a submerged polyvinylidene fluoride (PVDF) hollow-fiber membrane with a molecular weight cut-off (MWCO) of 100 kDa. At room temperature, pretreatment by CF-SED resulted in a LPM feed water with small sized dense flocs (3D fraction dimension, $D_{f,3}$ = 2.51) that agglomerated into foulant cakes with a narrower pore size (25.3 nm and 18.4 nm for settling times of 10 and 20 min, respectively) than those formed by C-IN. Without settling, the feed water contained more large-sized loose flocs which generated a thicker foulant cake (6.1 μm) of high porosity (pore size of 36.4 nm). The result was the existence of a critical settling time, with CF-SED requiring >30 min settling time to reduce UF fouling (in terms of TMP development) compared to C-IN. It is hypothesized that following 30 min of settling, the cake layer thickness was reduced sufficiently (decreasing from 5.4 μm to 0.3 μm) to offset the low porosity of the fouling cake, resulting in a net lower TMP increase than C-IN pretreatment. In contrast, at low temperature conditions, similar sized pores were formed in the foulant cake regardless of the settling duration (30.2, 28.4, and 25.3 nm for 0, 10, and 60 min settling), proposed to be a result of the looser floc structure formed at low temperatures ($D_{f,3}$= 2.22). Therefore, the final TMP after 12 d of operation was directly related to the foulant loading, with decreasing magnitude TMP for longer settling times as the cake thickness decreased (18.8, 10.9, and 4.1 μm for 0, 10, and 60 min settling). When the pH was adjusted to a value of 6 for low-temperature conditions, the flocs were observed to be small and have a higher density structure ($D_{f,3}$ = 2.41), which again created a critical settling time of a minimum 10 min for improved performance compared to C-IN. Ma et al. (2020a) also reported the existence of a critical settling time for CF-SED pretreatment. Like Ding et al. (2021), they considered a low DOC surface water with a submerged 100 kDa PVDF hollow-fiber membrane and investigated CF-SED performance for different settling lengths and water temperatures using aluminum chloride as coagulant. At room temperature conditions, the existence of a critical settling time was confirmed, with pretreatment by CF-SED resulting in a lower final TMP compared to C-IN for >10 min settling. In contrast, for low temperature conditions, CF-SED exhibited superior performance compared to C-IN regardless of the sedimentation time considered. For low temperatures, the foulant cake pore size (as determined from scanning electron microscope (SEM)

imaging of the fouled membrane surface) was found to be largely stable (values of 30.2, 28.4, and 25.3 nm following 0, 10, and 60 min of settling) leading to the relative performance being dictated by the cake thickness. Increasing sedimentation time led to a continuous decline in both the thickness of the formed fouling layer (from 18.8 μm to 4.1 μm after 60 min of settling) as well as the total fouling (i.e., TMP increase after 12 d of operation).

2.2.2. CF-DAF

In general, several researchers have reported that LPMs filtering CF-DAF pretreated water exhibit reduced fouling potential compared to when raw feed water is considered (Kang et al. 2021; Pissibanganga et al. 2016). However, other research studies have suggested that CF-DAF pretreatment for LPMs does not improve fouling reduction compared to when treating raw water alone, but may provide a superior quality product water (Amaral et al. 2013). Table 2.1 presents a summary of pertinent data for CF-DAF-LPM studies including information on the raw water quality, coagulation/flotation characteristics, and fouling metrics. Although there has been somewhat increased research interest in CF-DAF integration with LPMs in recent years, there remains a limited number of studies which directly compare the performance of CF-DAF pretreatment for LPMs with that of other coagulation approaches, including C-IN or CF-SED. A discussion of the relative performance of CF-DAF compared to these two alternative coagulation pretreatment strategies is warranted and provided in the next sub-sections.

Table 2.1. Summary of Pretreatment Parameters and Fouling Behavior for Selected CF-DAF-LPM Studies[a].

Mat.-Config. NPS or MWCO Scale	Raw Water Characteristics			Coagulation Characteristics		Flotation Characteristics			Fouling Measures			Ref. (see note)
	Water Type	DOC (mg L^{-1})	SUVA ($Lmg^{-1}m^{-1}$)	Coag. Type	Coag. Dose (mg L^{-1} metal)	Recycle Ratio (%)	Recycle Pressure (kPa)	Contact Time (min)	Permeability Decline Rate ($Lm^{-2}h^{-1}bar^{-1}d^{-1}$)	Hyd. Irrev. Fouling Rate (kPa h^{-1})	Chem. Irrev. Fouling Rate (kPa h^{-1})	
PVDF-FS 0.1 µm Bench	River	3.8	3.41	PACl	50 (as coag.)	10	517	N/A	6088	N/A	N/A	[1]
	Lake	2.2	1.53	PACl	12 (as coag.)	10	517	N/A	8645	N/A	N/A	
	Lake	2.0	1.58	PACl	18 (as coag.)	10	517	N/A	6391	N/A	N/A	
	Lake	2.2	1.15	PACl	20 (as coag.)	10	517	N/A	9912	N/A	N/A	
PVDF-PDO 0.1 µm Pilot	Lake	2.2	1.5	PACl	Variable[b]	10	N/A	N/A	N/A	0.248	N/A	[1]
	Lake	2.0	1.3	PACl	Variable[b]	10	N/A	N/A	N/A	1.87	N/A	
PP-PDO 0.2 µm Pilot	RES	6.9 (TOC)	2.3	Alum	45 (as coag.)	N/A	N/A	N/A	N/A	0.0937	N/A	[2]
PES-PDI 100 kDa Bench	River	8.16	3.92	Alum	3.18-3.36	N/A	N/A	N/A	N/A	1.53	0.143	[3]
		7.09	3.56	Alum	3.18-3.36	N/A	N/A	N/A	N/A	0.837	0.038	
		7.09	3.56	Alum	3.18-3.36	N/A	N/A	N/A	N/A	1.24[c]	0.398	
		7.09	3.56	Alum	3.18-3.36	N/A	N/A	N/A	N/A	2.14[d]	0.672	
PES-PDI 100 kDa Bench	River	6.07	4.16	Alum	2.99	N/A	N/A	N/A	N/A	1.045	0.643	[4]
PVDF-PDO 0.01 µm Pilot	RES	3.06	N/A	PACl	60 (as coag)	N/A	N/A	N/A	N/A	N/A	0.059	[5]
		3.06	N/A	PACl	60 (as coag)	N/A	N/A	N/A	N/A	N/A	0.027	
		3.06	N/A	PACl	40 (as coag)	N/A	N/A	N/A	N/A	N/A	0.007	
PAN-PDO 0.025 µm Pilot	River	3.37-6.64 (COD)	N/A	N/A	N/A	N/A	N/A	N/A	N/A	N/A	0.033	[6]

[a] COD=chemical oxygen demand; DOC = dissolved organic carbon; FS = flat sheet; N/A = not available; PACl = polyaluminum chloride; PAN = polyacrylonitrile; PDI = pressure-driven inside-out; PDO = pressure-driven outside-in; PVDF = polyvinylidene fluoride; RES = reservoir; SUVA = specific ultraviolet absorbance at 254nm; TOC = total organic carbon; WAC = aluminum polyhydroxichlorosulphate. [b]Coagulant dose was adjusted using influent feed water turbidity measurements. [c] Evaluated 60 min filtration cycle instead of 30 min. [d] Evaluated 90 min filtration cycle instead of 30 min. Note: refs [1] Van Benschoten et al. (2002); [2] Braghetta et al. (1997); [3] Xu and Narbaitz (2016); [4] Walker and Narbaitz (2016); [5] Kang et al. (2021); [6] Shi et al. (2017).

2.2.2.1. Comparison with C-IN

LPM pretreatment by C-IN involves the direct addition of coagulants (as well as pH adjusting chemicals and flocculants) to the feed stream prior to the membrane module without any clarification process. Instinctively, C-IN pretreatment should result in greater LPM fouling compared to CF-DAF as clarification by flotation significantly reduces the solids mass loading being delivered to the membrane. In fact, results from several studies (Braghetta et al. 1997; Hög et al. 2015; Van Benschoten et al. 2002) have indicated increased fouling by C-IN compared to CF-DAF using both lab- and pilot-scale filtration systems, whereby elevated fouling tendencies were purported to be a result of increased membrane solids loadings. For example, Braghetta et al. (1997) compared the performance of C-IN and CF-DAF for treatment of a reservoir water ahead of a polypropylene microfiltration (MF) membrane. In that study, following CF-DAF pretreatment with the addition of 45 mg L^{-1} alum (as coagulant), the MF membrane was found to operate stably at a flux of 120 L m^{-2} h^{-1} for a period of over 30 d without reaching the terminal TMP for initiating chemical cleaning (155 kPa). When coagulated feed water was delivered directly to the membrane module without clarification by flotation (using same coagulation chemistry as for CF-DAF), membrane fouling was found to be exacerbated, exceeding the terminal operating TMP within a short time (~1 d). Moreover, the recovery of membrane permeability by chemical cleaning was found to be incomplete, leading to reduced filter run times for each subsequent chemical clean cycle. It should be noted that, while the coagulant dose was kept consistent for comparative purposes, excessive coagulant usage may not be optimal for C-IN pretreatment of LPM-based systems and likely induced an additional resistance to filtration (Kimura et al. 2008; Lerch et al. 2003; Paar et al. 2011; Wray et al. 2016). Similar observations were also reported by Hög et al. (2015) when comparing CF-DAF and C-IN as pretreatment for a process intensified flotation-LPM unit. For ferric chloride pretreated river water at a dose of 10 mg-Fe L^{-1}, vacuum-driven ceramic MF membranes were found to reach the terminal operating TMP of -0.5 bar after only 4 h of filtration time, representing a total fouling rate of 6 kPa h^{-1}. In contrast, when CF-DAF was implemented using ferric chloride, a stable TMP of -0.28 bar was sustained for the gross operating flux of 112 L m^{-2} h^{-1}, with a total fouling rate only one third of that for C-IN pretreatment (i.e., 2 kPa h^{-1}).

Not all studies, however, have reported reduced LPM fouling by CF-DAF compared to C-IN. Van Benschoten et al. (2002) observed reduced fouling (measured as permeability decline) by

C-IN pretreatment compared to CF-DAF for a hydrophobic (HPO) reservoir water (as measured by the specific ultraviolet absorbance at 254 nm (SUVA) = 3.41 L mg^{-1} m^{-1}) and a flat sheet PVDF MF membrane, while for a lake water with a moderately high turbidity (67 NTU), CF-DAF and C-IN pretreatment performed equally well. The results of these studies seem to indicate a dependence of relative performance on LPM type/configuration and feed water quality. It is possible that each specific membrane type may have a unique threshold value above which the benefits of C-IN pretreatment (i.e., porous cake formation) are offset by the increased mass loading, resulting in elevated TMPs and increased irreversible fouling compared to CF-DAF.

2.2.2.2. Comparison with CF-SED

There exists relatively few studies comparing the performance of CF-SED and CF-DAF pretreatment for LPMs. In a bench-scale study by Walker and Narbaitz (2016), the performance of these two pretreatment alternatives was evaluated using colored water from the Ottawa River (Ottawa, Canada), which is predominated by HPO organics. This river has a large watershed (140,000 km^2), a large average flowrate (1,950 m^3 s^{-1}), and a low population density. Moreover, the river is fairly pristine (the nearest SE discharge point is nearly 80 km upstream from Ottawa) and the total phosphorus content is less than 0.03 mg-P L^{-1}, so it is not eutrophic. The Ottawa River is also representative of Northern Canadian surface waters, with a high NOM content and a low turbidity, alkalinity, and hardness. The pretreatment (i.e., CF-SED and CF-DAF) was performed at nearby full-scale facilities under different conditions (i.e., coagulation chemistry) which were optimized for the greatest removal of organics. Following multi-day filtration tests using inside-out polyethersulfone (PES) UF membranes, the TMP development for CF-SED pretreated water using alum as coagulant was found to be greater than for CF-DAF pretreated water with the same coagulant type. When ferric sulfate was used as coagulant for CF-SED pretreatment, the TMP increase was also reported to be more severe than for CF-DAF pretreatment (using alum), although it must be acknowledged that CF-SED pretreated water with ferric sulfate was produced using a pilot-plant facility which was not operating under optimized conditions. This resulted in elevated levels of CF-SED treated turbidity and DOC compared to CF-SED and CF-DAF pretreatment with alum as coagulant, possibly impacting the performance of this alternative.

Xu and Narbaitz (2016) used the same colored river water and inside-out hollow-fiber PES UF membranes as Walker and Narbaitz (2016) to investigate the superiority of CF-DAF

pretreatment compared to CF-SED during summer and winter seasons. To ensure differences in coagulation chemistry used by the full-scale facilities producing CF-DAF and CF-SED pretreated water were not responsible for observed performance differences, coagulated water from the flotation facility (which included the addition of a cationic polyacrylamide polymer) was also settled. The comparison of CF-DAF and CF-SED performance was assessed using resistance-in-series based fouling indices (Nguyen et al. 2011; Zupančič et al. 2014), where the total fouling index (TFI) describes the total fouling potential of the water-membrane configuration and the hydraulically irreversible fouling index (HIFI) describes the fraction of fouling which is not recoverable by hydraulic backwashing (i.e., physical cleaning methods). For both settled and floated waters the TFI was found to mirror the performance of the TMP profiles, although, for CF-DAF pretreatment the TFIs were three times lower than for CF-SED. Regarding the HIFI, CF-SED pretreated water was found to have consistently higher values (at least 1.8 times greater) than that for CF-DAF. It was proposed that the better performance of CF-DAF compared to CF-SED (in terms of TMP development and fouling indices) was a result of the greater removal of HPO organic material by the former. For the winter season tests, CF-DAF pretreatment was found to remove a significantly greater amount of HPO organics compared to pretreatment by CF-SED (75.6% vs. 63%, respectively). In fact, the TFI and HIFI during both seasons displayed strong positive linear correlations with the SUVA value (a surrogate for HPO NOM material).

2.2.2.3. Effects of Operating Parameters on Fouling of CF-DAF-LPM Systems

2.2.2.3.1. Water Quality. Van Benschoten et al. (2002) reported raw water turbidities of 67 NTU and 37 NTU for a reservoir water and a lake water, respectively, yet despite having the same DOC content the water with higher turbidity resulted in greater LPM permeability decline following CF-DAF pretreatment. Kang et al. (2021) considered average and maximum turbidity values as process controls for a CF-DAF-MF system. Under conditions of reduced raw water turbidity (average of 3.4 NTU) the MF module could be operated without CF-DAF pretreatment and with a week-long interval between chemical maintenance cleanings. When turbidity levels increased (average and maximum turbidity values reaching 10.1 NTU and 83 NTU, respectively), fouling mitigation could only be achieved with the implementation of optimized CF-DAF pretreatment in combination with enhanced physical backwashing and daily chemical maintenance cleaning. Therefore, for the hybrid system, it is suggested that raw water turbidity (in addition to the feed

water NOM) may also be critical in determining the fouling potential of a given source water. It is recommended that future CF-DAF-LPM studies distinguish between mineral and non-mineral turbidity when characterizing the raw water quality. As proposed by Valade et al. (2009), CF-DAF is most effectively employed for mineral turbidities (clays and silts) less than 10 NTU, while is recommended for average non-mineral turbidities (algae, particulate NOM) up to 100 NTU. When operated for feed waters with sustained turbidities above these levels, the CF-DAF effluent water quality may deteriorate, resulting in greater LPM fouling. Turbidity removals by CF-DAF amongst the literature surveyed in this review were found to be mostly greater than 75% and no relationships could be identified between raw water turbidity or CF-DAF treated turbidity and LPM irreversible fouling measures. It is likely, however, that the effects of turbidity on LPM fouling in the hybrid system are more important for hydraulically reversible fouling, which is less critical for long-term operation, and for which sufficient data was not available.

2.2.2.3.2. Membrane Configuration. The study by Van Benschoten et al. (2002) reported somewhat conflicting results when using bench- and pilot-scale membranes with different configurations (although the membrane pore size and principal polymer material were the same) to compare the performance of CF-DAF and C-IN. Lake Erie water (NY, USA) was used for all tests and was sampled in seasons of high (37 NTU) and low (1.65 NTU) average turbidity. At bench-scale, flat sheet PVDF membranes indicated that CF-DAF provided superior performance for the high turbidity season, while C-IN and CF-DAF performed equally well for the low turbidity season. When hollow-fiber PVDF membranes were used at the pilot-scale, CF-DAF pretreatment yielded reduced LPM fouling compared to C-IN regardless of the season. Therefore, in addition to feed water quality, membrane type/configuration may influence the performance of the hybrid system. However, there remains a dearth of studies which have investigated the impact of membrane material on LPM fouling following pretreatment by CF-DAF using the same water source. This should be the subject of future research studies.

2.2.2.3.3. CF-DAF Parameters. The influence of CF-DAF related parameters on LPM fouling in the hybrid system has not been adequately characterized. No study has systematically investigated whether the CF-DAF process parameters can influence the performance of the LPM in the hybrid system. For example, in the study by Minhalma and De Pinho (2001), although attempts are made

at optimizing the coagulation and CF-DAF process parameters (recycle ratio and saturation pressure) in terms of organics removals, these goals were not simultaneously balanced with membrane performance. The importance of CF-DAF process parameter optimization was shown in the study by Valade et al. (1996), where changes to the coagulant type, mixing intensity (i.e., mean velocity gradient), and flocculation characteristics (number of stages and mixer type) resulted in treated waters with different residual particle numbers and size distributions, which may lead to different LPM fouling tendencies. Gonzalez-Galvis and Narbaitz (2022) also reported that alteration of the flocculation mean velocity gradient (i.e., G value), the recycle ratio, or the saturator pressure may impact the removal of turbidity in CF-DAF, however, the degree to which differences in turbidity removal affected LPM fouling was not assessed. Concerning the removals of organics, this last study noted almost no impact by changing the flotation process conditions. Instead, coagulation chemistry (i.e., pH and coagulant dose) was noted as the most critical factor impacting the removal of organics. It is recommended that future studies undertake to systematically evaluate the impact of coagulation and DAF parameters on the hybrid system performance using a variety of water types. It is expected that, although CF-DAF is a robust clarification method, the alteration of operating conditions will result in a clarified feed water with different particle size distributions and/or different composition of organics which may influence LPM filterability.

2.2.3. C-IN

2.2.3.1. Type I Configuration

The focus of research on membrane fouling in the Type I C-IN configuration has centered around the effects of flocculation duration and mixing speed (intensity), pH, coagulant dose, and to a lesser extent coagulant type. Table 2.2 and Table 2.3 present a summary of the coagulation and mixing characteristics as well as LPM fouling measures for selected Type I C-IN bench- and pilot-scale studies, respectively.

Table 2.2. Selected Bench-Scale Studies in Type I C-IN Pretreatment.

Material Config. NPS or MWCO	Water Quality		Mixing Conditions				Coagulation Conditions			Fouling Measures			Ref. (See notes)
	DOC/TOC (mg L^{-1})	SUVA ($Lmg^{-1}m^{-1}$)	Rapid Mix Time (s)	Rapid Mix G (S^{-1})	Slow Mix Time (min)	Slow Mix G (s^{-1})	Coag. Type	Dose[a] (mg L^{-1})	pH	$(J/J_0)/t$ (h^{-1})	Tot. Fouling Rate (kPa d^{-1})	Hyd. Irrev Rate (kPa d^{-1})	
PVDF HF PDO 0.02 µm	4.5 (DOC)	3.11	540	150 rpm[b]	N/A	N/A	PACl	14	N/A	0.129	N/A	N/A	[1]
	4.5 (DOC)	3.11	540	150 rpm	N/A	N/A	PACl	28	N/A	0.105	N/A	N/A	
	4.5 (DOC)	3.11	540	50 rpm[b]	N/A	N/A	PACl	14	N/A	0.316	N/A	N/A	
	4.5 (DOC)	3.11	540	50 rpm	N/A	N/A	PACl	28	N/A	0.194	N/A	N/A	
PVDF HF SUB 0.04 µm	6.6	N/A	N/A	N/A[c]	16	30 rpm	Alum	30	N/A	N/A	N/A	5.28	[2]
	6.7	N/A	N/A	N/A	16	30 rpm	$FeCl_3$	45	N/A	N/A	N/A	12.0	
	6.2	N/A	N/A	N/A	16	30 rpm	PACl	40	N/A	N/A	N/A	9.36	
	6.4	N/A	N/A	N/A	16	30 rpm	PACl-70	50	N/A	N/A	N/A	10.3	
	2.8	N/A	N/A	N/A	16	30 rpm	Alum	15	N/A	N/A	N/A	6.48	
	2.6	N/A	N/A	N/A	16	30 rpm	$FeCl_3$	20	N/A	N/A	N/A	6.48	
	2.7	N/A	N/A	N/A	16	30 rpm	PACl	15	N/A	N/A	N/A	4.32	
	2.5	N/A	N/A	N/A	16	30 rpm	PACl-70	20	N/A	N/A	N/A	6.0	
	6.6	N/A	N/A	N/A	16	30 rpm	Alum	15	N/A	N/A	N/A	1.68	
	6.2	N/A	N/A	N/A	16	30 rpm	PACl	20	N/A	N/A	N/A	1.92	
	6.8	N/A	N/A	N/A	16	45 rpm	Alum	30	N/A	N/A	N/A	13.9	
	6.8	N/A	N/A	N/A	16	45 rpm	$FeCl_3$	45	N/A	N/A	N/A	13.4	
	6.8	N/A	N/A	N/A	16	45 rpm	PACl	40	N/A	N/A	N/A	14.6	
	6.8	N/A	N/A	N/A	16	45 rpm	PACl-70	50	N/A	N/A	N/A	16.6	
	6.8	N/A	N/A	N/A	16	30 rpm	Alum	30	5.5	N/A	N/A	13.7	
	6.8	N/A	N/A	N/A	16	30 rpm	$FeCl_3$	45	5	N/A	N/A	13.7	
	6.8	N/A	N/A	N/A	16	30 rpm	PACl	40	5.5	N/A	N/A	14.6	
	6.8	N/A	N/A	N/A	16	30 rpm	PACl-70	50	5	N/A	N/A	16.3	
PES HF PDI 150 kDa	N/A	N/A	N/A	N/A	N/A	N/A	PACl	2.7	5.25	0.0375	N/A	N/A	[3]
	N/A	N/A	N/A	N/A	N/A	N/A	PACl	13.5	6.75	0.025	N/A	N/A	
	N/A	N/A	N/A	N/A	N/A	N/A	PACl	2.7	6.75	0.0125	N/A	N/A	
	N/A	N/A	N/A	N/A	N/A	N/A	PACl	13.5	5.25	0.115	N/A	N/A	
	N/A	N/A	N/A	N/A	N/A	N/A	PACl	2.7	5.25	0.1	N/A	N/A	
	N/A	N/A	N/A	N/A	N/A	N/A	PACl	13.5	6.75	0.0175	N/A	N/A	
	N/A	N/A	N/A	N/A	N/A	N/A	PACl	2.7	6.75	0.01	N/A	N/A	
	N/A	N/A	N/A	N/A	N/A	N/A	PACl	13.5	5.25	0.06	N/A	N/A	
	N/A	N/A	N/A	N/A	N/A	N/A	$FeCl_3$	5.585	5.25	0.03	N/A	N/A	
	N/A	N/A	N/A	N/A	N/A	N/A	$FeCl_3$	27.92	6.75	0.125	N/A	N/A	
	N/A	N/A	N/A	N/A	N/A	N/A	$FeCl_3$	5.585	6.75	0.01	N/A	N/A	
	N/A	N/A	N/A	N/A	N/A	N/A	$FeCl_3$	27.92	5.25	0.1125	N/A	N/A	

	N/A	N/A	N/A	N/A	N/A	N/A	$FeCl_3$	5.585	5.25	0.045	N/A	N/A	
	N/A	N/A	N/A	N/A	N/A	N/A	$FeCl_3$	27.92	6.75	0.215	N/A	N/A	
	N/A	N/A	N/A	N/A	N/A	N/A	$FeCl_3$	5.585	6.75	0.07	N/A	N/A	
	N/A	N/A	N/A	N/A	N/A	N/A	$FeCl_3$	27.92	5.25	0.165	N/A	N/A	
PE HF PDO 0.1 µm	2.2	N/A	N/A	N/A[d]	N/A	N/A	Alum	30	7.5	N/A	134.4	N/A	[4]
	2.2	N/A	N/A	N/A	N/A	N/A	Alum	10	5	N/A	61.68	N/A	
PE HF SUB 0.1 µm	2.2	N/A	N/A	N/A[d]	N/A	N/A	Alum	30	7.5	N/A	16.56	N/A	

Note: DOC = dissolved organic carbon; HF = hollow fiber; MWCO = molecular weight cut-off; N/A = not available; NPS = nominal pore size; PACl = polyaluminum chloride; PDI = pressure driven inside-out; PDO = pressure driven outside-in; PE = polyethylene; PS = polysulfone; PVDF = polyvinylidene fluoride; SUB = vacuum submerged; TOC, total organic carbon. [a] dose as coagulant. [b] single mixing tank with different mixing intensity. [c] rapid blending by inline static mixer. [d] did not report mixing speed for single mixing tank. Refs.: [1] Dixon et al. (2013); [2] Ratajczak et al. (2012); [3](Lerch et al. 2003); [4] Lee et al. (2000).

Table 2.3. Selected Pilot-Scale Studies in Type I C-IN Pretreatment.

Material Config. NPS or MWCO	Water Quality		Mixing Conditions			Coagulation Conditions			Fouling Measures			Ref.
	DOC/TOC (mg L^{-1})	SUVA ($Lmg^{-1}m^{-1}$)	Slow Mix Method	Slow Mix Time (min)	Slow Mix G (s^{-1})	Coag. Type	Coag. Dose (mg L^{-1} metal)	pH	Final Perm. (L m^{-2} h^{-1} bar^{-1})	$(J/J_0)_f$	Hyd. Irrev Rate (kPa d^{-1})	
N/A												
HF PDI	N/A	N/A	VIST	3.3	N/A	PACl	15 (as PACl)	N/A	59	N/A	N/A	[1]
100 kDa												
	N/A	N/A	VIST	5	N/A	PACl	20 (as PACl)	N/A	56.6	N/A	N/A	
	N/A	N/A	VIST	5	N/A	PACl	10 (as PACl)	N/A	45.4	N/A	N/A	
	N/A	N/A	VIST	10	N/A	PACl	7 (as PACl)	N/A	64.6	N/A	N/A	
	N/A	N/A	VIST	10	N/A	PACl	15 (as PACl)	N/A	28.8-46.1[a]	N/A	N/A	
	N/A	N/A	VIST	10	N/A	PACl	22 (as PACl)	N/A	68.7	N/A	N/A	
	N/A	N/A	VIST	15	N/A	PACl	10 (as PACl)	N/A	68	N/A	N/A	
	N/A	N/A	VIST	15	N/A	PACl	20 (as PACl)	N/A	68.4	N/A	N/A	
	N/A	N/A	VIST	17	N/A	PACl	15 (as PACl)	N/A	56.5	N/A	N/A	
PS												
HF SUB	N/A	1.27	HFT[b]	N/A	N/A	Alum	1.8	5	N/A	0.4	N/A	[2]
68 kDa												
	N/A	1.27	HFT	N/A	N/A	Alum	1.8	10	N/A	0.2	N/A	
	N/A	3.3	HFT	N/A	N/A	Alum	1.8	5	N/A	0.23	N/A	
	N/A	3.3	HFT	N/A	N/A	Alum	1.8	10	N/A	0.32	N/A	
	N/A	1.27	HFT	N/A	N/A	Alum	3	5	N/A	0.63	N/A	
	N/A	1.27	HFT	N/A	N/A	Alum	3	10	N/A	0.18	N/A	
	N/A	3.3	HFT	N/A	N/A	Alum	3	5	N/A	0.746	N/A	
	N/A	3.3	HFT	N/A	N/A	Alum	3	10	N/A	0.658	N/A	
	N/A	2.29	HFT	N/A	N/A	Alum	2.4	2.5	N/A	0.512	N/A	
	N/A	2.29	HFT	N/A	N/A	Alum	2.4	12.5	N/A	0.201	N/A	
	N/A	0.26	HFT	N/A	N/A	Alum	2.4	7.5	N/A	0.607	N/A	
	N/A	4.31	HFT	N/A	N/A	Alum	2.4	7.5	N/A	0.747	N/A	
	N/A	2.29	HFT	N/A	N/A	Alum	1.2	7.5	N/A	0.222	N/A	
	N/A	2.29	HFT	N/A	N/A	Alum	3.6	7.5	N/A	0.527	N/A	
	N/A	2.29	HFT	N/A	N/A	Alum	2.4	7.5	N/A	0.537	N/A	
PVDF												
HF SUB	4-11		HFT[b]	15	N/A	Fe_2SO_4	8.5	5.2	N/A	N/A	4.32	[3]
0.04 µm		5.2-7.4										
	4-11	5.2-7.4	HFT	15	N/A	Fe_2SO_4	8.5	4.5	N/A	N/A	1.51	
	4-11	5.2-7.4	HFT	15	N/A	Fe_2SO_4	8.5	4.5	N/A	N/A	2.10	

Note: DOC = dissolved organic carbon; HF = hollow fiber; HFT = hydraulic flocculation tank; MWCO = molecular weight cut-off; N/A = not available; NPS = nominal pore size; PACl = polyaluminum chloride; PDI = pressure driven inside-out; PDO = pressure driven outside-in; PS = polysulfone; PVDF = polyvinylidene fluoride; SUB = vacuum submerged; VIST = vertical impeller stirred tank.[a] Repeated 5 times as center of central composite design. [b] Baffled end-over-end hydraulic flocculation tank. Refs.: [1] Arhin et al. (2018); [2] Zularisam et al. (2009); [3] Hillis (2006).

In the study by Arhin et al. (2018), preliminary jar testing identified 10 – 20 mg L^{-1} (as polyaluminum chloride (PACl)) and 5 to 15 min as suitable coagulant doses and flocculation hydraulic retention times (HRT), respectively, for use in their 2^2 central composite experimental design analysis. Using residual turbidity, ultraviolet absorbance at 254 nm (UV_{254}), and final permeability as response variables, results indicated that the treated water quality objectives did not necessarily align with membrane fouling objectives. High coagulant dose and low HRT led to the best UV_{254} removals, medium HRTs and high coagulant dose led to the lowest residual turbidity, while the final permeability was maximized by operation at high dose and either high or low HRT values (but not medium HRT). It was speculated that conditions resulting in greater NOM removal formed larger floc aggregates which could alleviate membrane cake resistance compared to those conditions that formed small sized flocs, however, no size measurements were actually performed in the study. Dixon et al. (2013) considered a fixed flocculation time of 9 min in their study, however, varied the mixing intensity by setting the flocculator speed to either 50 rpm or 150 rpm. The effect of flocculation speed on floc properties was assessed by considering the flocculation index (measured using a photometric dispersion analyzer) and its variance, which provide information regarding the floc size and size distribution (and indirectly floc strength). It was reported that a mixing speed of 150 rpm produced flocs with a reduced variance (indicating a high strength and uniform particle size distribution) and small size, which resulted in low specific flux decline compared to flocs formed at low mixing speed, which were characterized by a large, open structure that is susceptible to breakup (Table 2.2). This contradicts the results of the studies by Guan et al. (2001) and Park et al. (2006) where it was shown that that flocculation conditions that promoted large-sized flocs with low fractal dimension (i.e., loose structure) resulted in the lowest specific cake resistance (SCR). Ratajczak et al. (2012) also compared different flocculation intensities by varying the impeller speed from 30 rpm to 45 rpm in their bench-scale apparatus. Unlike Dixon et al. (2013), it was reported that increased mixing intensity led to a 20-40% increase in the final TMPs compared to the case where 30 rpm mixing intensity was used. However, it seems that the results of this study are due to differences in floc mass loading to the membrane as opposed to differences in the floc morphological properties, as greater floc carryover to the membrane tank was reported at higher mixing intensity.

Malkoske et al. (2023c) investigated the effects of flocculation intensity and mixing duration on membrane fouling resistance using a flat-sheet PVDF membrane and three coagulation

chemistries representing different coagulation mechanisms (i.e., sweep coagulation, adsorption, and combined). Coagulation was conducted in a modified jar-test system consisting of a dedicated rapid-mix unit (HRT = 2 min; G = 350 s^{-1}) followed by six jars arranged in series (and connected by overflow weirs) for flocculation. To assess the influence of flocculation intensity, the velocity gradient (G) was set to either 20 s^{-1} or 50 s^{-1} for a fixed HRT of 12 min. To provide reasonable HRT values, however, much larger flowrates were needed than required by the LPM filtration system. The effect of flocculation duration was evaluated by fixing G at 20 s^{-1} and reducing the system flow rate by 50 %, thereby increasing the flocculation HRT from 12 min to 24 min. Increasing the flocculation intensity from 20 s^{-1} to 50 s^{-1} resulted in higher total and hydraulically irreversible fouling resistance across all coagulation chemistries. Similarly, extending the flocculation HRT from 12 min to 24 min generally increased both total and hydraulically irreversible fouling resistance, although the adsorption-based coagulation chemistry exhibited overlapping confidence intervals with the baseline condition. These findings indicate that the effectiveness of flocculation as part of a Type I C-IN pretreatment configuration is sensitive to both flocculation intensity and retention time, with higher G values and longer HRTs potentially exacerbating membrane fouling.

In summary, for Type I C-IN pretreatment, the effects of mixing conditions on membrane performance are unclear. Regarding mixing intensity, Dixon et al. (2013) found the floc structure formed at higher speed (intensity) mixing could more effectively mitigate membrane TMP increase, while Ratajczak et al. (2012) and Malkoske et al. (2023c) reported increased fouling at higher mixing speeds. It is expected that, although varying flocculation HRT may have minimal impact on NOM removal (Zularisam et al. 2009), it can lead to significant differences in floc morphology and structure which can alter the foulant cake on the membrane surface. Furthermore, the use of different flocculation types (i.e., hydraulic flocculation vs. turbine impeller flocculation) may also be expected to influence floc structure (Saxena and Brighu 2020). A detailed mechanistic study regarding the effect of flocculation HRT and basin type on floc characteristics and subsequent membrane fouling is warranted.

For Type I C-IN pretreatment, the pH of coagulation seems to be critical in determining the LPM fouling behavior. In the study by Hillis (2006), sodium hydroxide and ferric sulphate were dosed inline and blended by means of static mixers prior to hydraulic flocculation with a mean HRT of 15 min. An initial malfunctioning of the pH control system led to a feed water pH of 5.2

instead of 4.5, which was found to be optimal during preliminary testing. With all other variables held constant (i.e., dose and HRT), the increased pH during coagulation led to a rapid fouling rate of 4.3 kPa d^{-1}, more than three times greater than the fouling rate of 1.5 kPa d^{-1} achieved with proper pH control (Table 2.3). Lee et al. (2000) and Zularisam et al. (2009) also emphasized the importance of pH on the coagulation mechanism and its influence on the system fouling behavior. Using alum as coagulant, Lee et al. (2000) reported that when the pH was reduced to ~5, charge-neutralization was achieved (as confirmed by zeta potential (ZP) measurements). This resulted in a lower degree of fouling compared to the sweep flocculation condition, which was achieved with a comparable coagulant dose (using alum) but a higher pH (above 7). In this last study, it was speculated that flocs formed by sweep flocculation are more compact and gelatinous (due to the presence of hydroxide precipitates) than those formed by charge neutralization, organizing into a membrane foulant cake with a lower porosity and a higher compressibility. Lerch et al. (2003) reported that for a river water with Type I C-IN pretreatment and flocculation by HCTF, the impact of feed water pH was dependent on the coagulant type and the filtration conditions. When PACl was used at a pH of either 5.25 or 6.75 and a dose of either 2.7 mg-Al L^{-1} or 13.5 mg-Al L^{-1}, conditions of low pH and high coagulant dose resulted in a severe normalized flux decline of nearly 50% over a four-hour period. When the filtration pressure was increased from 0.4 bar to 0.8 bar it was reported that only conditions of high pH (i.e., 6.75) were suitable, and that low pH conditions resulted in the formation of a highly compressible cake which exacerbated fouling at higher pressures. In contrast, when ferric chloride was used as the coagulant, the impact of pH was minimal and normalized flux decline seemed dependent on the dose alone. Regardless of pH, when the coagulant dose was high (27.9 mg-Fe L^{-1}) the flux decline was exacerbated compared to when low doses were considered (5.59 mg-Fe L^{-1}). It should be noted that in this last study, the effect of coagulant type was assessed by considering equivalent dosages on a molar basis, which resulted in different mass loadings (due to greater molecular weight of iron) to the membrane surface.

Ratajczak et al. (2012) studied the impact of pH on membrane fouling by comparing the performance using optimal coagulant dosages both with and without pH adjustment. For ferric- and aluminum-based coagulants the pH values were adjusted to 5 and 5.5, respectively, values which were selected to yield optimal total organic carbon (TOC) removal according to the literature. For all coagulant types, the final TMP values at the end of the three-day filtration tests were slightly lower when pH control was implemented compared to tests without pH adjustment

(e.g., the final TMP for alum decreased from 36.5 kPa to 33.1 kPa). Zularisam et al. (2009) also reported that for alum and low pH values (i.e., pH of 5), the permeability of a polysulfone UF membrane was enhanced compared to at high pH values (i.e., pH of 12.5). However, while Lee et al. (2000) reported that the enhanced performance was due to loose floc structure and better NOM removal by charge-neutralization compared to sweep flocculation, Zularisam et al. (2009) proposed that the enhanced permeability in the charge-neutralization zone was due to the formation of microflocs and more soluble complexes. Reduced cake formation and higher membrane permeability resulted from increased passage of these small sized and soluble compounds through the membrane. This hypothesis was corroborated by the NOM removal data, which indicated that the low pH condition had significantly lower NOM removals (50%) compared to the high pH condition (66.53%).

The effect of coagulant dose and type was investigated by several studies. Arhin et al. (2018) found that the final membrane permeability could be maximized by applying a high dose of 25 mg L^{-1} PACl (as coagulant), while lower dosages of 15-17 mg L^{-1} exacerbated the permeability decline. Zularisam et al. (2009) reported that the final membrane permeability increased, regardless of the pH, as the alum dose was increased from 1.8 mg-Al L^{-1} to 3 mg-Al L^{-1}. Dixon et al. (2013) compared an optimal dose determined from preliminary jar testing (14 mg L^{-1} as PACl) with an enhanced dose (28 mg L^{-1} as PACl) and found that, regardless of mixing condition, the enhanced dose resulted in a larger size floc size and lower fouling tendency than the optimal dose condition. Ratajczak et al. (2012) considered the effects of different coagulant types when implemented at optimal coagulation conditions determined from preliminary jar testing. Alum, ferric chloride, PACl SP (i.e., 50% basicity), and PACl SP-70 (i.e., 70% basicity) were considered for two natural waters with different levels of organics (Grand River with TOC of 5-6.9 mg-C L^{-1} and Lake Ontario with TOC of 1.5-2.9 mg-C L^{-1}). Notably, the coagulants that achieved the greatest removals of organics were not the same as those that resulted in the lowest level of membrane fouling. For the Grand River water, alum resulted in the greatest reduction in final TMP (57% reduction), although PACl SP and PACl SP-70 had 3% and 9% greater TOC removals (as determined from the preliminary jar tests). For Lake Ontario water, both PACl coagulants had the worst TOC reductions (i.e., 47% and 42% for PACl SP and PACL SP-70, respectively), although resulted in the lowest TMP increase over the three-day test period. Thus, organics removals as measured by DOC/TOC are not the sole determinant of the magnitude of

LPM fouling.

Malkoske et al. (2023c) evaluated the combined impact of pH and coagulant dose on the performance of Type I C-IN by examining three coagulation chemistries which corresponded to adsorption (0.23 mg-Al L^{-1}, pH =5.5), sweep (1.35 mg-Al L^{-1}, pH = 7), and combined (0.72 mg-Al L^{-1}, pH = 7.5) coagulation mechanisms. These conditions were selected according to the alum stability diagrams presented by Amirtharajah and Mills (1982) and Edwards and Amirtharajah (1985). Consistent with the finding of Choi and Dempsey (2004), "underdosing" of coagulant at acidic pH levels (i.e., adsorption mechanism) yielded improved reversibility of fouling, although, reduced fouling was accompanied by low TOC removals of only ~ 7%. Although sweep coagulation used almost twice the coagulant as for combined coagulation, which would reasonably be expected to deliver a greater mass loading to the membrane and yield increased fouling, combined coagulation yielded greater total and hydraulically irreversible fouling. Under identical mixing conditions, the combined coagulation mechanism produced significantly smaller flocs, which were hypothesized to form a denser, lower-porosity cake layer on the membrane surface.

2.2.3.2. Type II Configuration

As described in section 2.1.2.2, Type II C-IN pretreatment consists only of rapid mixing following coagulant addition without the inclusion of a dedicated flocculation stage. Selected bench- and pilot-scale Type II C-IN studies are presented in Tables 2.4 and 2.5, respectively, which provide a summary of water quality data, coagulation characteristics, and fouling measures.

Table 2.4. Selected Bench-Scale Studies in Type II C-IN Pretreatment.

Material Config. NPS or MWCO	Water Quality		Coagulation Conditions						Floc Properties		Fouling Measures		Ref. (see notes)
	DOC (mg L^{-1})	SUVA ($Lmg^{-1}m^{-1}$)	Rapid Mix Type	Transit time (s)	Pump Location	Coag. Type	Dose (mg L^{-1} metal)	pH	Mean Size (μm)	ZP (mV)	$(J/J_0)/t$ (h^{-1})	R_c ($\times 10^{11}$ m^{-1})	
PE					AC								
FS		N/A	IFM	N/A				N/A	N/A		0.812	N/A	[1]
0.1 μm	2					PACl	0.48			-19.9			
	2	N/A	IFM	N/A	AC	PACl	0.58	N/A	N/A	-14.2	0.521	N/A	
	2	N/A	IFM	N/A	AC	PACl	0.69	N/A	N/A	-9.6	0.707	N/A	
	2	N/A	IFM	N/A	AC	PACl	1.16	N/A	N/A	-3.8	0.812	N/A	
PVDF HF SUB 0.04 μm	6.8	N/A	SM + HCTF	N/A	BC	$FeCl_3$	3	N/A	N/A	N/A	0.24	N/A	[2]
PS FS 100 kDa	N/A	N/A	PF	40	BC	$FeCl_3$	2 (as $FeCl_3$)	N/A	44.9	N/A	N/A	0.65	[3]
	N/A	N/A	PF	40	BC	$FeCl_3$	5 (as $FeCl_3$)	N/A	59.9	N/A	N/A	1	
	N/A	N/A	PF	40	BC	$FeCl_3$	10 (as $FeCl_3$)	N/A	90	N/A	N/A	1.5	

Note: AC = after coagulation; BC = before coagulation; DOC = dissolved organic carbon; FS = flat sheet; HCTF = helically coiled tube flocculator; HF = hollow fiber; IFM = instantaneous flash mix; MWCO = molecular weight cut-off; N/A = not available; NPS = nominal pore size; PACl = polyaluminum chloride; PF = pipe flocculation; PS = polysulfone; PVDF = polyvinylidene fluoride; RMT = Rapid mix tank; SM = static mixer; SUB = vacuum submerged. Refs.: [1] (Oh and Lee 2005);[2] (Paar et al. 2011);[3] (Kamińska et al. 2020).

Table 2.5. Selected Pilot-Scale Studies in Type II C-IN Pretreatment.

Water Quality			Coagulation Conditions							Fouling Measures			
Material Config. NPS or MWCO	TOC (mg L^{-1})	SUVA ($Lmg^{-1}m^{-1}$)	Rapid Mix Type	Transit time (s)[a]	Pump Location	Coag. Type	Dose (mg L^{-1} metal)	pH	ZP (mV)	Perm. Decline (L m^{-2} h^{-1} bar^{-1} d^{-1})	Total Rate (kPa h^{-1})	Hyd. Irrev. Rate (kPa h^{-1})	Ref. (see notes)
PES HF PDI 0.1 µm	2.4	N/A	SM	20	BC	N/A	1	5.4		N/A	N/A	6.31	[1]
	2.4	N/A	SM	20	BC	N/A	1.5	5.4		N/A	N/A	5.93	
	2.4	N/A	SM	20	BC	N/A	2	5.4	-14.1	N/A	N/A	3.04	
	2.4	N/A	SM	20	BC	N/A	2.5	5.4	-9.1	N/A	N/A	2.06	
	2.4	N/A	SM	20	BC	N/A	3	5.4	-6.7	N/A	N/A	1.8	
	2.4	N/A	SM	20	BC	N/A	4	5.4	-0.3	N/A	N/A	0.4	
PVC HF N/A 0.05-0.07 µm	N/A	N/A	PF	N/A	N/A	$FeCl_3$	6 (as $FeCl_3$)	N/A	N/A	N/A	N/A	0	[2]
PVDF HF SUB 0.035 µm	2.43	N/A	RMT	N/A	N/A	Alum	4 (as alum)	5.9-6.2	N/A	N/A	N/A	0.1	[3]
	2.43	N/A	RMT	N/A	N/A	Alum	10 (as alum)	5.9-6.2	N/A	N/A	N/A	0.093	
PP HF PDO 0.2 µm	2.43	N/A	SM	N/A	N/A	PACl	2 (as PACl)	5.9-6.2	N/A	N/A	N/A	0.136	
	2.43	N/A	SM	N/A	N/A	PACl	4 (as PACl)	5.9-6.2	N/A	N/A	N/A	0.092	
	2.43	N/A	SM	N/A	N/A	PACl	10 (as PACl)	5.9-6.2	N/A	N/A	N/A	0.256	
PVDF HF SUB 0.04 µm	6.8 (DOC)	N/A	SM + HCTF[b]	30	BC	$FeCl_3$	1		N/A	9	N/A	N/A	[4]
PAN HF N/A 100 kDa	5 (DOC)	N/A	SM	60	BC	Alum	3.5	5	N/A	N/A	1.7	N/A	[5]
	5 (DOC)	N/A	SM	60	BC	Alum	3.5	7	N/A	N/A	0.62	N/A	

Note: AC = after coagulation; BC = before coagulation; DOC = dissolved organic carbon; HCTF = helically coiled tube flocculator; HF = hollow fiber; IFM = instantaneous flash mix; MWCO = molecular weight cut-off; N/A = not available; NPS = nominal pore size; PACl = polyaluminum chloride; PAN = polyacrylonitrile; PES = polyethersulfone; PDI = pressure-driven inside-out; PDO = pressure-driven outside-in; PF = pipe flocculation; PP = polypropylene; PVC = polyvinyl chloride; PVDF = polyvinylidene fluoride; RMT = Rapid mix tank; SM = static mixer; SUB = submerged. [a] transit time between coagulant addition point and membrane module. [b] static mixer used for coagulant injection followed by HCTF prior to contacting membrane module. Refs.: [1] Judd and Hillis (2001);[2] Xiangli et al. (2008);[3] Farahbakhsh and Smith (2002);[4] Paar et al. (2011);[5] Wang and Wang (2006).

Many of the studies available in the literature on Type II C-IN pretreatment were designed as proof-of-concept articles demonstrating the applicability of C-IN as a pretreatment alternative for LPMs and thus investigate only a limited number of conditions. Results of these studies indicate conflicting outcomes regarding the suitability of Type II C-IN for fouling mitigation. For example, the study by Xiangli et al. (2008) evaluated the long-term (7-month) performance of a large pilot-scale UF membrane system treating a river water with C-IN pretreatment at a dose of 6 mg-Fe L^{-1}. The coagulant dose for the study was selected according to chemical oxygen demand (COD) removal results from conventional jar testing. Compared to direct membrane filtration of the raw river water, which necessitated a plant shut-down and chemical cleaning after only 26 hours, Type II C-IN pretreatment using incidental pipe flocculation resulted in a stable membrane permeability and a chemical cleaning interval that exceeded the 7-month duration of the study. Unlike this last study, Galjaard et al. (2001) reported that Type II C-IN pretreatment using variable length incidental pipe flocculation and a coagulant dose of 2-4 mg-Fe L^{-1} resulted in a more rapid increase in membrane TMP compared to filtration of raw water or pre-coating with ferric hydroxide particles. Furthermore, the fouling was found to be largely chemically irreversible and membrane permeability could not be restored following 20 h of filtration. Paar et al. (2011) found that for a bench-scale pressure-driven outside-in (PDO) UF module with PVDF fibers, Type II C-IN pretreatment with ferric chloride at a dose of 3 mg-Fe L^{-1} could reduce the normalized specific flux loss from 20% to less than 10% (of original value) after 20 minutes of filtration. Here, it was suggested that coagulation could effectively agglomerate small colloidal particles into larger sized flocs which prevented pore blocking phenomena. When tests were performed at pilot-scale, however, this same study found that C-IN pretreatment with flocculation by HCTF and a 30 s residence time resulted in worsening of the membrane permeability decline rate, even when low dosages of 1 mg-Fe L^{-1} were considered. The likely reason for the observed difference between the bench- and pilot-scale studies is the inconsistent membrane configuration, with the pilot-scale system operated in a submerged dead-end configuration while the bench-scale system was operated in a cross-flow configuration. It should be noted that the bench-scale system used coagulated water from the pilot-scale system and so differences in mixing were not responsible for the observed performance differences.

Malkoske et al. (2023b) investigated the influence of rapid-mix duration on the performance of Type II C-IN pretreatment. The study was conducted using a low-TOC (< 2.1 mg-

C L^{-1}), low-hydrophobicity (SUVA < 1.6 L mg^{-1} m^{-1}) lake water and alum coagulant at either a low dose (0.76–1.3 mg-Al L^{-1}), defined as a 10% reduction in streaming current, or a high dose condition (6.5–7 mg-Al L^{-1}), which achieved a neutral streaming current. Rapid mixing was performed at a constant velocity gradient of 350 s^{-1} with HRTs of either 2 or 20 min, which were selected to represent both conventional full-scale operating conditions and the extended retention times often encountered in bench-scale studies operating at low flow rates. Increasing the rapid-mix HRT from 2 to 20 min significantly reduced both total and hydraulically irreversible fouling resistance under both coagulant dosing conditions. The extended HRT promoted the formation of larger and more compact flocs, as indicated by a significantly higher two-dimensional fractal dimension ($D_{f,2}$), which was hypothesized to produce a more porous cake layer that could be more readily removed by hydraulic cleaning. These findings contrast with those reported in many batch coagulation studies (e.g., (Yu et al. 2011; Yukselen and Gregory 2004)), where prolonged rapid mixing typically results in floc breakup and the formation of smaller re-aggregated flocs, and highlights important differences between batch and continuous-flow coagulation systems. It should be noted that, although the extended rapid-mix HRTs yielded improved fouling mitigation, such retention times are impractical for full-scale implementation. Nevertheless, the study provided valuable insight into how bench-scale reactor design may influence observed treatment performance relative to full-scale systems.

In a subsequent study, Malkoske et al. (2023c) compared the fouling mitigation performance of Type I (with flocculation) and Type II (without flocculation) C-IN configurations using three coagulation chemistries representing different destabilization mechanisms. Under conditions of rapid mixing alone (G = 350 s^{-1}, HRT = 2 min), both total and hydraulically irreversible fouling resistance were greater than when a flocculation stage was incorporated (G = 20 s^{-1}, HRT = 12 min), although flocculation with extended HRT (24 min vs. 12 min) led to overlapping confidence intervals for the adsorption destabilization chemistry. For the combined and sweep coagulation mechanisms, the inclusion of flocculation produced significantly larger flocs than rapid mixing alone, whereas for adsorption destabilization, flocculation primarily increased floc concentration. The larger flocs generated under Type I C-IN were proposed to form a more permeable and porous cake layer than the smaller aggregates produced under Type II conditions, while increased floc concentration was hypothesized to enhance the release of retained organic matter from the membrane surface, thereby contributing to fouling mitigation.

Other studies have considered the effects of coagulant dose on Type II C-IN pretreatment performance. In the study by Kamińska et al. (2020), which considered a humic acid (HA) spiked surface water treated with 2, 5, or 10 mg L^{-1} ferric chloride without pH adjustment, the lowest permeability decline was observed at 2 mg L^{-1}. It was proposed that for coagulant dosages greater than the optimal dose, thicker, denser, and more compressible cakes led to increased hydraulically irreversible fouling. Farahbakhsh and Smith (2002) likewise compared the effects of coagulant dosage on Type II C-IN-UF performance for two different membrane types. For the first, a submerged PVDF UF membrane with a nominal pore size of 0.035 μm, alum coagulation was evaluated at dosages of 4 mg L^{-1} and 10 mg L^{-1} (as coagulant) for a constant pH between 5.9 and 6.2. For the second, a PDO polypropylene MF membrane, PACl was evaluated at dosages of 2, 4, and 10 mg L^{-1} (as coagulant) with a constant pH. In the case of the submerged PVDF membrane, Type II C-IN pretreatment with alum at the lowest dose (4 mg L^{-1}) resulted in the lowest rate of TMP increase, a rate that was 5.2 times lower compared to when raw feed water was filtered. However, it could not be universally stated that the lowest coagulant dose results in the least rate of TMP increase since, for the PDO polypropylene membrane, 4 mg L^{-1} coagulant addition performed best compared to 2 mg L^{-1} and 10 mg L^{-1}. Oh and Lee (2005) also reported that the lowest coagulant dose does not always lead to lowest degree of membrane fouling. In their study, which investigated a range of PACl dosages between 0.48 mg-Al L^{-1} and 1.16 mg-Al L^{-1}, a dose of 0.58 mg-Al L^{-1} resulted in the lowest specific flux decline of a polyethylene flat sheet MF membrane. It was also demonstrated that the optimal coagulant dose for Type II C-IN pretreatment (i.e., 0.58 mg-Al L^{-1}) was obtained at conditions of neutral streaming potential where small colloidal and sub-micron flocs could more effectively agglomerate and prevent pore blocking. Judd and Hillis (2001) also reported that for conditions of neutral particle surface charge (as measured by the ZP) the rate of TMP increase could be minimized. In their study, the effects of varying coagulant dose and pH were separately assessed using a pilot-scale PES membrane module with a nominal pore size of 0.1 μm. For ferric-based coagulant at a fixed pH value of 5.5, the rate of TMP increase was found to be significantly greater (6.31 kPa h^{-1} vs. 0.4 kPa h^{-1}) at low coagulant doses of 1-2 mg-Fe L^{-1} where the coagulated ZP was between -18 mV and -14 mV, compared to at conditions where charge neutralization was achieved (i.e., 0 mV using 4 mg-Fe L^{-1}). Compared to the effects of varying coagulant dose, pH adjustment between 4.8 and 8.6 only resulted in a slight improvement in the observed SCR, although, it must be noted that this was evaluated only at an

alum dose of 6.75 mg-Al L^{-1} and not with an iron coagulant.

In general, for Type II C-IN pretreatment, the relationship between fouling measures and the applied coagulant dose is presented in Fig. 2.7. Note that the rate of normalized flux decline is given by Eqn. (2.1) below as described by others (Li et al. 2007a):

$$RNFD = \frac{\left(\frac{J_{t_i}}{J_0}\right) - \left(\frac{J_{t_f}}{J_0}\right)}{\Delta t} \tag{2.1}$$

where $RNFD$ is the rate of normalized flux decline in h^{-1}, J_{t_i} is the membrane flux at time t_i in L m^{-2} h^{-1}, J_{t_f} is the membrane flux at time t_f in L m^{-2} h^{-1}, J_0 is the initial clean water flux in L m^{-2} h^{-1}, and Δt is the difference in time between t_i and t_f in h (where $t_f > t_i$). It must be noted that the units of the abscissa in Fig. 2.7 have been presented on a molar basis (i.e., mmol L^{-1}) in order to account for differences in the inorganic coagulant species used in different studies. From Fig. 2.7 it can be seen that, for the lowest applied coagulant dosages, membrane fouling (measured as the irreversible fouling rate or the rate of normalized flux decline) is exacerbated, whereas for dosages greater than approximately 0.05 mmol L^{-1} (as metal), fouling measures appear to be minimized.

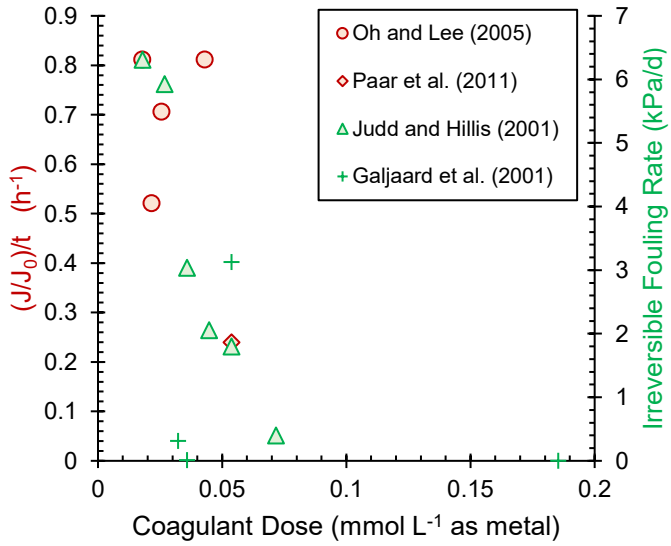


Fig. 2.7. Relationship between fouling measures and coagulant dose for Type II C-IN. Note: Oh and Lee (2005) used PACl, Paar et al. (2011) used ferric chloride, Judd and Hillis (2001) tested iron-based coagulant, and Galjaard et al. (2001) used ferric chloride.

To summarize, Type II C-IN is of particular interest for designers of new LPM facilities

since the lack of a flocculation basin reduces the retention time within the plant, and hence the required plant footprint. Although several authors have investigated the impacts of pH and coagulant dose on Type II C-IN pretreatment performance, there remains some important research gaps. Firstly, many researchers have employed proprietary pilot-scale test rigs which use inline static mixers, incidental pipe flocculation, HCTFs, or rapid mix tanks with limited operational flexibility. For example, Paar et al. (2011) considered 30 s of flocculation by HCTF, Judd and Hillis (2001) considered 20 s of pipe flocculation following static inline mixing, and Kamińska et al. (2020) used 40 s of pipe flocculation prior to contacting the membrane. No studies available in the literature appear to systematically evaluate the impact of the coagulation mixing method (i.e., static mixer, rapid mix tank, etc.) or its operating conditions (i.e., mean velocity gradient or length of pipe flocculation) on Type II pretreatment performance. Lastly, there remains a limited number of studies which present information on floc characteristics (mean size, zeta potential, fractal dimension) for Type II C-IN pretreatment. A lack of such information prevents a more critical comparison of the different coagulant mixing approaches and how their characteristics can influence those of the formed floc particles and finally membrane fouling behavior.

2.2.3.3. Type III Configuration

Type III C-IN (i.e., batch mixing) studies reported in the literature consider a fundamental science approach to the investigation of C-IN fouling phenomena. These studies systematically vary the coagulation chemistry (i.e., coagulant dose, coagulant type, pH) (Chen et al. 2020; Choi and Dempsey 2004; Jung and Kang 2003; Ma et al. 2014, 2017; Pikkarainen et al. 2004; Teng et al. 2020; Wang et al. 2010; Xie et al. 2016; Yao et al. 2015), mixing conditions (i.e., mean velocity gradient, flocculation time) (Amjad et al. 2015; Cho et al. 2006; Nan et al. 2016), and water quality (i.e., NOM, SUVA, ionic strength) (Choi et al. 2008; Long et al. 2021; Ma et al. 2013; Ren et al. 2021; Yan et al. 2021; You et al. 2021) to quantify the impact on floc structure (i.e., size, charge, and density), cake structure (i.e., porosity, thickness, roughness), and the membrane fouling potential. This section will summarize the reported impacts of each of the above-mentioned variables on floc characteristics and membrane fouling in the hybrid C-IN-LPM system. A survey of selected Type III (batch-mixing) studies from the literature using synthetic and natural waters is presented in Appendix A.

The relationship between coagulant dose and membrane fouling (measured as the

normalized specific flux (NSF) decline rate) for the Type III configuration is presented in Fig. 2.8. It should be noted that, in this figure, the coagulant dosages are reported in molar concentrations to account for the different coagulant types used by the studies consulted. From Fig. 2.8, the rate of NSF decline is initially low, reaching a maximum value at a dose of 0.005 mmol L^{-1} (0.15 mg L^{-1} as metal) before progressively decreasing with increasing coagulant dose. Based on this result, there are several comments to be made. First, there exists conflicting reports regarding the effectiveness of ultra-low coagulant dosages for mitigating LPM fouling following C-IN pretreatment. For example, Ma et al. (2014) considered synthetic feed synthetic waters containing 10 mg L^{-1} bovine serum albumin (BSA), 10 mg L^{-1} HA, or 5 mg L^{-1} HA + 5 mg L^{-1} BSA which were coagulated using aluminum chloride at dosages of 0.027 mg-Al L^{-1} to 0.81 mg-Al L^{-1} prior to filtration through a 100 kDa PVDF membrane. For the three feed waters investigated, C-IN pretreatment with a low coagulant dose resulted in a more severe NSF decline compared to the filtration of raw water, a finding which was proposed to be a result of pore blockage due to the formation of small sized floc particles with a similar diameter to the membrane pore size (39-41 nm). In contrast, several studies from other research groups (which use bench-scale hollow-fiber units as well as natural and synthetic waters with different organic character) have reported that coagulant dosages between 0.043 mg L^{-1} and 0.3 mg L^{-1} (as metal) can mitigate membrane irreversible fouling (Peleato et al. 2017; Tang et al. 2019; Wray and Andrews 2014). It was reported that the low coagulant dosages can induce conformational changes to the principle organic foulants in the raw water matrix leading to increased physical cleaning effectiveness as a result of altered membrane-foulant interactions (Peleato et al. 2017).

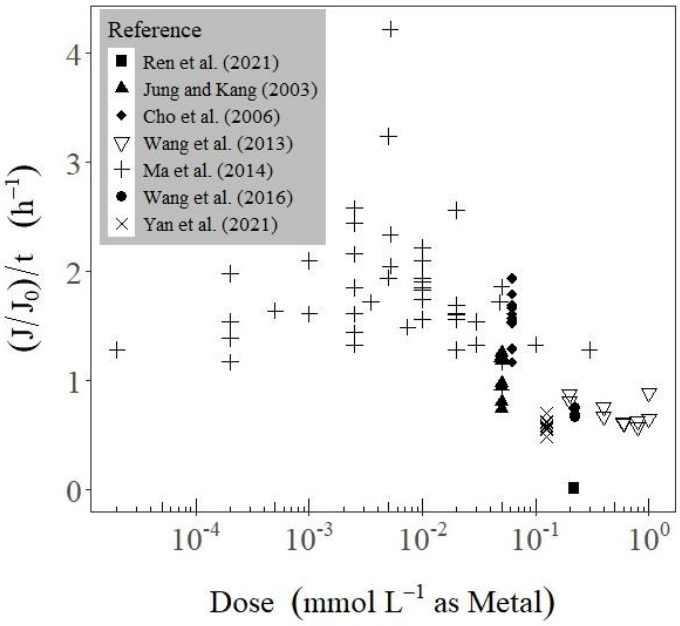


Fig. 2.8. Relationship between coagulant dose and rate of NSF decline for Type III C-IN. Note: References include Ren et al. (2021), Jung and Kang (2003), Cho et al. (2006), Wang et al. (2013), Ma et al. (2014), Wang et al. (2016), and Yan et al. (2021).

Akin to Fig. 2.8, Chen et al. (2020) and Teng et al. (2020) observed a monomodal relationship between coagulant dose and LPM fouling as measured in terms of the SCR. In both studies a 1 g L^{-1} sodium alginate (SA) solution was considered as the feed water for a 0.1 μm flat sheet PVDF membrane disc operating at a constant pressure. It must be noted that the concentrations of SA (which is used as a model foulant for high molecular weight polysaccharide-like foulants present in natural waters (Hao et al. 2012)) used in these two studies were extremely high compared to previous studies (De Angelis and de Cortalezzi 2013; Katsoufidou et al. 2008; Myat et al. 2014) (which considered concentrations < 25 mg L^{-1}) as well as what may be expected in the natural environment. In the study by Chen et al. (2020), the SCR of the challenge water was initially 1.46×10^{14} m kg^{-1} , although increased to 1.65×10^{14} m kg^{-1} following coagulation using a dose of 5.58 mg-Fe L^{-1}. Sequential increase in the coagulant dose from 5.58 mg-Fe L^{-1} to 140 mg-Fe L^{-1} resulted in a drastic reduction in SCR to a final value of 1.38×10^{12} m kg^{-1}. Teng et al. (2020) reported that the SCR increased from 5.2×10^{14} m kg^{-1} to 1.4×10^{15} m kg^{-1} upon addition of 100 mg L^{-1} PACl. A further increase in PACl up to 500 mg L^{-1} (as coagulant) resulted in a steep decline in SCR with a final value of 3.85×10^{13} m kg^{-1}. It was reported for both studies that at low

doses of coagulant, the positive metal ions complex with the terminal carboxyl groups of the SA molecule, which is the most thermodynamically stable configuration. The authors hypothesized that the low level of coagulant addition is unable to reduce the overall surface charge of the molecule and so its structure elongates and crosslinks with other SA molecules (Teng et al. 2020). This creates a dense gel layer with a chemical potential energy gap, resulting in higher SCR and higher filtration TMPs. At higher dosages they proposed that the electrostatic repulsion between chains of the molecule can be reduced which allows the SA to coil into a dense floc particle, producing a porous cake with a low SCR.

The progressive improvement in LPM fouling reduction with increasing coagulant dose has not, however, been universally reported. In the study by Ma et al. (2017), increasing the dose of aluminum chloride from 0 mg L^{-1} to 217.2 mg L^{-1} (as coagulant) for a 20 mg L^{-1} HA solution and 0 mg L^{-1} to 72.4 mg L^{-1} (as coagulant) for a 20 mg L^{-1} BSA solution resulted in the greatest reduction in membrane NSF decline. When the coagulant dose was increased further (up to 362 mg L^{-1}), improved organics removals were observed, although greater magnitude NSF decline occurred. In an earlier study by Ma et al. (2013), increasing the dose of alum from 2.7 mg-Al L^{-1} to 24.28 mg-Al L^{-1} worsened the NSF decline for a flat sheet regenerated cellulose membrane disc operating at a constant pressure. Wang et al. (2013) investigated Type III C-IN using ferric chloride or polymerized ferric sulfate for a 10 mg L^{-1} HA synthetic feed water. In their study, the addition of ferric chloride and ferric sulfate at dosages of 33.5 mg-Fe L^{-1} to 44.7 mg-Fe L^{-1} resulted in charge neutralization (i.e., ZP = 0 mV) and the lowest decline in NSF. When the coagulant dose was increased further to 55.9 mg-Fe L^{-1}, charge re-stabilization occurred (i.e., a ZP of +8 mV for ferric sulfate and 45 mV for ferric chloride) which promoted the formation of small sized and loose (low $D_{f,3}$) aggregates, resulting in a cake layer with low porosity and high compressibility.

The fractal dimension of a floc is a concept used to describe its structure and geometry by relating the aggregate volume or projected area to the size/length (Jiang 1993; Kim et al. 2001). In essence, it is a measure of the degree of occupation of the embedding space (Jiang and Logan 1996). For the most compact configuration, the fractal dimension is equal to the dimension space (i.e., Euclidean geometry), while those aggregates with the fractal dimension less than the dimension space are termed fractals (Li et al. 2007b; Waite 1999). Depending on the method employed to measure and report the floc fractal dimension, a 3-D (i.e., $D_{f,3}$) or 2-D (i.e., $D_{f,2}$) fractal dimension can be obtained. The character of the aggregate geometry is assessed by

imbedding the floc into either a two- or three-dimensional space using both $D_{f,2}$ and $D_{f,3}$ (Logan and Kilps 1995). In two-dimensions, the characteristic, or longest, dimension of the aggregate (l) is related to the projected area of the aggregate (A) through a power law relationship ($A \propto l^{D_{f,2}}$) (Bellouti et al. 1997; Chakraborti et al. 2000, 2003; Gorczyca and Ganczarczyk 1996; Kim et al. 2001; Stone and Krishnappan 2003; Zhu et al. 2018). Microscopy and other imaging techniques such as transmission electron microscopy are suited to the determination of the two-dimensional fractal dimension (Bushell and Amal 2000). The 3-D fractal dimension can be calculated from the power law relationship between the aggregate volume and characteristic dimension ($v \propto l^{D_{f,3}}$) (Chakraborti et al. 2000; Jiang 1993; Jiang and Logan 1996) and is often measured using small angle laser light scattering devices (Jefferson and Jarvis 2006).

Type III (batch) C-IN tests have been the most widely used test configuration for investigating the impact of floc properties (ZP, D_f, size) on C-IN membrane fouling. A relationship between $D_{f,3}$ and the coagulated floc ZP is shown in Fig. 2.9. From this figure it can be seen that as the ZP tends towards zero (i.e., conditions of neutral charge), $D_{f,3}$ tends towards its maximum value of 3. For conditions of increased positive or negative surface charge, the fractal dimension appears to become smaller, reaching values as low as 1.43. Wang et al. (2010) reported that, at a pH of 5, the structure of coagulated HA flocs was highly dependent on the applied coagulant dose. For an alum dose of 1.72 mg-Al L^{-1} to 3.43 mg-Al L^{-1}, the ZP of the coagulated suspension was depressed and dense flocs with 3-D fractal dimensions of 2.6-2.61 were achieved indicating a compact structure. When the alum dose was further increased to 5.14 mg-Al L^{-1}, charge reversion was observed with the ZP increasing to +14 mV. The greater magnitude positive charge led to charge repulsion amongst the chains of the HA-floc particles, finally resulting in a loose aggregate structure ($D_{f,3}$ of 1.54). Similarly, Wang et al. (2013) reported that for conditions of circumneutral ZP (i.e., ZP = 0 mV), the 3-D fractal dimension of the HA-floc aggregate floc was maximized ($D_{f,3}$ = 2.51). When the ferric chloride dosage was further increased to 55.9 mg-Fe L^{-1}, the ZP indicated re-stabilization (reaching +43.1 mV) and resulted in a loose aggregate structure with a low $D_{f,3}$ of 1.86.

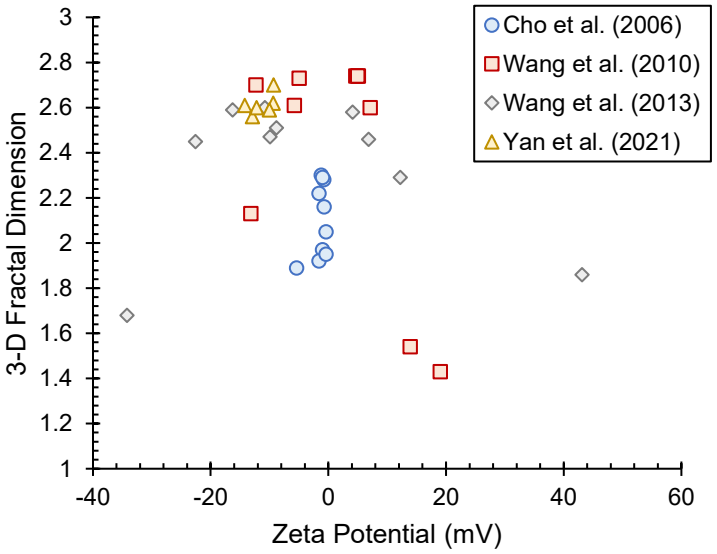


Fig. 2.9. Relationship between 3-D fractal dimension ($D_{f,3}$) and coagulated ZP for Type III C-IN. Note: References include Cho et al. (2006), Wang et al. (2010), Wang et al. (2013), and Yan et al. (2021).

The effects of ZP and $D_{f,3}$ on the rate of NSF decline for Type III C-IN tests are presented in Fig. 2.10a and Fig. 2.10b, respectively. From the studies by Wang et al. (2013), Wang et al. (2010), and Yan et al. (2021), the rate of NSF decline seems to be minimized at a ZP of 0 mV, while for increasing magnitude ZP (in the positive or negative direction) the membrane fouling becomes exacerbated (Fig. 2.10a). From Fig. 2.10b it is shown that for $D_{f,3}$ values of approximately 2.5 or greater the rate of NSF decline was minimized compared to when the value of $D_{f,3}$ was between 1.9-2.3. This finding is in agreement with that of Fig. 2.9 and Fig. 2.10a, suggesting that more compact floc structures (greater $D_{f,3}$) are achieved at conditions of low-magnitude ZP which result in reduced levels of LPM fouling. It should be mentioned that, while Fig. 2.10b shows improved performance for $D_{f,3}$ values less than 1.8 or greater than 2.5, the high rates of NSF decline for $D_{f,3}$ values of 1.9-2.3 were only observed for a single study (Cho et al. 2006).

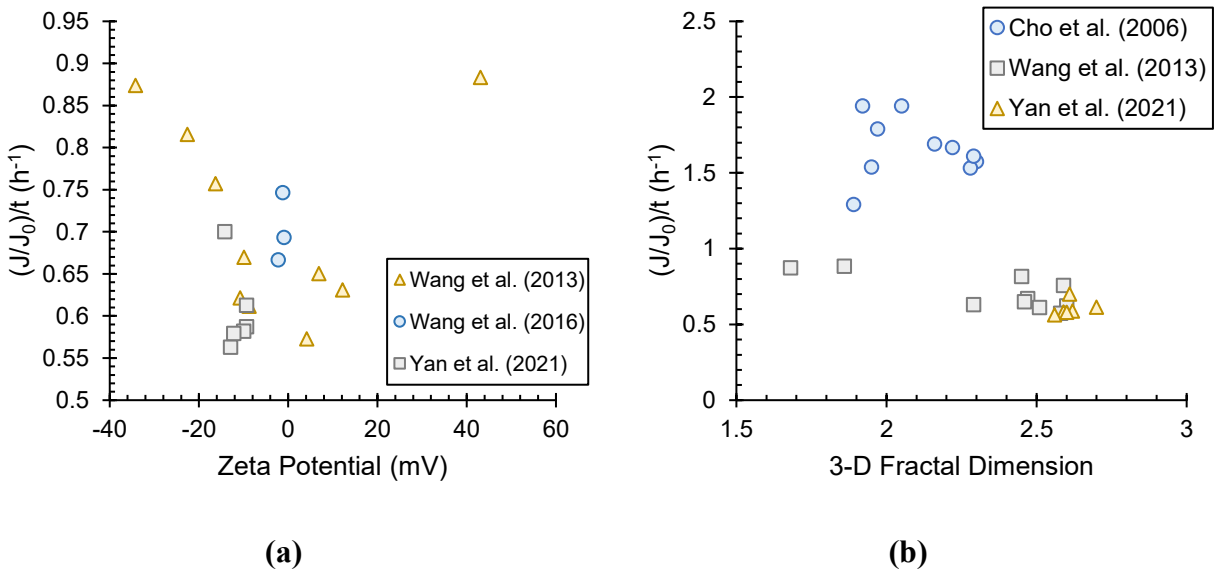


Fig. 2.10. Relationship between rate of NSF decline and: **(a)** ZP; **(b)** $D_{f,3}$. Note: References include Cho et al. (2006), Wang et al. (2013), Wang et al. (2016), and Yan et al. (2021).

While the relationship between the rate of NSF and fractal dimension was presented for the 3-D case in Fig. 2.10b, Fig. 2.11 presents the relationship for the 2-D case. From the figure it can be seen that the volume normalized rate of NSF decline displays a moderate correlation (R^2 = 0.64) with $D_{f,2}$, increasing for increasing values of $D_{f,2}$. This result is somewhat in agreement with the relationship presented for the 3-D fractal dimension in Fig. 2.10b, since the mass fractal in the three-dimensional space will scale with exactly the same dimension of the area projected fractal for fractal dimensions less than 2 (i.e., $D_{f,2} = D_{f,3}$ for $D_f < 2$). In both figures, reduced NSF decline is observed as the fractal dimension tends toward a value of 1, which is characterized by a linear floc structure (Nan et al. 2016; Yao et al. 2015) , while as D_f approaches a value of 2, the NSF decline rate is elevated. These findings suggest that conditions of linearly structured floc aggregates or compact flocs with Euclidean geometry (but not conditions in between) result in the lowest level of volume normalized NSF decline.

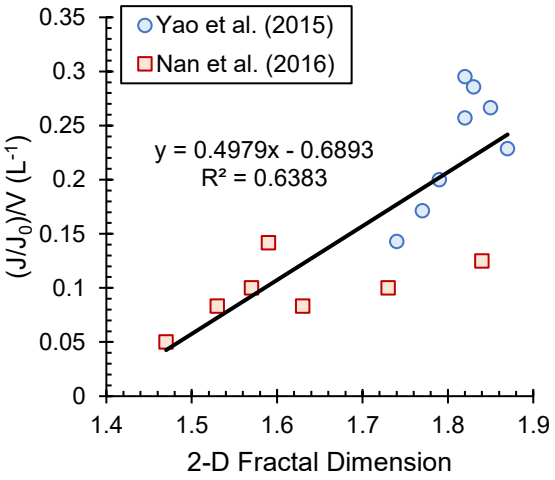


Fig. 2.11. Relationship between volume normalized rate of NSF decline and $D_{f,2}$.

An important research question that still remains is the influence of floc structure on LPM membrane fouling following C-IN pretreatment. From the literature consulted in this review, conflicting results concerning the effect of floc fractal dimension on membrane fouling were reported. These results are summarized in Table 2.6. Based on this, it is recommended that further research be performed systematically investigating the impact of a range of floc fractal dimensions on membrane fouling for the combined system. This study should investigate a range of water qualities with differing NOM matrices in order to bridge the gap between the current literature, which presents conflicting conclusions for a number of water types.

Table 2.6. Summary of Fractal Dimension Impact on Membrane Fouling for Type III C-IN Studies.

Ref.	Summary of Findings
	Better Performance by higher D_f
Feng et al. (2015)	Influence of both size and D_f. Flocs formed with Al_b had a higher $D_{f,3}$ (2.45) which led to a stronger floc that was more resistant to shear. It is suggested that stronger and more compact flocs avoid breakage when being incorporated into the fouling cake and have a lower compressibility. Low $D_{f,3}$ (1.82) resulted in loose floc structure which was susceptible to breakage and is highly compressible.
Wang et al. (2013)	Influence of both size and D_f. Conditions of charge neutralization formed flocs with higher $D_{f,3}$ (2.51) and a larger size, resulting in lower normalized flux decline. At conditions of over- or underdosing, the flocs formed were small and had a loose structure with a low $D_{f,3}$ (1.86). These flocs formed a compact cake layer with a low compressibility.
Yan et al. (2021)	Influence of both size and D_f. For Al_a sourced from both inorganic and polymeric coagulants, the flocs formed had the largest mean size and the greatest $D_{f,3}$ (2.62-2.7). These large, compact flocs were resistant to shear and arranged into a porous cake layer with a low resistance to filtration.
	Better Performance by lower D_f
Cho et al. (2006)	Influence of both floc size and D_f. When the floc size remained constant during rapid mix, decreasing fractal dimension was observed for longer mix times. This resulted in a more loose and open floc structure and a low resistance cake.
Wang et al. (2010)	Influence of both size and D_f. For conditions of near identical floc size, compact flocs (high $D_{f,3}$) formed during sweep flocculation resulted in a filtration resistance twice as high as that of the loose flocs (low $D_{f,3}$) formed through charge neutralization.
Ren et al. (2021)	Influence of both size and D_f. Flocs formed with the smallest size and the highest $D_{f,2}$ arranged into a low porosity, tightly packed cake that presented a high filtration resistance. Conditions resulting in loose, large sized flocs formed a fluffy cake layer which alleviated membrane fouling.
Amjad et al. (2015)	Influence of both size and D_f. Flocs with low $D_{f,3}$ (1.95) produced cakes with a lower D_f, indicating a loose structure and low resistance to filtration. Specific cake resistances of cakes formed by flocs with low and high $D_{f,3}$ were found to be statistically the same, owing to the differences in mean floc size between the conditions.
Xie et al. (2016)	Considered a 1:4 mixture (Fe:Al) of $FeCl_3$ and $AlCl_3$. Greatest reduction in membrane fouling was observed at a pH of 6 where the flocs formed were small and loose (low $D_{f,3}$ = 1.14). These arranged into a thin, dense cake with a high roughness that had greater NOM removal.
Ma et al. (2017)	For the same coagulant dose the impact of pH was critical. At a pH of 6, small sized, loose (low $D_{f,3}$ = 1.98) flocs formed a thin, dense cake layer that was positively charged and alleviated membrane fouling. At a pH of 8 large, dense (high $D_{f,3}$ = 2.45) flocs resulted in a cake with larger pores and worse normalized specific flux decline.
Yao et al. (2015)	At underdose conditions (based on UV_{254} removal), increasing calcium ion concentration led to the formation of larger floc with a lower $D_{f,2}$, resulting in a lower normalized flux decline. It is proposed that these flocs form a loose, porous cake layer with low resistance.
Nan et al. (2016)	Influence of size and D_f. When the flocculation duration was insufficient (5 min), a significant amount of small sized flocs remained in solution and promoted a rapid flux decline. Once the critical flocculation time had been exceeded, the $D_{f,2}$ of flocs increased with increasing flocculation duration, and resulted in increasingly dense cake layers. Flocs with lower $D_{f,2}$ were loose and formed a cake layer of higher porosity. Increasing flocculation G value led to flocs with higher $D_{f,2}$, resulting in a tightly structured cake with higher filtration resistance.

Note. D_f = fractal dimension; $D_{f,2}$ = 2-D fractal dimension; $D_{f,3}$ = 3-D fractal dimension; G = mean velocity gradient (s^{-1})

The surface charge of components within the feed water matrix (as measured by ZP) is the product of unique interaction between the quantity of DOC, the associated charge density of the organic and inorganic moieties, and the conditions used during coagulation to neutralize the charge (namely the pH and coagulant dose) (Smith et al. n.d.; Ulu et al. 2019). Fig. 2.12 presents the relationship between the ZP and the SCR for Type III C-IN tests. From this figure it can be concluded that for ZP values near 0 mV (i.e., charge neutralization) the SCR is minimized (10^{11}-10^{12} m kg^{-1}), while for increasing magnitude of ZP (i.e., up to -80 mV) the SCR increases, reaching greater than 10^{15} m kg^{-1}. The studies by Chen et al. (2020), Long et al. (2021), Teng et al. (2020), Long et al. (2020), and You et al. (2021) all considered a thermodynamic approach to explaining the observed phenomena. As aforementioned, it was proposed in these studies that at high magnitude values of ZP (corresponding to low coagulant dosages) the floc structure elongates and crosslinks with other floc aggregates creating a dense gel layer with a high resistance to filtration due to the creation of a chemical potential energy gap. For conditions of low magnitude ZP (corresponding to high coagulant dosages) the electrostatic repulsion between chains of the molecule can be reduced which allows the flocs to coil into a dense floc particle which produces a porous cake of low SCR.

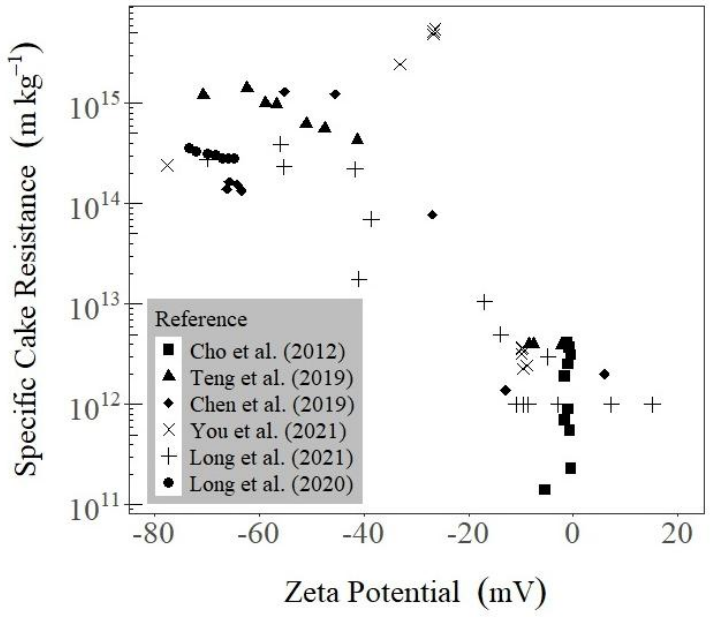


Fig. 2.12. Relationship between ZP and SCR for Type III C-IN.

Several authors have studied the impact of feed water quality on the Type III C-IN fouling behavior, primarily by comparing waters of different SUVA values. Choi et al. (2008) investigated LPM fouling for a "low SUVA" condition by using water from the Han River (Seoul, Korea) and for a "high SUVA" condition by spiking the Han River water with 4 mg L^{-1} HA. The resulting SUVA values of the low and high SUVA waters were 2 L mg^{-1} m^{-1} and 5.5 L mg^{-1} m^{-1}, respectively. PACl was selected as the coagulant, and optimal doses of 2.1 mg-Al L^{-1} and 4.2 mg-Al L^{-1} for the low and high SUVA conditions, respectively, were selected based on NOM and turbidity removals from conventional jar testing. For the low SUVA condition, the floc size was larger (flocculation index of 0.42 vs. 0.24 for high SUVA water), the floc structure was looser/more linear (lower $D_{f,2}$ of 1.64 compared to 1.87 for high SUVA water), and the compressibility (determined by regression of the TMP vs. SCR plot) was lower (0.54 vs. 0.81 for the high SUVA water). The resistance to filtration for a 0.2 μm flat sheet MF membrane was found to be significantly lower for the low SUVA water, resulting in 2.5 times the permeate throughput compared to the high SUVA water (prior to reaching the terminal TMP). In the study by Howe et al. (2006), batch MF tests were performed on 1 L of alum or ferric sulfate coagulated river waters using a 0.22 μm PVDF flat sheet membrane. The river waters considered were the Clackamas River (Oregon, USA) which had a SUVA value of 7.5 L mg^{-1} m^{-1}, the Chattahoochee River (Georgia, USA) which had a SUVA value of 2.5 L mg^{-1} m^{-1}, and finally the Waikato River (New Zealand) which had a SUVA of 3.6 L mg^{-1} m^{-1}. Optimized coagulant dosages were selected based on those used at the local water authorities. The results of the MF tests indicated that the alum coagulated Chattahoochee River water had the lowest NSF decline of 56%, followed by the Waikato River treated with alum (84%) and by ferric sulfate (89%), and finally the Clackamas River at 91% (using alum as coagulant). For increasing feed water SUVA, higher flux decline values were observed, although it must be acknowledged that the feed water DOC of each of the rivers also differed.

The effect of mixing conditions on floc characteristics and membrane fouling has been investigated by a number of authors (Amjad et al. 2015; Cho et al. 2006; Jung and Kang 2003; Nan et al. 2016). In the study by Nan et al. (2016) the effect of mixing duration and mixing intensity on floc characteristics and membrane fouling were separately assessed. Coagulation was performed in a rectangular coagulation tank using a rapid mix duration of 60 s and G value of 400 s^{-1} throughout the entire study. In the first portion of the study the mean G value was fixed at 20 s^{-1} while the flocculation time was set to either 5 min, 10 min, 15 min, and 20 min. In the second

part of the study, the flocculation duration was fixed at 15 min and the mixing intensity was set to either G= 8 s^{-1}, 10 s^{-1}, 15 s^{-1}, or 20 s^{-1}. At a flocculation time of 5 min, a large proportion of the flocs formed were microflocs, whose insufficient size caused rapid pore blockage. For increasing flocculation time beyond 10 min, the floc structure became denser (increasing $D_{f,2}$ from 1.59 to 1.84) and resulted in a greater NSF decline. When the flocculation intensity was varied, increasing intensity also led to an increasing $D_{f,2}$ and worsened NSF decline. It was proposed that increased flocculation mixing duration and intensity led to the formation of a more compact, dense floc structure which aggregated into a filter cake with a high resistance. In contrast, low velocity gradient of 8 s^{-1} and a shorter mixing time of 10 min resulted in a fluffy, loose floc structure which formed a porous filter cake. Amjad et al. (2015) also compared the influence of mixing duration and intensity on floc and foulant cake fractal dimensions by evaluating high (50,400), medium (17,820), and low (1,890) Gt values (i.e., product of mean velocity gradient and flocculation mixing time) for flocculation prior to UF membrane filtration using a 50 kDa PES flat sheet disc. The flocs formed under low Gt resulted in lower floc and cake fractal dimensions than those formed at high Gt values, however, the cake 3-D fractal dimension seemed to converge over a narrow range of 2.92-2.99 for all Gt conditions investigated. Although the floc fractal dimension was lower, indicating a more open structured/linear floc aggregate for the low Gt tests compared to the medium and high Gt tests, the particle size distribution indicated a smaller mean floc size which yielded a higher SCR – this suggests the importance of not only fractal dimension but also floc/particle size on the filterability of membrane fouling cakes. The influence of floc size on the SCR is presented in Fig. 2.13 below. Note that the abscissa plots the square of the mean floc diameter, as the Kozeny Carmen equation (Eqn. 2.2) outlines the inverse proportionality between the square of the mean floc diameter and the specific cake resistance (Endo and Alonso 2001; Fu and Dempsey 1998; Wang and Song 1999).

$$\alpha_{CR} = \frac{180(1-\varepsilon_c)}{\rho_{pp} d_{pp}^2 {\varepsilon_c}^3} \tag{2.2}$$

Where α is the specific cake resistance (m kg^{-1}), ε is the porosity of the cake, ρ_{pp} is the density of primary particles that form the cake (kg m^{-3}), and d_{pp} is the primary particle diameter (m). The studies by Cho et al. (2006) and You et al. (2021) appear to closely follow the relationship, with increasing square floc diameters leading to decreasing specific cake resistance. However, the study by Teng et al. (2020) does not follow such a linear pattern and instead exhibits a tendency to cluster

at a high or low SCR over a narrow range of square mean floc diameters. This points to the fact that floc size cannot be solely considered for C-IN process optimization and that other system parameters exert an influence on the fouling behavior.

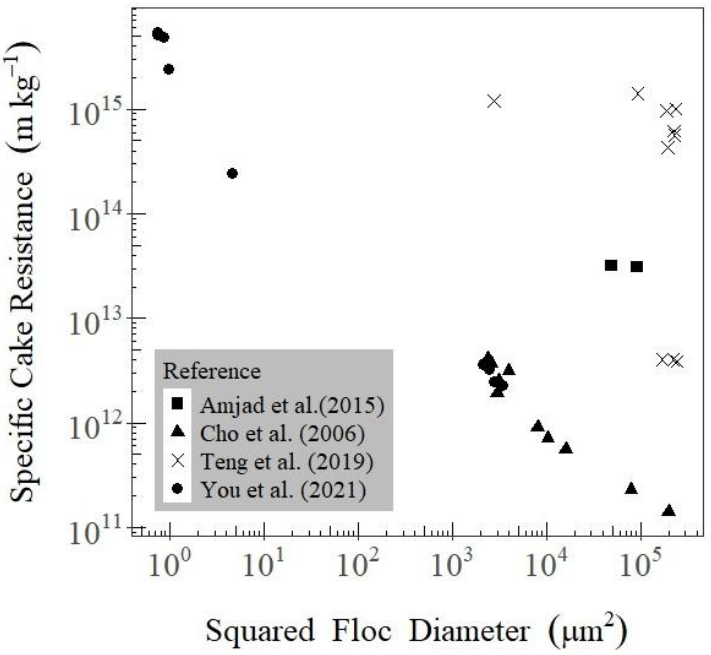


Fig. 2.13. Relationship between floc size and SCR.

2.2.4. C-IN-P

Studies involving C-IN-P pretreatment have, in general, considered the effects of the coagulant dose and the length of its addition (i.e., dosing time) on membrane fouling behavior. These two variables, as well as the membrane flux, can be encompassed within the membrane coating index (C-IDX), a coagulation parameter first introduced by Schweiger et al. (2018a) with potential application for C-IN-P operational control. The C-IDX is calculated using Eqn. 2.3 below.

$$C - IDX = J \times Q \times T \times \left(\frac{1}{60}\right) \tag{2.3}$$

where $C - IDX$ is the coating index (mg m^{-2}), J is the membrane gross flux (L m^{-2} h^{-1}), Q is the coagulant dose (as metal) (mg L^{-1}), and T is the duration of coagulant addition (min). For a LPM facility with a constant flux (as is typical in drinking water treatment (DWT) applications), lower values of the C-IDX suggest either a lower coagulant dose and/or a reduced dosing time. While a reduction in either of these factors is expected to lower the operating expense (OPEX) of a facility

due to decreased coagulant consumption, membrane fouling may become exacerbated, sacrificing the stability of operation and resulting in higher energy and chemical cleaning demand (Schweiger et al. 2018b). In contrast, a higher C-IDX for a constant flux facility suggests higher coagulant dosages and/or longer dosing times, which may lead to higher coagulant consumption without necessarily achieving any significant improvement in fouling reduction. More on the suitability of the C-IDX as a tool for controlling C-IN-P process performance will be discussed in Section 2.2.4.4.

In Table 2.7, pertinent data regarding raw water quality, coagulation characteristics, and fouling measures are presented for selected C-IN-P studies. Some of the most salient points that can be drawn from an analysis of the data contained within Table 2.7 are as follows. First, only a limited number of published studies have been reported regarding C-IN-P pretreatment for LPM technologies in DWT. For this reason, studies examining secondary effluent (SE) as source water (which account for 50% of reported studies) will be analyzed together with those that consider natural surface waters as LPM feed. Second, half of the studies presented in Table 2.7 used tubular multi-channel PES membranes with an inside-out pressure-driven configuration for the evaluation of C-IN-P performance, while only a single study evaluated an outside-in submerged membrane. Finally, owing to the disparate methods used in the literature for quantifying and reporting fouling development, several measures of LPM fouling are presented in Table 2.7, including fouling resistances (using resistance-in-series based models) and permeability decline rates. For this reason, a direct comparison of results between different studies is not always possible.

Table 2.7. C-IN-P Fouling Measures and Coagulation Characteristics.

Material Config. NPS or MWCO	Raw Water Characteristics			Coagulation Characteristics						Fouling Measures			Ref. (see Notes)
	Water Type	DOC (ppm)	SUVA ($Lmg^{-1}m^{-1}$)	Coag. Type	Mixing Type	Coag. Dose (mg L^{-1} metal	Dose Duration (min)	Fraction of Cycle (%)	Coating Index (mg/m^2)	Permeability Decline Rate ($Lm^{-2}h^{-1}bar^{-1}d^{-1}$)	Irrev. Resistance ($\times 10^{11}$ 1/m)	Total Resistance ($\times 10^{11}$ 1/m)	
PVDF													
SUB	Lake	3.9	0.73	PACl	INC	4 (as PACl)	10	8.3	N/A	N/A	0.5-2.72	N/A	[1]
0.02 µm													
	Lake	3.8	0.71	PACl	INC	4 (as PACl)	60	50	N/A	N/A	0.5-1.6	N/A	
	Lake	3.9	0.73	PACl	INC	4 (as PACl)	120	100	N/A	N/A	0.3-1.5	N/A	
PES													
PDI	SE	13.5	2.04	$FeCl_3$	RMCB [a]	20	15	50	300	1.34	N/A	N/A	[2]
50 kDa													
	SE	13.5	2.04	$FeCl_3$	RMCB	20	5	17	100	2.4	N/A	N/A	
	SE	13.5	2.04	$FeCl_3$	RMCB	20	2.5	8.3	50	24	N/A	N/A	
	SE	13.5	2.04	$FeCl_3$	RMCB	1	2.5	8.3	2.5	26.4	N/A	N/A	
PES													
PDI	SE	N/A	N/A	PACl	INC	5	40	100	233	2.88	N/A	N/A	[3,4]
0.02 µm													
	SE	N/A	N/A	PACl	INC	2	40	100	93	0	N/A	N/A	
	SE	N/A	N/A	PACl	INC	5	4	10	23	38.4	N/A	N/A	
	SE	N/A	N/A	PACl	INC	2	10	25	23	21.5	N/A	N/A	
PS													
PDI	River	2.3-2.9	1.27	PACl	N/A	0.53 [b]	1	5	N/A9	181.67	N/A	N/A	[5]
0.01 µm													
	River	2.3-2.9	1.27	PACl	N/A	1.06	1	5	N/A	251.22	N/A	N/A	
	River	2.3-2.9	1.27	PACl	N/A	2.17	1	5	N/A	268.7	N/A	N/A	
PES													
PDI	Lake	3.909	N/A	$FeCl_3$	N/A	2.0/1.0 [c]	30	50	N/A	N/A	N/A	5.3-10.4	[6]
100 kDa													

Note: INC = incidental; MWCO = molecular weight cut-off; NPS = nominal pore size; PACl = polyaluminum chloride; PDI = pressure driven inside-out; PES = polyethersulfone; PVDF = polyvinylidene fluoride; RMCB = rapid mix contact basin; SUB = vacuum submerged; SE = secondary effluent. [a] 10-21 s contact time. [b] dose reported as that which would deliver an equivalent mass for continuous coagulant addition. [c] 2ppm first cycle and 1ppm subsequent cycles for 30/60 mins. Refs.: [1] Lok et al. (2017);[2] Naim et al. (2014);[3] Buchta et al. (2019);[4] Schweiger et al. (2018a);[5] Park et al. (2002);[6] Pronk et al. (2016).

2.2.4.1. Effects of the Coagulation Process

Available studies in the literature exclusively compare the performance of C-IN-P pretreatment for LPM fouling mitigation to that of C-IN pretreatment (Buchta et al. 2019; Lok et al. 2017; Naim et al. 2014; Schweiger et al. 2018b). Lok et al. (2017) compared the irreversible fouling resistance (derived from the resistance-in-series model) of a submerged hollow-fiber UF membrane filtering a hydrophilic (as measured by the SUVA value) lake water following pretreatment by either C-IN or C-IN-P. For both C-IN and C-IN-P pretreatment alternatives, the filtration cycle duration was fixed at 120 min, while for C-IN-P the duration of coagulant addition was set to either 10 min or 60 min. This last study established that dosing coagulant for only the initial portion (fraction) of the filtration cycle did not result in a higher steady-state hydraulically irreversible fouling resistance compared to continuous coagulant addition. Furthermore, while the hydraulically irreversible fouling resistance increased rapidly initially, minimal increase was observed for both the 10 min and 60 min injection conditions after 10-20 h of operation, likely due to the establishment of a protective cake layer on the membrane surface. These findings were corroborated by Pronk et al. (2016), who found that phased addition of ferric chloride for only the initial 50% of the filtration cycle did not result in greater total membrane fouling resistance when compared to continuous coagulant injection. Moreover, the total fouling resistance for C-IN-P pretreated water stabilized (plateaued) after only five filtration cycles (Pronk et al. 2016).

Buchta et al. (2019) compared C-IN and C-IN-P pretreatment of two different SE samples using a tubular monolithic UF membrane made from hydrophilized PES material and operated inside-out. For both SE samples, PACl was added at either 2 mg-Al L^{-1} or 5 mg-Al L^{-1} continuously, or for only the initial portion of the filtration cycle to a fixed C-IDX value of 23 mg m^{-2}. They reported that C-IN-P pretreatment resulted in a higher degree of permeability variation between chemical cleanings compared to continuous inline dosing, although the permeability following chemically enhanced backwashing (CEB) was identical for the two conditions. These findings suggest that: a) the change in coagulant addition technique did not alter the fraction of foulants that were chemically irreversible; and b) that the phased addition of coagulant throughout the filtration cycle led to a reduced hydraulic backwash efficiency, which promoted a greater permeability decline.

Naim et al. (2014) also investigated the performance of C-IN-P for pretreatment of SE using the same tubular monolithic membrane (although with a different nominal molecular weight

cut-off) as Buchta et al. (2019). A single membrane module was employed for all tests, however, CEB cleaning performed following each experiment (which used different C-IDX values) was reported to eliminate any signs of cumulative irreversible fouling. This suggests that the observed performance for each tested C-IDX value was not due to poorly removed protective cake layers formed during earlier experiments. Results of the study indicate that, for a fixed ferric chloride dose of 20 mg-Fe L^{-1}, the permeability following CEB did not change significantly when the time of dosing was reduced from 15 min (out of a 30 min cycle) to 2.5 min (corresponding to a C-IDX reduction from 300 to 50 mg m^{-2}). When the time of dosing was fixed at 2.5 min and the coagulant dose was reduced from 20 mg-Fe L^{-1} to 1 mg-Fe L^{-1} (corresponding to a C-IDX decrease from 50 mg m^{-2} to 2.5 mg m^{-2}), the rate of permeability decline increased only slightly from 24 to 26.4 L m^{-2} h^{-1} bar^{-1} d^{-1}. Thus, significant savings in chemical coagulant are possible without greatly impacting the rate of membrane permeability decline.

In addition to details surrounding how the coagulant is added to the feed during C-IN-P (i.e., dosing time, dose, and C-IDX), the coagulant type is another parameter of the coagulation process whose impact on process performance merits discussion. All C-IN-P studies surveyed in Table 2.7 considered PACl and ferric chloride as coagulants. Importantly, no author has directly compared the effects of these two coagulants (or others) on fouling mitigation using the same membrane type, operating conditions, and water source despite the fact that coagulant type has been shown to exert an influence on LPM fouling in C-IN pretreatment (Aly et al. 2021; Arhin et al. 2016; Hatt et al. 2011). Therefore, based on the limited data available, it is difficult to arrive at any conclusion regarding the impact of coagulant type on fouling mitigation for C-IN-P. This should be the subject of future research.

2.2.4.2. Effects of the Cake Properties

For both the studies by Buchta et al. (2019) and Naim et al. (2014), properties of the cake layer including its thickness, roughness, and coverage of the fiber appear to be critical aspects governing LPM fouling (permeability decline and reversibility) in the C-IN-P-LPM process. In the study by Buchta et al. (2019), the reduced hydraulic backwash efficiency observed for pretreatment by C-IN-P compared to C-IN was postulated to be a result of incomplete coverage of the membrane fiber surface by the cake layer or due to the reduced thickness of the cake layer (Buchta et al. 2019). Complete coverage of the membrane fiber by the cake layer formed during the initial

fraction of the filtration cycle (i.e., with coagulant addition) may more effectively prevent membrane-foulant interactions (and promote foulant-foulant interactions) leading to improved hydraulic reversibility (De Angelis and de Cortalezzi 2013; Dong et al. 2007; Ye et al. 2011). An assessment of how modified operational strategies or altered C-IDXs affect coverage of the membrane fiber during C-IN-P pretreatment is thus warranted.

As the morphological properties of the cake could not be assessed for the tubular membranes used in their C-IN-P tests, Naim et al. (2014) collected atomic force microscopy micrographs for C-IN tests (using a flat-sheet membrane of identical polymer-dope solution and pore size as the tubular PES membrane) to help elucidate how properties of the cake layer impact fouling behavior in C-IN-P. When the coagulant dose was increased from 1 mg-Fe L^{-1} to 15 mg-Fe L^{-1}, the measured surface roughness of the fouled (but not cleaned) membranes decreased from 40 nm to 19 nm. This was postulated to be the result of a thicker and smoother cake layer formed at higher dosages, which led to reduced membrane fouling. Increased cake layer thickness at elevated coagulant dosages have also been reported by a number of other authors (e.g., Gu et al. (2018)). While this result considered continuous coagulant addition, it may suggest that C-IN-P conditions (i.e., C-IDX values) resulting in a more uniform and smooth cake layer could help to alleviate membrane fouling. It has been proposed by numerous authors that surface roughness exerts an important influence on fouling phenomena (Buisson et al. 2004; Tsuyuhara et al. 2010; Van Der Bruggen et al. 2003).

Despite these last studies demonstrating the importance of cake layer properties in governing C-IN-P-LPM fouling mitigation, there has been no investigation which explicitly studies how variable C-IDX values may impact the cake layer thickness, roughness, and coverage of the fiber. Moreover, while it was reported that reduced cake thickness led to greater foulant-membrane interaction and increased fouling, other studies investigating C-IN pretreatment have found that thicker cakes can result in reduced porosity and hydraulic permeability (Ma et al. 2020b; Yu et al. 2013). This can lead to the surface cake presenting its own significant resistance to filtration. A final consideration regarding cake thickness is that its value is likely to be different for different C-IDXs and for different source water qualities (i.e., high vs. low SUVA, high vs. low turbidity), even when these waters are treated using the same coagulant type and C-IDX. Regarding the coverage of the membrane fiber by the cake layer, the packing density of the membrane module is expected to be a critical factor for membranes operated with an outside-in

flow configuration, as higher densities may impair the ability to cover the entire fiber surface (Günther et al. 2012; Salinas-Rodriguez et al. 2016).

2.2.4.3. Effects of Other Parameters

A final word on fouling mitigation by C-IN-P is regarding the impact of several other process conditions, including membrane type/configuration and feed water type. The studies by Lok et al. (2017) and Pronk et al. (2016) both used resistance-in-series-based fouling measures to report that C-IN-P did not result in greater fouling (total and hydraulically irreversible) compared to C-IN and that the resistances stabilized after only a short period of time. The similar performance was despite the fact that the two studies considered membranes with disparate characteristics (submerged PVDF vs. pressure-driven inside-out PES), although, definitive conclusions regarding the impact of membrane configuration/type cannot be made owing to the differences in other operating conditions (coagulant type, dose, and duration of dosing). Moreover, comparison with studies using tubular multi-channeled membranes was not possible due to the different metrics used to quantify their performance. Regarding feed water quality, besides SE sources, only natural waters with relatively low DOC concentrations (< 3.9 mg L^{-1}) and HPI character (based on low SUVA values < 1.27 L mg^{-1} m^{-1}) have been investigated. While fouling mitigation by C-IN-P and C-IN exhibit similar performance for these water types, this has not been confirmed for waters with a greater hydrophobicity (> 3 L mg^{-1} m^{-1}) and DOC content (> 5 mg L^{-1}), which are present in many regions globally (Westerhoff et al. 1999; White et al. 1997).

2.2.4.4. The Coating Index for C-IN-P Operational Control

The reported trade-off between OPEX (i.e., as represented by the C-IDX) and membrane fouling is exhibited in Fig. 2.14a below where the rate of permeability decline reported from available literature follows a near asymptotic relationship. At high values of C-IDX (i.e., greater than 93 mg m^{-2}), the rate of permeability decline was found to be low (less than 2.88 L m^{-2} h^{-1} bar^{-1} d^{-1}), although as pointed out by Buchta et al. (2019), operation at such high C-IDX values leads to increased OPEX due to higher chemical coagulant consumption. In contrast, at low values of C-IDX the rate of permeability decline is exacerbated, exceeding 21.5 L m^{-2} h^{-1} bar^{-1} d^{-1} in all cases. While Schweiger et al. (2018a) proposed that, in terms of stable operational performance and

lowest OPEX, the optimal C-IDX lies within the range of 20 – 25 mg m^{-2}, the analysis in Fig. 2.14a seems to suggest that C-IDX values between 50 - 100 mg m^{-2} may be required for optimal performance. In fact, the range of C-IDXs evaluated by Naim et al. (2014) seem to suggest the possible existence of a threshold C-IDX value (which is likely dependent on the specific feed water, membrane type, and metal salt used) below which the thickness of the cake layer is insufficient and fouling becomes exacerbated. Given that the literature presents limited data for the various waters tested, there is a need to investigate to what C-IDX values the permeability decline rate remains low. This should be pursued for different membrane configuration/types, different raw water types, as well as different coagulant types to ascertain the variability of this apparent exponential drop in permeability decline rate with C-IDX values.

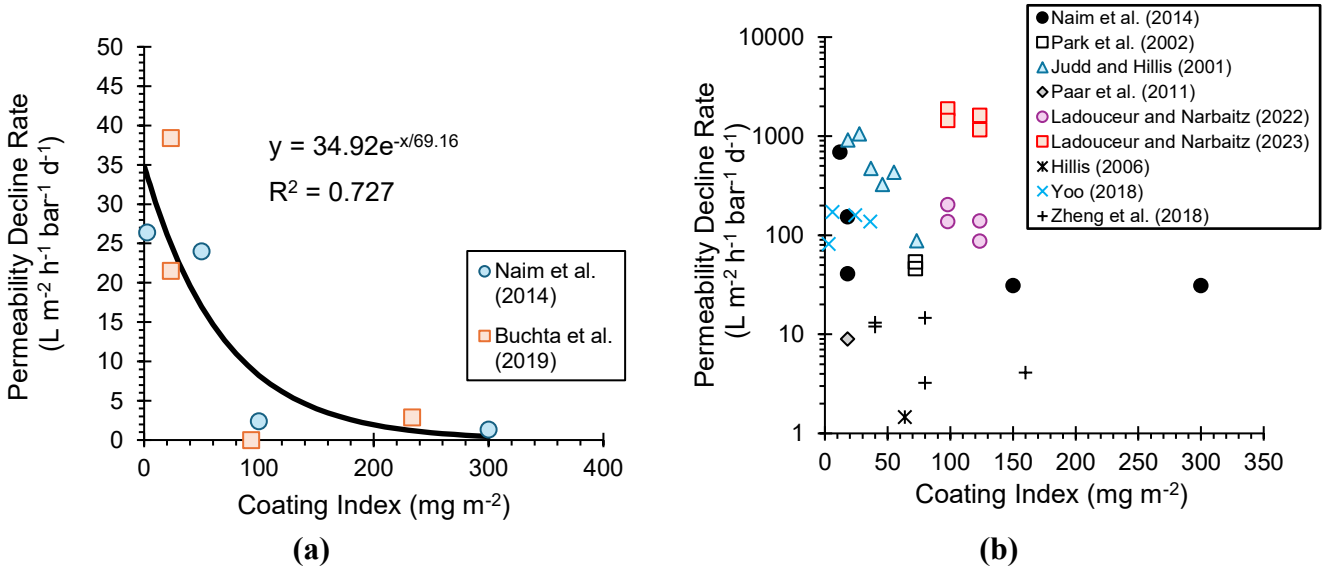


Fig. 2.14. Relationship between C-IDX and membrane permeability decline rate for: **(a)** C-IN-P; **(b)** C-IN. Note: plotted data obtained from articles (Hillis 2006; Judd and Hillis 2001; Ladouceur and Narbaitz 2022, 2023; Naim et al. 2014; Paar et al. 2011; Park et al. 2002; Yoo 2018; Zheng et al. 2017). See Chapter 3 for Ladouceur and Narbaitz (2023) and Chapter 4 for Ladouceur and Narbaitz (2022).

From a physical sense, the C-IDX represents the actual mass of coagulant coating the membrane per square meter of filtration area. Therefore, although the C-IDX was developed for C-IN-P operational control, the model given by Eqn. 2.3 can also be applied to studies considering C-IN pretreatment to help elucidate LPM behavior for different C-IDX values. Unlike for the

limited studies involving C-IN-P (Fig. 2.14a), no trend could be observed in the relationship between permeability decline rate and C-IDX for C-IN pretreatment (Fig. 2.14b). The observed differences between Fig. 2.14a and Fig. 2.14b highlight some of the limitations of using the current form of the C-IDX for operational control, which should be acknowledged. First, the C-IDX does not account for variable coagulant types, despite significant differences in the molecular weights of inorganic aluminum or iron species. For comparative reasons, it may be more appropriate in future to develop the C-IDX using a molar basis for the coagulant dose. Second, the current form of the C-IDX does not account for differences in membrane type (i.e., pore size, material, or configuration) nor does it consider the fact that facilities/studies employ filtration cycles with different durations. Variations in these last two may have led to the significant discrepancies in permeability decline rate observed for the same C-IDX value in Fig. 2.14b. A final limitation of the current C-IDX model worth noting is that it does not follow the principle of the single variable, making comparisons between studies difficult. The same C-IDX value may be arrived at by a number of facilities operating with different fluxes, coagulant dosages, and durations of coagulant addition. Therefore, future research should investigate the sensitivity of the C-IDX when different dosing time/coagulant dose combinations are used for the same C-IDX value, which to date has not been assessed.

2.3. Treated Water Quality by the Hybrid Coagulation-LPM System

The removal of organic matter by LPMs treating coagulated feed water is influenced by several factors, including coagulation conditions (e.g., coagulant type, dose, and pH), source-water characteristics, and membrane properties (including material and MWCO). Consequently, a wide range of NOM removals have been reported in the literature. When interpreting these results, two important considerations should be kept in mind. First, the LPMs used in conventional municipal applications have relatively large pore sizes (~100 kDa or approximately 10–20 nm) and therefore provide only limited removal of NOM in the absence of pretreatment, generally on the order of 5–20% (Pearce 2011). Second, the extent of NOM removal achievable through coagulation is inherently controlled by source-water quality, including factors such as the character of the organics (i.e., hydrophobicity, molecular weight), the alkalinity, and the pH (among others). This dependence is reflected in the U.S. Environmental Protection Agency's Enhanced Coagulation Guidance, which specifies TOC removal requirements ranging between only 10% for low (> 2-4

mg L^{-1}) TOC waters with > 120 mg $CaCO_3$ alkalinity to 50% for waters with high (> 8 mg-C L^{-1}) organics and low alkalinity (< 60 mg $CaCO_3$ L^{-1}) (Edzwald and Tobiason 1999; United States Environmental Protection Agency 1999).

The variability in reported NOM removals is further influenced by the heterogeneous nature of NOM itself, which can vary seasonally at the same location and whose composition is governed by local biogeochemical conditions (Sillanpaa 2015). In general, HPO NOM fractions are removed more effectively than HPI fractions, while high-molecular-weight NOM is removed to a greater extent than low-molecular-weight NOM (Chow et al. 2008; Matilainen et al. 2010). This behaviour is likely attributable to the greater aromaticity and predominantly hydrophobic character of high-molecular-weight organic fractions, which make them more amenable to coagulation (Świetlik et al. 2004).

Given these factors, substantial variability in reported treatment performance is expected across studies. The following subsections synthesize the available literature to identify the key removal trends associated with each coagulation-based pretreatment alternative examined in this review.

2.3.1. CF-SED

Generally, a number of different coagulant types (Alum, PACl, aluminum chloride, ferric chloride), coagulant dosages (1-20 mg L^{-1} as metal), and feed water qualities (SUVA from 1.52 to 4.16 L mg^{-1} m^{-1}) have been considered in tests evaluating the performance of CF-SED pretreatment, making it difficult to arrive at any general conclusions regarding trends in treated water quality. Fig. 2.15 reports the percent removal of bulk organic measures (DOC, UV_{254}, and SUVA) for select studies which encompass these variable operating conditions. For SUVA values between 2-4 L mg^{-1} m^{-1}, it has been reported that the removal of DOC from feed water by coagulation varies between 25-50% (Edzwald and Van Benschoten 1990). Pearce (2011) also reported that LPMs can remove an additional 5 to 20% of DOC without chemical pretreatment. Based on the literature consulted in this review, a mean DOC removal of 29.63% was reported following LPM filtration with pretreatment by CF-SED, with values ranging from 0.6% to 62% for the most HPI and HPO waters (based on SUVA), respectively. It should be noted that some removal values were determined using non-optimal pretreatment conditions as, for example, Jang et al. (2005) evaluated the performance of CF-SED by varying the PACl dose from a low value of 1 mg-Al L^{-1} to 16 mg-Al L^{-1}. Most

notably, it was reported in the studies by Ma et al. (2020a) and Ding et al. (2021) that the removal of organics by the combined CF-SED-LPM system was insensitive to the retention time within the sedimentation basin. Using a surface water with low DOC (2.5 mg L^{-1}), a moderate SUVA value (3.2 L mg^{-1} m^{-1}) and ferric chloride as coagulant, Ding et al. (2021) reported that the removal of DOC by the hybrid system varied between 26.1% and 26.5% (with overlapping 95% confidence intervals) for sedimentation times ranging between 0 to 60 min in either room- or low-temperature conditions (15 °C).

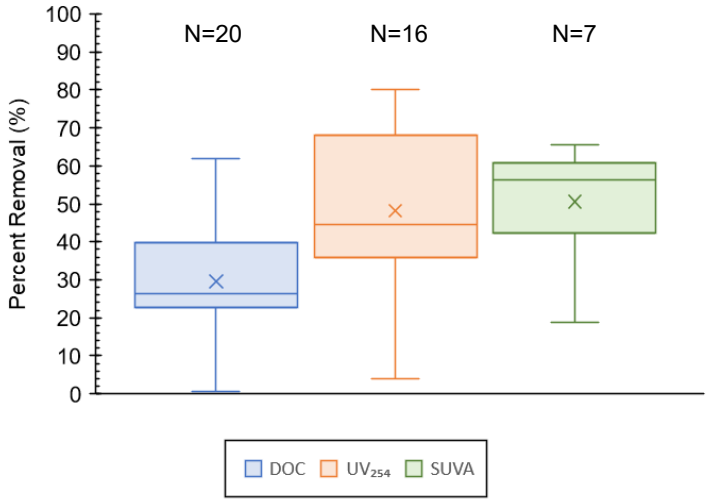


Fig. 2.15. Removal of DOC, UV_{254}, and SUVA following CF-SED pretreatment and LPM filtration for select studies. Note: Data from Liang et al. (2008), Ding et al. (2021), Minegishi et al. (2001), Jang et al. (2005), Walker and Narbaitz (2016), and Moon et al. (2009).

2.3.2 CF-DAF

Table 2.8 summarizes the removals of organic and particulate water quality measures following CF-DAF pretreatment and LPM filtration for selected studies. Important CF-DAF parameters as well as bulk measures of the raw water quality are also presented for each study.

Table 2.8. Removals of Bulk Water Quality Parameters for Selected CF-DAF-LPM Studies[a].

Coagulation/Flotation Characteristics				Raw Water Characteristics					Post CF-DAF Treatment[b]				Post Filtration[b]		
Coag. Type	Coag. Dose (mg L^{-1} metal)	Recycle Pressure (kPa)	Recycle Ratio (%)	Water Type	DOC (ppm)	SUVA ($Lmg^{-1}m^{-1}$)	Turbidity (NTU)	pH	DOC Removal (%)	Turbidity Removal (%)	UV_{254} Removal (%)	pH	DOC Removal (%)	Turbidity Removal (%)	Ref.
Alum	5	450	20	SE	9.85	2.5	3.2	8.2	N/A	N/A	N/A	N/A	10.0 (8.87)	N/A	[1]
CHIT	200 (as coag.)	600	19	CWW	3.35 (TOC)	N/A	N/A	4.9	12	N/A	N/A	3.0	Variable[c]	N/A	[2]
Alum	3.43	400	10	Lake	4.87	1.44	5.32	N/A	37.8 (3.03)	60.9 (2.08)	57.1 (0.03)	N/A	52.2 (2.33)	92 (0.43)	[3]
$FeCl_3$	10	200	N/A	River	6.25-10.1 (TOC)	N/A	>10	6.8-7.4	N/A	N/A	N/A	N/A	34	90	[4]
PACl	50 (as coag.)	517	10	River	3.8	3.41	2.3	7.0	N/A	78.3 (0.50)	69.9 (0.039)	N/A	59.2 (1.55)	97.8 (0.05)	[5]
PACl	12 (as coag.)	517	10	Lake	2.2	1.53	1.65	8.1	N/A	77.6 (0.37)	48.8 (0.017)	N/A	19.5 (1.77)	97.0 (0.05)	
PACl	18 (as coag.)	517	10	Lake	2.0	1.58	37	8.0	11.0 (1.79)	87.5 (4.61)	43.0 (0.018)	N/A	11.0 (1.78)	99.9 (0.04)	
PACl	20 (as coag.)	517	10	Lake	2.2	1.15	66	8.1	N/A	96.0 (2.7)	37.1 (0.016)	N/A	21.4 (1.73)	99.9 (0.04)	
PACl	Variable[d]	N/A	10	Lake	2.2	1.50	1.4	8.1	N/A	N/A	N/A	N/A	17.0 (1.83)	N/A	[6]
PACl	Variable[d]	N/A	10	Lake	2.0	1.30	15	8.0	N/A	N/A	N/A	N/A	N/A	N/A	
PACl	2	400	N/A	SYN	N/A	N/A	110-125	5.5	N/A	72	N/A	N/A	N/A	N/A	
PACl	2	400	N/A	SYN	N/A	N/A	110-125	5.5	N/A	72	N/A	N/A	N/A	N/A	
PACl	2	400	N/A	SYN	N/A	N/A	110-125	5.5	N/A	72	N/A	N/A	N/A	N/A	
PACl	2	400	N/A	SYN	N/A	N/A	50-70	5.0	N/A	29	N/A	N/A	N/A	N/A	
PACl	2	400	N/A	SYN	N/A	N/A	50-70	5.0	N/A	29	N/A	N/A	N/A	N/A	
PACl	2	400	N/A	SYN	N/A	N/A	50-70	5.0	N/A	29	N/A	N/A	N/A	N/A	
Alum	45 (as coag.)	N/A	N/A	RES	6.9 (TOC)	2.3	2.7	7.3	(3.5-5.3)	(0.3-1.0)	43.8 (0.09)	6.2	2.6-11.1[e]	(<0.03)	[7]
Alum	3.18-3.36	N/A	N/A	River	8.16	3.92	3.56	7.7	62.4 (3.07)	85.4 (0.52)	81.3 (0.06)	7.54	73.7	N/A	[8]
Alum	3.18-3.36	N/A	N/A	River	7.09	3.56	1.63	6.77	72.4 (1.96)	82.2 (0.29)	88.0 (0.03)	6.48	N/A	N/A	[9]
Alum	2.99	N/A	N/A	River	6.07	4.16	1.52	6.97	65.9 (2.07)	75.7 (0.37)	80.0 (0.05)	6.46	69 (1.88)	N/A	
PACl	60 (as coag.)	N/A	N/A	RES	3.06	N/A	8.3	N/A	41.2 (1.8)	(<1)	N/A	N/A	N/A	N/A	[10]

[a] CHIT = chitosan; CWW = cork processing wastewater; DOC = dissolved organic carbon; PACl = polyaluminum chloride; RES = reservoir; SE = secondary effluent; SUVA = specific ultraviolet absorbance at 254nm; SW= seawater; SYN = synthetic water; TOC = total organic carbon. [b] Residual values in brackets. [c] Performed critical flux testing with five membrane types reporting 15-99% rejection. [d] Coagulant dose was adjusted using influent feed water turbidity measurements. [e] Removal by MF membrane only. Refs.: [1] Goh et al. (2010);[2] Minhalma and De Pinho (2001);[3] Amaral et al. (2013);[4] Hög et al. (2015);[5] Van Benschoten et al. (2002);[6] Pissibanganga et al. (2016);[7] Braghetta et al. (1997);[8] Xu and Narbaitz (2016);[9] Walker and Narbaitz (2016);[10] Kang et al. (2021).

Analysis of this hybrid system's product water quality will be made by considering the performance in terms of organics, particulate, and algae removals. It can be seen from Table 2.8 that the removal of organics (measured as DOC) by LPMs following CF-DAF pretreatment varies between 0-14.4% (calculated by subtracting the post-CF-DAF DOC removal from the post-filtration DOC removal in Table 2.8). Although this is within the range of removals (5-20%) suggested by Pearce (2011), it has been it has been proposed that the removal of organics by the LPM following CF-DAF pretreatment will be lower than what is typical for LPMs without pretreatment or even with alternative coagulation pretreatment strategies (i.e., CF-SED) (Guastalli et al. 2013; Minhalma and De Pinho 2001; Shi et al. 2017). The propensity of CF-DAF pretreatment for removing HPO organic materials results in a membrane feed water with a more hydrophilic character and greater proportions of low-molecular weight organics, which are poorly retained by LPMs. This was observed in the study by Shi et al. (2017), where the UF membranes reduced the organics (measured as COD) by only 6.4%, as well as in the study by Guastalli et al. (2013) where only 6% of low-molecular weight organics (measured by liquid chromatography organic carbon detection (LC-OCD)) were retained by the UF membrane.

The hybrid system has been shown to effectively reduce turbidity in treated water, with a number of studies reporting finished water qualities < 0.06 NTU (Braghetta et al. 1997; Van Benschoten et al. 2002). The hybrid system has also proven to effectively manage variable feed water quality. Braghetta et al. (1997) reported that, despite a variable average feed water turbidity ranging between 2-5 NTU, CF-DAF pretreatment was able to produce a LPM feed water with a consistent quality < 0.5 NTU. Kang et al. (2021) also reported that for an average feed water turbidity of 10.1 NTU, but variable conditions reaching a maximum value of 83 NTU, the hybrid system could produce an effluent with a consistent quality.

A few authors have monitored the removal of algal cells throughout the various stages of the hybrid system. Amaral et al. (2013) reported that for a freshwater lagoon source known to contain high densities of microalgae (cyanobacterial density of 39,000 ind mL^{-1}), CF-DAF pretreatment could remove 71% of the organisms, while CF-DAF integrated with MF consistently achieved complete cyanobacterial cell removal. This finding was corroborated by Goh et al. (2010) who reported negligible Chlorophyll-a concentration following CF-DAF-MF of a SE spiked with *M. aeruginosa*. Regarding the removal of algae, it would be of interest to evaluate the seasonality of the CF-DAF performance and its effect on LPM fouling. Many studies have indicated that their

source water is subject to seasonal algal blooms yet only report average values for bulk parameters and do not adequately discuss any observed performance differences (in terms of fouling and water quality) between conditions of normal and algal impacted water quality. It would also be of interest to investigate whether the hybrid system requires continuous optimization or whether the CF-DAF process is robust enough to satisfy fouling and water quality objectives during all water quality events.

2.3.3 C-IN

In general, it has been widely reported that C-IN pretreatment of LPM feed water can achieve improved NOM removal compared to direct filtration (Farahbakhsh and Smith 2002; Kabsch-Korbutowicz 2005; Kimura et al. 2008; Lee et al. 2000; Ren et al. 2021). The improvement in the removal of organics by LPMs following pretreatment by C-IN is attributed to the destabilization, complexation, and precipitation of NOM moieties followed by their agglomeration into flocs of sufficiently large size to be rejected by the membrane (Huang et al. 2009; Wang et al. 2013). Not all studies, however, have reported improved removals of organics following C-IN pretreatment. For example, a number of studies have considered ultra-low coagulant dosages (<1 mg L^{-1} as alum) as a means to alter LPM foulant interactions with the membrane surface. These ultra-low dose conditions, although reported to be effective in fouling mitigation (especially by biopolymers) (Peleato et al. 2017; Wray et al. 2016; Wray and Andrews 2014), have not demonstrated an ability to remove significantly greater levels of NOM compared to direct filtration (Hatt et al. 2011; Tang et al. 2019). Fig. 2.16 presents the NOM removal following coagulation and LPM filtration as a function of coagulant dose for select Type I (with dedicated flocculation), Type II (without/incidental flocculation), and Type III (batch mixing) C-IN studies. It can be seen that when all mixing types are considered together, NOM removal increased with coagulant dose up to approximately 0.15 mmol L^{-1} (as metal), beyond which removal plateaued at approximately 80–90%. The relatively high removal observed at this plateau is largely attributable to the source waters examined, which consisted of either synthetic humic acid solutions or natural waters with high SUVA values (~5.7 L mg^{-1} m^{-1}). Owing to their predominantly hydrophobic, aromatic, and high-molecular-weight NOM fractions, these waters are highly amenable to coagulation (Edzwald 1993; Edzwald and Van Benschoten 1990). It should also be noted that the NOM removal data presented in this figure include both TOC and DOC reductions, as relatively few studies report

both NOM removal performance and coagulant dose expressed on a metal basis. The 10-20% of NOM which cannot be removed by the hybrid C-IN-LPM system, despite increasing coagulant dose up to 0.5 mmol L^{-1}, is in agreement with the findings of previous studies who have reported the existence of a recalcitrant portion of NOM resistant to removal by coagulation (Chow et al. 1999; Fabris et al. 2004; van Leeuwen et al. 2002; Randtke 1988).

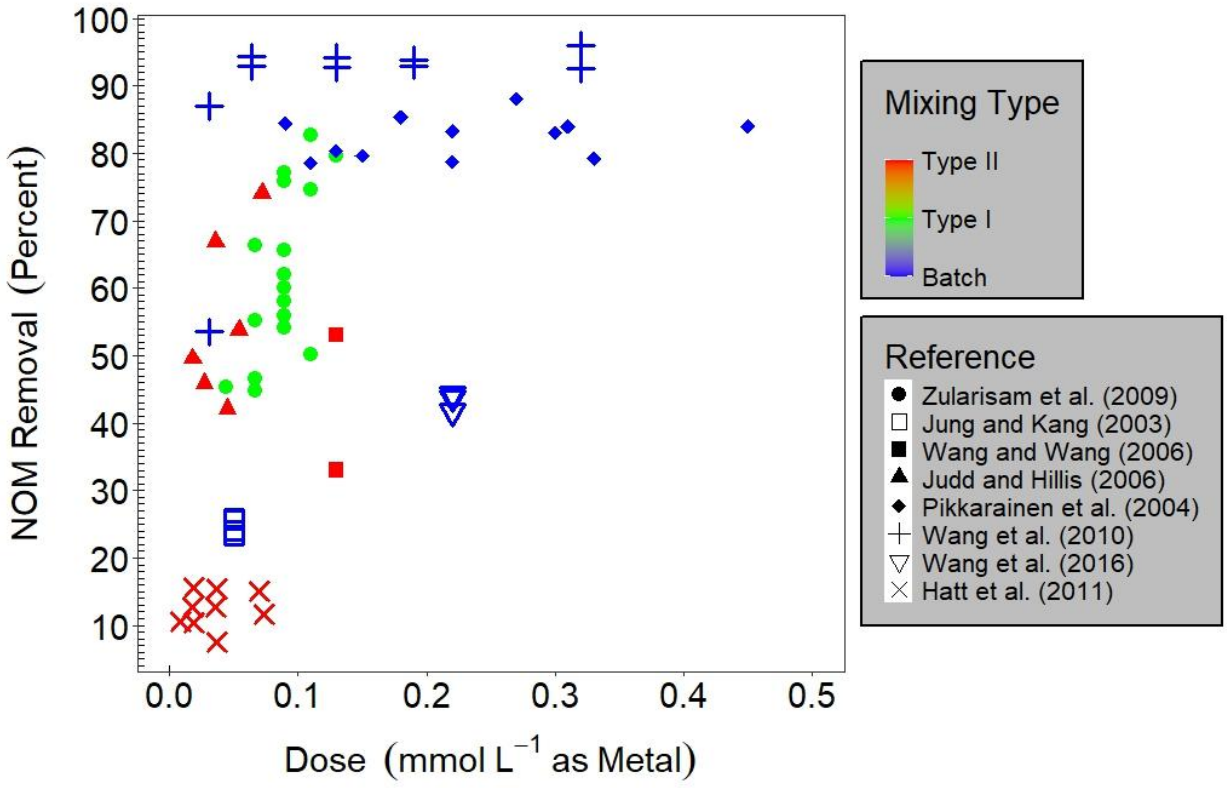


Fig. 2.16. Relationship between applied coagulant dose and filtered removal of organics for pretreatment by Type I, Type II, and Type III C-IN.

Relationships between NOM removal and pH, coagulant type (i.e., iron or aluminum based), and feed water SUVA are presented in Appendix B. Regarding the impact of coagulated pH, no trends could be observed from consideration of Type I, Type II, and Type III studies together. Several authors, however, have emphasized the importance of coagulated pH on the performance of the C-IN-LPM system. Lee et al. (2000) reported that, for pH of 5 corresponding to charge neutralization conditions, the removal of TOC was superior (35.3% vs. 23.5%) compared to conditions of sweep flocculation at a pH of 7. Meyn et al. (2008) observed that for coagulation

by ferric chloride, the greatest removal of DOC was at the lowest tested pH value of 4.5 where conditions of charge neutralization were expected. In contrast, Malkoske et al. (2023a) found that conditions of sweep coagulation (pH=7) promoted greater reduction in TOC compared to adsorption destabilization (pH 5.5) for a lake water (Lake Simcoe, ON, Canada) with moderate DOC content (4 mg L^{-1}). Both Meyn and Leiknes (2010) and Kimura et al. (2008) reported that for precoagulation with alum, the effect of pH on NOM removal was more significant than that of coagulant dose and that pH values of 5.5-6 resulted in the best reduction in organics. It was also noted that for low pH conditions below a value of 5 the residual aluminum concentration in the permeate water increased greatly (Health Canada specifies an operational guideline of 0.1 mg L^{-1} total aluminum), likely due to the formation of small microflocs. Furthermore, with decreasing pH the solubility of aluminum and iron increases. Operation at such low pH values, even if it presents advantages in terms of organics removal, may not be feasible due to the inability to meet local regulatory standards relating to residual metal concentration.

When the impact of feed water SUVA value on the variation of NOM removal was assessed, it was clearly shown that the lowest removal values occurred for feed waters with the lowest SUVA values. It has been previously well established that waters with high SUVA values are composed of aromatic, hydrophobic, aquatic humic substances which are preferentially removed by coagulation (Archer and Singer 2006; Cornelissen et al. 2008; Edzwald and Van Benschoten 1990).

Interesting results were reported regarding the impact of flocculation duration on removal of organics in the hybrid C-IN-LPM system by Type I and Type III tests. Zularisam et al. (2009) investigated the effect of flocculation HRT on the combined coagulation LPM process by using an end-over-end hydraulic flocculator with an HRT of either 5 min or 15 min. ANOVA analysis of a 2^4 full-factorial design found that the HRT had minimal impact on the removal of NOM and in fact the secondary impacts of pH, coagulant dose, and feed water SUVA value were all more significant that the primary impact of HRT. Based on these findings, it was proposed that following short duration flocculation microflocs had already aggregated to sufficiently large size to be excluded by the LPM. Pikkarainen et al. (2004) observed similar insensitivity of NOM removal in the hybrid system to flocculation HRT when evaluating flocculation times of 30, 60, and 90 s. Despite variable cake resistance for different flocculation durations, trends in NOM removal were not observed and it was reported that following only 30 s of flocculation the microflocs had grown to

sufficient size to be removed by the membrane.

2.3.4 C-IN-P

The removal of organic matter by LPMs with C-IN-P pretreatment must also be assessed as an important parameter in the integrated design process of drinking water and wastewater facilities. Several studies have reported similar removals of bulk organics measures by LPM systems with C-IN-P and C-IN pretreatment for both natural waters and SEs. Lok et al. (2017) reported that when PACl was dosed for 50% of the filtration cycle (i.e., 60 min out of 120 min) the average DOC and SUVA removal rates in the permeate were 13.2% and 7%, respectively, for a low SUVA (0.73 L mg^{-1} m^{-1}) lake water. When the dosing time was reduced from 60 min to 10 min for the same water, the average DOC and SUVA removals decreased to 7.7% and 6.8%, respectively. Surprisingly, for both C-IN-P conditions, the average SUVA removals exceeded those obtained using C-IN pretreatment with continuous coagulant addition, while dosing for 50% of the cycle was sufficient to achieve greater bulk DOC removal. Park et al. (2002) considered the low SUVA (1.27 L mg^{-1} m^{-1}) Han River (Seoul, Korea) as the source water for their study and reported the removal of UV_{254} absorbance (UVA_{254}) to be 44.1% following C-IN pretreatment with a PACl dose of 2.17 mg-Al L^{-1}. When C-IN-P pretreatment was investigated using coagulant dosages equivalent to continuous addition of 0.53, 1.06, and 2.17 mg-Al L^{-1}, the corresponding UV_{254} removals were found to be 27.3%, 38.8%, and 49.6%. Therefore, compared to C-IN pretreatment, C-IN-P with an equivalent mass loading of coagulant improved UV_{254} removals by 5.5% and could achieve comparable removals with half the coagulant dose. In the study by Buchta et al. (2019), the two SE sources considered had different levels of bulk organics, as displayed by COD values of 17.6 mg L^{-1} and 35 mg L^{-1}. When comparing the removals of organics by continuous and phased coagulant addition, different tendencies were reported depending on the source water. For the first SE (with a COD of 17.6 mg L^{-1}), continuous and phased coagulant addition (using a C-IDX of 23 mg m^{-2}) resulted in nearly identical COD removals of 43% and 41%, respectively. In contrast, for the second SE (with a COD of 35 mg L^{-1}), continuous coagulant addition resulted in a 10% greater (30% vs. 20%) removal of COD than C-IN-P.

In summary, similar removals of bulk organics can be achieved by C-IN-P and C-IN pretreatment of LPM feed waters, although the removals appear to be dependent on a unique interaction between the membrane type, the source water quality, as well as the dose and fraction

of cycle it is applied (i.e., coating index). For some waters the removals of organics by C-IN or C-IN-P were found to be similar, however, the water types and organic loadings for which this is true have not been properly elucidated. Future studies should consider advanced characterization/fractionation techniques of organics for natural waters or synthetic waters with a controlled composition to identify which water quality indicators govern the removals of organics in the C-IN-P scheme. Results from Lok et al. (2017) suggest that a reduction in the C-IDX (by reducing the dosing time from 60 min to 10 min) had minimal effect on the removal of HPO organic materials (as measured by SUVA). This fact may be critical to the applicability of C-IN-P for LPM pretreatment in DWT facilities as these organics have been suggested as the main precursor to trihalomethanes and haloacetic acids (Hua and Reckhow 2007; Jung and Kang 2003), which are regulated in North America and Europe.

2.4. Conclusions of Literature Review

This review compiled the results of studies investigating the performance of coagulation pretreatment (including CF-SED, CF-DAF, C-IN, and C-IN-P) for LPMs in water treatment. Based on the literature surveyed, the key findings are summarized as follows:

1. For a single membrane and water type, CF-DAF was found to exhibit superior performance (in terms of fouling mitigation) compared to pretreatment by CF-SED. When compared to pretreatment by C-IN, the relative performance of CF-DAF appears to be dependent on unique interactions between the feed water quality and the membrane type/configuration.
2. For C-IN pretreatment, it has been reported for both Type I and Type II configurations that coagulation conditions optimized for the removal of NOM (i.e., coagulant type, dose, and pH) do not necessarily coincide with those optimal for LPM fouling reduction.
3. Conditions of low or high (but not intermediate) floc fractal dimension appear to result in the greatest reduction in LPM fouling for C-IN pretreatment. According to identified relationships, ZP appears to exert an important influence on the floc structure following coagulation and may be suitable as a process control tool for the hybrid C-IN-LPM system.
4. Besides floc structure (determined by fractal dimension), floc size also is seen to exert an influence on membrane fouling following pretreatment by C-IN. Although many authors

report on the importance of both floc structure and size in determining LPM fouling, conflicting results exist in the literature regarding optimal conditions.

5. Although mixing conditions during coagulation (i.e., length and type of mixing) have not been reported to influence removal of NOM following pretreatment by C-IN, it is expected that they will alter character of the formed flocs and hence the LPM surface cake. A wide variety of water types and mixing configurations (i.e., static mixer, HCTF) are reported without adequate assessment of their impact on the characteristics of the resulting floc and LPM fouling mitigation.
6. Studies evaluating C-IN-P performance have only investigated a limited number of conditions. Compared to C-IN, similar (or improved) fouling mitigation and removal of bulk organics has been observed following C-IN-P pretreatment, although this has only been evaluated using low SUVA waters (≤ 2.04 L mg^{-1} m^{-1}). It seems that regulation of the coating layer thickness, roughness and coverage of the membrane fiber surface may be critical to the success of C-IN-P for fouling mitigation.
7. The membrane C-IDX may be a suitable tool for C-IN-P operational control, with existing studies suggesting fouling becomes exacerbated at low C-IDXs. Optimal operation, which must balance considerations of fouling mitigation, operating expenditure, and product water quality, is likely dependent on the membrane type and the source water characteristics.

2.5. Research Needs

Based on the literature consulted in this review, the following research needs were identified which guided the work performed in subsequent chapters of this thesis.

1. *Examine the impact of both membrane material and configuration on the performance of the hybrid CF-DAF-LPM system.*

   Comparatively few studies have investigated the effectiveness of CF-DAF as pretreatment for LPMs in DWT. Of these studies, only a limited number have undertaken to directly compare the performance of CF-DAF with other coagulation pretreatment alternatives including C-IN and CF-SED. Furthermore, available studies have only compared the relative performance of each pretreatment alternative using a

single membrane material/configuration. Accordingly, there is a need to directly evaluate their relative performance of CF-DAF compared to alternative coagulation pretreatment strategies using membranes with different properties.

2. *Development of bench-scale continuous-flow coagulation system with low water volume requirements for LPM filtration studies.*

   One of the key focuses of this thesis is to investigate C-IN-P pretreatment for LPM systems, however, this is only possible with the development of a continuous-flow coagulation system that can operate at very low flowrates. Considering existing Type I, Type II, and Type II C-IN studies surveyed in this review, they have employed a multitude of strategies for coagulant mixing, including primarily batch mixing, which may produce flocs with distinct properties and, consequently, differing fouling propensities. These same studies, however, do not assess how the choice of mixing technique may impact the conclusions of the work, potentially complicating comparisons across studies. Therefore, there is a need to compare the performance of C-IN pretreatment with mixing by a batch-reactor to continuous-flow C-IN, which is representative of the conditions experienced in practice. Moreover, the few existing reports of continuous-flow bench-scale coagulation systems required the use of relatively high flowrates and significant volumes of water, limiting their practicality for laboratory-scale studies. Accordingly, there is a need to develop systems which can perform coagulation/flocculation at the low flowrates that can be accommodated by lab studies.

3. *Study the suitability of HCTFs for continuous-flow coagulation at bench-scale and elucidate the impact the helical geometry and flow hydrodynamics have on floc properties.*

   The secondary flows generated within HCTFs offer a promising means of promoting effective floc formation at the low flow rates typical of laboratory-scale continuous-flow coagulation systems. However, the lack of widely established design guidelines, coupled with the limited understanding of how coil geometry influences floc properties, presents a barrier to their effective design and implementation. Systematic investigation is therefore needed to establish the relationship between HCTF geometry

and floc characteristics and to aid in the development of practical design guidelines.

4. *Evaluate the performance of C-IN-P, in terms of fouling mitigation and permeate water quality, using different water types and durations of coagulant addition.*

   Currently, studies evaluating C-IN-P performance only investigate a limited number of operating conditions. Owing to the relative novelty of the C-IN-P approach and the lack of scientific studies investigating its application, there remains a number of important gaps in our understanding of the effects of (1) membrane configuration, (2) varying operational conditions, and (3) feed water quality. In order to provide definitive guidance regarding the operation of C-IN-P-LPM facilities, more research is required. The performance of C-IN-P pretreatment needs to be evaluated in terms of both fouling reduction and organics removals using a range of C-IDXs (especially in the range of 20 – 100 mg m^{-2} which has limited data), different coagulant types, and waters with different organic makeup. Moreover, it would be of interest to investigate C-IN-P performance using waters with SUVA values > 2 L mg^{-1} m^{-1} (for which high NOM removals may be critical for reduced DBP formation potential and LPM fouling).

5. *For C-IN-P systems, determine whether different combinations of coagulant dose and dosing time, which yield the same C-IDX, result in the same membrane performance in terms of permeate quality and fouling mitigation.*

   It has been suggested by previous authors that the operation of C-IN-P may be controlled by the C-IDX value. For constant flux operation, typical of drinking water facilities, the coagulant dose and length of coagulant addition can be simultaneously adjusted to yield the same coating index. Whether the performance of C-IN-P depends solely on the mass of coagulant delivered to the membrane or the particular dosing strategy employed remains to be elucidated.

2.6. References

Aly, S. A., W. B. Anderson, and P. M. Huck. 2021. "In-line coagulation assessment for ultrafiltration fouling reduction to treat secondary effluent for water reuse." *Water Science and Technology*, 83 (2): 284–296. https://doi.org/10.2166/wst.2020.571.

Amaral, P. A. P. do, L. A. Coral, M. E. Nagel-Hassemer, T. J. Belli, and F. R. Lapolli. 2013. "Association of dissolved air flotation (DAF) with microfiltration for cyanobacterial removal in water supply." *Desalination and Water Treatment*, 51 (7–9): 1664–1671. https://doi.org/10.1080/19443994.2012.715128.

Amirtharajah, A., and K. M. Mills. 1982. "Rapid-mix design for mechanisms of alum coagulation." *Journal AWWA*, 74 (4): 210–216. https://doi.org/10.1002/j.1551-8833.1982.tb04890.x.

Amjad, H., Z. Khan, and V. V. Tarabara. 2015. "Fractal structure and permeability of membrane cake layers: Effect of coagulation–flocculation and settling as pretreatment steps." *Separation and Purification Technology*, 143: 40–51. https://doi.org/10.1016/j.seppur.2015.01.020.

Archer, A. D., and P. C. Singer. 2006. "Effect of SUVA and enhanced coagulation on removal of TOX precursors." *Journal AWWA*, 98 (8): 11.

Arhin, S. G., N. Banadda, A. J. Komakech, I. Kabenge, and J. Wanyama. 2016. "Membrane fouling control in low pressure membranes: A review on pretreatment techniques for fouling abatement." *Environmental Engineering Research*, 21 (2): 109–120. https://doi.org/10.4491/eer.2016.017.

Arhin, S. G., N. Banadda, A. J. Komakech, W. Pronk, and S. J. Marks. 2018. "Optimization of hybrid coagulation-ultrafiltration process for potable water treatment using response surface methodology." *Water Supply*, 18 (3): 862–874. https://doi.org/10.2166/ws.2017.159.

AWWA Membrane Process Committee. 2008. "Microfiltration and ultrafiltration membranes for drinking water." *Journal AWWA*, 100 (12): 84–97. https://doi.org/10.1002/j.1551-8833.2008.tb09801.x.

Barbot, E., S. Moustier, J. Bottero, and P. Moulin. 2008. "Coagulation and ultrafiltration: Understanding of the key parameters of the hybrid process." *Journal of Membrane Science*, 325 (2): 520–527. https://doi.org/10.1016/j.memsci.2008.07.054.

Bellouti, M., M. M. Alves, J. M. Novais, and U. Minho. 1997. "FLOCS VS GRANULES: DIFFERENTIATION BY FRACTAL DIMENSION." *Water Research*, 31 (5): 1227–1231.

Best, G., M. Singh, D. Mourato, and Y. J. Chang. 2001. "Application of immersed ultrafiltration membranes for organic removal and disinfection by-product reduction." *Water Supply*, 1 (5–6): 221–231. https://doi.org/10.2166/ws.2001.0118.

Braghetta, A., J. G. Jacangelo, S. Chellam, B. A. Utne, and M. L. Hotaling. 1997. "DAF pretreatment: its effect on MF performance." *Journal AWWA*, 89 (10): 90–101.

Buchta, P., P. Berg, A. Schweiger, and D. Vial. 2019. "In-line coagulation upstream ultrafiltration - comparison of continuous vs. intermittent addition." 8. New Orleans, LA: American Water Works Association.

Buchta, P., A. Kripahle, D. Vial, R. Winkler, and P. Berg. 2017. "In-out ultrafiltration in tertiary wastewater applications- Comparison of different operational strategies." *Desalination and Water Treatment*, 73: 145–154.

Buisson, H., N. Lee, G. Amy, and J. Croue. 2004. "Identification and understanding of fouling in low-pressure membrane (MF / UF) filtration by natural organic." *Water Research*, 38: 4511–4523. https://doi.org/10.1016/j.watres.2004.08.013.

Bushell, G., and R. Amal. 2000. "Measurement of Fractal Aggregates of Polydisperse Particles Using Small-Angle Light Scattering." *Journal of Colloid and Interface Science*, 221 (2): 186–194. https://doi.org/10.1006/jcis.1999.6532.

Carroll, T., S. King, S. R. Gray, B. A. Bolto, and N. A. Booker. 2000. "The fouling of microfiltration membranes by NOM after coagulation treatment." *Water Research*, 34 (11): 2861–2868. https://doi.org/10.1016/S0043-1354(00)00051-8.

Chakraborti, R. K., J. F. Atkinson, and J. E. Van Benschoten. 2000. "Characterization of alum floc by image analysis." *Environmental Science & Technology*, 34 (18): 3969–3976. https://doi.org/10.1021/es990818o.

Chakraborti, R. K., K. H. Gardner, J. F. Atkinson, and J. E. Van Benschoten. 2003. "Changes in fractal dimension during aggregation." *Water Research*, 37 (4): 873–883. https://doi.org/10.1016/S0043-1354(02)00379-2.

Chen, Y., J. Teng, B.-Q. Liao, R. Li, and H. Lin. 2020. "Molecular insights into the impacts of iron(III) ions on membrane fouling by alginate." *Chemosphere*, 242: 125232. https://doi.org/10.1016/j.chemosphere.2019.125232.

Cho, M.-H., C.-H. Lee, and S. Lee. 2006. "Effect of flocculation conditions on membrane permeability in coagulation–microfiltration." *Desalination*, 191 (1–3): 386–396. https://doi.org/10.1016/j.desal.2005.08.017.

Choi, K. Y. J., and B. A. Dempsey. 2004. "In-line coagulation with low-pressure membrane filtration." *Water Research*, 38 (19): 4271–4281. https://doi.org/10.1016/j.watres.2004.08.006.

Choi, Y. H., H. S. Kim, and J. H. Kweon. 2008. "Role of hydrophobic natural organic matter flocs on the fouling in coagulation-membrane processes." *Separation and Purification Technology*, 62 (3): 529–534. https://doi.org/10.1016/j.seppur.2008.03.001.

Chow, C. W. K., R. Fabris, J. V. Leeuwen, D. Wang, and M. Drikas. 2008. "Assessing Natural Organic Matter Treatability Using High Performance Size Exclusion Chromatography." *Environmental Science & Technology*, 42 (17): 6683–6689. https://doi.org/10.1021/es800794r.

Chow, C. W. K., J. A. van Leeuwen, M. Drikas, R. Fabris, K. M. Spark, and D. W. Page. 1999. "The impact of the character of natural organic matter in conventional treatment with alum." *Water Science and Technology*, 40 (9): 97–104. https://doi.org/10.2166/wst.1999.0452.

Citulski, J., K. Farahbakhsh, F. Kent, and H. Zhou. 2008. "The impact of in-line coagulant addition on fouling potential of secondary effluent at a pilot-scale immersed ultrafiltration plant." *Journal of Membrane Science*, 325 (1): 311–318. https://doi.org/10.1016/j.memsci.2008.07.053.

Cornelissen, E. R., N. Moreau, W. G. Siegers, A. J. Abrahamse, L. C. Rietveld, A. Grefte, M. Dignum, G. Amy, and L. P. Wessels. 2008. "Selection of anionic exchange resins for removal of natural organic matter (NOM) fractions." *Water Research*, 42 (1–2): 413–423. https://doi.org/10.1016/j.watres.2007.07.033.

De Angelis, L., and M. M. F. de Cortalezzi. 2013. "Ceramic membrane filtration of organic compounds: Effect of concentration, pH, and mixtures interactions on fouling." *Separation and Purification Technology*, 118: 762–775. https://doi.org/10.1016/j.seppur.2013.08.016.

De Oliveira, D. S., and E. C. Teixeira. 2017. "Experimental evaluation of helically coiled tube flocculators for turbidity removal in drinking water treatment units." *Water SA*, 43 (3): 378. https://doi.org/10.4314/wsa.v43i3.02.

Deka, B. J., J. Guo, S. Jeong, M. Kumar, and A. K. An. 2020. "Control of membrane fouling by dissolved algal organic matter using pre-oxidation with coagulation as seawater pretreatment." *Environmental Science: Water Research and Technology*, 6 (4): 935–944. Royal Society of Chemistry. https://doi.org/10.1039/c9ew00955h.

Ding, Y., T. Li, K. Qiu, B. Ma, and R. Wu. 2021. "Membrane fouling performance of Fe-based coagulation-ultrafiltration process: Effect of sedimentation time." *Environmental Research*, 195: 110756. https://doi.org/10.1016/j.envres.2021.110756.

Dixon, M., C. Staaks, R. Fabris, V. Vimonses, C. W. K. Chow, S. Panglisch, J. A. van Leeuwen, and M. Drikas. 2013. "The impact of optimised coagulation on membrane fouling for coagulation/ultrafiltration process." *Desalination and Water Treatment*, 51 (13–15): 2718–2725. https://doi.org/10.1080/19443994.2012.749367.

Dong, B., Y. Chen, N. Gao, and J. Fan. 2007. "Effect of coagulation pretreatment on the fouling of ultrafiltration membrane." *Journal of Environmental Sciences*, 19 (3): 278–283. https://doi.org/10.1016/S1001-0742(07)60045-X.

Edwards, G. A., and A. Amirtharajah. 1985. "Removing color caused by humic acids." *Journal AWWA*, 77 (3): 50–57. https://doi.org/10.1002/j.1551-8833.1985.tb05508.x.

Edzwald, J. K. 1993. "Coagulation in drinking water treatment: Particles, organics and coagulants." *Water Science and Technology*, 27 (11): 21–35. https://doi.org/10.2166/wst.1993.0261.

Edzwald, J. K., and J. Haarhoff. 2012. *Dissolved Air Flotation for Water Clarification*. New York, NY: McGraw-Hill.

Edzwald, J. K., and J. E. Tobiason. 1999. "Enhanced coagulation: US requirements and a broader view." *Water Science and Technology*, 40 (9): 63–70. IAWQ. https://doi.org/10.1016/S0273-1223(99)00641-1.

Edzwald, J. K., and J. E. Van Benschoten. 1990. "Aluminum coagulation of natural organic matter." *Chemical Water and Wastewater Treatment*, edited by H. H. Hahn and R. Klute, 341–359. Berlin, Heidelberg: Springer Berlin Heidelberg.

Endo, Y., and Manuel. Alonso. 2001. "Physical Meaning of Specific Cake Resistance and Effects of Cake Properties in Compressible Cake Filtration." *Filtration & Separation*, 38 (7): 42–46. https://doi.org/10.1016/S0015-1882(01)80447-X.

Fabris, R., C. W. K. Chow, and M. Drikas. 2004. "Practical application of a combined treatment process for removal of recalcitrant NOM - alum and PAC." *Water Supply*, 4 (4): 89–94. https://doi.org/10.2166/ws.2004.0065.

Farahbakhsh, K., and D. W. Smith. 2002. "Performance comparison and pretreatment evaluation of three water treatment membrane pilot plants treating low turbidity water." *Journal of Environmental Engineering and Science*, 1 (2): 113–122. https://doi.org/10.1139/S02-006.

Feng, L., W. Wang, R. Feng, S. Zhao, H. Dong, S. Sun, B. Gao, and Q. Yue. 2015. "Coagulation performance and membrane fouling of different aluminum species during coagulation/ultrafiltration combined process." *Chemical Engineering Journal*, 262: 1161–1167. Elsevier B.V. https://doi.org/10.1016/j.cej.2014.10.078.

Formato, G., R. Romano, A. Formato, J. Sorvari, T. Koiranen, A. Pellegrino, and F. Villecco. 2019. "Fluid–structure interaction modeling applied to peristaltic pump flow simulations." *Machines*, 7 (3): 50. https://doi.org/10.3390/machines7030050.

Fu, L. F., and B. A. Dempsey. 1998. "Modeling the effect of particle size and charge on the structure of the filter cake in ultrafiltration." *Journal of Membrane Science*, 149: 20.

Galjaard, G., J. van Paassen, P. Buijs, and F. Schoonenberg. 2001. "Enhanced pre-coat engineering (EPCE) for micro- and ultrafiltration: the solution for fouling?" *Water Supply*, 1 (5–6): 151–156. https://doi.org/10.2166/ws.2001.0109.

García-Ávila, F., D. Tenesaca-Pintado, F. Novoa-Zamora, E. A. Alfaro-Paredes, A. Avilés-Añazco, A. Guanuchi-Quito, M. D. Tonon-Ordoñez, and C. Zhindón-Arévalo. 2023. "Vertical tubular flocculator: Alternative technology for the improvement of drinking water treatment processes in rural areas." *Journal of Environmental Management*, 331: 117342. https://doi.org/10.1016/j.jenvman.2023.117342.

Goh, Y. T., J. L. Harris, and F. A. Roddick. 2010. "Reducing the effect of cyanobacteria in the microfiltration of secondary effluent." *Water Science and Technology*, 62 (7): 1682–1688. https://doi.org/10.2166/wst.2010.482.

Gonzalez-Galvis, J. P., and R. M. Narbaitz. 2022. "Large batch bench-scale dissolved air flotation system for simulating full-scale turbidity removal." *Environmental Technology*, 43 (12): 1791–1804. https://doi.org/10.1080/09593330.2020.1852317.

Gorczyca, B., and J. Ganczarczyk. 1996. "Image Analysis of Alum Coagulated Mineral Suspensions." *Environmental Technology*, 17 (12): 1361–1369. https://doi.org/10.1080/09593331708616505.

Gu, H., A. Rahardianto, L. X. Gao, X. P. Caro, J. Giralt, R. Rallo, P. D. Christofides, and Y. Cohen. 2018. "Fouling indicators for field monitoring the effectiveness of operational strategies of ultrafiltration as pretreatment for seawater desalination." *Desalination*, 431: 86–99. https://doi.org/10.1016/j.desal.2017.11.038.

Guan, J., R. Amal, and T. D. Waite. 2001. "Effect of aggregate size and structure on specific resistance of biosolids filter cakes." *Water Science and Technology*, 44 (10): 215–220. https://doi.org/10.2166/wst.2001.0624.

Guastalli, A. R., F. X. Simon, Y. Penru, A. de Kerchove, J. Llorens, and S. Baig. 2013. "Comparison of DMF and UF pre-treatments for particulate material and dissolved organic matter removal in SWRO desalination." *Desalination*, 322: 144–150. Elsevier B.V. https://doi.org/10.1016/j.desal.2013.05.005.

Günther, J., D. Hobbs, C. Albasi, C. Lafforgue, A. Cockx, and P. Schmitz. 2012. "Modeling the effect of packing density on filtration performances in hollow fiber microfiltration module: A spatial study of cake growth." *Journal of Membrane Science*, 389: 126–136. https://doi.org/10.1016/j.memsci.2011.10.055.

Hao, Y., C. Liang, A. Moriya, H. Matsuyama, and T. Maruyama. 2012. "Visualization of protein fouling inside a hollow fiber ultrafiltration membrane by fluorescent microscopy." *Industrial and Engineering Chemistry Research*, 51 (45): 14850–14858. https://doi.org/10.1021/ie302111w.

Harvey, N. J., Z. ur Rehman, T. O. Leiknes, N. Ghaffour, H. Urakawa, and T. M. Missimer. 2020. "Organic compounds and microbial assessment of a seawater reverse osmosis facility at Tampa Bay Water, USA." *Desalination*, 496 (August): 114735–114735. Elsevier. https://doi.org/10.1016/j.desal.2020.114735.

Hatt, J. W., E. Germain, and S. J. Judd. 2011. "Precoagulation-microfiltration for wastewater reuse." *Water Research*, 45 (19): 6471–6478. https://doi.org/10.1016/j.watres.2011.09.039.

Hillis, P. 2006. "Enhanced coagulation, flocculation and immersed ultrafiltration for treatment of low alkalinity and highly coloured upland water." *Journal of Water Supply: Research and Technology-Aqua*, 55 (7–8): 549–558. https://doi.org/10.2166/aqua.2006.043.

Hög, A., J. Ludwig, and M. Beery. 2015. "The use of integrated flotation and ceramic membrane filtration for surface water treatment with high loads of suspended and dissolved organic matter." *Journal of Water Process Engineering*, 6: 129–135. Elsevier Ltd. https://doi.org/10.1016/j.jwpe.2015.03.010.

Howe, K. J., A. Marwah, K.-P. Chiu, and S. S. Adham. 2006. "Fouling of microfiltration and ultrafiltration membranes by natural waters." *Environmental Science & Technology*, 40 (24): 7908–7913. https://doi.org/10.1021/es0616480.

Hu, M., L. Zhao, N. Yu, Z. Tian, Z. Yin, Z. Yang, W. Yang, and N. J. D. Graham. 2021. "Application of ultra-low concentrations of moderately-hydrophobic chitosan for ultrafiltration membrane fouling mitigation." *Journal of Membrane Science*, 635: 119540. https://doi.org/10.1016/j.memsci.2021.119540.

Hua, G., and D. A. Reckhow. 2007. "Characterization of disinfection byproduct precursors based on hydrophobicity and molecular size." *Environmental Science & Technology*, 41 (9): 3309–3315. https://doi.org/10.1021/es062178c.

Huang, H., K. Schwab, and J. G. Jacangelo. 2009. "Pretreatment for low pressure membranes in water treatment: A review." *Environmental Science and Technology*, 43 (9): 3011–3019. https://doi.org/10.1021/es802473r.

Huttl, T. J., and R. Friedrich. 2000. "Infuence of curvature and torsion on turbulent flow in helically coiled pipes." *International Journal of Heat and Fluid Flow*, 345–353.

Jang, H. N., D. S. Lee, and S. O. Ko. 2010. "The effects of coagulation with MF/UF membrane filtration in drinking water treatment." *Desalination and Water Treatment*, 19 (1–3): 138–145. https://doi.org/10.5004/dwt.2010.1906.

Jang, N.-Y., Y. Watanabe, and S. Minegishi. 2005. "Performance of ultrafiltration membrane process combined with coagulation/sedimentation." *Water Science and Technology*, 51 (6–7): 209–219. https://doi.org/10.2166/wst.2005.0640.

Jefferson, B., and P. R. Jarvis. 2006. "Practical application of fractal dimension." *Interface Science and Technology*, 45–61. Elsevier.

Jiang, Q. 1993. "Fractal structure of aggregates induced by shear motion." Ph.D. Thesis, The University of Arizona.

Jiang, Q., and B. E. Logan. 1996. "Fractal dimensions of aggregates from shear devices." *Journal AWWA*, 88 (2): 100–113. https://doi.org/10.1002/j.1551-8833.1996.tb06506.x.

Judd, S. J., and P. Hillis. 2001. "Optimisation of combined coagulation and microfiltration for water treatment." *Water Research*, 35 (12): 2895–2904. https://doi.org/10.1016/S0043-1354(00)00586-8.

Jung, C. W., and L. S. Kang. 2003. "Application of combined coagulation-ultrafiltration membrane process for water treatment." *Korean Journal of Chemical Engineering*, 20 (5): 855–861. https://doi.org/10.1007/BF02697288.

Kabsch-Korbutowicz, M. 2005. "Application of ultrafiltration integrated with coagulation for improved NOM removal." *Desalination*, 174 (1): 13–22. https://doi.org/10.1016/j.desal.2004.08.037.

Kamińska, G., W. Pronk, and J. Traber. 2020. "Effect of coagulant dose and backflush pressure on NOM membrane fouling in inline coagulation-ultrafiltration." *Desalination and Water Treatment*, 199: 188–197. https://doi.org/10.5004/dwt.2020.25657.

Kang, J., J. Seong, J. Yoo, P. Kim, K. Park, J. Lee, J. Cheon, H. Kim, and S. Lee. 2021. "Applicability of a combined DAF-MF process to respond to changes in reservoir water quality through a two-year pilot plant operation." *Membranes*, 11 (12): 964. https://doi.org/10.3390/membranes11120964.

Katsoufidou, K., S. G. Yiantsios, and A. J. Karabelas. 2008. "An experimental study of UF membrane fouling by humic acid and sodium alginate solutions: the effect of backwashing on flux recovery." *Desalination*, 220 (1–3): 214–227. https://doi.org/10.1016/j.desal.2007.02.038.

Keucken, A., G. Heinicke, K. M. Persson, and S. J. Köhler. 2017. "Combined coagulation and ultrafiltration process to counteract increasing NOM in brown surface water." *Water*, 9 (9): 697. Multidisciplinary Digital Publishing Institute. https://doi.org/10.3390/w9090697.

Khanzada, N. K., S. J. Khan, and P. A. Davies. 2017. "Performance evaluation of reverse osmosis (RO) pre-treatment technologies for in-land brackish water treatment." *Desalination*, 406: 44–50. https://doi.org/10.1016/j.desal.2016.06.030.

Kim, H.-C., J.-H. Hong, and S. Lee. 2006. "Fouling of microfiltration membranes by natural organic matter after coagulation treatment: A comparison of different initial mixing conditions." *Journal of Membrane Science*, 283 (1–2): 266–272. https://doi.org/10.1016/j.memsci.2006.06.041.

Kim, S.-H., B.-H. Moon, and H.-I. Lee. 2001. "Effects of pH and dosage on pollutant removal and floc structure during coagulation." *Microchemical Journal*, 68 (2–3): 197–203. https://doi.org/10.1016/S0026-265X(00)00146-6.

Kimura, K., T. Maeda, H. Yamamura, and Y. Watanabe. 2008. "Irreversible membrane fouling in microfiltration membranes filtering coagulated surface water." *Journal of Membrane Science*, 320 (1–2): 356–362. https://doi.org/10.1016/j.memsci.2008.04.018.

Kimura, K., K. Tanaka, and Y. Watanabe. 2014. "Microfiltration of different surface waters with/without coagulation: Clear correlations between membrane fouling and hydrophilic biopolymers." *Water Research*, 49: 434–443. https://doi.org/10.1016/j.watres.2013.10.030.

Kinser, K. 2021. "Membrane Filtration: Past, Present, and Future." *Journal AWWA*, 113 (8): 72–75. https://doi.org/10.1002/awwa.1791.

Ladouceur, J. D., and R. M. Narbaitz. 2022. "Reduced low–pressure membrane fouling by inline coagulation pretreatment for a colored river water." *Membranes*, 12 (11): 1028. https://doi.org/10.3390/membranes12111028.

Ladouceur, J. D., and R. M. Narbaitz. 2023. "Comparing sedimentation, flotation, and inline pre-treatment for low-pressure membrane fouling reduction." *Journal of Environmental Engineering (United States)*, 149 (4).

Lebeau, T., C. Lelièvre, H. Buisson, D. Cléret, L. W. Van de Venter, and P. Côté. 1998. "Immersed membrane filtration for the production of drinking water: combination with PAC for NOM and SOCs removal." *Desalination*, 117 (1–3): 219–231. https://doi.org/10.1016/S0011-9164(98)00101-5.

Lee, J. D., S. H. Lee, M. H. Jo, P. K. Park, C. H. Lee, and J. W. Kwak. 2000. "Effect of coagulation conditions on membrane filtration characteristics in coagulation - Microfiltration process for water treatment." *Environmental Science and Technology*, 34 (17): 3780–3788. https://doi.org/10.1021/es9907461.

van Leeuwen, J., C. Chow, R. Fabris, N. Withers, D. Page, and M. Drikas. 2002. "Application of a fractionation technique for better understanding of the removal of natural organic matter

by alum coagulation." *Water Supply*, 2 (5–6): 427–433. https://doi.org/10.2166/ws.2002.0200.

Lerch, A., G. Hagmeyer, R. Gimbel, and J. Fehn. 2003. "A comparison of laboratory and pilot plant experiments on the combination of flocculation/ultrafiltration for direct potable water treatment of river water." *Water Supply*, 3 (5–6): 345–352. https://doi.org/10.2166/ws.2003.0187.

Li, Q., Z. Xu, and I. Pinnau. 2007a. "Fouling of reverse osmosis membranes by biopolymers in wastewater secondary effluent: Role of membrane surface properties and initial permeate flux." *Journal of Membrane Science*, 290 (1–2): 173–181. https://doi.org/10.1016/j.memsci.2006.12.027.

Li, T., Z. Zhu, D. Wang, C. Yao, and H. Tang. 2007b. "The strength and fractal dimension characteristics of alum–kaolin flocs." *International Journal of Mineral Processing*, 82 (1): 23–29. https://doi.org/10.1016/j.minpro.2006.09.012.

Liang, H., W. Gong, and G. Li. 2008. "Performance evaluation of water treatment ultrafiltration pilot plants treating algae-rich reservoir water." *Desalination*, 221 (1–3): 345–350. https://doi.org/10.1016/j.desal.2007.01.093.

Logan, B. E., and J. R. Kilps. 1995. "Fractal dimensions of aggregates formed in different fluid mechanical environments." *Water Research*, 29 (2): 443–453. https://doi.org/10.1016/0043-1354(94)00186-B.

Lok, A., H. Wray, P. Bérubé, and R. C. Andrews. 2017. "Optimization of air sparging and in-line coagulation for ultrafiltration fouling control." *Separation and Purification Technology*, 188: 60–66. https://doi.org/10.1016/j.seppur.2017.06.064.

Long, Y., X. You, Y. Chen, H. Hong, B.-Q. Liao, and H. Lin. 2020. "Filtration behaviors and fouling mechanisms of ultrafiltration process with polyacrylamide flocculation for water treatment." *Science of The Total Environment*, 703: 135540. https://doi.org/10.1016/j.scitotenv.2019.135540.

Long, Y., G. Yu, L. Dong, Y. Xu, H. Lin, Y. Deng, X. You, L. Yang, and B.-Q. Liao. 2021. "Synergistic fouling behaviors and mechanisms of calcium ions and polyaluminum chloride associated with alginate solution in coagulation-ultrafiltration (UF) process." *Water Research*, 189: 116665. https://doi.org/10.1016/j.watres.2020.116665.

Ma, B., Y. Ding, B. Wang, Z. Qi, Y. Bai, R. Liu, H. Liu, and J. Qu. 2020a. "Influence of sedimentation with pre-coagulation on ultrafiltration membrane fouling performance." *Science of the Total Environment*, 708: 134671–134671. Elsevier B.V. https://doi.org/10.1016/j.scitotenv.2019.134671.

Ma, B., X. Wang, C. Hu, W. A. Jefferson, H. Liu, and J. Qu. 2017. "Antifouling by pre-deposited Al hydrolytic flocs on ultrafiltration membrane in the presence of humic acid and bovine serum albumin." *Journal of Membrane Science*, 538: 34–40. https://doi.org/10.1016/j.memsci.2017.05.029.

Ma, B., W. Xue, Y. Bai, R. Liu, W. Chen, H. Liu, and J. Qu. 2020b. "Enhanced alleviation of ultrafiltration membrane fouling by regulating cake layer thickness with pre-coagulation during drinking water treatment." *Journal of Membrane Science*, 596 (November 2019): 117732–117732. Elsevier B.V. https://doi.org/10.1016/j.memsci.2019.117732.

Ma, B., W. Yu, H. Liu, and J. Qu. 2014. "Effect of low dosage of coagulant on the ultrafiltration membrane performance in feedwater treatment." *Water Research*, 51: 277–283. https://doi.org/10.1016/j.watres.2013.10.069.

Ma, B., W. Yu, H. Liu, J. Yao, and J. Qu. 2013. "Effect of iron/aluminum hydrolyzed precipitate layer on ultrafiltration membrane." *Desalination*, 330: 16–21. https://doi.org/10.1016/j.desal.2013.09.019.

Malkoske, T. A., R. C. Andrews, and P. R. Bérubé. 2023a. "20+ years of drinking water related coagulation/flocculation-MF/UF studies: Knowledge gaps and recommendations for future research." Knoxville, TN.

Malkoske, T. A., P. R. Bérubé, and R. C. Andrews. 2023b. "Impact of extended versus typical rapid mixing HRTs on continuous-flow coagulation-ultrafiltration." *Separation and Purification Technology*, 319: 124041. https://doi.org/10.1016/j.seppur.2023.124041.

Malkoske, T. A., P. R. Bérubé, and R. C. Andrews. 2023c. "Leveraging coagulation mechanisms to reduce fouling and increase natural organic matter removal during coagulation/flocculation-ultrafiltration treatment." *Separation and Purification Technology*, 327: 124877. https://doi.org/10.1016/j.seppur.2023.124877.

Malkoske, T. A., P. R. Bérubé, and R. C. Andrews. 2025. "Hydraulic and chemical cleaning efficiency for the release of microplastics retained during coagulation/flocculation-ultrafiltration." *Water Research*, 282: 123601. https://doi.org/10.1016/j.watres.2025.123601.

Mansour, M., P. Khot, D. Thévenin, K. D. P. Nigam, and K. Zähringer. 2020a. "Optimal Reynolds number for liquid-liquid mixing in helical pipes." *Chemical Engineering Science*, 214: 114522. https://doi.org/10.1016/j.ces.2018.09.046.

Mansour, M., Z. Liu, G. Janiga, K. D. P. Nigam, K. Sundmacher, D. Thévenin, and K. Zähringer. 2017. "Numerical study of liquid-liquid mixing in helical pipes." *Chemical Engineering Science*, 172: 250–261. https://doi.org/10.1016/j.ces.2017.06.015.

Mansour, M., K. Zähringer, K. D. P. Nigam, D. Thévenin, and G. Janiga. 2020b. "Multi-objective optimization of liquid-liquid mixing in helical pipes using genetic algorithms coupled with computational fluid dynamics." *Chemical Engineering Journal*, 391: 123570. https://doi.org/10.1016/j.cej.2019.123570.

Matilainen, A., M. Vepsäläinen, and M. Sillanpää. 2010. "Natural organic matter removal by coagulation during drinking water treatment: A review." *Advances in Colloid and Interface Science*, 159 (2): 189–197. https://doi.org/10.1016/j.cis.2010.06.007.

Meyn, T., J. Altmann, and T. Leiknes. 2012. "In-line coagulation prior to ceramic microfiltration for surface water treatment—minimisation of flocculation pre-treatment." *Desalination and Water Treatment*, 14.

Meyn, T., A. Bahn, and T. O. Leiknes. 2008. "Significance of flocculation for NOM removal by coagulation–ceramic membrane microfiltration." *Water Supply*, 8 (6): 691–700. https://doi.org/10.2166/ws.2008.148.

Meyn, T., and T. Leiknes. 2010. "Comparison of optional process configurations and operating conditions for ceramic membrane MF coupled with coagulation/flocculation pre-treatment for the removal of NOM in drinking water production." *Journal of Water Supply: Research and Technology-Aqua*, 59 (2–3): 81–91. https://doi.org/10.2166/aqua.2010.044.

Minegishi, S., N.-Y. Jang, Y. Watanabe, S. Hirata, and G. Ozawa. 2001. "Fouling mechanism of hollow fiber ultrafiltration membrane with pretreatment by coagulation/sedimentation process." *Water Supply*, 1 (4): 49–56. https://doi.org/10.2166/ws.2001.0066.

Minhalma, M., and M. N. De Pinho. 2001. "Flocculation/flotation/ultrafiltration integrated process for the treatment of cork processing wastewaters." *Environmental Science and Technology*, 35 (24): 4916–4921. https://doi.org/10.1021/es010119n.

Moon, J., M.-S. Kang, J.-L. Lim, C.-H. Kim, and H.-D. Park. 2009. "Evaluation of a low-pressure membrane filtration for drinking water treatment: pretreatment by coagulation/sedimentation for the MF membrane." *Desalination*, 247 (1–3): 271–284. https://doi.org/10.1016/j.desal.2008.12.030.

Myat, D. T., M. B. Stewart, M. Mergen, O. Zhao, J. D. Orbell, and S. Gray. 2014. "Experimental and computational investigations of the interactions between model organic compounds and subsequent membrane fouling." *Water Research*, 48 (1): 108–118. Elsevier Ltd. https://doi.org/10.1016/j.watres.2013.09.020.

Naim, R., R. Epsztein, A. Felder, M. Heyer, M. Heijnen, and V. Gitis. 2014. "Rethinking the role of in-line coagulation in tertiary membrane filtration of municipal effluents." *Separation and Purification Technology*, 125: 11–20. Elsevier B.V. https://doi.org/10.1016/j.seppur.2014.01.036.

Nan, J., M. Yao, Q. Li, D. Zhan, T. Chen, Z. Wang, and H. Li. 2016. "The role of shear conditions on floc characteristics and membrane fouling in coagulation/ultrafiltration hybrid process – the effect of flocculation duration and slow shear force." *RSC Advances*, 6 (1): 163–173. https://doi.org/10.1039/C5RA18328F.

Neama, M.-A. A. M., W. A. Elbarki, M. Fayed, and S. Aly. 2024. "Upgrading the eastern wastewater treatment plant effluent quality in Egypt for reuse by means of in-line coagulation followed by ultrafiltration." *Water Practice & Technology*, 19 (12): 4754–4772. London, UK: IWA Publishing. https://doi.org/10.2166/wpt.2024.285.

Nguyen, A. H., J. E. Tobiason, and K. J. Howe. 2011. "Fouling indices for low pressure hollow fiber membrane performance assessment." *Water Research*, 45 (8): 2627–2637. Elsevier Ltd. https://doi.org/10.1016/j.watres.2011.02.020.

Oh, J., and S. Lee. 2005. "Influence of streaming potential on flux decline of microfiltration with in-line rapid pre-coagulation process for drinking water production." *Journal of Membrane Science*, 254 (1–2): 39–47. https://doi.org/10.1016/j.memsci.2004.12.030.

Paar, H., J. Benecke, M. Ernst, and M. Jekel. 2011. "Pre-coagulation and ultrafiltration of effluent impaired surface water for phosphorus removal and fouling control." *Water Supply*, 11 (2): 211–218. https://doi.org/10.2166/ws.2011.037.

Palmada, N., J. E. Cater, L. K. Cheng, and V. Suresh. 2022. "Experimental and computational studies of peristaltic flow in a duodenal model." *Fluids*, 7 (1): 40. https://doi.org/10.3390/fluids7010040.

Park, P. K., C. H. Lee, S. J. Choi, K. H. Choo, S. H. Kim, and C. H. Yoon. 2002. "Effect of the removal of DOMs on the performance of a coagulation-UF membrane system for drinking water production." *Desalination*, 145 (1–3): 237–245. https://doi.org/10.1016/S0011-9164(02)00418-6.

Park, P.-K., C.-H. Lee, and S. Lee. 2006. "Permeability of collapsed cakes formed by deposition of fractal aggregates upon membrane filtration." *Environmental Science & Technology*, 40 (8): 2699–2705. https://doi.org/10.1021/es0515304.

Pearce, G. K. 2011. *UF/MF Membrane Water Treatment: Principles and Design*. 387. 1st ed. Bangkok: Water Treatment Academy.

Peleato, N. M., R. L. Legge, and R. C. Andrews. 2017. "Characterization of UF foulants and fouling mechanisms when applying low in-line coagulant pre-treatment." *Water Research*, 126: 1–11. Elsevier Ltd. https://doi.org/10.1016/j.watres.2017.08.064.

Pikkarainen, A. T., S. J. Judd, J. Jokela, and L. Gillberg. 2004. "Pre-coagulation for microfiltration of an upland surface water." *Water Research*, 38 (2): 455–465. https://doi.org/10.1016/j.watres.2003.09.030.

Pissibanganga, O. G. M., J. Jung, Y. Choi, S. Lee, J. Sohn, and N. Cho. 2016. "Influence of microbial floatation on membrane fouling due to particles and organic matters in submerged microfiltration." *Desalination and Water Treatment*, 57 (51): 24557–24565. Taylor & Francis. https://doi.org/10.1080/19443994.2016.1152645.

Poje, C. 2023. "How ceramic flat membrane solutions are changing the status quo of water and sewage treatment." Knoxville, TN.

Pronk, W., J. Traber, and G. Kamińska. 2016. "Optimization of process parameters of the coagulation/ultrafiltration process for the reduction of membrane fouling." In: *Advances in Particle Science and Separation: Meeting Tomorrow's Challenges*, 198–205. Oslo, Norway: International Water Association.

Randtke, S. J. 1988. "Organic contaminant removal by coagulation and related process combinations." *Journal AWWA*, 80 (5): 40–56. https://doi.org/10.1002/j.1551-8833.1988.tb03037.x.

Ratajczak, M. J., K. N. Exall, and P. M. Huck. 2012. "Factors affecting coagulation as a pretreatment to ultrafiltration membranes." *Water Quality Research Journal*, 47 (2): 103–116. https://doi.org/10.2166/wqrjc.2012.010.

Ren, L., C. Liu, T. Meng, and Y. Sun. 2021. "Effects of micro-flocculation pretreatment on the ultrafiltration membrane fouling caused by different dissolved organic matters in treated wastewater." *Journal of Water Reuse and Desalination*, 11 (4): 597–609. https://doi.org/10.2166/wrd.2021.051.

Salinas-Rodriguez, S. G., A. Prabowo, A. Abushaban, F. Battes, J. C. Schippers, and M. D. Kennedy. 2016. "Pre-coating of outside-inside capillary UF membranes with iron hydroxide particles to limit non-backwashable fouling during seawater algal blooms." *Desalination and Water Treatment*, 57 (55): 26730–26740. https://doi.org/10.1080/19443994.2016.1190111.

Sartori, M., D. S. Oliveira, E. C. Teixeira, W. B. Rauen, and N. C. Reis. 2015. "CFD modelling of helically coiled tube flocculators for velocity gradient assessment." *Journal of the Brazilian Society of Mechanical Sciences and Engineering*, 37 (1): 187–198. https://doi.org/10.1007/s40430-014-0141-3.

Saxena, K., and U. Brighu. 2020. "Comparison of floc properties of coagulation systems: Effect of particle concentration, scale and mode of flocculation." *Journal of Environmental Chemical Engineering*, 8 (5): 104311. https://doi.org/10.1016/j.jece.2020.104311.

Schimmoller, L., B. McEwen, and J. Fisher. 2000. "Membrane pilot results for Denver's new 30 MGD water reclamation plant." *Proceedings of the Water Environment Federation*, 2000 (13): 410–431. https://doi.org/10.2175/193864700784607767.

Schweiger, A., P. Buchta, D. Vial, and P. Berg. 2018a. "Coating of ultrafiltration membranes - the solution to improve the efficiency of the pre-treatment." In: *Desalination for the Environment - Clean Water and Energy*. Athens.

Schweiger, A., C. Starke, D. Vial, P. Buchta, and P. Berg. 2018b. "Coating - a dramatic change in ultrafiltration treatment of secondary effluent." Valencia, Spain.

Shi, Y., J. Ma, D. Wu, and Q. Pan. 2017. "Dessolved air flotation in combination with ultrafiltration membrane modules in surface water treatment." *Journal of Harbin Institute of Technology*, 24 (3).

Sillanpaa, M. 2015. *Natural Organic Matter in Water*. 1st ed. Oxford, UK: Butterworth-Heinemann.

Smith, R., F. Hassard, E. L. Sharp, P. Jarvis, L. Montalban, T. Worley, P. Liu, and B. Jefferson. n.d. "Coagulation control using on-line zeta potential measurements: Can it save money and improve performance?" *Institute of Water Journal*, (3): 10–13.

Stone, M., and B. G. Krishnappan. 2003. "Floc morphology and size distributions of cohesive sediment in steady-state flow." *Water Research*, 37 (11): 2739–2747. https://doi.org/10.1016/S0043-1354(03)00082-4.

Świetlik, J., A. Dąbrowska, U. Raczyk-Stanisławiak, and J. Nawrocki. 2004. "Reactivity of natural organic matter fractions with chlorine dioxide and ozone." *Water Research*, 38 (3): 547–558. https://doi.org/10.1016/j.watres.2003.10.034.

Tabatabai, S. A. A., M. D. Kennedy, G. L. Amy, and J. C. Schippers. 2009. "Optimizing inline coagulation to reduce chemical consumption in MF/UF systems." *Desalination and Water Treatment*, 6 (1–3): 94–101. https://doi.org/10.5004/dwt.2009.653.

Tang, C. K., N. M. Peleato, P. R. Bérubé, and R. C. Andrews. 2019. "Impact of low coagulant dosages on protein fouling of ultrafiltration membranes." *Journal of Water Process Engineering*, 31: 100801. https://doi.org/10.1016/j.jwpe.2019.100801.

Tang, L., Y. Tang, and S. Parameswaran. 2016. "A numerical study of flow characteristics in a helical pipe." *Advances in Mechanical Engineering*, 8 (7): 168781401666024. https://doi.org/10.1177/1687814016660242.

Tao, C., W. Parker, and P. Bérubé. 2024. "The impact of secondary operating temperature on in-line coagulation/flocculation and fouling of membranes used in tertiary treatment." *Environmental Science: Water Research & Technology*, 10 (7): 1676–1687. https://doi.org/10.1039/D4EW00239C.

Teng, J., Y. Chen, G. Ma, H. Hong, T. Sun, B.-Q. Liao, and H. Lin. 2020. "Membrane fouling by alginate in polyaluminum chloride (PACl) coagulation/microfiltration process: Molecular insights." *Separation and Purification Technology*, 236: 116294. https://doi.org/10.1016/j.seppur.2019.116294.

Tsuyuhara, T., Y. Hanamoto, T. Miyoshi, K. Kimura, and Y. Watanabe. 2010. "Influence of membrane properties on physically reversible and irreversible fouling in membrane bioreactors." *Water Science and Technology*, 61 (9): 2235–2240. https://doi.org/10.2166/wst.2010.122.

Ulu, F., E. Gengec, and M. Kobya. 2019. "Removal of natural organic matter from Lake Terkos by EC process: Studying on removal mechanism by floc size and zeta potential measurement and characterization by HPSEC method." *Journal of Water Process Engineering*, 31: 100831. https://doi.org/10.1016/j.jwpe.2019.100831.

United States Environmental Protection Agency. 1999. "Enhanced Coagulation and Enhanced Precipitative Softening Guidance Manual."

Valade, M. T., W. C. Becker, and J. K. Edzwald. 2009. "Treatment selection guidelines for particle and NOM removal." *Journal of Water Supply: Research and Technology - AQUA*, 58 (6): 424–432. https://doi.org/10.2166/aqua.2009.201.

Valade, M. T., J. K. Edzwald, J. E. Tobiason, J. Dahlquist, T. Hedberg, and T. Amato. 1996. "Particle removal by flotation and filtration: Pretreatment effects." *Journal AWWA*, 88 (12): 35–47. https://doi.org/10.1002/j.1551-8833.1996.tb06660.x.

Van Benschoten, J. E., C. Martin, J. Schaefer, L. Xu, and S. Franceschini. 2002. "Evaluation of dissolved air flotation and membrane filtration for drinking water treatment." Niagara Falls: ASCE.

Van Der Bruggen, B., C. Vandecasteele, T. Van Gestel, W. Doyen, and R. Leysen. 2003. "A review of pressure-driven membrane processes in wastewater treatment and drinking water production." *Environmental Progress*, 22 (1): 46–56. https://doi.org/10.1002/ep.670220116.

Waite, T. D. 1999. "Measurement and implications of floc structure in water and wastewater treatment." *Colloids and Surfaces A: Physicochemical and Engineering Aspects*, 151 (1–2): 27–41. https://doi.org/10.1016/S0927-7757(98)00634-7.

Walker, S., and R. M. Narbaitz. 2016. "Hollow fiber ultrafiltration of Ottawa River water: Floatation versus sedimentation pre-treatment." *Chemical Engineering Journal*, 288: 228–237. Elsevier B.V. https://doi.org/10.1016/j.cej.2015.11.064.

Wang, F., B. Gao, D. Ma, Q. Yue, R. Li, and Q. Wang. 2016. "Reduction of disinfection by-product precursors in reservoir water by coagulation and ultrafiltration." *Environmental Science and Pollution Research*, 23 (22): 22914–22923. https://doi.org/10.1007/s11356-016-7496-1.

Wang, J., J. Guan, S. R. Santiwong, and T. D. Waite. 2010. "Effect of aggregate characteristics under different coagulation mechanisms on microfiltration membrane fouling." *Desalination*, 258 (1–3): 19–27. https://doi.org/10.1016/j.desal.2010.03.056.

Wang, J., S. Pan, and D. Luo. 2013. "Characterization of cake layer structure on the microfiltration membrane permeability by iron pre-coagulation." *Journal of Environmental Sciences*, 25 (2): 308–315. https://doi.org/10.1016/S1001-0742(12)60025-4.

Wang, J., and X. Wang. 2006. "Ultrafiltration with in-line coagulation for the removal of natural humic acid and membrane fouling mechanism." *Journal of Environmental Sciences*, 18 (5): 880–884. https://doi.org/10.1016/S1001-0742(06)60008-9.

Wang, L., and L. Song. 1999. "Flux decline in crossflow microfiltration and ultrafiltration: Experimental verification of fouling dynamics." *Journal of Membrane Science*, 160 (1): 41–50. https://doi.org/10.1016/S0376-7388(99)00075-7.

Westerhoff, P., G. Aiken, G. Amy, and J. Debroux. 1999. "Relationships between the structure of natural organic matter and its reactivity towards molecular ozone and hydroxyl radicals." *Water Research*, 33 (10): 2265–2276. https://doi.org/10.1016/S0043-1354(98)00447-3.

White, M. C., J. D. Thompson, G. W. Harrington, and P. C. Singer. 1997. "Evaluating criteria for enhanced coagulation compliance." *Journal AWWA*, 89 (5): 64–77. American Water Works Association.

Wray, H. E., and R. C. Andrews. 2014. "Optimization of coagulant dose for biopolymer removal: Impact on ultrafiltration fouling and retention of organic micropollutants." *Journal of Water Process Engineering*, 1: 74–83. https://doi.org/10.1016/j.jwpe.2014.03.007.

Wray, H. E., R. C. Andrews, and P. R. Bérubé. 2016. "Coagulation optimization for DOC removal: pilot-scale analysis of UF fouling and disinfection byproduct formation potential." *Water Supply*, 16 (2): 473–480. https://doi.org/10.2166/ws.2015.157.

Wu, S., B. Ma, C. Hu, X. Hua, H. Fan, M. Ulbricht, and J. Qu. 2023. "Cake layer 3D structure regulation to optimize water channels during Al-based coagulation-ultrafiltration process." *Water Research*, 236: 119941. https://doi.org/10.1016/j.watres.2023.119941.

Xiangli, Q., Z. Zhenjia, W. Nongcun, V. Wee, M. Low, C. S. Loh, and N. Teck Hing. 2008. "Coagulation pretreatment for a large-scale ultrafiltration process treating water from the

Taihu River." *Desalination*, 230 (1–3): 305–313. https://doi.org/10.1016/j.desal.2007.11.032.

Xie, Y., B. Ma, X. Zhang, H. Liu, and J. Qu. 2016. "Modification of ultrafiltration membrane with iron/aluminum mixed hydrolyzed precipitate layer for humic acid fouling reduction." *Desalination and Water Treatment*, 57 (54): 26022–26030. https://doi.org/10.1080/19443994.2016.1159991.

Xu, B., and R. M. Narbaitz. 2016. "Improved membrane pretreatment of high hydrophobic natural organic matter (NOM) waters by floatation." *Journal of Membrane Science*, 518: 120–130. Elsevier. https://doi.org/10.1016/j.memsci.2016.02.056.

Yamamoto, K., A. Aribowo, Y. Hayamizu, T. Hirose, and K. Kawahara. 2002. "Visualization of the flow in a helical pipe." *Fluid Dynamics Research*, 30 (4): 251–267. https://doi.org/10.1016/S0169-5983(02)00043-6.

Yan, M., X. Shen, B. Gao, K. Guo, and Q. Yue. 2021. "Coagulation-ultrafiltration integrated process for membrane fouling control: Influence of Al species and SUVA values of water." *Science of The Total Environment*, 793: 148517. https://doi.org/10.1016/j.scitotenv.2021.148517.

Yao, M., J. Nan, Q. Li, D. Zhan, T. Chen, Z. Wang, and H. Li. 2015. "Effect of under-dosing coagulant on coagulation–ultrafiltration process for treatment of humic-rich water with divalent calcium ion." *Journal of Membrane Science*, 495: 37–47. https://doi.org/10.1016/j.memsci.2015.08.001.

Ye, Y., V. Chen, and P. Le-Clech. 2011. "Evolution of fouling deposition and removal on hollow fibre membrane during filtration with periodical backwash." *Desalination*, 283: 198–205. Elsevier B.V. https://doi.org/10.1016/j.desal.2011.03.087.

Yoo, S. S. 2018. "Operating cost reduction of in-line coagulation/ultrafiltration membrane process attributed to coagulation condition optimization for irreversible fouling control." *Water (Switzerland)*, 10 (8). https://doi.org/10.3390/w10081076.

You, X., J. Zhang, L. Shen, R. Li, Y. Xu, M. Zhang, H. Hong, L. Yang, Y. Ma, and H. Lin. 2021. "Thermodynamic mechanisms of membrane fouling during filtration of alginate solution in coagulation-ultrafiltration (UF) process in presence of different ionic strength and iron(III) ion concentration." *Journal of Membrane Science*, 635: 119532. https://doi.org/10.1016/j.memsci.2021.119532.

Yu, W., J. Gregory, L. Campos, and G. Li. 2011. "The role of mixing conditions on floc growth, breakage and re-growth." *Chemical Engineering Journal*, 171 (2): 425–430. https://doi.org/10.1016/j.cej.2011.03.098.

Yu, W. zheng, N. Graham, H. juan Liu, and J. hui Qu. 2013. "Comparison of FeCl3 and alum pre-treatment on UF membrane fouling." *Chemical Engineering Journal*, 234: 158–165. Elsevier B.V. https://doi.org/10.1016/j.cej.2013.08.105.

Yukselen, M. A., and J. Gregory. 2004. "The effect of rapid mixing on the break-up and re-formation of flocs." *Journal of Chemical Technology & Biotechnology*, 79 (7): 782–788. https://doi.org/10.1002/jctb.1056.

Zheng, X., F. Zietzschmann, S. Plume, H. Paar, M. Ernst, Z. Wang, and M. Jekel. 2017. "Understanding and control of biopolymer fouling in ultrafiltration of different water types." *Water (Switzerland)*, 9 (4). https://doi.org/10.3390/w9040298.

Zhu, Z., D. Peng, and J. Dou. 2018. "Changes in the two-dimensional and perimeter-based fractal dimensions of kaolinite flocs during flocculation: a simple experimental study." *Water Science and Technology*, 77 (4): 861–870. https://doi.org/10.2166/wst.2017.603.

Zularisam, A. W., A. F. Ismail, M. R. Salim, M. Sakinah, and T. Matsuura. 2009. "Application of coagulation – ultrafiltration hybrid process for drinking water treatment : Optimization of operating conditions using experimental design." 65: 193–210. https://doi.org/10.1016/j.seppur.2008.10.018.

Zupančič, M., D. Novak, J. Diaci, and I. Golobič. 2014. "An evaluation of industrial ultrafiltration systems for surface water using fouling indices as a performance indicator." *Desalination*, 344: 321–328. https://doi.org/10.1016/j.desal.2014.04.002.

CHAPTER 3

Comparing Sedimentation, Flotation, and Inline Pretreatment for Low-Pressure Membrane Fouling Reduction

Context: Coagulation pretreatment for low-pressure membranes can be employed in a number of different configurations, with and without particle separation prior to filtration. Despite its high-rate operation and compact footprint, comparatively few studies have investigated coagulation/flocculation/dissolved-air-flotation (CF-DAF) for low-pressure membrane pretreatment, and none have directly compared the performance of coagulation/flocculation/sedimentation (CF-SED), CF-DAF, and inline coagulation (C-IN) for the same source water. This chapter compares the performance of these alternative coagulation pretreatment strategies for a single membrane type and colored river water.

The work in this chapter was performed prior to fast-tracking to the Ph.D. program and was initially intended to be a part of the requirements of the M.A.Sc degree.

A version of this manuscript has been published as:

Ladouceur, J.D., & Narbaitz, R.M. (2023). Comparing sedimentation, flotation, and in-line pretreatment for low-pressure membrane fouling reduction. *Journal of Environmental Engineering (ASCE), 149 (4), 04023002.*

List of Abbreviations

BWE	Hydraulic backwash efficiency
CEB	Chemically enhanced backwash
CF-DAF	Coagulation/flocculation/dissolved air flotation
CF-SED	Coagulation/flocculation/sedimentation
CI	Confidence interval
CIFI	Chemically irreversible fouling index
C-IN	Inline coagulation
CIP	Clean-in-place
DBP	Disinfection by-product
DOC	Dissolved organic carbon
HIFI	Hydraulically irreversible fouling index
HPI	Hydrophilic
HPO	Hydrophobic
HRFI	Hydraulically reversible fouling index
LB-DAF	Large bench-scale dissolved air flotation unit
LC-OCD	Liquid chromatography organic carbon detection
NOM	Natural organic matter
nTMP	Normalized transmembrane pressure
ORW	Ottawa River water
ORW_s	Summer season Ottawa River water
ORW_w	Winter season Ottawa River water
PES	Polyethersulfone
PVDF	Polyvinylidene fluoride
SUVA	Specific ultraviolet absorbance at 254nm
TFI	Total fouling index
TOC	Total organic carbon
UF	Ultrafiltration
UV_{254}	Ultraviolet absorbance at 254nm
WQI	Water quality indicators
WTP	Water treatment plant

ZP	Zeta potential

List of Variables

Variable	Description
FI	Fouling index ($m^2\ L^{-1}$)
J_s'	Normalized specific flux (dimensionless)
L_{NP}	Normalized permeability (dimensionless)
$L_{p,0}$	Clean water steady-state membrane permeability ($L\ m^{-2}\ h^{-1}\ Bar^{-1}$)
$L_{p,t}$	Permeability at time t ($L\ m^{-2}\ h^{-1}\ Bar^{-1}$)
$nTMP$	Normalized transmembrane pressure (dimensionless)
TMP_o	Clean water steady-state transmembrane pressure (mBar)
$TMP_{n-1,f}$	TMP at the end of cycle *n-1* (mBar)
$TMP_{n,i}$	TMP at the beginning of cycle *n* (mBar)
$TMP_{n-1,i}$	TMP at the beginning of cycle *n-1* (mBar)
TMP_t	Transmembrane pressure at time *t* (Bar)
V_s	specific volume ($L\ m^{-2}$)

3.1. Abstract

Feed water pretreatment is commonly required for low-pressure membrane technologies employed in drinking water treatment applications to reduce membrane fouling and create stable operating conditions. Comparatively few studies have investigated coagulation/flocculation/dissolved-air-flotation (CF-DAF) pretreatment for drinking water applications, and none have compared CF-DAF, coagulation/flocculation/sedimentation (CF-SED), and inline coagulation (C-IN) pretreatments using the same water. This study compares these three pretreatments for the filtration of a high dissolved organic carbon (DOC), high hydrophobic (HPO) surface water using a hydrophilic polyvinylidene fluoride (PVDF) ultrafiltration (UF) fiber. Multi-day filtration tests were carried out using an automated bench-scale testing system operated in an outside-in configuration. CF-SED and CF-DAF were found to be equally effective at mitigating membrane fouling, in spite of CF-DAF pre-treated water having a lower residual DOC and the greatest removal of UV_{254} absorbent organics. Compared to CF-DAF and CF-SED, C-IN pretreatment resulted in higher levels of total and irreversible fouling, regardless of the applied coagulant dose.

For all the pretreatments studied, irreversible membrane fouling was found to be strongly dependent on both the hydrophobicity of the feed water (as measured by specific ultraviolet absorbance at 254 nm (SUVA)) and the concentration of the 5-10 kDa DOC fraction, suggesting that the HPO humic organics were the principal foulant for this membrane/water combination. C-IN pretreatment performance was also strongly impacted by the feed water zeta potential, suggesting that the characteristics of the formed flocculant particles are critical to the fouling behavior of the hybrid C-IN-UF system.

3.2. Introduction

Following large outbreaks of waterborne diseases at Milwaukee and Walkerton, membrane technologies have become increasingly popular, likely due to their effective removal of microorganisms, pathogens, and protozoa (American Water Works Association 2005). Degrading water quality, coupled with increasing demand in water stressed areas due to population and economic growth, and increasingly stringent water quality standards are further driving rapid growth in membrane installations worldwide (Amjad et al. 2015; Pearce 2011). An additional driver for the increased use of low-pressure membrane filtration systems is that they consistently produce a superior quality effluent compared to deep bed filtration units and the product water quality is not as impacted by fluctuating feed water quality (Crittenden et al. 2012). Membranes, however, are susceptible to fouling; particulates, dissolved organic and inorganic compounds, and microorganisms in the feed water cause the membrane to foul. While synergistic fouling effects have been reported between natural organic matter (NOM) and particulate matter (Schulz et al. 2016), many studies have reported NOM as the primary membrane foulant in surface waters (Zularisam et al. 2011).

NOM is ubiquitous in natural waters and is composed of a complex heterogenous matrix of organic macromolecules with a wide range of functional groups (Sillanpaa 2015). Hydrophobic (HPO) acids constitute the major fraction (>50%) of aquatic NOM in typical surface waters, with humic substances (humic and fulvic acids) being the largest component (Aiken et al. 1985). The remaining NOM is described as non-humic and includes substances such as low molecular weight neutrals, proteins, and other hydrophilic (HPI) biopolymers (Sillanpaa 2015; Zularisam et al. 2011). The composition of aquatic NOM is known to be highly dependent on the biogeochemical cycles of the surrounding environment, and can even vary seasonally at the same location

(Matilainen et al. 2011). Inconsistent findings have been reported by researchers regarding which fraction of NOM is primarily responsible for low-pressure membrane fouling. Some studies have suggested that humic substances are responsible for severe membrane fouling (Peiris et al. 2013; Xu and Narbaitz 2016), while others, particularly more recent studies employing liquid chromatography organic carbon detection (LC-OCD) analysis, have suggested that the HPI biopolymer fraction is the primary membrane foulant (Kimura and Kume 2020; Tian et al. 2013).

Fouling can be classified as either hydraulically reversible or irreversible in nature. Hydraulically reversible fouling can be controlled by frequent backwashing and physical cleaning operations (Kimura and Kume 2020), while hydraulically irreversible fouling necessitates the use of more aggressive chemical cleaning agents (Shi et al. 2014). While fouling increases membrane operational costs, chemical cleaning may alter the membranes and hasten the need for membrane replacement- a capital expenditure. Besides physical and chemical cleaning, feed water pretreatment may be used to mitigate membrane fouling.

Coagulation pretreatment has been the most extensively researched and implemented pretreatment due to its simple application and relative low cost (Gao et al. 2011). Instinctively, inline coagulation (C-IN) without solids separation should lead to a higher particulate/foulant loading and greater membrane fouling. This was observed by several researchers who found that C-IN worsened fouling behavior (Schäfer et al. 2001), however, a number of other research studies have reported that C-IN pretreatment can mitigate membrane fouling in some cases (Kamińska et al. 2020; Ratajczak et al. 2012). There recently has been an increased interest in C-IN as a membrane pretreatment strategy due to its shorter coagulation time (and corresponding smaller footprint) and reduced process complexity (Kamińska et al. 2020). More importantly, several authors have suggested that C-IN can be successful at mitigating irreversible membrane fouling even at very low coagulant doses in the range of 0.3-1 mg L^{-1} as alum (Peleato et al. 2017; Wray et al. 2014). Successful implementation of low coagulant dosages can greatly reduce the cost associated with pretreatment as well as reduce the sludge processing costs when compared with conventional processes. However, this is likely accompanied by a decrease in the NOM removal which may be critical to water treatment plants (WTP) with disinfection by-product (DBP) challenges, as NOM is a well-known DBP precursor.

Conventional coagulation/flocculation/sedimentation (CF-SED) pretreatment has been reported to be successful at mitigating membrane fouling in a number of studies (Amjad et al.

2015; Ma et al. 2020). The effectiveness of CF-SED pretreatment has largely been attributed to the reduced foulant load it imparts on the membrane surface, although cakes of low porosity are formed during filtration (Yu et al. 2015). Coagulation/flocculation/dissolved-air-flotation (CF-DAF) has been proposed as an alternative to CF-SED because DAF units are characterized by a small footprint, and therefore compliment the compactness of membrane installations well. Furthermore, CF-DAF is known to be more efficient than CF-SED for the removal of low-density flocs, such as NOM flocs and algal matter (Edzwald and Haarhoff 2012). There remains, however, comparatively few studies regarding the effectiveness of DAF as pretreatment to low-pressure membrane technologies (Amaral et al. 2013; Hög et al. 2015). Even fewer are the number of studies comparing the effectiveness of CF-DAF and CF-SED (Walker and Narbaitz 2016; Xu and Narbaitz 2016), C-IN and CF-SED (Amjad et al. 2015; Yu et al. 2015), or CF-DAF and C-IN (Braghetta et al. 1997) as pretreatment alternatives. Furthermore, available studies often only evaluate pretreatment performance for a single membrane fiber material and configuration. It is known that membrane configuration differences can greatly influence the fouling behavior observed during membrane filtration (Howe et al. 2007). Additionally, the different hydrophilicities and surface charges of membrane materials can result in differing degrees of foulant-membrane interactions at the membrane surface, even when using the same water source (Kumar and Ismail 2015). Based on this, it is of interest to evaluate whether the superior performance of CF-DAF pretreatment observed by Walker and Narbaitz (2016) and Xu and Narbaitz (2016) is membrane material/membrane configuration dependent.

A comparison of CF-SED, CF-DAF, and C-IN pretreatment using the same water source does not appear to have been studied until now. Thus, the main objectives of this study are therefore to: a) determine whether the reported superiority of CF-DAF compared to CF-SED is independent of membrane material/configuration type; and b) investigate the suitability of C-IN pretreatment, using both a standard and a low coagulant dose, as an alternative to CF-SED and CF-DAF pretreatment.

3.3. Materials and Methods

3.3.1. Waters Tested

Ottawa River Water (ORW) was selected for the challenge water as it was previously used by Walker and Narbaitz (2016) and Xu and Narbaitz (2016) in their comparison of CF-SED and CF-

DAF pretreatment. ORW represents typical northern surface waters in Canadian environments; low turbidity, low hardness, high NOM content, high HPO fraction, and high color (Dang et al. 2010). The high color and NOM levels of ORW also make it representative of climate change impacted waters: elevated NOM and color have been reported in natural waterways as a result of flood and drought cycles associated with climate change (Sillanpaa 2015).

Raw ORW samples were collected at the Britannia WTP (Ottawa, Canada). To achieve optimum organics removal, the Britannia WTP doses 34 mg L^{-1} as alum (3.09 mg L^{-1} as Al), 8.50 mg L^{-1} sulfuric acid (H_2SO_4), and 1.25 mg L^{-1} activated silicate (SiO_2) to reduce the raw water pH to around 6 upstream of inclined plate clarifiers. Due to provincial health guidelines during the COVID-19 pandemic, it was not possible to access floated water samples from the nearby Aylmer WTP, so floated ORW was produced using a large volume bench-scale dissolved air flotation system (LB-DAF) (Gonzalez-Galvis and Narbaitz 2020). To best simulate the conditions at the Aylmer facility, ORW was dosed with 37 mg L^{-1} as alum (ALS, Kemira, Varennes, QC) and 0.1 mg L^{-1} cationic polyacrylamide polymer (Superfloc C-492PWG, Kemira, Varennes, QC), while the flotation parameters were as recommended by Gonzalez-Galvis and Narbaitz (2020).

Samples of ORW were collected in both the winter (ORW_w) and summer (ORW_s) season on days that constitute "normal" conditions (i.e., not following large rainfall or runoff events). Following collection, the water samples were transferred to a walk-in refrigerator and stored at 4 °C to minimize biological degradation. Prior to UF tests, the water samples were transferred to the laboratory and allowed to reach room temperature (~20 °C). Therefore, any observed difference in performance during the seasonal assessment is due to differences in water quality and not temperature. The ORW_w sample was used to evaluate membrane fouling performance for raw ORW, CF-SED, CF-DAF and C-IN pretreated waters. The ORW_s sample was used to test the membrane performance following C-IN pretreatment so that a seasonal performance comparison could be made.

3.3.2. Filtration Apparatus and Membrane Module

Evaluation of membrane performance was conducted using an automated bench-scale filtration system with data acquisition capabilities (Fig. 3.1) adapted from that described by Xu and Narbaitz (2016). In Fig. 3.1, the hydraulic piping of the filtration subsystem is shown as solid black lines while the backwash system is illustrated using a zig-zag pattern. Pressure-driven, dead-end

membrane modules (Fig. 3.2) were fabricated using hollow fiber membranes. The modules housed five hydrophilized polyvinylidene fluoride (PVDF) fibers (FG fiber, Kuraray, Kurakishi Okayama, Japan) and operated with an outside-in flow pattern, which is the same flow pattern as used by the manufacturer in its full-scale modules. It is acknowledged that many outside-in PVDF systems also operate under a submerged, vacuum-driven arrangement. The fibers have a nominal pore size of 0.02 μm, a lumen diameter of 0.75 mm, an outside diameter of 1.15 mm, and a pure water permeability of approximately 5,000 L m^{-2} h^{-1} bar^{-1} (reported by the manufacturer). Given that the pure water permeability of conventional low-pressure membranes range from 500 to 1,500 L m^{-2} h^{-1} bar^{-1}, the membrane fibers used in this study have a very high permeability (Pearce 2011).

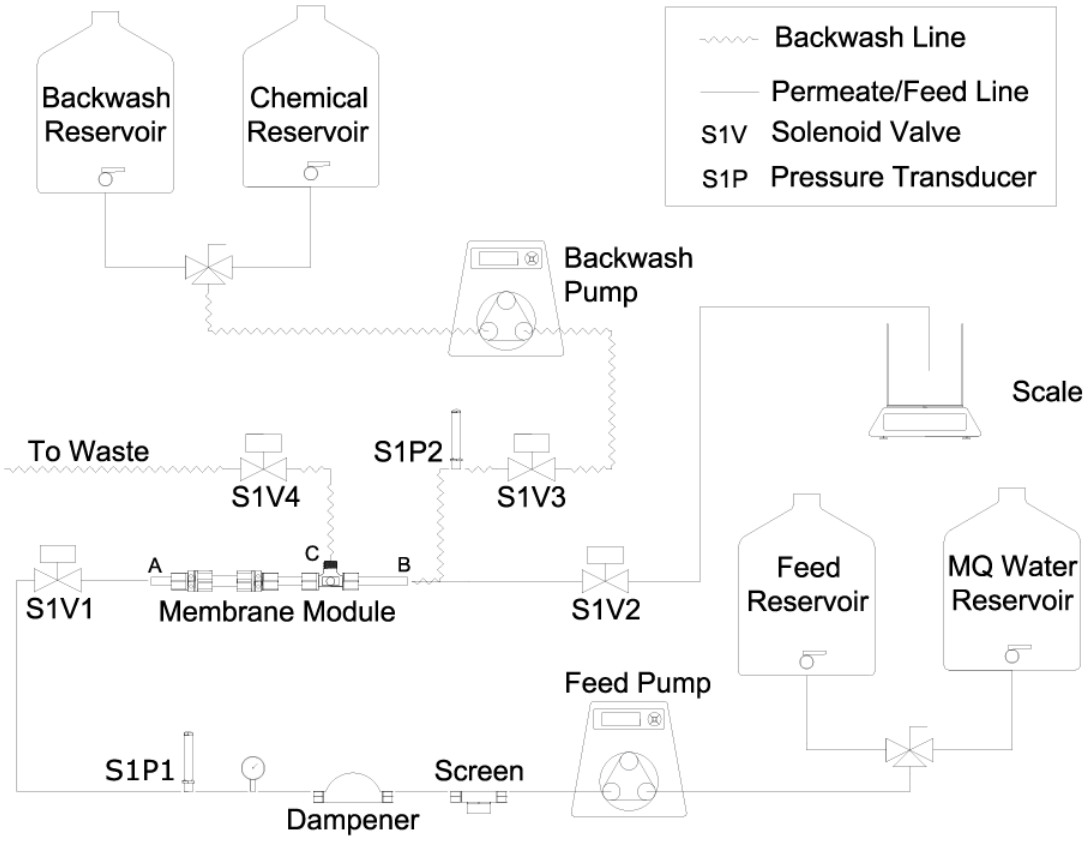


Fig. 3.1. Outside-in membrane filtration system.

Modules were constructed in-house using five fibers, each cut to 20 cm, with a total casing length of approximately 30 cm (Fig. 3.2). The fibers were potted using a high strength epoxy resin.

The potting sealed the fiber lumen shut at the module entrance (end A in Fig. 3.2) as well as the cavity space between the casing and the fibers at the module exit (end B in Fig. 3.2). This forced the challenge water (which enters at end A in Fig. 3.2) to cross the membrane skin and enter the lumen, from where the product water will exit the module and be collected for analysis. Each run was conducted using a newly potted module.

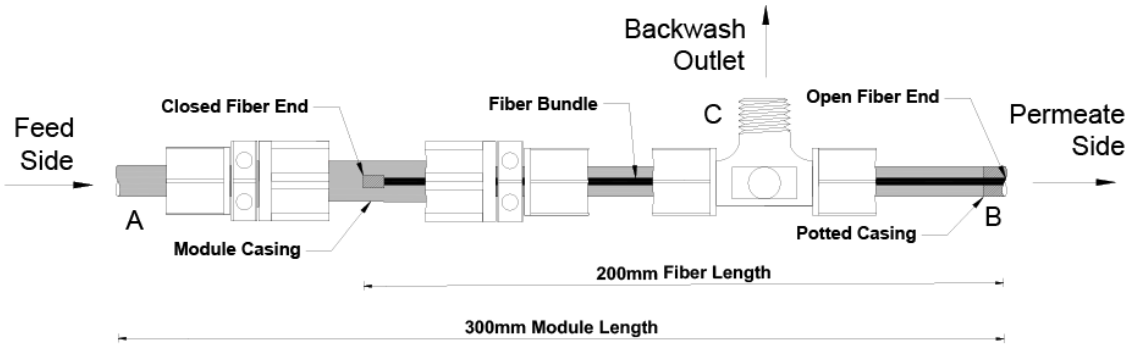


Fig. 3.2. Schematic diagram of the outside-in lab-scale module.

3.3.3. Inline Coagulation

In the current study, C-IN pretreatment was performed using a batch-wise approach, an approach that has previously been used by a number of authors (Choi and Dempsey 2004; Peleato et al. 2017). Raw ORW was placed inside the LB-DAF where alum coagulation was performed at G=296 s^{-1} for 2 min with the addition of sulphuric acid to a pH of 6. The adjustment of pH was done for two reasons: first, it was previously reported that optimal NOM removal for ORW could be obtained near this pH (Waterman 2008), and second, to match the acidity of the CF-SED water. Two different coagulant dosages were used: i) 34 mg L^{-1} as alum, which was the optimal coagulant dose for organics removal based on jar tests and was also the dose used at the Britannia WTP; and ii) a 20% reduced dose (27 mg L^{-1} as alum). The latter was used because Konieczny et al. (2009) found that for coagulation with alum, doses 20% lower than the optimal dose determined by jar testing resulted in the lowest decrease in membrane permeability. Furthermore, Choi and Dempsey (2004) found that the acidic under-dosed coagulation condition resulted in the lowest fouling resistance during filtration. Following the rapid mix period, the mixer speed was reduced to provide a constant mean velocity gradient of 200 s^{-1}. In order to minimize the settling of solids and fluctuating feed water quality, Peleato et al. (2017) and Tang et al. (2019) similarly provided continuous intense mixing to the coagulated feed water when investigating C-IN pretreatment.

3.3.4. Multi-day Filtration Test Protocol

Three-day bench-scale fouling tests were conducted as it has previously been suggested that longer duration bench-scale tests are required to be more representative of full-scale operation (Ayache et al. 2013). The assessment of all pretreatments (for raw ORW, CF-SED, CF-DAF, and C-IN) were conducted in replicate using winter water samples, while those evaluating C-IN pretreatment during the summer season were limited to single runs. Each experiment involved continuous cyclical operation with 30 min filtration cycles and 2 min hydraulic backwash cycles. Following membrane conditioning, filtration was performed at a flux of 80 L m^{-2} h^{-1}. This value was chosen so that the membrane would operate in the subcritical range based on preliminary critical flux tests conducted using the flux stepping method proposed by Le Clech et al. (2003). Intermittent hydraulic backwashing was performed at a flux of 200 L m^{-2} h^{-1} without air scouring. Air scouring was omitted due to the difficulty in purging the small-scale pressure-driven module of trapped air bubbles following each backwash cycle. Chemically enhanced backwash (CEB) was performed daily using a 100 ppm NaOCl solution; the dose being optimized in preliminary testing. The CEB cycle consisted of two components: in the first stage, the chemical solution was backwashed through the membrane module for a period of 20 min, which is typical for UF membrane facilities (Shi et al. 2014). In the second phase, the backwash feed line was switched from CEB chemicals to reverse osmosis water and backwashing continued for 20 min to flush remaining chemicals and foulants from the module. Chemical clean-in-place (CIP) was performed at the end of every three-day test using the same protocol as CEB cleaning but with a 0.1 N NaOH + 200 ppm NaOCl solution, as recommended by Xu and Narbaitz (2016) for ORW. It is acknowledged that the CIP used in the present study has a much greater frequency and reduced intensiveness than those used in full-scale systems (Pearce 2011). Following CIP cleaning, pure water permeability tests were conducted for 1 hour using type 1 reagent grade water (Barnstead, MicroPure, ThermoFisher Scientific, Waltham, MA) water to assess the permeability restoration. A summary of the operating conditions is presented in Table D.1.

3.3.5. Analytical Methods

The water samples collected were analyzed for total organic carbon (TOC), dissolved organic carbon (DOC), pH, zeta potential (ZP), turbidity, UV_{254}, alkalinity, total hardness, and true and apparent color. TOC was measured using a TOC analyzer (Pheonix 8000, Tekmar-Dohrmann,

Cincinnati, OH) according to Standard Method 5310/5310C, the UV-persulfate oxidation method (APHA et al. 2012). Samples used for DOC measurement were first filtered using a 0.45 µm polyethersulfone (PES) membrane filter (Supor 47 mm, 60043, Pall, Mississauga, ON) and then measured in the same manner as for TOC. Ultraviolet absorbance was measured according to Standard Methods 5910/5910A (APHA et al. 2012) using a UV-Vis spectrophotometer (DR6000, Hach, Loveland, CO) at a wavelength of 254 nm. The samples for UV absorbance measurements were prepared by filtering through a 0.45-µm PES membrane (Supor 47 mm, 60043, Pall, Mississauga, ON). ZP was measured with a zetasizer nano particle analyzer (Nano ZS Series, Malvern Instruments Ltd., Worcestershire, UK). All other parameters were measured according to Standard Methods (APHA et al. 2012). The molecular weight distribution of each pre-treated water was determined using serial membrane fractionation as outlined by Nilson and DiGiano (1996) and is detailed in Appendix D. Amicon 8400 stirred filtration cells (Millipore, Bedford, MA) were used in conjunction with membranes of nominal molecular weight cut-offs of 100,000, 30,000, 10,000, 5,000 and 3,000 Daltons (Millipore, MA).

3.3.6. Membrane Performance Indicators

3.3.6.1. Normalized TMP and Permeability Profiles

At the commencement of each three-day experiment, pure water permeability testing was conducted until stability was reached. The average steady-state flux and TMP were used to compute the corresponding clean membrane permeability. The TMP and permeability profiles throughout the three-day testing period were then normalized against these initial clean water steady-state values. The normalized nTMP was calculated using Eqn. 3.1.

$$nTMP = \frac{TMP_t}{TMP_o} \tag{3.1}$$

Where TMP_t is the transmembrane pressure at time *t* (Bar) and TMP_o is clean water steady-state transmembrane pressure (Bar). The normalized permeability (L_{NP}) can similarly be calculated using Eqn. 3.2.

$$L_{NP} = \frac{L_{p,t}}{L_{p,0}} \tag{3.2}$$

Where $L_{p,t}$ is the permeability at time t (L m^{-2} h^{-1} Bar^{-1}), and $L_{p,0}$ is the clean water steady-state membrane permeability (L m^{-2} h^{-1} Bar^{-1}). Normalization was performed in order to reduce the

effects of membrane variability when comparing the results of different testing conditions. Slight differences in the porosity, thickness, or pore size during the manufacturing process and variability in the membrane hydrophilization process may result in slightly different clean membrane permeabilities (Crittenden et al. 2012).

3.3.6.2. Fouling Index Modeling

Resistance-in-series based fouling indices were computed using a modified version of the unified membrane fouling index (UMFI) presented by Nguyen et al. (2011). The general form of the fouling index (FI) model is:

$$\frac{1}{J_s'} = 1 + (FI)V_s \tag{3.3}$$

Where $\frac{1}{J_s'}$ is the inverse normalized specific flux and V_s is the specific volume (L m^{-2}). The FI computed will depend on the operational cycles that are considered during the analysis. The total fouling index (TFI) is used to describe the data for a single cycle between hydraulic backwashes. When numerous hydraulic backwash cycles without chemical cleaning are considered, the hydraulically irreversible fouling index (HIFI) is computed. The hydraulically reversible fouling index (HRFI) is calculated as the difference between the TFI and the HIFI. When the total data is considered following chemical CIP, the chemically irreversible fouling index (CIFI) is determined. Based on preliminary analysis, the linear regression method was applied to determine the respective FI as opposed to the 2-point method. A detailed presentation of the operational cycles for the FI calculations, and their linear regression analysis are shown in Fig. D.2a-Fig. D.2d.

3.3.6.3. Backwash Efficiency

The backwash efficiency (BWE) was used to determine the percentage recovery of the TMP increase for each filtration cycle. The BWE is formulated according to Chellam et al. (1998) and presented in Eqn. 3.4 below.

$$BWE\ (\%) = \frac{TMP_{n-1,f} - TMP_{n,i}}{TMP_{n-1,f} - TMP_{n-1,i}} \times 100 \tag{3.4}$$

Where $TMP_{n,i}$ is the measured TMP at the beginning of cycle *n* (mBar), $TMP_{n-1,f}$ is the measured TMP at the end of cycle *n-1* (mBar), and $TMP_{n-1,i}$ is the measured TMP at the beginning of cycle *n-1* (mBar).

3.4. Results and Discussion

3.4.1. Challenge Water Quality

The water quality data for the raw and pre-treated feed waters is presented in Table 3.1. The characteristics of the winter sample (ORW_w) will be discussed first. The ORW_w sample had a high DOC concentration of 6.54 ± 0.01 mg L^{-1} and a UV_{254} of 0.276 ± 0.001 cm^{-1} yielding a specific UV absorbance (SUVA) of 4.22 L mg^{-1} m^{-1}. Elevated SUVA values above 4 L mg^{-1} m^{-1} have been reported by other authors for ORW during the winter season (Dang et al. 2010; Waterman 2008). Such a high SUVA value indicates a strong aromatic character of the NOM, as waters with SUVA values in excess of 4 L mg^{-1} m^{-1} are known to be composed largely of aquatic humic substances that are HPO in nature (Edzwald and Haarhoff 2012). Such a presence of HPO organic matter has previously been confirmed by Xu and Narbaitz (2016), who used XAD resin fractionation and reported that over 77.5% of DOC in raw ORW was HPO in nature.

When comparing the winter and summer season ORW, the most notable difference was related to the character of the organics. While the raw water's DOC and TOC levels for the summer sample are similar to those during the winter sample, the UV_{254} (0.226 ± 0.001 cm^{-1}) and true color (34.3 Pt. Co.) were both lower for the summer sample. The corresponding SUVA value for ORW_s was found to be 3.41 L mg^{-1} m^{-1}, supporting the conclusion of a lower aromaticity during the summer season. Seasonal differences in the aromatic character of ORW were also reported by Xu and Narbaitz (2016).

From Table 3.1 it can be seen that all pretreatments were effective in the removal of DOC and UV_{254}, however, the relatively greater removals of UV_{254} indicate a preferential removal of HPO, aromatic, organic components. Such a preferential removal has previously been reported (Crittenden et al. 2012). Compared to the other pretreatments, CF-DAF had the greatest propensity for removal of DOC (mean removal of 65.9%) and UV absorbent compounds (mean removal of 85.1%). The higher effectiveness of CF-DAF at removing HPO components of the organic matrix was also reported by Amaral et al. (2013) using a highly colored water, and is thought to be a result of HPO interactions at the air bubble surface (Braghetta et al. 1997). Accordingly, based on bulk organics removals alone, one would expect CF-DAF to result in reduced membrane fouling compared to other pretreatment alternatives.

Table 3.1. Water Quality Data for Raw ORW and Pre-treated ORW

Parameter	Raw ORW		CF-DAF	CF-SED	C-IN (34 mg L^{-1})		C-IN (27 mg L^{-1})	
	Winter	**Summer**	**Winter**	**Winter**	**Winter**	**Summer**	**Winter**	**Summer**
Turbidity (NTU)	4.92 ± 0.01[a]	1.89 ± 0.02	0.546 ± 0.02	2.41 ± 0.03	9.17 ± 0.07	5.88 ± 0.01	10.02 ± 0.65	5.58 ± 0.02
pH (unit)	7.76 ± 0.02	7.76 ± 0.02	6.24 ± 0.02	6.07 ± 0.01	6.01 ± 0.01	6.01 ± 0.01	6.03 ± 0.02	6.02 ± 0.01
UV_{254} (cm^{-1})	0.276 ± 0.001	0.226 ± 0.001	0.041 ± 0.001	0.057 ± 0.001	0.053 ± 0.02	0.049 ± 0.01	0.06 ± 0.001	0.056 ± 0.001
App. Color (Pt. Co.)	83 ± 0.9	54.3 ± 2.1	8.7 ± 0.5	30.3 ± 1.1	NA	NA	NA	NA
True Color (Pt. Co.)	53.3 ± 0.5	34.3 ± 0.5	2 ± 0	2.3 ± 0.5	1.8 ± 0.3	2.7 ± 0.5	1.8 ± 0.3	3 ± 0
Total Hardness (mg $CaCO_3$ L^{-1})	31.3 ± 1.4	32.7 ± 0.5	29.7 ± 0.5	31.3 ± 1.4	30.3 ± 0.5	30.3 ± 0.5	31.3 ± 0.5	31.7 ± 0.5
Alkalinity (mg $CaCO_3$ L^{-1})	28.2 ± 0.4	28.5 ± 0.3	NA	9.5 ± 0.07	NA	NA	NA	NA
Zeta Potential (mV)	-21.4 ± 2.77	-21.7 ± 2.99	-6.5 ± 0.44	-8.5 ± 0.46	-6.4 ± 0.45	-5.93 ± 0.69	-15.93 ± 0.51	-8.51 ± 0.65
DOC (mg L^{-1})	6.54 ± 0.01	6.62 ± 0.01	2.23 ± 0.01	2.94 ± 0.02	2.31 ± 0.01	2.35 ± 0.01	2.84 ± 0.01	2.67 ± 0.01
TOC (mg L^{-1})	6.95 ± 0.08	7.01 ± 0.01	2.58 ± 0.01	3.05 ± 0.01	2.48 ± 0.01	NA	NA	NA
SUVA (L mg^{-1} m^{-1})	4.22	3.41	1.85	1.95	2.30	2.06	2.39	2.11
DOC Removal (%)	NA	NA	65.90	55.05	64.68	64.50	56.57	59.67
UV_{254} Removal (%)	NA	NA	85.14	79.35	80.80	78.31	73.45	75.22

[a]μ ± 95% Confidence Interval

3.4.2. Winter Backwash Efficiency Evaluation

As shown in Fig. 3.3a below, average BWEs greater than 90% were observed for all pretreatment alternatives, including raw ORW, which is within the range observed for full-scale facilities. For the fibers used in this study, the raw ORW runs had lower BWEs, while most of the runs with the various pretreatments had overlapping 95% confidence intervals (CI). For all ORW_w tests, the BWE showed substantial variability, presumably occurs because some foulants may remain on the membrane until a certain amount of cake is formed prior to being effectively removed by later backwash cycles (Walker and Narbaitz 2016). Fig. 3.3b shows there was a strong negative linear relationship between the average BWE and SUVA, suggesting that for waters with increasing SUVA (and therefore aromaticity), lower average BWEs are expected. Decreasing BWEs inherently result in greater proportions of hydraulically irreversible fouling. Therefore, Fig. 3.3b also indirectly associates greater hydraulically irreversible fouling with aromatic, HPO NOM (which have high SUVA values). This will be discussed further in Section 3.4.5.

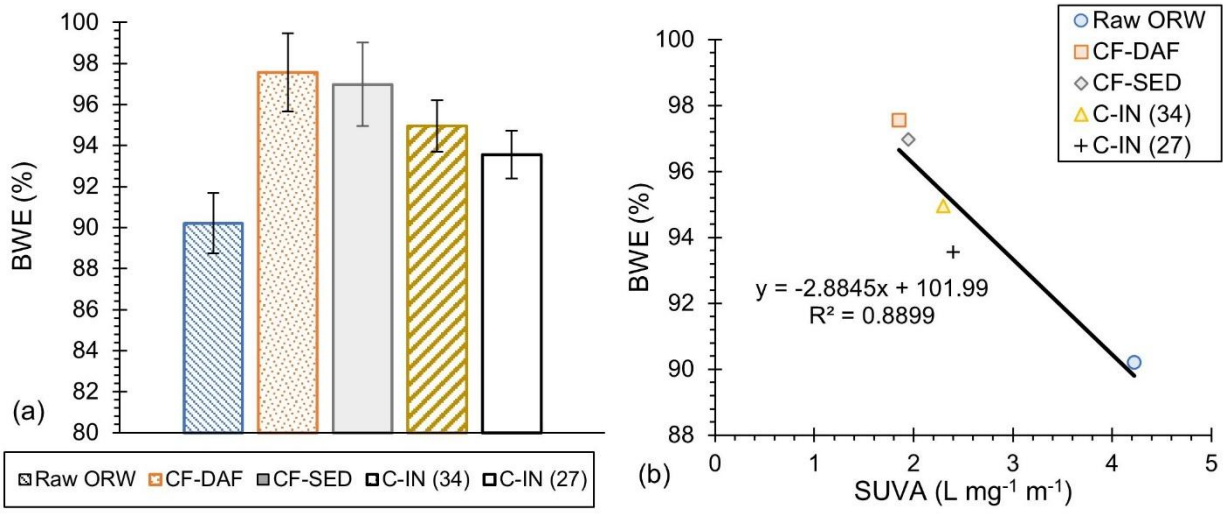


Fig. 3.3. ORW_w backwash evaluation: **(a)** Average BWEs; **(b)** Relationship between average BWE and SUVA.

3.4.3. Comparison of CF-DAF and CF-SED Pretreatment During Winter Season

Fig. 3.4a shows the nTMP profiles for the CF-SED, CF-DAF, and raw ORW filtration tests using ORW_w. It should be noted that the filtration time in the figure does not include time spent backwashing, and that all nTMP profiles have been generated using a representative test from the

replicates for each pretreatment. Furthermore, the effectiveness of the CEB can be observed from the drop in nTMP after the 22nd and 44th hours (which occur at 24 and 48 h of real time). The pre-treated waters had substantially lower nTMP increases than the raw ORW indicating the beneficial impact of feed water pretreatment. For example, the raw ORW reached a final nTMP of 19.25, while the CF-DAF and CF-SED pre-treated waters only reached nTMP values of 1.62 and 1.67, respectively. Such a reduction in membrane fouling may be attributed to the lower foulant load reaching the membrane surface for both pretreated waters. In both cases, the particle loading (measured by turbidity) and the organic loading (as measured by DOC and UV_{254}) were greatly reduced compared to that for raw ORW. The beneficial impact of CF-SED pretreatment was also reported by Amjad et al. (2015) who found that the lower mass deposited on the membrane surface for CF-SED pretreatment could result in a lower membrane flux decline, regardless of the cake porosity. Braghetta et al. (1997) similarly reported that the effectiveness of the CF-DAF pretreatment process in removing particulate matter and DOC results in a membrane feed water that has a lower fouling potential compared to untreated water. To better compare the performance of the CF-DAF and CF-SED pretreatments, Fig. 3.4b presents their filtration profiles without that of raw ORW. This figure shows that even at a smaller scale the two profiles are very similar. In fact, over the first day the profiles cannot be distinguished from one another (overlapping 95% CIs for mean nTMP), and it is only the second and third days where the CF-DAF pretreatment results in a slightly reduced nTMP. Analysis of the FIs (see Table D.2) supports this finding, with the HIFI values of CF-DAF and CF-SED pretreatment having overlapping 95% CIs, indicating their values are statistically the same.

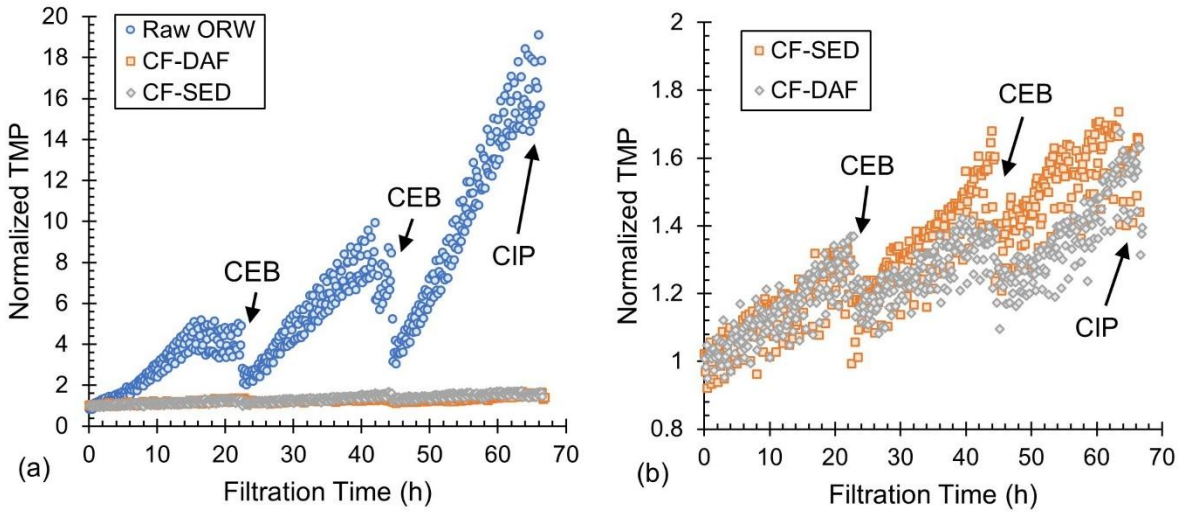


Fig. 3.4. Comparison of nTMP profiles for pre-treated ORW_w: **(a)** raw, CF-DAF, and CF-SED; **(b)** CF-DAF and CF-SED.

The finding of similar CF-SED and CF-DAF nTMP profiles is in contrast to the results presented by both Walker and Narbaitz (2016) and Xu and Narbaitz (2016) who used the same water source, but a different membrane type (which also had a 0.02 µm pore size). Their ORW_w studies found that the TMP for CF-SED pretreated water was nearly two times larger than that for CF-DAF. Several factors may account for the differences in behavior. The most obvious reason supporting the observed superiority of CF-DAF pretreatment in their studies is related to the membrane material properties. Xu and Narbaitz (2016) reported that the measured contact angle for the hydrophilic PES membrane used in their study was 65.8 ± 2° while for the PVDF fiber used in the current study the contact angle was 45°, indicating a significantly higher hydrophilicity. Unfortunately, it was not possible to verify this membrane-causation hypothesis relating to membrane materials as the other membrane type is no longer available. Additionally, it must also be noted that the effects of membrane fiber material and configuration could not be separated in the current study.

A second contributing factor to the differences in results between the studies is water quality. While the raw water qualities were not identical during the three studies, they are quite consistent. For example, the current study and that by Xu and Narbaitz (2016) found similar increased removal of UV_{254} by CF-DAF compared to CF-SED (i.e., 5.8% and 7.5% greater UV_{254} removal by CF-DAF, respectively). However, in the current study the CF-DAF and CF-SED SUVA

values were found to be quite similar (1.85 vs 1.95 L mg^{-1} m^{-1}, respectively), while in the study by Xu and Narbaitz (2016) the CF-SED SUVA value was found to be 33% greater than that of CF-DAF. This may explain the difference in the level of fouling between the two studies. An additional consideration is that in the studies by Walker and Narbaitz (2016) and Xu and Narbaitz (2016) the pretreatment was performed at the Aylmer (CF-DAF) and Britannia (CF-SED) WTPs. In contrast, in the current study, the CF-DAF pretreatment was performed using the LB-DAF system, which has slightly lower UV_{254} removals than the Aylmer plant (Gonzalez-Galvis and Narbaitz 2020), and the Britannia WTP now has a more effective inclined plate clarifier system that covers the entire clarifier surface area.

A third possibility explaining the observed discrepancies is the bench-scale testing system. The filtration system was modified to improve the BWE by reducing the length of hydraulic piping that contacted both the backwash and feed waters. A significant improvement in the BWE (greater than 90% vs. less than 70%) should affect the hydraulically irreversible fouling, and is a possible source of the discrepancies observed between the results of the current study and those by Walker and Narbaitz (2016) and Xu and Narbaitz (2016).

A final comment regarding CF-DAF and CF-SED pretreatment performance is that Fig. 3.4a makes it clear that a pseudo steady state was not reached within the three-day membrane filtration test period. The absence of filtration stability may have been caused by the membrane fiber's very high clean membrane permeability or the lack of air assistance during hydraulic backwashing. Due to the extremely high initial permeability of the fibers used in this study, the time period required to reach the lower, stable, reference permeability typical of long-term operation is expected to take longer. Additionally, the fibers used in this study have been developed for use in a full-scale module that employs air-based backwashing. The lack of such backwashing in the bench-scale modules may have prolonged the stabilization period.

3.4.4. C-IN Pretreatment During Winter Season

Fig. 3.5 shows that the CF-SED and CF-DAF pretreatments yielded very similar and low nTMP profiles (final nTMPs of 1.67 and 1.62, respectively) while C-IN pretreatment at dosages of 34 mg L^{-1} and 27 mg L^{-1} as alum yielded significantly higher final nTMPs of 5.30 and 10.95, respectively. Using FI analysis (Table D.2), the performance of the CF-SED and CF-DAF pretreatments (in terms of TFI and HIFI) were also found to be superior to pretreatment by C-IN for ORW. These

findings suggest that the order of increasing effectiveness for pretreatment of ORW is C-IN (27) < C-IN (34) < CF-SED < CF-DAF, although CF-SED and CF-DAF exhibited similar behavior as discussed in Section 3.4.3. It appears that for ORW and the PVDF fibers used in this study, C-IN is not a suitable pretreatment as it was unable to mitigate membrane fouling to the levels seen for CF-SED and CF-DAF pre-treated waters. While many authors have proposed that C-IN pretreatment generates a porous and low hydraulic resistance surface cake (Amjad et al. 2015; Cho et al. 2006), this expected porosity was offset for ORW by the larger mass of deposited flocculant particles, resulting in higher nTMP values than CF-DAF and CF-SED pretreatments. Concerning the two C-IN pretreatments, thick cakes were observed to form on the membrane surface during the three-day filtration cycles, as evidenced by the increasing in-cycle variation of the nTMP profile (Fig. 3.5) and the high TFI values (Table D.2). While the C-IN pretreatment at a dose of 34 mg L^{-1} as alum logically delivers a greater mass loading of flocs to the membrane surface compared to 27 mg L^{-1} as alum, its lower nTMP values suggest that the addition of a higher coagulant dose in-line formed a more porous cake layer on the membrane surface.

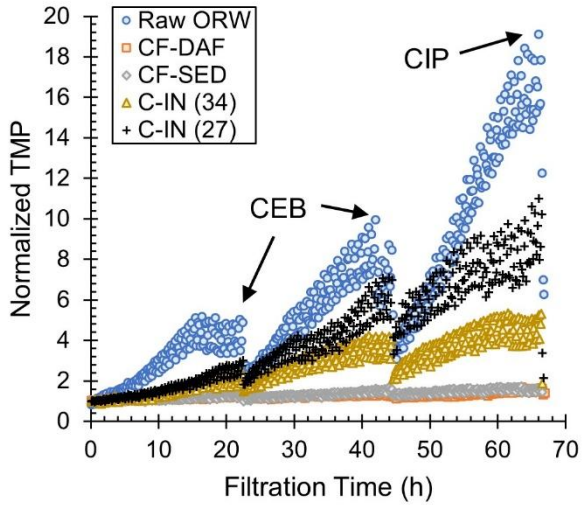


Fig. 3.5. Comparison of C-IN pretreatment with CF-DAF and CF-SED during winter season.

Although C-IN pretreatment caused thick surface cakes to be formed, the CEB and CIP cleanings were seen to be highly effective (Fig. 3.5), resulting in low CIFI/TFI values of 0.4-1.1%. Visually, the 100 ppm NaOCl CEB solution was able to remove the entire cake from the membrane surface at the termination of the CEB cycles (Fig. D.3). Furthermore, although complete recovery

of the nTMP increase was not achieved, C-IN (34) averaged 77.8% and 87.8% recovery for CEB and CIP, respectively, whereas for C-IN (27) these recoveries were 72.2% and 87.6%, respectively.

3.4.5. C-IN Seasonality Comparison and Relevant Correlations

The effects of seasonal variations in feed water quality were assessed for C-IN in Fig. 3.6a and Fig. 3.6b. From the nTMP profiles, it can be seen that the summer season resulted in a greatly reduced fouling compared to the winter season when using the same pretreatment conditions. For example, at the end of the third day, the nTMP for C-IN (27) was 10.95 in the winter compared to 5.01 in the summer (Fig. 3.6a), while for C-IN (34) it was 5.31 in the winter compared to 2.69 in the summer (Fig. 3.6b). Brinkman and Hozalski (2011) also reported that the permeability was negatively correlated to the raw feed water SUVA value in the summer and autumn seasons for an inside-out PES membrane. Higher autumnal SUVA values resulted in greater membrane TMP increases compared to the summer season.

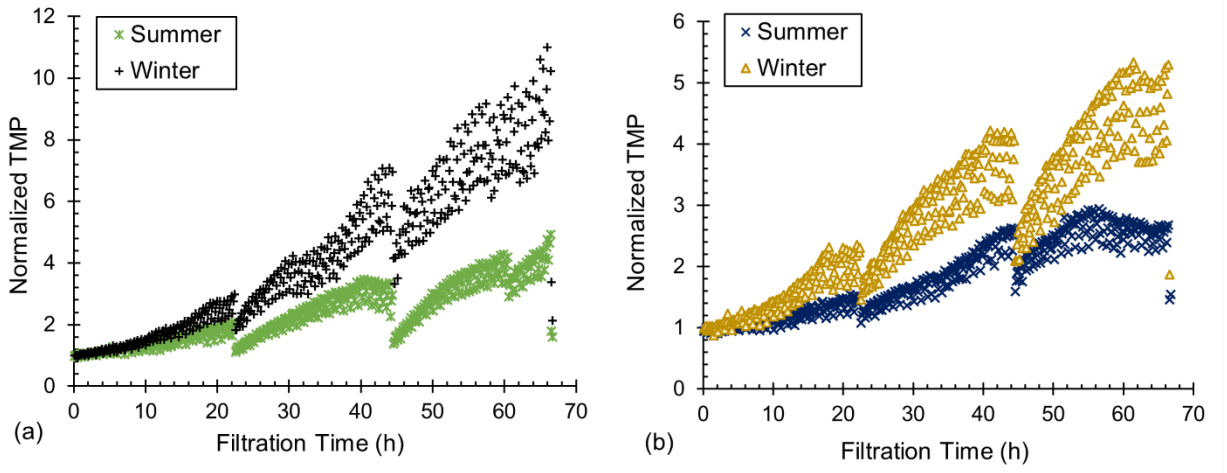


Fig. 3.6. Comparison of summer and winter C-IN pretreatment: **(a)** 27 mg L^{-1} alum; **(b)** 34 mg L^{-1} alum.

Like Xu and Narbaitz (2016), the current study also identified a linear relationship between HIFI and SUVA as well as between CIFI and SUVA when all winter and summer season feed waters were considered (Fig. 3.7a and Fig. 3.7b). Notably, the regressed linear equation between HIFI and SUVA in the current study was remarkably similar to that from the study by Xu and Narbaitz (2016), possibly suggesting that this relationship is dependent on the feed water, though

not necessarily on membrane materials. The observed correlations indicate that higher SUVA values, which are representative of the HPO NOM fraction, seem to result in higher levels of hydraulically and chemically irreversible fouling. Indeed, UF molecular weight fractionation of all pretreated waters appears to support this finding, with serial fractionations revealing that elevated irreversible fouling measures were most strongly correlated with the fraction between 5 kDa and 10 kDa (Fig. 3.8a and Fig. 3.8b). This size fraction has previously been associated with the highly aromatic humic acid fraction (between 1 kDa - 10 kDa) using LC-OCD analysis by Liu et al. (2020). This finding is of interest as it is in contrast to much of the recent literature which suggests that HPI biopolymers, which have much higher molecular weights, are the primary cause of irreversible membrane fouling (Kimura and Kume 2020; Peleato et al. 2017; Tang et al. 2019; Tian et al. 2013). However, it should be noted that for CF-SED pre-treated ORW from the Britannia WTP, Croft (2012) reported very low HPI biopolymer concentrations (~80 µg L^{-1}). In many of the studies reporting the HPI NOM fraction as the primary membrane foulant, higher biopolymer concentrations were observed. Another point from the analysis of Fig. 3.8 is that the CF-DAF pre-treated water had a slightly higher concentration of the 5 kDa and 10 kDa DOC fraction than the CF-SED pre-treated water, in spite of having a lower SUVA value: this difference may contribute to the similarity in the fouling arising from these two pretreatments.

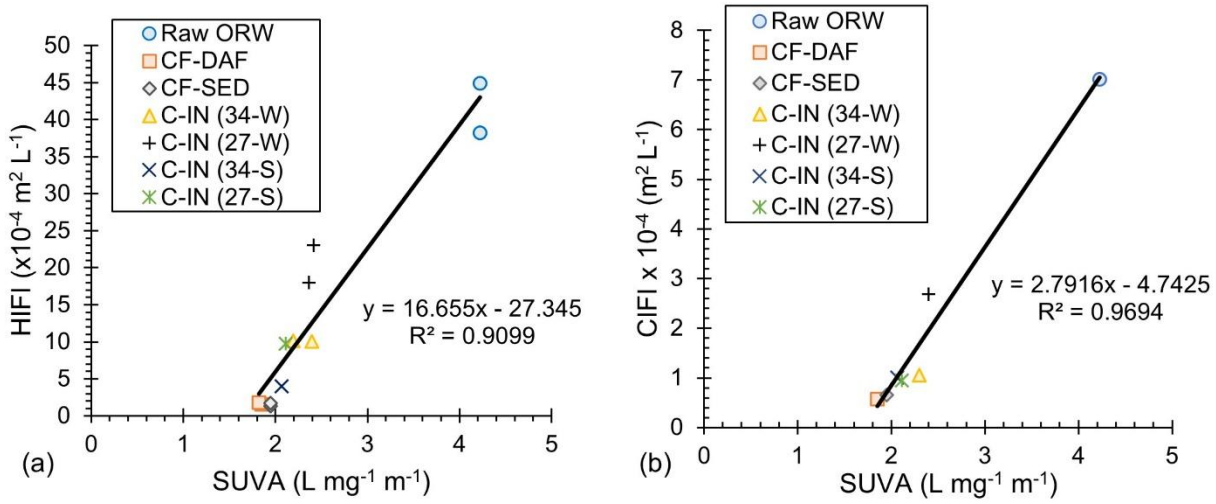


Fig. 3.7. Relationship between average fouling indices and SUVA: **(a)** HIFI and SUVA; **(b)** CIFI and SUVA.

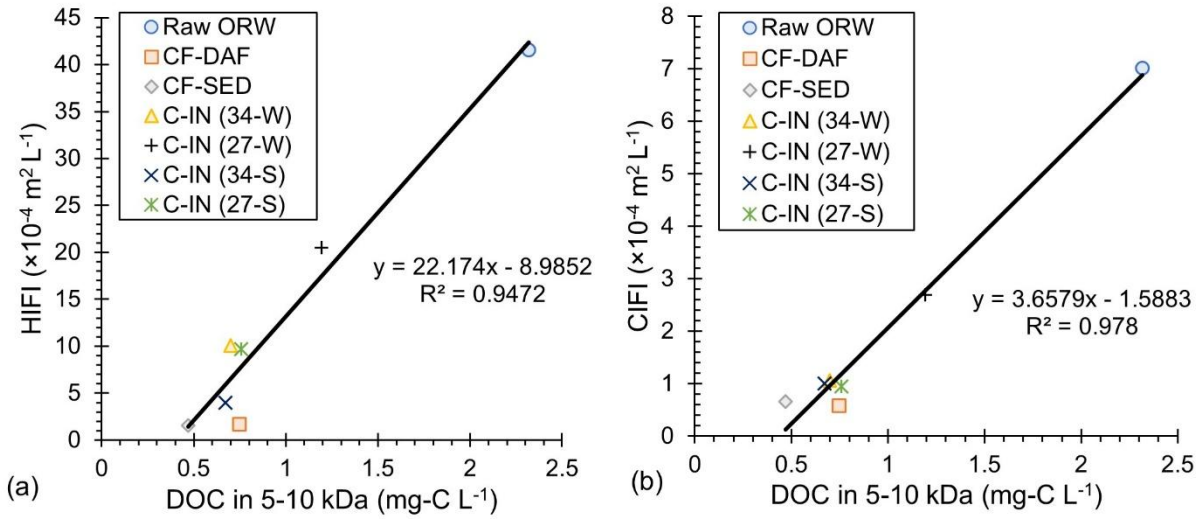


Fig. 3.8. Relationship between the 5-10 kDa organic fraction and: **(a)** HIFI; **(b)** CIFI.

While the feed water SUVA value appeared to determine the extent of the irreversible fouling for ORW, the performance of C-IN pretreatment appeared to be strongly influenced by other characteristics as well. Strong relationships were identified between HIFI and ZP as well as CIFI and ZP for C-IN tests conducted with water from both seasons (Fig. 3.9a and Fig. 3.9b). From these relationships, it is observed that lower magnitudes of ZP result in lower levels of hydraulically irreversible fouling. This is consistent with the findings of Wang et al. (2013), who reported that the structure of the cake layer is related to the floc structure, size, and compressibility. Importantly, they note that higher magnitudes of ZP (i.e., higher charge repulsion) led to the formation of small floc particles with lower values of fractal dimension (i.e., loose structure), which aggregated into a compact cake of high compressibility and low porosity. In contrast, they reported that conditions near zero zeta potential resulted in larger floc particles with higher fractal dimensions, forming a low compressibility and high porosity surface cake. The influential role ZP plays in governing the performance of C-IN pretreatment for both membranes may therefore not have been entirely unexpected. Compared to CF-SED and CF-DAF, C-IN pretreatment delivers much higher floc particle loading to the membrane surface. The characteristics of the C-IN flocs govern the nature of the cake structure formed on the membrane surface, which is thought to control the membrane fouling (Kamińska et al. 2020; Maeng et al. 2017; Shen et al. 2020).

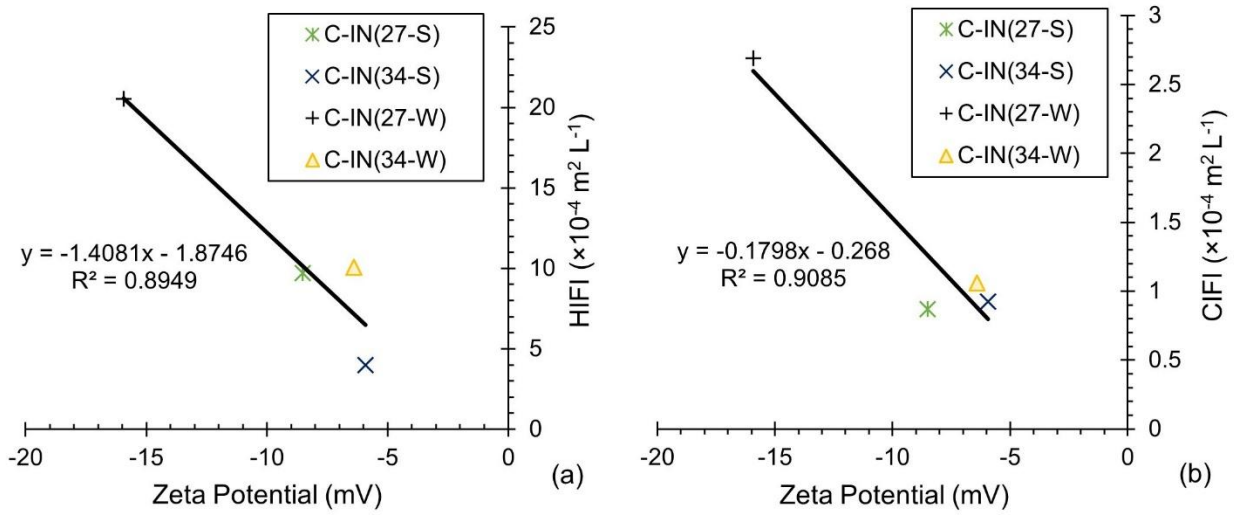


Fig. 3.9. Relationships between Zeta Potential and: **(a)** HIFI; **(b)** CIFI.

Although no imaging of the cake structure was performed in this study, the performance of C-IN pretreatment supports the concept described above. The best performing C-IN pretreatment was under conditions of reduced ZP magnitude. Such conditions were found to be associated with higher coagulant doses and were more easily achieved during the summer season than in the winter season. Based on the current study, it appears that the structure of the two cakes formed at 34 mg L^{-1} and 27 mg L^{-1} alum pretreatment differed, with the cake formed at higher dosage presenting a reduced hydraulic resistance to flow. The low porosity and high hydraulic resistance of the cake layer formed following C-IN (27) pretreatment in the winter is clearly evident from the high nTMP values, the high TFI value (which exceeded that of ORW), and the high HIFI values (which had overlapping 95% CI with ORW). Unlike some reports in the literature lower coagulant dose resulted in greater fouling, it seems that the contradiction in the results arises from the characteristics of ORW, the different membranes used, and possibly the differences in the membrane filtration apparatus.

3.5. Practical Implications

In contrast to the results of earlier studies, CF-DAF and CF-SED pretreatment performed equally well. This was in spite of CF-DAF having the lowest residual DOC and the greatest preference for removal of UV_{254} absorbent organics. Based on the FI vs SUVA relationships presented in Section

3.4.5, this is likely due to their similar SUVA values. Practically, these findings indicate that the selection of either flotation or sedimentation as pretreatment in low-pressure membrane WTPs should not be solely based on the gross organic removals. Any improvement in membrane fouling tendency from these pretreatments appears to be based on a unique interaction between feed water quality, membrane material, and membrane configuration. Thus, the pretreatment selection should also be based on considerations of integrated design such as reduced plant footprint, process complexity, susceptibility of source water to algal blooms, and disinfection by-product goals. For example, HPO NOM has been shown to have higher potential for trihalomethane and trihaloacetic acid formation during the subsequent chemical disinfection process (Crittenden et al. 2012; Hua and Reckhow 2007). Considering that the PVDF fibers used in this study removed less than 10% of DOC in all cases (which is typical for UF membranes), the increased DOC and UV_{254} absorbent organic removal exhibited by CF-DAF pretreatment may help MF/UF WTPs in the attainment of their DBP treatment goals.

An important consideration for C-IN pretreatment of ORW is that because of the high NOM levels present, the lower coagulant dosages (0.3-1 mg L^{-1}) reported by other authors (Peleato et al. 2017; Wray et al. 2014) may not be feasible for an integrated facility design. Subsequent downstream processes would likely be required for NOM removal to meet DBP regulations. The suitability of C-IN pretreatment, particularly at low coagulant dosages, should be subject to further testing using different water types, especially those with lower DOC and higher HPI-NOM content. The pronounced seasonal differences in membrane performance observed in the current study suggest that C-IN pretreatment may require continuous process control/optimization throughout the year. The correlations between ZP and measures of irreversible fouling indicate that ZP is likely a critical parameter that may be used for process control. Future studies should further investigate the impact of ZP on controlling C-IN performance for a range of waters and membrane types.

3.6. Conclusions

Bench-scale multi-day filtration tests were conducted using modules housing PVDF fibers operated in an outside-in, dead-end configuration to assess the impact of membrane pretreatment for a river water with a high HPO NOM fraction. The findings of the study are as follows:

1) CF-DAF and CF-SED pretreatments yielded similar levels of fouling for the PVDF fibers used in this study in-spite of CF-DAF having greater DOC removal and preferential removal of HPO foulants. This finding contradicts those of earlier studies that used the same river water but a different membrane type. The selection of either CF-DAF or CF-SED as pretreatment for low-pressure membrane WTPs should therefore not be based solely on the gross removal of organics, but rather on considerations of integrated design.
2) C-IN pretreatment was unable to mitigate fouling to levels seen for CF-DAF and CF-SED. Unlike findings reported in some earlier studies, C-IN pretreatment using a 20% lower coagulant dosage than suggested by jar tests resulted in greater fouling. This suggests that the applicability of such a pretreatment strategy is dependent on the raw water quality.
3) For C-IN pretreatment, strong relationships were identified between ZP and HIFI and between ZP and CIFI. Favorable conditions of low magnitude zeta potential were more easily achieved during the summer season, leading to distinct seasonal differences in fouling behavior. As suggested by others, it seems that the differences in ZP impacted the cake structure, which in turn impacted the irreversibility of fouling. Accordingly, a coagulant dosing control system could be developed to optimize C-IN performance through zeta potential adjustment across different seasons.
4) For ORW, which has a low HPI NOM concentration, strong correlations were observed between irreversible FIs and SUVA as well as between irreversible FIs and the DOC in the 5 to 10 kDa fraction. These findings suggest that for this river water and PVDF fibers, the HPO NOM fraction is the primary irreversible membrane foulant for ORW.

To facilitate comparison of results with earlier research, this study used 30-minute filtration cycles. Due to the fiber differences between studies, this led to smaller TMPs than observed in full-scale systems. Accordingly, future studies should investigate if the significant differences in the fouling of membranes is independent the degree of taxing (i.e., the filtration cycle duration) and if the patterns persist when a pseudo steady-state is reached during longer tests. Additionally, further research should consider waters with a higher hydrophilic NOM content water to evaluate if the observed correlations of irreversible fouling with SUVA and the similarity in CF-SED and CF-DAF performance persist.

3.7. Acknowledgements

The authors thank the Natural Sciences and Engineering Research Council of Canada for their scholarship to the lead author as well as their support through the Discovery Grant program. Furthermore, the authors extend their gratitude to Andy Campbell at the Britannia Water Purification Facility for his assistance during the complexities of the COVID-19 pandemic, Catherine Brosseau from Kemira for providing the study coagulants, and Kuraray Ltd. for providing membrane fibers.

3.8. References

Aiken, G. R., D. M. McKnight, R. L. Wershaw, and P. MacCarthy. 1985. *Humic Substances in Soil, Sediment, and Water: Geochemistry, Isolation, and Characterization*. 1st ed. Toronto: John Wiley & Sons.

Amaral, P. A. P. do, L. A. Coral, M. E. Nagel-Hassemer, T. J. Belli, and F. R. Lapolli. 2013. "Association of dissolved air flotation (DAF) with microfiltration for cyanobacterial removal in water supply." *Desalination and Water Treatment*, 51 (7–9): 1664–1671. https://doi.org/10.1080/19443994.2012.715128.

American Water Works Association. 2005. *Microfiltration and Ultrafiltration Membranes for Drinking Water: Manual of Water Supply Practices 53*. 1st ed. Denver, CO: American Water Works Association.

Amjad, H., Z. Khan, and V. V. Tarabara. 2015. "Fractal structure and permeability of membrane cake layers: Effect of coagulation–flocculation and settling as pretreatment steps." *Separation and Purification Technology*, 143: 40–51. https://doi.org/10.1016/j.seppur.2015.01.020.

APHA, WEF, and AWWA. 2012. *Standard Methods for the Examination of Water and Wastewater*. Edited by L. Clesceri, A. Greenberg, and A. Eaton. 22nd Editi. Washington, D.C.: American Public Health Association, Water Environment Federation, American Water Works Association.

Ayache, C., M. Pidou, J.-P. Croue, J. Labanowski, Y. Poussade, A. Tazi-Pain, J. Keller, and W. Gernjak. 2013. "Impact of effluent organic matter on low-pressure membrane fouling in tertiary treatment." *Water Research*, 47 (8): 2633–2642. https://doi.org/10.1016/j.watres.2013.01.043.

Braghetta, A., J. G. Jacangelo, S. Chellam, B. A. Utne, and M. L. Hotaling. 1997. "DAF pretreatment: its effect on MF performance." *Journal AWWA*, 89 (10): 90–101.

Brinkman, B. M., and R. M. Hozalski. 2011. "Temporal variation of NOM and its effects on membrane treatment." *Journal AWWA*, 103 (2): 98–106. https://doi.org/10.1002/j.1551-8833.2011.tb11405.x.

Chellam, S., J. G. Jacangelo, and T. P. Bonacquisti. 1998. "Modeling and Experimental Verification of Pilot-Scale Hollow Fiber, Direct Flow Microfiltration with Periodic Backwashing." *Environmental Science & Technology*, 32 (1): 75–81. https://doi.org/10.1021/es9610040.

Cho, M. H., C. H. Lee, and S. Lee. 2006. "Effect of flocculation conditions on membrane permeability in coagulation-microfiltration." *Desalination*, 191 (1–3): 386–396. https://doi.org/10.1016/j.desal.2005.08.017.

Choi, K. Y. J., and B. A. Dempsey. 2004. "In-line coagulation with low-pressure membrane filtration." *Water Research*, 38 (19): 4271–4281. https://doi.org/10.1016/j.watres.2004.08.006.

Crittenden, J. C., R. R. Trussell, D. W. Hand, K. J. Howe, and G. Tchobanoglous. 2012. *Water Treatment: Principles and Design*. 3rd ed. New York, NY: McGraw-Hill.

Croft, J. 2012. "Natural Organic Matter Characterization of Different Source and Treated Waters; Implications for Membrane Fouling Control." M.A.S.c Thesis, University of Waterloo.

Dang, H. T., R. M. Narbaitz, and T. Matsuura. 2010. "Evaluation of apparatus for membrane cleaning tests." *Journal of Environmental Engineering*, 136 (10): 1161–1170. https://doi.org/10.1061/(ASCE)EE.1943-7870.0000254.

Edzwald, J. K., and J. Haarhoff. 2012. *Dissolved Air Flotation for Water Clarification*. 1st ed. New York, NY: McGraw-Hill.

Gao, W., H. Liang, J. Ma, M. Han, Z. Chen, Z. Han, and G. Li. 2011. "Membrane fouling control in ultrafiltration technology for drinking water production: A review." *Desalination*, 272 (1–3): 1–8. Elsevier B.V. https://doi.org/10.1016/j.desal.2011.01.051.

Gonzalez-Galvis, J. P., and R. M. Narbaitz. 2020. "Large batch bench-scale dissolved air flotation system (LB-DAF) for drinking water treatability tests." *Environmental Science: Water Research and Technology*, 6 (4): 1004–1017. Royal Society of Chemistry. https://doi.org/10.1039/c9ew00935c.

Hög, A., J. Ludwig, and M. Beery. 2015. "The use of integrated flotation and ceramic membrane filtration for surface water treatment with high loads of suspended and dissolved organic matter." *Journal of Water Process Engineering*, 6: 129–135. Elsevier Ltd. https://doi.org/10.1016/j.jwpe.2015.03.010.

Howe, K. J., A. Marwah, K. Chiu, and S. S. Adham. 2007. "Effect of membrane configuration on bench-scale MF and UF fouling experiments." 41: 3842–3849. https://doi.org/10.1016/j.watres.2007.05.025.

Hua, G., and D. A. Reckhow. 2007. "Characterization of disinfection byproduct precursors based on hydrophobicity and molecular size." *Environmental Science & Technology*, 41 (9): 3309–3315. https://doi.org/10.1021/es062178c.

Kamińska, G., W. Pronk, and J. Traber. 2020. "Effect of coagulant dose and backflush pressure on NOM membrane fouling in inline coagulation-ultrafiltration." *Desalination and Water Treatment*, 199: 188–197. https://doi.org/10.5004/dwt.2020.25657.

Kimura, K., and K. Kume. 2020. "Irreversible fouling in hollow-fiber PVDF MF / UF membranes filtering surface water: Effects of precoagulation and identification of the foulant." *Journal of Membrane Science*, 602 (February): 117975–117975. Elsevier B.V. https://doi.org/10.1016/j.memsci.2020.117975.

Konieczny, K., M. Rajca, D. Sakol, J. Plonka, and M. Bodzek. 2009. "Coagulation-ultrafiltration system for river water treatment." *Desalination*, 240 (September 2007): 2–6. https://doi.org/10.1016/j.desal.2007.11.072.

Kumar, R., and A. F. Ismail. 2015. "Fouling control on microfiltration/ultrafiltration membranes: Effects of morphology, hydrophilicity, and charge." *Journal of Applied Polymer Science*, 132 (21): n/a-n/a. https://doi.org/10.1002/app.42042.

Le Clech, P., B. Jefferson, I. S. Chang, and S. J. Judd. 2003. "Critical flux determination by the flux-step method in a submerged membrane bioreactor." *Journal of Membrane Science*, 227 (1–2): 81–93. https://doi.org/10.1016/j.memsci.2003.07.021.

Liu, J., E. Yang, T. Huang, Z. Wang, and B. Dong. 2020. "Correlation of chemically irreversible fouling with organic constituents of feed water during membrane filtration." *Colloids and Surfaces A: Physicochemical and Engineering Aspects*, 597 (January): 124790–124790. Elsevier. https://doi.org/10.1016/j.colsurfa.2020.124790.

Ma, B., Y. Ding, B. Wang, Z. Qi, Y. Bai, R. Liu, H. Liu, and J. Qu. 2020. "Influence of sedimentation with pre-coagulation on ultrafiltration membrane fouling performance." *Science of the Total Environment*, 708: 134671–134671. Elsevier B.V. https://doi.org/10.1016/j.scitotenv.2019.134671.

Maeng, S. K., T. C. Timmes, and H.-C. Kim. 2017. "Characteristics of flocs formed by polymer-only coagulation in water treatment and their impacts on the performance of downstream membrane separation." *Environmental Technology*, 38 (20): 2601–2610. https://doi.org/10.1080/09593330.2016.1271460.

Matilainen, A., E. T. Gjessing, T. Lahtinen, L. Hed, A. Bhatnagar, and M. Sillanpää. 2011. "An overview of the methods used in the characterisation of natural organic matter (NOM) in relation to drinking water treatment." *Chemosphere*, 83 (11): 1431–1442. https://doi.org/10.1016/j.chemosphere.2011.01.018.

Nguyen, A. H., J. E. Tobiason, and K. J. Howe. 2011. "Fouling indices for low pressure hollow fiber membrane performance assessment." *Water Research*, 45 (8): 2627–2637. Elsevier Ltd. https://doi.org/10.1016/j.watres.2011.02.020.

Nilson, J. A., and F. A. DiGiano. 1996. "Influence of NOM composition on nanofiltration." *Journal AWWA*, 88 (5): 53–66. https://doi.org/10.1002/j.1551-8833.1996.tb06555.x.

Pearce, G. K. 2011. *UF/MF Membrane Water Treatment: Principles and Design*. 387. 1st ed. Bangkok: Water Treatment Academy.

Peiris, R. H., M. Jaklewicz, H. Budman, R. L. Legge, and C. Moresoli. 2013. "Assessing the role of feed water constituents in irreversible membrane fouling of pilot-scale ultrafiltration drinking water treatment systems." *Water Research*, 47 (10): 3364–3374. Elsevier Ltd. https://doi.org/10.1016/j.watres.2013.03.015.

Peleato, N. M., R. L. Legge, and R. C. Andrews. 2017. "Characterization of UF foulants and fouling mechanisms when applying low in-line coagulant pre-treatment." *Water Research*, 126: 1–11. Elsevier Ltd. https://doi.org/10.1016/j.watres.2017.08.064.

Ratajczak, M. J., K. N. Exall, and P. M. Huck. 2012. "Factors affecting coagulation as a pretreatment to ultrafiltration membranes." *Water Quality Research Journal*, 47 (2): 103–116. https://doi.org/10.2166/wqrjc.2012.010.

Schäfer, A. I., A. G. Fane, and T. D. Waite. 2001. "Cost factors and chemical pretreatment effects in the membrane filtration of waters containing natural organic matter." *Water Research*, 35 (6): 1509–1517. https://doi.org/10.1016/S0043-1354(00)00418-8.

Schulz, M., A. Soltani, X. Zheng, and M. Ernst. 2016. "Effect of inorganic colloidal water constituents on combined low-pressure membrane fouling with natural organic matter (NOM)." *Journal of Membrane Science*, 507: 154–164. Elsevier. https://doi.org/10.1016/j.memsci.2016.02.008.

Shen, X., B. Gao, K. Guo, and Q. Yue. 2020. "Characterization and influence of floc under different coagulation systems on ultrafiltration membrane fouling." *Chemosphere*, 238. https://doi.org/10.1016/j.chemosphere.2019.124659.

Shi, X., G. Tal, N. P. Hankins, and V. Gitis. 2014. "Fouling and cleaning of ultrafiltration membranes: A review." *Journal of Water Process Engineering*, 1: 121–138. Elsevier Ltd. https://doi.org/10.1016/j.jwpe.2014.04.003.

Sillanpaa, M. 2015. *Natural Organic Matter in Water*. 1st ed. Oxford, UK: Butterworth-Heinemann.

Tang, C. K., N. M. Peleato, P. R. Bérubé, and R. C. Andrews. 2019. "Impact of low coagulant dosages on protein fouling of ultrafiltration membranes." *Journal of Water Process Engineering*, 31: 100801. https://doi.org/10.1016/j.jwpe.2019.100801.

Tian, J. yu, M. Ernst, F. Cui, and M. Jekel. 2013. "Correlations of relevant membrane foulants with UF membrane fouling in different waters." *Water Research*, 47 (3): 1218–1228. Elsevier Ltd. https://doi.org/10.1016/j.watres.2012.11.043.

Walker, S., and R. M. Narbaitz. 2016. "Hollow fiber ultrafiltration of Ottawa River water: Floatation versus sedimentation pre-treatment." *Chemical Engineering Journal*, 288: 228–237. Elsevier B.V. https://doi.org/10.1016/j.cej.2015.11.064.

Wang, J., S. Pan, and D. Luo. 2013. "Characterization of cake layer structure on the microfiltration membrane permeability by iron pre-coagulation." *Journal of Environmental Sciences*, 25 (2): 308–315. https://doi.org/10.1016/S1001-0742(12)60025-4.

Waterman, D. 2008. "Bench Scale Analysis of Ultrafiltration Membranes for Investigation of Fouling by Natural Organic Matter in Surface Waters." *Analysis*. M.A.S.c Thesis, University of Ottawa.

Wray, H. E., R. C. Andrews, P. R. Bérubé, H. E. Wray, R. C. Andrews, and P. R. Bérubé. 2014. "Ultrafiltration organic fouling control: Comparison of air-sparging and coagulation." 106 (2).

Xu, B., and R. M. Narbaitz. 2016. "Improved membrane pretreatment of high hydrophobic natural organic matter (NOM) waters by floatation." *Journal of Membrane Science*, 518: 120–130. Elsevier. https://doi.org/10.1016/j.memsci.2016.02.056.

Yu, W., J. Qu, and J. Gregory. 2015. "Pre-coagulation on the submerged membrane fouling in nano-scale: Effect of sedimentation process." *Chemical Engineering Journal*, 262: 676–682. https://doi.org/10.1016/j.cej.2014.09.102.

Zularisam, A. W., A. Ahmad, M. Sakinah, A. F. Ismail, and T. Matsuura. 2011. "Role of natural organic matter (NOM), colloidal particles, and solution chemistry on ultrafiltration performance." *Separation and Purification Technology*, 78 (2): 189–200. Elsevier B.V. https://doi.org/10.1016/j.seppur.2011.02.001.

CHAPTER 4

Reduced Low-Pressure Membrane Fouling by Inline Coagulation Pretreatment for a Colored River Water

Context: Chapter 3 investigated the performance of alternative coagulation pretreatment strategies for low-pressure membranes including coagulation/flocculation/sedimentation (CF-SED), coagulation/flocculation/dissolved-air-flotation (CF-DAF), and inline coagulation (C-IN) using a single outside-in hollow-fiber polyvinylidene fluoride (PVDF) ultrafiltration membrane. In the present chapter, this analysis is extended by comparing the performance of these same pretreatment strategies using the identical colored river water, but a different membrane type with an inside-out tubular multichannel configuration and polyethersulfone base polymer. Although the relative performance of these alternative coagulation-based pretreatment strategies has been evaluated to some extent by previous authors, all three strategies had not been directly compared using the same source water prior to the work presented in this thesis. Furthermore, the importance of membrane type (i.e., configuration and material properties) on the relative performance of these pretreatment strategies remains insufficiently understood. Accordingly, this chapter seeks to evaluate whether the performance of alternative coagulation-based pretreatment strategies is consistent across different membrane types, providing insight into the role of membrane characteristics on determining pretreatment effectiveness.

The work in this chapter was performed prior to fast-tracking to the Ph.D. program and was initially intended to be a part of the requirements of the M.A.Sc degree.

A version of this manuscript has been published as:

Ladouceur, J.D., & Narbaitz, R.M. (2022). Reduced low-pressure membrane fouling by inline coagulation pretreatment for a colored river water. *Membranes, 12(11), 1028*.

The supporting information for this chapter is presented in Appendix E of this thesis.

List of Abbreviations

CEB	Chemically enhanced backwash
CF-DAF	Coagulation/flocculation/dissolved air flotation
CF-SED	Coagulation/flocculation/sedimentation
CI	Confidence interval
C-IN	Inline coagulation
CIP	Clean-in-place
DAF	Dissolved air flotation
DOC	Dissolved organic carbon
DOM	Dissolved organic matter
FR_{hr}	Hydraulically reversible fouling rate
FR_{hirr}	Hydraulically irreversible fouling rate
HPO	Hydrophobic
LPM	Low-pressure membrane
NOM	Natural organic matter
ORW	Ottawa River water
ORW_s	Summer season Ottawa River water
ORW_w	Winter season Ottawa River water
PES	Polyethersulfone
PVDF	Polyvinylidene fluoride
SUVA	Specific ultraviolet absorbance at 254nm
TMC	Tubular multichannel
TMP	Transmembrane pressure
TOC	Total organic carbon
UF	Ultrafiltration
WTP	Water treatment plant
ZP	Zeta potential

List of Variables

Variable	**Description**
FR_{CEB}	Irreversible fouling rate over CEB cycle (mBar h^{-1})

FR_{CIP}	Irreversible fouling rate over CIP cycle (mBar h^{-1})
FR_{hirr}	Hydraulically irreversible fouling rate (mBar h^{-1})
FR_{hr}	Hydraulically reversible fouling rate (mBar h^{-1})
$nTMP$	Normalized transmembrane pressure (dimensionless)
t_3	Length of one CIP cycle (h)
t_k	Filtration time at the start of CEB cycle *k*
t_{k-1}	Filtration time following CEB cycle *k-1*
$t_{n-1,f}$	Filtration time at the end of cycle *n-1*
$t_{n-1,i}$	Filtration time at the start of cycle *n-1*
TMP_3	TMP (mBar) following CIP cleaning on day 3
TMP_o	Clean water steady-state transmembrane pressure (mBar)
TMP_k	TMP (mBar) following CEB cleaning on day *k* (for *k* =1, 2)
TMP_{k-1}	TMP (mBar) following pure water permeability testing on day *k-1* (for *k* = 1) and following CEB cleaning on day *k-1* (for *k* = 2)
$TMP_{n-1,f}$	TMP at the end of cycle *n-1* (mBar)
$TMP_{n,i}$	TMP at the beginning of cycle *n* (mBar)
$TMP_{n-1,i}$	TMP at the beginning of cycle *n-1* (mBar)
TMP_t	Transmembrane pressure at time *t* (Bar)

4.1. Abstract

Drinking water treatment (DWT) using low-pressure membranes (LPM) has become increasingly popular due to their many reported advantages compared to conventional technologies. Productivity decline due to fouling has prevented LPMs from becoming the technology of choice in DWT, however, coagulation pretreatment either with or without particle separation mitigates fouling phenomena. The effectiveness of coagulation/flocculation/sedimentation (CF-SED), coagulation/flocculation/dissolved-air-flotation (CF-DAF), and inline coagulation (C-IN) as technologies for pretreatment of feed water has rarely been investigated using the same water source. In this study, CF-SED, CF-DAF, and C-IN are directly compared as pretreatment of a tubular multi-channel ultrafiltration (UF) membrane using the same highly colored river water. Three-day long filtration tests were performed using an automated bench-scale filtration apparatus

with an inside-out configuration. Although CF-DAF had the greatest removal of dissolved organic matter (DOM) and hydrophobic organics, CF-SED pretreatment resulted in a similar level of total fouling. Compared to CF-DAF and CF-SED, C-IN pretreatment resulted in lower fouling. The hydraulic and chemical reversibility of C-IN fouling was seen to be strongly influenced by the feed water zeta potential, suggesting the importance of floc electrostatic and morphological characteristics on inline coagulation performance.

4.2. Introduction

Low-pressure membranes (LPMs) have become increasingly popular in drinking water treatment (DWT) due to their effectiveness in particle and bacterial separation (Anis et al. 2019; Li et al. 2019; Malkoske et al. 2020; Peters et al. 2021; Xu et al. 2022). Since the late 1990s, technology advancement, increasingly stringent treated water regulations, increased water demand and scarcity, and degrading source water quality have helped to drive the growth of LPM technologies for DWT (Amjad et al. 2015; Kinser 2021; Pearce 2011). This growth has been aided by the fact that LPMs are known to be less susceptible to raw water quality fluctuations when compared to deep bed filters and produce a superior quality effluent (Crittenden et al. 2012; Kinser 2021). Despite their numerous advantages, the more widespread implementation of LPMs in DWT remains a challenge due to membrane fouling, which results in a progressive worsening of membrane productivity, higher energy costs, and a potential reduction in membrane lifespan (Hatt et al. 2011; Kimura et al. 2014; Sun et al. 2013). Particulate matter, dissolved organic and inorganic substances, and microorganisms (i.e., biofouling) have all been reported to cause LPM productivity decline (Arhin et al. 2016; Guo et al. 2012). Although synergistic fouling by particulates and natural organic matter (NOM) has been reported in the literature (Jermann et al. 2008; Schulz et al. 2016), NOM has been identified by many researchers as the principle foulant of LPMs (Amy 2008; Buisson et al. 2004; Fan et al. 2001). Accordingly, there has been a concerted effort to develop membranes/membrane materials, as well as best-practices for LPM operation, which help to alleviate fouling by NOM. Concerning LPM best-practices, the most common approaches followed have been: a) adjustment of operating conditions (such as reduction of membrane flux or alteration/optimization of membrane cleaning strategies) (Ehsani et al. 2021; Hatt et al. 2011; Lee et al. 2008; Lin et al. 2010; Miller et al. 2014; Porcelli and Judd 2010); and b) implementation of feed water pretreatment processes (Farahbakhsh et al. 2004; Gao et al. 2011). This article will

consider the latter approach.

The selection of a given pretreatment strategy will depend on cost, considerations of integrated design, and most importantly on the raw water quality (Ang et al. 2015; Kumar and Ismail 2015). The selection is further complicated when LPM operating conditions and material/configuration characteristics are considered (Aly 2015). For surface waters low in particulate and organic matter, LPM facilities can often efficiently operate without the use of any pretreatment in a scheme known as direct filtration (Côté et al. 1998; Schneider and Freeman 2005; Thompson 2001). Higher particulate and/or organic concentrations, typical of many highly colored river waters, are problematic for LPM systems. For such waters, pretreatment is often necessary to maintain stable and economic operation as well as to achieve enhanced removals of contaminants (i.e., disinfection by-product precursors) within the framework of an integrated design (Moon et al. 2009; Zydney and Zeman 1996). Amongst numerous possible alternatives, pre-coagulation is the most commonly employed pretreatment approach for controlling LPM membrane fouling due to its relative low cost, its reported effectiveness, and its familiarity to plant operators (Fabris et al. 2007; Farahbakhsh et al. 2004; Gao et al. 2011; Huang et al. 2009; Peters et al. 2021). Pre-coagulation of LPM feeds has been performed both with and without particle separation processes (Gao et al. 2011; Liang et al. 2008). For concentrations of particles and/or organics resulting in a moderate fouling load on the membrane surface, coagulation/flocculation without particle separation (i.e., inline coagulation (C-IN)) can be employed before the LPM (Ding et al. 2021; Ma et al. 2020). If elevated NOM or highly variable turbidity levels exist in the source water, then coagulation/flocculation/sedimentation (CF-SED) is often considered for feed water pretreatment (American Water Works Association 2011; Thompson 2001). For algal impacted waters, dissolved air flotation (DAF) may be selected as the pretreatment separation process as it is more adept for the removal of low-density molecules (like algae) than sedimentation and can accomplish the removal in a smaller footprint (Edzwald and Haarhoff 2012; Teixeira and Rosa 2006).

Feed water pretreatment by C-IN has garnered increased attention over the past decade (Long et al. 2021; Ren et al. 2021; Teng et al. 2020), likely due to the cost savings its offers water purveyors through its reduction in facility footprint (Ding et al. 2016; Lebeau et al. 1998). This is achieved through elimination of the flocculation and sedimentation basins, which are not required since the flocs are delivered to the membrane surface and their size needs only to be larger than

the membrane pore, not settleable (Jung and Kang 2003; Keucken et al. 2017; Naim et al. 2014). Compared to direct filtration, several authors have found that C-IN pretreatment can mitigate irreversible membrane fouling (Kamińska et al. 2020; Ratajczak et al. 2012). Some studies have even reported improved performance at sub-optimal coagulant dosages as low as 0.2 mg L^{-1} as alum (Peleato et al. 2017; Tabatabai et al. 2009; Wray et al. 2014). The relative performance of C-IN compared to other pretreatment approaches, however, has not been extensively investigated. A limited number of studies comparing CF-DAF and C-IN (Braghetta et al. 1997) or CF-SED and C-IN (Amjad et al. 2015; Jang et al. 2005; Yu et al. 2015) are available in the literature, but present conflicting results. Amjad et al. (2015), who compared C-IN and CF-SED, and Braghetta et al. (1997), who compared CF-DAF and C-IN, both found that the C-IN pre-treated water had a higher fouling potential compared to waters whose pretreatment involved a particle separation step. In contrast, Yu et al. (2015) reported that CF-SED pretreatment resulted in the development of a dense cake layer of low porosity which gave rise to a rapid increase in transmembrane pressure (TMP) compared to C-IN pretreatment.

Although there have been number of studies which investigate CF-SED (Liang et al. 2008; Ma et al. 2020) and CF-DAF (Amaral et al. 2013; Goh et al. 2010) pretreatments individually, there remains a very limited number of research studies that directly compare their performance for LPM fouling mitigation. The earliest studies comparing CF-DAF and CF-SED, which considered pressure-driven inside-out polyethersulfone (PES) hollow fiber membranes and a colored river water, reported that CF-DAF resulted in somewhat better organics removal (both in terms of bulk dissolved organic carbon (DOC) and specific ultraviolet absorbance at 254 nm (SUVA)) and reduced membrane fouling compared to CF-SED (Walker and Narbaitz 2016; Xu and Narbaitz 2016). In our recent work (Chapter 3) using the same highly colored river water and a high permeability pressure-driven outside-in polyvinylidene fluoride (PVDF) hollow fiber membrane, it was shown that, although CF-DAF pretreatment yielded slightly better removal of organics, both pretreatment schemes (i.e., CF-SED and CF-DAF) resulted in very similar levels of fouling (see Chapter 3). The study also showed that C-IN pretreatment led to greater fouling than CF-SED and CF-DAF pretreatment, likely due to the higher foulant loads imparted on the membrane surface.

Based on the above findings, it is of interest to ascertain whether the differences in LPM fouling behavior following pretreatment of highly colored waters were a result of the distinct

membrane material/configuration used in each study. Accordingly, the objectives of this study are to: a) directly compare the fouling of a different PES UF membrane following CF-SED, CF-DAF, and C-IN pretreatment; b) investigate the suitability of sub-optimal (based on jar testing) coagulant dosages on the performance of the integrated C-IN-UF membrane system; and c) assess the impact of seasonality on C-IN pretreatment performance.

4.3. Materials and Methods

4.3.1. Raw Water

Ottawa River Water (ORW) was selected for the challenge water in order to minimize the effects of water quality differences when comparing to the results of our previous study (Chapter 3). ORW is typical of northern waters in the Canadian context but also in many regions throughout the globe (Goslan et al. 2004; Irvine et al. 2019; Klante et al. 2021; White et al. 2003). Furthermore, ORW is also representative of waters impacted by climate change (Dang et al. 2010; Sillanpaa 2015), which are characterized by elevated NOM and color levels due to increased flood and drought cycles as well as changing precipitation patterns (Johansson et al. 2010; Sillanpaa 2015). Raw ORW samples were collected at the intake of the Britannia water treatment plant (WTP) (Ottawa, Canada). ORW samples were collected during both the winter (ORW_w) and summer (ORW_s) season on days where the water quality was representative of average conditions (i.e., not following large rainfall or runoff events). The water samples were transferred to a walk-in refrigerator immediately following collection and were stored in the dark at 4 °C to minimize biological degradation. Prior to the filtration experiments, the water samples were placed in the laboratory for 24 h and allowed to reach room temperature (~20 °C) (Kimura et al. 2015). Therefore, any observed difference in performance during the seasonal assessment is a result of water quality differences and not temperature. The ORW_w sample was used to evaluate membrane fouling for raw ORW, CF-SED, CF-DAF and C-IN pretreated waters while an evaluation of seasonality effects using ORW_s was limited to C-IN pretreatment.

4.3.2. Filtration Apparatus and Membrane Module

An automated bench-scale filtration apparatus (Fig. 4.1) was used to investigate membrane fouling following pretreatment by different methods. The filtration apparatus possessed two subsystems (filtration and backwash), each of which could be independently programmed using a LabView

software (National Instruments, TX, USA).

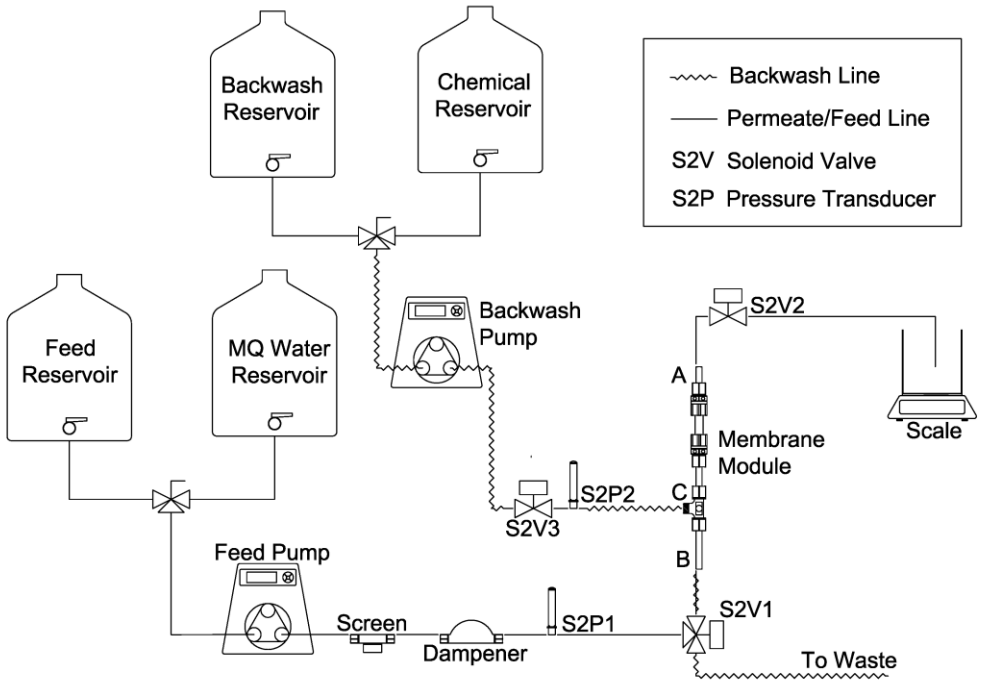
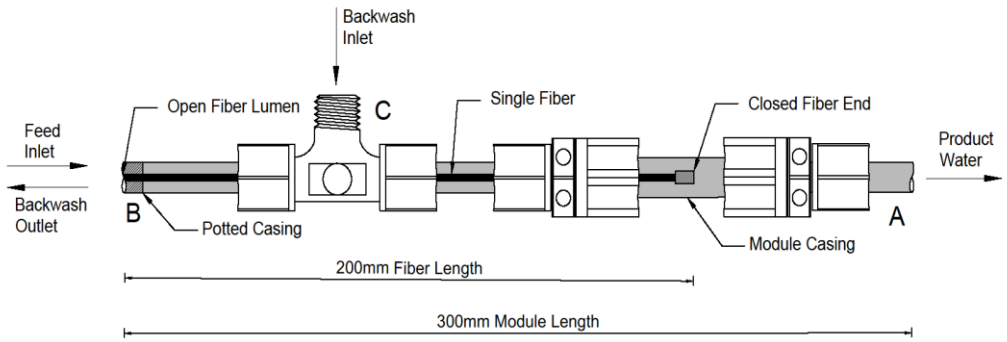


Fig. 4.1. Inside-out filtration apparatus.

Pressure-driven inside-out, dead-end membrane modules (Fig. 4.2a) were fabricated using tubular multi-channel (TMC) membrane fibers. The modules housed a single hydrophilized PES fiber (Multibore, Inge GmbH, Germany) and operated with the same inside-out flow pattern as used by the manufacturer in its full-scale modules. The tubular fibers have an outside diameter of approximately 4 mm and consist of 7 concentrically positioned capillaries (each capillary with a diameter of 0.9 mm) with a 300 µm porous foam-like support layer between them (Fig. 4.2b). The pure water permeability of a new membrane fiber is reported to be 700-1,000 L m^{-2} h^{-1} bar^{-1} (Inge GmbH 2020).

(a)



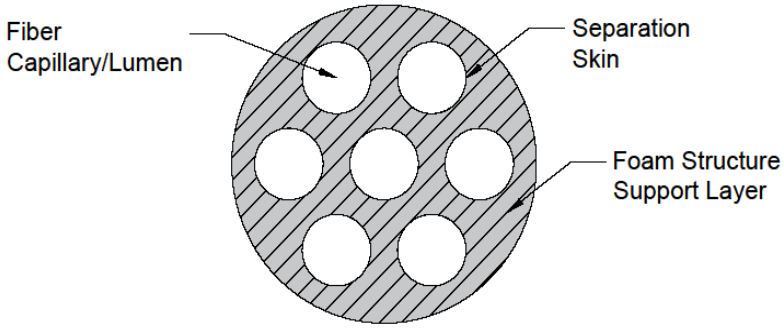


Fig. 4.2. Pressure-driven inside-out membrane: **(a)** module; **(b)** fiber cross-section.

Modules were constructed in-house using a single TMC fiber cut to a total length of 20 cm yielding a surface area of approximately 35 cm^2 (Fig. 4.2a). The fibers were potted within the 30 cm long module using a high strength epoxy resin. The potting sealed the annular cavity space between the membrane fiber and the module casing at the module entrance (end B in Fig. 4.2a) as well as the fiber capillaries at the module exit (end A in Fig. 4.2a). The highly porous foam-like support structure (hatched region in Fig. 4.2b) located between the fiber capillaries at the module entrance also needed to be sealed to force the challenge water to enter the capillaries (as opposed to the foam structure directly). This was accomplished by placing a very fine layer of epoxy resin on the face of the fiber (hatched area in Fig. 4.2b) at the module entrance with the help of a 21-gauge needle attached to a compressed air line. The needle was inserted into the capillary of the membrane fiber at end A (Fig. 4.2a), with the resulting air flow ensuring that epoxy did not seal the capillary entrance on the membrane face. The potting process forced the challenge water to enter the fiber capillaries at end B (Fig. 4.2a), cross the separation skin and pass through the foam-like support structure, prior to exiting the module at end A (Fig. 4.2a) for collection and analysis. Stereoscopic images (Stemi 305, Carl Zeiss, Germany) verifying the effectiveness of the potting process are shown in Fig. E.1. Each run was conducted using a newly potted module.

4.3.3. Pretreatment Methods

CF-SED pre-treated water was collected from the Britannia WTP's pilot facility, which draws water from the outlet of the sedimentation basin. To achieve optimal removal of organics at the time the winter CF-SED sample was collected, the Britannia WTP dosed 34 mg L^{-1} alum (3.09 mg L^{-1} as Al), 8.50 mg L^{-1} sulfuric acid (H_2SO_4), and 1.25 mg L^{-1} activated silicate (SiO_2) to reduce the raw water pH to around 6 ahead of hydraulic flocculation and inclined plate clarifiers. CF-DAF

pre-treated ORW was produced using a large volume bench-scale dissolved air flotation system (LB-DAF) (Gonzalez-Galvis and Narbaitz 2020) as local COVID-19 pandemic guidelines prevented access to the nearby full-scale Aylmer DAF facility. To best simulate the optimized conditions at the Aylmer WTP, raw ORW was conditioned using the same chemicals and dosages used at the full-scale facility (i.e., 37 mg L^{-1} alum (Kemira ALS) and 0.1 mg L^{-1} cationic polyacrylamide polymer (Superfloc C-492PWG, Kemira)). All flotation parameters were as recommended by the LB-DAF system developers (Gonzalez-Galvis and Narbaitz 2020).

C-IN pretreatment was simulated at the lab-scale using a batch-wise approach (Jung and Kang 2003; Peleato et al. 2017; Tang et al. 2019). Aliquots of raw ORW were placed in a 20 L baffled mixing tank and rapid mixed at G=296 s^{-1} for 2 min following the addition of sulfuric acid and alum. The pH was adjusted to a value of 6 to match that of the CF-SED pre-treated water and because it has previously been reported that optimal removal of organics could be achieved near this pH for ORW (Waterman 2008). Two different coagulant dosages were used: i) 34 mg L^{-1} as alum, which was the optimal coagulant dose for organics removal based on jar tests and was also the dose used at the Britannia WTP; and ii) 27 mg L^{-1} as alum (a 20% reduced dose). The latter dose was selected because Konieczny et al. (2009) found that for coagulation with alum, the lowest permeability decline was achieved at a 20% reduced coagulant dose compared to the optimal determined from jar testing. Furthermore, Choi and Dempsey (2004) found that the acidic under-dosed coagulation condition resulted in the lowest fouling resistance during filtration. It should be noted that the same coagulant doses were used during the winter and summer seasons for C-IN pretreatment for a consistent analysis. Following the rapid mix period, the mixer speed was reduced to provide a constant mean velocity gradient of 200 s^{-1}. Like Peleato et al. (2017) and Tang et al. (2019), this study provided continuous intense mixing to the coagulated feed water in order to prevent fluctuating feed water quality due to the settling of flocs.

4.3.4. Multi-day Filtration Test Protocol

Filtration conditions used in this study are similar to those used in our previous study (see Chapter 3) and are briefly described below. A three-day duration was selected for all experiments as longer duration filtration tests are reported to be more representative of full-scale behavior (Ayache et al. 2013; Walker and Narbaitz 2016). Filtration tests for raw ORW, as well as CF-DAF and CF-SED pre-treated waters, were conducted in replicate using winter water samples, while those evaluating

C-IN pretreatment during both seasons were limited to single runs. For all experiments the filtration flux was fixed at 80 L m^{-2} h^{-1}, which was chosen so that the membrane would operate in the subcritical range based on preliminary critical flux tests (Fig. E.2a) conducted using the flux stepping method proposed by Le Clech et al. (2003). Hydraulic backwashing was performed using reverse osmosis (RO) water after every 30 min filtration cycle. Each backwash cycle continued for a duration of 2 min at a flux of 300 L m^{-2} h^{-1} without air scouring. Chemically enhanced backwash (CEB) was performed daily using a 0.05 N NaOH + 50 mg L^{-1} Cl^- solution, which was optimized during preliminary testing (Fig. E.2b). The daily CEB cycle was divided into two components: in the first stage, the chemical solution was backwashed through the membrane module for a period of 20 min, which is typical for UF membrane facilities (Shi et al. 2014). In the second phase, the backwash feed line was switched from CEB chemicals to RO water and backwashing continued for 20 min to flush remaining chemicals and foulants from the module. Chemical clean-in-place (CIP) was performed at the end of every three-day test using the same protocol as CEB cleaning but with a more aggressive chemical solution of 0.1 N NaOH + 200 mg L^{-1} Cl^- solution. It is acknowledged that the CIP used in the present study has a much greater frequency and reduced intensiveness than those used in full-scale systems (Pearce 2011). Following CIP cleaning, pure water permeability tests were conducted for 1 hour using type 1 reagent grade water (Barnstead, MicroPure, ThermoFisher Scientific, Waltham, MA) to assess the permeability restoration. A summary of the operating conditions is presented in Table 4.1.

Table 4.1. Summary of Multi-day Testing Parameters.

Characteristic	**Value**
Pore Size, µm	0.02[1]
Permeability, L m^{-2} h^{-1} bar^{-1}	700-1000[1]
Fiber Material	h-PES[1]
Operation	Pressure driven inside-out
Filtration Flux, L m^{-2} h^{-1}	80
Backwash Flux, L m^{-2} h^{-1}	300
Filtration Cycle Duration, min	30
Backwash Cycle Duration, min	2
CEB Interval, day	1
CEB Chemicals	0.05 N NaOH + 50 mg L^{-1} Cl^-
CIP Interval, day	3
CIP Chemicals	0.1 N NaOH + 200 mg L^{-1} Cl^-

[1]Obtained from Inge GmbH (Inge GmbH 2020).

4.3.5. Membrane Performance Measures

4.3.5.1. Normalized TMP (nTMP) Profiles

Prior to each three-day filtration experiment, pure water permeability testing was conducted with each new membrane module until stability (as determined by TMP variation less than 5%) was reached (Howe et al. 2006). For each filtration test, the resulting TMP profiles were normalized against the initial clean water steady-state TMP value. Normalization was performed to reduce the effects of membrane variability when comparing the results following different pretreatment. Slight differences in the porosity, thickness, or pore size during the manufacturing process may result in slightly different clean membrane permeabilities (Crittenden et al. 2012). The nTMP was calculated using Eqn. (4.1).

$$nTMP = \frac{TMP_t}{TMP_o} \tag{4.1}$$

where TMP_t is the transmembrane pressure at time *t* (Bar) and TMP_o is clean water steady-state transmembrane pressure (Bar).

4.3.5.2. Fouling Rates

Hydraulically reversible and irreversible fouling rates (FR) were computed following the approach of Aly et al. (2021). The general form of the FRs is presented below and in the schematic diagram of Fig. E.3a).

$$FR_{hr} = \frac{TMP_{n-1,f} - TMP_{n,i}}{t_{n-1,f} - t_{n-1,i}} \tag{4.2}$$

$$FR_{hirr} = \frac{TMP_{n,i} - TMP_{n-1,i}}{t_{n-1,f} - t_{n-1,i}} \tag{4.3}$$

where FR_{hr} is the hydraulically reversible fouling rate (mBar h^{-1}), FR_{hirr} is the hydraulically irreversible fouling rate (mBar h^{-1}), $TMP_{n,i}$ is the measured TMP at the beginning of cycle *n* (mBar), $TMP_{n-1,f}$ is the measured TMP at the end of cycle *n-1* (mBar), $TMP_{n-1,i}$ is the measured TMP at the beginning of cycle *n-1* (mBar), and $t_{n-1,f}$ and $t_{n-1,i}$ are the end of cycle filtration time and the beginning of cycle filtration time, respectively. The fouling that is reversible in nature is therefore considered to be that which is recovered by the hydraulic backwash. The fouling that is hydraulically irreversible in nature is then determined as the difference between the initial TMP following hydraulic backwash and the initial TMP of the preceding cycle. The total fouling rate

(FR_{TOT}) is considered to be the sum of the hydraulically reversible and irreversible fouling rates. The analysis in the current study was based on the three-day average FR_{hr}, FR_{hirr}, and FR_{TOT} values. The fouling rates can also be determined for the chemically irreversible fouling, both following CEB and CIP cleanings, as shown in Eqn. (4.4) and Eqn. (4.5) below and in Fig. E.3b).

$$FR_{CEB} = \frac{TMP_k - TMP_{k-1}}{t_k - t_{k-1}} \quad (4.4)$$

where FR_{CEB} is the irreversible fouling rate following CEB (mBar h^{-1}), TMP_k is the measured TMP (mBar) following CEB cleaning on day k (for k =1, 2), TMP_{k-1} is the measured TMP (mBar) following pure water permeability testing on day *k-1* (for k = 1) and following CEB cleaning on day *k-1* (for k = 2), t_k and t_{k-1} are the filtration times (measured in h) corresponding to TMP_k and TMP_{k-1}, respectively. In this study t_k was every 22.5 h.

$$FR_{CIP} = \frac{TMP_3 - TMP_0}{t_3} \quad (4.5)$$

where FR_{CIP} is the irreversible fouling rate following CIP (mBar h^{-1}), TMP_{CIP} is the measured TMP (mBar) following CIP cleaning on day 3, TMP_0 is the measured TMP (mBar) following pure water permeability testing at the commencement of the test (i.e., day 0), and t_3 is the length of the CIP cycle which, in this study, was 67.5 h.

4.3.6. Analytical Methods

Raw and pre-treated ORW was analyzed for DOC, pH, zeta potential (ZP), turbidity, UV_{254}, and true color. Samples used for DOC and UV_{254} measurement were pre-filtered using a 0.45 µm PES membrane filter (Supor 47 mm, 60043, Pall, Mississauga, ON, Canada). The filter material was selected to minimize adsorption of organics, as recommended by Karanfil et al. (2003). A total organic carbon (TOC) analyzer (Pheonix 8000, Tekmar-Dohrmann, Cincinnati, OH, USA) was used for analysis of DOC according to Standard Method 5310/5310C, the UV-persulfate oxidation method (APHA et al. 2012). Ultraviolet absorbance was measured at a wavelength of 254 nm according to Standard Methods 5910/5910A (APHA et al. 2012) using a UV-Vis spectrophotometer (DR6000, Hach, Loveland, CO, USA). The feed water SUVA values were determined by dividing the UV_{254} absorbance by the DOC. ZP was measured with a zetasizer nano particle analyzer (Nano ZS Series, Malvern Instruments Ltd., Worcestershire, UK). Turbidity was measured according to Standard Methods 2130/2130B (APHA et al. 2012) using a Hach 2100AN nephelometric laboratory turbidimeter (4700100, Hach, Loveland, CO, USA). The pH of all

samples was measured using a benchtop meter (Symphony B10P, VWR, Mississauga, ON, Canada) and electrode (Red Rod, 89-321-580, VWR, Mississauga, ON, Canada).

4.4. Results

4.4.1. Water Quality

The measured water quality indicators for all raw and pre-treated waters are presented in Table 4.2. Raw ORW is characterized by its high true color, SUVA, and relatively high DOC. From the table, it can be seen that all pretreatments were effective in the removal of DOC, color, and UV_{254}, although to different extents. CF-DAF resulted in the greatest removal of organics (as measured by DOC) and hydrophobic (HPO) organics (as measured by SUVA), which is consistent with the findings of earlier studies with this river water (Xu and Narbaitz 2016). The propensity of CF-DAF pretreatment for removing HPO organics was also reported by Braghetta et al. (1997) and Wang et al. (2022), who proposed that enhanced HPO interaction occurs at the bubble surface in order to reduce its interface energy.

Although the mean DOC of the ORW_s and ORW_w samples were practically identical, the character of the two waters was notably different, especially in terms of hydrophobicity (as quantified in terms of SUVA and UV_{254}). The ORW_s sample had a UV_{254} absorbance value of 0.225 cm^{-1} yielding a SUVA of 3.41 L mg^{-1} m^{-1}, compared to 4.16 L mg^{-1} m^{-1} during the winter season. The true color of the ORW also dropped from 55.3 Pt. Co. units during the winter to 32.3 Pt. Co. units during the summer season. Concerning the C-IN pre-treated waters, several differences could be observed. Regardless of season, pre-coagulation at the 34 mg L^{-1} dose resulted in a higher feedwater turbidity compared to coagulation at 27 mg L^{-1}. For both seasons, pretreatment at 34 mg L^{-1} resulted in a lower residual DOC and UV_{254} levels compared to when 27 mg L^{-1} was used. It can also be observed that, compared to the winter season, C-IN pretreatment at both dosages during the summer resulted in a more HPI feed water (based on a reduced SUVA and UV_{254} absorbance).

Table 4.2. Water Quality Data for Raw and Pre-treated ORW

Parameter	Raw ORW		CF-DAF	CF-SED	C-IN (34 mg L^{-1})		C-IN (27 mg L^{-1})	
	Winter	**Summer**	**Winter**	**Winter**	**Winter**	**Summer**	**Winter**	**Summer**
Turbidity (NTU)	4.88 ± 0.01[a]	1.94 ± 0.01	0.591 ± 0.02	2.42 ± 0.01	9.11 ± 0.07	5.4 ± 0.01	8.15 ± 0.04	4.76 ± 0.03
pH (unit)	7.52 ± 0.02	7.70 ± 0.03	6.28 ± 0.02	6.08 ± 0.01	6.02 ± 0.01	5.99 ± 0.01	5.98 ± 0.03	6.05 ± 0.03
UV_{254} (cm^{-1})	0.276 ± 0.001	0.225 ± 0.001	0.042 ± 0.001	0.054 ± 0.001	0.051 ± 0.02	0.047 ± 0.01	0.058 ± 0.001	0.055 ± 0.001
True Color (Pt. Co.)	55.3 ± 0.5	32.3 ± 0.5	2.0 ± 0	2.3 ± 0.5	2.0 ± 0	2.0 ± 0	2.3 ± 0.3	3.3 ± 0.3
Zeta Potential (mV)	-22 ± 0.8	-19.3 ± 0.25	-6.31 ± 0.20	-7.23 ± 0.24	-6.21 ± 0.22	-5.48 ± 0.13	-15.17 ± 0.37	-8.69 ± 0.14
DOC (mg-C $L^{-1)}$	6.64 ± 0.02	6.58 ± 0.01	2.27 ± 0.01	2.67 ± 0.01	2.29 ± 0.01	2.33 ± 0.01	2.55 ± 0.01	2.63 ± 0.01
SUVA (L mg^{-1} m^{-1})	4.16	3.41	1.85	2.03	2.21	1.99	2.26	2.08
DOC Removal (%)	N/A	N/A	65.81	59.79	65.51	64.59	61.60	60.03
UV_{254} Removal (%)	N/A	N/A	84.78	80.43	81.52	79.11	78.98	75.56

[a]μ±95% Confidence Interval

4.4.2. Comparison of CF-SED, CF-DAF, and C-IN Pretreatment During Winter Season

The performance of the TMC membrane following pretreatment by CF-DAF, CF-SED, and C-IN is shown in Fig. 4.3a and Fig. 4.3b, which present the nTMP profiles for all ORW_w filtration tests. It should be noted that the CEB was performed daily (after 22.5 h of real filtration time), while the CIP was performed at the termination of each three-day test (after 67.5 h of filtration time). Additionally, while the TMP was measured every 2 s, the data in Fig. 4.3a and Fig. 4.3b was reduced to intervals of 7.5 min to facilitate interpretation and visualization. Direct filtration of raw ORW resulted in the greatest nTMP increase, reaching a final nTMP of 2.27 after three-days. Compared to direct filtration of ORW, CF-DAF and CF-SED pretreatment resulted in lower levels of membrane fouling, with final nTMPs of 1.60 and 1.49, respectively. Fig. 4.3b presents a comparison of the C-IN nTMP profiles with those of raw ORW during the winter season. At the end of the third day, C-IN pretreatment with 34 mg L^{-1} and 27 mg L^{-1} alum reached final nTMPs of 1.20 and 1.73, respectively. The order of increasing pretreatment effectiveness in terms of final nTMP is therefore: Raw ORW < C-IN (27) < CF-DAF < CF-SED < C-IN (34). It should be noted that, although the nTMP profile for CF-SED pretreatment in the current study was slightly lower than that of CF-DAF initially, the final nTMP values at the end of the three-day filtration tests were quite similar.

Selected three-day FRs are presented in Fig. 4.3c and Fig. 4.3d, while all of the rates are presented in Table E.2. CF-DAF and CF-SED pretreatments showed similar levels of total fouling (10.8 ± 0.61 versus 10.2 ± 0.55 mBar h^{-1}, respectively) despite CF-DAF pretreatment resulting in a feed water with the lowest residual DOC and SUVA, which is consistent with the results of our previous study (see Chapter 3).

A notable difference between the results of the current study and those of past studies using ORW (i.e., Chapter 3) is the performance of C-IN (34) pretreatment, which resulted in the smallest increase in nTMP compared to all other alternatives (including those with particle separation). It should be noted that the FR_{TOT} for C-IN (34) pre-treatment was not the lowest amongst all alternatives because FR_{TOT} does not incorporate the benefits of the daily CEB cleaning. If instead it had been calculated using the first and last nTMP values, then the order of the fouling rates would have matched that of the final nTMPs. Thus, the final nTMP is expected to be a better indicator of overall fouling performance compared to the FR_{TOT} as calculated in Table E.2. In summary, the most salient point of the tests conducted with ORW_w is that the C-IN (34) condition

performed even better than CF-SED and CF-DAF pretreatment.

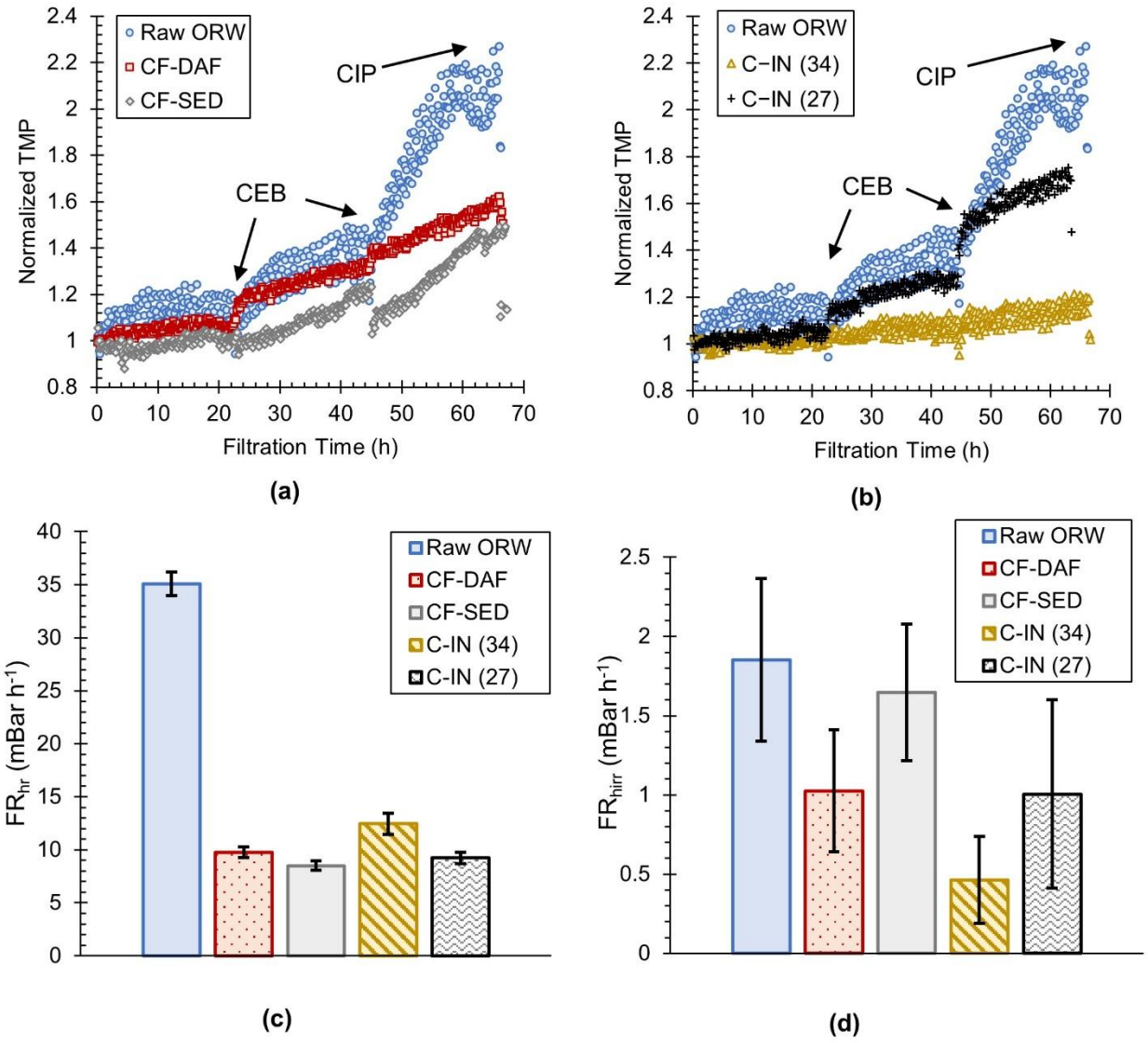


Fig. 4.3. Comparison of ORWw filtration tests: **(a)** Raw ORW, CF-SED, CF-DAF nTMP profile; **(b)** Raw ORW and C-IN nTMP profile; **(c)** Three-day average total FR; **(d)** Three-day average hydraulically irreversible FR.

As a reference, it should be noted that the Raw ORW FR_{hr} and FR_{hirr} values were in the same order of magnitude (35.1 ± 1.1 mBar h^{-1} and 1.85 ± 0.5 mBar h^{-1}) as those reported by Croft (2012) for ORW using a PVDF membrane.

4.4.3. C-IN Seasonality Assessment

To assess the effects of seasonal water quality differences on C-IN performance, ORW was sampled in both the summer and winter seasons. The nTMP profiles for C-IN pretreatment during both seasons at alum dosages of 27 mg L^{-1} and 34 mg L^{-1} are presented in Fig. 4.4a and Fig. 4.4b, respectively. According to these figures, the relative performance of C-IN pretreatment at two different doses was dependent on the season. The addition of 27 mg L^{-1} alum (final nTMP of 1.73) resulted in a steeper nTMP increase during the winter season compared to the summer (final nTMP of 1.28), although the greatest difference was only observed on the third day of operation. Furthermore, besides the increased FR_{hirr} observed for 27 mg L^{-1} pretreatment during the winter season (see Fig. 4.5b), the final nTMP was exacerbated by the high FR_{CEB} values, which will be discussed later. At the 34 mg L^{-1} alum dose, the C-IN pretreatment during the winter season resulted in a lower final nTMP (1.20) compared to the summer season (1.34). The better performance of C-IN pretreatment at 27 mg L^{-1} compared to 34 mg L^{-1} during the summer season suggests that the coagulant dose for fouling mitigation does not necessarily correspond to that which is better for organics/turbidity removal (See Table 4.2). This is in agreement with the findings of Kimura et al. (2008) and Ding et al. (2016).

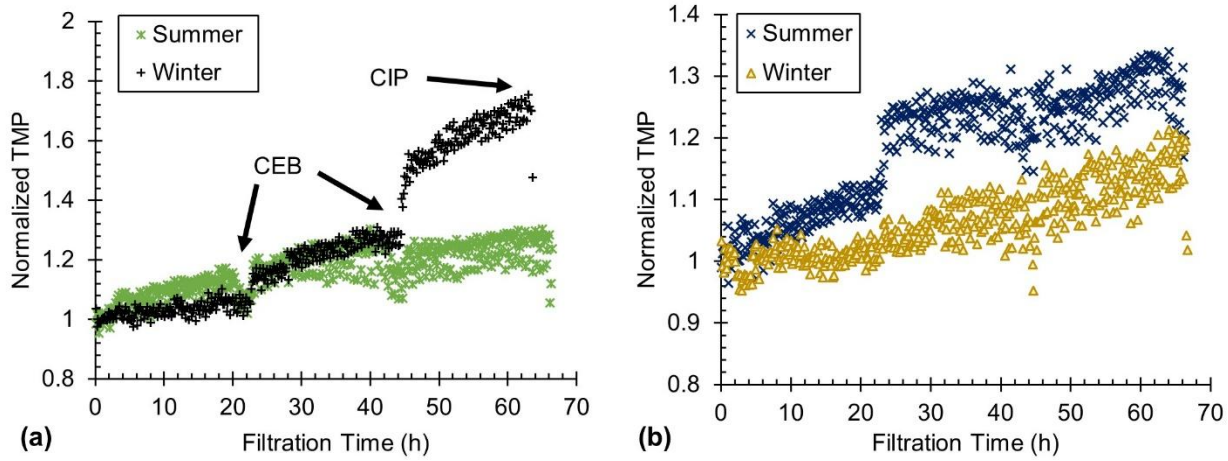


Fig. 4.4. Comparison of summer and winter C-IN pretreatment at alum dose of: **(a)** 27 mg L^{-1}; **(b)** 34 mg L^{-1}.

For a further comparison of the effects of seasonality on C-IN performance, the hydraulically reversible and irreversible fouling rates for C-IN (34) and C-IN (27) pretreated

waters during the summer and winter seasons are presented in Fig. 4.5a and Fig. 4.5b, respectively. C-IN pretreatment at 34 mg L^{-1} during both the summer and winter season results in hydraulically reversible fouling rates which were statistically the same (overlapping 95% confidence intervals (CIs). Although the mean FR_{hirr} is lower for C-IN (34) during summer season compared to the winter season, the 95% CIs are overlapping, and the observed difference in final nTMP can be attributed to the differences in chemically reversible foulants. It can also be observed from Fig. 4.5a and Fig. 4.5b that there is a much greater difference in seasonal fouling performance (in terms of nTMP, FR_{hr}, and FR_{hirr}) for C-IN pretreatment at 27 mg L^{-1} compared to 34 mg L^{-1}. While the mean FR_{hr} and FR_{hirr} values were similar during both the summer and winter season for C-IN pretreatment at 34 mg L^{-1}, pretreatment at 27 mg L^{-1} during the winter season resulted in a significantly lower FR_{hr} and a higher mean FR_{hirr} than during the summer season. In Fig. 4.5c the FR_{hirr} could be quadratically related to the feed water ZP for C-IN pretreatment, although it must be acknowledged that the inherent variability associated with the FR_{hirr} makes the relationship not so rigidly defined. Maeng et al. (2017) similarly reported a quadratic relationship between feed ZP and the hydraulically irreversible fouling resistance, with minimal resistance found at slightly negative ZP values.

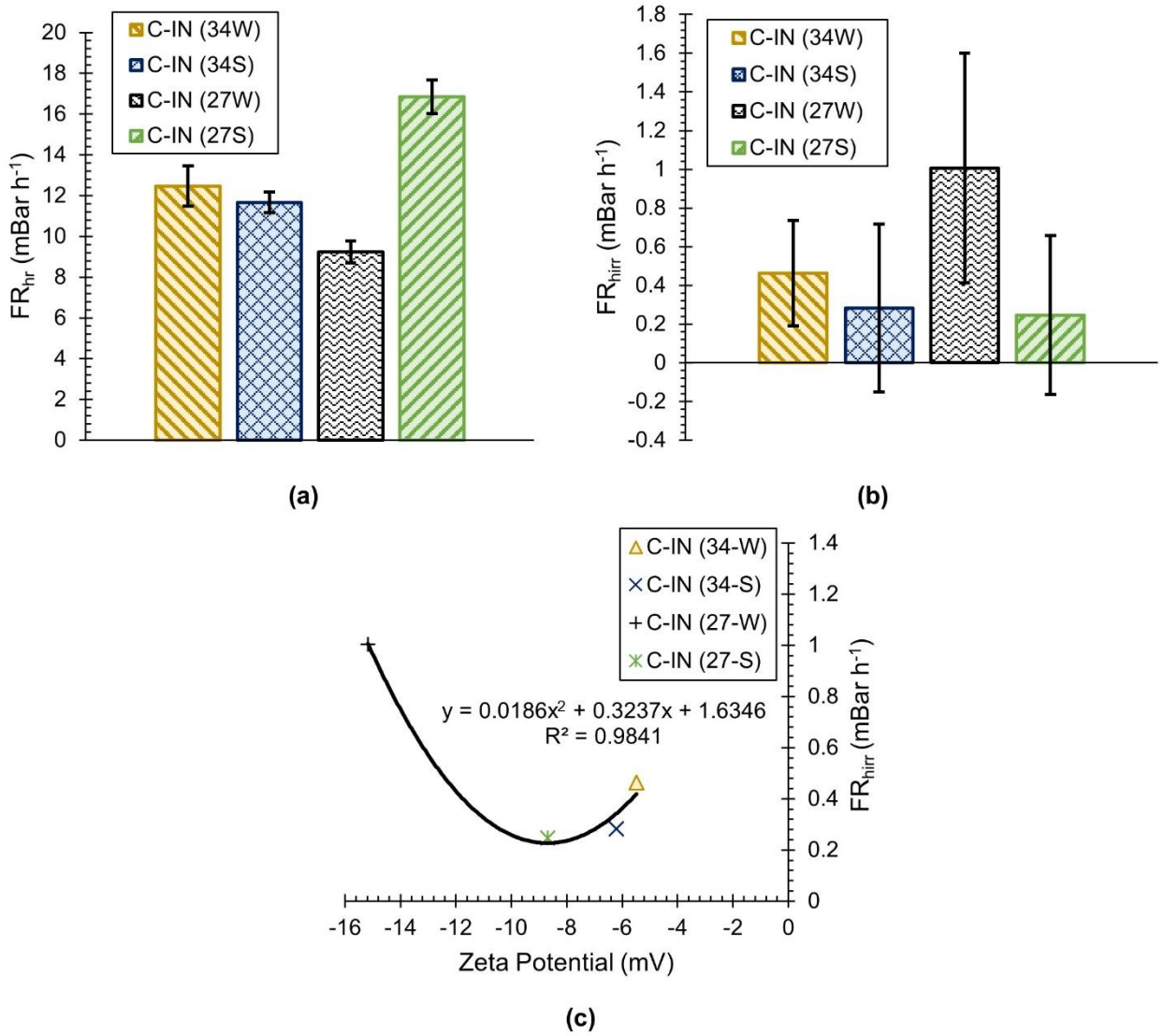


Fig. 4.5. Comparison of seasonal C-IN fouling rates: **(a)** hydraulically reversible; **(b)** hydraulically irreversible; **(c)** relationship between ZP and hydraulically irreversible.

A possible explanation for the worsened FR_{hirr} performance of C-IN (27W) pretreatment in the current study is the floc characteristics and the nature of their deposition and transport. Based on the ZP measures (Table 4.2), it appears that for the same coagulation conditions it is more difficult to achieve optimal conditions during the winter season than during the summer. This is especially true for C-IN (27) pretreatment where the ZP during the winter season was -15.17 mV, while in the summer season reached -8.69 mV. The increased difficulty in achieving optimal conditions during the winter season may be due to the greater feed water turbidity levels (i.e., 4.88

NTU in winter and 1.94 NTU in summer), as Black and Hannah reported that the alum dose required for charge neutralization was significantly affected by the exchange capacity (and hence concentration) of the particle matrix (Black and Hannah 1961). Additionally, Sharp et al. (2006) reported that the higher charge density of HPO organics (which were present in greater quantity during the winter season for ORW according to SUVA measures) necessitates higher coagulant dosages for optimum conditions of charge neutralization. Given the discussion above and the fact that the summer ORW had a lower turbidity and lower HPO NOM content, it is therefore likely that pretreatment at 27 mg L^{-1} is closer to the optimal coagulant dose during the summer than during the winter.

The higher magnitude ZP that results for C-IN (27W) is thought to lead to the development of small-sized flocs of low fractal dimension (i.e., loose in nature) (Wang et al. 2013). It has been shown by others using the multi-channel PES membrane (Arkhangelsky et al. 2011; Lerch et al. 2007) that small flocs will deposit more or less homogenously along a greater length of the capillary wall compared to large flocs, which are deposited principally at the capillary dead-end. Therefore, a greater proportion of the fiber capillary is coated by a flocculated suspension which is highly susceptible to compression – this likely explains the rapid TMP increase that occurred following the daily CEB (Fig. 4.4a). Lorenzen et al. (2017) also reported that the cake compressibility greatly increased for conditions of higher magnitude ZP. In contrast, the more favorable conditions of ZP reported during the summer season and C-IN (34) pre-treatment during the winter season are thought to have resulted in the formation of larger sized flocs which were deposited at the capillary dead-end. The portion of the fiber affected by flocculated irreversible foulants is thus likely very small, with the remainder of the fiber length experiencing minimal relative flux decline.

Fig. 4.6 presents the correlation between ZP and the chemically irreversible fouling rates following CEB and CIP cleaning (i.e., FR_{CEB} and FR_{CIP}). In Fig. 4.6a, a moderate correlation exists ($R^2 = 0.7623$) relating lower magnitude FR_{CEB} to lower magnitude feed water ZP. From Fig. 4.6b, a relatively stronger correlation ($R^2 = 0.8946$) is observed demonstrating reduced FR_{CIP} at lower magnitudes of feed water ZP. Electrostatic and morphological differences in floc character are the likely reason behind the observed behavior. Kim (2015) investigated the impact of calcium and polymer (pDADMAC) addition to a high SUVA (> 5 L mg^{-1} m^{-1}) synthetic water ahead of LPM filtration. In this last study it was also reported that the chemical reversibility of fouling was

greatest at low magnitudes of ZP, which were achieved through increased polymer and calcium addition (Kim 2015). Kim (2015) hypothesized reduced electrostatic repulsion facilitated coiling of the humic NOM molecules, which produced flocs of higher fractal dimension and greater density, which were more amenable to removal by hydraulic and chemical cleaning.

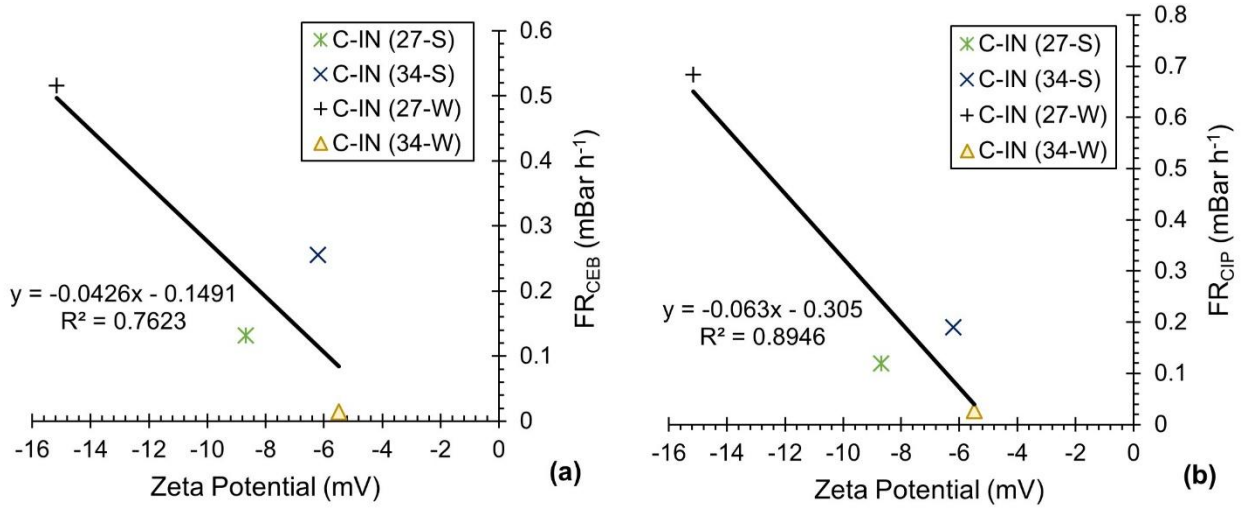


Fig. 4.6. Relationships between zeta potential and chemically irreversible fouling: **(a)** following CEB; **(b)** following CIP.

4.5. Discussion

For ORW_W and this membrane type, C-IN pretreatment at 34 mg L^{-1} was found to be the most suitable pretreatment alternative. This finding suggests that membrane material/type is critical in the selection of an appropriate pretreatment regime, as in our previous study (which used ORW from the same season but a different membrane type) C-IN pretreatment performed worse than both CF-SED and CF-DAF (see Chapter 3). The importance of membrane material/type is further supported by the fact that for the PVDF membrane used in our previous study the hydraulically irreversible fouling was strongly correlated with the SUVA, while in the current study no such relationship existed (see Fig. E.4). Therefore, for the same water, it can be concluded that the relative performance of a given pretreatment is uniquely dependent on the membrane material/type.

For economic long-term performance of the membrane, control of the hydraulically and chemically irreversible fouling is critical (Yamamura et al. 2007). The pronounced seasonal

differences in membrane performance observed in the current study suggest that C-IN pretreatment will likely benefit from continuous process control/optimization throughout the year. For C-IN pretreatment of ORW, the FR_{hirr} as well as both the FR_{CEB} and FR_{CIP} seem to be reasonably well correlated with the feed water ZP. These correlations between ZP and measures of irreversible fouling indicate that ZP is likely a critical parameter that may be used for process control. Future research studies should investigate the implementation of online ZP instrumentation for optimized control of C-IN pretreatment of LPMs. Such real-time monitoring has the potential to lead to significant savings in energy, chemical, and sludge disposal costs (Yoo 2018).

4.6. Conclusions

In this study, a PES multi-channel UF membrane was used to directly compare the performance of CF-DAF, CF-SED, and C-IN pretreatment for LPM fouling mitigation in the treatment of a high color, high DOC river water. The main findings for the membrane/membrane configuration used in this study are summarized as follows:

1. For the winter water samples, C-IN pretreatment at 34 mg L^{-1} could more effectively mitigate membrane fouling compared to CF-DAF and CF-SED. This is in contrast to the findings of previous studies using the same highly colored river water but a different membrane type. This finding is an indication of the uniqueness of the interaction between membrane material/configuration and feed water quality and points to the necessity for preliminary testing when verifying the impact of pretreatment for a given membrane.
2. The chemical reversibility of fouling for C-IN tests seems to be strongly influenced by the ZP of the challenge waters. For C-IN conditions with lower magnitude ZP, irreversibility of fouling following CEB and CIP was minimized.
3. Distinct seasonal differences in C-IN performance were observed. For the winter season, C-IN pretreatment at a high dose led to reduced fouling, while for the summer season the low dose performed better. The better performance at the low dose is linked to the lower turbidity and HPO NOM concentrations in the summer water. The effect of these intra-annual variations should be the subject of future research.
4. CF-SED pretreatment of the highly colored ORW resulted in a similar level of fouling as CF-DAF using the h-PES TMC UF membrane. This was despite the fact that CF-DAF exhibited preferential removal of DOC and HPO organics (as measured by SUVA).

4.7. Acknowledgments

The authors wish to thank the Natural Sciences and Engineering Research Council of Canada for their scholarship to the lead author as well as their support through the Discovery Grant program. Furthermore, our gratitude is extended to Andy Campbell at the Britannia Water Purification Facility for his assistance during the complexities of the COVID-19 pandemic, Catherine Brosseau from Kemira for providing the study coagulants, and Dr. Peter Berg of Inge AG for providing membrane fibers.

4.8. References

Aly, S. 2015. “Pre-Treatment Evaluation Prior to Ultrafiltration in Secondary Effluent Treatment for Water Reuse.” Ph.D. Thesis, University of Waterloo.

Aly, S. A., W. B. Anderson, and P. M. Huck. 2021. “In-line coagulation assessment for ultrafiltration fouling reduction to treat secondary effluent for water reuse.” *Water Science and Technology*, 83 (2): 284–296. https://doi.org/10.2166/wst.2020.571.

Amaral, P. A. P. do, L. A. Coral, M. E. Nagel-Hassemer, T. J. Belli, and F. R. Lapolli. 2013. “Association of dissolved air flotation (DAF) with microfiltration for cyanobacterial removal in water supply.” *Desalination and Water Treatment*, 51 (7–9): 1664–1671. https://doi.org/10.1080/19443994.2012.715128.

American Water Works Association. 2011. *Water Quality & Treatment: A Handbook on Drinking Water*. Edited by J. K. Edzwald. 6th ed. New York, NY: McGraw-Hill.

Amjad, H., Z. Khan, and V. V. Tarabara. 2015. “Fractal structure and permeability of membrane cake layers: Effect of coagulation–flocculation and settling as pretreatment steps.” *Separation and Purification Technology*, 143: 40–51. https://doi.org/10.1016/j.seppur.2015.01.020.

Amy, G. 2008. “Fundamental understanding of organic matter fouling of membranes.” *Desalination*, 231 (1–3): 44–51. https://doi.org/10.1016/j.desal.2007.11.037.

Ang, W. L., A. W. Mohammad, N. Hilal, and C. P. Leo. 2015. “A review on the applicability of integrated/hybrid membrane processes in water treatment and desalination plants.” *Desalination*, 363: 2–18. https://doi.org/10.1016/j.desal.2014.03.008.

Anis, S. F., R. Hashaikeh, and N. Hilal. 2019. “Microfiltration membrane processes: A review of research trends over the past decade.” *Journal of Water Process Engineering*, 32: 100941. https://doi.org/10.1016/j.jwpe.2019.100941.

APHA, WEF, and AWWA. 2012. *Standard Methods for the Examination of Water and Wastewater*. Edited by L. Clesceri, A. Greenberg, and A. Eaton. 22nd Editi. Washington, D.C.: American Public Health Association, Water Environment Federation, American Water Works Association.

Arhin, S. G., N. Banadda, A. J. Komakech, I. Kabenge, and J. Wanyama. 2016. “Membrane fouling control in low pressure membranes: A review on pretreatment techniques for fouling abatement.” *Environmental Engineering Research*, 21 (2): 109–120. https://doi.org/10.4491/eer.2016.017.

Arkhangelsky, E., A. Lerch, W. Uhl, and V. Gitis. 2011. “Organic fouling and floc transport in capillaries.” *Separation and Purification Technology*, 80 (3): 482–489. https://doi.org/10.1016/j.seppur.2011.06.001.

Ayache, C., M. Pidou, J.-P. Croue, J. Labanowski, Y. Poussade, A. Tazi-Pain, J. Keller, and W. Gernjak. 2013. “Impact of effluent organic matter on low-pressure membrane fouling in tertiary treatment.” *Water Research*, 47 (8): 2633–2642. https://doi.org/10.1016/j.watres.2013.01.043.

Black, A. P., and S. A. Hannah. 1961. “Electrophoretic Studies of Turbidity Removal by Coagulation with Aluminum Sulfate.” *Journal AWWA*, 53 (4): 438–452. https://doi.org/10.1002/j.1551-8833.1961.tb00689.x.

Braghetta, A., J. G. Jacangelo, S. Chellam, B. A. Utne, and M. L. Hotaling. 1997. “DAF pretreatment: its effect on MF performance.” *Journal AWWA*, 89 (10): 90–101.

Buisson, H., N. Lee, G. Amy, and J. Croue. 2004. “Identification and understanding of fouling in

low-pressure membrane (MF / UF) filtration by natural organic." *Water Research*, 38: 4511–4523. https://doi.org/10.1016/j.watres.2004.08.013.

Choi, K. Y. J., and B. A. Dempsey. 2004. "In-line coagulation with low-pressure membrane filtration." *Water Research*, 38 (19): 4271–4281. https://doi.org/10.1016/j.watres.2004.08.006.

Côté, P., D. Mourato, C. Güngerich, J. Russell, and E. Houghton. 1998. "Immersed membrane filtration for the production of drinking water: Case studies." *Desalination*, 117 (1–3): 181–188. https://doi.org/10.1016/S0011-9164(98)00090-3.

Crittenden, J. C., R. R. Trussell, D. W. Hand, K. J. Howe, and G. Tchobanoglous. 2012. *Water Treatment: Principles and Design*. 3rd ed. New York, NY: McGraw-Hill.

Croft, J. 2012. "Natural Organic Matter Characterization of Different Source and Treated Waters; Implications for Membrane Fouling Control." M.A.S.c Thesis, University of Waterloo.

Dang, H. T., R. M. Narbaitz, and T. Matsuura. 2010. "Evaluation of apparatus for membrane cleaning tests." *Journal of Environmental Engineering*, 136 (10): 1161–1170. https://doi.org/10.1061/(ASCE)EE.1943-7870.0000254.

Ding, Q., H. Yamamura, N. Murata, N. Aoki, H. Yonekawa, A. Hafuka, and Y. Watanabe. 2016. "Characteristics of meso-particles formed in coagulation process causing irreversible membrane fouling in the coagulation-microfiltration water treatment." *Water Research*, 101: 127–136. https://doi.org/10.1016/j.watres.2016.05.076.

Ding, Y., T. Li, K. Qiu, B. Ma, and R. Wu. 2021. "Membrane fouling performance of Fe-based coagulation-ultrafiltration process: Effect of sedimentation time." *Environmental Research*, 195: 110756. https://doi.org/10.1016/j.envres.2021.110756.

Edzwald, J. K., and J. Haarhoff. 2012. *Dissolved Air Flotation for Water Clarification*. New York, NY: McGraw-Hill.

Ehsani, M., H. Doan, and A. Lohi. 2021. "A comprehensive review of membrane fouling and cleaning methods with emphasis on ultrasound-assisted fouling control processes." *Korean Journal of Chemical Engineering*, 38 (8): 1531–1555. https://doi.org/10.1007/s11814-021-0832-2.

Fabris, R., E. K. Lee, C. W. K. Chow, V. Chen, and M. Drikas. 2007. "Pre-treatments to reduce fouling of low pressure micro-filtration (MF) membranes." *Journal of Membrane Science*, 289 (1–2): 231–240. https://doi.org/10.1016/j.memsci.2006.12.003.

Fan, L., J. L. Harris, F. A. Roddick, and N. I. C. A. Booker. 2001. "Influence of the Characterstics of Natural Organic Matter on the Fouling of Microfiltration Membranes." *Water Research*, 35 (18): 4455–4463.

Farahbakhsh, K., C. Svrcek, R. K. Guest, and D. W. Smith. 2004. "A review of the impact of chemical pretreatment on low-pressure water treatment membranes." *Journal of Environmental Engineering and Science*, 3 (4): 237–253. https://doi.org/10.1139/S03-078.

Gao, W., H. Liang, J. Ma, M. Han, Z. Chen, Z. Han, and G. Li. 2011. "Membrane fouling control in ultrafiltration technology for drinking water production: A review." *Desalination*, 272 (1–3): 1–8. Elsevier B.V. https://doi.org/10.1016/j.desal.2011.01.051.

Goh, Y. T., J. L. Harris, and F. A. Roddick. 2010. "Reducing the effect of cyanobacteria in the microfiltration of secondary effluent." *Water Science and Technology*, 62 (7): 1682–1688. https://doi.org/10.2166/wst.2010.482.

Gonzalez-Galvis, J. P., and R. M. Narbaitz. 2020. "Large batch bench-scale dissolved air flotation system (LB-DAF) for drinking water treatability tests." *Environmental Science: Water Research and Technology*, 6 (4): 1004–1017. Royal Society of Chemistry.

https://doi.org/10.1039/c9ew00935c.

Goslan, E. H., S. Voros, J. Banks, D. Wilson, P. Hillis, A. T. Campbell, and S. A. Parsons. 2004. "A model for predicting dissolved organic carbon distribution in a reservoir water using fluorescence spectroscopy." *Water Research*, 38 (3): 783–791. https://doi.org/10.1016/j.watres.2003.10.027.

Guo, W., H.-H. Ngo, and J. Li. 2012. "A mini-review on membrane fouling." *Bioresource Technology*, 122: 27–34. https://doi.org/10.1016/j.biortech.2012.04.089.

Hatt, J. W., E. Germain, and S. J. Judd. 2011. "Precoagulation-microfiltration for wastewater reuse." *Water Research*, 45 (19): 6471–6478. https://doi.org/10.1016/j.watres.2011.09.039.

Howe, K. J., A. Marwah, K.-P. Chiu, and S. S. Adham. 2006. "Fouling of microfiltration and ultrafiltration membranes by natural waters." *Environmental Science & Technology*, 40 (24): 7908–7913. https://doi.org/10.1021/es0616480.

Huang, H., K. Schwab, and J. G. Jacangelo. 2009. "Pretreatment for low pressure membranes in water treatment: A review." *Environmental Science and Technology*, 43 (9): 3011–3019. https://doi.org/10.1021/es802473r.

Inge GmbH. 2020. *Inge Product Series: Dizzer XL Series Modules. Process and Design Guidelines*. 66–66. Greifenberg.

Irvine, E., D. Welch, A. Smith, and T. Rachwal. 2019. "Nanofiltration for colour removal – 8 years' operational experience in Scotland." *Water Science and Technology: Water Supply*, 11 (5/6): 10.

Jang, N.-Y., Y. Watanabe, and S. Minegishi. 2005. "Performance of ultrafiltration membrane process combined with coagulation/sedimentation." *Water Science and Technology*, 51 (6–7): 209–219. https://doi.org/10.2166/wst.2005.0640.

Jermann, D., W. Pronk, R. Ka, M. Halbeisen, and M. Boller. 2008. "Influence of interactions between NOM and particles on UF fouling mechanisms." *Water Research*, 42: 3870–3878. https://doi.org/10.1016/j.watres.2008.05.013.

Johansson, L., J. Temnerud, J. Abrahamsson, and D. B. Kleja. 2010. "Variation in Organic Matter and Water Color in Lake Mälaren during the Past 70 Years." *AMBIO*, 39 (2): 116–125. https://doi.org/10.1007/s13280-010-0019-2.

Jung, C. W., and L. S. Kang. 2003. "Application of combined coagulation-ultrafiltration membrane process for water treatment." *Korean Journal of Chemical Engineering*, 20 (5): 855–861. https://doi.org/10.1007/BF02697288.

Kamińska, G., W. Pronk, and J. Traber. 2020. "Effect of coagulant dose and backflush pressure on NOM membrane fouling in inline coagulation-ultrafiltration." *Desalination and Water Treatment*, 199: 188–197. https://doi.org/10.5004/dwt.2020.25657.

Karanfil, T., I. Erdogan, and M. Schlautman. 2003. "Selecting filter membranes for measuring DOC and UV254." *Journal AWWA*, 95 (3): 86–100.

Keucken, A., G. Heinicke, K. M. Persson, and S. J. Köhler. 2017. "Combined coagulation and ultrafiltration process to counteract increasing NOM in brown surface water." *Water*, 9 (9): 697. Multidisciplinary Digital Publishing Institute. https://doi.org/10.3390/w9090697.

Kim, H.-C. 2015. "Microfiltration of humic-rich water coagulated with cationic polymer: The effects of particle characteristics on the membrane performance." *Journal of Membrane Science*, 475: 349–356. https://doi.org/10.1016/j.memsci.2014.10.041.

Kimura, K., T. Maeda, H. Yamamura, and Y. Watanabe. 2008. "Irreversible membrane fouling in microfiltration membranes filtering coagulated surface water." *Journal of Membrane Science*, 320 (1–2): 356–362. https://doi.org/10.1016/j.memsci.2008.04.018.

Kimura, K., K. Tanaka, and Y. Watanabe. 2014. "Microfiltration of different surface waters with/without coagulation: Clear correlations between membrane fouling and hydrophilic biopolymers." *Water Research*, 49: 434–443. https://doi.org/10.1016/j.watres.2013.10.030.

Kimura, K., K. Tanaka, and Y. Watanabe. 2015. "Confirmation of the correlation between membrane fouling in microfiltration and biopolymer concentrations in various Japanese surface waters." *Water Science and Technology: Water Supply*, 15 (2): 288–293. https://doi.org/10.2166/ws.2014.112.

Kinser, K. 2021. "Membrane Filtration: Past, Present, and Future." *Journal AWWA*, 113 (8): 72–75. https://doi.org/10.1002/awwa.1791.

Klante, C., M. Larson, and K. M. Persson. 2021. "Brownification in Lake Bolmen, Sweden, and its relationship to natural and human-induced changes." *Journal of Hydrology: Regional Studies*, 36: 100863. https://doi.org/10.1016/j.ejrh.2021.100863.

Konieczny, K., M. Rajca, D. Sakol, J. Plonka, and M. Bodzek. 2009. "Coagulation-ultrafiltration system for river water treatment." *Desalination*, 240 (September 2007): 2–6. https://doi.org/10.1016/j.desal.2007.11.072.

Kumar, R., and A. F. Ismail. 2015. "Fouling control on microfiltration/ultrafiltration membranes: Effects of morphology, hydrophilicity, and charge." *Journal of Applied Polymer Science*, 132 (21): n/a-n/a. https://doi.org/10.1002/app.42042.

Le Clech, P., B. Jefferson, I. S. Chang, and S. J. Judd. 2003. "Critical flux determination by the flux-step method in a submerged membrane bioreactor." *Journal of Membrane Science*, 227 (1–2): 81–93. https://doi.org/10.1016/j.memsci.2003.07.021.

Lebeau, T., C. Lelièvre, H. Buisson, D. Cléret, L. W. Van de Venter, and P. Côté. 1998. "Immersed membrane filtration for the production of drinking water: combination with PAC for NOM and SOCs removal." *Desalination*, 117 (1–3): 219–231. https://doi.org/10.1016/S0011-9164(98)00101-5.

Lee, E. K., V. Chen, and A. G. Fane. 2008. "Natural organic matter (NOM) fouling in low pressure membrane filtration — effect of membranes and operation modes." *Desalination*, 218 (September 2006): 257–270. https://doi.org/10.1016/j.desal.2007.02.021.

Lerch, A., W. Uhl, and R. Gimbel. 2007. "CFD modelling of floc transport and coating layer build-up in single UF/MF membrane capillaries driven in inside-out mode." *Water Supply*, 7 (4): 37–47. https://doi.org/10.2166/ws.2007.141.

Li, K., G. Wen, S. Li, H. Chang, S. Shao, T. Huang, G. Li, and H. Liang. 2019. "Effect of pre-oxidation on low pressure membrane (LPM) for water and wastewater treatment: A review." *Chemosphere*, 231: 287–300. https://doi.org/10.1016/j.chemosphere.2019.05.081.

Liang, H., W. Gong, and G. Li. 2008. "Performance evaluation of water treatment ultrafiltration pilot plants treating algae-rich reservoir water." *Desalination*, 221 (1–3): 345–350. https://doi.org/10.1016/j.desal.2007.01.093.

Lin, J. C.-T., D.-J. Lee, and C. Huang. 2010. "Membrane Fouling Mitigation: Membrane Cleaning." *Separation Science and Technology*, 45 (7): 858–872. https://doi.org/10.1080/01496391003666940.

Long, Y., G. Yu, L. Dong, Y. Xu, H. Lin, Y. Deng, X. You, L. Yang, and B.-Q. Liao. 2021. "Synergistic fouling behaviors and mechanisms of calcium ions and polyaluminum chloride associated with alginate solution in coagulation-ultrafiltration (UF) process." *Water Research*, 189: 116665. https://doi.org/10.1016/j.watres.2020.116665.

Lorenzen, S., K. Keiding, and M. L. Christensen. 2017. "The effect of particle surface charge density on filter cake properties during dead-end filtration." *Chemical Engineering Science*, 163: 155–166. https://doi.org/10.1016/j.ces.2017.01.044.

Ma, B., Y. Ding, B. Wang, Z. Qi, Y. Bai, R. Liu, H. Liu, and J. Qu. 2020. "Influence of sedimentation with pre-coagulation on ultrafiltration membrane fouling performance." *Science of The Total Environment*, 708: 134671. https://doi.org/10.1016/j.scitotenv.2019.134671.

Maeng, S. K., T. C. Timmes, and H.-C. Kim. 2017. "Characteristics of flocs formed by polymer-only coagulation in water treatment and their impacts on the performance of downstream membrane separation." *Environmental Technology*, 38 (20): 2601–2610. https://doi.org/10.1080/09593330.2016.1271460.

Malkoske, T. A., P. R. Bérubé, and R. C. Andrews. 2020. "Coagulation/flocculation prior to low pressure membranes in drinking water treatment: A review." *Environmental Science: Water Research and Technology*, 6 (11): 2993–3023. Royal Society of Chemistry. https://doi.org/10.1039/d0ew00461h.

Miller, D. J., S. Kasemset, D. R. Paul, and B. D. Freeman. 2014. "Comparison of membrane fouling at constant flux and constant transmembrane pressure conditions." *Journal of Membrane Science*, 454: 505–515. https://doi.org/10.1016/j.memsci.2013.12.027.

Moon, J., M.-S. Kang, J.-L. Lim, C.-H. Kim, and H.-D. Park. 2009. "Evaluation of a low-pressure membrane filtration for drinking water treatment: pretreatment by coagulation/sedimentation for the MF membrane." *Desalination*, 247 (1–3): 271–284. https://doi.org/10.1016/j.desal.2008.12.030.

Naim, R., R. Epsztein, A. Felder, M. Heyer, M. Heijnen, and V. Gitis. 2014. "Rethinking the role of in-line coagulation in tertiary membrane filtration of municipal effluents." *Separation and Purification Technology*, 125: 11–20. Elsevier B.V. https://doi.org/10.1016/j.seppur.2014.01.036.

Pearce, G. K. 2011. *UF/MF Membrane Water Treatment: Principles and Design*. 387. 1st ed. Bangkok: Water Treatment Academy.

Peleato, N. M., R. L. Legge, and R. C. Andrews. 2017. "Characterization of UF foulants and fouling mechanisms when applying low in-line coagulant pre-treatment." *Water Research*, 126: 1–11. Elsevier Ltd. https://doi.org/10.1016/j.watres.2017.08.064.

Peters, C. D., T. Rantissi, V. Gitis, and N. P. Hankins. 2021. "Retention of natural organic matter by ultrafiltration and the mitigation of membrane fouling through pre-treatment, membrane enhancement, and cleaning - A review." *Journal of Water Process Engineering*, 44: 102374. https://doi.org/10.1016/j.jwpe.2021.102374.

Porcelli, N., and S. Judd. 2010. "Chemical cleaning of potable water membranes: The cost benefit of optimisation." *Water Research*, 44 (5): 1389–1398. Elsevier Ltd. https://doi.org/10.1016/j.watres.2009.11.020.

Ratajczak, M. J., K. N. Exall, and P. M. Huck. 2012. "Factors affecting coagulation as a pretreatment to ultrafiltration membranes." *Water Quality Research Journal*, 47 (2): 103–116. https://doi.org/10.2166/wqrjc.2012.010.

Ren, L., C. Liu, T. Meng, and Y. Sun. 2021. "Effects of micro-flocculation pretreatment on the ultrafiltration membrane fouling caused by different dissolved organic matters in treated wastewater." *Journal of Water Reuse and Desalination*, 11 (4): 597–609. https://doi.org/10.2166/wrd.2021.051.

Schneider, O., and S. M. Freeman. 2005. "Recent advances in MF/UF membrane treatment."

Journal of the New England Water Works Association, 119 (2): 98–104.
Schulz, M., A. Soltani, X. Zheng, and M. Ernst. 2016. "Effect of inorganic colloidal water constituents on combined low-pressure membrane fouling with natural organic matter (NOM)." *Journal of Membrane Science*, 507: 154–164. Elsevier. https://doi.org/10.1016/j.memsci.2016.02.008.
Sharp, E. L., S. A. Parsons, and B. Jefferson. 2006. "Seasonal variations in natural organic matter and its impact on coagulation in water treatment." *Science of The Total Environment*, 363 (1–3): 183–194. https://doi.org/10.1016/j.scitotenv.2005.05.032.
Shi, X., G. Tal, N. P. Hankins, and V. Gitis. 2014. "Fouling and cleaning of ultrafiltration membranes: A review." *Journal of Water Process Engineering*, 1: 121–138. Elsevier Ltd. https://doi.org/10.1016/j.jwpe.2014.04.003.
Sillanpaa, M. 2015. *Natural Organic Matter in Water*. 1st ed. Oxford, UK: Butterworth-Heinemann.
Sun, W., J. Liu, H. Chu, and B. Dong. 2013. "Pretreatment and membrane hydrophilic modification to reduce membrane fouling." *Membranes*, 3 (3): 226–241. https://doi.org/10.3390/membranes3030226.
Tabatabai, S. A. A., M. D. Kennedy, G. L. Amy, and J. C. Schippers. 2009. "Optimizing inline coagulation to reduce chemical consumption in MF/UF systems." *Desalination and Water Treatment*, 6 (1–3): 94–101. https://doi.org/10.5004/dwt.2009.653.
Tang, C. K., N. M. Peleato, P. R. Bérubé, and R. C. Andrews. 2019. "Impact of low coagulant dosages on protein fouling of ultrafiltration membranes." *Journal of Water Process Engineering*, 31: 100801. https://doi.org/10.1016/j.jwpe.2019.100801.
Teixeira, M. R., and M. J. Rosa. 2006. "Comparing dissolved air flotation and conventional sedimentation to remove cyanobacterial cells of Microcystis aeruginosa. Part I: The key operating conditions." *Separation and Purification Technology*, 52 (1): 84–94. https://doi.org/10.1016/j.seppur.2006.03.017.
Teng, J., Y. Chen, G. Ma, H. Hong, T. Sun, B.-Q. Liao, and H. Lin. 2020. "Membrane fouling by alginate in polyaluminum chloride (PACl) coagulation/microfiltration process: Molecular insights." *Separation and Purification Technology*, 236: 116294. https://doi.org/10.1016/j.seppur.2019.116294.
Thompson, M. A. 2001. "Membrane filtration of high turbidity sources." *Water Supply*, 1 (5–6): 325–330. https://doi.org/10.2166/ws.2001.0129.
Walker, S., and R. M. Narbaitz. 2016. "Hollow fiber ultrafiltration of Ottawa River water: Floatation versus sedimentation pre-treatment." *Chemical Engineering Journal*, 288: 228–237. Elsevier B.V. https://doi.org/10.1016/j.cej.2015.11.064.
Wang, J., S. Pan, and D. Luo. 2013. "Characterization of cake layer structure on the microfiltration membrane permeability by iron pre-coagulation." *Journal of Environmental Sciences*, 25 (2): 308–315. https://doi.org/10.1016/S1001-0742(12)60025-4.
Wang, Y., H. Ma, X. Wang, L. Ju, L. Tian, H. Qi, H. Yu, G. He, and J. Li. 2022. "Study on the operation performance and floc adhesion mechanism of dissolved air flotation equipment." *Environmental Science and Pollution Research*, 29 (36): 54219–54233. https://doi.org/10.1007/s11356-022-19359-9.
Waterman, D. 2008. "Bench Scale Analysis of Ultrafiltration Membranes for Investigation of Fouling by Natural Organic Matter in Surface Waters." *Analysis*. M.A.S.c Thesis, University of Ottawa.
White, D. M., D. S. Garland, J. Narr, and C. R. Woolard. 2003. "Natural organic matter and DBP

formation potential in Alaskan water supplies." *Water Research*, 37 (4): 939–947. https://doi.org/10.1016/S0043-1354(02)00425-6.

Wray, H. E., R. C. Andrews, and P. R. Bérubé. 2014. "Ultrafiltration organic fouling control: Comparison of air-sparging and coagulation." *Journal - American Water Works Association*, 106 (2): E76–E85. https://doi.org/10.5942/jawwa.2014.106.0018.

Xu, B., and R. M. Narbaitz. 2016. "Improved membrane pretreatment of high hydrophobic natural organic matter (NOM) waters by floatation." *Journal of Membrane Science*, 518: 120–130. Elsevier. https://doi.org/10.1016/j.memsci.2016.02.056.

Xu, X., Y. Yang, T. Liu, and B. Chu. 2022. "Cost-effective polymer-based membranes for drinking water purification." *Giant*, 10: 100099. https://doi.org/10.1016/j.giant.2022.100099.

Yamamura, H., K. Okimoto, K. Kimura, and Y. Watanabe. 2007. "Influence of calcium on the evolution of irreversible fouling in microfiltration/ultrafiltration membranes." *Journal of Water Supply: Research and Technology-Aqua*, 56 (6–7): 425–434. https://doi.org/10.2166/aqua.2007.018.

Yoo, S. S. 2018. "Operating cost reduction of in-line coagulation/ultrafiltration membrane process attributed to coagulation condition optimization for irreversible fouling control." *Water (Switzerland)*, 10 (8). https://doi.org/10.3390/w10081076.

Yu, W., J. Qu, and J. Gregory. 2015. "Pre-coagulation on the submerged membrane fouling in nano-scale: Effect of sedimentation process." *Chemical Engineering Journal*, 262: 676–682. https://doi.org/10.1016/j.cej.2014.09.102.

Zydney, A. L., and L. Zeman J. 1996. *Microfiltration and ultrafiltration: principles and applications*. 1st ed. New York, NY: Marcel Dekker.

CHAPTER 5

Characterizing the Impact of Geometry on the Performance of Inline-Coagulation Pretreatment Systems with Helical Flocculators

Context: The work completed in Chapter 3 and Chapter 4 compared the performance of alternative coagulation pretreatment strategies and, in Chapter 4, it was noted that for one particular tubular multi-channel membrane and water combination, continuous inline-coagulation (C-IN) yielded improved performance compared to more sophisticated treatment technologies involving particle separation. This finding motivated further investigation into alternative/novel continuous-inline dosing strategies, namely phased inline coagulation (C-IN-P), where the coagulant is added during only the initial portion of the filtration cycle rather than continuously throughout its entire length. Compared with C-IN, C-IN-P offers the potential to simultaneously reduce membrane fouling while improving process sustainability through reduced coagulant usage and sludge disposal requirements.

To investigate C-IN-P pretreatment, a bench-scale system capable of implementing continuous-flow inline coagulation was required. Although systems of this type have been developed in previous studies limitations related to cost, hydraulic retention time, and water volume requirements motivated the development of an improved system, this is the subject of Chapter 5 and Chapter 6 of this thesis.

Implementing inline coagulation for continuous-flow bench-scale systems, including those used for low-pressure membrane studies, remains a significant challenge due to the low flowrates that can be managed by these systems. Helically coiled tube flocculators offer a promising solution as they have been reported to promote efficient mixing even when operated firmly within the laminar flow regime. However, existing evidence suggests that the helical coil geometry can influence the size and structure of the resulting flocs, which are known to govern the performance of downstream treatment processes.

Accordingly, this chapter uses a designed experimental approach to systematically evaluate and characterize the impact of helical coil geometry on floc properties generated by a bench-scale continuous-flow system. Insights regarding the effect of system hydrodynamics are also provided

in terms of reduced (scalable) parameters. Based on the findings, design recommendations are developed to support the selection of appropriate helical coil geometries for coagulation pretreatment in low-pressure membrane systems, as well as in conventional treatment trains incorporating coagulation/flocculation/sedimentation.

A version of this work has been published as:

Ladouceur, J.D., Narbaitz, R.M., & Lan, C.Q. (2026). Characterizing the impact of geometry on the performance of inline-coagulation pretreatment systems with helical flocculators. *Environmental Science: Water Research & Technology, 12(8), 2423-2438. 10.1039/D6EW00221H*

The supporting information for this chapter of the thesis can be found in Appendix F

Artwork associated with this chapter was also featured on the outside-front cover of the journal issue, which is reproduced on the next page, and which was published as:

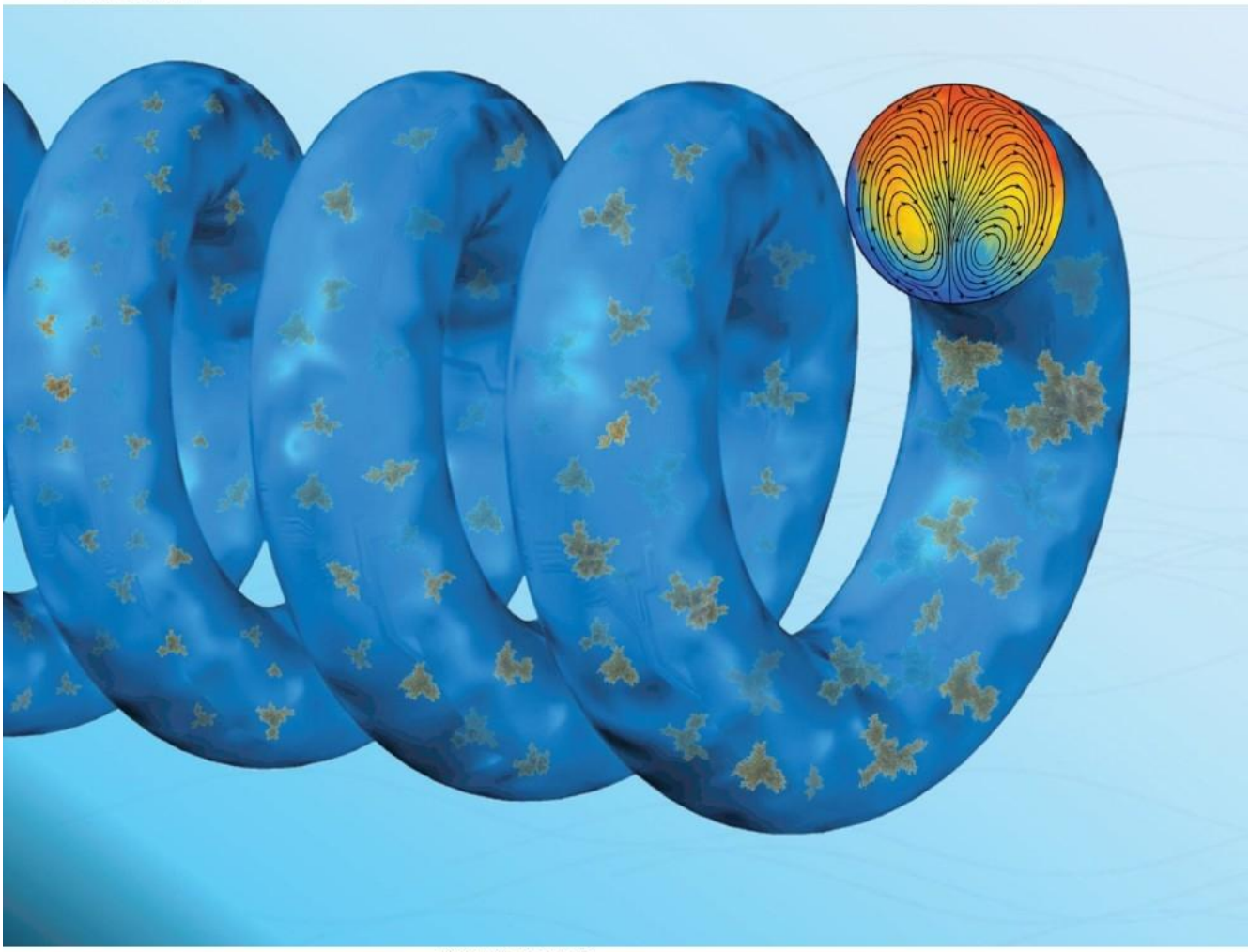
Ladouceur, J.D., Narbaitz, R.M., & Lan, C.Q. (2026). Front cover. *Environmental Science: Water Research & Technology, 12(8), 2267-2268*

.

Volume 12
Number 8
August 2026
Pages 2267–2648

Environmental Science
Water Research & Technology

rsc.li/es-water



ISSN 2053-1400

ROYAL SOCIETY OF CHEMISTRY

PAPER
Joseph D. Ladouceur *et al.*
Characterizing the impact of geometry on the performance of inline-coagulation pretreatment systems with helical flocculators

List of Abbreviations

ANOVA	Analysis of variance
BSA	Bovine serum albumin
C-IN	Inline coagulation
D_e	Dean number
DOC	Dissolved organic carbon
D_p	Perimeter-based fractal dimension
ECD	Equivalent circular diameter
FFD	Full-factorial design
G	Mean velocity gradient
HA	Humic acid
HCTF	Helically coiled tube flocculator
HRT	Hydraulic retention time
ISM	Inline static mixer
LPM	Low-pressure membrane
NIH	National Institutes of Health
NOM	Natural organic matter
R^2	Coefficient of determination
R_e	Reynolds number
SA	Sodium alginate
SUVA	Specific ultraviolet absorbance at 254nm
TRE	Turbidity removal efficiency

List of Variables

Variable	**Description**
$\beta_{i,FFD}$	Regression coefficient for the i^{th} predictor variable (factor) in 2^k factorial design (varies)
$\beta_{ij,FFD}$	Regression coefficient for the interaction of factors i and j $(i \neq j)$ in 2^k factorial design (varies)
$\beta_{0,FFD}$	Intercept of regression model for 2^k factorial design (varies)
γ	Dimensionless helical coil pitch

δ_{nd}	Dimensionless curvature of HCTF
ε_{FFD}	Random error component for 2^k factorial design (varies)
λ	HCTF torsion/curvature ratio (dimensionless)
$A_{p,floc}$	Projected area of the floc (μm^2)
b_{ps}	HCTF helical pitch slope (mm rad^{-1})
C_{floc}	Floc concentration (#/mL)
c_R	HCTF curvature ratio (dimensionless)
ECD	Equivalent circular diameter (μm)
D_e	Dean number (dimensionless)
N_{floc}	Number of flocs counted per grid area of the Sedgewick-Rafter cel
p	HCTF coil pitch (mm)
P_{floc}	Floc perimeter (μm)
r_c	HCTF helical coil radius (mm)
R_c	Modified coil radius of curvature (mm)
R_e	Reynolds number (dimensionless)
r_p	HCTF pipe radius (mm)
y_{FFD}	Response variable for 2^k factorial design (varies)

5.1. Abstract

Inline-coagulation (C-IN), where coagulant is added to the feed without solids separation prior to filtration, is a widely applied pretreatment strategy for low-pressure membrane fouling mitigation. At bench-scale, simulating C-IN has proven difficult due to the low flowrates involved. One promising approach to achieve continuous-flow operation in these small-scale systems is the helically coiled tube flocculator (HCTF), a coiled section of pipe. However, the impact of changing helical geometry on the properties of flocs formed by HCTFs, which can significantly affect membrane performance, has yet to be quantitatively characterized. Moreover, there are currently no widely accepted design guidelines for HCTFs. Accordingly, the current study uses a continuous-flow bench-scale system and a 2^3 full-factorial experimental design approach to investigate the impact of HCTF geometry on the properties of flocs produced. The results showed that the floc size and concentration were most significantly impacted by the pipe length (i.e., retention time),

while the floc fractal dimension demonstrated a relative insensitivity to helical geometry for all tested configurations. The Reynolds number was also shown to exert a critical impact on the properties of flocs, likely the result of a trade-off between mixing strength and retention time. When compared to a batch-reactor, the tested HCTF configurations produced smaller sized flocs in greater concentrations, while relative to a commercial inline static mixer, HCTFs yielded larger sized flocs in lower concentrations. The size of the flocs formed indicate that HCTFs are suitable for continuous-flow C-IN, with pipe length and system hydrodynamics being the most important parameters in their design. Additionally, the choice of mixer type significantly impacts floc properties, which are expected to alter the performance of downstream unit operations.

5.2. Introduction

Low-pressure membrane (LPM) technologies for drinking water treatment have benefitted from rapid growth over the past two decades owing to their numerous advantages (Alresheedi et al. 2022; Kinser 2021; Pearce 2018). Membrane fouling, however, which leads to a loss of productivity with time, is one of the main impediments preventing a more widespread application of LPMs in potable water treatment (Zietzschmann et al. 2014;Appendix B). To help mitigate the fouling of LPMs, which is primarily caused by natural organic matter (NOM) (Amy 2008; AWWA 2005; Howe et al. 2006), coagulation pretreatment has been established as an effective strategy capable of removing organics across a wide range of molecular weights and surface functional groups (Kimura and Kume 2020). While coagulation pretreatment can be performed in a number of different configurations both with and without particle separation (Huang et al. 2009; Malkoske et al. 2020), inline coagulation (C-IN), where the flocs are delivered to the membrane surface without pre-separation, has become the most popular approach owing to its reduced process complexity and smaller footprint (American Water Works Association 2018; Kamińska et al. 2020).

The popularity of C-IN pretreatment has garnered increased attention among academic studies and industrial research and design, however, simulating the continuous-flow operation of full-scale facilities at bench-scale has proven very challenging due to the low flow rates that can be managed by small-scale filtration processes (Malkoske et al. 2023). As a result, a number of studies have performed coagulation using a batch-wise approach (Tang et al. 2019;Chapter 3;Chapter 4), which is experimentally simpler to implement compared to continuous-flow systems.

In such batch configurations, the feed tank/reactors had to be continuously stirred for the entire duration of the test to prevent floc settling, meaning the flocs were subjected to moderately high shear rates for considerably longer durations than typical of full-scale practice. To address this limitation, Malkoske et al. (2023) developed a modified jar test apparatus to simulate bench-scale continuous-flow C-IN. Although effective, the flowrate required to maintain reasonable hydraulic retention times (HRT) in the coagulation and flocculation jars was much larger than that needed to operate the downstream LPMs at conventional/reasonable flux rates (owing to the small membrane surface areas used at bench-scale). Consequently, over 96% of the coagulated feed water had to be wasted. Therefore, there is a need for an effective, low-cost alternative that can simulate the continuous-flow operation of C-IN pretreatment from full-scale facilities at the low flow rates used for bench-scale LPM studies.

To this end, helically coiled tube flocculators (HCTFs), a helically wound pipe (Fig. 5.1), represent a promising option due to their reported ability to achieve complete and efficient mixing even when operated firmly within the laminar flow range, which is expected for small-scale studies (Mansour et al. 2017, 2020a; Zhang et al. 2019). This feature of HCTFs stems from the presence of strong secondary flows, that is, fluid flow towards the outer radius of curvature, normal to the direction of flow. This causes bifurcation of the flow and the formation of a pair of recirculating vortices (Huttl and Friedrich 2000). HCTFs further offer flexibility in design for bench-scale operations as their structural simplicity allows them to be easily fabricated with any geometry based on the needs of the user. However, the helical coil geometry, including the coil pitch (p), coil diameter (d_c), and pipe diameter (d_p), has been shown to alter the hydrodynamic flow pattern within the flocculator (Cioncolini and Santini 2006; Liou 1992; Mansour et al. 2020a; Sartori et al. 2015; Tang et al. 2016; Yamamoto et al. 1995, 2002), which is expected to influence the properties of flocculated aggregates. Several studies (Cahyana et al. 2021; De Oliveira and Teixeira 2017; Maraschin et al. 2020) have reported altered floc settleability, which is known to be dependent on both the size and morphology (i.e., fractal dimension) of the formed flocs (Vahedi and Gorczyca 2011, 2012), as a result of changing helical coil geometry. To date, however, only a single study (Carissimi et al. 2018) has reported how changing HCTF geometry impacts floc size and none have characterized the impact on floc structure.

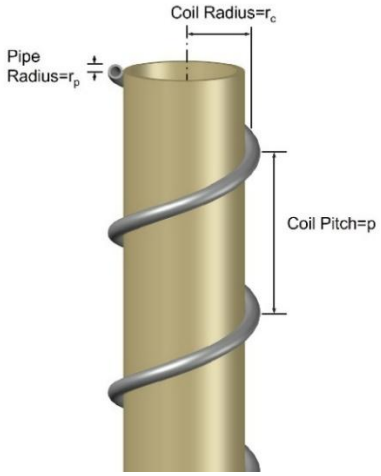


Fig. 5.1. Geometrical description of a helically coiled tube flocculator (HCTF)

Given the relatively large number of geometric and hydraulic parameters shown to affect the overall performance of HCTFs, a designed experiment is necessary to elucidate the relative importance of these parameters on the properties of flocs formed by the HCTF. Moreover, understanding the relationship between HCTF geometry and floc properties is critical for its application within integrated systems. For example, in the C-IN-LPM system, it is well understood that cake properties, which are significantly impacted by the size and fractal dimension of the formed floc aggregates, dictate the degree of LPM fouling (Amjad et al. 2015; Du et al. 2019; Liu et al. 2024; Nan et al. 2016; Shen et al. 2020). Although HCTFs offer considerable advantages over conventional flocculators, including markedly reduced HRTs and footprints as well as the possibility for low-energy mixing at full-scale (De Oliveira and Teixeira 2017; García-Ávila et al. 2023), there remains a lack of clear design guidance for their application as part of continuous-flow coagulation-based systems.

Accordingly, the objectives of the current study were to: (a) demonstrate that continuous-flow C-IN in low flow bench-scale systems can be achieved using HCTFs; (b) employ a designed experimental approach to identify which geometric and operational properties of the HCTF exert the greatest impact on the characteristics of the formed flocs, including their size and structure, and to; (c) directly compare the properties of the flocs generated by HCTFs with those formed by alternative coagulation/flocculation strategies used in bench-scale studies, including a commercial inline static mixer (ISM) and batch reactor with vertical shaft turbine. The novelty of this study is

that it is the first to comprehensively characterize the impact of helical geometry on the properties of flocs formed by HCTFs. Furthermore, a comparison between the performance of different C-IN mixing conditions is expected to provide important guidance for future researchers conducting continuous-flow lab-scale coagulation as pretreatment for different separation processes such as LPMs, sedimentation, dissolved air flotation, etc.

5.3. Materials and Methods

5.3.1. Synthetic Water

To eliminate the possibility for inter- and intra-annual variations in water quality typical of natural water sources (Winterdahl 2013), a synthetic water was prepared by combining stock solutions of humic acid (HA) (H16752, Sigma-Aldrich, St. Louis, MO), bovine serum albumin (BSA) (A7906, Sigma-Aldrich, St. Louis, MO), and sodium alginate (SA) (180947, Sigma-Aldrich, St. Louis, MO), which were selected to represent humic substances, proteins, and polysaccharides, respectively. These model foulants have been previously used by a number of studies to simulate the organic matrix of natural waters (Mallya et al. 2023; Schulz et al. 2016). Details regarding the preparation of the model organic stock solutions are presented in Appendix F (Section F.1.1).

The applied concentration of each model organic component was 5 mg L^{-1} HA, 4 mg L^{-1} BSA, and 4 mg L^{-1} SA yielding a water with a dissolved organic carbon (DOC) content of approximately 5 mg-C L^{-1}, which is within the range of typical concentrations for natural surface waters (Crittenden et al. 2012), and a moderate hydrophobicity, as defined by the specific ultraviolet absorbance at 254 nm (SUVA) (Edzwald and Tobiason 1999). To simulate the more complex nature of natural waters, kaolin clay (~5 mg L^{-1}, corresponding to a turbidity of 5.5 NTU, Laboratory Grade 75185, Fisher Scientific, Hampton, NH), calcium chloride (0.6 mM, 97%, Thermo Scientific, Hampton, NH), and sodium bicarbonate (0.9 mM, Certified ACS, Fisher Scientific, Hampton, NH) were added to provide low levels of turbidity, hardness, and alkalinity, respectively (Alresheedi and Basu 2019). Prior to commencing any testing, the pH of the raw water was adjusted to 7.5 and the turbidity was verified using a turbidimeter (2100AN, Hach, Loveland, CO). A summary of the key organic and inorganic characteristics of the synthetic water is provided in Table 5.1.

Table 5.1. Synthetic Water Quality

Parameter	pH	Organic Measures			Inorganic Measures		
		DOC	UV_{254}	SUVA	Turbidity	Hardness	Alkalinity
	(Unit)	(mg-C L^{-1})	(cm^{-1})	(L mg^{-1} m^{-1})	(NTU)	(mg-$CaCO_3$ L^{-1})	(mg-$CaCO_3$ L^{-1})
	7.52±0.05	4.98±0.01	0.108±0.006	2.17±0.12	5.44±0.08	61.83±0.53	52.17±2.27

Note: ± represents the 95% confidence interval calculated based on two-tailed Students t-Test, $\mu \pm t_{0.025,n}\frac{s}{\sqrt{n}}$

5.3.2. Experimental Procedure

The effects of HCTF geometry as well as coagulation chemistry, which are expected to influence the properties of the formed flocs, were initially screened using an unreplicated fractional factorial design of resolution IV (2_{IV}^{6-2}). This design was selected because the six main effects are confounded only with three-factor or higher interactions (not with two-factor interactions), which are almost always small in magnitude and can be neglected, allowing clear estimation of the main effects of each factor using only 16 tests (Montgomery 2020). Based on these results, the HCTF geometrical factors with the greatest significance were further studied using a two-level full-factorial design (FFD) to characterize their effects on floc size, structure (fractal dimension), and concentration. Finally, the properties of flocs formed by the various HCTF geometries in the full factorial study were compared with those formed by a commercial ISM using the same continuous-flow C-IN system, as well as flocs formed by batch coagulation using a conventional jar test apparatus. Details regarding the designed experiments, the continuous-flow bench-scale system, and the characterization of flocs are provided in the subsequent sections. Due to space limitations, details regarding the design and outcome of the preliminary screening experiments are presented in Appendix F (Section F.2.).

5.3.2.1. Full-Factorial Study

The full-factorial experiments considered a replicated 2^3 design with three center points (i.e., factors are set midway between their low and high levels), yielding a total of 22 runs. Based on the results of the screening study, the coil pitch (x_1), pipe length (x_2), and coil diameter (x_3) were chosen as HCTF geometrical factors of interest. The high and low factor settings for the coil pitch and coil diameter were typical of reported values from the literature (Cahyana et al. 2021; De Oliveira and Teixeira 2017; Mansour et al. 2020a) and selected to be within the range of Pareto-

optimal values identified in the study by Mansour et al. (2020b). The pipe diameter was fixed at 3.175 mm (1/8") as, from a practical perspective, the small cross-section helped to prevent settling of flocs within the pipe due to the higher axial flow velocity. Moreover, fixing the pipe diameter also constrained the range of theoretical HRT values between 1.6-3.2 min for the chosen pipe lengths (Table F.1), thereby reducing its potential confounding effects on floc properties. While the geometric factors were selected based on the practical considerations noted above, it must be acknowledged that changes in their values did not affect the mean velocity gradient (i.e., G value), which remained ~18 s^{-1} (according to the model by Tse et al. (2011)) for all tested configurations. Although floc properties are also dependent on coagulant type (Yu et al. 2015), alum (see Table F.2; ALS, Kemira, Varennes, QC) was used throughout this study to minimize the number of tests and because it was shown to have a high efficiency for this synthetic water type, yielding equally good zeta potential and DOC reduction as specialty blend pre-polymerized types (see Fig. F.1). Despite the coagulation chemistry being shown to exert an important influence on floc properties during preliminary screening experiments (see Tables F.6-F.8), the objectives of the current study were to characterize the impact of helical geometry on floc properties. Accordingly, for the FFD, the alum coagulant dose and pH were fixed at 3 mg-Al L^{-1} and 6, respectively, corresponding to the jar test optimal conditions for this synthetic water (Fig. F.2). A summary of the factor settings for the FFD is provided in Table 5.2.

Table 5.2. Factor Level Settings for 2^3 FFD.

Factors	Unit	Levels		
		(–1)	**(0)**	**(+1)**
$\boldsymbol{x_1}$: Coil Pitch	(mm)	15	30	45
$\boldsymbol{x_2}$: Pipe Length	(mm)	1000	1500	2000
$\boldsymbol{x_3}$: Coil Diameter	(mm)	50	67.5	75

The response variables were selected to characterize the floc size and structure (fractal dimension), which were shown by others to be impacted by changing HCTF geometry, as well as the floc concentration, which was reported by Malkoske et al. (2023) to impact the reversibility of the fouling layer in LPM systems. Details regarding the calculation of these floc properties are provided in Section 5.3.4. The general form of the regression model used for the 2^k factorial design is given in Eqn. (5.1) (Montgomery 2020):

$$y_{FFD} = \beta_{0,FFD} + \sum_{i=1}^{k} \beta_{i,FFD} x_i + \sum \sum_{i<j=2}^{k} \beta_{ij,FFD} x_i x_j + \varepsilon_{FFD} \quad (5.1)$$

Where: y_{FFD} is the response variable, $\beta_{0,FFD}$ is the intercept, $\beta_{i,FFD}$ is the regression coefficient for the ith predictor variable (factor), $\beta_{ij,FFD}$ is the regression coefficient for the interaction of factors i and j $(i \neq j)$, x_i is the predictor variable (factor), and ε_{FFD} is the random error component. In this study, the response variables include the floc size (measured as the equivalent circular diameter (ECD)), floc concentration, and fractal dimension, the calculation of which is described in Section 5.3.4.2.

5.3.2.2. Bench-Scale Coagulation Systems

Continuous-flow C-IN by the HCTFs, as well as a commercial ISM, was evaluated using the bench-scale system shown in Fig. 5.2. The synthetic water was stored in a glass reservoir positioned on a magnetic stirrer in order to prevent settling of the suspended clay particles. A precision metering pump (Optos 3HM, Eldex, Napa, CA) was used to withdraw the feedwater from the reservoir through 3.175 mm (1/8") stainless steel piping (SS-T2-S-028-20, Swagelok, Solon, OH) at a flowrate of 5 mL min^{-1} (Re= 33.3), which is low but representative of flowrates encountered in bench-scale LPM studies (see Chapter 3 and Chapter 4). After passing through a pulse dampener (MFLX0759620, Avantor Inc., Radnor, PA), coagulant was added inline at a junction just upstream of the mixer using a syringe pump (Pump 22, Harvard Apparatus, Cambridge, MA), which was required for accurate delivery of low volumes of coagulant. The ISM was purchased from Koflo Corporation and had a 316L stainless steel housing with an inside diameter of 8.1 mm (~5/16") and 21 helical elements (3/8-21, Koflo, Cary, IL). The mean G-value for the ISM was estimated to be 25.8 s^{-1} based on differential pressure measurements (see Section F.3.). HCTFs were manufactured in-house with varying geometries defined by the fractional- and full-factorial designs. The polyethylene tubing was wound around a central acrylonitrile butadiene styrene pipe, which ensured a constant coil diameter, and was affixed at pre-measured locations according to the HCTF pitch. Prior to the sampling of flocs for a given test condition, the system was allowed to run for a period of 1 h to achieve steady-state floc properties, which is in excess of the 5 HRTs required to achieve steady state operation in continuous-flow reactors noted by Malkoske et al. (2023) and Crittenden et al. (2012) for constant rate kinetics.

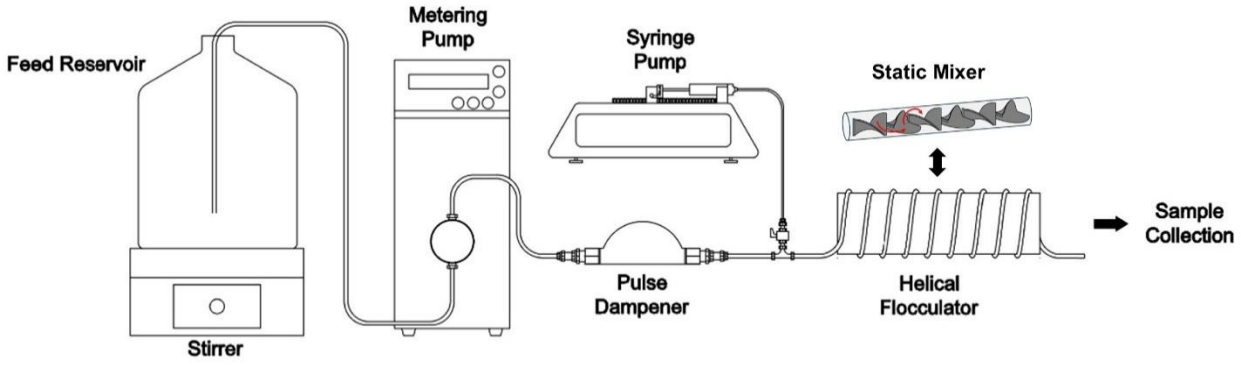


Fig. 5.2. Schematic of bench-scale system.

For batch coagulation tests, a conventional jar test apparatus was used (Model 7790-400, Phipps and Bird, Richmond, VA). Coagulant was added to the gator jar and rapid mixed for 2 min at 164 rpm (G ~ 296 s^{-1}) prior to the mixer speed being reduced to 127 rpm to provide a constant mean velocity gradient of 200 s^{-1} (to prevent floc settling) for the duration of the test. Mixer speeds were calculated according to the model presented by Bratby (2016) to match the G values used in our previous batch coagulation study (see Chapter 3) and are representative of the conditions used by previous bench-scale LPM studies with coagulation performed by batch reactors (Neama et al. 2024; Peleato et al. 2017; Tang et al. 2019). As LPM tests with pretreatment by C-IN using batch coagulation involve significantly longer HRTs than for continuous-flow systems, floc samples were collected and analyzed every 60 min over a period of 3 h to evaluate whether the constant mixing led to kinetic changes in floc properties.

5.3.3. HCTF Geometrical Characterization

While the factorial analysis in this study considered the coil pitch, coil diameter, and pipe length as factors describing HCTF geometry, many previous studies have related the flow hydrodynamics in coiled pipes to the degree of curvature, which measures the within-plane deviation from a straight line, and the torsion, which describes the out-of-plane twisting of the pipe. To quantify the curvature of each HCTF configuration, Eqns. (5.2)–(5.5) were used, with all parameters defined according to the geometry presented in Fig. 5.1 (Mansour et al. 2020b; Mishra and Gupta 1979; Yamamoto et al. 2002):

$$\delta_{nd} = \frac{r_p r_c}{{b_{ps}}^2 + r_c^2} \tag{5.2}$$

$$c_R = \frac{r_p}{r_c} \tag{5.3}$$

$$R_c = r_c \left[1 + \left(\frac{p}{2\pi r_c}\right)^2\right] \tag{5.4}$$

$$D_e = \sqrt{\frac{r_p}{R_c}} R_e \tag{5.5}$$

Where δ_{nd} is the dimensionless curvature, c_R is the curvature ratio, R_c is the modified coil radius of curvature (mm), D_e is the Dean number, which is the ratio of inertial to viscous forces, R_e is the Reynolds number, and b_{ps} is the pitch slope (mm rad^{-1}). The degree of torsion in the various HCTFs was characterized according to Eqns. (5.6)–(5.8) as defined by Liou (1992), Yamamoto et al. (2002), and Mansour et al. (2020a):

$$\beta_0 = \frac{\lambda}{\sqrt{2\delta_{nd}}} \tag{5.6}$$

$$\lambda = \frac{b_{ps}}{r_c} \tag{5.7}$$

$$\gamma = \frac{p}{2\pi r_c} \tag{5.8}$$

Where β_0 is the torsion parameter, λ is the torsion/curvature ratio, and γ is the dimensionless pitch. HCTF geometrical parameters were again defined according to Fig. 5.1.

5.3.4. Floc Characterization

5.3.4.1. Floc Sample Collection, Image Acquisition, and Processing

Samples acquired from the outlet of the continuous-flow system were immediately taken for analysis. A 1000 µL mechanical pipettor was fitted with a wide orifice pipette tip (Finntip, Thermo Scientific, Hampton, NH) for sample transfer. This approach was previously shown to impart minimal shear on flocs during the transfer of sample (Malkoske et al. 2023). The sample was carefully transferred to a 1 mm x 1 mm gridded Sedgewick-Rafter cell (1801-G20, Wildco, France) for imaging analysis using an optical microscope (Zeiss Standard, Zeiss, Germany) affixed with 3.2x and 10x objective pieces. The ocular tube of the microscope was fitted with a 0.5x reduction

lens (A3RDF50, OMAX, WA) and a 10 MP camera (A35100U, OMAX, WA) connected to a computer with image acquisition software (ToupTek, China). Sufficient images were obtained from random locations throughout the counting cell to permit the characterization of 100 flocs for each tested condition. The length of 1 pixel was considered the limit of detection for linear measurements and, using a calibration slide (A36CALM1, OMAX, WA) it was determined to be 0.33 μm. It should be noted that, while large sample sizes are desired to ensure representative characterization of the floc population for each experimental condition, the extensive amount of time required for image acquisition/processing using the microscopic approach imposed practical limitations on the number analyzed. The floc image analysis of a single experiment took half a day's work, longer than conducting the actual flocculation test. Image processing was performed using ImageJ by the U.S. National Institutes of Health (NIH) as in the work by Malkoske (2023). Collected images were processed by subtraction of the image background using a rolling-ball technique with a ball radius of 50-80 pixels and thresholding. The validity of using thresholding in ImageJ for image processing has been previously shown by Balay-Karperinen (2004).

5.3.4.2. Floc Size, Concentration, and Fractal Dimension

The ECD of the floc was determined by back calculating for the diameter of a circle with an equivalent area to the floc, as determined from ImageJ analysis of the 2D projection, according to the following equation (Jarvis et al. 2005):

$$ECD = \sqrt{\frac{4A_{p,floc}}{\pi}} \tag{5.9}$$

Where ECD is the equivalent circular diameter (μm) and $A_{p,floc}$ is the projected area of the floc (μm^2). This procedure is shown graphically in Fig. 5.3.

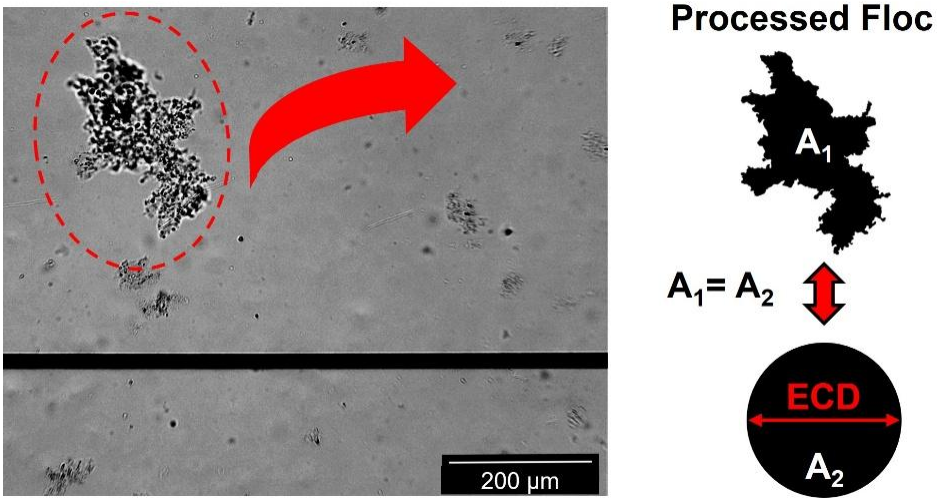


Fig. 5.3. Microscopic analysis of floc ECD

Using images of the Sedgewick-Rafter cell acquired with the 3.2x objective, the floc concentration was determined by dividing the number of flocs in each 1 mm x 1 mm grid by the grid volume according to:

$$C_{floc} = \frac{N_{floc}}{V_{grid}} = \frac{N_{floc}}{1mm^3} \times \frac{10^3 mm^3}{1\ cm^3} \times \frac{1\ cm^3}{mL} = 1000 \times N_{floc} \quad (5.10)$$

Where C_{floc} is the estimate for floc concentration (#/mL) and N_{floc} is the number of flocs counted per grid area of the Sedgewick-Rafter cell. The structure of the individual flocs was assessed using the perimeter-based fractal dimension according to the power law relationship presented by Liu et al. (2021):

$$A_{p,floc} \propto {P_{floc}}^{\frac{2}{D_p}} \quad (5.11)$$

where $A_{p,floc}$ is the projected area of the floc (µm^2), P_{floc} is the floc perimeter (µm), and D_p is the perimeter-based fractal dimension, which was determined by regression of the log-log plot of floc perimeter vs. projected area as in Spicer et al. (1996). For Euclidian objects such as a perfect sphere, D_p is equal to 1, while for more highly irregular objects approaches a value of 2.

5.3.5. Statistical Analysis for FFD

Statistical treatment of the FFD was performed using JMP® Pro 18 (SAS Institute Inc., Cary, NC). All statistical tests were conducted at a significance level of α=0.05 and the statistical significance of the regressed models was determined using the analysis of variance (ANOVA) and F-test.

5.4. Results and Discussion

5.4.1. Model Fitting and Adequacy Assessment

A total of 22 experiments were conducted following a replicated three-factor two-level FFD with three center point runs. The experiments were carried out in a randomized order (Table F.9) to determine the effects of the factors and their interactions on three responses describing floc characteristics: ECD, D_p, and concentration. The statistical significance of the developed models and individual factors for each of the three response variables considered in the FFD was assessed using the ANOVA and the F-test. As shown in Table 5.3, the *p*-values derived from the F-test indicate that the three models are significant with greater than 95% confidence ($p < 0.0035$ in all cases). Among the three response variables, the floc concentration model was found to have the best fit with a coefficient of determination, R^2, greater than 0.88, suggesting that more than 88% of the variability in the response data could be accounted for by the developed model. The regressed model for the floc ECD demonstrated a good fit (R^2=0.775), whereas only a moderate fit was found for D_p (R^2 = 0.686). Model adequacy was further evaluated by examining the normality of the residuals. The residual normal quantile plots (see Fig. F.3) demonstrated an approximately linear trend for all responses, with residuals falling within the Lilliefors confidence bounds, indicating no significant deviation from normality (Conover 1999). Finally, although interaction effects allow for the developed models to account for some degree of non-linearity, the validity of the linearity assumption inherent to the least-squares regression was also assessed to determine whether pure second-order (quadratic) effects warranted inclusion through an expanded design (i.e., central composite design). Using the procedure outlined by Montgomery (2020), a *t*-test was conducted to test the null hypothesis that the mean of the responses at the center point was equal to that of the factorial points. For all three response variables, the null hypothesis failed to be rejected (Section F.4.3.), indicating that the first-order model with interaction shown in Eqn. (5.1) was sufficient to describe the observed relationships.

Table 5.3. ANOVA Analysis and Model Adequacy for 2^3 FFD

Response	Factor	Model Coefficient Estimate	SSE	DF	MSE	*F*-Ratio	*p*-Value
ECD	Intercept	54.6772 [c]	-	-	-	-	-
	x_1: Coil Pitch	-0.4889	3.824	1	3.824	0.087	0.772
	x_2: Pipe Length	9.333	1393.734	1	1393.734	31.744	<.0001 [a]
	x_3: Coil Diameter	2.415	93.335	1	93.335	2.126	0.166
	x_1x_2	-6.825	745.265	1	745.265	16.974	0.0009 [a]
	x_1x_3	0.906	13.126	1	13.126	0.299	0.593
	x_2x_3	1.248	24.922	1	24.922	0.568	0.463
	Model		2274.206	6	379.034	8.633	0.0004
	Residual Error		658.585	15	43.906		
	R^2		0.775				
	RMSE		6.626				
D_p	Intercept	1.5651	-	-	-	-	-
	x_1: Coil Pitch	-0.0104	0.001744	1	0.001744	3.766	0.0713 [b]
	x_2: Pipe Length	-0.0252	0.010188	1	0.010188	21.999	0.0003 [a]
	x_3: Coil Diameter	-0.00549	0.000482	1	0.000482	1.041	0.3237
	x_1x_2	0.01167	0.002179	1	0.002179	4.705	0.0465 [a]
	x_1x_3	0.005095	0.000415	1	0.000415	0.897	0.3586
	x_2x_3	-0.00353	0.000199	1	0.000199	0.430	0.522
	Model		0.01520784	6	0.002535	5.4729	0.0035
	Residual Error		0.00694683	15	0.000463		
	R^2		0.686439				
	RMSE		0.02152				
Floc Concentration	**Intercept**	15705.75	-	-	-	-	-
	x_1: Coil Pitch	-404.488	2,617,762	1	2,617,762	1.942	0.1838
	x_2: Pipe Length	-2229.76	79,549,572	1	79,549,572	59.012	<.0001 [a]
	x_3: Coil Diameter	-1725.46	47,635,560	1	47,635,560	35.337	<.0001 [a]
	x_1x_2	-164.26	431,708	1	431,708	0.320	0.5798
	x_1x_3	-756.75	9,162,710	1	9,162,710	6.797	0.0198 [a]
	x_2x_3	1071.44	18,367,721	1	18,367,721	13.626	0.0022 [a]
	Model		157,765,033	6	26,294,172	19.5056	<.0001
	Residual Error		20,220,466	15	1,348,031		
	R^2		0.88639				
	RMSE		1161.047				

Note: [a] denotes significant with > 95% confidence; [b] denotes significant with > 90% confidence; [c] Model coefficient estimates in terms of coded design variables; SSE = sum of squared errors; DF = degrees of freedom; MSE = mean square error; *F*-Ratio is the test statistic for the F-test.

5.4.1.1. Main and Interaction Effects

The least-squares estimates of the coded factor coefficients for the models describing the three response variables are summarized in Table 5.3. Fig. 5.4 - Fig. 5.6 depict the main and interaction effects of factors on the ECD, D_p, and floc concentration, respectively, in the form of three-dimensional surface plots. For the floc ECD, the pipe length and the interaction between pipe length and coil pitch were found to be statistically significant. Considering the interaction factor seen in Fig. 5.4b as well as the interaction diagrams presented in Fig. F.4, the effect of increasing the pipe length is greater at the low factor setting of coil pitch compared to at the high factor setting. Moreover, the effect of coil pitch on the ECD is seen to change depending on the factor setting of pipe length. At the high factor setting for pipe length, the floc ECD increases with decreasing coil pitch, while at the low factor setting the opposite is true. From Fig. 5.4c, floc ECD is seen to increase primarily as a function of pipe length with minimal interaction between the pipe length and coil diameter as confirmed by a *p*-value of 0.463 (Table 5.3).

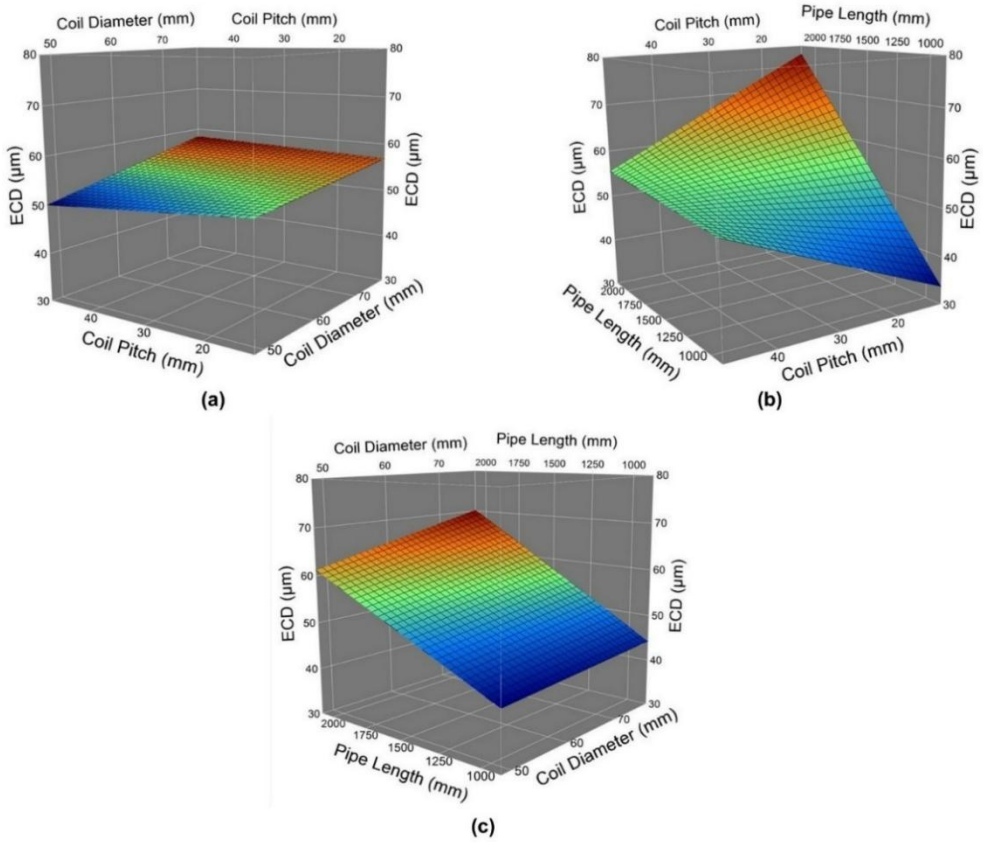


Fig. 5.4. Response surface plots for ECD showing the interaction between: **(a)** d_c and p; **(b)** Length and p; **(c)** Length and d_c.

The response surfaces for D_p are presented in Fig. 5.5 where, it should be noted, the range of the D_p axis was kept at a minimum to better illustrate the effects of flocculator geometry. Floc D_p was found to vary only slightly between 1.512-1.622 (or less than 8%), suggesting that the floc structure remained relatively constant despite changing HCTF geometry (Fig. 5.5). The use of other fractal definitions, including the one-dimensional and two-dimensional forms (see Jiang (1993)), also yielded similar results in that their values were not particularly sensitive to changing HCTF geometry. From Table 5.3, the main effect of pipe length, as well as its interaction with the coil pitch, were found to have small (but statistically significant) effects, with D_p increasing for smaller pitch and shorter pipe length (Fig. 5.5b). Recall, a D_p of 1 indicates a perfect Euclidean geometry while more highly irregular objects have a D_p value closer to 2. Thus, it seems that stronger secondary flow produced by more tightly wound HCTFs generated increased particle

collision frequency for the aggregation of primary particles, leading to more highly branched floc structures with higher D_p. The effect of pipe length may be related to the HRT: as the residence time inside the flocculator is increased from 1.6 min to 3.2 min (as pipe length increases from 1000 to 2000 mm), the floc structure may re-organize to become more compact with a concomitant decrease in the porosity. In the current study the G value for HCTFs was ~ 18 s^{-1}, Selomulya et al. (2001) also reported floc re-organization, without breakup, as flocculation time increased under conditions of moderate mixing intensity (G= 30-80 s^{-1}).

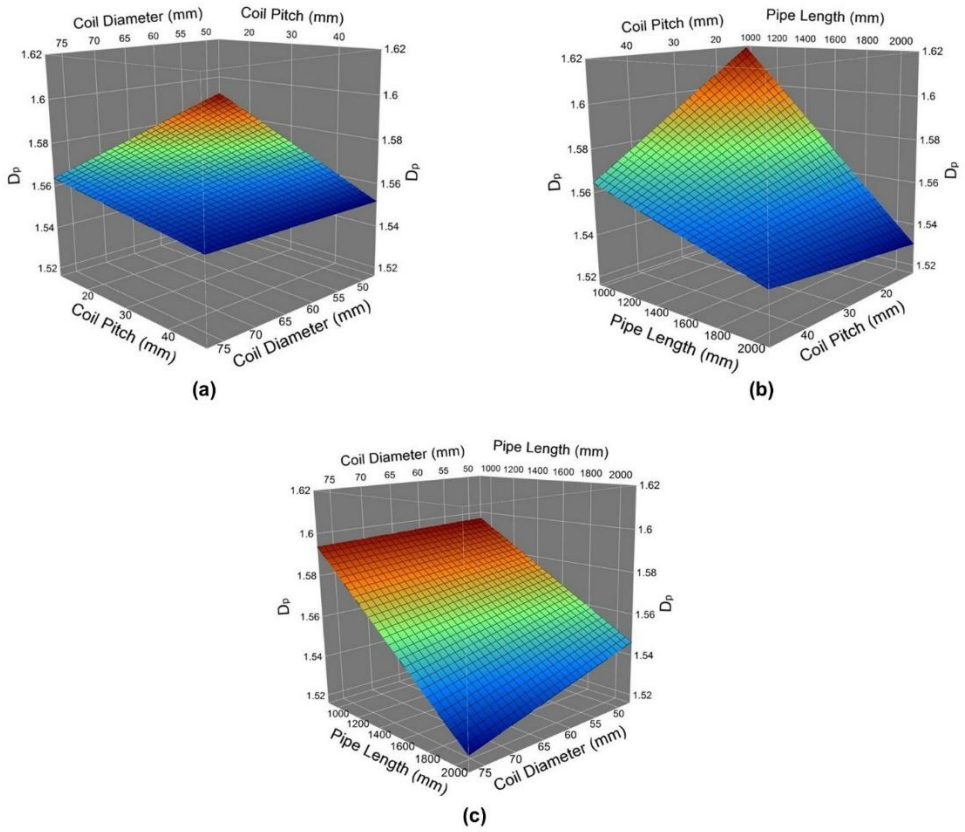


Fig. 5.5. Response surface plots for D_p showing the interaction between: **(a)** d_c and p; **(b)** Length and p; **(c)** Length and d_c.

Finally, in the model for floc concentration, the main effects the coil diameter and pipe length were found to be highly significant ($p < 0.001$, Table 5.3), while the interactions between coil diameter and pipe length (p =0.0022, Table 5.3) as well as coil diameter and coil pitch (p

=0.0198, Table 5.3) were also found to be significant with greater than 95% confidence. In general (Fig. 5.6), the floc concentration increased with decreasing pitch, coil diameter, and pipe length. Considering Fig. 5.6a as well as the interaction diagrams (Fig. F.5 and Fig. F.6), the effect of coil pitch changed depending on the factor setting of the coil diameter. For the low coil diameter conditions, increasing pitch led to a slight increase in floc concentration, whereas at the high setting increasing coil pitch reduced the floc concentration. From Fig. 5.6c the interaction effect between the coil diameter and pipe length is clearly seen, with simultaneous decreases in both parameters resulting in increasing floc concentration. Comparing these results with those of the model for ECD, it is apparent that the higher pipe length setting yields a longer HRT and permits greater opportunities for floc-floc and floc-particle collisions, forming larger sized flocs (ECD significantly increases with pipe length) in lower concentration.

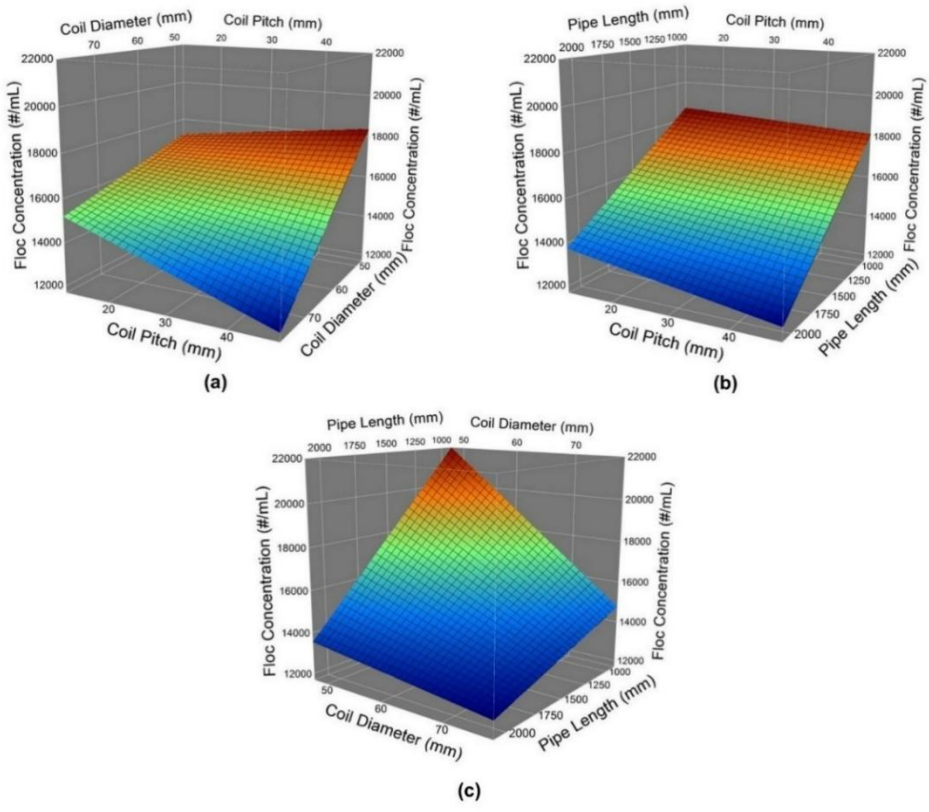


Fig. 5.6. Response surface plots for floc concentration showing the interaction between: **(a)** d_c and p; **(b)** Length and p; **(c)** Length and d_c.

5.4.2. Impact of Torsion and Curvature on HCTF Performance

The findings of the FFD were also supported by those of a multivariate regression analysis relating the response variables to measures of torsion and curvature. Recall that these parameters, which were introduced in Section 5.3.3, have been widely used to describe the impact of geometry on flow in helical pipes. Given the strong effect of pipe length on HCTF performance observed in Table 5.3, the regression analysis was restricted to HCTFs with identical lengths (and thus identical HRTs). For the floc ECD, the effect of coil pitch was seen to change depending on the factor setting of pipe length. This finding was corroborated by the multivariate regression analysis (Fig. 5.7 and Table F.11 – F.12) where, at the high factor setting of pipe length, the ECD was found to have strong and statistically significant negative correlations with β_0 ($p = 0.06$) and γ ($p = 0.03$), while at the low factor setting (i.e., 1000 mm) had a strong positive correlation with β_0 ($p = 0.09$) and γ ($p = 0.15$). The decrease in floc size with increasing torsion, seen for the 2000 mm pipe length setting in the current study (HRT = 3.16 min), was also observed by Carissimi et al. (2018) for an HCTF with a length of 12 m (HRT = 18 s) and operated within the laminar-transitional flow zone. In that study, as γ increased from 0.057-0.452, the observed floc diameter was found to decrease from approximately 3 mm to non-detect. The disparate effect of coil torsion on the ECD for different pipe lengths may be related to the HRT and the number of coil rotations. Tang et al. (2016) reported that the secondary flow in helically coiled tubes is fully developed within the first rotation while Mansour et al. (2020a) reported that, for conditions similar to those used in the current study (Re < 50 and coil pitch < 60 mm), complete mixing was achieved within approximately three complete revolutions of the HCTF. Thus, for the 2000 mm pipe length, the primary particles experience 7-11 complete rotations of fully developed secondary flow, affording them sufficient opportunity for collisions and aggregate growth. Increasing the coil torsion at this condition serves to destabilize the secondary flow, deteriorating the twin-vortex structure and even delaying their development to higher R_e(Yamamoto et al. 2002). In contrast, for the 1000 mm condition, the floc growth is limited by the relatively shorter HRT (only 1.6 min) and lower number of rotations (3-5) with fully developed secondary flow. For these HCTFs, it may be that the increased torsion arising from greater coil pitch values led to enhanced vorticity (curl of the local velocity profile) in the pipe, facilitating improved floc growth compared to conditions with lower torsion. The increase in vorticity with torsion was also reported by Wang (1981) for low flow conditions (Re < 40) like those used in this bench-scale system.

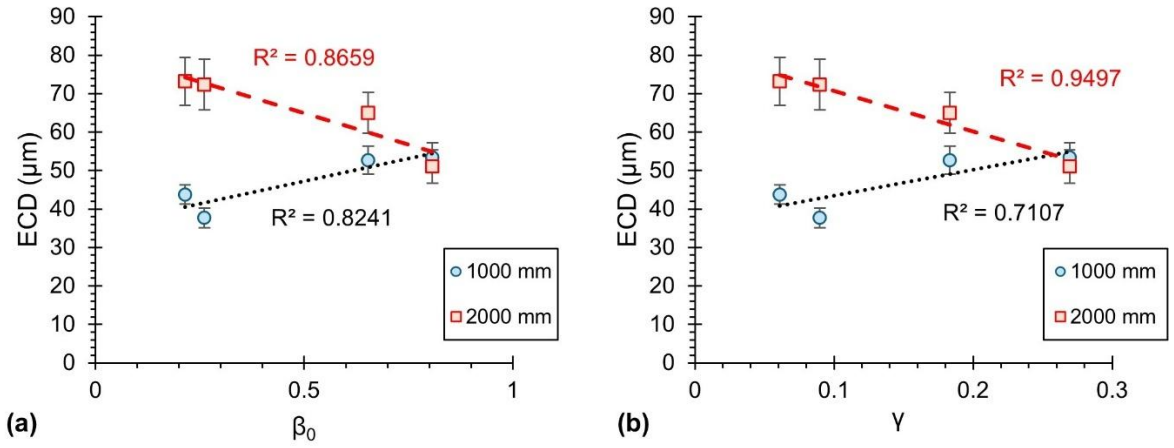


Fig. 5.7. Relationship between floc ECD and measures of torsion for HCTFs with high and low pipe length settings: **(a)** ECD vs. torsion parameter (β_0); **(b)** ECD vs. dimensionless pitch (γ)

For floc concentration, the FFD results were also corroborated by the analysis of HCTF curvature (Fig. 5.8). As the HCTF coil diameter, coil pitch, or the combination of coil pitch and diameter were decreased, the curvature increases and higher floc concentrations were observed. Increased curvature has been shown to generate a larger magnitude centrifugal force, thus a more intense and improved secondary flow that yields more efficient mixing (Kumar et al. 2006; Mansour et al. 2017). Therefore, for flocculation with the short setting of pipe length where, as noted above, the floc growth can be hindered by the low HRT and number of coil rotations with fully developed flow, it is possible that the improved secondary flow yields greater aggregation efficiency of primary particles, leading to a larger number of detectable/measurable flocs.

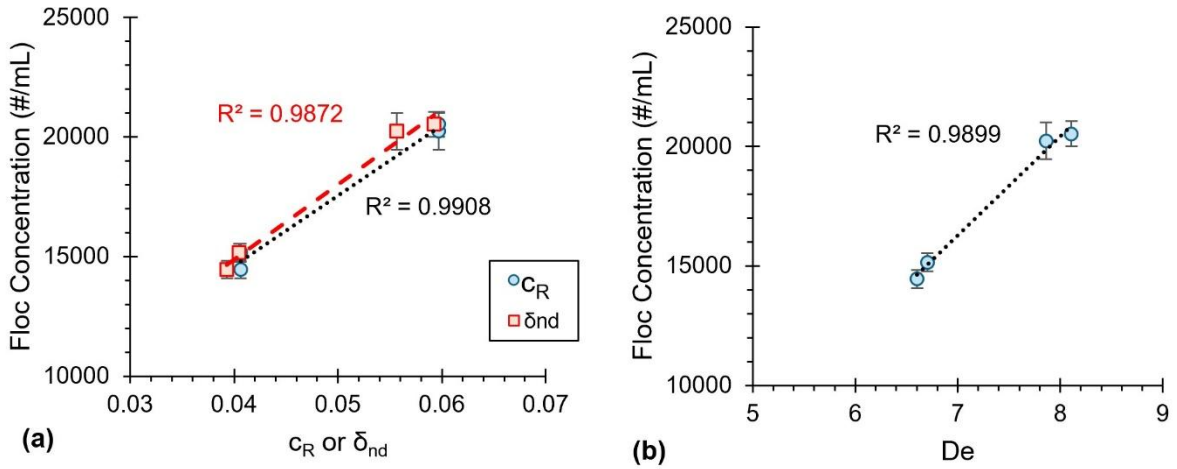


Fig. 5.8. Relationship between floc concentration and measures of curvature for HCTFs with 1000 mm pipe length: **(a)** Concentration vs. curvature ratio (c_R) or dimensionless curvature (δ_{nd}); **(b)** Concentration vs. Dean number (D_e)

5.4.3. Comparison with Alternative C-IN Mixer Types

Fig. 5.9 compares the floc ECD, concentration, and D_p of the nine HCTF configurations with those of the batch reactor and commercial ISM. Although there were significant differences in floc size for the alternative helical flocculators (mean size ranging between 37.7 μm and 73.1 μm), the flocs produced by batch mixing and the ISM were significantly larger (140.1 μm) and smaller (19.8 μm), respectively, than those formed by the HCTFs. Moreover, the size of flocs formed by the batch reactor were found to be stable over a three-hour period following the initial rapid mixing (Fig. F.7). When floc concentration was considered, the values for the different HCTFs (10,485-20,529 mL^{-1}) again lay between those for batch (4,904 mL^{-1}) and the ISM (26,444 mL^{-1}), although this time the batch mixer yielded the lowest concentration while the ISM yielded the greatest. While statistically significant differences in D_p were observed between the different HCTF configurations and the batch reactor, D_p remained relatively constant and the variations were small, suggesting a similar structure. D_p for the ISM, however, was found to be 6.5-15.2 % greater than for the various HCTFs and batch reactor (1.72 vs. 1.52-1.59), suggesting a structure with a less compact geometry with a looser and more elongated structure. These findings confirm that, while many C-IN-LPM studies in the literature have used different mixing approaches based on what is

available to them or experimentally convenient, the properties of the flocs formed by these mixers differ significantly. As many previous studies have reported that floc size and concentration can impact the properties of the cake layer in C-IN-LPM systems (Amjad et al. 2015), the degree of fouling reported by bench-scale filtration studies is likely to be impacted by the choice of coagulant mixing. Accordingly, future research should compare the fouling tendency of LPMs pre-treated by C-IN with each of these three mixing approaches. This work should characterize the developed foulant cake so that the measured properties of the flocs and the cake layer can be related to the observed fouling potential.

Comparing the HCTFs with the ISM, both exhibit toroidal flow patterns. In fact, much like HCTFs, Jones et al. (2002) reported that the helical elements within the ISM produce complex secondary flow patterns with several pairs of counter-rotating vortices formed at the intersection of the elements within the mixer. Despite the apparent similarity in flow pattern, the ISM was seen to have poorer flocculation performance resulting in smaller sized steady-state floc aggregates. As HCTFs with shorter pipe length produced larger flocs (in lower concentration) compared to the ISM, despite having a slightly shorter effective HRT (1.6 min vs. 2.58 min), residence time alone could not account for the differences in performance. Rather, the disparity likely reflects differences in the hydrodynamics and secondary flow intensity. It must be acknowledged that, in practice, ISMs are primarily used for coagulant blending with high intensity mixing (Edzwald 2013) while HCTFs are employed to promote floc growth under comparatively low shear. Although the ISM may be a suitable flocculator for bench-scale studies (the manufacturer reports that complete mixing can be achieved by the ISM in the fully laminar flow regime), the slightly larger cross-sectional diameter led to a lower axial flow velocity which likely weakened the secondary flow pattern compared to the HCTFs. Consequently, the potential for cluster-cluster collisions within the ISM would be limited, resulting in the observed smaller sized steady-state floc aggregates. Therefore, ISMs may be more appropriate for bench-scale flocculation studies conducted at higher flowrates, although further investigation is required to confirm this hypothesis and to identify the operational range of flow conditions for which they are appropriate.

The differences in floc properties between the batch reactor and the two types of continuous-flow mixers is likely due to the absence of rapid (intense) mixing in the latter two alternatives. Based on the aluminum speciation diagram proposed by Amirtharajah and Mills (1982), the coagulation chemistry used in the current study falls within the sweep coagulation

zone, however, is influenced by adsorption-destabilization. Although the performance of sweep flocculation is largely independent of the mixing intensity (Kawamura 2000), adsorption destabilization reactions are estimated to occur in less than 1 s. Accordingly, the dispersal of the small coagulant flow across the entire cross-section of the process flow as rapidly as possible is necessary to prevent either incomplete or extensive local adsorption of the metal hydroxide species (Bratby 2016). For the HCTFs and ISM in the continuous-flow system, the low flowrate condition was possibly inadequate to fully distribute the coagulant within the feedwater. This may have led to local regions where the coagulant concentration was high enough to cause restabilization or too low to destabilize the suspension, resulting in the observed smaller sized floc aggregates as compared to the batch reactor (Letterman et al. 1973).

The larger flocs formed by the batch-reactor seem to suggest that the inclusion of a dedicated rapid mixing unit is necessary for optimal flocculation performance in continuous-flow bench-scale systems. Accordingly, future work should undertake to develop an inline rapid mixing unit for bench-scale studies and evaluate its impact on the properties of flocs formed by the continuous-flow mixing approaches (i.e., HCTFs and ISM). In addition, although the ISM generated small-sized flocs on its own, its reported ability to achieve complete mixing under firmly laminar conditions suggests that it could be an effective tool for coagulant distribution across the feed upstream of flocculation by HCTFs. This hypothesis should be evaluated by future studies.

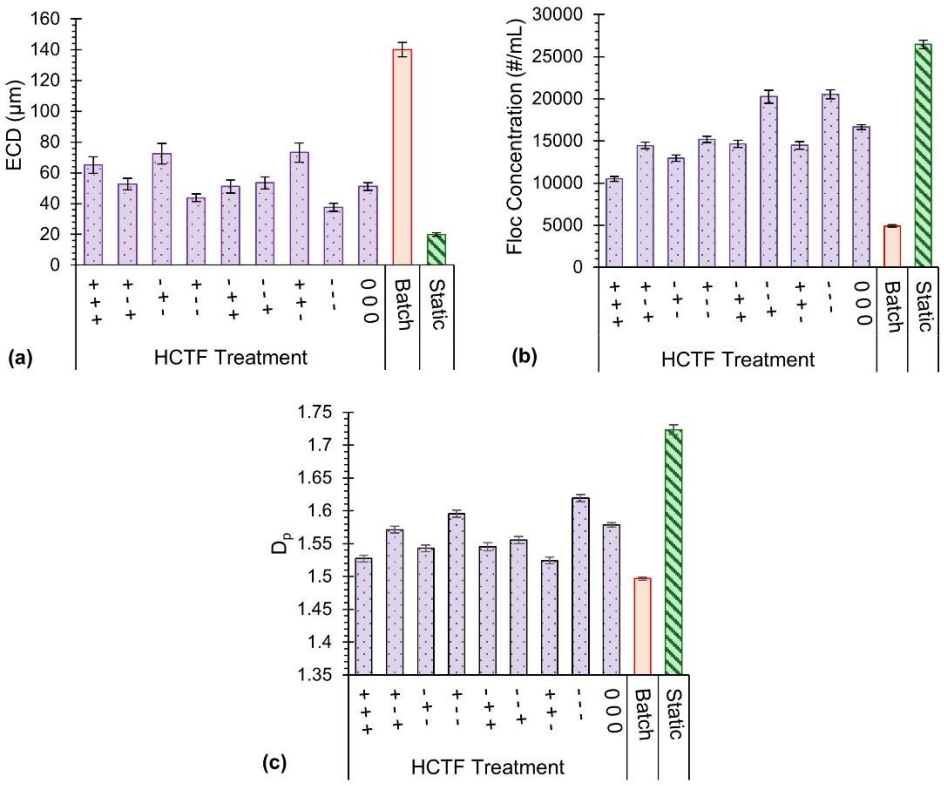


Fig. 5.9. Comparison of HCTF floc properties with mixing by batch reactor or ISM: **(a)** ECD; **(b)** Floc concentration; **(c)** D_p. Note that the HCTF Treatments are coded by the factor levels for coil diameter, pipe length, and coil pitch (in that order) where +, 0, and – refer to the high, center-point, and low factor settings, respectively (see Table F.9).

5.4.4. Effect of Reynolds Number on HCTF Performance

All the experiments presented to this point used the same flowrate and a constant helical tube diameter, thus, they had the same axial flow velocity and R_e. To evaluate the impact of R_e on the properties of the flocs formed by HCTFs, the system was operated at three different flowrates. Fig. 5.10 compares the ECD and floc concentration found for the HCTF at the center point of the FFD (HRT = 2.4 min, R_e = 33.3) with those for the same HCTF operated at flowrates of 10 mL min^{-1} (HRT = 1.2 min, R_e = 66.6) and 20 mL min^{-1} (HRT = 0.6 min, R_e = 133.3). While the D_p was found to vary narrowly between 1.55-1.6 for the three studied R_e values, the mean ECD was found to initially increase (from 51.1 μm to 108.8 μm) as the R_e increased from 33.3 to 66.6, before decreasing to 33.9 μm as the R_e was further increased to 133.3. Opposite to ECD, the floc

concentration initially decreased with increasing R_e before increasing as the R_e was increased from 66.6 to 133.3. This unimodal pattern was also observed in the studies by De Oliveira and Teixeira (2017) and De Oliveira et al. (2020) where the turbidity removal efficiency (TRE) was measured as a surrogate for HCTF flocculation performance at different flowrates and HRTs. In the current study, given that the floc fractal dimension remains nearly constant for the three different R_e conditions, achieved by changing the flowrate, the ECD would be expected to represent the TRE given the well-established relationships between TRE and settling velocity as well as settling velocity and size/fractal dimension (Vahedi and Gorczyca 2011, 2012). Given that the variation in floc ECD was much greater for changing R_e compared to the average effect of pipe length (i.e., $\overline{ECD_{2000}} - \overline{ECD_{1000}} = 18.5\ \mu m$), which was shown to be the most significant HCTF geometrical parameter, the tubular flow R_e (which is directly related to the flowrates studied) should be considered as the most important variable in the design of HCTFs.

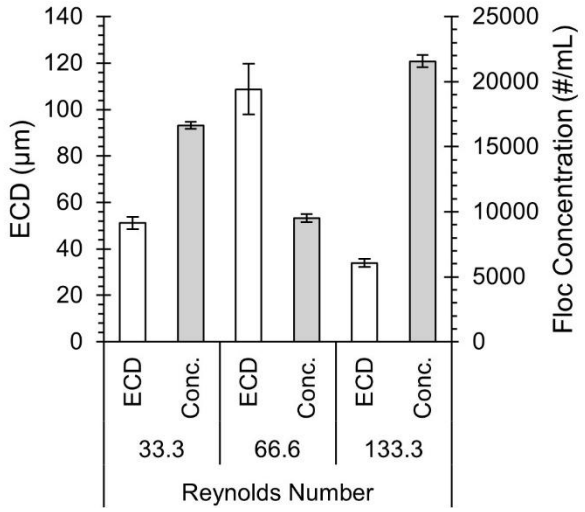


Fig. 5.10. Effect of Reynolds number on ECD and floc concentration at FFD center point ($Length$ = 1500 mm; d_c = 67.5 mm; p = 30 mm)

The unimodal pattern is likely the result of a trade-off between the mixing intensity and the HRT of the flocculator. As the R_e is increased from 33.3 to 66.6, increasing Dean number (7.25→14.49) and G value (18 s^{-1}→36 s^{-1}) suggests a stronger secondary flow, which should lead

to improved mixing characteristics. In fact, Serra et al. (2008) reported that floc size increased with G values up to ~ 30 s^{-1} due to aggregation dominated flocculation. This was seen in the current study by the increased floc ECD and the concomitant lower floc concentration as more primary particles and small flocs are aggregated into larger sized flocs. As the R_e increased to 133.3 the secondary flow pattern is again strengthened (D_e=14.49→29), however, the magnitude of the Dean number actually exceeds the region (5≤ D_e ≤21) identified by Mansour et al. (2019) for optimal mixing across a wide range of HCTF geometries. Moreover, the G value, which reached ~ 75 s^{-1}, suggests shear-induced breakage of floc aggregates, which led to smaller sized particles as in the study by Yu et al. (2011). The increased flowrate associated with the highest R_e also led to a decrease in flocculator HRT to only 0.6 min, which affords little opportunity for collisions between the flocs, yielding a suspension with a larger concentration of small sized flocs. This hypothesis should be confirmed by future testing which compares the effect of varying flowrate for HCTFs of the same geometry, but also with the same HRT.

5.4.5. Experimental Design Guidelines

As shown in this study, irrespective of the geometry, HCTFs are an effective means to achieve flocculation in bench-scale continuous-flow systems with low R_e. A distinct advantage of HCTFs is the flexibility that they provide in design, with a completely customizable geometry capable of producing flocs of differing character according to the downstream technology choice and experimental requirements. The system flowrate (i.e., R_e) was shown to exert the greatest effect on floc ECD, with the trade-off between shear intensity and mixing HRT governing the potential for floc agglomeration and growth. Therefore, the design of HCTFs should select pipe diameter accordingly to provide R_e, D_e, G, and HRT values (for the corresponding flowrate) that facilitate the formation of flocs with the desired properties. The helical pipe length and, by extension, HRT were found to be the geometrical parameters that have the most significant impact on floc ECD and thus should also be carefully considered in future work. It is suggested that the scalability of these guidelines also be tested in full-scale units.

For LPM pretreatment, Malkoske et al. (2023) reported that increased floc concentration improved the hydraulic reversibility of fouling and the release of retained NOM from the membrane surface. However, Amjad et al. (2015) noted the importance of mass loading during

filtration and larger floc sizes are known to reduce the cake resistance to filtration (Guan et al. 2001). For conventional coagulation/flocculation/sedimentation large sized flocs are also desired to enable rapid settling times (see Chapter 3). Therefore, to produce the largest sized flocs HCTFs with longer pipes (higher HRTs) and small coil pitch values should be specified, although, for LPM pretreatment applications the inverse proportionality between the floc ECD and floc concentration should be kept in mind. According to the results of Section 5.4.4, the HCTF pipe diameter should be selected to provide R_e, D_e and G values near 67, 15 and 30 s^{-1}, respectively, which were optimal for floc growth. These conditions produced flocs with an average ECD greater than 100 μm, which Edzwald (2011) as well as Edzwald and Haarhoff (2012) have noted is the minimum size required to provide reasonable settling velocities in downstream settling basins. For LPM filtration applications, Park et al. (2006) have also reported that the specific cake layer resistance is minimized for flocs larger than 100 μm in size.

5.5. Conclusions

In this study, as a result of their strong secondary flow pattern, HCTFs were shown to provide sufficient mixing for good floc development under laminar flow conditions with Reynolds numbers as low as 33.3. Through the use of a 2^3 FFD, this work represents the first effort to comprehensively and systematically investigate the impact of helical geometry on the properties of flocs formed in continuous-flow coagulation systems typical of those used for LPM fouling mitigation studies. The performance of the HCTFs was additionally compared with that of a commercial ISM and batch coagulation reactor, which have also been extensively used in C-IN-LPM studies. The results of the study may be summarized as:

1. Helical geometry was confirmed to have a statistically significant impact on the properties of flocs formed by HCTFs. The floc size was significantly impacted by the pipe length and the interaction between pipe length and coil pitch. When the floc concentration was considered, the main effects of coil diameter and pipe length, their interaction, as well as the interaction between coil diameter and coil pitch were the significant factors. In contrast, the floc structure remained relatively constant for all geometries considered, with only the pipe length and its interaction with coil pitch exhibiting small, but statistically significant, effects.

2. The variation in floc properties produced by HCTFs in the FFD could also be correlated well to measures of pipe curvature and torsion. For HCTFs at the high factor setting of pipe length, the torsion parameter displayed a strong negative correlation with floc size, likely due to its disruptive effect on the secondary flow pattern. In contrast, for HCTFs with a short pipe length, increased torsion led to greater ECD possibly due to increased vorticity in the secondary flow.
3. Statistically significant differences existed in the mean floc ECD and concentration for the three mixer types investigated with batch mixing yielding the largest flocs in the lowest concentration, while the commercial ISM produced the smallest flocs in the largest concentration. The flocs produced by the ISM were also found to have a significantly looser structure compared to those of the HCTFs and batch reactor.
4. Compared to parameters describing helical geometry, Reynolds number exhibited the greatest impact on floc properties. For three different flowrates with Reynolds numbers between 33.3 and 133.3, the ECD initially showed an increasing, then decreasing trend, while the floc concentration changed in inverse. The unimodal pattern was likely the result of a trade-off between the mixing intensity (G value), the secondary flow strength (D_e number), and the flocculation HRT. Initial floc size increase was promoted by stronger secondary flow (D_e 7.25→14.49) and aggregation-dominated flocculation (G < ~ 30 s^{-1}) at reasonable HRTs, however, shear induced floc breakup (G ~ 75 s^{-1}) and decreasing flocculation HRT (2.4 min → 0.6 min) likely led to smaller flocs in greater concentrations as the system flowrate increased. Accordingly, the impact of Reynolds number for HCTFs with constant HRT should be studied further. The Reynolds number is critical to the design of future HCTFs and appropriate selection of pipe diameter is required for the system to operate within optimal regions of D_e, G, and HRT.

Future studies should investigate how the altered floc properties seen for each mixing approach impact LPM fouling in the integrated C-IN-LPM system. Moreover, it would be of interest to characterize the fouling layer in the C-IN-LPM system so that the observed fouling potential and cake layer properties may be related to the characteristics of the flocs formed by each mixing type. Finally, rapid mixing in the batch coagulation approach seemed to have an important effect on floc growth. Accordingly, future work should consider the development of an inline rapid

mixing unit with reasonable HRTs for bench-scale systems and evaluate its impact on floc properties and membrane fouling for continuous-flow C-IN with the HCTFs and ISM used in this study.

5.6. Acknowledgements

This work was supported by the Natural Sciences and Engineering Research Council of Canada (NSERC) under grant RGPIN 2018-06571 as well as the NSERC Canada Graduate Scholarship-Doctoral Program (ID 579943-2023). The authors would also like to acknowledge financial support provided to the lead author by the American Membrane Technology Association (AMTA) through their Ian C. Watson Fellowship and by the American Water Works Association (AWWA) through the Dr. James K. Edzwald Scholarship. Finally, the authors extend their thanks to Catherine Brosseau (Kemira Water Solutions Canada) for providing coagulants for this study as well as Mr. Julian Fino for his help in the lab.

5.7. References

Alresheedi, M. T., and O. D. Basu. 2019. "Effects of feed water temperature on irreversible fouling of ceramic ultrafiltration membranes." *Journal of Water Process Engineering*, 31: 100883. https://doi.org/10.1016/j.jwpe.2019.100883.

Alresheedi, M. T., S. L. D. Kenari, B. Barbeau, and O. D. Basu. 2022. "Flux modulation: A novel approach for ultrafiltration fouling control." *Journal of Water Process Engineering*, 46: 102551. https://doi.org/10.1016/j.jwpe.2021.102551.

American Water Works Association. 2018. *Manual of Water Supply Practices - M62: Membrane Applications for Water Reuse*. 1st ed. Denver, CO: American Water Works Association.

Amirtharajah, A., and K. M. Mills. 1982. "Rapid-mix design for mechanisms of alum coagulation." *Journal AWWA*, 74 (4): 210–216. https://doi.org/10.1002/j.1551-8833.1982.tb04890.x.

Amjad, H., Z. Khan, and V. V. Tarabara. 2015. "Fractal structure and permeability of membrane cake layers: Effect of coagulation–flocculation and settling as pretreatment steps." *Separation and Purification Technology*, 143: 40–51. https://doi.org/10.1016/j.seppur.2015.01.020.

Amy, G. 2008. "Fundamental understanding of organic matter fouling of membranes." *Desalination*, 231 (1–3): 44–51. https://doi.org/10.1016/j.desal.2007.11.037.

AWWA. 2005. "Committee Report: Recent advances and research needs in membrane fouling." *Journal AWWA*, 97 (8): 79–89. https://doi.org/10.1002/j.1551-8833.2005.tb07452.x.

Balay-Karperinen, A. 2004. "Defining Microglial Morphology: Form, Function, and Fractal Dimension." M.Sc, Charles Sturt University.

Bratby, J. 2016. *Coagulation and Flocculation in Water and Wastewater Treatment*. 3rd ed. London, UK: IWA Publishing.

Cahyana, G. H., P. Suwandhi, and T. Mulyani. 2021. "Novel helical or coiled flocculator for turbidity reduction in drinking water treatment: a performance study." *IOP Conference Series: Earth and Environmental Science*, 623 (1): 012009. https://doi.org/10.1088/1755-1315/623/1/012009.

Carissimi, E., D. G. Sanagiotto, E. B. C. Schettini, and J. Rubio. 2018. "Revisiting coiled flocculator performance for particle aggregation." *Water Environment Research*, 90 (4): 322–328. https://doi.org/10.2175/106143017X14902968254935.

Cioncolini, A., and L. Santini. 2006. "An experimental investigation regarding the laminar to turbulent flow transition in helically coiled pipes." *Experimental Thermal and Fluid Science*, 30 (4): 367–380. https://doi.org/10.1016/j.expthermflusci.2005.08.005.

Conover, W. J. 1999. *Practical Nonparametric Statistics*. 3rd ed. Hoboken, NJ, USA: Wiley.

Crittenden, J. C., R. R. Trussell, D. W. Hand, K. J. Howe, and G. Tchobanoglous. 2012. *Water Treatment: Principles and Design*. 3rd ed. New York, NY: McGraw-Hill.

De Oliveira, D. S., and E. C. Teixeira. 2017. "Experimental evaluation of helically coiled tube flocculators for turbidity removal in drinking water treatment units." *Water SA*, 43 (3): 378. https://doi.org/10.4314/wsa.v43i3.02.

De Oliveira, D. S., E. C. Teixeira, and C. B. Donadel. 2020. "Novel approaches for predicting efficiency in helically coiled tube flocculators using regression models and artificial neural networks." *Water and Environment Journal*, 34 (4): 550–562. https://doi.org/10.1111/wej.12484.

Du, P., X. Li, Y. Yang, Z. Su, H. Li, N. Wang, T. Guo, T. Zhang, and Z. Zhou. 2019. "Optimized coagulation pretreatment alleviates ultrafiltration membrane fouling: The role of floc

properties and slow-mixing speed on mechanisms of chitosan-assisted coagulation." *Journal of Environmental Sciences*, 82: 82–92. https://doi.org/10.1016/j.jes.2019.02.027.

Edzwald, J. K., ed. 2011. *Water quality & treatment: A handbook on drinking water*. 6th ed. Denver, CO: American Water Works Association.

Edzwald, J. K. 2013. "Coagulant mixing revisited: theory and practice." *Journal of Water Supply: Research and Technology-Aqua*, 62 (2): 67–77. https://doi.org/10.2166/aqua.2013.142.

Edzwald, J. K., and J. Haarhoff. 2012. *Dissolved Air Flotation for Water Clarification*. 1st ed. New York, NY: McGraw-Hill.

Edzwald, J. K., and J. E. Tobiason. 1999. "Enhanced coagulation: US requirements and a broader view." *Water Science & Technology*, 40 (9): 63–70. https://doi.org/10.1016/S0273-1223(99)00641-1.

García-Ávila, F., D. Tenesaca-Pintado, F. Novoa-Zamora, E. A. Alfaro-Paredes, A. Avilés-Añazco, A. Guanuchi-Quito, M. D. Tonon-Ordoñez, and C. Zhindón-Arévalo. 2023. "Vertical tubular flocculator: Alternative technology for the improvement of drinking water treatment processes in rural areas." *Journal of Environmental Management*, 331: 117342. https://doi.org/10.1016/j.jenvman.2023.117342.

Guan, J., R. Amal, and T. D. Waite. 2001. "Effect of aggregate size and structure on specific resistance of biosolids filter cakes." *Water Science and Technology*, 44 (10): 215–220. https://doi.org/10.2166/wst.2001.0624.

Howe, K. J., A. Marwah, K.-P. Chiu, and S. S. Adham. 2006. "Effect of coagulation on the size of MF and UF membrane foulants." *Environmental Science & Technology*, 40 (24): 7908–7913. https://doi.org/10.1021/es0616480.

Huang, H., K. Schwab, and J. G. Jacangelo. 2009. "Pretreatment for low pressure membranes in water treatment: A review." *Environmental Science and Technology*, 43 (9): 3011–3019. https://doi.org/10.1021/es802473r.

Huttl, T. J., and R. Friedrich. 2000. "Infuence of curvature and torsion on turbulent flow in helically coiled pipes." *International Journal of Heat and Fluid Flow*, 345–353.

Jarvis, P., B. Jefferson, and S. A. Parsons. 2005. "Measuring floc structural characteristics." *Reviews in Environmental Science and Bio/Technology*, 4 (1–2): 1–18. https://doi.org/10.1007/s11157-005-7092-1.

Jiang, Q. 1993. "Fractal structure of aggregates induced by shear motion." Ph.D. Thesis, The University of Arizona.

Jones, S. C., F. Sotiropoulos, and A. Amirtharajah. 2002. "Numerical modeling of helical static mixers for water treatment." *Journal of Environmental Engineering*, 128 (5): 431–440. https://doi.org/10.1061/(ASCE)0733-9372(2002)128:5(431).

Kamińska, G., W. Pronk, and J. Traber. 2020. "Effect of coagulant dose and backflush pressure on NOM membrane fouling in inline coagulation-ultrafiltration." *Desalination and Water Treatment*, 199: 188–197. https://doi.org/10.5004/dwt.2020.25657.

Kawamura, S. 2000. *Integrated Design and Operation of Water Treatment Facilities*. New York, NY: John Wiley & Sons.

Kimura, K., and K. Kume. 2020. "Irreversible fouling in hollow-fiber PVDF MF / UF membranes filtering surface water: Effects of precoagulation and identification of the foulant." *Journal of Membrane Science*, 602 (February): 117975–117975. Elsevier B.V. https://doi.org/10.1016/j.memsci.2020.117975.

Kinser, K. 2021. "Membrane Filtration: Past, Present, and Future." *Journal AWWA*, 113 (8): 72–75. https://doi.org/10.1002/awwa.1791.

Kumar, V., M. Aggarwal, and K. D. P. Nigam. 2006. "Mixing in curved tubes." *Chemical Engineering Science*, 61 (17): 5742–5753. https://doi.org/10.1016/j.ces.2006.04.040.

Letterman, R. D., J. E. Quon, and R. Gemmell S. 1973. "Influence of rapid-mix parameters on flocculation." *Journal AWWA*, 65 (11): 716–722. Hoboken, NJ, USA: Wiley.

Liou, T. M. 1992. "Flow visualization and LDV measurement of fully developed laminar flow in helically coiled tubes." *Experiments in Fluids*, 13 (5): 332–338. https://doi.org/10.1007/BF00209507.

Liu, Y., Z. Wang, M. Xu, F. Qi, C. Li, D. Sun, J. Nan, W. Li, X. Guan, and A. Ikhlaq. 2024. "Unveiling the role of cake layer in coagulation-ultrafiltration on membrane fouling and emerging application as dynamic membrane before ultrafiltration." *Separation and Purification Technology*, 350: 127932. https://doi.org/10.1016/j.seppur.2024.127932.

Liu, Y., X. Zhang, W. Jiang, M. Wu, and Z. Li. 2021. "Comprehensive review of floc growth and structure using electrocoagulation: Characterization, measurement, and influencing factors." *Chemical Engineering Journal*, 417: 129310. https://doi.org/10.1016/j.cej.2021.129310.

Malkoske, T. A. 2023. "Coagulation/Flocculation-Ultrafiltration Optimization in Drinking Water Treatment." Ph.D. Thesis, University of Toronto.

Malkoske, T. A., P. R. Bérubé, and R. C. Andrews. 2020. "Coagulation/flocculation prior to low pressure membranes in drinking water treatment: A review." *Environmental Science: Water Research and Technology*, 6 (11): 2993–3023. Royal Society of Chemistry. https://doi.org/10.1039/d0ew00461h.

Malkoske, T. A., P. R. Bérubé, and R. C. Andrews. 2023. "Impact of extended versus typical rapid mixing HRTs on continuous-flow coagulation-ultrafiltration." *Separation and Purification Technology*, 319: 124041. https://doi.org/10.1016/j.seppur.2023.124041.

Mallya, D. S., S. Abdikheibari, L. F. Dumée, S. Muthukumaran, W. Lei, and K. Baskaran. 2023. "Removal of natural organic matter from surface water sources by nanofiltration and surface engineering membranes for fouling mitigation – A review." *Chemosphere*, 321: 138070. https://doi.org/10.1016/j.chemosphere.2023.138070.

Mansour, M., P. Khot, D. Thévenin, K. D. P. Nigam, and K. Zähringer. 2020a. "Optimal Reynolds number for liquid-liquid mixing in helical pipes." *Chemical Engineering Science*, 214: 114522. https://doi.org/10.1016/j.ces.2018.09.046.

Mansour, M., Z. Liu, G. Janiga, K. D. P. Nigam, K. Sundmacher, D. Thévenin, and K. Zähringer. 2017. "Numerical study of liquid-liquid mixing in helical pipes." *Chemical Engineering Science*, 172: 250–261. https://doi.org/10.1016/j.ces.2017.06.015.

Mansour, M., D. Thévenin, K. D. P. Nigam, and K. Zähringer. 2019. "Generally-valid optimal Reynolds and Dean numbers for efficient liquid-liquid mixing in helical pipes." *Chemical Engineering Science*, 201: 382–385. https://doi.org/10.1016/j.ces.2019.03.003.

Mansour, M., K. Zähringer, K. D. P. Nigam, D. Thévenin, and G. Janiga. 2020b. "Multi-objective optimization of liquid-liquid mixing in helical pipes using genetic algorithms coupled with computational fluid dynamics." *Chemical Engineering Journal*, 391: 123570. https://doi.org/10.1016/j.cej.2019.123570.

Maraschin, M., K. F. S. H. Ferrari, A. P. H. da Silva, and E. Carissimi. 2020. "Aluminum sludge thickening: Novel helical pipes for aggregation by dual flocculation and thickening by filtration applied to water treatment plants." *Separation and Purification Technology*, 241: 116560. https://doi.org/10.1016/j.seppur.2020.116560.

Mishra, P., and S. N. Gupta. 1979. "Momentum transfer in curved pipes. 1. Newtonian fluids."

Industrial & Engineering Chemistry Process Design and Development, 18 (1): 130–137. https://doi.org/10.1021/i260069a017.

Montgomery, D. C. 2020. *Design and Analysis of Experiments*. 10th ed. Hoboken, NJ, USA: Wiley.

Nan, J., M. Yao, Q. Li, D. Zhan, T. Chen, Z. Wang, and H. Li. 2016. "The role of shear conditions on floc characteristics and membrane fouling in coagulation/ultrafiltration hybrid process – the effect of flocculation duration and slow shear force." *RSC Advances*, 6 (1): 163–173. https://doi.org/10.1039/C5RA18328F.

Neama, M.-A. A. M., W. A. Elbarki, M. Fayed, and S. Aly. 2024. "Upgrading the eastern wastewater treatment plant effluent quality in Egypt for reuse by means of in-line coagulation followed by ultrafiltration." *Water Practice & Technology*, 19 (12): 4754–4772. London, UK: IWA Publishing. https://doi.org/10.2166/wpt.2024.285.

Park, P.-K., C.-H. Lee, and S. Lee. 2006. "Permeability of collapsed cakes formed by deposition of fractal aggregates upon membrane filtration." *Environmental Science & Technology*, 40 (8): 2699–2705. https://doi.org/10.1021/es0515304.

Pearce, G. K. 2018. "Is the Water Membrane Market in a State of Flux?" *Water World*.

Peleato, N. M., R. L. Legge, and R. C. Andrews. 2017. "Characterization of UF foulants and fouling mechanisms when applying low in-line coagulant pre-treatment." *Water Research*, 126: 1–11. https://doi.org/10.1016/j.watres.2017.08.064.

Sartori, M., D. S. Oliveira, E. C. Teixeira, W. B. Rauen, and N. C. Reis. 2015. "CFD modelling of helically coiled tube flocculators for velocity gradient assessment." *Journal of the Brazilian Society of Mechanical Sciences and Engineering*, 37 (1): 187–198. https://doi.org/10.1007/s40430-014-0141-3.

Schulz, M., A. Soltani, X. Zheng, and M. Ernst. 2016. "Effect of inorganic colloidal water constituents on combined low-pressure membrane fouling with natural organic matter (NOM)." *Journal of Membrane Science*, 507: 154–164. Elsevier. https://doi.org/10.1016/j.memsci.2016.02.008.

Selomulya, C., R. Amal, G. Bushell, and T. D. Waite. 2001. "Evidence of shear rate dependence on restructuring and breakup of latex aggregates." *Journal of Colloid and Interface Science*, 236 (1): 67–77. https://doi.org/10.1006/jcis.2000.7372.

Serra, T., J. Colomer, and B. E. Logan. 2008. "Efficiency of different shear devices on flocculation." *Water Research*, 42 (4–5): 1113–1121. https://doi.org/10.1016/j.watres.2007.08.027.

Shen, X., B. Gao, K. Guo, and Q. Yue. 2020. "Characterization and influence of floc under different coagulation systems on ultrafiltration membrane fouling." *Chemosphere*, 238.

Spicer, P. T., W. Keller, and S. E. Pratsinis. 1996. "The effect of impeller type on floc size and structure during shear-induced flocculation." *Journal of Colloid and Interface Science*, 184 (1): 112–122. https://doi.org/10.1006/jcis.1996.0601.

Tang, C. K., N. M. Peleato, P. R. Bérubé, and R. C. Andrews. 2019. "Impact of low coagulant dosages on protein fouling of ultrafiltration membranes." *Journal of Water Process Engineering*, 31: 100801. https://doi.org/10.1016/j.jwpe.2019.100801.

Tang, L., Y. Tang, and S. Parameswaran. 2016. "A numerical study of flow characteristics in a helical pipe." *Advances in Mechanical Engineering*, 8 (7): 168781401666024. https://doi.org/10.1177/1687814016660242.

Tse, I. C., K. Swetland, M. L. Weber-Shirk, and L. W. Lion. 2011. "Method for quantitative analysis of flocculation performance." *Water Research*, 45 (10): 3075–3084.

https://doi.org/10.1016/j.watres.2011.03.021.

Vahedi, A., and B. Gorczyca. 2011. "Application of fractal dimensions to study the structure of flocs formed in lime softening process." *Water Research*, 45 (2): 545–556. https://doi.org/10.1016/j.watres.2010.09.014.

Vahedi, A., and B. Gorczyca. 2012. "Predicting the settling velocity of flocs formed in water treatment using multiple fractal dimensions." *Water Research*, 46 (13): 4188–4194. https://doi.org/10.1016/j.watres.2012.04.031.

Wang, C. Y. 1981. "On the low-Reynolds-number flow in a helical pipe." *Journal of Fluid Mechanics*, 108: 185–194. https://doi.org/10.1017/S0022112081002073.

Winterdahl, M. 2013. "Intra-Annual Variability of Natural Organic Matter in Boreal Streams." Doctoral Dissertation, Swedish University of Agricultural Science.

Yamamoto, K., T. Akita, H. Ikeuchi, and Y. Kita. 1995. "Experimental study of the flow in a helical circular tube." *Fluid Dynamics Research*, 16 (4): 237–249. https://doi.org/10.1016/0169-5983(95)00022-6.

Yamamoto, K., A. Aribowo, Y. Hayamizu, T. Hirose, and K. Kawahara. 2002. "Visualization of the flow in a helical pipe." *Fluid Dynamics Research*, 30 (4): 251–267. https://doi.org/10.1016/S0169-5983(02)00043-6.

Yu, W., J. Gregory, L. C. Campos, and N. Graham. 2015. "Dependence of floc properties on coagulant type, dosing mode and nature of particles." *Water Research*, 68: 119–126. https://doi.org/10.1016/j.watres.2014.09.045.

Yu, W., J. Gregory, L. Campos, and G. Li. 2011. "The role of mixing conditions on floc growth, breakage and re-growth." *Chemical Engineering Journal*, 171 (2): 425–430. https://doi.org/10.1016/j.cej.2011.03.098.

Zhang, C., A. R. Ferrell, and K. Nandakumar. 2019. "Study of a toroidal-helical pipe as an innovative static mixer in laminar flows." *Chemical Engineering Journal*, 359: 446–458. https://doi.org/10.1016/j.cej.2018.11.048.

Zietzschmann, F., M. Ernst, M. Godehardt, H. Paar, X. Zheng, and M. Jekel. 2014. "Linking UF reversible and irreversible fouling to the water quality of surface water and treated municipal wastewater." *Desalination and Water Treatment*, 52 (40–42): 7598–7608. https://doi.org/10.1080/19443994.2013.834271.

CHAPTER 6

Impact of Flocculator Type on Continuous Inline Coagulation for Low-Pressure Membrane Pretreatment in Drinking Water Production

Context: Due to the low flow rates that can be accommodated by the small-scale low-pressure membrane (LPM) filtration systems commonly used in industrial design and academic research, simulating continuous-flow coagulation remains a significant challenge. Consequently, previous studies have adopted a range of coagulant mixing strategies, including batch coagulation (which is experimentally simpler to implement), commercial inline static mixers (ISMs), and modified jar-test apparatuses. In Chapter 5, helically coiled tube flocculators (HCTFs) were shown to provide sufficient mixing for strong floc development under low Reynolds flow conditions. Moreover, While floc size and concentration varied with HCTF geometry, distinct differences were observed relative to the flocs generated using batch reactors and ISMs.

Building on the findings of Chapter 5, this chapter evaluates membrane fouling associated with two HCTFs previously shown to generate flocs with disparate properties. Fouling behavior and floc characteristics were also compared against a straight-pipe control that provided incidental flocculation and a commercial ISM. In addition, a new small-scale inline rapid mixer was developed, enabling comparison of all flocculator configurations with and without rapid mixing. Collectively, this work aims to elucidate the relationship between the mixer configuration, floc characteristics, and membrane fouling and is expected to provide important insights on the impact of mixer selection for optimal performance in integrated inline coagulation LPM filtration systems.

A version of this work has been published as:

Ladouceur, J.D., Narbaitz, R.M., Lan, C.Q. (2026). Impact of flocculator type on continuous inline coagulation for low-pressure membrane pretreatment in drinking water production. *Separation and Purification Technology, 10.1016/j.seppur.2026.140504*

The supporting information for this chapter is presented in Appendix G of this thesis.

List of Abbreviations

AMTA	American Membrane Technology Association
ANOVA	Analysis of variance
AWWA	American Water Works Association
CI	Confidence interval
C-IN	Inline coagulation
D_e	Dean number
$D_{f,3}$	3-D fractal dimension (volume-based)
DOC	Dissolved organic carbon
D_p	Perimeter-based fractal dimension
DW-RO	Distilled water passed through 5-stage reverse osmosis unit
ECD	Equivalent circular diameter
FLOCC	Flocculation only
FR_{hr}	Hydraulically reversible fouling rate
FR_{hirr}	Hydraulically irreversible fouling rate
FR_{TOT}	Total fouling rate
G	Mean velocity gradient
HCTF	Helically coiled tube flocculator
HF-1000-⅛	Helically coiled tube flocculator with pipe inside diameter of ⅛” and pipe length of 1000 mm
HF-2000-⅛	Helically coiled tube flocculator with pipe inside diameter of ⅛” and pipe length of 2000 mm
HF-3000-⅛	Helically coiled tube flocculator with pipe inside diameter of ⅛” and pipe length of 3000 mm
HF-1000-¼	Helically coiled tube flocculator with pipe inside diameter of ¼” and pipe length of 1000 mm
HF-2000-¼	Helically coiled tube flocculator with pipe inside diameter of ¼” and pipe length of 2000 mm
HRT	Hydraulic retention time
ISM	Inline static mixer
LPM	Low-pressure membrane

NOM	Natural organic matter
R_e	Reynolds number
RM	Rapid mixing
RM+FLOCC	Rapid mixing and flocculation
UV_{254}	Ultraviolet absorbance at 254nm
WQI	Water quality indicators

List of Variables

Variable	Description
β_0	HCTF torsion parameter (dimensionless)
δ_{nd}	Dimensionless curvature of HCTF
λ	HCTF torsion/curvature ratio (dimensionless)
ν	kinematic viscosity ($m^2\ s^{-1}$)
$A_{p,floc}$	Projected area of the floc (μm^2)
b_{ps}	HCTF helical pitch slope ($mm\ rad^{-1}$)
C_{floc}	Floc concentration (#/mL)
D_e	Dean number (dimensionless)
D_p	Perimeter-based fractal dimension (dimensionless)
ECD	Equivalent circular diameter (μm)
$\frac{f_c}{f_s}$	Curvature correction factor
FR_{hirr}	Hydraulically irreversible fouling rate ($mBar\ h^{-1}$)
FR_{hr}	Hydraulically reversible fouling rate ($mBar\ h^{-1}$)
G_c	Corrected mean velocity gradient for laminar flow through a curved pipe (s^{-1})
G_s	Mean velocity gradient for laminar flow through a straight pipe (s^{-1})
N_{floc}	Number of flocs counted per grid area of the Sedgewick-Rafter cell
P_{floc}	Floc perimeter (μm)
Q_s	Volumetric flowrate through straight pipe segment ($m^3\ s^{-1}$)
r_c	HCTF helical coil radius (mm)
R_c	Modified coil radius of curvature (mm)

R_e	Reynolds number (dimensionless)
r_p	HCTF pipe radius (mm)
$t_{n-1,f}$	Filtration time at the end of cycle *n-1*
$t_{n-1,i}$	Filtration time at the start of cycle *n-1*
$TMP_{n-1,f}$	TMP at the end of cycle *n-1* (mBar)
$TMP_{n,i}$	TMP at the beginning of cycle *n* (mBar)
$TMP_{n-1,i}$	TMP at the beginning of cycle *n-1* (mBar)
u	Axial pipe velocity (m s^{-1})

6.1. Abstract

Due to the low flowrates involved, bench-scale testing of continuous-flow inline-coagulation (C-IN) for low-pressure membrane (LPM) pretreatment remains a significant challenge. Consequently, previous studies have employed a large number of mixer configurations, however, the influence of mixing strategy on membrane performance is not well established. Accordingly, this study used a bench-scale system to compare floc properties and LPM fouling for C-IN pretreatment using batch and continuous-flow mixing strategies. Continuous-flow configurations included incidental flocculation by a straight pipe, an inline static mixer, and different helically coiled tube flocculators (HCTFs), all operated with and without a rapid mixer. Batch coagulation yielded the lowest fouling rate amongst alternatives whereas for continuous-flow strategies, rapid mixing with flocculation resulted in lower fouling than rapid mixing or flocculation alone. LPM fouling was found to be strongly influenced by floc characteristics, with higher fouling rates associated with large concentrations of small, more circular flocs. For HCTFs, the Reynolds number was the most important factor affecting floc growth and fouling mitigation, while extended retention times resulted in smaller-sized flocs and greater fouling propensity. Finally, for the zeta-potential-based optimal coagulant dose used, the removal of organics was found to be independent of the employed mixer configuration. This suggests that mixing conditions for C-IN pretreatment can be configured to produce optimized floc properties without compromising the treated water quality. The findings from this study emphasize the importance of mixer selection on C-IN-LPM performance and highlight the need for a more standardized experimental approach to reduce uncertainty in the comparison of results between studies.

6.2. Introduction

Despite their numerous advantages, low-pressure membranes (LPMs) are highly susceptible to fouling by natural organic matter (NOM) (Amy 2008), which leads to a loss of productivity over time (Yamamura et al. 2019). To mitigate NOM-induced LPM fouling and improve system efficiency, feed water pretreatment by coagulation is the most commonly employed approach due to its relative low cost and familiarity among facility operators (Huang et al. 2009). While conventional coagulation-flocculation-sedimentation has a proven effectiveness as LPM pretreatment (Guigui et al. 2002), inline-coagulation (C-IN), where the coagulant is applied continuously without prior separation of the flocs before the membrane module, has become the most common strategy owing to its small footprint and reduced process complexity (Kamińska et al. 2020). Moreover, for at least one membrane-water treatment combination, bench-scale testing indicated that C-IN yielded reduced LPM fouling compared to when more sophisticated treatment involving particle separation by flotation or sedimentation was considered (see Chapter 4).

It is now well understood that the performance of C-IN as LPM pretreatment is dependent on the nature of the cake layer formed by the retained floc aggregates on the membrane surface (Liu et al. 2024). In fact, Amjad et al. (2015) reported that cake layers formed by C-IN pretreatment retained a "memory" of the floc aggregate properties, highlighting their importance in controlling the fouling of LPMs. Realizing that floc size alone was insufficient to fully describe LPM performance, Guan et al. (2001) and Park et al. (2006) proposed modified Carman-Kozeny models that accounted for the floc structure by incorporating the three-dimensional floc fractal dimension ($D_{f,3}$), a measure of the degree to which particles occupy the embedding space within the aggregate structure (Jiang and Logan 1996). In these models, the specific cake layer resistance increased as the floc size decreased and $D_{f,3}$ increased (indicative of a compact floc geometry), however, demonstrated a relative insensitivity to $D_{f,3}$ for large sized flocs (greater than approximately 100 μm). The dependency of specific cake resistance on both floc size and fractal dimension in these modified models was corroborated experimentally by Lee et al. (2005), who reported that large and loosely structured hematite flocs formed by the hydrolysis of ferric chloride led to lower specific cake resistance compared to flocs with a smaller size and more compact structure.

Based on this understanding, many authors have studied the effect of floc size and fractal dimension on the fouling propensity of cakes formed following C-IN pretreatment by varying the coagulation chemistry or rapid-mixing/flocculation conditions, including shear intensity and

mixing hydraulic retention time (HRT) (e.g., Nan et al. 2016; Wang et al. 2010). However, the appropriate mixer configuration and operating condition depend on the coagulation mechanism, as well as on raw-water characteristics and the requirements of downstream treatment processes (Amirtharajah et al. 1991). For alum coagulation via adsorption/destabilization, the most effective destabilizing species, namely the highly positively charged hydrolysis products, form within 0.01-1 s of coagulant addition (Amirtharajah and Mills 1982). In contrast, amorphous hydroxide precipitates form more slowly, over approximately 1-7 s following coagulant addition (Hahn and Stumm 1968). Thus, the relative importance of rapid mixing depends on the coagulation mechanism. For sweep flocculation, maintaining chemical conditions that provide sufficient degree of supersaturation with respect to the metal ion is critical for precipitate formation, whereas the coagulation performance has been reported to be relatively insensitive to rapid-mixing intensity over a broad range of velocity gradients (G) (300 s^{-1} to 16,000 s^{-1}) (Amirtharajah and Mills 1982). In contrast, for adsorption/destabilization, rapid and complete dispersion of the coagulant through the bulk flow is essential to promote adsorption of the hydrolysis products formed within the first second after dosing (Amirtharajah et al. 1991; Amirtharajah and Mills 1982; Johnson and Amirtharajah 1983). Accordingly, high-intensity, plug-flow-type reactors, such as static mixers or radial turbine blenders, may be particularly suitable for this application.

Besides the operational parameters, two features of C-IN pretreatment systems, namely, the presence/absence of rapid mixing (RM) and the choice of flocculator type, can also impact floc formation. Concerning the presence of RM, it has been shown by several studies that coagulation (i.e., RM only) vs. coagulation/flocculation (i.e., rapid mix + slow mix) results in differing floc properties that alter the performance of downstream LPM filtration. Malkoske et al. (2023b) reported that for coagulation chemistries associated with combined adsorption/destabilization and sweep flocculation mechanisms, the addition of dedicated flocculation stage following RM resulted in flocs with a larger mean size that packed into a more permeable cake layer. This corresponded to a lower degree of total and hydraulically irreversible membrane fouling compared to C-IN treatment by RM only. Cho et al. (2006) similarly found that, compared to RM only, the addition of a dedicated flocculation stage yielded larger sized flocs which led to reduced LPM permeability decline and a significantly lower specific cake resistance. Both of these studies, however, used vertical-turbine impeller systems for coagulation/flocculation: it is, however, unclear whether alternative flocculator types would similarly benefit from prior intensive mixing.

The choice of flocculator type itself can also strongly influence floc formation. Our recent work (see Chapter 5), as well as those of Spicer et al. (1996) and Serra et al. (2008), demonstrated that different mixer types can lead to disparate floc properties even when operated using identical conditions of HRT and G. Previous studies of LPM pretreatment by C-IN have considered a variety of conventional flocculator types including vertical-shaft turbine mixers, hydraulic pipe flocculators consisting of straight pipe sections (to provide incidental inline flocculation) (Kamińska et al. 2020), and commercial inline static mixers (ISMs) (Wang and Wang 2006), however, none appear to have investigated how the choice of flocculator type will impact fouling in downstream LPMs. Among alternative flocculator types, there remains an extremely limited number of studies that have considered helically coiled tube flocculators (HCTFs) (a coiled segment of pipe) as part of the integrated C-IN-LPM system (e.g., Lerch et al. 2003) despite their numerous advantages compared to conventional flocculator types. These include considerably lower HRTs, which results in a very compact footprint, and effective floc generation arising from their strong secondary flow (García-Ávila et al. 2023). Moreover, no previous studies have considered the impact of controlled helical geometry, which has been shown to alter the size and structure of the formed flocs (Carissimi et al. 2018;Chapter 5), on downstream LPM fouling.

Given that flocculation conditions, including the mixing time, shear intensity, and flocculator type have been shown to impact the properties of floc aggregates, it raises concerns as to the fairness of comparisons between LPM fouling studies using C-IN pretreatment with alternative mixing strategies. This concern is particularly relevant because some studies have directly compared LPM fouling in C-IN-LPM systems using disparate mixing types without accounting for potential differences in floc properties (e.g., Cho et al. 2006; Paar et al. 2011). Accordingly, there is a need to evaluate whether the choice of flocculator type impacts the degree of membrane fouling in the C-IN-LPM hybrid system. Based on this, the objectives of the study were to: (a) investigate whether the inclusion of inline RM alters floc properties and the degree of LPM fouling compared to hydraulic flocculation only; (b) determine whether different flocculator types (batch vs. various continuous-flow alternatives) used in C-IN pretreatment impact the degree of LPM fouling, and; (c) assess the effectiveness of HCTFs as flocculators for C-IN pretreatment systems and evaluate the impact their geometry has on floc properties and LPM fouling. To the authors' knowledge, this study represents the first effort to directly compare the impact of continuous-flow C-IN with RM vs. RM + flocculation has on floc properties and on downstream

LPM fouling for a variety of continuous-flow hydraulic flocculator types, including helical flocculators. This is particularly useful because helical flocculators have received only limited attention for potable water treatment applications, yet could lead to substantially more economical units. The results of this study are expected to provide important insights regarding the selection of mixing configuration for C-IN pretreatment to optimize LPM performance.

6.3. Materials and Methods

6.3.1. Synthetic Water

A synthetic water, which had the same composition as in our previous work (see Chapter 5) was used throughout this study to minimize the inter- and intra-annual variations in water quality expected of natural water sources throughout the duration of the lead author's doctoral studies. Briefly, 5 mg L^{-1} humic acid (H16752, Sigma-Aldrich, St. Louis, MO), 4 mg L^{-1} bovine serum albumin (A7906, Sigma-Aldrich, St. Louis, MO), and 4 mg L^{-1} sodium alginate (180947, Sigma-Aldrich, St. Louis, MO) were added to distilled water that had been passed through a commercial five-stage reverse-osmosis-based system (TGI-525-NO. 92821, TGI Pure Water Systems, Brea, CA), abbreviated as DW-RO water. These model organics were selected to represent humic substances, proteins, and polysaccharides, respectively, which are major NOM components and known to cause significant fouling of LPMs (Alresheedi 2023). Their use as representative model organic compounds has been well established by a number of previous studies (e.g., Alresheedi et al. 2019; Schulz et al. 2016). To better simulate natural waters, an inorganic background consisting of 5 mg L^{-1} kaolin clay (Laboratory Grade 75185, Fisher Scientific, Hampton, NH), 0.6 mM calcium chloride (97%, Thermo Scientific, Hampton, NH), and 0.9 mM sodium bicarbonate (Certified ACS, Fisher Scientific, Hampton, NH) were added. This resulted in a turbidity of 5.45 ± 0.04 NTU, a hardness of 61.25 ± 1.17 mg-$CaCO_3$ L^{-1}, and an alkalinity of 51.75 ± 1.84 mg-$CaCO_3$ L^{-1}. The water was characterized by a moderately low dissolved organic carbon (DOC) of 4.95 ± 0.05 mg-C L^{-1} and a medium hydrophobicity, as determined by a specific ultraviolet absorbance at 254 nm (Edzwald and Tobiason 1999), of 2.21 ± 0.04 L mg^{-1} m^{-1}.

6.3.2. Filtration Experiments

6.3.2.1. Bench-Scale Filtration Apparatus and Test Protocol

Lab-scale membrane modules (surface area: ~0.0035 m^2) were fabricated in-house using a single inside-out tubular multi-channel (TMC) membrane fiber that has seven concentrically positioned capillaries (Multibore 0.9, Inge GmbH, Greiffenberg, Germany). The hydrophilized polyethersulfone TMC membranes had a molecular weight cutoff of approximately 100 kDa and a pure water permeability (PWP) of 700 – 1000 L m^{-2} h^{-1} bar^{-1}. A new module was prepared for every test.

Day-long dead-end filtration tests were conducted in replicate using the bench-scale filtration apparatus shown in Fig. 6.1. LPM pretreatment by C-IN was performed using a fixed coagulation chemistry and different flocculator types (Section 6.3.2.3) either with or without RM. The filtration system was the same as in our previous studies (see Chapter 3 and Chapter 4), however, was modified to provide continuous-flow chemical addition, coagulation, and flocculation. The chemical addition was performed using a syringe pump (Pump 22, Harvard Apparatus, Cambridge, MA). This is a unique feature of this study as continuous-flow coagulation is rarely practiced at bench-scale because it is more challenging to implement. Malkoske et al. (2023a; b), for example, devised a novel bench-scale continuous-flow system based on a modified jar test apparatus, however, to provide reasonable HRT values much larger flowrates (20 times greater) were needed than required by LPM filtration tests. The syringe pump used a gastight syringe (1010 TLL-SAL, Hamilton Co., Reno, NV) to accurately deliver low volumes of alum coagulant (ALS, Kemira Water Solutions, Varennes, QC) to the feed water, which had been pH adjusted (0.05 N H_2SO_4, Honeywell, Charlotte, NC) to yield a final pH of 6, at a pre-calculated rate equivalent to 3 mg-Al L^{-1}. This coagulation chemistry corresponded to the jar test optimal condition for this water type based on DOC removal and zeta potential reduction (coagulated value of -3.6±0.6 mV). The LabView program (National Instruments, Austin, TX) used to automate the cyclical operation of the system was modified so that the syringe pump extruded coagulant only during the filtration cycle and not during hydraulic backwashing. For tests with flocculation only (abbreviated as FLOCC), the coagulant from the syringe pump was added directly inline at a point just upstream of the flocculator. For tests with RM and flocculation (abbreviated as RM+FLOCC), the coagulant was added to the small-scale inline rapid mixer described in the following section.

All tests were conducted using a constant flux mode of operation at 80 L m^{-2} h^{-1}, which was selected based on the results of preliminary critical flux testing for this membrane-water combination (108 L m^{-2} h^{-1}, see Section G.1.1.) to ensure operation at a sub-critical flux. To assess

the reversibility of fouling, a 2 min-long hydraulic backwash was performed following every 30 min filtration cycle at a flux of 300 L m^{-2} h^{-1} using DW-RO water (due to the low volumes of permeate produced). Prior to commencing each filtration experiment, the PWP of the membrane module was verified by filtering Type I deionised water (ZenoPure Quatra 90LC, Zenon Environmental Inc., Burlington, ON) for a duration of 60 min. Following the PWP test, the feed water was switched to the pH-adjusted synthetic challenge water and the syringe pump was engaged. The system was allowed to run for a period of two hours prior to the commencement of the experiment to establish steady-state floc properties, which is in excess of the 5 HRTs reported by Malkoske et al. (2023b) for steady-state to be achieved. It should be noted that, during this stabilization period, the manual bypass valves were used to route the coagulated/flocculated water through the sampling port (and not the membrane module) to prevent the continuous deposition of flocs on the membrane surface. At the end of the two-hour period, floc samples were collected for analysis (Section 6.3.3.), the bypass valves were set to route the coagulated/flocculated water to the membrane module, and the membrane filtration test was begun.

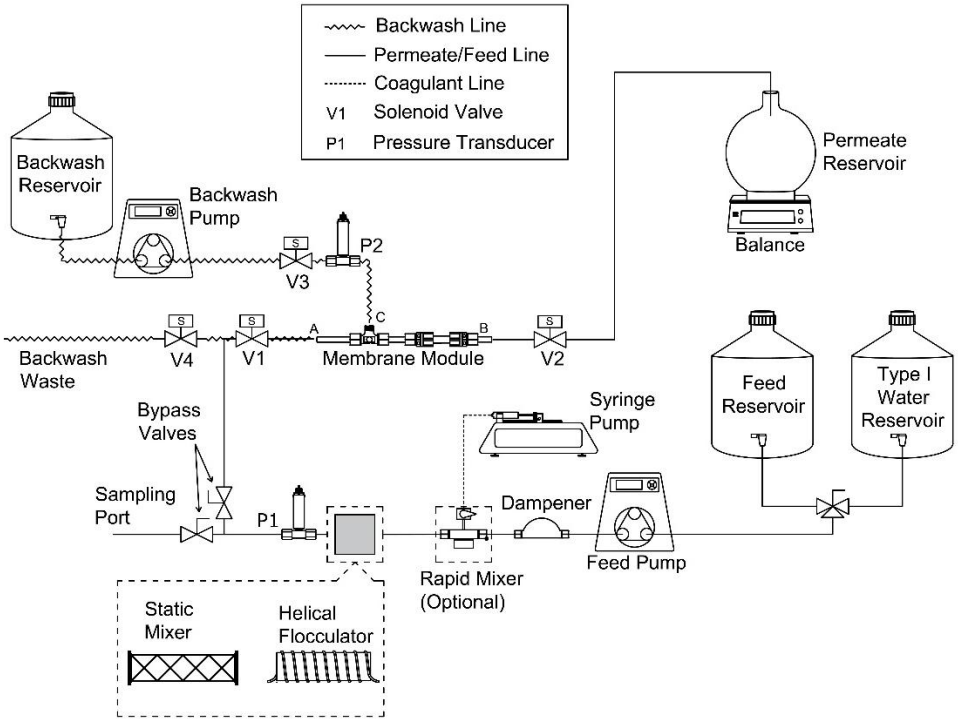


Fig. 6.1. Bench-scale filtration system

The performance of these continuous-flow C-IN approaches was additionally compared with that of a batch reactor which, due to its experimental simplicity, has been used by a number of previous studies to simulate C-IN at bench-scale (e.g., Neama et al. 2024; Tang et al. 2019). For batch coagulation, a large baffled reactor developed by Gonzalez-Galvis and Narbaitz (2020) replaced the feed reservoir in the bench-scale filtration system (Fig. 6.1). In this approach, the coagulant was added to the reactor and following 2 min of rapid mixing at G = 296 s^{-1}, the motor was slowed to provide a constant G = 200 s^{-1} (to prevent floc settling) for the duration of the membrane filtration test. Flocs were sampled for characterization from a sampling port located at the mid-depth of the reactor immediately following RM. Additional floc sampling was not conducted because our previous work demonstrated that the properties of flocs produced in the batch reactor were independent of the stirring duration (see Chapter 5)

6.3.2.2. Small-Scale Rapid Mixer

Full-scale rapid-mix basins commonly have design contact times of less than 1 min (Amirtharajah et al. 1991; Kawamura 2000). Given the low flow rates of bench-scale LPM systems (~5 mL min^{-1} in this study), a scaled-down rapid mixer would require a volume of less than 5 mL. Designing and constructing an inline mixer at this scale, without pumping feed water to waste, presents an extreme challenge. In this study, the rapid blending of coagulant was accomplished by an in-house designed inline rapid mixer that consisted of a low-profile cylindrical inline strainer housing (GY-29595-05, Cole Parmer, Montreal, QC) with the strainer mesh removed and a magnetic stir-bar driven by a disc stirrer (3907500, IKA, Wilmington, NC). A detailed description of the rapid mixer is provided in Appendix G Section G.1.2. Preliminary tracer studies (Section G.1.3.) showed that the rapid mixer operated like a continuous-flow stirred tank reactor, consistent with its intended design. These same tests showed that it has a mean residence time of approximately 4 min. This is comparable to other bench-scale studies which have reported rapid mix durations of up to 5 min (e.g., Kimura et al. 2008). Additionally, although full-scale facilities commonly have a design RM contact time less than 1 min (Kawamura 2000), in practice they are frequently operated below the design flowrate meaning they may experience longer actual RM times. The authors acknowledge that prolonged rapid-mixing times may delay or otherwise adversely affect floc formation in downstream flocculators, as previously reported by Letterman et al. (1973) and Bratby (2016). Therefore, the findings of this study (detailed in Section 6.4) should be further validated using

lower rapid mixing HRTs that are more representative of typical full-scale operating conditions employed in practice.

6.3.2.3. Flocculator Types

Using the bench-scale system described in Section 6.3.2.1., the performance of different continuous-flow flocculators, namely, a section of straight pipe, a commercial ISM, and two HCTFs, was evaluated both with and without the inclusion of the inline rapid mixer ahead of the flocculation unit. The segment of straight pipe (SS-T6-S-065-20, Swagelok, Solon, OH) was used as a control (denoted as "control") to simulate incidental pipe flocculation. The ISM was purchased from Koflo Corporation and had a 316L stainless steel housing with an inside diameter of 8.1 mm (~5/16") and 21 helical elements (3/8-21, Koflo, Cary, IL). Although ISMs are primarily used at full-scale for inline blending of treatment chemicals with the feed water at high intensities (Edzwald 2013), their reported ability to achieve flow-independent mixing, even when operated firmly within the laminar flow regime (Koflo Corp., personal communication, 01 Jan 2021), may make them suitable for application as a flocculator for bench-scale continuous-flow C-IN systems.

To further investigate whether different flocculator types alter LPM performance following pretreatment by C-IN, two HCTFs were selected which, based on the results of our previous work (see Chapter 5), produced the largest and smallest sized floc aggregates among twenty-five different helical configurations. A schematic describing the HCTF geometry is provided in Fig. 6.2. Both these flocculators had a pipe radius (r_p) of 1.5875 mm (⅛" I.D.), a coil radius (r_c) of 26.5875 mm, and a coil pitch ($p=2\pi b_{ps}$) of 15 mm (where b_{ps} is the coil pitch slope), however, differed in their pipe length. That which produced the largest size flocs had a pipe length of 2000 mm (abbreviated as HF-2000-⅛) while the HCTF that produced the smallest size flocs had a pipe length of 1000 mm (abbreviated as HF-1000-⅛).

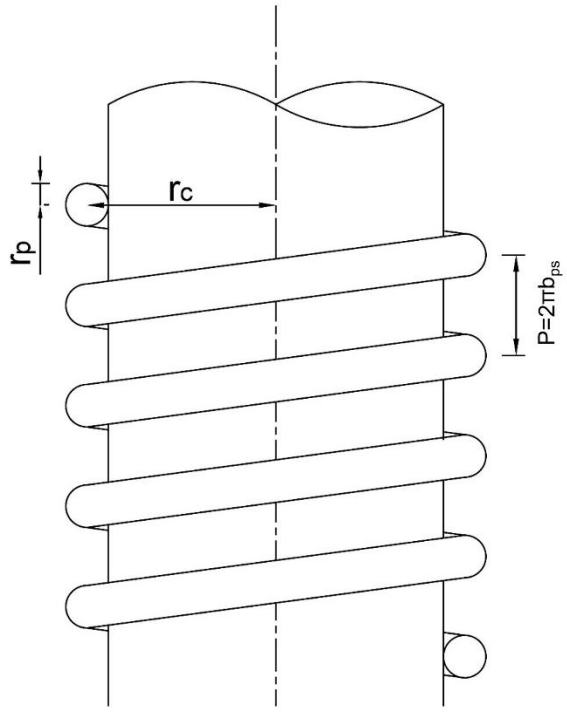


Fig. 6.2. HCTF geometry

The helical pipe length (and consequently the HRT), together with the hydrodynamic condition have been reported to be the most significant factors governing the performance of HCTFs (Maraschin et al. 2020). Accordingly, to study the impact of HRT on the floc properties and LPM fouling, a third HCTF was prepared with the same geometry as the HF-1000-⅛ and HF-2000-⅛ flocculators, but a length of 3000 mm (HF-3000-⅛). The influence of hydrodynamic condition on the performance of HCTFs was assessed using HCTFs with a pipe radius of 3.175 mm (abbreviated as HF-1000-¼ and HF-2000-¼, respectively), thereby reducing the axial flow velocity and corresponding Reynolds number. A summary of the flocculator geometries used in the present study is provided in Table G.2.

6.3.2.4. Mixer and HCTF Operational Properties

To facilitate improved comparisons among the different mixer types, their operation was characterized using a series of hydrodynamic and operational parameters. The effective HRT was evaluated using tracer studies (i.e., $\boldsymbol{\tau_{Experimental}}$), conducted according to the methodology outlined in Benjamin and Lawler (2013) and described in detail in Section G.1.3.

Additional hydrodynamic parameters were used to describe the different helical geometries. For flow through a curved pipe, the Dean number (D_e) is used to describe the strength of the secondary flow and is defined as the ratio of the centrifugal force to the inertial force (Dean 1928). Mathematically, D_e can be determined using the Reynolds number (R_e) and the modified radius of curvature proposed by Mishra and Gupta (1979):

$$R_e = \frac{2ur_p}{\nu} \tag{6.1}$$

$$R_c = r_c\left[1 + \left(\frac{b_{ps}}{r_c}\right)^2\right] \tag{6.2}$$

$$D_e = \sqrt{\frac{r_p}{R_c}}R_e \tag{6.3}$$

Where R_e is the Reynolds number, u is the axial flow velocity (m s^{-1}), ν is the kinematic viscosity (m^2 s^{-1}), R_c is the modified coil radius of curvature (mm), D_e is the Dean number, b_{ps} is the pitch slope (mm rad^{-1}), r_c is the coil radius (mm), and r_p is the pipe radius (mm). The model proposed by Gregory (1981) for the mean velocity gradient is limited to laminar flow through a straight pipe section. Therefore, this expression is updated to include a correction factor that accounts for the effect of centrifugal forces acting on the flow in curved pipe (Mishra and Gupta 1979; Tse et al. 2011):

$$G_s = \frac{8Q_s}{3\pi r_p^3} \tag{6.4}$$

$$\frac{f_c}{f_s} = 1 + 0.033\big(log(D_e)\big)^4 \tag{6.5}$$

$$G_c = G_s\sqrt{\frac{f_c}{f_s}} \tag{6.6}$$

Where G_s is the mean velocity gradient for laminar flow through a straight pipe (s^{-1}), Q is the system volumetric flowrate (m^3 s^{-1}), $\frac{f_c}{f_s}$ is the curvature correction factor, and G_c is the corrected mean velocity gradient for laminar flow through a curved pipe (s^{-1}). HCTFs can further be described by their degree of torsion and curvature, characterized according to Eqs. (6.7) – (6.9) as defined by Liou (1992) and Yamamoto et al. (2002):

$$\lambda = \frac{b_{ps}}{r_c} \tag{6.7}$$

$$\beta_0 = \frac{\lambda}{\sqrt{2\delta_{nd}}} \tag{6.8}$$

$$\delta_{nd} = \frac{r_p r_c}{{b_{ps}}^2 + r_c^2} \tag{6.9}$$

Where β_0 is the torsion parameter, λ is the torsion/curvature ratio, δ_{nd} is the dimensionless curvature and all other parameters have previously been defined.

A summary of the hydrodynamic and operational properties for all mixer configurations is provided in Table 6.1. The increased pipe diameter for the HF-1000-¼ and HF-2000-¼ flocculators (relative to the corresponding ⅛-in. configurations) resulted in longer HRTs as well as lower Reynolds number (and by extension Dean number) and mean velocity gradients.

Table 6.1. Summary of Mixer Hydrodynamic Properties

Mixer Type	$\tau_{Experimental}$ (min)	G_c (s^{-1})	Gt[b]	β_0	δ_{nd}	R_e	D_e
Batch	∞	296/200[a]	86.4×10^5 [c]				
Rapid Mixer	4.08	-	N/A	-	-	-	-
Inline Static Mixer	2.29	25.8[d]	3,545	-	-	-	-
Control-¼	2.74	2.21	363	-	-	-	-
HF-1000-⅛	2.00		2,146				
HF-2000-⅛	4.00	17.88[d]	4,291	0.26	0.06	33.32	8.11
HF-3000-⅛	5.24		5,621				
HF-1000-¼	6.15	2.22[d]	819	0.18	0.11	16.66	5.57
HF-2000-¼	12.75	2.22	1,698				

[a]Batch coagulation performed with rapid mixing for 2 min at G=296 s^{-1} followed by mixing at G=200 s^{-1} for the remainder of the day-long test. [b]Gt value, which is widely used in mixer design, computed by multiplying the mean experimental retention time (in s) with G_c. [c]The mean retention time for continuous-stirred reactor considered to be half the total time, as some flocs exit immediately and some are retained for the whole day [d]see Chapter 5.

6.3.3. Floc Characterization

The floc properties were characterized in terms of size, concentration, structure, and shape for the replicated filtration tests conducted with each combination of rapid mixer and flocculator. Flocs collected from the sampling port at the end of the system stabilization period were immediately taken for analysis. Using a wide orifice pipette tip (Finntip, Thermo Scientific, Hampton, NH) to minimize the shear imparted to flocs, the coagulated/flocculated samples were carefully transferred from the sampling beaker to a gridded Sedgewick-Rafter cell (1801-G20, Wildco, France) for image analysis using an optical microscope (Zeiss Standard, Zeiss, Germany) fitted with 3.2x and 10x objective lenses. Manual optical microscopy was selected for floc analysis because of the inherent limitations associated with microscopic flow-imaging technologies (see Section G.1.4). Floc images were acquired using a 10 MP eye-piece camera (A35100U, OMAX, WA) and were processed using ImageJ software from the U.S National Institute of Health as in the work by Malkoske et al. (2023b). Image processing and analysis associated with this microscopic technique proved extremely laborious, which practically limited the sample size to 100 flocs for each replicate. Similar population sizes have been reported in previous studies using microscopic techniques for alum floc size characterization, including those of Gorczyca and Ganczarczyk (1999) and Chakraborti et al. (2003). The equivalent circular diameter (ECD) was determined by back calculating for the diameter of a circle with an equivalent area to that of the 2D floc projection (as measured using ImageJ software) according to the following equation (Jarvis et al. 2005):

$$ECD = \sqrt{\frac{4A_{p,floc}}{\pi}} \tag{6.10}$$

where ECD is the equivalent circular diameter (μm) and $A_{p,floc}$ is the projected area of the floc (μm^2). Using images of the Sedgewick-Rafter cell acquired with the 3.2x objective, the floc concentration was determined by dividing the number of flocs in each 1 mm x 1 mm grid by the grid volume according to:

$$C_{floc} = \frac{N_{floc}}{V_{grid}} = \frac{N_{floc}}{1mm^3} \times \frac{10^3 mm^3}{1\ cm^3} \times \frac{1\ cm^3}{mL} = 1000 \times N_{floc} \tag{6.11}$$

where C_{floc} is the estimate for floc concentration (#/mL), V_{grid} is the volume of each grid (mm^3), and N_{floc} is the number of flocs counted per grid area. The structure of the individual flocs was

characterized using the perimeter-based fractal dimension according to the power law relationship presented by Liu et al. (2021):

$$A_{p,floc} \sim P_{floc}^{\frac{2}{D_p}} \tag{6.12}$$

where $A_{p,floc}$ is the projected area of the floc (μm^2), P_{floc} is the floc perimeter (μm), and D_p is the perimeter-based fractal dimension, which was determined by regression of the log-log plot of floc perimeter vs. projected area as in Spicer and Pratsinis (1996). The shape of the flocs was also characterized using the floc circularity (Iskander and Li 2024):

$$Circularity = \sqrt{\frac{4\pi A_{p,floc}}{P_{floc}^{\ 2}}} \tag{6.13}$$

where all parameters have already been defined. The closer the circularity is to unity, the more similar the projected contour of the floc is to that of a circle.

6.3.4. Membrane Fouling Assessment

Hydraulically reversible and irreversible fouling rates were computed following the approach of Aly et al. (2021):

$$FR_{hr} = \frac{TMP_{n-1,f} - TMP_{n,i}}{t_{n-1,f} - t_{n-1,i}} \tag{6.14}$$

$$FR_{hirr} = \frac{TMP_{n,i} - TMP_{n-1,i}}{t_{n-1,f} - t_{n-1,i}} \tag{6.15}$$

where FR_{hr} is the hydraulically reversible fouling rate (mBar h^{-1}), FR_{hirr} is the hydraulically irreversible fouling rate (mBar h^{-1}), $TMP_{n,i}$ is the measured transmembrane pressure (TMP) at the beginning of cycle n (mBar), $TMP_{n-1,f}$ is the measured TMP at the end of cycle n–1 (mBar), $TMP_{n-1,i}$ is the measured TMP at the beginning of cycle n–1 (mBar), and $t_{n-1,f}$ and $t_{n-1,i}$ are the end of cycle filtration time and the beginning of cycle filtration time, respectively. The total fouling rate (FR_{TOT}) is considered to be the sum of the hydraulically reversible and irreversible fouling rates. Although it was of great interest to compliment the above fouling analyses with characterization of the cake layer, this was not pursued in this study because based on the

equipment at our disposal, it was not possible to ensure the collection of undisturbed samples from the fiber lumen, which are within the membrane.

6.3.5. Analytical Methods and Statistical Analysis

Statistical treatment was performed using JMP® Student 19 (SAS Institute Inc., Cary, NC) and, unless otherwise indicated, all statistical tests were conducted at a significance level of α=0.05. The measurement of all water quality indicators were performed in accordance with APHA/AWWA Standard Methods (American Public Health Association et al. 2012).

6.4. Results and Discussion

6.4.1. Validation of Continuous-Flow Bench-Scale Inline Rapid Mixer

Bratby (2016) has noted that the RM stage during the coagulation/flocculation process exerts a critically important impact on destabilization reactions and the formation of primary floc particles, both of which influence flocculation kinetics and, consequently, the performance of downstream unit operations. Evidence from our previous study (see Chapter 5) comparing the properties of flocs formed by a batch reactor to those from a continuous-flow bench-scale system suggested that the low Reynolds flow conditions used in the latter configuration were insufficient to provide immediate and complete dispersal of the coagulant into the feed stream. This likely resulted in localized regions of incomplete or extensive adsorption of the metal hydrolysis species (Bratby 2016; Letterman et al. 1973) which caused particle restabilization, yielding poorer flocculation efficiency and smaller sized flocs. Based on this, the current study developed the inline rapid mixer described in Section 6.3.2.2. as a means to address the significant challenges involved with conducting continuous-flow coagulation at small-scale.

Fig. 6.3 compares floc properties, including ECD, concentration, and D_p for RM alone as well as for the control, ISM, HF-1000-⅛, and HF-2000-⅛ flocculators with and without the inline rapid mixer. Representative microscopic images of flocs collected for each flocculator type, with and without RM, are also shown in Fig. G.4. RM alone produced flocs with a mean ECD of 59.0 ± 5.50 µm, whereas the addition of flocculation led to significantly larger aggregates (Fig. 6.3a). This observation is consistent with previous studies (Amjad et al. 2015; Malkoske et al. 2023b). For all flocculator types, the inclusion of the small-scale rapid mixer (RM+FLOCC) resulted in a statistically significant increase in floc ECD (based on 95% confidence intervals (CIs)) compared

to C-IN treatment with flocculation alone (FLOCC) (Fig. 6.3a). For the control, ISM, and HF-1000-⅛ flocculators, RM+FLOCC yielded significantly lower floc concentrations (Fig. 6.3b) as well as smaller D_p values (Fig. 6.3c) than FLOCC, indicating the formation of more compact aggregate structures. In contrast, for the HF-2000-⅛ flocculator, the floc concentration and D_p values for RM+FLOCC and FLOCC exhibited overlapping 95% CIs. The significantly larger ECD for HF-2000-⅛ under RM+FLOCC conditions, despite having almost identical floc compactness (based on D_p values) and floc concentration, suggests that the increase in floc size did not arise from the creation of more open, loose floc structures or from enhanced aggregation of the same particle pool. If the size increase was driven solely by improved cluster-cluster aggregation of a constant particle population, a corresponding reduction in floc concentration would have been expected. Instead, the comparable floc concentrations suggest that the addition of RM increased the total number of primary particles available for aggregation. This is consistent with the self-similar fractal framework described by Meakin (1987) where, for aggregates with a constant fractal dimension, an increase in floc diameter necessarily requires an increase in the number of particles within the structure. Further evidence supporting this interpretation is provided by the relationship between the percent increase in floc ECD and the percent decrease in floc concentration (Fig. G.5), where the size increase associated with the addition of rapid mixing was ~ 2.99 times greater than the corresponding decrease in floc concentration. This relationship implies a greater number of particles incorporated within the flocs as, if the floc growth was due to improved agglomeration of the same primary particle pool, the floc ECD would have been expected to increase by the same amount as the decrease in floc concentration (i.e., 1:1 slope). Similar findings were previously reported by Hudson Jr. (1965) who observed that flocs produced by RM+FLOCC contained approximately 2.5 times more solids than those formed by FLOCC alone.

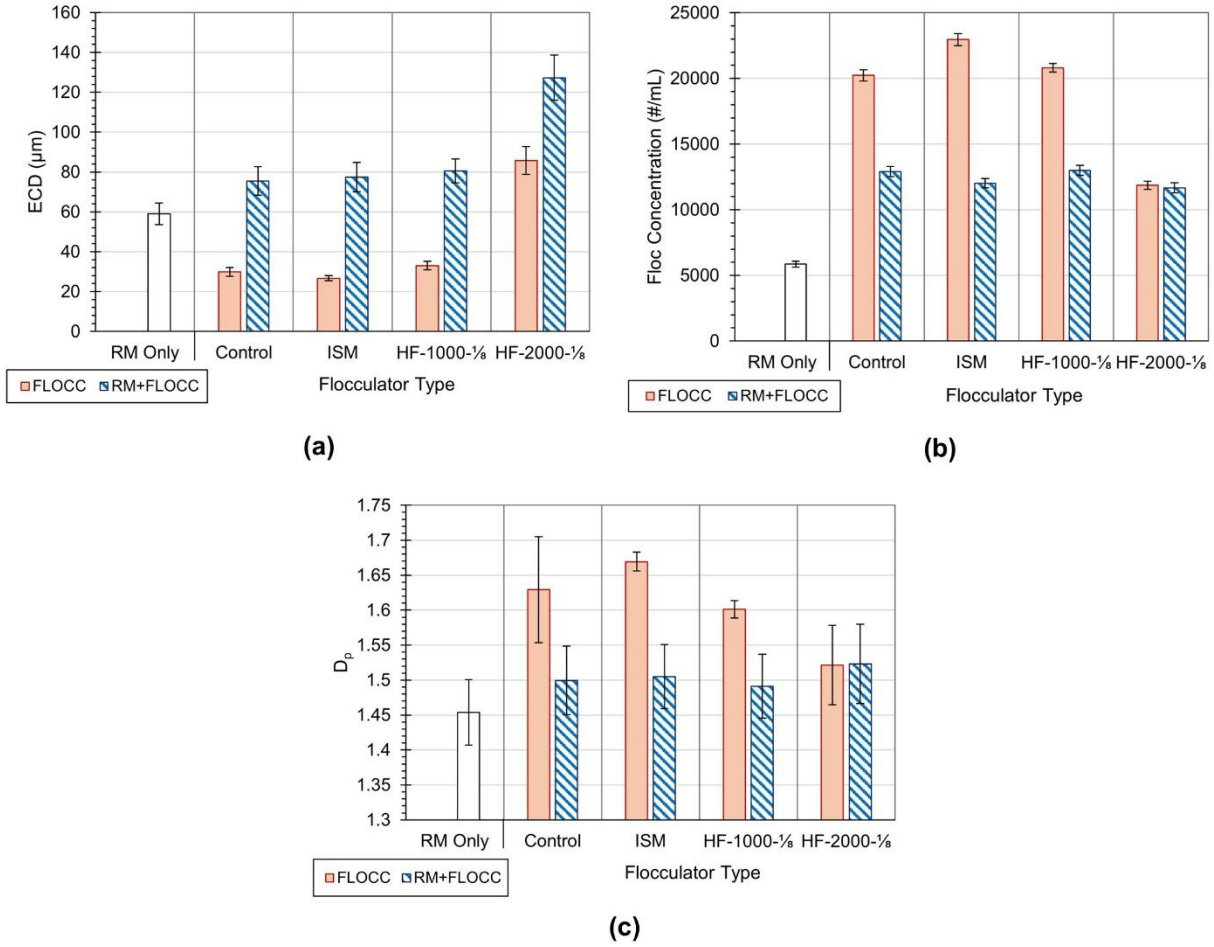


Fig. 6.3. Comparison of floc properties for various flocculator types with and without inline rapid mixer: **(a)** ECD; **(b)** Floc concentration; **(c)** Perimeter-based fractal dimension (D_p). Note: Error bars represent the 95% confidence interval calculated using the Student's *t*-test as $\mu \pm t_{n-1,0.025}\frac{s}{\sqrt{n}}$ where $n = 200$ for replicated tests.

Fig 6.3c shows the variation in D_p for all mixing configurations where, for Euclidian objects D_p is equal to 1, and for more highly irregular objects approaches a value of 2. It should be noted that, although the 95% CIs seem wide, the scale of the vertical axis is relatively narrow and they represent less than 5% of the mean D_p in all cases. For FLOCC only, the HF-2000-⅛ flocculator was found to have the most compact floc structure while the ISM generated the loosest floc structure, although the ISM and control had overlapping 95% CIs. Differences in floc structure arising from changing flocculation parameters including G and HRT have been previously reported by a number of studies (He et al. 2012a; Nan et al. 2016). Moreover, without RM, the

relatively greater compactness of the flocs formed by the HF-2000-⅛ flocculator is consistent with its longer HRT compared to the alternative flocculator types (Table G.2), as prolonged shear exposure can promote structural rearrangement of flocs towards denser configurations (Selomulya et al. 2001). When RM preceded flocculation, however, D_p exhibited no dependency on flocculator type, with overlapping 95% CIs for all configurations. Based on this, it seems likely that the greater incorporation of primary particles formed during RM exerts a stronger influence on the degree of floc compactness than structural rearrangement occurring within the low-shear flocculator. Comparison of the D_p values for RM+FLOCC and RM (without flocculation) also appears to support this finding, as the addition of flocculation did not significantly change the D_p compared to RM only. The insensitivity of D_p to flocculator type for RM+FLOCC suggests that, for this small-scale continuous-flow system, the rapid mixer governs the overall degree of floc compactness. This hypothesis should be further evaluated in future work through systematic variation of G and HRT during both RM and flocculation for different coagulant dosages under alternative coagulation mechanisms.

Overall, the results demonstrate that incorporating RM prior to flocculation in the low Reynolds flow bench-scale system significantly improved coagulation/flocculation performance, yielding larger sized flocs for all flocculator types. Furthermore, the rapid mixer not only promoted the formation of larger flocs but, based on the discussion above, also increased the solids content within each aggregate. The enhanced performance of RM+FLOCC compared to FLOCC alone is likely attributable to the improved initial coagulant dispersion illustrated schematically in Fig. 6.4.

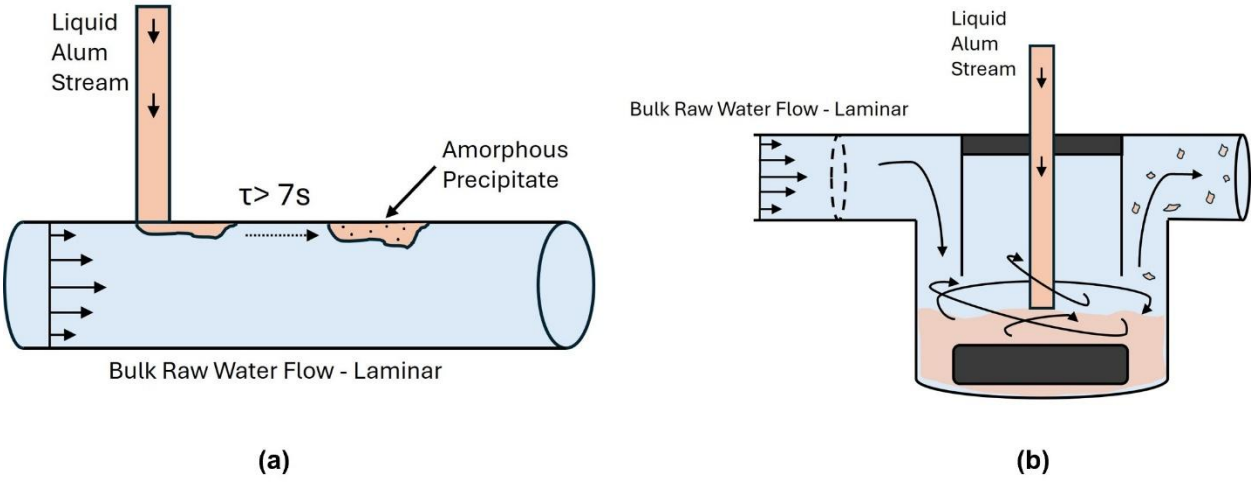


Fig. 6.4. Hypothesized coagulant dispersion mechanisms for: **(a)** FLOCC; **(b)** RM+FLOCC

For direct injection of coagulant into the low-Reynolds laminar flow upstream of flocculators, calculation of the Peclet number indicated that advective transport governs the mixing (P_e=32,880, Section G.2.1.2) (Ekambara and Joshi 2004). Under these conditions, limited radial and axial diffusion across the pipe cross-section causes the injected coagulant to remain concentrated within a localized region, with the slug of coagulant carried downstream prior to becoming fully dispersed. Furthermore, the amorphous aluminum-hydroxide precipitate has been shown to form within ~ 7 s of addition (Amirtharajah and Mills 1982; Letterman et al. 1973), but due to the poor mixing coupled with laminar flow, would be constrained to a small pocket in the pipe cross section. Consistent with this interpretation, Mansour et al. (2022) previously demonstrated the limited mixing efficiency of horizontally oriented straight pipe segments under laminar conditions (Re=593, while for the HF-2000-⅛ was only ~33). For the HF-2000-⅛, the improved performance relative to the other FLOCC-only mixer configurations may be attributed to enhanced radial mixing associated with the formation of a pair of rotating vortices, in combination with its longer HRT. Together, these features likely promote greater transverse redistribution of coagulant and improved contact between the coagulant and the bulk raw water.

In contrast, the rapid mixer is expected to produce a swirling flow field with chaotic eddies driven by the formation of a turbulent vortex. Although Rushton and Mahony (1954) reported limited vertical exchange of fluid streamlines for similar configurations, the continuous flow-through design of the RM coupled with the center baffle promoted a downward entrant velocity profile and an upward profile on exit. This flow structure should therefore enhance the vertical mixing of fluid and promote a more uniform distribution of the injected coagulant stream throughout the bulk raw water. Therefore, compared to laminar flow with FLOCC only, the addition of the RM promotes the rapid distribution of the small coagulant flow across the entire bulk raw water flow, which Bratby (2016) identified as the most important parameter affecting coagulation performance.

The equilibrium alum domain diagrams developed by Amirtharajah and Mills (1982) suggest that the main coagulation mechanism in the present study was sweep flocculation. It has been previously reported that for sweep coagulation, rapid mixing is less important than for adsorption/destabilization mechanism (Johnson and Amirtharajah 1983). Indeed, Amirtharajah and Mills (1982) and Amirtharajah et al. (1991) reported that the hydrolysis species most effective for adsorption/destabilization form within approximately 0.01–1.0 s following alum addition.

Under adsorption/destabilization conditions, mononuclear and small polynuclear species must be rapidly and uniformly distributed throughout the bulk water because adsorption can occur on timescales as short as 10^{-10} s. Delayed or prolonged hydrolysis can instead favor formation of aluminum hydroxide precipitates that are less effective for adsorption-based destabilization. Thus, the enhanced initial coagulant dispersion provided by the RM should have a greater influence on floc formation under adsorption-destabilization conditions than under the sweep-flocculation conditions evaluated here. This hypothesis warrants further investigation.

Collectively, these results demonstrate the potential of the small-scale rapid mixer developed in this study as a simple, customizable, and cost-effective means to improve coagulation/flocculation performance in bench-scale continuous-flow experiments. The lower experimental HRT relative to the theoretical value (Table G.2) suggests the presence of a dead volume within the current design. Reducing this volume by filling the void space behind the inlet baffle, for example, may improve hydraulic efficiency. Additional modifications, including the use of wall baffles recommended for circular mixing basins (Crittenden et al. 2012), and reducing the HRT by filling the volume with epoxy, may further enhance mixing performance. A schematic illustrating a revised design for the RM which incorporates these improvements is presented in Fig. G.6. Future work focused on optimizing the reactor geometry could leverage 3-D printing technology to enable the fabrication of smaller, baffled units with tailored geometries.

6.4.2. Comparison of LPM Fouling with Alternative Mixing Types

The hydraulically reversible (FR_{hr}) and irreversible (FR_{hirr}) fouling rates obtained from the replicated day-long filtration experiments are presented in Fig. 6.5. Elevated FR_{hr} and FR_{hirr} were observed during the first ~ 4 h of filtration, after which a pseudo-steady state operation was observed for the remainder of the day-long test. Accordingly, the FR values in the present study were calculated using only data collected after 4 h of operation (i.e., from the 9^{th} to 45^{th} filtration cycle). Moreover, the data was screened for potential outliers using a boxplot approach with upper and lower fences specified by a distance of three interquartile ranges from the first and third quartiles. As shown in Fig 6.5a, the FR_{hirr} were low (< 3 mBar h^{-1}) for all configurations and, using a one-way analysis of variance (ANOVA), no significant differences (p=.9657) were identified between the mean FR_{hirr} for all tested configurations, including direct filtration of raw water. Furthermore, the 95% CIs for all FR_{hirr} values included zero, indicating that the hydraulically

irreversible fouling was not statistically significant. Based on this, alternative means of quantifying hydraulically irreversible fouling were also considered: Section G.2.2. attempted to use the hydraulically irreversible fouling index defined by Nguyen et al. (2011), but it also yielded values which were mostly statistically indistinguishable from zero (Fig. G.7). In contrast to the hydraulically irreversible fouling, FR_{hr} (Fig. 6.5b) was found to be substantially larger, ranging from 7.88 mBar h^{-1} for batch coagulation to over 110 mBar h^{-1} for direct filtration (i.e., raw water filtration). Consequently, the fouling was predominantly reversible in nature, with FR_{hr} accounting for more than 94.83% of the total fouling rate ($FR_{TOT}=FR_{hr}+FR_{hirr}$) across all configurations (Table G.4). This is consistent with the operation of LPMs at full-scale, where high hydraulic reversibility of fouling is required to enable extended filtration periods between intensive chemical cleanings. Because the control of irreversible fouling is critical for the sustainable long-term operation of LPM systems, the day-long filtration tests used in this study may not fully capture the long-term trajectory of irreversible fouling (Ayache et al. 2013). To also quantify irreversible fouling, it would have been necessary to conduct additional tests with accelerated irreversible fouling development using greater permeation flux, longer filtration cycles, or much longer test duration. Such conditions may have permitted a clearer analysis of the potential impact of mixer configuration on FR_{hirr}. However, given the observed cycle-to-cycle variability of FR_{hirr} as well as the fact that it is calculated from adjacent filtration cycles, it remains unclear whether these adjustments would have produced statistically significant differences. Given the negligible contribution of FR_{hirr} to the total fouling development under the conditions tested in this study, as well as its lack of statistical significance, subsequent comparisons among configurations will focus on FR_{hr} as the primary indicator of fouling behavior.

Pooled *t*-tests were used to help elucidate the impact of C-IN pretreatment, flow configuration, RM, and flocculation on FR_{hr}. A summary of the statistical data is presented in Section G.2.3. As shown in Fig. 6.5b as well as Table G.5, regardless of the mixer configuration, C-IN pretreatment using the jar-test optimal coagulation chemistry yielded reduced magnitude LPM fouling compared to direct filtration. The improvement in fouling mitigation by C-IN pretreatment is consistent with the findings from many previous studies in the literature (e.g., Choi and Dempsey 2004; Naim et al. 2014). Compared to mixing by a batch reactor, all continuous-flow configurations (both with and without RM) resulted in significantly higher FR_{hr} values (Table G.6). Therefore, not only does the batch coagulation configuration have unrealistic operation (with

GT values up to ~10^4 times greater than for continuous-flow approaches as shown in Table 6.1) with long HRTs (compared to full-scale facilities), but it also appears to provide an optimistic fouling assessment. This should be confirmed in future work using data from a full- or pilot-scale system.

For the four flocculator types considered in the continuous-flow system, RM+FLOCC yielded mean FR_{hr} values that were significantly lower than for FLOCC only (see the *p*-values on the difference in means presented in Table G.7). This highlights the beneficial impact of RM for the complete dispersal of coagulant within the feed stream prior to these low Reynolds bench-scale flocculators. Compared to RM only, the addition of flocculation (i.e., RM+FLOCC) led to significantly lower FR_{hr} for all flocculator types (Table G.8). These results are consistent with the findings of Malkoske et al. (2023b), who reported similar trends in total and irreversible fouling when comparing RM+FLOCC with a vertical shaft flocculator to RM only. While pretreatment with mixing by RM only may be desirable from a cost perspective in terms of minimization of plant footprint, the data from this study suggests that the inclusion of a dedicated flocculation stage leads to a statistically significant reduction in FR_{hr}. This will serve to reduce operating and maintenance costs, which represent the most significant component of the present value cost for a LPM installation (Judd and Carra 2021).

The differences in FR_{hr} arising from mixing configuration have important implications for the design of C-IN-LPM studies and the interpretation of their data. Because no standardized methodology exists for simulating C-IN pretreatment at bench-scale, researchers have employed a variety of mixing configurations based largely on the equipment at their disposal as well as experimental convenience. The results of this study indicate that the selection of mixer configuration can significantly influence the propensity for LPM fouling, something that experimenters must be aware of when designing their studies. Furthermore, extreme caution should be exercised when interpreting the results from previous C-IN-LPM studies as the reported differences may reflect not only the influence of coagulation chemistry, membrane type, and membrane operating conditions, but also the differences in mixing configuration. These observations give rise to several important research needs. First, the comparison of batch and continuous-flow coagulation should be extended to natural waters and different membrane types to validate the generalizability of this finding. Second, future work should endeavor to compare the LPM fouling in full- or pilot-scale systems with that observed in bench-scale simulations

employing both batch and continuous-flow coagulation to determine which approach more accurately represents full-scale operation. It would also be of interest to ascertain whether the most appropriate bench-scale alternative is dependent on the particular mixing configuration employed at full-scale.

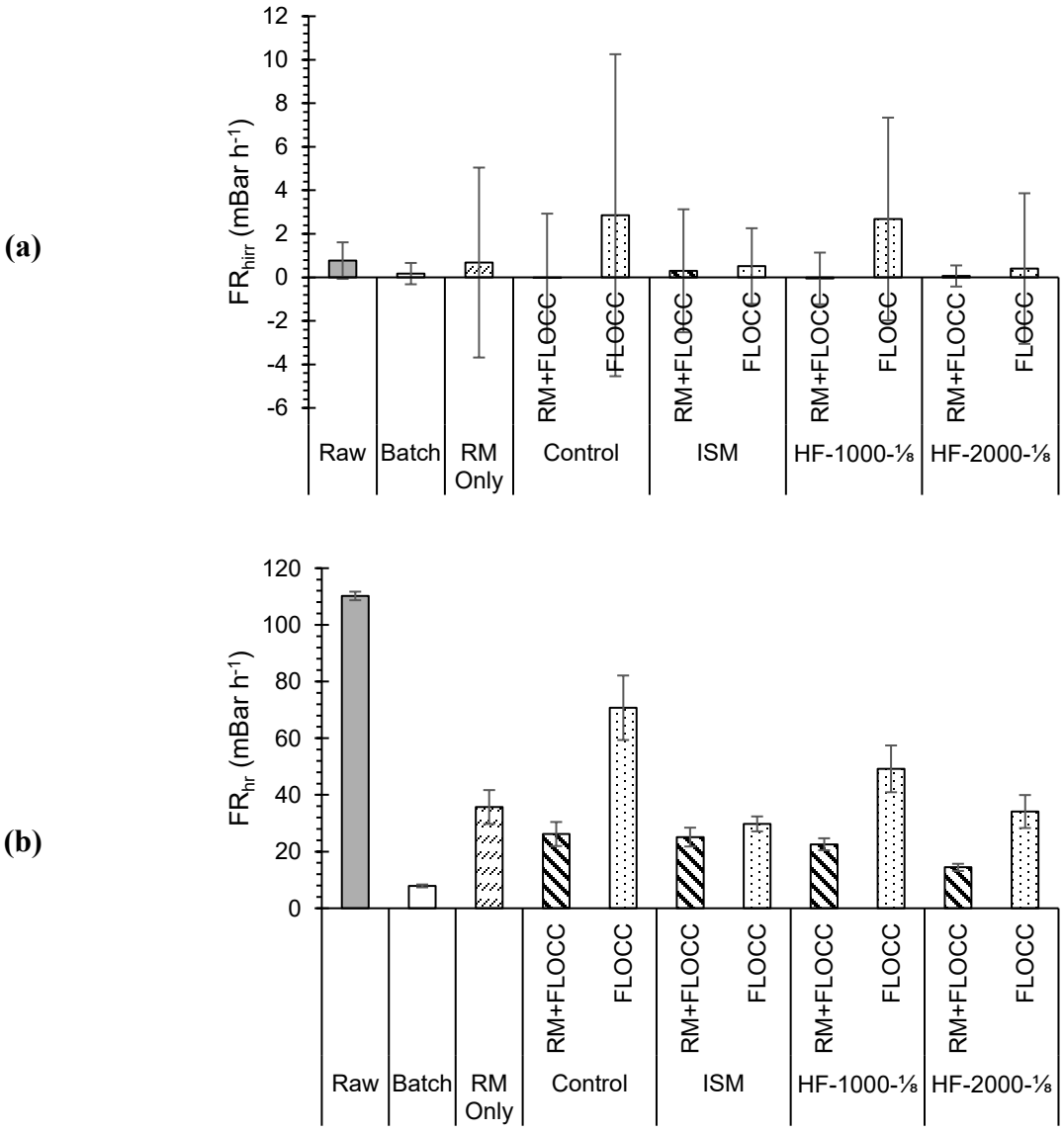


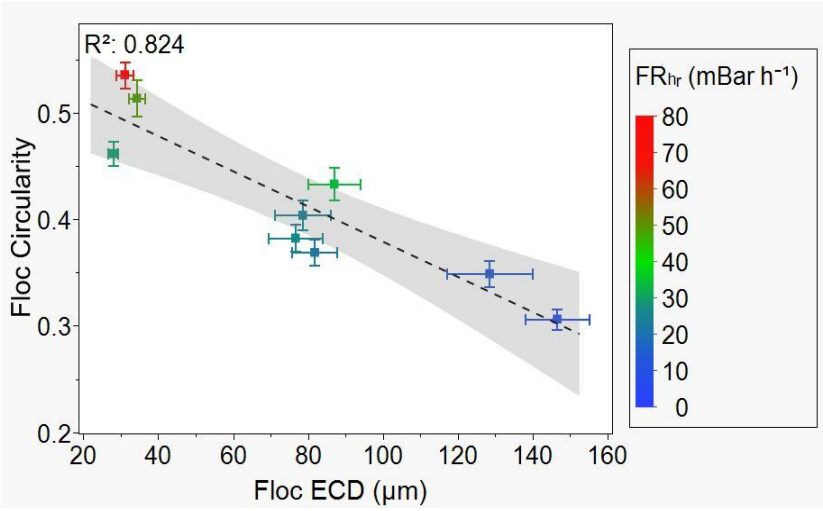
Fig. 6.5. Impact of rapid mixing and flocculator type on: **(a)** FR_{hirr}; **(b)** FR_{hr}**.** Note: Error bars represent the 95% confidence interval calculated using the Student's *t*-test as $\mu \pm t_{n-1,0.025}\frac{s}{\sqrt{n}}$ where $n = 72$ for replicated day-long filtration tests

The effect of floc aggregate properties, which varied among mixer configurations as described in Section 6.4.1., on fouling potential was further evaluated. Fig 6.6 presents scatter plots illustrating the relationships between FR_{hr}, floc ECD, and either floc circularity (Fig. 6.6a) or floc concentration (Fig. 6.6b). In each subplot, the dashed line represents the regressed linear relationship between floc ECD and the corresponding floc property while the shaded grey region represents the 95% prediction interval. The color of the data points is representative of the magnitude of FR_{hr}, with the scale shown on the right of the plots. In Fig. 6.6a, a moderately strong (R^2=0.824) and significant (p=.0002) relationship was identified between the floc circularity and floc ECD, with decreasing circularity as the floc size increased. Floc growth is brought about by particle-cluster or cluster-cluster aggregation via a mechanism that resembles the cluster-cluster aggregation model. For mixer configurations that brought about more effective flocculation, the small clusters formed during the initial stages of coagulation combine to produce large-sized flocs with highly branched, fractal structure. When the flocculation was poor, which led to lower collision frequencies, or absent, and only the small initial aggregates formed under the high shear stress conditions of the rapid mixer were present, smaller sized flocs with a more regular/compact structure were formed. The variation in FR_{hr} shows that lower magnitude fouling occurred for large, irregular shaped flocs while FR_{hr} was maximized for small-sized flocs with high circularity. This is in agreement with the findings of previous studies who have reported lower magnitude fouling resistance for large-sized flocs with a loose structure (Wang et al. 2010). Moreover, they are also in agreement with the explicit form of the Carman-Kozeny expression where the specific cake resistance was shown to be inversely proportional to the square of the floc size (Section G.2.4., Supplemental Materials) (Amjad et al. 2015; Carman 1997).

The relationship between floc ECD and floc concentration, which was moderately strong (R^2=0.873) and statistically significant (p=.0002), is presented in Fig 6.6b. As floc ECD increased, the measured floc concentration decreased. This trend likely reflects the progressive incorporation of smaller particle clusters into growing flocs, resulting in fewer, but larger, aggregates in suspension. The highest FR_{hr} values were seen to occur for conditions characterized by small flocs at high concentration, whereas larger flocs in lower concentration were associated with reduced fouling potential. This finding is in contrast to that of Malkoske et al. (2023a; b), who reported lower fouling resistance for increased floc concentrations. However, Amjad et al. (2015) also emphasized the importance of particle concentration on LPM fouling and proposed that a critical

threshold exists at which increased floc/particle loading to the membrane surface offsets the benefits of large and loosely structured aggregates, leading to greater LPM fouling. Accordingly, these results suggest that optimal C-IN-LPM operation is achieved when the pretreatment configuration is tailored to form a relatively low number of large sized, loose flocs.

(a)



(b)

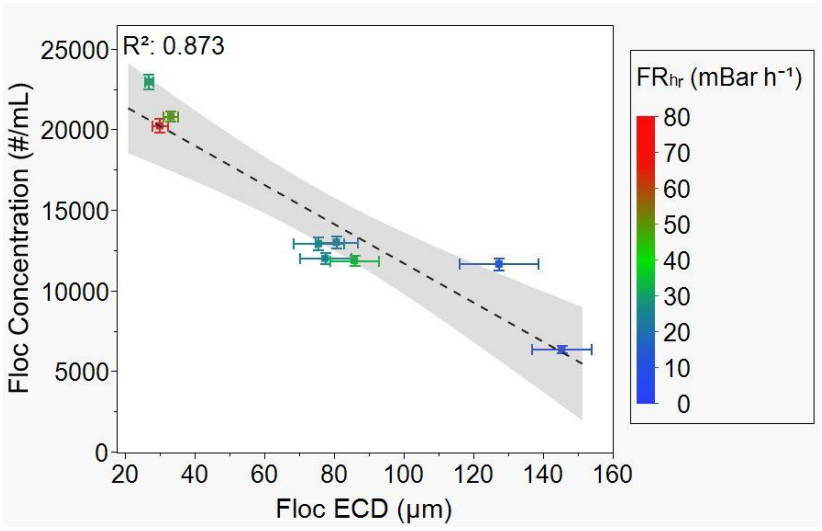


Fig. 6.6. Relationships between floc FR_{hr}, Floc ECD, and: **(a)** Floc circularity; **(b)** Floc concentration for batch tests and FLOCC or RM+FLOCC. Note: Error bars represent the 95% confidence interval calculated using the Student's *t*-test as $\mu \pm t_{n-1,0.025}\frac{s}{\sqrt{n}}$ where $n = 200$ for replicated tests.

6.4.3. Impact of HCTF Properties on LPM Fouling in RM+FLOCC

To elucidate the impact of helical geometry, experiments were also conducted using HCTFs with varying pipe length and pipe diameters. Fig. 6.7a and Fig. 6.7b show that FR_{hr} decreased with increasing floc size and decreasing floc circularity for HCTFs with varying pipe length and pipe diameters, consistent with the trends observed across all mixing configurations shown in Fig. 6.5. Increasing pipe diameter (□→○ and ■→●) produced smaller flocs with a more circular geometry that led to higher FR_{hr} whereas increasing pipe length (○→● and □→■) generated larger flocs with reduced circularity and lower FR_{hr}. The influence of pipe length was more pronounced for the 3.175 mm pipe diameter HCTF ($\overline{FR}_{hr_{2000,3.175}} - \overline{FR}_{hr_{1000,3.175}} = 8.14\ mBar\ h^{-1}$; $\overline{FR}_{hr_{2000,6.35}} - \overline{FR}_{hr_{1000,6.35}} = 5.4\ mBar\ h^{-1}$), likely due to the more favorable hydrodynamic conditions (Fig. 6.6c). For this configuration, the Dean number (D_e ~ 8.11), which describes the strength of the secondary flow pattern in curved pipes (see Table 6.1) and Reynolds number (R_e ~ 33.32) fell within the optimal ranges reported by Mansour et al. (2020) (7≤ D_e ≤15 and 25≤ R_e ≤60), while the velocity gradient (G ~17.8 s^{-1}) corresponded to the aggregation-dominated regime described by Serra et al. (2008). In contrast, the larger pipe diameter HCTFs exhibited lower D_e (~ 5.57) and G (~ 2.22 s^{-1}), conditions that have been associated with reduced collision frequencies and smaller sized floc formation (He et al. 2012b). Furthermore, Mansour et al. (2020) demonstrated that for R_e < ~20 (R_e = 16.7 for the HF-1000-¼ and HF-2000-¼ configurations), mixing efficiency becomes highly sensitive to pipe diameter due to the weakening of the secondary flow structures.

Therefore, in summary, increasing the pipe length for the 3.175 mm pipe diameter HCTF increased the HRT (refer to Table 6.1) under near optimal mixing conditions, promoting the formation of larger and more highly branched floc structures that led to reduced FR_{hr}. For the larger diameter HCTF, the benefit of increased HRT was limited by the sub-optimal hydrodynamic conditions. These results indicate that FR_{hr} is governed not only by the secondary flow strength, characterized by D_e or R_e, but also by the HRT and further reinforce previous findings that HCTF design should be guided primarily by these parameters (see Chapter 5).

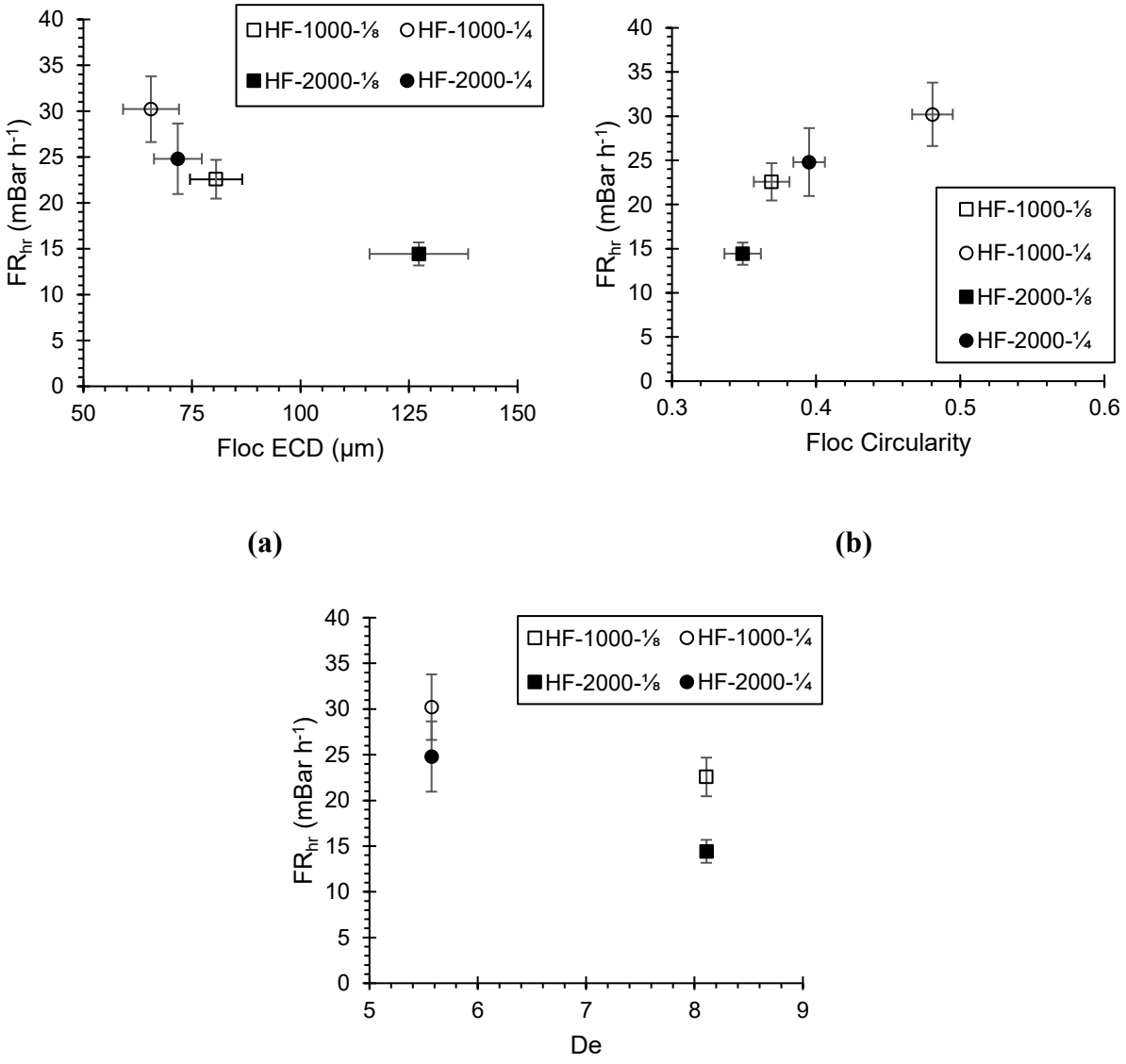


Fig. 6.7. Relationships between FR_{hr} and: **(a)** ECD; **(b)** Floc circularity; **(c)** D_e for helical flocculators with varying length and pipe diameter. Note that ○→● and □→■ represent the impact of pipe length while ○→□ and ●→■ represent the impact of pipe diameter. Error bars represent the 95% confidence intervals calculated using the Student's t-test as $\mu \pm t_{n-1,0.025}\frac{s}{\sqrt{n}}$ where $n = 200$ for floc properties and $n = 72$ for fouling rates.

One limitation of the preceding analysis is that increasing the HCTF pipe diameter simultaneously increased the flocculator HRT, convoluting the interpretation of the results. To

address this, three HCTFs with identical geometry but different pipe lengths (1000 mm, 2000 mm, 3000 mm) were compared in order to isolate the impact of HRT. As shown in Fig. 6.8a, FR_{hr} exhibited a unimodal response to increasing HRT. Specifically, FR_{hr} decreased (22.57 $mBarh^{-1}$ → 14.43 mBar h^{-1}) with the increase in HRT from 2 min to 4 min, before increasing to 25.52 mBar h^{-1} as the HRT was further increased to 5.22 min. The floc ECD showed the opposite behavior, reaching a maximum at an HRT of 4 min, whereas the trends in floc concentration and floc circularity closely mirrored that of FR_{hr}. These results suggest the existence of an optimal HRT for a given R_e and G whereby floc growth is maximized and the corresponding degree of LPM fouling is minimized. Similar trends in floc properties with variable HRT have been reported in previous studies of HCTF systems. For example, De Oliveira and Teixeira (2017) observed that the turbidity removal by sedimentation following flocculation initially increased with increasing HRT, reaching a maximum that was dependent on the employed G value, before declining at longer retention times. Given the strong dependence of settling velocity (turbidity removal) on floc size (Vahedi and Gorczyca 2012), their findings are consistent with the trends in ECD observed in the present study.

The unimodal response in ECD observed in this study likely reflects the combined impact of HRT and the characteristic secondary flow pattern in HCTFs. According to the two-zone transport model proposed by Sartori et al. (2015), floc growth predominantly occurs in the low-shear central core of the flow, while the high-shear region near the pipe wall induces floc breakup. Based on this model and the results presented in Fig. 6.8 it is hypothesized that at moderate retention times, conditions favor floc aggregation within the central region, resulting in flocs with large ECDs and lower fouling rates. However, as the retention time increases further, the large-sized flocs are more frequently transported to the high-shear wall region where they become susceptible to shear-induced fragmentation. This should be confirmed in future studies by using computation fluid dynamics coupled with discrete element methods (i.e., CFD-DEM) to model the transport of flocculating aggregates flowing in complex pipe flow. For the conditions employed in the current study, the structure of the large flocs is presumably more fragile due to the inherent weakness in their bonds (Selomulya 2002), making them especially susceptible to shear-induced breakup near the wall of the HCTF. This led to the pronounced impact of HRT on floc properties and LPM performance in the integrated system. In contrast, for higher G values, the floc structure would be expected to be more tenable due to the breakup and re-aggregation that occurs at elevated

hydrodynamic shear levels, reducing the impact of HRT on system performance. This hypothesis should be confirmed by future work which characterizes the change in floc properties for HCTFs with variable HRT values across a range of high and low G values.

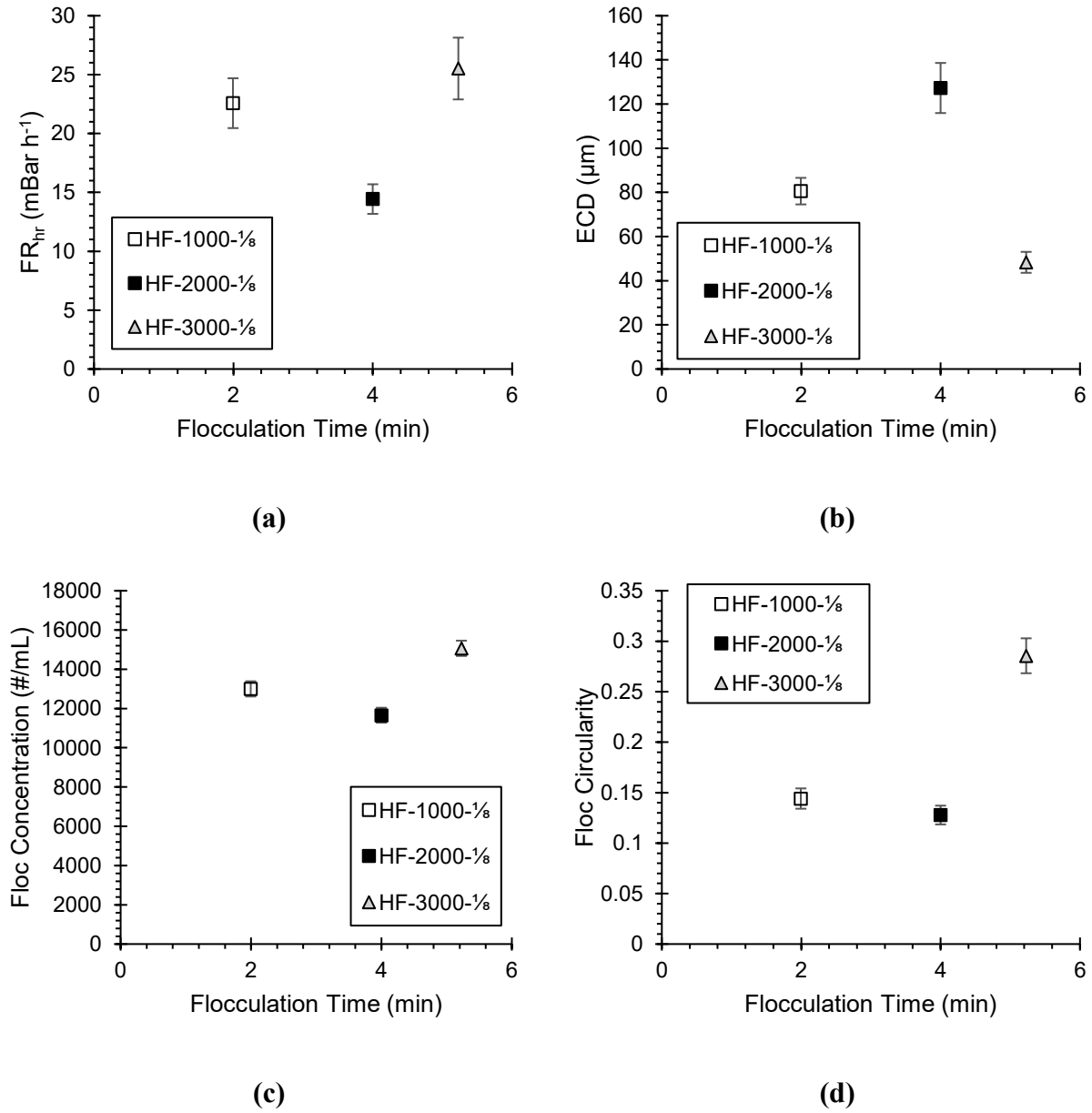


Fig. 6.8. Impact of HCTF HRT on: **(a)** FR$_{hr}$; **(b)** Floc ECD; **(c)** Floc concentration; **(d)** Floc circularity. Note: Error bars represent the 95% confidence interval calculated using the Student's t-test as $\mu \pm t_{n-1,0.025}\frac{s}{\sqrt{n}}$ where $n = 200$ for replicated tests.

6.4.4. Treated Water Quality

The treated water quality, including the percentage removal of turbidity, true and apparent color, as well as UV_{254}, was assessed for all test conditions. Considering first the removal of turbidity, a Student's *t*-test demonstrated that direct filtration had overlapping 95% CIs with most C-IN pretreatment approaches (Table G.9). This finding was not unexpected as the organics in this study were already pre-filtered through a 0.45 µm membrane. As a result, the particulate/colloidal material consisted principally of kaolin clay, which had a median diameter of 1-2 µm and was therefore removed sterically by the LPM to a similar extent regardless of whether C-IN pretreatment was applied or not. For direct filtration, the mean removal of UV_{254} across replicated tests was 44.38%, while the removals of true and apparent color were 53.44% and 75.3%, respectively. These removals of organic water quality indicators (WQIs) are much greater than those typically reported for direct filtration when natural water sources are used, where removals are often below 20% (Pearce 2011). This discrepancy highlights an important limitation of the use of synthetic waters for LPM studies. Although considerable efforts were made in the current study to simulate the conditions of natural waters by using a more complex multi-component organic matrix with added alkalinity, hardness, and turbidity, synthetic waters do not represent the behavior of natural waters so well. Consequently, results obtained from studies using synthetic waters should be carefully considered in future as system performance may differ significantly compared to what would be expected when natural water is used.

Compared to direct filtration, a one-way ANOVA confirmed that C-IN pretreatment improved the removal of organics regardless of the employed mixing configuration (*p*-values <0.05 in Table G.10). Many previous studies have similarly reported coagulation pretreatment as an effective means to enhance organics removals in LPM systems compared to direct filtration of raw waters (e.g., Keucken et al. 2017; Yu et al. 2021). When the removal of the four WQIs were compared for tests with C-IN pretreatment using different mixing configurations, the *F*-test indicated no statistical difference in the mean removals regardless of flocculator type or the presence/absence of the inline rapid mixer (Table G.11). This finding is in agreement with Malkoske et al. (2020) who, in their review of over 60 C-IN-LPM studies from the literature, reported that there was no clear trend between the removal of DOC and the configuration of mixers used in C-IN pretreatment. The removal of organics by the integrated C-IN-LPM system therefore appears to be dependent principally on the coagulation chemistry (dose and pH) and the applied

Al^{3+}/DOC ratio, which govern conventional coagulation performance, rather than the specific mixing configuration. This finding has important implications in the design of future C-IN-LPM systems as the mixer configuration can be optimized to yield favorable floc size and structure for fouling mitigation without adversely affecting the removal of organics.

In addition to the impact of flocculator type, the impact of HRT on organics removal was assessed using the HF-1000-⅛, HF-2000-⅛, and HF-3000-⅛ flocculators. An *F*-test indicated no statistically significant impact (p>0.05) of HRT on the removal of the four WQIs (Table G.12). This is in agreement with the findings of Meyn et al. (2012) who also reported that the organics removal (measured in terms of DOC) was not dependent on the HRT of a hydraulic pipe flocculator when varied between 10-240 s. In contrast, Malkoske et al. (2023a) found that extending the HRT of a vertical turbine flocculator from 12 min to 24 min increased the total organic carbon removal under adsorption coagulation, but decreased removal under combined adsorption/destabilization and sweep coagulation chemistries. Walsh et al. (2009) noted that for C-IN pretreatment, the removal of DOC and true color were relatively unchanged as the HRT increased up to 10 min, however, decreased slightly when the HRT increased further to 25 min. The results of these last studies may indicate the presence of a threshold HRT below which changes in retention time do not influence the removal of organics. It seems likely that the insensitivity of organics removal to HRT reported by the current study and that of Meyn et al. (2012) is due to the fact that hydraulic flocculators were operated with shorter retention times (typical of LPM pretreatment), which fall below this critical threshold value. For extended flocculation times more typical of conventional processes with clarification by sedimentation (which range between 15-45 min) (Kawamura 2000), the HRT may exceed this threshold and impact the removal of organics. Future work should directly compare the removals achieved by both hydraulic and turbine flocculators over a range of HRT conditions to confirm this hypothesis.

6.4.5. Engineering Significance

Presently, no standardized testing methodology or apparatus exists for bench-scale evaluation of LPMs. Consequently, studies investigating C-IN pretreatment of LPMs have employed a wide range of mixing configurations, with many adopting continuous-stirred batch reactors because of their relative ease of implementation and the practical challenges associated with scaling down continuous-flow systems. The findings of this study demonstrate that mixer configuration can

significantly influence floc properties and membrane performance in integrated C-IN–LPM systems. Although continuous-flow coagulation resulted in greater LPM fouling than batch coagulation under the conditions investigated, continuous-flow systems more closely represent the hydraulic conditions encountered in full-scale treatment facilities. In particular, implementation of batch coagulation at full-scale would require substantially greater reactor volumes and, consequently, a larger treatment footprint. Continuous-flow coagulation should therefore be considered when developing benchmark configurations for bench-scale evaluation of C-IN pretreatment.

This study developed and validated a continuous-flow inline rapid mixer and demonstrated the importance of rapid mixing to coagulation efficiency and subsequent LPM performance under low-Reynolds-number flocculation conditions. Accordingly, rapid mixing should be incorporated into future bench-scale investigations rather than relying solely on the mixing provided by the flocculation stage. Among the flocculator configurations evaluated, the HF-2000-⅛ performed well with an optimal Re~33 (corresponding G value ~18 s^{-1}) and an HRT of ~4 min. This can serve as a useful benchmark for the design of future low-Reynolds-number coagulation studies. The selection of HCTFs as a candidate benchmark flocculator also capitalizes on their strong secondary flow, which promotes improved radial and transverse transport of coagulant under low-Reynolds-number conditions. Furthermore, HCTFs are relatively simple and inexpensive to construct, particularly compared with the custom continuous-flow jar-test apparatuses reported by other authors in the literature (Malkoske et al. 2023b). This accessibility makes HCTFs a practical option for establishing more consistent and reproducible bench-scale testing methodologies across research groups.

Although standardizing a single mixing configuration for the evaluation of C-IN pretreatment of LPMs may not be practical given the range of research objectives and experimental constraints across different research groups, a more achievable approach is to improve consistency in the reporting of hydraulic and hydrodynamic mixing conditions. To facilitate meaningful comparison among studies, future bench-scale investigations should report, at minimum, the presence or absence of rapid mixing; rapid-mixing intensity and HRT; flow rate; and flocculator geometry and type. More consistent reporting of these parameters would enable more critical comparisons amongst literature studies.

Finally, the bench-scale system used in the present study demonstrated that operation should be adjusted according to the research objectives, whether they be assessment of hydraulically reversible or irreversible fouling development. For reversible fouling assessment, continuous-flow bench-scale systems should be designed to simulate normal full-scale operation by incorporating the following considerations: (a) hollow-fiber membranes, although complimentary flat-sheet tests should be considered for foulant cake investigations; (b) test durations of at least one day, as the present study demonstrated that the performance during the initial 4 hours of operation was not representative of pseudo-steady-state operation; (c) sufficiently long hydraulic backwash periods to ensure high backwash efficiency; and (d) operation at sub-critical fluxes with conventional filtration cycle durations. For quantification of hydraulically irreversible fouling development, accelerated fouling tests should be designed with higher flux values, longer filtration cycle lengths, and/or greater durations. The relevant values of these parameters, however, would depend on the specific interaction of the raw water, coagulant chemistry, and membrane type.

6.5. Conclusions

Day-long bench-scale filtration tests were conducted using a dead-end TMC membrane to evaluate the impact of mixing configuration on the performance of C-IN pretreatment for LPMs. The floc properties, fouling development, and treated water quality for mixing by a batch reactor were compared with those for different continuous-flow flocculators with or without RM. The results of the study can be summarized as:

1. The most significant contribution of this study was the development of a novel small-scale inline rapid mixer and coagulant dosing system. This system permitted continuous-flow C-IN LPM testing without requiring excessive flowrates and volumes of water.
2. Using a novel small-scale inline rapid mixer, the importance of RM for bench-scale studies was confirmed. For the four flocculator types considered in the study, RM+FLOCC led to significantly increased floc size compared to FLOCC only. Moreover, for RM+FLOCC, the floc compactness was unaffected by the choice of flocculator type but instead appeared to be governed by the presence of RM.
3. Hydraulically reversible LPM fouling was strongly influenced by the choice of C-IN mixing configuration. Batch coagulation resulted in the lowest fouling rates while all

continuous-flow C-IN configurations yielded higher FR_{hr} values. Among continuous-flow approaches, RM+FLOCC resulted in reduced membrane fouling compared to RM or flocculation alone. These significant differences in LPM fouling amongst C-IN mixing configurations highlight the potential for mixing strategy to confound comparisons across studies and underscore the necessity of accounting for mixing conditions when interpreting fouling results from different studies.

4. HCTFs proved effective for continuous-flow flocculation at bench-scale with the RM+HF-2000-⅛ configuration generating the largest sized flocs and lowest FR_{hr} amongst tested flocculator types. This configuration therefore represents a promising approach for bench-scale simulation of continuous-flow C-IN systems, while avoiding the key limitation associated with existing designs, namely, the large raw water demand.
5. The performance of HCTFs was governed by the hydrodynamic condition as well as HRT. For the larger diameter HCTF operated under sub-optimal hydrodynamic conditions (Reynolds number of 16.7), increasing HRT offered limited benefits in terms of floc aggregation and LPM fouling reduction. In contrast, for the smaller diameter HCTF with operation at a Reynolds number of 33.3 and varying HRT between 2 min and 5.22 min, the floc ECD showed an increasing, then decreasing trend while the floc concentration and circularity changed in inverse. The unimodal pattern was likely the result of increased interaction of floc particles with the high shear region located near the pipe wall, characteristic of the secondary flow pattern in HCTFs.
6. Under zeta-potential-based jar-test optimal conditions, the removal of bulk organic WQIs by the integrated C-IN-LPM system was found to be unaffected by the employed mixer configuration, including flocculator type and the presence/absence of RM. This indicates that the mixing configuration can be optimized to produce flocs with low fouling propensity without adversely affecting the treated water quality. However, these results were for conditions governed by sweep flocculation, the effectiveness of which is known to be relatively insensitive to mixing. The impact of mixing configuration on organics reduction may be more pronounced for sub-optimal coagulation chemistries with reduced dosages, the effectiveness of which are dependent on highly efficient mixing.

The most salient finding from this study is that the choice of mixing configuration exerts an important influence on the performance of LPMs in the integrated C-IN-LPM system. Based on this, future studies should carefully consider how their experimental system design may bias results by selecting a given mixing configuration. Moreover, the interpretation and analysis of literature data must consider that reported performance differences may arise not only from differences in coagulation chemistry or membrane operation, but also from the employed mixing strategy. This study was conducted using a synthetic water and a single TMC membrane, the performance of which may not be fully representative of natural waters and/or membrane types. Consequently, experiments conducted using natural waters with different characteristics may yield somewhat different results, and further investigation using similar experiments and real waters are therefore warranted. It must also be acknowledged that, due to the day-long duration of the LPM filtration tests, the hydraulically irreversible fouling was not quantifiable. As irreversible fouling is critical for the long-term operation of full-scale LPM systems, similar C-IN pretreatment comparisons should be conducted using long-term pilot-scale tests or, at a minimum, longer duration bench-scale tests with longer filtration cycles and possibly higher filtration rates. Finally, the performance of the various bench-scale configurations should be compared with that of full-scale facilities to identify the optimal configuration for replicating full-scale plant performance.

6.6. Acknowledgements

This work was supported by the Natural Sciences and Engineering Research Council of Canada (NSERC) under grant RGPIN 2018-06571 as well as the NSERC Canada Graduate Scholarship Doctoral Program (ID 579943-2023). The authors would also like to acknowledge financial support provided to the lead author by the American Membrane Technology Association (AMTA) through their Ian C. Watson Fellowship and by the American Water Works Association (AWWA) through the Dr. James K. Edzwald Scholarship. Finally, the authors extend their thanks to Catherine Brosseau and Kemira Water Solutions Canada for providing coagulant for this study.

6.7. References

Alresheedi, M. T. 2023. "Understanding protein and polysaccharide fouling with silicon dioxide and aluminum oxide in low-pressure membranes." *Membranes*, 13 (5): 476. https://doi.org/10.3390/membranes13050476.

Alresheedi, M. T., B. Barbeau, and O. D. Basu. 2019. "Comparisons of NOM fouling and cleaning of ceramic and polymeric membranes during water treatment." *Separation and Purification Technology*, 209: 452–460. https://doi.org/10.1016/j.seppur.2018.07.070.

Aly, S. A., W. B. Anderson, and P. M. Huck. 2021. "In-line coagulation assessment for ultrafiltration fouling reduction to treat secondary effluent for water reuse." *Water Science and Technology*, 83 (2): 284–296. https://doi.org/10.2166/wst.2020.571.

American Public Health Association, Water Environment Foundation, and American Water Works Association. 2012. *Standard Methods for the Examination of Water and Wastewater*. 1496. Edited by L. Clesceri, A. Greenberg, and A. Eaton. 22nd Editi. Washington: APHA Press.

Amirtharajah, A., M. M. Clark, and R. R. Trussell, eds. 1991. *Mixing in Coagulation and Flocculation*. Denver, CO: American Water Works Association Research Foundation.

Amirtharajah, A., and K. M. Mills. 1982. "Rapid-mix design for mechanisms of alum coagulation." *Journal AWWA*, 74 (4): 210–216. https://doi.org/10.1002/j.1551-8833.1982.tb04890.x.

Amjad, H., Z. Khan, and V. V. Tarabara. 2015. "Fractal structure and permeability of membrane cake layers: Effect of coagulation–flocculation and settling as pretreatment steps." *Separation and Purification Technology*, 143: 40–51. https://doi.org/10.1016/j.seppur.2015.01.020.

Amy, G. 2008. "Fundamental understanding of organic matter fouling of membranes." *Desalination*, 231 (1–3): 44–51. https://doi.org/10.1016/j.desal.2007.11.037.

Ayache, C., M. Pidou, J.-P. Croue, J. Labanowski, Y. Poussade, A. Tazi-Pain, J. Keller, and W. Gernjak. 2013. "Impact of effluent organic matter on low-pressure membrane fouling in tertiary treatment." *Water Research*, 47 (8): 2633–2642. https://doi.org/10.1016/j.watres.2013.01.043.

Benjamin, M. M., and D. Lawler. 2013. *Water Quality Engineering: Physical/Chemical Treatment Processes*. 1st ed. Hoboken, NJ, USA: John Wiley & Sons.

Bratby, J. 2016. *Coagulation and Flocculation in Water and Wastewater Treatment*. 3rd ed. London, UK: IWA Publishing.

Carissimi, E., D. G. Sanagiotto, E. B. C. Schettini, and J. Rubio. 2018. "Revisiting coiled flocculator performance for particle aggregation." *Water Environment Research*, 90 (4): 322–328. https://doi.org/10.2175/106143017X14902968254935.

Carman, P. C. 1997. "Fluid flow through granular beds." *Chemical Engineering Research and Design*, 75: S32–S48. https://doi.org/10.1016/S0263-8762(97)80003-2.

Chakraborti, R. K., K. H. Gardner, J. F. Atkinson, and J. E. Van Benschoten. 2003. "Changes in fractal dimension during aggregation." *Water Research*, 37 (4): 873–883. https://doi.org/10.1016/S0043-1354(02)00379-2.

Cho, M. H., C. H. Lee, and S. Lee. 2006. "Effect of flocculation conditions on membrane permeability in coagulation-microfiltration." *Desalination*, 191 (1–3): 386–396. https://doi.org/10.1016/j.desal.2005.08.017.

Choi, K. Y. J., and B. A. Dempsey. 2004. "In-line coagulation with low-pressure membrane filtration." *Water Research*, 38 (19): 4271–4281. https://doi.org/10.1016/j.watres.2004.08.006.

Crittenden, J. C., R. R. Trussell, D. W. Hand, K. J. Howe, and G. Tchobanoglous. 2012. *Water Treatment: Principles and Design*. 3rd ed. New York, NY: McGraw-Hill.

De Oliveira, D. S., and E. C. Teixeira. 2017. "Experimental evaluation of helically coiled tube flocculators for turbidity removal in drinking water treatment units." *Water SA*, 43 (3): 378. https://doi.org/10.4314/wsa.v43i3.02.

Dean, W. R. 1928. "The stream-line motion of fluid in a curved pipe." *The London, Edinburgh, and Dublin Philosophical Magazine and Journal of Science*, 5 (30): 673–695. https://doi.org/10.1080/14786440408564513.

Edzwald, J. K. 2013. "Coagulant mixing revisited: theory and practice." *Journal of Water Supply: Research and Technology-Aqua*, 62 (2): 67–77. https://doi.org/10.2166/aqua.2013.142.

Edzwald, J. K., and J. E. Tobiason. 1999. "Enhanced coagulation: US requirements and a broader view." *Water Science and Technology*, 40 (9): 63–70. IAWQ. https://doi.org/10.1016/S0273-1223(99)00641-1.

Ekambara, K., and J. B. Joshi. 2004. "Axial mixing in laminar pipe flows." *Chemical Engineering Science*, 59 (18): 3929–3944. https://doi.org/10.1016/j.ces.2004.05.025.

García-Ávila, F., D. Tenesaca-Pintado, F. Novoa-Zamora, E. A. Alfaro-Paredes, A. Avilés-Añazco, A. Guanuchi-Quito, M. D. Tonon-Ordoñez, and C. Zhindón-Arévalo. 2023. "Vertical tubular flocculator: Alternative technology for the improvement of drinking water treatment processes in rural areas." *Journal of Environmental Management*, 331: 117342. https://doi.org/10.1016/j.jenvman.2023.117342.

Gonzalez-Galvis, J. P., and R. M. Narbaitz. 2020. "Large batch bench-scale dissolved air flotation system (LB-DAF) for drinking water treatability tests." *Environmental Science: Water Research and Technology*, 6 (4): 1004–1017. Royal Society of Chemistry. https://doi.org/10.1039/c9ew00935c.

Gorczyca, B., and J. Ganczarczyk. 1999. "Structure and porosity of alum coagulation flocs." *Water Quality Research Journal of Canada*, 34 (4).

Gregory, J. 1981. "Flocculation in laminar tube flow." *Chemical Engineering Science*, 36 (11): 1789–1794. https://doi.org/10.1016/0009-2509(81)80126-1.

Guan, J., R. Amal, and T. D. Waite. 2001. "Effect of aggregate size and structure on specific resistance of biosolids filter cakes." *Water Science and Technology*, 44 (10): 215–220. https://doi.org/10.2166/wst.2001.0624.

Guigui, C., J. C. Roucha, L. Durand-Bourlierb, V. Bonnelyeb, and P. Aptel. 2002. "Impact of coagulation conditions on the in-line coagulationKJF process for drinking water production." 6.

Hahn, H. H., and W. Stumm. 1968. "Kinetics of coagulation with hydrolyzed Al (III)." *Journal of Colloid and Interface Science*, 28: 133.

He, W., J. Nan, H. Li, and S. Li. 2012a. "Characteristic analysis on temporal evolution of floc size and structure in low-shear flow." *Water Research*, 46 (2): 509–520. https://doi.org/10.1016/j.watres.2011.11.040.

He, W., J. Nan, H. Li, and S. Li. 2012b. "Characteristic analysis on temporal evolution of floc size and structure in low-shear flow." *Water Research*, 46 (2): 509–520. https://doi.org/10.1016/j.watres.2011.11.040.

Huang, H., K. Schwab, and J. G. Jacangelo. 2009. "Pretreatment for low pressure membranes in water treatment: A review." *Environmental Science and Technology*, 43 (9): 3011–3019. https://doi.org/10.1021/es802473r.

Hudson Jr., H. E. 1965. "Physical aspects of flocculation." *Journal AWWA*, 57 (7).

Iskander, M., and L. Li. 2024. *Dynamic Image Analysis of Granular Materials: Particle Granulometry for Geotechnical, Material, and Geological Applications*. 1st ed. Cham, Switzerland: Springer.

Jarvis, P., B. Jefferson, and S. A. Parsons. 2005. "Measuring floc structural characteristics." *Reviews in Environmental Science and Bio/Technology*, 4 (1–2): 1–18. https://doi.org/10.1007/s11157-005-7092-1.

Jiang, Q., and B. E. Logan. 1996. "Fractal dimensions of aggregates from shear devices." *Journal AWWA*, 88 (2): 100–113. https://doi.org/10.1002/j.1551-8833.1996.tb06506.x.

Johnson, P. N., and A. Amirtharajah. 1983. "Ferric Chloride and Alum As Single and Dual Coagulants." *Journal AWWA*, 75 (5): 232–239. https://doi.org/10.1002/j.1551-8833.1983.tb05122.x.

Judd, S. J., and I. Carra. 2021. "Low-pressure membrane technology for potable water filtration: true costs." *Water Research*, 191: 116826. https://doi.org/10.1016/j.watres.2021.116826.

Kamińska, G., W. Pronk, and J. Traber. 2020. "Effect of coagulant dose and backflush pressure on NOM membrane fouling in inline coagulation-ultrafiltration." *Desalination and Water Treatment*, 199: 188–197. https://doi.org/10.5004/dwt.2020.25657.

Kawamura, S. 2000. *Integrated Design and Operation of Water Treatment Facilities*. New York, NY: John Wiley & Sons.

Keucken, A., G. Heinicke, K. Persson, and S. Köhler. 2017. "Combined coagulation and ultrafiltration process to counteract increasing NOM in brown surface water." *Water*, 9 (9): 697. https://doi.org/10.3390/w9090697.

Kimura, K., T. Maeda, H. Yamamura, and Y. Watanabe. 2008. "Irreversible membrane fouling in microfiltration membranes filtering coagulated surface water." *Journal of Membrane Science*, 320 (1–2): 356–362. https://doi.org/10.1016/j.memsci.2008.04.018.

Lee, S. A., A. G. Fane, and T. D. Waite. 2005. "Impact of natural organic matter on floc size and structure effects in membrane filtration." *Environmental Science & Technology*, 39 (17): 6477–6486. https://doi.org/10.1021/es050148o.

Lerch, A., G. Hagmeyer, R. Gimbel, and J. Fehn. 2003. "A comparison of laboratory and pilot plant experiments on the combination of flocculation/ultrafiltration for direct potable water treatment of river water." *Water Supply*, 3 (5–6): 345–352. https://doi.org/10.2166/ws.2003.0187.

Letterman, R. D., J. E. Quon, and R. Gemmell S. 1973. "Influence of rapid-mix parameters on flocculation." *Journal AWWA*, 65 (11): 716–722. Hoboken, NJ, USA: Wiley.

Liou, T. M. 1992. "Flow visualization and LDV measurement of fully developed laminar flow in helically coiled tubes." *Experiments in Fluids*, 13 (5): 332–338. https://doi.org/10.1007/BF00209507.

Liu, Y., Z. Wang, M. Xu, F. Qi, C. Li, D. Sun, J. Nan, W. Li, X. Guan, and A. Ikhlaq. 2024. "Unveiling the role of cake layer in coagulation-ultrafiltration on membrane fouling and emerging application as dynamic membrane before ultrafiltration." *Separation and Purification Technology*, 350: 127932. https://doi.org/10.1016/j.seppur.2024.127932.

Liu, Y., X. Zhang, W. Jiang, M. Wu, and Z. Li. 2021. "Comprehensive review of floc growth and structure using electrocoagulation: Characterization, measurement, and influencing

factors." *Chemical Engineering Journal*, 417: 129310. https://doi.org/10.1016/j.cej.2021.129310.

Malkoske, T. A., P. R. Bérubé, and R. C. Andrews. 2020. "Coagulation/flocculation prior to low pressure membranes in drinking water treatment: A review." *Environmental Science: Water Research and Technology*, 6 (11): 2993–3023. Royal Society of Chemistry. https://doi.org/10.1039/d0ew00461h.

Malkoske, T. A., P. R. Bérubé, and R. C. Andrews. 2023a. "Impact of extended versus typical rapid mixing HRTs on continuous-flow coagulation-ultrafiltration." *Separation and Purification Technology*, 319: 124041. https://doi.org/10.1016/j.seppur.2023.124041.

Malkoske, T. A., P. R. Bérubé, and R. C. Andrews. 2023b. "Leveraging coagulation mechanisms to reduce fouling and increase natural organic matter removal during coagulation/flocculation-ultrafiltration treatment." *Separation and Purification Technology*, 327: 124877. https://doi.org/10.1016/j.seppur.2023.124877.

Mansour, M., S. Kasetti, D. Thévenin, K. D. P. Nigam, and K. Zähringer. 2022. "Numerical study of the separation of two immiscible liquids in helical and straight pipes." *Chemical Engineering and Processing - Process Intensification*, 180: 108654. https://doi.org/10.1016/j.cep.2021.108654.

Mansour, M., P. Khot, D. Thévenin, K. D. P. Nigam, and K. Zähringer. 2020. "Optimal Reynolds number for liquid-liquid mixing in helical pipes." *Chemical Engineering Science*, 214: 114522. https://doi.org/10.1016/j.ces.2018.09.046.

Maraschin, M., K. F. S. H. Ferrari, A. P. H. da Silva, and E. Carissimi. 2020. "Aluminum sludge thickening: Novel helical pipes for aggregation by dual flocculation and thickening by filtration applied to water treatment plants." *Separation and Purification Technology*, 241: 116560. https://doi.org/10.1016/j.seppur.2020.116560.

Meakin, P. 1987. "Fractal aggregates." *Advances in Colloid and Interface Science*, 28: 249–331. https://doi.org/10.1016/0001-8686(87)80016-7.

Meyn, T., J. Altmann, and T. Leiknes. 2012. "In-line coagulation prior to ceramic microfiltration for surface water treatment—minimisation of flocculation pre-treatment." *Desalination and Water Treatment*, 14.

Mishra, P., and S. N. Gupta. 1979. "Momentum transfer in curved pipes. 1. Newtonian fluids." *Industrial & Engineering Chemistry Process Design and Development*, 18 (1): 130–137. https://doi.org/10.1021/i260069a017.

Naim, R., R. Epsztein, A. Felder, M. Heyer, M. Heijnen, and V. Gitis. 2014. "Rethinking the role of in-line coagulation in tertiary membrane filtration of municipal effluents." *Separation and Purification Technology*, 125: 11–20. Elsevier B.V. https://doi.org/10.1016/j.seppur.2014.01.036.

Nan, J., M. Yao, Q. Li, D. Zhan, T. Chen, Z. Wang, and H. Li. 2016. "The role of shear conditions on floc characteristics and membrane fouling in coagulation/ultrafiltration hybrid process – the effect of flocculation duration and slow shear force." *RSC Advances*, 6 (1): 163–173. https://doi.org/10.1039/C5RA18328F.

Neama, M.-A. A. M., W. A. Elbarki, M. Fayed, and S. Aly. 2024. "Upgrading the eastern wastewater treatment plant effluent quality in Egypt for reuse by means of in-line coagulation followed by ultrafiltration." *Water Practice & Technology*, 19 (12): 4754–4772. London, UK: IWA Publishing. https://doi.org/10.2166/wpt.2024.285.

Nguyen, A. H., J. E. Tobiason, and K. J. Howe. 2011. "Fouling indices for low pressure hollow fiber membrane performance assessment." *Water Research*, 45 (8): 2627–2637. Elsevier Ltd. https://doi.org/10.1016/j.watres.2011.02.020.

Paar, H., J. Benecke, M. Ernst, and M. Jekel. 2011. "Pre-coagulation and ultrafiltration of effluent impaired surface water for phosphorus removal and fouling control." *Water Supply*, 11 (2): 211–218. https://doi.org/10.2166/ws.2011.037.

Park, P.-K., C.-H. Lee, and S. Lee. 2006. "Permeability of collapsed cakes formed by deposition of fractal aggregates upon membrane filtration." *Environmental Science & Technology*, 40 (8): 2699–2705. https://doi.org/10.1021/es0515304.

Pearce, G. K. 2011. *UF/MF Membrane Water Treatment: Principles and Design*. 387. 1st ed. Bangkok: Water Treatment Academy.

Rushton, J. H., and L. H. Mahony. 1954. "Fundamentals of mixing and agitation with applications to extractive metallurgy." *Journal of Metals*, 6 (11): 1199–1206. https://doi.org/10.1007/BF03398358.

Sartori, M., D. S. Oliveira, E. C. Teixeira, W. B. Rauen, and N. C. Reis. 2015. "CFD modelling of helically coiled tube flocculators for velocity gradient assessment." *Journal of the Brazilian Society of Mechanical Sciences and Engineering*, 37 (1): 187–198. https://doi.org/10.1007/s40430-014-0141-3.

Schulz, M., A. Soltani, X. Zheng, and M. Ernst. 2016. "Effect of inorganic colloidal water constituents on combined low-pressure membrane fouling with natural organic matter (NOM)." *Journal of Membrane Science*, 507: 154–164. Elsevier. https://doi.org/10.1016/j.memsci.2016.02.008.

Selomulya, C. 2002. "The Effect of Shear on Flocculation and Floc Size/Structure." UNSW Sydney. https://doi.org/10.26190/UNSWORKS/20227.

Selomulya, C., R. Amal, G. Bushell, and T. D. Waite. 2001. "Evidence of shear rate dependence on restructuring and breakup of latex aggregates." *Journal of Colloid and Interface Science*, 236 (1): 67–77. https://doi.org/10.1006/jcis.2000.7372.

Serra, T., J. Colomer, and B. E. Logan. 2008. "Efficiency of different shear devices on flocculation." *Water Research*, 42 (4–5): 1113–1121. https://doi.org/10.1016/j.watres.2007.08.027.

Spicer, P. T., W. Keller, and S. E. Pratsinis. 1996. "The effect of impeller type on floc size and structure during shear-induced flocculation." *Journal of Colloid and Interface Science*, 184 (1): 112–122. https://doi.org/10.1006/jcis.1996.0601.

Spicer, P. T., and S. E. Pratsinis. 1996. "Shear-induced flocculation: The evolution of floc structure and the shape of the size distribution at steady state." *Water Research*, 30 (5).

Tang, C. K., N. M. Peleato, P. R. Bérubé, and R. C. Andrews. 2019. "Impact of low coagulant dosages on protein fouling of ultrafiltration membranes." *Journal of Water Process Engineering*, 31: 100801. https://doi.org/10.1016/j.jwpe.2019.100801.

Tse, I. C., K. Swetland, M. L. Weber-Shirk, and L. W. Lion. 2011. "Method for quantitative analysis of flocculation performance." *Water Research*, 45 (10): 3075–3084. https://doi.org/10.1016/j.watres.2011.03.021.

Vahedi, A., and B. Gorczyca. 2012. "Predicting the settling velocity of flocs formed in water treatment using multiple fractal dimensions." *Water Research*, 46 (13): 4188–4194. https://doi.org/10.1016/j.watres.2012.04.031.

Walsh, M. E., N. Zhao, S. L. Gora, and G. A. Gagnon. 2009. "Effect of coagulation and flocculation conditions on water quality in an immersed ultrafiltration process."

Environmental Technology, 30 (9): 927–938. https://doi.org/10.1080/09593330902971287.

Wang, J., J. Guan, S. R. Santiwong, and T. D. Waite. 2010. "Effect of aggregate characteristics under different coagulation mechanisms on microfiltration membrane fouling." *Desalination*, 258 (1–3): 19–27. https://doi.org/10.1016/j.desal.2010.03.056.

Wang, J., and X. C. Wang. 2006. "Ultrafiltration with in-line coagulation for the removal of natural humic acid and membrane fouling mechanism." *Journal of Environmental Sciences (China)*, 18 (5): 880–884. https://doi.org/10.1016/S1001-0742(06)60008-9.

Yamamoto, K., A. Aribowo, Y. Hayamizu, T. Hirose, and K. Kawahara. 2002. "Visualization of the flow in a helical pipe." *Fluid Dynamics Research*, 30 (4): 251–267. https://doi.org/10.1016/S0169-5983(02)00043-6.

Yamamura, H., Q. Ding, and Y. Watanabe. 2019. "Solid-phase fluorescence excitation emission matrix for in-situ monitoring of membrane fouling during microfiltration using a polyvinylidene fluoride hollow fiber membrane." *Water Research*, 164: 114928. https://doi.org/10.1016/j.watres.2019.114928.

Yu, H., W. Huang, H. Liu, T. Li, N. Chi, H. Chu, and B. Dong. 2021. "Application of coagulation–membrane rotation to improve ultrafiltration performance in drinking water treatment." *Membranes*, 11 (8): 643. https://doi.org/10.3390/membranes11080643.

CHAPTER 7

Phased-Inline-Coagulation Pretreatment for Low-Pressure Membrane Fouling Reduction

Context: To investigate C-IN-P pretreatment, a bench-scale system capable of implementing continuous-flow inline coagulation was required. Although systems of this type have been developed in previous studies limitations related to cost, hydraulic retention time, and water volume requirements motivated the development of an improved system, as described and evaluated in Chapter 5 and Chapter 6.

Phased inline coagulation (C-IN-P) is a novel operating strategy in which coagulant is added only during the initial portion of a filtration cycle rather than continuously throughout its entire length. Despite its potential advantages, C-IN-P as a pretreatment strategy for low-pressure membrane systems has received limited attention, and previous studies have examined only a narrow range of operating conditions. Accordingly, this study systematically investigates the influence of water type, coagulant type, length of coagulant addition, and dosing strategy (i.e., the combination of coagulant dose and dosing time) to elucidate the impact of these key process parameters on C-IN-P performance. Advanced organic characterization techniques are also employed to track the removal of individual model organic foulants to identify the organic fractions most critical to C-IN-P effectiveness.

A version of this work is currently being prepared for submission to the Separation and Purification Technology as:

Ladouceur, J.D., Narbaitz, R.M., Lan, C.Q. (2026). Phased-inline-coagulation pretreatment for low-pressure membrane fouling reduction.

The supporting information for this chapter is presented in Appendix H.

List of Abbreviations

ACH	Aluminum chlorohydrate
ANOVA	Analysis of variance
BSA	Bovine serum albumin
BSA^*	FEEM-derived DOC concentration of bovine serum albumin
BWE	Hydraulic backwash efficiency
CI	Confidence interval
C-IDX	Coating index
C-IN	Inline coagulation
C-IN-P	Phased-inline coagulation
C-IN-S	Stepped-inline coagulation
COD	Chemical oxygen demand
DOC	Dissolved organic carbon
FEEM	Fluorescence excitation-emission matrices
FR_{hr}	Hydraulically reversible fouling rate
FR_{hirr}	Hydraulically irreversible fouling rate
HA	Humic acid
HA^*	FEEM-derived DOC concentration of humic acid
H-SUVA	High SUVA synthetic water
L-SUVA	Low SUVA synthetic water
LPM	Low-pressure membrane
M-SUVA	Medium hydrophobicity synthetic water
NOM	Natural organic matter
PARAFAC	Parallel factor analysis
PWP	Pure water permeability
SA	Sodium alginate
SA^*	FEEM-derived DOC concentration of sodium alginate
SUVA	Specific ultraviolet absorbance at 254nm
TMC	Tubular multichannel
WQI	Water quality indicators
ZP	Zeta potential

List of Variables

Variable	Description
a, b, c	Adjustable model fitting parameters
a_{ir}	Sample score for the rth component and ith sample in FEEM model
b_{jr}	Mode for the jth emission wavelength and rth component in FEEM model
c_{kr}	Mode for the kth excitation wavelength and rth component in FEEM model
e_{ijk}	Residual term of unexplained variation for FEEM model
FR_{hirr}	Hydraulically irreversible fouling rate (mBar h^{-1})
FR_{hr}	Hydraulically reversible fouling rate (mBar h^{-1})
P_d	Coagulant dosing time as a percent of the cycle length (%)
$t_{n-1,f}$	Filtration time at the end of cycle *n-1*
$t_{n-1,i}$	Filtration time at the start of cycle *n-1*
$TMP_{n-1,f}$	TMP at the end of cycle *n-1* (mBar)
$TMP_{n,i}$	TMP at the beginning of cycle *n* (mBar)
$TMP_{n-1,i}$	TMP at the beginning of cycle *n-1* (mBar)
x_{ijk}	Fluorescence intensity of the i^{th} sample at the k^{th} excitation and j^{th} emission wavelength

7.1. Abstract

Phased-inline-coagulation (C-IN-P), where coagulant is added only during the initial portion of the filtration cycle, represents a promising alternative to continuous inline-coagulation (C-IN) for reducing treatment costs and improving sustainability in low-pressure membrane (LPM) systems. However, its performance across a broad range of operational conditions remains poorly understood. Accordingly, this study evaluated the performance of C-IN-P across three model waters and varying membrane coating indices (C-IDXs), defined as the surface-area normalized mass of coagulant delivered to the membrane. For all waters, LPM fouling decreased exponentially with increasing C-IDX. For the intermediate- and high-hydrophobicity waters, bulk organics removals plateaued near C-IDXs of 75 mg m^{-2}, corresponding to chemical addition for half the filtration cycle, whereas treatment of the low-hydrophobicity water resulted in reduced organics removals and greater fouling potential. Fluorescence analysis suggests that fouling behaviour was

strongly associated with humic acid and sodium alginate removal, with a critical removal threshold of 60-70% occurring near a C-IDX of 75 mg m^{-2}. Finally, experiments employing different combinations of coagulant dose-dosing time for a fixed C-IDX revealed that identical C-IDXs did not necessarily produce equivalent fouling behaviour, despite similar organics removals. Membrane performance was significantly impacted by both coagulant type and dosing strategy, indicating that fouling depends not only on the C-IDX magnitude but also on the temporal mode of coagulant addition. Overall, the findings establish the C-IDX as a useful framework for C-IN-P optimization, however, the optimal C-IDX is not universal and depended on the raw water quality, coagulant type, and coagulant dosing strategy.

7.2. Introduction

Coagulation pretreatment has been shown by many studies to be effective at mitigating low-pressure membrane (LPM) fouling (Kamińska et al. 2020) due to its ability to remove a wide range of natural organic matter (NOM) fractions (Kimura and Kume 2020), the consensus principle foulant of LPMs (Cui and Choo 2014; Howe and Clark 2002). While coagulation pretreatment can be implemented with particle separation by sedimentation (Ma et al. 2020a; Moon et al. 2009) or flotation (Kang et al. 2021;Chapter 3), continuous inline-coagulation (C-IN) has become a popular alternative due to its reduced process complexity and smaller footprint (Kamińska et al. 2020; Tao et al. 2024; Yoo 2018). In this approach, coagulant is applied continuously, inline, during the entire filtration cycle and floc agglomerates are delivered directly to the membrane without any particle separation, forming a cake layer on its surface. This cake layer, the effectiveness of which is governed by its thickness, porosity, roughness, and uniformity (Liu et al. 2024; Ma et al. 2020b), has been reported to lead to an improvement in LPM performance by acting as a protective layer, limiting the interactions between the membrane and primary foulants (Chen and Nan 2023; Kimura and Kume 2020). However, despite the reported success of C-IN at mitigating membrane fouling for a variety of water and membrane types (Lee and Kim 2015;Chapter 4), the continuous dosing of the hydrolysing metal salts commonly used as inorganic coagulants can generate large quantities of sludge, incurring significant disposal costs (Keeley et al. 2016). Moreover, discounting membrane replacement costs, the cost of membrane pretreatment represents an important component of LPM operating expenditures (OPEX) and, depending on the size of the plant, can reach as high as 50% of the total OPEX (Campinas et al. 2021; Schweiger et al. 2018a).

Accordingly, there is a need to improve process sustainability and economy by mitigating irreversible membrane fouling (a key driver of long-term LPM OPEX) while simultaneously minimizing coagulant usage to reduce LPM pretreatment and sludge disposal costs.

Phased-inline-coagulation (C-IN-P), a novel variation of C-IN where the coagulant is added only for the initial portion of the filtration cycle, represents a promising operational approach for achieving these goals (Buchta et al. 2019). Compared to C-IN, several studies have demonstrated that coagulant usage could be reduced by at least half without any appreciable increase in the degree of total or irreversible membrane fouling. For identical membrane type, water type, and coagulant dosing rate, Lok et al. (2017) found that C-IN-P with coagulant addition for either the first 8.3% or 50% of the filtration cycle resulted in a hydraulically irreversible fouling resistance that stabilized at the same level as for pretreatment by C-IN. Similarly, Pronk et al. (2016) reported that for C-IN-P pretreatment with ferric chloride addition during the first 50% of the filtration cycle, the total fouling resistance stabilized at a similar magnitude as for C-IN.

To control the operation of C-IN-P, Schweiger et al. (2018b) introduced the membrane coating index (C-IDX), defined as the surface area normalized mass of coagulant delivered to the membrane (i.e., product of the membrane flux, coagulant dose, and dosing time). Based on studies using treated secondary effluents (SEs) with chemical oxygen demands (CODs) of 20-30 mg L^{-1}, an optimal C-IDX range of 20-25 mg m^{-2} was proposed to minimize LPM fouling while reducing operating costs (Buchta et al. 2019; Schweiger et al. 2018a; b). In fact, Buchta et al. (2017) demonstrated that the baseline permeability with C-IN-P pretreatment at a C-IDX of 23 mg m^{-2} (representing coagulant addition for only 10% of the filtration cycle) decreased by only ~5.9% compared to C-IN, while achieving OPEX savings of 83.5%. Despite these promising results, several limitations constrain the broader application of the C-IDX for C-IN-P operational control. Almost all studies to date have employed a single membrane type (modified polyethersulfone tubular multichannel (TMC) fibers) and a single coagulant type (polyaluminum chloride). In addition, the C-IDX was developed exclusively using treated SEs, waters known to possess elevated concentrations of soluble microbial products and biopolymers (Kim and Dempsey 2013), while studies involving natural waters have similarly been restricted to those with a hydrophilic character (Lok et al. 2017; Park et al. 2002), as defined by the specific ultraviolet absorbance (SUVA) at 254 nm. Consequently, the suitability of the C-IDX for C-IN-P operational control and its proposed optimal range require further validation across a broader range of conditions including

waters with a greater hydrophobicity and for alternative coagulant types. Furthermore, for a constant-flux facility (as is typical in municipal potable water production), the C-IDX is dependent on the product of the coagulant dose and dosing time meaning that different combinations of these two parameters can yield identical C-IDX values. It remains unclear, however, whether the effectiveness of C-IN-P pretreatment is solely dependent on the total coagulant mass delivered to the membrane surface or whether it also depends on the specific combination of coagulant dose and dosing time.

Besides fouling mitigation, the removal of NOM is also an important consideration in the design of integrated treatment systems. For aluminum-based coagulation, optimal NOM removal has been linked to a pseudo-stoichiometric relationship between the applied metal dose and dissolved organic carbon (DOC) concentration (Edzwald and Van Benschoten 1990), suggesting that the removal of bulk organics under C-IN-P may be lower than for C-IN. This was observed by Buchta et al. (2019) who, for a SE with a COD of 50 mg L^{-1}, reported ~10% lower removal of COD with pretreatment by C-IN-P compared to C-IN. However, for a lower strength SE (COD=17.6 mg L^{-1}), this same study found that C-IN-P and C-IN achieved comparable reduction (~41%) in COD, despite C-IN-P using only 10% of the coagulant mass. Similarly, Lok et al. (2017) reported comparable or slightly improved removals of organics for a moderate-DOC (3.9 mg-C L^{-1}), hydrophilic (SUVA < 1 L mg^{-1} m^{-1}) river water, even when coagulant dosing was limited to 8.3% of the filtration cycle. The range of outcomes reported by previous studies seem to suggest that the performance of C-IN-P is dependent on the specific composition of the organics in the feedwater: additional research is merited to elucidate which components of the organic matrix govern the performance of this strategy. Furthermore, as pointed out in our recent review article (see Appendix C), existing studies have been limited to waters dominated by hydrophilic organics, and the organics removals obtained by C-IN-P for waters with greater hydrophobicity remains unclear. Given the role of hydrophobic NOM as a precursor to carcinogenic disinfection byproducts (Hua and Reckhow 2007), further investigation is needed to assess the suitability of C-IN-P for application across a broader range of water types.

Owing to the relative novelty of the C-IN-P approach, there remains a number of important gaps in our understanding of the effects of different feed water qualities and operating conditions (i.e., C-IDX) on fouling mitigation and product water quality. Based on this, the objectives of the study were to: (a) examine the generalizability of the C-IDX as an operational tool for C-IN-P

pretreatment using different feed waters; (b) elucidate for which conditions the removals of organics by C-IN-P and C-IN are comparable; and (c) evaluate the sensitivity of the C-IDX to different combinations of coagulant dose/dosing time and coagulant type. This study represents the first attempt to systematically evaluate the performance of C-IN-P across a range of controlled operating conditions.

7.3. Materials and Methods

7.3.1. Synthetic Water

To avoid potential inter- and intra-annual variations in natural water quality influencing the study results (Sillanpaa 2015), synthetic challenge waters composed of model organic foulants were used throughout this study. Humic acid (HA) (Humic Acid Sodium Salt, H16752, Sigma-Aldrich, St. Louis, MO), bovine serum albumin (BSA) (Bovine Serum Albumin, A7906, Sigma-Aldrich, St. Louis, MO), and sodium alginate (SA) (Alginic Acid Sodium Salt, 180947, Sigma-Aldrich, St. Louis, MO) were selected to represent humic substances, proteins, and polysaccharides, respectively, classes of organics that are typical of the NOM in surface waters used for potable water production (Mallya et al. 2023).

To investigate the suitability of C-IN-P for treating different water types, multi-component mixtures of model organics were prepared by combining HA with BSA and SA in varying concentrations to be representative of waters with high (SUVA> 4 L mg^{-1} m^{-1}), medium (SUVA=2-4 L mg^{-1} m^{-1}), and low (SUVA< 2 L mg^{-1} m^{-1}) hydrophobicity, according to the ranges proposed by Edzwald and Tobiason (1999). These water types will be identified by the acronyms H-SUVA, M-SUVA, and L-SUVA, respectively, throughout this chapter. To prevent the organic loading from impacting the study results, all three challenge waters were designed to have a DOC content of approximately 5 mg-C L^{-1}, which is within the range of typical concentrations for natural water sources (Crittenden et al. 2012) and closely approximated the average DOC value from a literature survey of natural waters used in global research studies (see Appendix H, Section H.1.1). The concentrations of each model organic that were required for the three water types are summarized in Table 7.1 and were determined during preliminary work (see Appendix H, Section H.1.3).

Table 7.1. Composition of Organic Matrix in Three Synthetic Waters

	Water Type		
Component	**L-SUVA**	**M-SUVA**	**H-SUVA**
HA (mg L^{-1})	2	5	10
BSA (mg L^{-1})	4	4	2
SA (mg L^{-1})	7	4	2

All three synthetic waters were prepared in a background of distilled water which has been passed through a five-stage commercial reverse osmosis-activated carbon system (TGI-525 NO. 92821, TGI Pure Water Systems, Brea, California), abbreviated at DW-RO water. To better simulate the more complex nature of natural waters, 5 mg L^{-1} kaolin clay (Laboratory Grade 75185, Fisher Scientific, Hampton, NH, USA), 0.6 mM calcium chloride (Dried Powder 97%, Thermo Scientific, Hampton, NH, USA), and 0.9 mM sodium bicarbonate (Certified ACS, Fisher Scientific, Hampton, NH, USA) were added to provide turbidity, hardness, and alkalinity, respectively. The pH of the feed waters was adjusted to a value of 7.5 prior to any testing. Like for the DOC content, the concentrations for the inorganic background components were selected based on the results of a literature survey of natural waters (Section H.1.1) and closely matched those of Alresheedi et al. (2019). Additional details regarding the preparation of the stock model organic solutions as well as the three synthetic challenge waters are provided in Section H.1.2.

A summary of the primary water quality indicators (WQI) for the three water types is provided in Table 7.2 while details regarding their measurement are given in Section 7.3.3.2. It should be acknowledged that the measured DOC for the three water types was slightly lower (10.57% – 13.30%) than the design values calculated based on the standard curves generated for each organic compound (Fig. H.2). This may suggest that by combining the three organic compounds and background matrix, the combined sample presented greater difficulty in oxidation for the UV-persulfate DOC analyzer used in the present study compared to when the compounds were analyzed individually. This hypothesis should be the subject of future research work where the additivity of the individual components in the synthetic water is evaluated, and the carbon recovery for each compound is compared using different analytical approaches. In the present study, the DOC was measured for the raw (untreated) and permeate waters, meaning that the removal values could be uniquely determined for each test.

Table 7.2. Summary of Primary WQIs for Synthetic Challenge Waters

Water Type	DOC (mg-C L^{-1})	SUVA (L mg^{-1} m^{-1})	True Color (Pt. Co.)	Turbidity (NTU)	Alkalinity (mg-$CaCO_3$ L^{-1})	Hardness (mg-$CaCO_3$ L^{-1})
L-SUVA	4.47±0.07	0.91±0.02	22.63±0.37	5.52±0.05	50.25±1.24	60.58±1.17
M-SUVA	4.35±0.07	2.45±0.08	55.53±1.24	5.56±0.03	52.17±3.06	60.83±1.43
H-SUVA	4.46±0.03	4.83±0.06	115.23±0.71	5.62±0.03	52.92±3.19	61.17±1.54

Note. ± represents the 95% confidence interval calculated based on two-tailed Students *t*-Test, $\mu \pm t_{0.025,n}\frac{s}{\sqrt{n}}$

7.3.2. Filtration Experiments

7.3.2.1. Coagulation/Flocculation

Simulating continuous-flow inline coagulation at bench-scale remains a significant challenge due to the low flowrates that can be accommodated by the small-scale filtration systems commonly used in academic studies and industrial research and design. A unique feature of the present study is that continuous-flow coagulant addition was implemented using a syringe pump (Pump 22, Harvard Apparatus, Holliston, MA) in combination with an in-house constructed mini-inline rapid mixer and helical flocculator (coil pitch = 15 mm; coil diameter = 50 mm; pipe length = 2000 mm) (selected according to the results of Chapter 6). Alum (ALS, Kemira Water Solutions, Varennes, QC) was used throughout most of the study and was pumped by the syringe pump (during the filtration cycle only) to the inline rapid mixer, where it was introduced to the synthetic challenge water, at a rate equivalent to a dose of 3 mg-Al L^{-1}. Prior to coagulation, all three water types were pH-adjusted using pre-determined (via titration) volumes of 0.05 N H_2SO_4 (Honeywell, Charlotte, NC) to achieve a coagulated pH of 6. Based on preliminary jar testing (Appendix H, Section H.1.4.), the selected coagulant dose and pH represented the optimal coagulation chemistry for all three water types in terms of zeta potential (ZP) reduction and DOC elimination. The similarity of the optimal coagulation chemistries across water types, however, was somewhat unexpected. The effectiveness of this continuous-flow coagulation system for floc generation at low Reynolds conditions was verified in our previous study (i.e., Chapter 6). For the flow rate used in the current study (~ 5.6 mL min^{-1}), the hydraulic retention times (HRT) for the rapid mixer and helical flocculator were found to be approximately 3.66 min and 3.11 min, respectively, as determined from preliminary tracer studies (Appendix H, Section H.1.5).

7.3.2.2. Continuous-Flow Bench-Scale System and Test Protocol

Mini membrane modules were fabricated in-house according to previously validated procedures (see Chapter 4) using a single TMC membrane fiber with seven concentrically arranged 0.9 mm diameter capillaries and a length of 0.17 m, yielding an effective filtration area of approximately 0.0033 m^2. The membranes (Multibore 0.9, Dupont, Wilmington, DE) were made from a proprietary modified polyethersulfone blend and had a nominal pore size of 20 nm.

Day-long filtration tests were performed using the automated bench-scale filtration system shown in Fig. 7.1 which was controlled using a LabView program (National Instruments, Austin, TX, USA) that permitted cyclical operation between permeation and backwash cycles as well as automated data acquisition (USB-6361, National Instruments, Austin, TX, USA). Prior to use, the membranes were conditioned by filtering deionised water (DI) (Quatra 90LC, Zenon Environmental, Burlington, ON, CA) for a period of 2 hours followed by repeated 10 min-long filtration and backwash cycles at elevated fluxes of 200 L m^{-2} h^{-1} and 400 L m^{-2} h^{-1}, respectively. Once all air had been purged from the membrane module and the permeability had stabilized within the manufacturer specified range (700 – 1000 L m^{-2} h^{-1} bar^{-1}) (Inge GmbH 2020), the pure water permeability (PWP) of the module was determined by filtering DI for a period of 1 h.

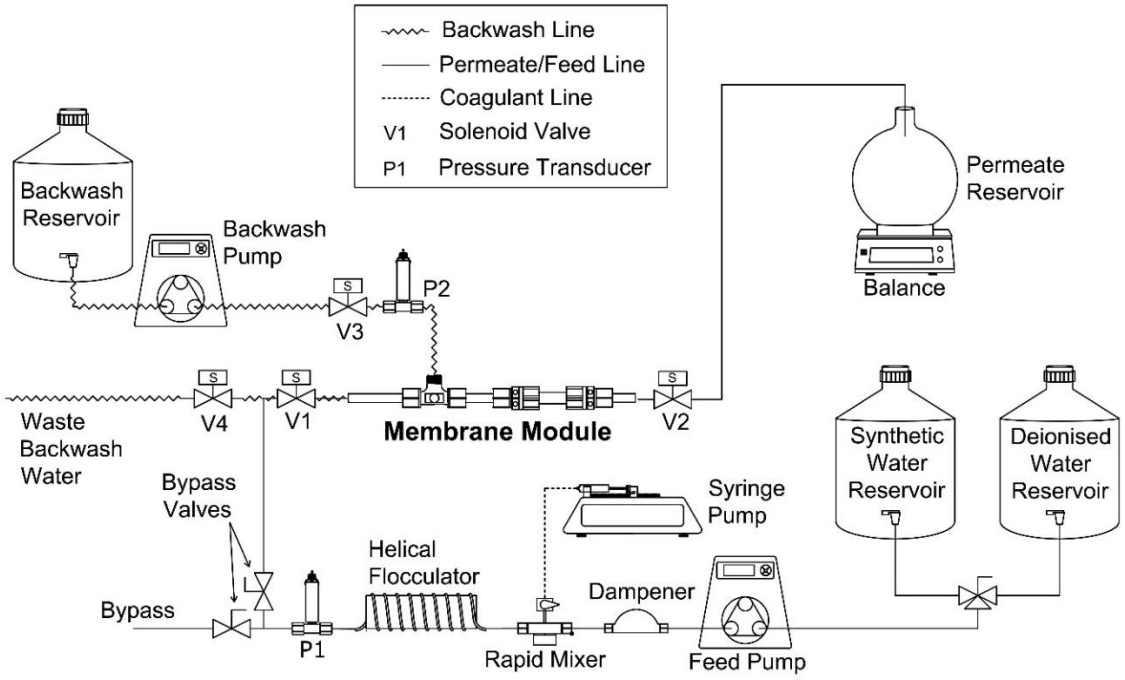


Fig. 7.1. Schematic of bench-scale continuous-flow filtration system.

Following the PWP test, but prior to the commencement of the filtration test, the feed source was switched from DI to the synthetic water reservoir and the syringe pump was activated at the user-defined delivery rate. To achieve steady state floc formation, as recommended by Malkoske et al. (2023), the system was allowed to run for a period of 120 min prior to the start of the filtration test. During this stabilization period, the bypass valves located downstream of the helical flocculator were set to route the coagulated/flocculated feedwater to the permeate reservoir, without passing through the membrane module. This permitted constant-flux operation, which is dependent on the continuous feedback loop between the permeate balance and LabView software, while also preventing continuous floc deposition on the membrane. Following the stabilization period, the bypass valves were returned to their original position, which directed the coagulated/flocculated water to the membrane module, and the filtration test was begun.

Each experiment was conducted in replicate and involved continuous cyclical operation with 30 min long filtration cycles and 2 min long hydraulic backwash cycles. The filtration flux was set to 100 L m^{-2} h^{-1}. This value was selected based on the results of preliminary critical flux testing (see Appendix H, Section H.1.6) conducted using the flux-stepping approach proposed by Le Clech et al. (2003). Moreover, the permeate flux was increased relative to Chapter 6 with the goal of achieving greater irreversible fouling. Based on the manufacturer's recommendations, hydraulic backwashing was performed at a flux of 300 L m^{-2} h^{-1} using DW-RO water due to the small amount of permeate generated by the bench-scale system and the volume requirements for water quality analyses of the permeate water.

7.3.2.3. C-IN-P Pretreatment

The performance of C-IN-P across varying C-IDX values was studied for the three water types using alum and a fixed dosing rate equivalent to 3 mg-Al L^{-1} (as noted in Section 7.3.2.1). To change the C-IDX value, the length of time that the coagulant was added to the feed was varied. For the L-SUVA and M-SUVA waters, the coagulant was dosed for 20, 50, 75, and 100% (i.e., C-IN) of the filtration cycle length, corresponding to C-IDXs of 30, 75, 112.5, and 150 mg m^{-2}, respectively. For the high SUVA water, an additional set of replicate tests was conducted with coagulant dosing for 33% of the cycle, corresponding to a C-IDX of 50 mg m^{-2}.

7.3.2.4. Evaluation of C-IDX for C-IN-P Operational Control

Using only the H-SUVA water and a fixed C-IDX value of 75 mg m^{-2}, additional tests were conducted in replicate to evaluate the sensitivity of the C-IDX to different combinations of coagulant dose/dosing time and coagulant types. This combination of C-IDX and feed water type were selected because of their low FR_{hr} (discussed in Section 7.4.1.1), which was expected to facilitate discrimination of potential performance differences arising from alternative coagulant dosing strategies. The length of coagulant addition was varied from the baseline condition of 50% of the cycle length (denoted as Alum-3.0) to either 3.3% (corresponding to 1 min) or 100% (corresponding to 30 min), representing opposite extremes of the dosing time parameter. To maintain a constant C-IDX value, the coagulant dose was adjusted accordingly to 45 mg-Al L^{-1} (denoted as Alum-45) and 1.5 mg L^{-1} (denoted Alum-1.5) for the 1 min and 30 min conditions, respectively.

The impact of coagulant type was assessed by comparing alum with aluminum chlorohydrate (ACH) (PAX-XL 1900, Kemira, Varennes, QC), which was selected based on its demonstrated treatment efficiency (Section H.1.4), favorable sludge characteristics (Bratby 2016) and broad effective pH range (Omar and Aziz 2021). Comparisons were conducted for both the baseline dosing condition of 3 mg-Al L^{-1}, applied over 50% of the filtration cycle (denoted ACH-3.0 for ACH coagulant), as well as for the addition of 45 mg-Al L^{-1} applied during only the first minute of the cycle (denoted as ACH-45 for ACH coagulant). Membrane filtration system operation was the same as described in Section 7.3.2.2.

7.3.3. Analytical Methods

7.3.3.1. Fouling Assessment

Hydraulically reversible and irreversible fouling rates were computed following the approach of Aly et al. (2021):

$$FR_{hr} = \frac{TMP_{n-1,f} - TMP_{n,i}}{t_{n-1,f} - t_{n-1,i}} \tag{7.1}$$

$$FR_{hirr} = \frac{TMP_{n,i} - TMP_{n-1,i}}{t_{n-1,f} - t_{n-1,i}} \tag{7.2}$$

where FR_{hr} is the hydraulically reversible fouling rate (mBar h^{-1}), FR_{hirr} is the hydraulically irreversible fouling rate (mBar h^{-1}), $TMP_{n,i}$ is the measured transmembrane pressure (TMP) at the beginning of cycle *n* (mBar), $TMP_{n-1,f}$ is the measured TMP at the end of cycle n–1 (mBar), $TMP_{n-1,i}$ is the measured TMP at the beginning of cycle n–1 (mBar), and $t_{n-1,f}$ and $t_{n-1,i}$ are the end of cycle filtration time and the beginning of cycle filtration time, respectively. The total fouling rate (FR_{TOT}) is considered to be the sum of the hydraulically reversible and irreversible fouling rates.

7.3.3.2. Water Quality Assessment

Feed water and permeate were assessed for DOC, true and apparent color, ultraviolet absorbance at 254 nm (UV_{254}), as well as turbidity. All measurements were performed in triplicate. Prior to analysis, samples for DOC, true color, and UV_{254} were filtered using 0.45 µm membrane filter discs (GN-6 Metricel, Cytiva, Marlborough, MA). DOC was measured using a UV-persulfate analyzer (Phoenix 8000, Tekmar-Dohrmann, Cincinnati, OH) in accordance with Standard Methods 5310C (American Public Health Association et al. 2012) (additional information is provided in Section H.1.7). UV_{254} measurements were obtained using a UV-VIS spectrophotometer (DR6000, Hach, Loveland, CO) and a 50 mm pathlength quartz cell. True and apparent color were measured using the UV-VIS spectrophotometer and Hach method 8025 (Hach Company 2014), while turbidity was measured using a bench-top turbidimeter (2100AN, Hach, Loveland, CO) according to standard method 2130B (American Public Health Association et al. 2012). To facilitate comparison with available literature, the COD of the synthetic waters was also measured using Hach reactor digestion method (Method 8000) and ultra-low range digestion vials (2415815, Hach, Loveland, CO).

Fluorescence analysis was used to generated 3-D fluorescence excitation-emission matrices (FEEM) for feed and permeate waters. FEEM analysis was conducted using a fluorescence spectrometer (Aqualog, HORIBA Instruments Inc., Piscataway, NJ) which simultaneously measures the UV absorbance and fluorescence of a sample. Details concerning the collection of FEEM data and its processing are provided in Section H.2.4. Parallel factor analysis (PARAFAC) was used to develop a mathematic model capable of deconvoluting the FEEM data into its various components (Stedmon and Bro 2008). The analysis considered the model presented

in Eqn. 7.3 (Smilde et al. 2004) and was performed using SOLO software (Eigenvector Research Inc., Mason, WA, USA).

$$x_{ijk} = \sum_{r=1}^{R} a_{ir} b_{jr} c_{kr} + e_{ijk} \quad (7.3)$$

Where x_{ijk} is the fluorescence intensity of the i^{th} sample at the k^{th} excitation and j^{th} emission wavelength, r is the component number, R is the number of components used in the PARAFAC model, e_{ijk} is the residual term containing the unexplained variation, a, b, c are three modes of the model related to the sample score, the emission wavelength, and the excitation wavelength, respectively; i, j, k are the individual sample number, the specific emission wavelength, and the specific excitation wavelength, respectively (Wells et al. 2022). Core consistency and split-half validation was used to assess the adequacy of the model.

7.3.3.3. Statistical Treatment

Statistical treatment was performed using JMP® Student 19 (SAS Institute Inc., Cary, NC) and, unless otherwise indicated, all statistical tests were conducted at a significance level of α=0.05.

7.4. Results and Discussion

7.4.1. Evaluation of C-IN-P Performance

7.4.1.1. Fouling Mitigation

The hydraulically reversible (FR_{hr}) and irreversible (FR_{hirr}) fouling rates for each water type and pretreatment condition are shown in Fig. 7.2a and Fig. 7.2b, respectively. For each water type, baseline conditions corresponding to the direct filtration of raw water (i.e., C-IDX = 0) as well as C-IN, where the coagulant was applied for the entire filtration cycle (C-IDX = 150 mg m^{-2}), were established. C-IN-P pretreatment was investigated by varying the length of coagulant addition between 20% and 75% of the filtration cycle length, corresponding to C-IDXs of 30 to 112.5 mg m^{-2}, respectively. Throughout this chapter, the water type and length of coagulant addition (as a percentage of the filtration cycle) will be used to reference specific test conditions.

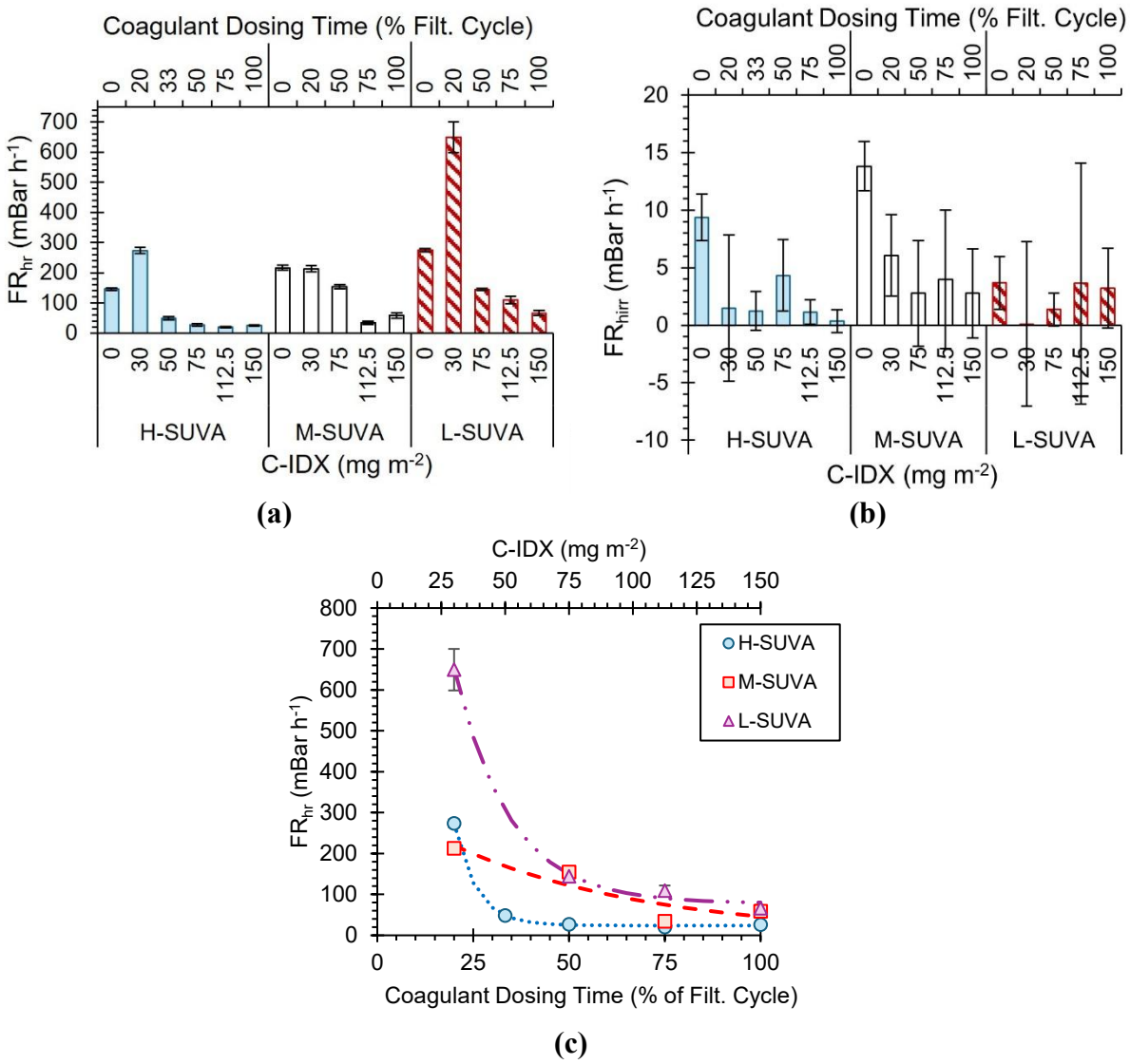


Fig. 7.2. C-IN-P for LPM pretreatment: **(a)** Impact of water type and C-IDX on FR_{hr}; **(b)** Impact of water type and C-IDX on FR_{hirr}; **(c)** Relationship between FR_{hr} and C-IDX or coagulant dosing time. Note: C-IDX=150 mg m^{-2} represents C-IN; error bars represent 95% confidence intervals calculated using a two-sided Student's *t*-test, $\mu \pm t_{0.025,n}\frac{s}{\sqrt{n}}$.

Considering first the FR_{hirr} (Fig. 7.2b), direct filtration (i.e., untreated water) led to low, but statistically significant levels of fouling for all water types. The FR_{hirr} was greatest for the M-SUVA water (13.81±2.13 mBar h^{-1}), whereas significantly lower values were observed for the H-SUVA (9.37±2.04 mBar h^{-1}) and L-SUVA (3.67±2.28 mBar h^{-1}) waters. Compared to direct filtration, coagulation pretreatment using either C-IN-P or C-IN reduced the mean FR_{hirr} values across all water types and C-IDXs. Moreover, the overlapping 95% confidence intervals (CIs) for

these two pretreatment strategies indicate that C-IN-P did not produce significantly greater hydraulically irreversible fouling development than for C-IN. This is in contrast to the study by Buchta et al. (2019) where, using the hydraulically irreversible permeability decline rate (L_{DR}) as a metric of irreversible fouling, it was reported that the L_{DR} for C-IN-P was 9.34 and 11.76 times greater than those for C-IN when coagulant dosages of 5 mg-Al L^{-1} and 2 mg-Al L^{-1} (respectively) were applied to SEs with COD values of 24 mg L^{-1} and 50 mg L^{-1}. Buchta et al. (2019) attributed this behaviour to the reduced coagulant mass delivered to the LPM surface during C-IN-P operation, which produced a thinner cake layer that enhanced foulant-membrane interactions and reduced hydraulic backwash efficiency (BWE). In the present study, however, no reduction in BWE was observed for C-IN-P compared to C-IN; indeed, the M-SUVA and L-SUVA waters were found to have BWEs that were equal to, or greater, than those for C-IN (Fig. H.8). The differing results between studies likely arise from differences in challenge water characteristics and treatment conditions. Specifically, the waters considered in the current study had a much lower organic content (COD ~17.03 mg L^{-1}) than the SEs examined by Buchta et al. (2019). Furthermore, as discussed later, the C-IDXs used in the present study were greater than those used by Buchta et al. (2019) and Schweiger et al. (2018a; b), which likely reduced FR_{hirr} due to the higher coagulant:organic ratio.

It must be acknowledged that, except for M-SUVA-20 and H-SUVA-50, the 95% CIs for FR_{hirr} encompassed zero across all water types and C-IDXs, indicating that the measured values were not statistically significant. Furthermore, substantial variability was observed in the FR_{hirr} measurements, with the 95% CIs reaching up to seven times the corresponding mean FR_{hirr} values (Table H.6). Moreover, except for the M-SUVA-75 condition, FR_{hirr} accounted for less than 10% of the total fouling resistance (i.e., $FR_{TOT}=FR_{hr}+FR_{hirr}$). Although the permeate flux in the present study was increased relative to our previous work (see Chapter 6) from 80 to 100 L m^{-2} h^{-1} in an effort to promote greater irreversible fouling development and facilitate more meaningful and significant comparisons among the coagulation pretreatment alternatives, FR_{hirr} remained low and statistically insignificantly for all conditions. Given the minimal contribution of FR_{hirr} to the overall fouling development under the tested conditions, together with its high variability and lack of statistical significance, the remaining comparisons between C-IN and C-IN-P in this chapter will focus on FR_{hr} as the primary indicator of fouling behavior.

The FR_{hr} data (Fig. 7.2a) provided insight into the effects of water type and C-IDX on the performance of C-IN-P. The FR_{hr} profiles for the replicated tests were seen to increase rapidly over the first ~ 4 h of operation, corresponding to 8 filtration cycles, after which FR_{hr} plateaued and remained at a pseudo-steady state for the remainder of the test duration (Appendix H, Fig. H.9). This is consistent with the findings of Lok et al. (2017) and Pronk et al. (2016), who noted that C-IN-P pretreatment resulted in a rapid initial increase in fouling, but stabilized after ~5-8 cycles of operation. As a result of this pattern, the mean FR_{hr} values in the current study were calculated using only data collected after 4 h of operation (i.e., 9^{th} to 45^{th} filtration cycles). Moreover, the data was screened for potential outliers using a boxplot approach with upper and lower fences specified by a distance of three interquartile ranges from the first and third quartiles. For the H-SUVA water and C-IDXs of 50 mg m^{-2} or higher, the FR_{hr} decreased substantially compared to direct filtration or C-IN-P at 30 mg m^{-2}. A Student's *t*-Test indicated that a C-IDX of 112.5 mg m^{-2} (addition for 75% of the cycle) resulted in significantly lower FR_{hr} than for C-IDXs of 150 mg m^{-2} or 75 mg m^{-2}, corresponding to coagulant addition for 100% and 50% of the cycle length, respectively. Notably, limiting coagulant addition to only half the filtration cycle did not increase FR_{hr} compared to continuous addition throughout the filtration cycle. This finding is consistent with the observations of Lok et al. (2017) and Pronk et al. (2016) who similarly reported that the fouling resistance for C-IN-P with addition for half the filtration cycle was not greater than for continuous addition. A similar trend was observed for the M-SUVA water where FR_{hr} was also minimized when coagulant was applied for only 75% of the cycle length. The lower FR_{hr} observed for M-SUVA-75 and H-SUVA-75 conditions compared to continuous coagulant dosing may suggest a de-coupling of the optimal coagulation chemistry based on organics reduction determined via jar testing (which is consistent with the chemistry applied for C-IN) and LPM fouling mitigation. Furthermore, the increased FR_{hr} observed at coagulant loadings greater than 112.5 mg m^{-2} suggests that the aluminum hydrolysis species may themselves become important LPM foulants at elevated loadings. This is in agreement with the findings of Ladouceur et al. (2024) (see Appendix C), where it was shown that for C-IN pretreatment, membrane fouling worsened with increasing coagulant dose beyond 0.1 mmol-Al L^{-1}. For the M-SUVA water, further reductions in dosing duration below 75% resulted in statistically significant increases in the mean FR_{hr}, with values increasing by a factor of 4.47 and 6.17 for M-SUVA-50 and M-SUVA-20, respectively, compared to M-SUVA-75. For C-IN, the L-SUVA water yielded the highest FR_{hr}

amongst the three water types and each successive reduction in dosing duration resulted in statistically significant increases in FR_{hr}.

Table H.7 presents the results of a pooled *t*-test on the difference in means between FR_{hr} for each water type at constant C-IDX conditions. Except for the M-SUVA vs. L-SUVA comparison at a C-IDX of 150 mg m^{-2}, the differences in mean FR_{hr} between water types were statistically significant, meaning water type exerts an important influence on C-IN-P performance. Fig. 7.2a shows that for the same C-IDX value, the H-SUVA water exhibited the lowest fouling potential whereas the L-SUVA water generally produced the highest FR_{hr}, suggesting that hydrophilic waters with elevated biopolymer concentrations posed the greatest challenge for this membrane type under C-IN-P operation. Previous studies using C-IN pretreatment have also noted that proteins and polysaccharides are a critical foulant of LPMs (Kimura et al. 2015; Kimura and Ando 2016; Yamamura et al. 2014). Katsoufidou et al. (2010) noted that SA accumulation on the membrane surface can form a hydrated gel layer of low permeability, but a high hydraulic reversibility, which is consistent with the findings of this study. Zhao et al. (2020) also noted that in mixtures with HA and coagulation pretreatment, SA can act as a natural flocculant, generating thick cakes which presented their own significant resistance to filtration.

Fig. 7.2c presents the developed models relating the coagulant dosing time (or equivalently C-IDX) to the FR_{hr} for each water type. For all three water types, the relationship between dosing time and FR_{hr} could be modeled using an exponential model of the form $FR_{hr} = ae^{P_d/b} + c$ where P_d is the coagulant dosing time as a percent of the cycle length (%) and a, b, and c are adjustable parameters that were determined using Excel's built-in Solver tool and minimization of the sum of squared errors criterion. A summary of the regressed model parameters as well as goodness-of-fit criteria is presented in Section H.2.2. The exponential decrease in LPM fouling with increasing C-IDX is consistent with the findings from several previous studies for C-IN-P (Naim et al. 2014; Appendix C), however, it must be acknowledged that in these studies the hydraulically reversible fouling was not quantified and the reported trends were based instead on alternative measures of hydraulically irreversible fouling.

Previous studies by Schweiger et al. (2018a; b) have reported that for this same TMC membrane type treating SEs with COD values ranging between 24 and 50 mg L^{-1} the optimal C-IDX value, in terms of fouling mitigation and OPEX reduction, was between 20-25 mg m^2. The results of the current study, however, suggest that the threshold C-IDX value is unique to each

water type and is greater than previously reported. For the H-SUVA water, a C-IDX value of 50 mg m^{-2} was required to prevent severe LPM fouling, while 75 mg m^{-2} could mitigate fouling as effectively as C-IN. For the M-SUVA and L-SUVA waters, a C-IDX of 112.5 mg m^{-2}, which was the highest C-IDX evaluated for C-IN-P in this study, was required for acceptable fouling reduction. Therefore, based on the results of this study, it is likely that the optimal C-IDX range is 75-112.5 mg m^{-2}, where comparable FR_{hr} values to C-IN are achieved, but coagulant savings of 25-50% are realized. It would be of interest for future studies to investigate the cake layer morphology, which is expected to govern the observed fouling behaviour, to ascertain whether the threshold C-IDX value for each water type is related to the coverage of the membrane fiber by the coagulant layer, the thickness of the coating layer, or whether structural changes in the cake layer itself are responsible for the exponential increase in FR_{hr} observed below the threshold C-IDX.

7.4.1.2. Organics Removal by C-IN-P

The removals of bulk measures of organics, namely, true color, DOC, and UV_{254} are presented in Fig. 7.3. For true color, the removal efficiency increased with increasing C-IDX up to 112.5 mg m^{-2} where, for all three water types, the 95% CIs were overlapping with C-IN. For the H-SUVA and M-SUVA waters, the removals of DOC and UV_{254} with pretreatment by C-IN-P at 112.5 mg m^{-2} were either statistically the same as C-IN or had 95% CIs which were nearly overlapping. For the L-SUVA water, however, C-IN-P could not achieve comparable removals of DOC and UV_{254} to C-IN regardless of the applied C-IDX. This is in contrast to the findings of the study by Lok et al. (2017) who found the addition of coagulant for only half the filtration cycle could achieve improved DOC reduction compared to C-IN for a lake water with a low DOC (~3.9 mg-C L^{-1}) and a low SUVA value (0.73 L mg^{-1} m^{-1}). The discrepancy in the removal trends between that study and the present one, despite the hydrophilic character of the organic matrix in both studies, is likely related to differences in the organic composition, specifically the nature of the biopolymers, whose molecular properties have been reported to significantly impact coagulation performance (Kimura and Ando 2016).

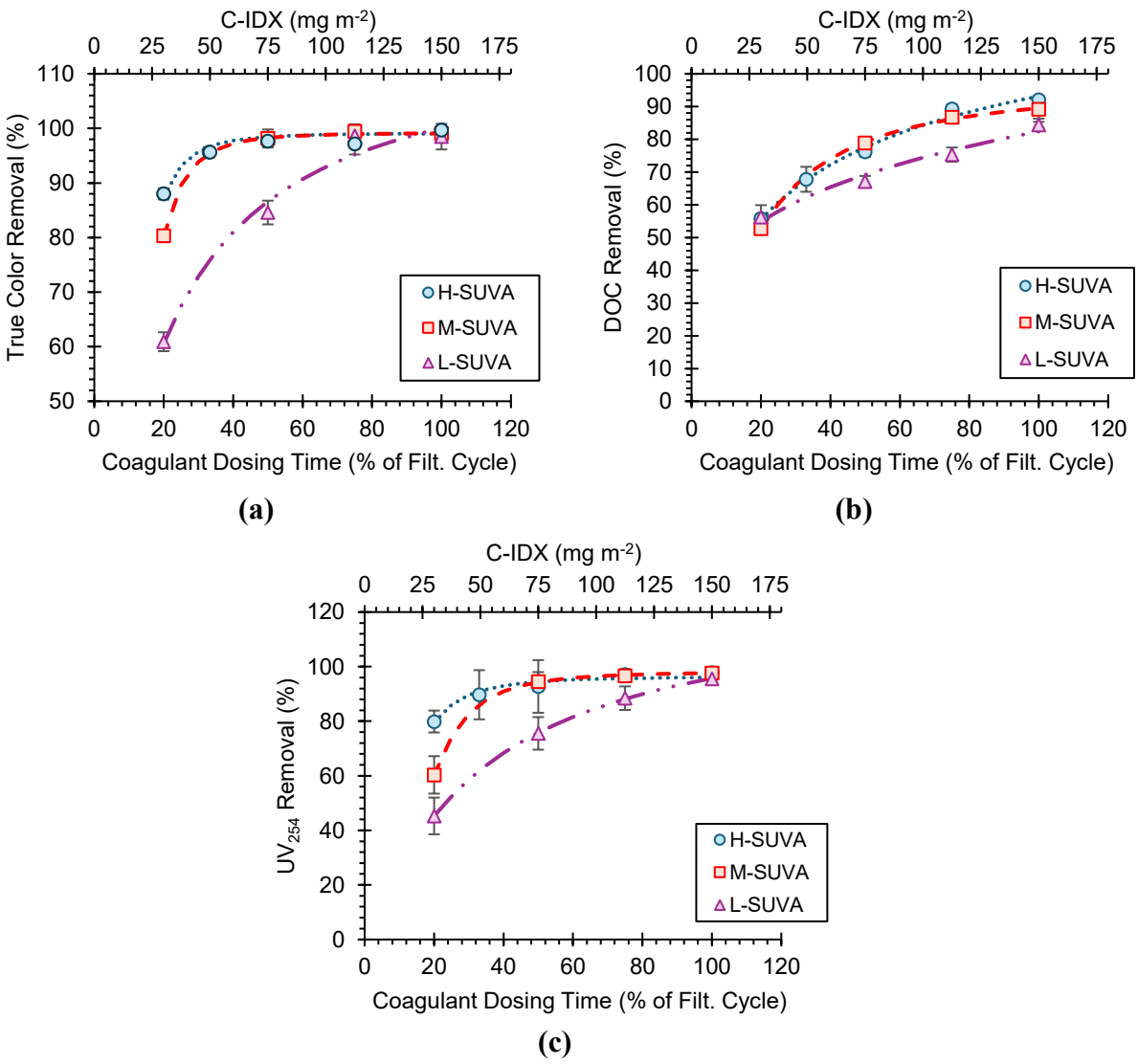


Fig. 7.3. Percent removal of bulk measures of organics by C-IN-P across C-IDX values and water types: **(a)** True color; **(b)** DOC; **(c)** UV_{254}. Note, Sips model used to plot lines of best fit.

For all three water types, the relationship between the mean percent removal and the dosing time (or C-IDX) was modeled using the Sips model (Aguareles et al. 2023), which was selected as the best model amongst a number of alternatives based on comparison of statistical performance indicators (Appendix H, Section H.2.3). The fitted model parameters as well as the model adequacy data for each WQI across the three water types are summarized in Tables H.10-Table H.12 (Appendix H). The nature of these models suggests a possible mechanism for the observed trends in organics removals for C-IN-P. It is hypothesized that sorption is a critical mechanism of organics removal in C-IN-P and that there exists a critical cake/coating layer mass needed to

provide sufficient sites for the removal of organic foulants. For C-IDX values below this threshold, there is insufficient coagulant to capture these foulants, whereas beyond this threshold there is only limited additional benefit in organics removals. Increasing the C-IDX would imply that a thicker cake layer is formed, yet the degree of fouling didn't increase proportionally, likely a result of the porous characteristics of the cake layer (see H-SUVA and M-SUVA waters in Fig. 7.2).

Generally, as shown in Fig. 7.3, the removals achieved by the M-SUVA and H-SUVA waters were practically identical, while the L-SUVA water yielded somewhat lower removals except under continuous dosing. The lower organics removals for the L-SUVA water may not have been entirely unexpected, however, as Kimura and Ando (2016) reported that extremely high coagulant dosages were required to achieve maximal biopolymer removal for three Japanese river waters. Moreover, the lower charge density of the hydrophilic organic fraction has been shown to make it more difficult to coagulate than for the hydrophobic fraction (Sillanpää et al. 2018; Volk 2000). Accordingly, it is reasonable that the removal of bulk organics for the L-SUVA water, whose organic matrix was dominated by biopolymers (specifically polysaccharides), exhibited greater sensitivity to the reduced coagulant addition during C-IN-P pretreatment than for the M-SUVA or H-SUVA waters. It is likely that following the cessation of coagulant addition, the resulting pH drift and lower effective coagulant dose reduced the removal efficiency for biopolymers.

In contrast to the above mentioned need for higher coagulant dosages in the pretreatment of hydrophilic waters, several authors (Tang et al. 2019; Wray and Andrews 2014) have reported that optimal fouling mitigation for waters with elevated biopolymer concentrations is achieved using ultra-low coagulant dosages (~0.3-0.5 mg-Al L^{-1}). However, these lower dosages result in minimal DOC removal and may therefore necessitate additional downstream treatment to remove organics prior to disinfection. One possible solution to address this apparent trade-off is a novel operating scheme termed stepped inline coagulation (C-IN-S), introduced in our previous study (see Appendix C), where the coagulant dose is reduced (not set to zero) in the latter portion of the filtration cycle. By integrating the higher initial dosing with sustained low-level coagulant addition during the latter portion of the cycle, the C-IN-S strategy may be better suited to the treatment of hydrophilic waters than C-IN-P, offering a potential means of reconciling the competing objectives of effective biopolymer removal and fouling mitigation within a single treatment framework. This should be the subject of future research.

One final comment concerns the collection of samples for WQI measurement. It must be acknowledged that the removal of bulk organic WQIs in this study was determined using a composite sample collected from the permeate reservoir: the reported removal values therefore represent an average value for the test and provides no information regarding the time dependent removal of each indicator. It would be of interest for future studies to evaluate the feed and permeate quality using advanced organic characterization methods throughout the filtration cycle. Such a study could elucidate whether coagulation chemistry changes lead to altered biopolymer removals in the initial and latter portions of the filtration cycle and how these contribute to the observed fouling phenomena noted in Section 7.4.1.1.

7.4.1.3. FEEM Analysis

PARAFAC modeling was used in the current study to de-convolute the FEEM spectra of the various components into three modes, namely, the sample score, the emission loadings, and the excitation loadings according to the model presented in Eqn. 7.3. The most appropriate PARAFAC model (see Section H.2.4. for a detailed discussion of its validation) for the FEEM data contained three components which were assigned, in order of increasing emission loadings peak wavelengths, as protein-like/tryptophan-like substances (Ex/Em=280/335), humic-like I (Ex/Em=245/435), and humic-like II (Ex/Em=260/540) (see Fig. H.13). It should be mentioned that, although there are only two components in the synthetic water mixtures that exhibit spectral/fluorescent properties (i.e., HA & BSA), a three-component model is appropriate as Mealio et al. (2024) have reported that Aldrich HA exhibits an additional terrestrial humic component at a peak emission loading of 530-540 nm.

Using the developed PARAFAC model, a one-point calibration was performed using HA and BSA standards of known concentration to relate the sample scores to the measured DOC content. The single point method was deemed appropriate as the concentrations for both components were maintained within the linear Beer-Lambert range (see Section H.2.4.4). Using this calibration factor and the sample scores obtained from the validated FEEM model, the concentration of HA and BSA were directly calculated, while the concentration of SA was determined by subtracting the calculated HA and BSA concentrations from the measured bulk DOC. To differentiate FEEM-derived DOC concentrations from references to the model organic components, the former are denoted using an asterisk (see Eqn. 7.4- Eqn. 7.6) throughout the

remainder of this text. Using this approach, the percent removal values of each model organic were computed across all C-IDXs for the three water types, the results of which are presented in Fig 7.4.

$$HA^* = DOC\ corresponding\ to\ FEEM\ humic\text{-}like\ I\ and\ humic\text{-}like\ II\ component \quad (7.4)$$

$$BSA^* = DOC\ corresponding\ to\ FEEM\ protein\text{-}like\ component \quad (7.5)$$

$$SA^* = Measured\ Bulk\ DOC - HA^* - BSA^* \quad (7.6)$$

For HA^* (Fig. 7.4a), the removals increased with increasing C-IDX, reaching a plateau near 90% following C-IN-P pretreatment at 75 mg m^{-2} for M-SUVA and 112.5 mg m^{-2} for H-SUVA and L-SUVA. In contrast, BSA^* removals remained relatively high across all operating conditions (Fig. 7.4b), generally exceeding 80% for all waters and C-IDX values. These results suggest that significant protein removal can be achieved under conditions where limited effective coagulant dose is added to the system (i.e., coagulant addition for only a limited duration). This is in contrast to the findings of Tang et al. (2019) who reported that ultra-low dosing conditions favorable for irreversible fouling mitigation led to the lowest protein rejection by the integrated system. Moreover, the insignificant improvement in BSA^* removal observed beyond a C-IDX of 75-112.5 mg m^{-2} suggests the existence of a point of diminishing returns for protein removal under C-IN-P operation. The removals of SA^* (Fig. 7.4c) increased nearly linearly with increasing C-IDX. The greater difficulty in removing SA^* compared to BSA^* in the current study seems to suggest that polysaccharides, and not proteins, are the critical biopolymer fraction responsible the reduced DOC removal for the L-SUVA water with C-IN-P pretreatment.

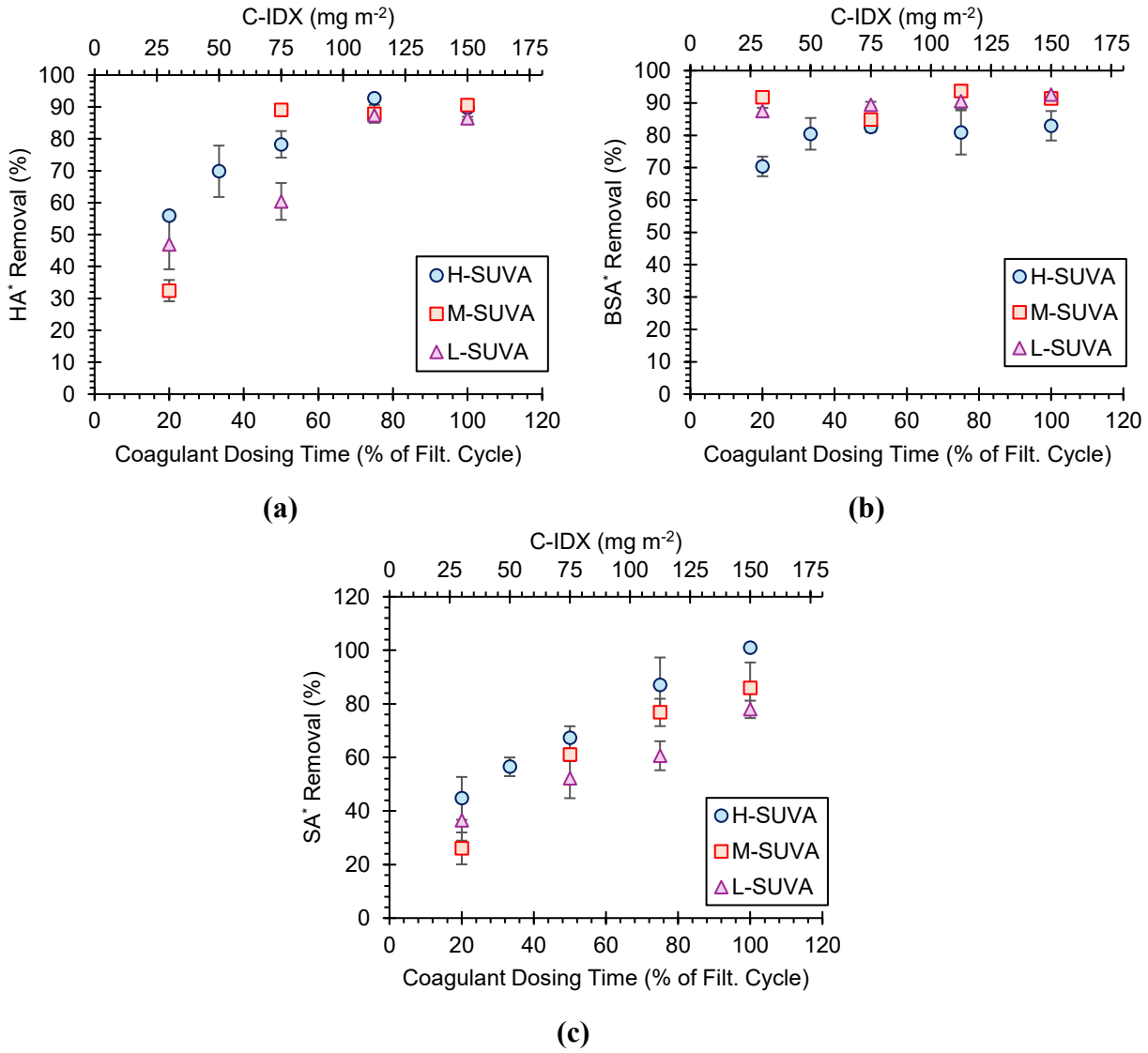
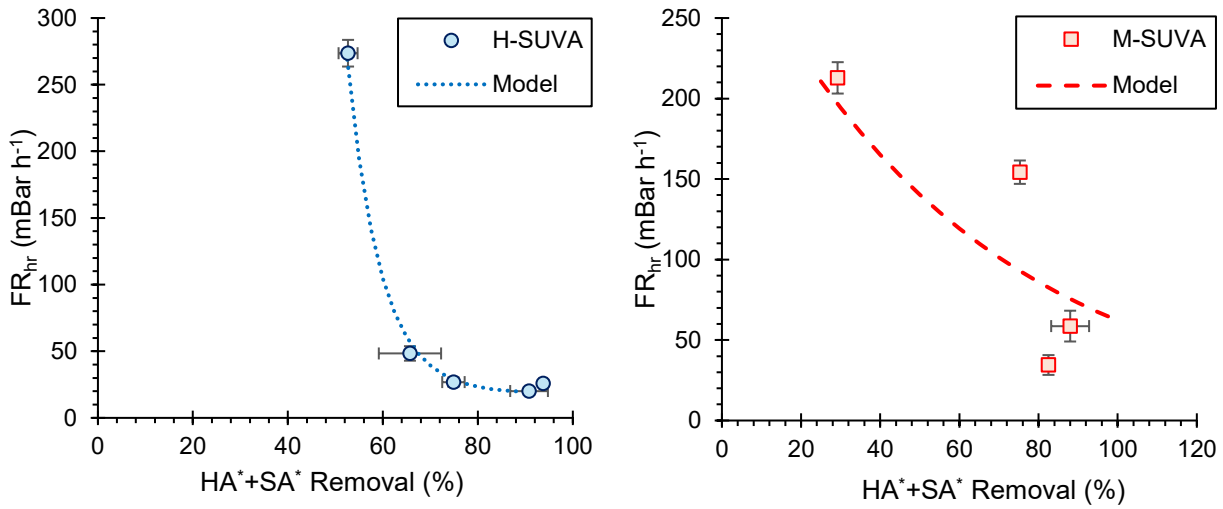


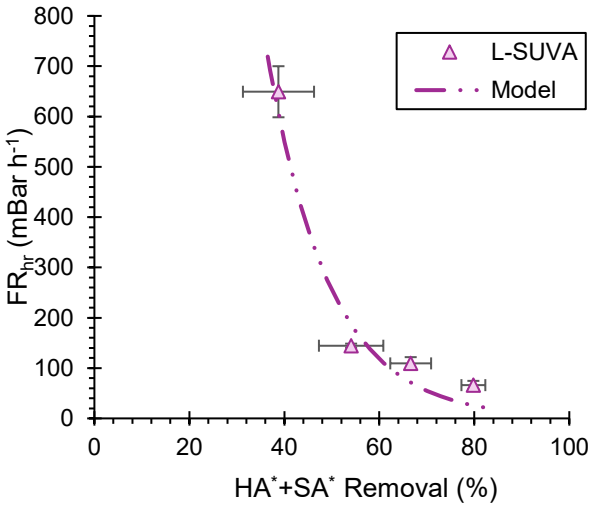
Fig. 7.4. Trends in the removal of model organic compounds by C-IN-P with varying C-IDX and water type: **(a)** HA*; **(b)** BSA*; **(c)** SA*

The relationships between HA*+SA* removal and FR_{hr} were plotted for each water type and are shown in Fig. 7.5. In all cases, the data were modeled following the same approach as in Section 7.4.2.1 but with the percent HA*+SA* removal as the dependent variable, which was selected as the best single, overall parameter for FR_{hr} simulation (see Section H.2.5). As shown in Fig. 7.5a and Fig. 7.5c, the developed models exhibited a strong agreement with the experimental data for the H-SUVA and L-SUVA waters (R^2>0.96), with FR_{hr} increasing exponentially as HA*+SA* removal decreased. In contrast, the relationship for the M-SUVA water was quite different, which resulted in a poor model fit for this water type. Although FR_{hr} generally decreased

with increasing removal of these two components, the trend was not exponential as was the case for the H-SUVA and L-SUVA waters. This difference may be related to the dominance of HA^* and SA^* within the organic makeup of the H-SUVA and L-SUVA waters (respectively), however, further research is needed to verify this hypothesis.

For both the H-SUVA and L-SUVA waters, Fig. 7.5 suggests the existence of a threshold HA^*+SA^* removal of approximately 60-70% required to maintain reasonable FR_{hr} values. Based on Fig. 7.4, these removals correspond to minimum C-IDX values of approximately 75 mg m^{-2}, while additional removals brought about only a small improvement in fouling reduction. The similarity of this threshold value across disparate water types suggests that the reduction of humic substances and polysaccharides may provide a useful basis for selecting appropriate C-IDX values during C-IN-P optimization. Future studies should evaluate the generalizability of this finding using natural waters and advanced organic characterization techniques (such as liquid chromatography organic carbon detection) to quantify the removal of these fractions. It is likely that for natural waters, the threshold HA^*+SA^* removal value will be lower than for the synthetic waters used in the current study due to the presence of recalcitrant NOM fractions.





(c)

Fig. 7.5. Relationship between FR_{hr} and the removal of HA^{*}+SA^{*} for: **(a)** H-SUVA; **(b)** M-SUVA; **(c)** L-SUVA

7.4.2. Sensitivity Analysis of C-IDX

In this section, the impact of several combinations of coagulant dose and dosing time on LPM performance was investigated for a fixed C-IDX of 75 mg m^{-2} and the H-SUVA water. This analysis was performed using two coagulant types.

7.4.2.1. Fouling Performance

The FR_{hr} values obtained from the replicated day-long filtration experiments for each treatment condition are presented in Fig. 7.6. Pooled *t*-tests were used to help elucidate the impact of dose/dosing time and coagulant type on FR_{hr}, with a summary of the statistical data presented in Section H.2.6. As shown in Fig. 7.6, regardless of the coagulant type, altered combinations of coagulant dose/dosing time led to statistically significant (p <.0001) differences in FR_{hr}. For alum coagulant, the lowest FR_{hr} was observed for Alum-3.0 (26.85 mBar h^{-1}), whereas significantly greater values were seen for Alum-1.5 (108.33 mBar h^{-1}) and Alum-45 (183.26 mBar h^{-1}). For ACH, as was seen for alum coagulant, altered combinations of coagulant dose/dosing time led to significant differences in FR_{hr}. However, unlike for alum where Alum-45 resulted in the highest FR_{hr} amongst alternatives, ACH-45 yielded improved performance compared to ACH-3.0 (64.93 mBar h^{-1} vs. 104.24 mBar h^{-1}).

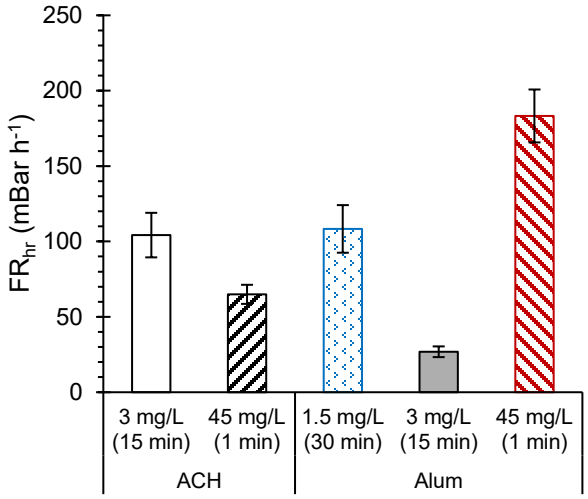


Fig. 7.6. Impact of coagulant dose/dosing time and coagulant type on FR_{hr} for H-SUVA water and a C-IDX of 75 mg m^{-2}

The superior performance of Alum-3.0 relative to ACH-3.0 may be related to the differences in ZP at these dosages. The 3 mg-Al L^{-1} condition was selected using the alum coagulant based (in part) on ZP minimization. However, Fig. H.5c indicates that ZP neutralization for the ACH coagulant required a slightly higher dosage in the range of 4 mg-Al L^{-1} for the H-SUVA water. Consequently, the ACH-3.0 condition likely represented a slight underdose relative to Alum-3.0 during the first half of the filtration cycle. Furthermore, our previous work (Chapter 4) demonstrated that for this membrane type and a natural water with a moderate DOC content (6.64 mg-C L^{-1}) and high hydrophobicity (4.16 L mg^{-1} m^{-1}), circumneutral ZP values led to the lowest irreversible fouling potential. Despite the overlapping 95% CIs for all dose/dosing time combinations (Table H.19), the mean FR_{hirr} in the current study was more than two times greater for ACH-3.0 than Alum-3.0, which is consistent with these previous findings (Chapter 4).

Floc characteristics may also have contributed to the observed differences in FR_{hr} between ACH-3.0 and Alum-3.0. Our previous study (see Chapter 6) showed that the combined small-scale rapid mixer and helical flocculator produced relatively large-sized flocs (127.27 μm) with a perimeter-based fractal dimension of 1.52 using Alum at 3 mg-Al L^{-1}, indicative of a moderately loose/open structure. In contrast, Yao et al. (2015) reported that ACH coagulation near the ZP-optimized dose produced substantially more compact flocs, with a perimeter-based fractal dimension of 1.27. Dense flocs have previously been associated with the formation of low-porosity

cake layers that exhibit elevated fouling resistance (Park et al. 2006). Additional research is therefore needed to characterize the cake layers formed under different dose/dosing time conditions, including their porosity, thickness, and surface roughness, in order to more definitively relate dosing strategy, floc characteristics, cake-layer properties, and LPM fouling potential.

Overall, these findings demonstrate C-IN-P performance for a given water type depends not only on the normalized mass of coagulant delivered to the membrane, but also on the coagulant type and the dosing strategy. Consequently, each C-IDX value corresponds to a range of possible FR_{hr} values governed by coagulant dose, dosing time, and coagulant type (in addition to water type, which was shown earlier to exhibit a statistically significant impact on FR_{hr}). Based on Alum-3.0 yielding the lowest FR_{hr} values, it seems likely that the best performing C-IDX value is defined using the jar-test optimal coagulation chemistry, although, this should be confirmed by future work.

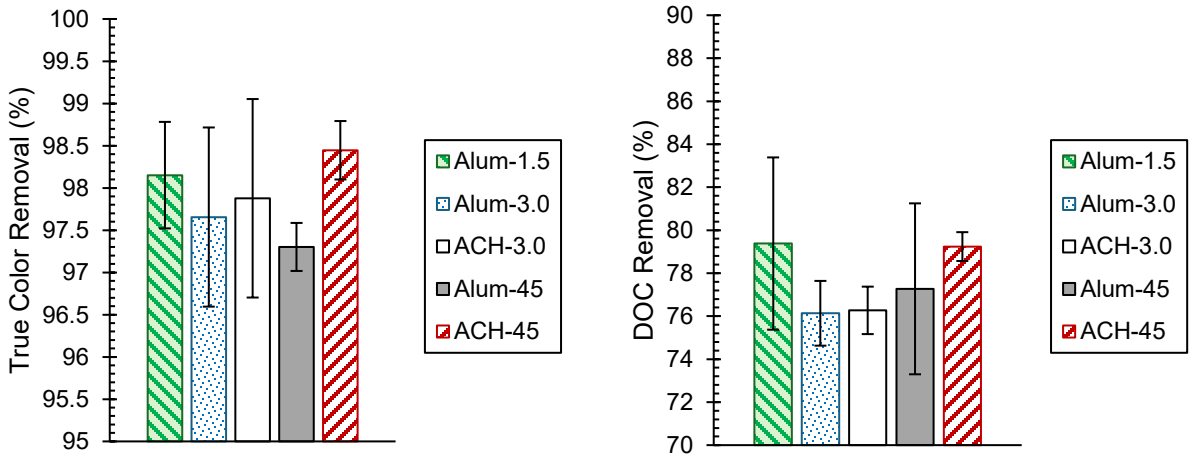
7.4.2.2. Organics Removals

The treated water quality, including the true color, DOC, UV_{254}, and SUVA was assessed for both coagulant types and all combinations of coagulant dose/dosing time. A summary of the percent removal of each WQI is presented in Fig. 7.7. It should be noted that in this figure, while the 95% CIs may appear substantial, this is largely a result of the scale of the ordinate axis. For alum coagulant, Alum-1.5, Alum-3.0, and Alum-45 were found to have overlapping 95% CIs for all four WQIs. When the coagulant type was changed to ACH, the removal of all four WQIs was similarly unaffected by the change in dose/dosing time. In fact, a one-way analysis of variance (ANOVA) test confirmed that there were no significant differences in the removal of the four WQIs with changing dose/dosing time or coagulant type (Table H.21). This finding suggests that the removal of organics achieved by C-IN-P pretreatment at a specific C-IDX value is dependent solely on the mass of coagulant used during the filtration cycle and not on the method of coagulant addition. This is consistent with the findings of Edzwald and Kaminski (2009) as well as Black et al. (1963) who have previously reported that for these low-alkalinity colored water types, a stoichiometry exists between the initial NOM concentration and the required coagulant dose for optimal performance.

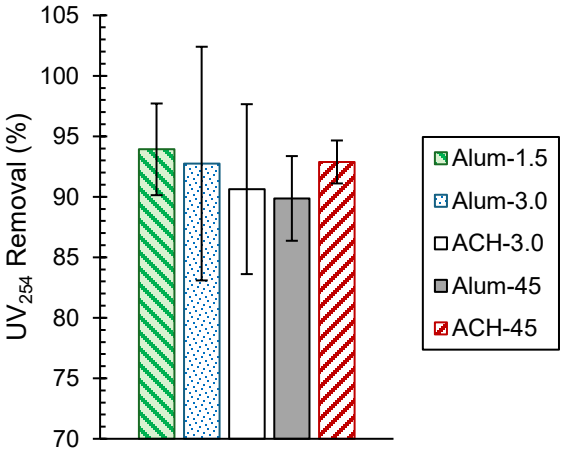
Based on the 95% CIs, the removals of HA^*, BSA^*, and SA^* were also found to be quite similar for all treatments (Fig. 7.7e – Fig. 7.7g). While the removal of HA^*+SA^* was proposed to

exert an important impact on C-IN-P across C-IDXs and water type, for fixed C-IDX the combined removal was not indicative of the FR_{hr}. This further supports the hypothesis that differences in cake layer morphological properties are responsible for the observed performance differences.

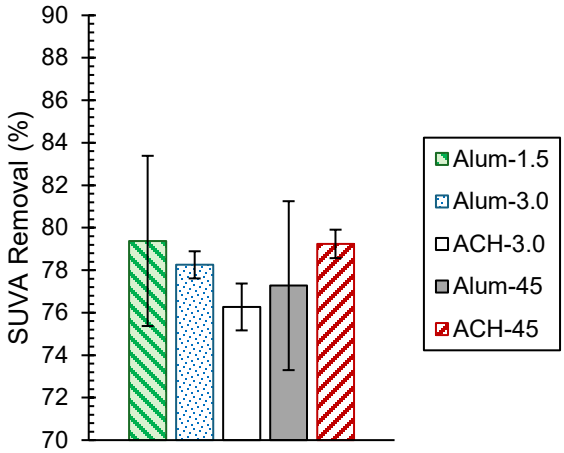
The similar removal of all components by both ACH and alum coagulant types is in contrast to the study by Papineau et al. (2019) where ACH was shown to yield improved removals of biopolymers compared to alternative coagulant types and, for neutral pH values, led to the greatest removals of HA. The differences in removal trends between studies is likely related to the differences in water quality. The high-basicity, pre-polymerized ACH coagulant is reported to improve NOM-coagulant reactions for NOM fractions that are recalcitrant to coagulation by aluminum- or ferric-based coagulants. This feature of ACH may not be significant for the synthetic challenge waters used in the current study, which were shown to have high coagulation efficacy. Therefore, the similarity of the removal of different organic components for different combinations of dose/dosing time should be verified for natural waters which possess a more complex NOM matrix with recalcitrant organic fractions.



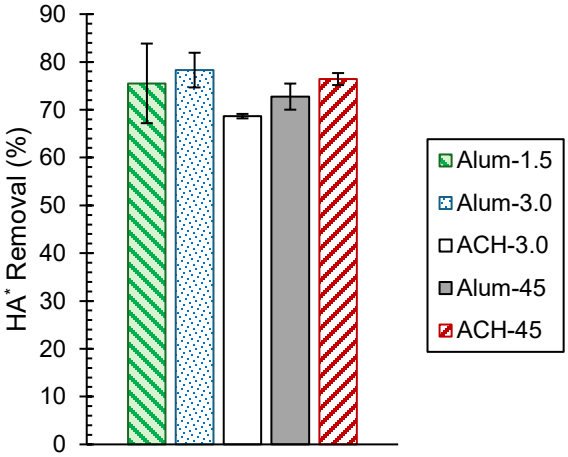
(a) **(b)**


105
100
95
90
85
80
75
70
UV254 Removal (%)
Alum-1.5
Alum-3.0
ACH-3.0
Alum-45
ACH-45

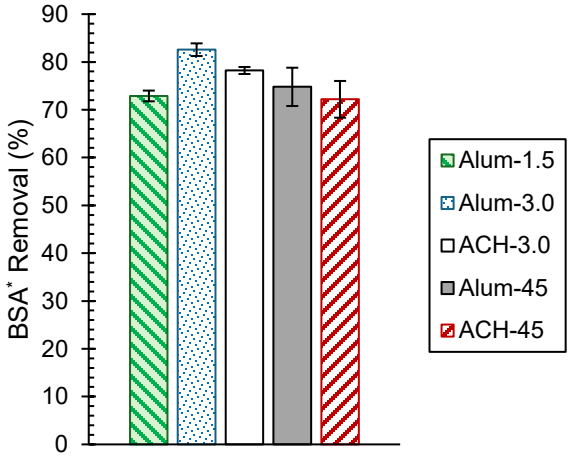
(c)


90
88
86
84
82
80
78
76
74
72
70
SUVA Removal (%)
Alum-1.5
Alum-3.0
ACH-3.0
Alum-45
ACH-45

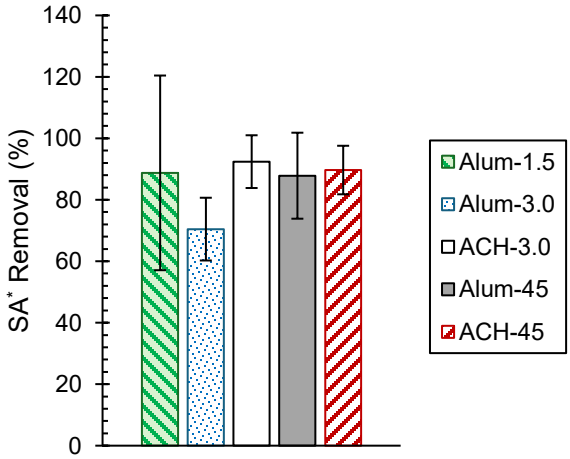
(d)


90
80
70
60
50
40
30
20
10
0
HA* Removal (%)
Alum-1.5
Alum-3.0
ACH-3.0
Alum-45
ACH-45

(e)


90
80
70
60
50
40
30
20
10
0
BSA* Removal (%)
Alum-1.5
Alum-3.0
ACH-3.0
Alum-45
ACH-45

(f)


140
120
100
80
60
40
20
0
SA* Removal (%)
Alum-1.5
Alum-3.0
ACH-3.0
Alum-45
ACH-45

(g)

Fig. 7.7. Impact of different combinations of coagulant dose/dosing time and coagulant type on the removal of water quality indices when treating H-SUVA water: **(a)** True color; **(b)** DOC; **(c)** UV_{254}; **(d)** SUVA; **(e)** HA*; **(f)** BSA*; **(g)** SA*

The insensitivity of the removal of organic WQIs to changing combinations of coagulant dose/dosing time and coagulant type was also seen using FEEMs captured for each treatment combination. Fig. 7.8 presents the FEEMs for the raw (untreated) H-SUVA water as well as the permeate from the ALS-1.5 and ACH-45 tests. From Fig. 7.8c and Fig. 7.8d, the permeate fluorescence patterns could both be seen to center around the Humic-like I peak and were practically identical, with a significant reduction in the DOC fingerprint. These conditions were selected for illustrative purposes to emphasize the similarity in the observed permeate FEEM despite disparate coagulant type and drastically different coagulant dosing conditions.

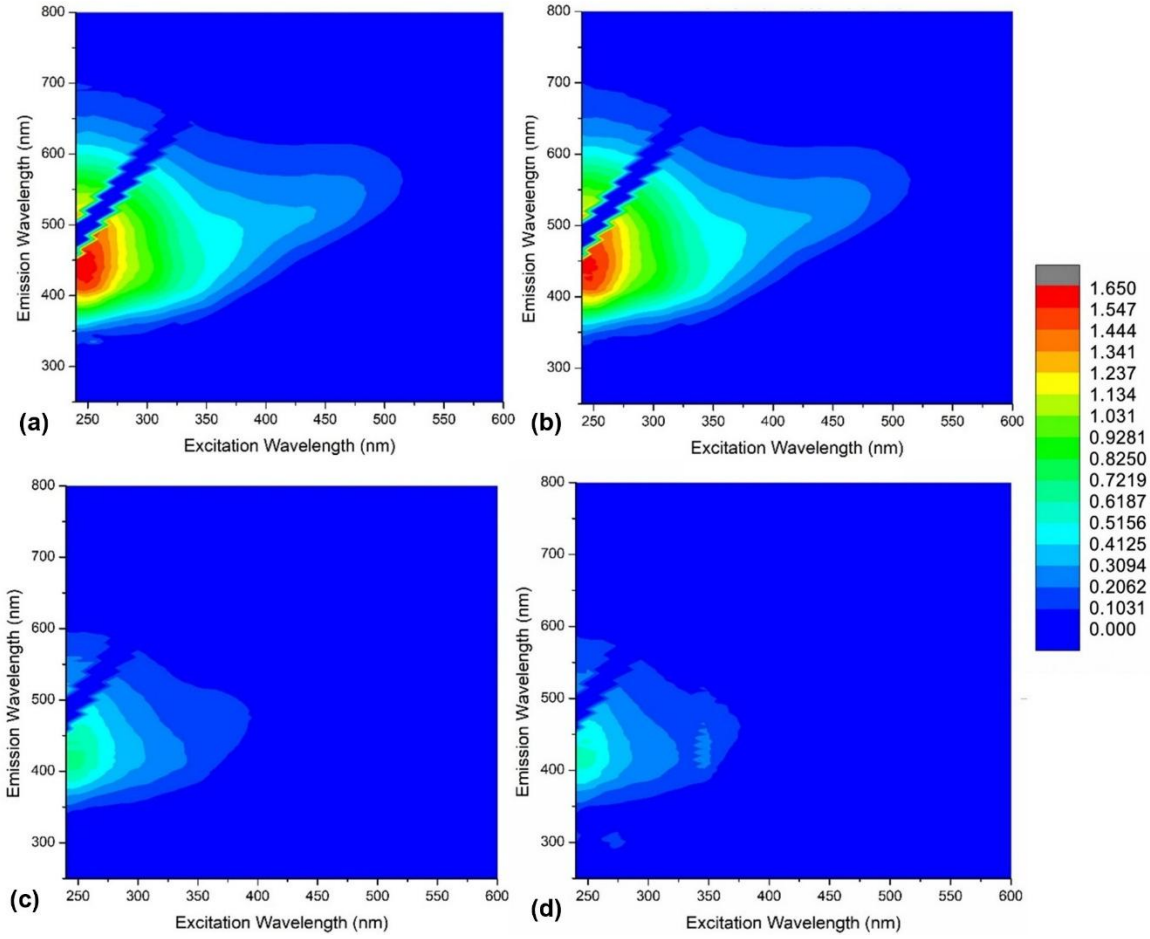


Fig. 7.8. FEEM contour plot for C-IDX sensitivity analysis: **(a)** ALS-1.5 raw H-SUVA water; **(b)** ACH-45 raw H-SUVA water; **(c)** ALS-1.5 permeate; **(d)** ACH-45 permeate

7.5. Conclusions

Day-long bench-scale filtration tests were conducted using synthetic challenge waters with varying hydrophobicities to evaluate the suitability of C-IN-P for LPM pretreatment in terms of fouling mitigation and organics reduction. The results of this study can be summarized as:

1. For pretreatment by C-IN-P, LPM fouling was strongly influenced by both the C-IDX value as well as the feed water characteristics. For the three water types considered in the study, FR_{hr} decreased exponentially as the length of coagulant addition (or C-IDX value) increased. Among the three water types, FR_{hr} was lowest for the H-SUVA water and highest for the L-SUVA water, suggesting that hydrophilic biopolymers were the critical foulant for C-IN-P operation and this membrane type.
2. The removals of bulk measures of organics for the H-SUVA and M-SUVA waters were practically identical and plateaued around a threshold C-IDX value of 75 mg m^{-2}. For L-SUVA water, the removals were lower across all C-IDX values. As suggested by others, it is likely that optimal biopolymer removal necessitates elevated coagulant addition: C-IN-P pretreatment may therefore be incompatible for these water types.
3. The removal of HA^{*}+SA^{*} was strongly associated with fouling mitigation for the H-SUVA and L-SUVA waters, with FR_{hr} increasing exponentially as HA^{*}+SA^{*} removal decreased. A threshold HA^{*}+SA^{*}removal of approximately 60-70% corresponded to minimum effective C-IDX values near 75 mg m^{-2} for these water types. The similarity of this threshold value across disparate water types suggests that the reduction of humic substances and polysaccharides may provide a useful basis for selecting appropriate C-IDX values during C-IN-P optimization with natural water types.
4. Filtration of the H-SUVA water at a fixed C-IDX of 75 mg m^{-2} demonstrated that equivalent C-IDX values did not necessarily produce similar fouling behaviour for different dosing strategies. Although comparable removals of bulk organics and individual foulant fractions were achieved, FR_{hr} varied significantly with coagulant type and dosing approach, with alum at the jar-test optimal dose providing the best performance. These results suggest that membrane fouling in C-IN-P is governed not only by the applied mass of coagulant (i.e., C-IDX), but also by the applied combinations of coagulant dose/dosing time which likely give rise to altered cake/floc morphological properties.

To the knowledge of the authors, this study is the first to comprehensively and systematically investigate the performance of C-IN-P pretreatment across different water types and C-IDX values. Several limitations of the present work should be acknowledged. First, this study considered three different synthetic water types and the results, therefore, may not be fully representative of those that would be obtained with natural waters. Second, although the flux was increased relative to our previous study (Chapter 6), the day-long filtration test and 30 min filtration cycle did not generate sufficient fouling to permit good appraisal of the impact of C-IN-P pretreatment on irreversible fouling development. Finally, the result of this study are for a single tubular multichannel membrane type, and may change for membranes with different configuration and/or material type.

Future studies should focus on a number of research needs that have been identified in this work. Firstly, the apparent dependence of optimal C-IN-P performance on the combined removal of HA+SA (i.e., humic substances and polysaccharides) should be confirmed for alternative membrane types and for natural waters with more complex organic matrices. For L-SUVA waters which presented significant operational challenges for C-IN-P, the novel C-IN-S strategy should be investigated as a means to simultaneously optimize biopolymer removal and fouling mitigation. Lastly, it would be of interest to characterize the properties of the fouling layer formed for different combinations of dose/dosing time to elucidate whether different methods of addition bring about structural changes to the coating layer.

7.6. Acknowledgements

This work was supported by the Natural Sciences and Engineering Research Council of Canada (NSERC) under grant RGPIN 2018-06571 as well as the NSERC Canada Graduate Scholarship-Doctoral Program (ID 579943-2023). The authors would also like to acknowledge financial support provided to the lead author by the American Membrane Technology Association (AMTA) through their Ian C. Watson Fellowship and by the American Water Works Association (AWWA) through the Dr. James K. Edzwald Scholarship. The authors extend their thanks to Catherine Brosseau and Kemira Water Solutions Canada for providing coagulants for this study as well as to Adam Gilmore (Horiba) and Dr. Onita Basu (Carleton University) for training in the use of the fluorescence spectrophotometer as well as their assistance in interpretation of fluorescence data.

7.7. References

Aguareles, M., E. Barrabés, T. Myers, and A. Valverde. 2023. "Mathematical analysis of a Sips-based model for column adsorption." *Physica D: Nonlinear Phenomena*, 448: 133690. https://doi.org/10.1016/j.physd.2023.133690.

Alresheedi, M. T., O. D. Basu, and B. Barbeau. 2019. "Chemical cleaning of ceramic ultrafiltration membranes – Ozone versus conventional cleaning chemicals." *Chemosphere*, 226: 668–677. https://doi.org/10.1016/j.chemosphere.2019.03.188.

Aly, S. A., W. B. Anderson, and P. M. Huck. 2021. "In-line coagulation assessment for ultrafiltration fouling reduction to treat secondary effluent for water reuse." *Water Science and Technology*, 83 (2): 284–296. https://doi.org/10.2166/wst.2020.571.

American Public Health Association, Water Environment Foundation, and American Water Works Association. 2012. *Standard Methods for the Examination of Water and Wastewater*. 1496. Edited by L. Clesceri, A. Greenberg, and A. Eaton. 22nd Editi. Washington: APHA Press.

Black, A. P., J. E. Singley, G. P. Whittle, and J. S. Maulding. 1963. "Stoichiometry of the coagulation of color-causing organic compounds with ferric sulfate." *Journal AWWA*, 55 (10): 1347–1366. https://doi.org/10.1002/j.1551-8833.1963.tb01151.x.

Bratby, J. 2016. *Coagulation and Flocculation in Water and Wastewater Treatment*. 3rd ed. London, UK: IWA Publishing.

Buchta, P., P. Berg, A. Schweiger, and D. Vial. 2019. "In-line coagulation upstream ultrafiltration - comparison of continuous vs. intermittent addition." 8. New Orleans, LA: American Water Works Association.

Buchta, P., A. Kripahle, D. Vial, R. Winkler, and P. Berg. 2017. "In-out ultrafiltration in tertiary wastewater applications- Comparison of different operational strategies." *Desalination and Water Treatment*, 73: 145–154.

Campinas, M., R. M. C. Viegas, C. Silva, H. Lucas, and M. J. Rosa. 2021. "Operational performance and cost analysis of PAC/ceramic MF for drinking water production: Exploring treatment capacity as a new indicator for performance assessment and optimization." *Separation and Purification Technology*, 255: 117443. https://doi.org/10.1016/j.seppur.2020.117443.

Chen, Y., and J. Nan. 2023. "A strategy to alleviate membrane fouling by optimizing the structure of the cake layer formed by flocs deposited directly on the membrane in the ultrafiltration process through coagulation and nanoscale Fe3O4/Fe3O4@SiO2 load." *Journal of Membrane Science*, 680: 121729. https://doi.org/10.1016/j.memsci.2023.121729.

Crittenden, J. C., R. R. Trussell, D. W. Hand, K. J. Howe, and G. Tchobanoglous. 2012. *Water Treatment: Principles and Design*. 3rd ed. New York, NY: McGraw-Hill.

Cui, X., and K. H. Choo. 2014. "Natural organic matter removal and fouling control in low-pressure membrane filtration for water treatment." *Environmental Engineering Research*, 19 (1): 1–8. https://doi.org/10.4491/eer.2014.19.1.001.

Edzwald, J. K., and G. S. Kaminski. 2009. "A practical method for water plants to select coagulant dosing." *Journal NEWWA*, 123 (1): 15–31.

Edzwald, J. K., and J. E. Tobiason. 1999. "Enhanced coagulation: US requirements and a broader view." *Water Science & Technology*, 40 (9): 63–70. https://doi.org/10.1016/S0273-1223(99)00641-1.

Edzwald, J. K., and J. E. Van Benschoten. 1990. "Aluminum coagulation of natural organic matter." *Chemical Water and Wastewater Treatment*, edited by H. H. Hahn and R. Klute, 341–359. Berlin, Heidelberg: Springer Berlin Heidelberg.

Hach Company. 2014. "Color, True and Apparent, Method 8025."

Howe, K. J., and M. M. Clark. 2002. "Fouling of Microfiltration and Ultrafiltration Membranes by Natural." 36 (16): 3571–3576. https://doi.org/10.1021/es025587r.

Hua, G., and D. A. Reckhow. 2007. "Characterization of disinfection byproduct precursors based on hydrophobicity and molecular size." *Environmental Science & Technology*, 41 (9): 3309–3315. https://doi.org/10.1021/es062178c.

Inge GmbH. 2020. *Inge Product Series: Dizzer XL Series Modules. Process and Design Guidelines*. 66–66. Greifenberg.

Kamińska, G., W. Pronk, and J. Traber. 2020. "Effect of coagulant dose and backflush pressure on NOM membrane fouling in inline coagulation-ultrafiltration." *Desalination and Water Treatment*, 199: 188–197. https://doi.org/10.5004/dwt.2020.25657.

Kang, J., J. Seong, J. Yoo, P. Kim, K. Park, J. Lee, J. Cheon, H. Kim, and S. Lee. 2021. "Applicability of a combined DAF-MF process to respond to changes in reservoir water quality through a two-year pilot plant operation." *Membranes*, 11 (12): 964. https://doi.org/10.3390/membranes11120964.

Katsoufidou, K. S., D. C. Sioutopoulos, S. G. Yiantsios, and A. J. Karabelas. 2010. "UF membrane fouling by mixtures of humic acids and sodium alginate: Fouling mechanisms and reversibility." *Desalination*, 264 (3): 220–227. https://doi.org/10.1016/j.desal.2010.08.017.

Keeley, J., P. Jarvis, A. D. Smith, and S. J. Judd. 2016. "Coagulant recovery and reuse for drinking water treatment." *Water Research*, 88: 502–509. https://doi.org/10.1016/j.watres.2015.10.038.

Kim, H. C., and B. A. Dempsey. 2013. "Membrane fouling due to alginate, SMP, EfOM, humic acid, and NOM." *Journal of Membrane Science*, 428: 190–197. Elsevier. https://doi.org/10.1016/j.memsci.2012.11.004.

Kimura, K., and N. Ando. 2016. "Maximizing biopolymer removal by coagulation for mitigation of fouling in the following membrane process." *Separation and Purification Technology*, 163: 8–14. Elsevier B.V. https://doi.org/10.1016/j.seppur.2016.02.013.

Kimura, K., and K. Kume. 2020. "Irreversible fouling in hollow-fiber PVDF MF / UF membranes filtering surface water: Effects of precoagulation and identification of the foulant." *Journal of Membrane Science*, 602 (February): 117975–117975. Elsevier B.V. https://doi.org/10.1016/j.memsci.2020.117975.

Kimura, K., K. Tanaka, and Y. Watanabe. 2015. "Confirmation of the correlation between membrane fouling in microfiltration and biopolymer concentrations in various Japanese surface waters." *Water Science and Technology: Water Supply*, 15 (2): 288–293. https://doi.org/10.2166/ws.2014.112.

Ladouceur, J. D., R. M. Narbaitz, and C. Q. Lan. 2024. "Phased-inline coagulation for low-pressure membranes in water and wastewater treatment: a review of fouling mitigation, process control, and water quality." *Environmental Technology Reviews*, 13 (1): 305–324. https://doi.org/10.1080/21622515.2024.2343128.

Le Clech, P., B. Jefferson, I. S. Chang, and S. J. Judd. 2003. "Critical flux determination by the flux-step method in a submerged membrane bioreactor." *Journal of Membrane Science*, 227 (1–2): 81–93. https://doi.org/10.1016/j.memsci.2003.07.021.

Lee, S.-J., and J.-H. Kim. 2015. "Effects of coagulation on the ceramic membrane fouling during surface water treatment." *Journal of Environmental Engineering*, 141 (5): 04014087. https://doi.org/10.1061/(ASCE)EE.1943-7870.0000918.

Liu, Y., Z. Wang, M. Xu, F. Qi, C. Li, D. Sun, J. Nan, W. Li, X. Guan, and A. Ikhlaq. 2024. "Unveiling the role of cake layer in coagulation-ultrafiltration on membrane fouling and emerging application as dynamic membrane before ultrafiltration." *Separation and Purification Technology*, 350: 127932. https://doi.org/10.1016/j.seppur.2024.127932.

Lok, A., H. Wray, P. Bérubé, and R. C. Andrews. 2017. "Optimization of air sparging and in-line coagulation for ultrafiltration fouling control." *Separation and Purification Technology*, 188: 60–66. https://doi.org/10.1016/j.seppur.2017.06.064.

Ma, B., Y. Ding, B. Wang, Z. Qi, Y. Bai, R. Liu, H. Liu, and J. Qu. 2020a. "Influence of sedimentation with pre-coagulation on ultrafiltration membrane fouling performance." *Science of the Total Environment*, 708: 134671–134671. Elsevier B.V. https://doi.org/10.1016/j.scitotenv.2019.134671.

Ma, B., W. Xue, Y. Bai, R. Liu, W. Chen, H. Liu, and J. Qu. 2020b. "Enhanced alleviation of ultrafiltration membrane fouling by regulating cake layer thickness with pre-coagulation during drinking water treatment." *Journal of Membrane Science*, 596: 117732. https://doi.org/10.1016/j.memsci.2019.117732.

Malkoske, T. A., P. R. Bérubé, and R. C. Andrews. 2023. "Leveraging coagulation mechanisms to reduce fouling and increase natural organic matter removal during coagulation/flocculation-ultrafiltration treatment." *Separation and Purification Technology*, 327: 124877. https://doi.org/10.1016/j.seppur.2023.124877.

Mallya, D. S., S. Abdikheibari, L. F. Dumée, S. Muthukumaran, W. Lei, and K. Baskaran. 2023. "Removal of natural organic matter from surface water sources by nanofiltration and surface engineering membranes for fouling mitigation – A review." *Chemosphere*, 321: 138070. https://doi.org/10.1016/j.chemosphere.2023.138070.

Mealio, K. N., M. J. M. Wells, K. Y. Bell, D. Wolgemuth, and H. A. Stretz. 2024. "Fluorescent EEM-PARAFAC considerations of Aldrich humic acid salt as an aquatic or terrestrial organic matter surrogate." *Journal of Environmental Chemical Engineering*, 12 (5): 113864. https://doi.org/10.1016/j.jece.2024.113864.

Moon, J., M.-S. Kang, J.-L. Lim, C.-H. Kim, and H.-D. Park. 2009. "Evaluation of a low-pressure membrane filtration for drinking water treatment: pretreatment by coagulation/sedimentation for the MF membrane." *Desalination*, 247 (1–3): 271–284. https://doi.org/10.1016/j.desal.2008.12.030.

Naim, R., R. Epsztein, A. Felder, M. Heyer, M. Heijnen, and V. Gitis. 2014. "Rethinking the role of in-line coagulation in tertiary membrane filtration of municipal effluents." *Separation and Purification Technology*, 125: 11–20. Elsevier B.V. https://doi.org/10.1016/j.seppur.2014.01.036.

Omar, I. A., and S. Q. Aziz. 2021. "Optimization of ACH Coagulant, Settling Time and Powdered Activated Carbon as Coagulant Aid with Economic Analysis." *Global NEST Journal*, 23 (3). https://doi.org/10.30955/gnj.003797.

Papineau, I., M. Lapointe, N. M. Peleato, S. Peldszus, and B. Barbeau. 2019. "Selecting the best coagulant for NOM removal: Conventional monometric hydroxide vs. polynuclear Al-species."

Park, P. K., C. H. Lee, S. J. Choi, K. H. Choo, S. H. Kim, and C. H. Yoon. 2002. "Effect of the removal of DOMs on the performance of a coagulation-UF membrane system for drinking water production." *Desalination*, 145 (1–3): 237–245. https://doi.org/10.1016/S0011-9164(02)00418-6.

Park, P.-K., C.-H. Lee, and S. Lee. 2006. "Permeability of collapsed cakes formed by deposition of fractal aggregates upon membrane filtration." *Environmental Science & Technology*, 40 (8): 2699–2705. https://doi.org/10.1021/es0515304.

Pronk, W., J. Traber, and G. Kamińska. 2016. "Optimization of process parameters of the coagulation/ultrafiltration process for the reduction of membrane fouling." In: *Adv. Part. Sci. Sep. Meet. Tomorrows Chall.*, 198–205. Oslo, Norway: International Water Association.

Schweiger, A., P. Buchta, D. Vial, and P. Berg. 2018a. "Coating of ultrafiltration membranes - the solution to improve the efficiency of the pre-treatment." In: *Desalination Environ. - Clean Water Energy*. Athens.

Schweiger, A., C. Starke, D. Vial, P. Buchta, and P. Berg. 2018b. "Coating - a dramatic change in ultrafiltration treatment of secondary effluent." Valencia, Spain.

Sillanpaa, M. 2015. *Natural Organic Matter in Water*. 1st ed. Oxford, UK: Butterworth-Heinemann.

Sillanpää, M., M. C. Ncibi, A. Matilainen, and M. Vepsäläinen. 2018. "Removal of natural organic matter in drinking water treatment by coagulation: A comprehensive review." *Chemosphere*, 190: 54–71. https://doi.org/10.1016/j.chemosphere.2017.09.113.

Smilde, A., R. Bro, and P. Geladi. 2004. *Multi-Way Analysis with Applications in the Chemical Sciences*. 1st ed. Wiley.

Stedmon, C. A., and R. Bro. 2008. "Characterizing dissolved organic matter fluorescence with parallel factor analysis: a tutorial." *Limnology and Oceanography: Methods*, 6 (11): 572–579. https://doi.org/10.4319/lom.2008.6.572.

Tang, C. K., N. M. Peleato, P. R. Bérubé, and R. C. Andrews. 2019. "Impact of low coagulant dosages on protein fouling of ultrafiltration membranes." *Journal of Water Process Engineering*, 31: 100801. https://doi.org/10.1016/j.jwpe.2019.100801.

Tao, C., W. Parker, and P. Bérubé. 2024. "The impact of secondary operating temperature on in-line coagulation/flocculation and fouling of membranes used in tertiary treatment." *Environmental Science: Water Research & Technology*, 10 (7): 1676–1687. https://doi.org/10.1039/D4EW00239C.

Volk, C. 2000. "Impact of enhanced and optimized coagulation on removal of organic matter and its biodegradable fraction in drinking water." *Water Research*, 34 (12): 3247–3257. https://doi.org/10.1016/S0043-1354(00)00033-6.

Wells, M. J. M., J. Hooper, G. A. Mullins, and K. Y. Bell. 2022. "Development of a fluorescence EEM-PARAFAC model for potable water reuse monitoring: Implications for inter-component protein–fulvic–humic interactions." *Science of The Total Environment*, 820: 153070. https://doi.org/10.1016/j.scitotenv.2022.153070.

Wray, H. E., and R. C. Andrews. 2014. "Optimization of coagulant dose for biopolymer removal: Impact on ultrafiltration fouling and retention of organic micropollutants." *Journal of Water Process Engineering*, 1: 74–83. https://doi.org/10.1016/j.jwpe.2014.03.007.

Yamamura, H., K. Okimoto, K. Kimura, and Y. Watanabe. 2014. "Hydrophilic fraction of natural organic matter causing irreversible fouling of microfiltration and ultrafiltration membranes." *Water Research*, 54: 123–136. Elsevier Ltd. https://doi.org/10.1016/j.watres.2014.01.024.

Yao, M., J. Nan, T. Chen, D. Zhan, Q. Li, Z. Wang, and H. Li. 2015. "Influence of flocs breakage process on membrane fouling in coagulation/ultrafiltration process—Effect of additional

coagulant of poly-aluminum chloride and polyacrylamide." *Journal of Membrane Science*, 491: 63–72. https://doi.org/10.1016/j.memsci.2015.05.018.

Yoo, S. S. 2018. "Operating cost reduction of in-line coagulation/ultrafiltration membrane process attributed to coagulation condition optimization for irreversible fouling control." *Water (Switzerland)*, 10 (8). https://doi.org/10.3390/w10081076.

Zhao, C., T. Song, Y. Yu, L. Qu, J. Cheng, W. Zhu, Q. Wang, P. Li, and W. Tang. 2020. "Insight into the influence of humic acid and sodium alginate fractions on membrane fouling in coagulation-ultrafiltration combined system." *Environmental Research*, 191: 110228. https://doi.org/10.1016/j.envres.2020.110228.

CHAPTER 8

General Conclusions and Directions for Future Research

This chapter presents the most significant findings from the research performed as a part of this thesis as well as some potential directions for future research. The reader is referred to the conclusions section of each individual chapter for more specific conclusions pertaining to the work.

8.1. General Conclusions and Engineering Significance

Chapter 3 and Chapter 4 investigated the influence of membrane type on the performance of alternative coagulation pretreatment strategies for a colored river water. The principal finding from this work was that the optimal low-pressure membrane (LPM) pretreatment strategy depends on the membrane type (i.e., material and configuration). While, in Chapter 3, coagulation strategies with clarification (i.e., CF-DAF or CF-SED) provided superior performance, inline coagulation (C-IN) resulted in the lowest fouling potential for the identical colored water when membrane type was switched from outside-in hollow-fiber polyvinylidene fluoride (PVDF) to inside-out polyethersulfone (PES) tubular multichannel. These findings demonstrate that the effectiveness of a given pretreatment strategy cannot be determined solely from feedwater characteristics but must also be evaluated in the context of the membrane being used.

Although membrane suppliers commonly propose treatment configurations based on raw water quality characteristics and historical performance data from their existing installations, the results of this research demonstrate that membrane performance is governed by complex interactions between the membrane surface chemistry and the feedwater composition. Consequently, reliance on generalized design recommendations likely will not necessarily produce optimal outcomes. Preliminary testing can provide significant economic benefits by identifying opportunities to implement simpler and less costly pretreatment approaches, such as C-IN, in place of coagulation processes requiring clarification. Conversely, where clarification is necessary to achieve sustainable fouling control, failure to identify this requirement during the conceptual

and/or detailed design phase may result in increased operational risk, unanticipated capital expenditures, and substantial challenges associated with retrofitting treatment infrastructure within existing plant footprints and hydraulic constraints.

Chapter 5 and Chapter 6 focused on developing a bench-scale system capable of performing continuous-flow coagulation, which was required to investigate phased-inline coagulation (C-IN-P). In Chapter 5, helically coiled tube flocculators (HCTFs) were investigated as a promising strategy to achieve improved mixing during flocculation under low-flowrate conditions. While the impact of helical geometry was systematically assessed using a replicated full-factorial design, the hydrodynamic characteristics of flow, namely the Reynolds number, had the greatest impact on the properties of flocs formed by HCTFs. These findings indicate that future HCTF design should be guided primarily by hydrodynamic considerations rather than geometric characteristics alone. According to the results of this study, the Reynolds number should be the basis for design of future HCTFs with pipe sizing selected to provide a Reynolds number, Dean number, and mean velocity gradient near 67, 15 and 30 s^{-1}, respectively, conditions which were optimal for floc growth.

Chapter 6 extended the work of Chapter 5 by comparing the performance of HCTFs to alternative continuous-flow hydraulic flocculator types and developing a novel small-scale inline rapid mixer. The rapid mixer developed in this study overcame the key limitation of previous approaches by providing effective coagulation without requiring large volumes of water. This represents one of the main contributions of this thesis.

A key finding of the work from Chapter 6 was that the choice of coagulant mixing strategy used to conduct C-IN at bench-scale significantly impacted the observed fouling potential, even when identical coagulation chemistries and membrane types were employed. Incorporating rapid mixing upstream flocculation significantly improved coagulation performance under low-Reynolds flow conditions and had a greater impact on floc properties than hydraulic flocculator type. Across the four continuous-flow flocculator types considered in this research, combined rapid mixing and flocculation generated larger sized flocs than either rapid mixing or flocculation alone.

Although batch coagulation has been widely used in previous studies, the results of this research indicate that it may not be appropriate for future LPM studies intended to investigate continuous-flow coagulation/flocculation pretreatment. Batch mixing produced flocs with

different characteristics from those formed under continuous-flow conditions, resulting in altered membrane fouling. These findings emphasize that mixing strategy can itself introduce significant experimental bias and may influence the conclusions drawn regarding pretreatment performance. Consequently, greater consideration should be devoted to the design and selection of coagulant mixing systems during experimental planning. Extreme caution must be exercised in the comparison of results from various studies in the literature as the findings from the present work suggest that reported performance differences may arise not only as a result of altered system operation, but also from the employed mixing strategy. The substantially altered experimental outcomes with changing mixing configuration highlight the need for a more standardized experimental approach to reduce the uncertainty in the comparison of results between studies.

Chapter 7 compared the performance of C-IN-P pretreatment to C-IN across three different synthetic water types and a range of coating index (C-IDX) values. For the three synthetic challenge waters considered in this work, C-IN-P could achieve coagulant savings of 25-50% with essentially no changes in the degree of LPM fouling and only minimal/small decreases in permeate quality. This represents a promising alternative for full-scale plants to achieve their goals of improved process sustainability and reduced operating expenses (due to lower coagulant demand and lower sludge processing requirements). The effectiveness of C-IN-P, however, was not equally effective for all three water types: even with coagulant addition for 75% of the cycle, C-IN-P was unable to achieve comparable fouling mitigation and organics reduction as continuous C-IN for the low SUVA water. Furthermore, while some previous authors suggested that optimal LPM operation in terms of fouling mitigation and reduced OPEX could be achieved near C-IDXs of 20-25 mg m^{-2}, this work indicated that higher values were required for effective fouling mitigation across the three different synthetic water types.

Finally, although the C-IDX may be a useful tool for C-IN-P operational control, experiments using the high SUVA water demonstrated that it is insufficient to fully characterize process behaviour. Despite maintaining a constant C-IDX, membrane fouling varied significantly with both the dosing strategy (i.e., the combination of coagulant dose and dosing time) as well as the coagulant type (Alum and ACH in this study). Optimal C-IDX values are therefore not universal, but instead correspond to a range of possible fouling outcomes that are dependent on raw water quality, coagulant dose, dosing time, coagulant type, and likely the membrane

characteristics. Thus, preliminary testing is required to determine the optimal C-IDX for the membrane, water quality, and coagulant being considered.

8.2. Recommendations for Future Research

1. Comparison of CF-DAF and CF-SED Pretreatment Strategies

Given that CF-DAF yielded the best performance for the PVDF membrane investigated in this research, and the relative dearth of studies on its application for LPM pretreatment, further investigation of this approach is warranted. A key priority is the assessment of long-term process robustness under highly variable water quality conditions, particularly during algal bloom events. Specifically, future studies should determine whether continuous optimization is required during such events or whether CF-DAF systems are robust enough to satisfy water quality and fouling objectives during all water quality events under normal operating conditions.

The present work, together with several previous studies from our research group using the same source water, have consistently demonstrated enhanced removal of hydrophobic organic matter by CF-DAF compared to CF-SED. It would be of interest for a future study to directly compare the removals of different organic fractions by CF-DAF and CF-SED using advanced organic characterization techniques (e.g., LC-OCD and FEEM) for identical coagulation chemistry and mixing conditions so that any resulting differences in removals can be attributed solely to the difference in separation mechanism. Using a mass balance approach and these same advanced organic characterization techniques, the differences in removal of the various organic fractions could be related to the observed LPM fouling and permit identification of the key hydraulically reversible and irreversible foulants. Additional work could be performed to evaluate whether the alteration of key DAF operating parameters (i.e., recycle ratio, saturator pressure and separation zone contact time) significantly impacts the removal of the key foulant fraction, to inform on DAF system optimization for implementation as part of an integrated DAF-LPM system.

2. Bench-Scale Continuous-Flow Coagulation System Development

Based on the significantly altered floc properties and membrane fouling characteristics generated by intensive batch mixing for long periods compared to those generated by continuous-flow inline coagulation/flocculation, it is recommended that future studies should not use batch mixing approaches for investigating LPM fouling following coagulation pretreatment. Future research should focus on evaluating the scalability of the HCTF design guidelines presented in this thesis using pilot-scale systems. Additionally, by considering pipe diameter as a variable of interest in the present work, the impact of system hydrodynamics became convoluted with the hydraulic retention time (HRT) – future studies should investigate the impact of Reynolds number and HRT independently

Several other important research needs emerged from this work. First, detailed characterization of membrane cake layers should be undertaken to establish stronger mechanistic links between the observed LPM fouling and the disparate floc properties formed using different coagulant mixing strategies. Second, future investigations should directly compare fouling behavior observed in full-scale and pilot-scale systems with that measured in bench-scale simulations employing both batch and continuous-flow coagulation approaches. Such work would help identify the bench-scale methodologies that most accurately replicate full-scale performance. Finally, it would be valuable to ascertain whether the most appropriate bench-scale simulation strategy depends on the specific mixing configuration employed at full scale.

3. C-IN-P Pretreatment for LPMs

Future research should focus on improving the understanding of the specific organic fractions governing membrane fouling during C-IN-P pretreatment. Based on results of the FEEM analysis, polysaccharides, not proteins, were the critical biopolymer fraction for this membrane type, however, the relative importance of the polysaccharides should be confirmed using natural waters and advanced organic characterization techniques.

Across the three synthetic water types, effective fouling mitigation for C-IN-P pretreatment necessitated 60-70% removal of the combined humic acid and sodium alginate

fraction. This suggests that removal targets for critical foulant fractions may provide a more meaningful basis for process optimization (i.e., C-IDX selection) than bulk water quality parameters alone, however, additional research using natural waters containing recalcitrant NOM fractions is required to determine the broader applicability of this proposed threshold.

For the H-SUVA water and a fixed C-IDX, membrane fouling was significantly influenced by both the dosing strategy (i.e., the combination of coagulant dose and dosing duration) and the coagulant type (Alum and ACH). This is despite similar removals of bulk organic matter and specific organic foulants across all dosing strategies, suggesting that variations in cake layer properties, rather than differences in organic removal, were responsible for the observed performance differences. Future research should therefore investigate how changes in dosing strategy influence cake layer characteristics and how these characteristics relate to membrane fouling behavior. Particular attention should also be given to determining whether significant changes in cake layer structure occur as C-IDX decreases from optimal values to the lower ranges associated with accelerated fouling.

Due to the significant challenges that the low hydrophobicity water presented in terms of organics reduction and fouling mitigation for C-IN-P at all C-IDX values, further optimization is required for theses water types. Previous authors have reported that biopolymers require elevated coagulant dosages for effective removal, while others have shown that ultra-low coagulant addition can alter the biopolymer conformation or interaction with the membrane surface, reducing fouling. Based on these, a novel coagulation strategy termed stepped-inline coagulation (C-IN-S) was proposed whereby the coagulant dose is reduced, not set to zero, in the latter portion of the filtration cycle. Based on the results of the present study and those of previous authors, the novel C-IN-S approach may be able to more effectively manage low SUVA waters by integrating a higher initial dose with a sustained low-level addition during the latter portion of the cycle. However this hypothesis must be tested. Furthermore, it should be confirmed whether low-dose addition in the latter portion of the cycle is sufficient for effective fouling mitigation or whether the dose must be adjusted to maintain a C-IDX corresponding to the aforementioned 60-70% removal threshold for humics and polysaccharides. Finally, it would be of interest to develop an adaptive operational control tool (perhaps using artificial intelligence based approaches) for the integrated C-IN-S-LPM system. The intent of this predictive model would be to provide dynamic operation by

forecasting at what point during the filtration cycle the coagulant dose needs to be reduced, and by how much, in order to achieve optimal C-IN-S operation in the face of variable feedwater quality.

4. *Irreversible Fouling for Bench-Scale LPM Studies*

For both the C-IN tests performed in Chapter 6 as well as the C-IN-P studies performed as a part of Chapter 7, FR_{hirr} was found to be low and the 95% confidence intervals mostly included zero within their range. As hydraulically irreversible fouling is a key driver of long-term OPEX for LPM facilities, future work should focus on the development of alternative bench-scale testing systems and procedures to permit realistic assessment of LPM irreversible fouling development in bench-scale studies.

APPENDIX A

Supplemental Information for Chapter 2

Context: This appendix presents supporting information associated with Chapter 2 of this thesis – the literature review.

A.1. Fouling Data for Type III C-IN-Studies

Table A-1. Results of Selected Type III C-IN Studies Using Synthetic Challenge Waters.

Bench Scale - Synthetic													
	Coagulation Conditions			Floc Characteristics			Fouling Measures						
Material Config. NPS/MWCO	Type	Dose (mg L^{-1} metal)	pH	D_f	Mean Size (μm)	ZP (mV)	$(J/J_0)/t$ (h^{-1})	$(J/J_0)/V$ (mL^{-1})	α ($\times10^{12}$ m/kg)	R_{irr} ($\times10^{11}$ m^{-1})	R_r ($\times10^{11}$ m^{-1})	Ref.
PVDF FS 100 kDa	$AlCl_3$	0.067	7	N/A	N/A	N/A	1.33	0.87	N/A	N/A	N/A	Ma et al. (2014)
	$AlCl_3$	0.2	7	N/A	N/A	N/A	1.49	0.97	N/A	N/A	N/A	
	$AlCl_3$	0.27	7	N/A	N/A	N/A	1.85	1.2	N/A	N/A	N/A	
	$AlCl_3$	0.54	7	N/A	N/A	N/A	1.69	1.1	N/A	N/A	N/A	
	$AlCl_3$	0.81	7	N/A	N/A	N/A	1.54	1	N/A	N/A	N/A	
	$AlCl_3$	0.067	7	N/A	N/A	N/A	1.44	0.87	N/A	N/A	N/A	
	$AlCl_3$	0.0094	7	N/A	N/A	N/A	1.72	1.03	N/A	N/A	N/A	
	$AlCl_3$	0.135	7	N/A	N/A	N/A	1.94	1.17	N/A	N/A	N/A	
	$AlCl_3$	0.27	7	N/A	N/A	N/A	1.56	0.93	N/A	N/A	N/A	
	$AlCl_3$	0.54	7	N/A	N/A	N/A	1.28	0.77	N/A	N/A	N/A	
	$AlCl_3$	0.027	7	N/A	N/A	N/A	2.1	1.17	N/A	N/A	N/A	
	$AlCl_3$	0.067	7	N/A	N/A	N/A	2.58	1.43	N/A	N/A	N/A	
	$AlCl_3$	0.135	7	N/A	N/A	N/A	3.24	1.8	N/A	N/A	N/A	
	$AlCl_3$	0.27	7	N/A	N/A	N/A	2.22	1.23	N/A	N/A	N/A	
	$AlCl_3$	0.540	7	N/A	N/A	N/A	1.56	0.87	N/A	N/A	N/A	
	$AlCl_3$	0.0067	6	N/A	N/A	N/A	1.54	1	N/A	N/A	N/A	
	$AlCl_3$	0.067	6	N/A	N/A	N/A	1.85	1.2	N/A	N/A	N/A	
	$AlCl_3$	0.14	6	N/A	N/A	N/A	2.05	1.33	N/A	N/A	N/A	
	$AlCl_3$	0.270	6	N/A	N/A	N/A	1.90	1.23	N/A	N/A	N/A	
	$AlCl_3$	1.35	6	N/A	N/A	N/A	0.92	0.6	N/A	N/A	N/A	
	$AlCl_3$	0.0067	6	N/A	N/A	N/A	1.98	1.1	N/A	N/A	N/A	
	$AlCl_3$	0.067	6	N/A	N/A	N/A	2.16	1.2	N/A	N/A	N/A	
	$AlCl_3$	0.14	6	N/A	N/A	N/A	2.34	1.3	N/A	N/A	N/A	
	$AlCl_3$	0.27	6	N/A	N/A	N/A	2.1	1.17	N/A	N/A	N/A	
	$AlCl_3$	1.35	6	N/A	N/A	N/A	1.86	1.03	N/A	N/A	N/A	
	$AlCl_3$	0.027	6	N/A	N/A	N/A	1.61	0.97	N/A	N/A	N/A	
	$AlCl_3$	0.067	6	N/A	N/A	N/A	2.44	1.47	N/A	N/A	N/A	
	$AlCl_3$	0.14	6	N/A	N/A	N/A	4.22	2.53	N/A	N/A	N/A	
	$AlCl_3$	0.54	6	N/A	N/A	N/A	2.56	1.53	N/A	N/A	N/A	

	$AlCl_3$	1.35	6	N/A	N/A	N/A	1.17	0.7	N/A	N/A	N/A	
	$AlCl_3$	0.0067	8	N/A	N/A	N/A	1.39	0.83	N/A	N/A	N/A	
	$AlCl_3$	0.067	8	N/A	N/A	N/A	1.61	0.97	N/A	N/A	N/A	
	$AlCl_3$	0.27	8	N/A	N/A	N/A	1.83	1.1	N/A	N/A	N/A	
	$AlCl_3$	0.54	8	N/A	N/A	N/A	1.56	0.93	N/A	N/A	N/A	
	$AlCl_3$	8.09	8	N/A	N/A	N/A	1.28	0.77	N/A	N/A	N/A	
	$AlCl_3$	0.0067	8	N/A	N/A	N/A	1.17	0.7	N/A	N/A	N/A	
	$AlCl_3$	0.13	8	N/A	N/A	N/A	1.72	1.03	N/A	N/A	N/A	
	$AlCl_3$	0.27	8	N/A	N/A	N/A	1.94	1.17	N/A	N/A	N/A	
	$AlCl_3$	0.54	8	N/A	N/A	N/A	1.61	0.97	N/A	N/A	N/A	
	$AlCl_3$	2.7	8	N/A	N/A	N/A	1.33	0.8	N/A	N/A	N/A	
	$AlCl_3$	0.0067	8	N/A	N/A	N/A	1.28	0.83	N/A	N/A	N/A	
	$AlCl_3$	0.013	8	N/A	N/A	N/A	1.64	1.07	N/A	N/A	N/A	
	$AlCl_3$	0.27	8	N/A	N/A	N/A	1.74	1.13	N/A	N/A	N/A	
	$AlCl_3$	0.54	8	N/A	N/A	N/A	1.59	1.03	N/A	N/A	N/A	
	$AlCl_3$	0.81	8	N/A	N/A	N/A	1.33	0.87	N/A	N/A	N/A	
PES FS 100 kDa	Al_a	6	N/A	2.16	221	N/A	0.21	N/A	N/A	N/A	N/A	Feng et al. (2015)
	Al_b	6	N/A	2.45	167	N/A	0.21	N/A	N/A	N/A	N/A	
	Al_c	6	N/A	1.82	211	N/A	0.22	N/A	N/A	N/A	N/A	
PVDF FS 0.22 µm	Alum	10	7	2.13	N/A	-13.2	N/A	2.10	N/A	N/A	N/A	Wang et al. (2010)
	Alum	20	7	2.73	N/A	-4.94	N/A	1.38	0.0000275	N/A	N/A	
	Alum	40	7	2.74	N/A	5.12	N/A	1.5	0.0000254	N/A	N/A	
	Alum	60	7	2.74	N/A	4.65	N/A	1.67	0.0000251	N/A	N/A	
	Alum	100	7	2.74	N/A	5	N/A	1.95	0.0000321	N/A	N/A	
	Alum	10	5	2.7	N/A	-12.3	N/A	1.40	0.0000362	N/A	N/A	
	Alum	20	5	2.61	N/A	-5.76	N/A	1.12	0.0000169	N/A	N/A	
	Alum	40	5	2.6	N/A	7.11	N/A	1.05	0.0000130	N/A	N/A	
	Alum	60	5	1.54	N/A	13.9	N/A	1.83	0.0000450	N/A	N/A	
	Alum	100	5	1.43	N/A	19		1.95	0.0000334	N/A	N/A	
PVDF FS 0.22 µm	$FeCl_3$	11.2	7.14	2.45	N/A	-22.6	0.82	3.65	N/A	N/A	N/A	Wang et al. (2013)
	$FeCl_3$	22.3	6.6	2.47	N/A	-9.9	0.67	3	N/A	N/A	N/A	
	$FeCl_3$	33.5	6.21	2.51	N/A	-8.8	0.61	2.74	N/A	N/A	N/A	
	$FeCl_3$	44.68	5.5	2.29	N/A	12.2	0.63	2.83	N/A	N/A	N/A	
	$FeCl_3$	55.9	3.9	1.86	N/A	43.1	0.88	3.96	N/A	N/A	N/A	
	Fe_2SO_4	11.2	7	1.68	N/A	-34.2	0.87	3.91	N/A	N/A	N/A	
	Fe_2SO_4	22.3	6.4	2.59	N/A	-16.3	0.76	3.39	N/A	N/A	N/A	
	Fe_2SO_4	33.5	6.05	2.6	N/A	-10.8	0.62	2.79	N/A	N/A	N/A	

	Fe_2SO_4	44.68	5.3	2.58	N/A	4.12	0.57	2.57	N/A	N/A	N/A	
	Fe_2SO_4	55.9	4.8	2.46	N/A	6.85	0.65	2.91	N/A	N/A	N/A	
PVDF FS 0.1 μm	$FeCl_3$	0.1mM	6.54	N/A	N/A	-65.8	N/A	N/A	165	N/A	N/A	Chen et al. (2020)
	$FeCl_3$	0.2mM	5.75	N/A	N/A	-64.2	N/A	N/A	155	N/A	N/A	
	$FeCl_3$	0.3mM	5.5	N/A	N/A	-66.2	N/A	N/A	140	N/A	N/A	
	$FeCl_3$	0.4mM	5.08	N/A	N/A	-63.4	N/A	N/A	134	N/A	N/A	
	$FeCl_3$	0.5mM	4.93	N/A	N/A	-55.2	N/A	N/A	1300	N/A	N/A	
	$FeCl_3$	1mM	3.79	N/A	N/A	-45.5	N/A	N/A	1230	N/A	N/A	
	$FeCl_3$	1.5mM	3.46	N/A	N/A	-26.9	N/A	N/A	78.0	N/A	N/A	
	$FeCl_3$	2mM	3.12	N/A	N/A	-12.9	N/A	N/A	1.38	N/A	N/A	
	$FeCl_3$	2.5mM	3.04	N/A	N/A	5.97	N/A	N/A	2.00	N/A	N/A	
PVDF FS 0.1 μm	PACl	1.1mM	N/A	N/A	N/A	-69.9	N/A	N/A	277	N/A	N/A	Long et al. (2021)
	PACl	2.2mM	N/A	N/A	N/A	-55.3	N/A	N/A	233	N/A	N/A	
	PACl	3.3mM	N/A	N/A	N/A	-41.7	N/A	N/A	220	N/A	N/A	
	PACl	4.4mM	N/A	N/A	N/A	-38.7	N/A	N/A	70.0	N/A	N/A	
	PACl	5.6mM	N/A	N/A	N/A	-4.89	N/A	N/A	3.00	N/A	N/A	
	PACl	1.1mM	N/A	N/A	N/A	-56	N/A	N/A	393	N/A	N/A	
	PACl	2.2mM	N/A	N/A	N/A	-41	N/A	N/A	17.8	N/A	N/A	
	PACl	3.3mM	N/A	N/A	N/A	-13.9	N/A	N/A	5.00	N/A	N/A	
	PACl	4.4mM	N/A	N/A	N/A	-10.9	N/A	N/A	1.00	N/A	N/A	
	PACl	5.6mM	N/A	N/A	N/A	7.22	N/A	N/A	1.00	N/A	N/A	
	PACl	1.1mM	N/A	N/A	N/A	-17	N/A	N/A	10.5	N/A	N/A	
	PACl	2.2mM	N/A	N/A	N/A	-9.6	N/A	N/A	1.00	N/A	N/A	
	PACl	3.3mM	N/A	N/A	N/A	-8.7	N/A	N/A	1.00	N/A	N/A	
	PACl	4.4mM	N/A	N/A	N/A	-2.87	N/A	N/A	1.00	N/A	N/A	
	PACl	5.6mM	N/A	N/A	N/A	15.1	N/A	N/A	1.00	N/A	N/A	
RC FS 10 kDa	PACl	6	6.45	0.879 (2D)	4.99	N/A	0.0088	N/A	N/A	N/A	N/A	Ren et al. (2021)
	PACl	6	6.48	0.977 (2D)	3.12	N/A	0.014	N/A	N/A	N/A	N/A	
	PACl	6	6.19	0.816 (2D)	7.54	N/A	0.016	N/A	N/A	N/A	N/A	
RC FS 100 kDa	Al_a	3.375	N/A	2.62	1.38	-9.34	0.59	N/A	N/A	620	N/A	Yan et al. (2021)
	Al_b	3.375	N/A	2.59	1.18	-10	0.58	N/A	N/A	130	N/A	
	Al_c	3.375	N/A	2.56	1.26	-12.9	0.56	N/A	N/A	380	N/A	
	Al_a- P	3.375	N/A	2.7	1.39	-9.32	0.61	N/A	N/A	540	N/A	
	Al_b- P	3.375	N/A	2.6	1.38	-12.2	0.58	N/A	N/A	290	N/A	
	Al_c- P	3.375	N/A	2.61	1.23	-14.2	0.7	N/A	N/A	160	N/A	
	Al_a	3.375	N/A	2.67	N/A	N/A	0.55	N/A	N/A	N/A	N/A	

	Al_a	3.375	N/A	2.49	N/A	N/A	0.49	N/A	N/A	N/A	N/A	
	Al_a- P	3.375	N/A	2.58	N/A	N/A	0.56	N/A	N/A	N/A	N/A	
	Al_a- P	3.375	N/A	2.49	N/A	N/A	0.63	N/A	N/A	N/A	N/A	
PVDF FS 0.1 μm	PACl	50 (as PACl)	5.9	N/A	52.6	-70.8	N/A	N/A	1200	N/A	N/A	Teng et al. (2020)
	PACl	100 (as PACl)	5.6	N/A	305	-62.4	N/A	N/A	1400	N/A	N/A	
	PACl	150 (as PACl)	5.1	N/A	486	-58.9	N/A	N/A	1000	N/A	N/A	
	PACl	200 (as PACl)	4.8	N/A	435	-56.7	N/A	N/A	960	N/A	N/A	
	PACl	250 (as PACl)	4.7	N/A	477	-51.1	N/A	N/A	620	N/A	N/A	
	PACl	300 (as PACl)	4.3	N/A	480	-47.5	N/A	N/A	560	N/A	N/A	
	PACl	350 (as PACl)	4	N/A	441	-41.3	N/A	N/A	430	N/A	N/A	
	PACl	400 (as PACl)	3.4	N/A	411	-8.45	N/A	N/A	4.00	N/A	N/A	
	PACl	450 (as PACl)	3.5	N/A	471	-7.63	N/A	N/A	4.00	N/A	N/A	
	PACl	500 (as PACl)	3.5	N/A	495	-2.21	N/A	N/A	3.85	N/A	N/A	
PVDF FS 0.1 μm	PAM	10 (as polymer)	6.3	N/A	N/A	-68.4	N/A	N/A	305	N/A	N/A	Long et al. (2020)
	PAM	15 (as polymer)	6.23	N/A	N/A	-65.9	N/A	N/A	285	N/A	N/A	
	PAM	20 (as polymer)	6.15	N/A	N/A	-64.9	N/A	N/A	279	N/A	N/A	
	PAM	25 (as polymer)	6.21	N/A	N/A	-67.1	N/A	N/A	285	N/A	N/A	
	PAM	30 (as polymer)	6.35	N/A	N/A	-70	N/A	N/A	315	N/A	N/A	
	PAM	40 (as polymer)	6.33	N/A	N/A	-72.1	N/A	N/A	330	N/A	N/A	
	PAM	50 (as polymer)	6.4	N/A	N/A	-73.4	N/A	N/A	355	N/A	N/A	
PES FS 50 kDa	Alum	70 (as alum)	5.5	2.56	303	N/A	N/A	0.31	31.0	N/A	N/A	Amjad et al. (2015)
	Alum	70 (as alum)	5.5	2.46	222	N/A	N/A	0.37	31.7	N/A	N/A	

	Alum	70 (as alum)	4.8	1.95		N/A	N/A	0.25	31.7	N/A	N/A	
PVDF FS 0.1 μm	$FeCl_3$	5.58	N/A	N/A	2.16	-77.7	N/A	N/A	240	N/A	N/A	You et al. (2021)
	$FeCl_3$	5.58	N/A	N/A	0.98	-33.1	N/A	N/A	2440	N/A	N/A	
	$FeCl_3$	5.58	N/A	N/A	0.92	-26.8	N/A	N/A	4870	N/A	N/A	
	$FeCl_3$	5.58	N/A	N/A	0.86	-26.8	N/A	N/A	5160	N/A	N/A	
	$FeCl_3$	5.58	N/A	N/A	0.86	-26.4	N/A	N/A	5460	N/A	N/A	
	$FeCl_3$	111.7	N/A	N/A	58.3	-9.6	N/A	N/A	2.25	N/A	N/A	
	$FeCl_3$	111.7	N/A	N/A	52.5	-8.9	N/A	N/A	2.45	N/A	N/A	
	$FeCl_3$	111.7	N/A	N/A	50	-9.95	N/A	N/A	3.20	N/A	N/A	
	$FeCl_3$	111.7	N/A	N/A	46.7	-9.78	N/A	N/A	3.70	N/A	N/A	
	$FeCl_3$	111.7			46.4	-9.95			3.60			
PES FS 100 kDa	Alum	0.59	7.47	N/A	N/A	-22.6	N/A	N/A	N/A	1.5	N/A	Choi and Dempsey (2004)
	Alum	0.59	8.73	N/A	N/A	-24.2	N/A	N/A	N/A	0.043	N/A	
	Alum	1.17	4.81	N/A	N/A	-11.9	N/A	N/A	N/A	0.064	N/A	
	Alum	1.76	5.27	N/A	N/A	-4.6	N/A	N/A	N/A	0.25	N/A	
	Alum	2.34	6.78	N/A	N/A	-1	N/A	N/A	N/A	0.18	N/A	
	Alum	2.93	7.14	N/A	N/A	2.7	N/A	N/A	N/A	0.18	N/A	
				N/A	N/A		N/A	N/A	N/A		N/A	
PES FS 100 kDa	PACl	0.025 mM	N/A	1.82 (2D)	130	-20	N/A	0.26	N/A	N/A	N/A	Yao et al. (2015)
	PACl	0.1 mM	N/A	1.87 (2D)	155	-13.7	N/A	0.23	N/A	N/A	N/A	
	PACl	0.025 mM	N/A	1.79 (2D)	145	-16.9	N/A	0.2	N/A	N/A	N/A	
	PACl	0.025 mM	N/A	1.77 (2D)	164	-13.2	N/A	0.17	N/A	N/A	N/A	
	PACl	0.025 mM	N/A	1.74 (2D)	172	-11.7	N/A	0.14	N/A	N/A	N/A	
	PACl	0.1 mM	N/A	1.85 (2D)	162	-11.1	N/A	0.27	N/A	N/A	N/A	
	PACl	0.1 mM	N/A	1.83 (2D)	167	-6.48	N/A	0.29	N/A	N/A	N/A	
	PACl	0.1 mM	N/A	1.82 (2D)	182	-3.19	N/A	0.30	N/A	N/A	N/A	
PES FS 100 kDa	PACl	2.16	N/A	1.59 (2D)	36.5	N/A	N/A	0.14	N/A	N/A	N/A	Nan et al. (2016)
	PACl	2.16	N/A	1.63 (2D)	55.1	N/A	N/A	0.125	N/A	N/A	N/A	
	PACl	2.16	N/A	1.73 (2D)	73.1	N/A	N/A	0.1	N/A	N/A	N/A	
	PACl	2.16	N/A	1.84 (2D)	81.1	N/A	N/A	0.083	N/A	N/A	N/A	
	PACl	2.16	N/A	1.47 (2D)	62.9	N/A	N/A	0.05	N/A	N/A	N/A	
	PACl	2.16	N/A	1.53 (2D)	70.7	N/A	N/A	0.083	N/A	N/A	N/A	
	PACl	2.16	N/A	1.57 (2D)	92.1	N/A	N/A	0.1	N/A	N/A	N/A	
PES FS 100 kDa	$AlCl_3$	0.3 mM	6	1.98	60.3	N/A	1.24	N/A	N/A	N/A	N/A	Ma et al. (2017)

$AlCl_3$	0.3 mM	7	2.32		N/A	1.71	N/A	N/A	N/A	N/A
$AlCl_3$	0.3 mM	8	2.45	422.3	N/A	2.06	N/A	N/A	N/A	N/A
$AlCl_3$	0.3 mM	6	N/A	N/A	N/A	1.12	N/A	N/A	N/A	N/A
$AlCl_3$	0.3 mM	7	N/A	N/A	N/A	1.29	N/A	N/A	N/A	N/A
$AlCl_3$	0.3 mM	8	N/A	N/A	N/A	1.59	N/A	N/A	N/A	N/A

Note: Al_a-P = Al_a- PolyDMDAAC; FS = flat sheet; MWCO = molecular weight cutoff; NPS = nominal pore size; PAM = polyacrylamide; PES = polyethersulfone; PVDF = polyvinylidene fluoride; RC = regenerate cellulose;

Table A-2. Results of Selected Type III C-IN Studies Using Natural Challenge Waters.

Bench Scale – Real Waters											
	Water Quality		Coagulation Conditions		Floc Characteristics			Fouling Measures			
Material Config. NPS/MWCO	Water Source	SUVA (L/mg/m)	Type	Dose (mg L^{-1} metal)	D_f	Mean Size (μm)	ZP (mV)	(J/J_0)	$(J/J_0)/t$ (1/h)	α ($\times 10^{11}$ m/kg)	Ref.
RC FS	River	1.21-1.40	PACl	1.35	N/A	N/A	N/A	N/A	0.80	N/A	Jung and Kang (2003)
RC FS		1.21-1.40	Alum	1.35	N/A	N/A	N/A	N/A	0.94	N/A	
PS FS		1.21-1.40	PACl	1.35	N/A	N/A	N/A	N/A	1.21	N/A	
PS FS		1.21-1.40	Alum	1.35	N/A	N/A	N/A	N/A	1.26	N/A	
RC FS		1.21-1.40	PACl	1.35	N/A	N/A	N/A	N/A	0.74	N/A	
RC FS		1.21-1.40	Alum	1.35	N/A	N/A	N/A	N/A	0.97	N/A	
PS FS		1.21-1.40	PACl	1.35	N/A	N/A	N/A	N/A	1.18	N/A	
PS FS		1.21-1.40	Alum	1.35	N/A	N/A	N/A	N/A	1.23	N/A	
PVDF FS 0.22 μm	River	N/A	PACl	1.68	N/A	N/A	-0.5	N/A	1.17	N/A	Cho et al. (2006)
		N/A	PACl	1.68	2.3	49	-1.2	N/A	1.57	41.0	
		N/A	PACl	1.68	2.28	51	-0.8	N/A	1.53	37.0	
		N/A	PACl	1.68	2.05	63	-0.4	N/A	1.94	31.0	
		N/A	PACl	1.68	1.97	56	-1	N/A	1.79	25.0	
		N/A	PACl	1.68	1.92	55	-1.6	N/A	1.94	19.0	
		N/A	PACl	1.68	2.29	90	-1	N/A	1.61	9	
		N/A	PACl	1.68	2.22	102	-1.6	N/A	1.67	7	
		N/A	PACl	1.68	2.16	127	-0.7	N/A	1.69	5.5	
		N/A	PACl	1.68	1.95	282	-0.4	N/A	1.54	2.3	
		N/A	PACl	1.68	1.89	447	-5.4	N/A	1.29	1.4	
N/A FS 0.2 μm	River	2	PACl	2.12	1.64 (2D)	N/A	N/A	N/A	N/A	0.03	Choi et al. (2008)

	River	5.5	PACl	4.24	1.87 (2D)	N/A	N/A	N/A	N/A	0.29	
PS FS 100 kDa	River	2.3	$FeCl_3$	7.1	N/A	N/A	N/A	0.36	N/A	N/A	Howe et al. (2006)
		3.9	$Fe_2(SO_4)_3$	6.9	N/A	N/A	N/A	0.61	N/A	N/A	
		7.5	$Fe_2(SO_4)_3$	0.94	N/A	N/A	N/A	0.38	N/A	N/A	
		7.5	Alum	0.45	N/A	N/A	N/A	0.39	N/A	N/A	
PVDF FS 0.22 µm		2.5	Alum	0.7	N/A	N/A	N/A	0.44	N/A	N/A	
		3.6	Alum	2.3	N/A	N/A	N/A	0.16	N/A	N/A	
		7.5	$Fe_2(SO_4)_3$	0.94	N/A	N/A	N/A	0.11	N/A	N/A	
		7.5	Alum	0.45	N/A	N/A	N/A	0.09	N/A	N/A	
CA FS 0.2 µm	River	5.71	Alum	0.11 mM	N/A	N/A	N/A	N/A	N/A	0.59	Pikkarainen et al. (2004)
		5.71	Alum	0.22 mM	N/A	N/A	N/A	N/A	N/A	0.65	
		5.71	Alum	0.33 mM	N/A	N/A	N/A	N/A	N/A	0.7	
		5.71	PACl	0.15 mM	N/A	N/A	N/A	N/A	N/A	0.89	
		5.71	PACl	0.3 mM	N/A	N/A	N/A	N/A	N/A	1.36	
		5.71	PACl	0.45 mM	N/A	N/A	N/A	N/A	N/A	1.51	
		5.71	$Fe_2(SO_4)_3$	0.13 mM	N/A	N/A	N/A	N/A	N/A	1.07	
		5.71	$Fe_2(SO_4)_3$	0.22 mM	N/A	N/A	N/A	N/A	N/A	0.8	
		5.71	$Fe_2(SO_4)_3$	0.31 mM	N/A	N/A	N/A	N/A	N/A	0.94	
		5.71	$FeCl_3$	0.09 mM	N/A	N/A	N/A	N/A	N/A	0.87	
		5.71	$FeCl_3$	0.18 mM	N/A	N/A	N/A	N/A	N/A	1.02	
		5.71	$FeCl_3$	0.27 mM	N/A	N/A	N/A	N/A	N/A	1.06	
		5.71	Alum	0.11 mM	N/A	N/A	N/A	N/A	N/A	0.42	
		5.71	Alum	0.22 mM	N/A	N/A	N/A	N/A	N/A	0.65	
		5.71	Alum	0.33 mM	N/A	N/A	N/A	N/A	N/A	0.68	
		5.71	PACl	0.15 mM	N/A	N/A	N/A	N/A	N/A	0.89	
		5.71	PACl	0.3 mM	N/A	N/A	N/A	N/A	N/A	1.25	
		5.71	PACl	0.45 mM	N/A	N/A	N/A	N/A	N/A	1.70	
		5.71	$Fe_2(SO_4)_3$	0.13 mM	N/A	N/A	N/A	N/A	N/A	1.02	
		5.71	$Fe_2(SO_4)_3$	0.22 mM	N/A	N/A	N/A	N/A	N/A	0.75	
		5.71	$Fe_2(SO_4)_3$	0.31 mM	N/A	N/A	N/A	N/A	N/A	0.84	
		5.71	$FeCl_3$	0.09 mM	N/A	N/A	N/A	N/A	N/A	0.86	
		5.71	$FeCl_3$	0.18 mM	N/A	N/A	N/A	N/A	N/A	1.21	
		5.71	$FeCl_3$	0.27 mM	N/A	N/A	N/A	N/A	N/A	1.21	
		5.71	Alum	0.11 mM	N/A	N/A	N/A	N/A	N/A	0.47	
		5.71	Alum	0.22 mM	N/A	N/A	N/A	N/A	N/A	0.57	
		5.71	Alum	0.33 mM	N/A	N/A	N/A	N/A	N/A	0.81	
		5.71	PACl	0.15 mM	N/A	N/A	N/A	N/A	N/A	0.88	

		5.71	PACl	0.3 mM	N/A	N/A	N/A	N/A	N/A	1.06	
		5.71	PACl	0.45 mM	N/A	N/A	N/A	N/A	N/A	1.14	
		5.71	$Fe_2(SO_4)_3$	0.13 mM	N/A	N/A	N/A	N/A	N/A	1.02	
		5.71	$Fe_2(SO_4)_3$	0.22 mM	N/A	N/A	N/A	N/A	N/A	0.073	
		5.71	$Fe_2(SO_4)_3$	0.31 mM	N/A	N/A	N/A	N/A	N/A	4.23	
		5.71	$FeCl_3$	0.09 mM	N/A	N/A	N/A	N/A	N/A	1.09	
		5.71	$FeCl_3$	0.18 mM	N/A	N/A	N/A	N/A	N/A	1.27	
		5.71	$FeCl_3$	0.27 mM	N/A	N/A	N/A	N/A	N/A	1.23	
PVDF FS 150 kDa	River	1.7	Alum	4	N/A	N/A	N/A	N/A	0.055	N/A	Chen et al. (2007)
		1.7	Alum	10	N/A	N/A	N/A	N/A	0.038	N/A	

Note: CA = cellulose acetate; FS = flat sheet; MWCO = molecular weight cutoff; NPS = nominal pore size; PS = polysulfone; PVDF = polyvinylidene fluoride; RC = regenerate cellulose.

Fig. A.1 to Fig. A.3 present relationships between the removal of bulk organics by the C-IN-LPM system and the feed water pH, SUVA value, and coagulant type (i.e., Al- or Fe-based).

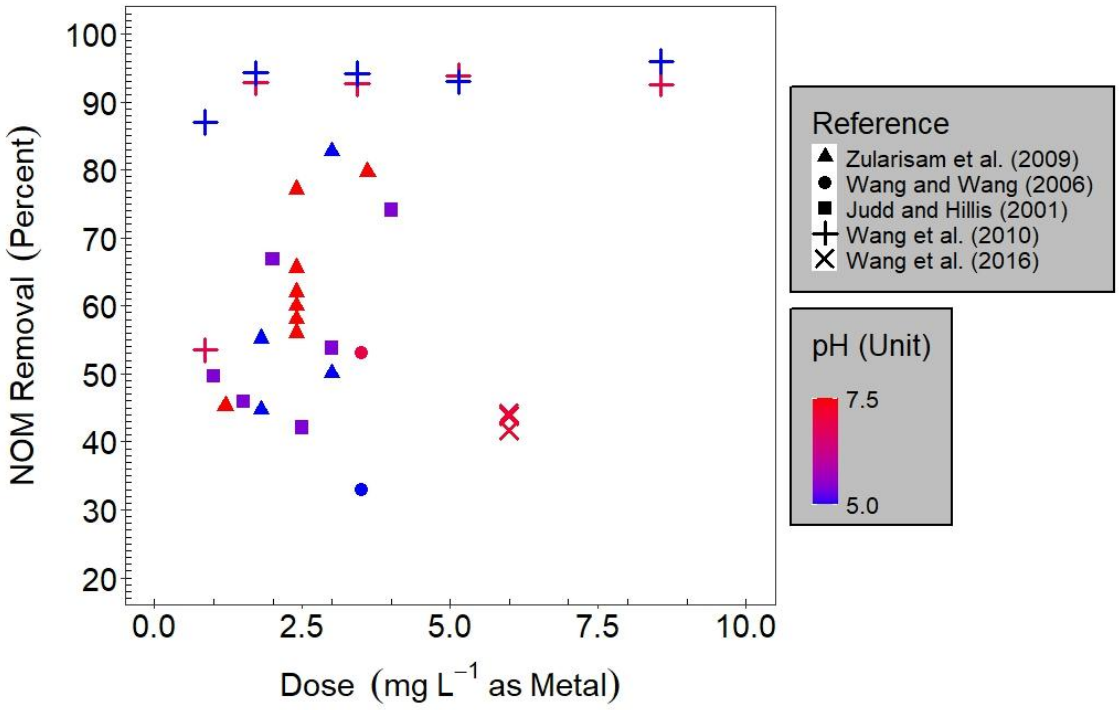


Fig. A.1. Relationship between applied coagulant dose, pH, and filtered removal of organics for pretreatment by Type I, Type II, and Type III C-IN. Note: References include Zularisam et al. (2009), (Wang and Wang 2006), Judd and Hillis (2001), Wang et al. (2010), and Wang et al. (2016),

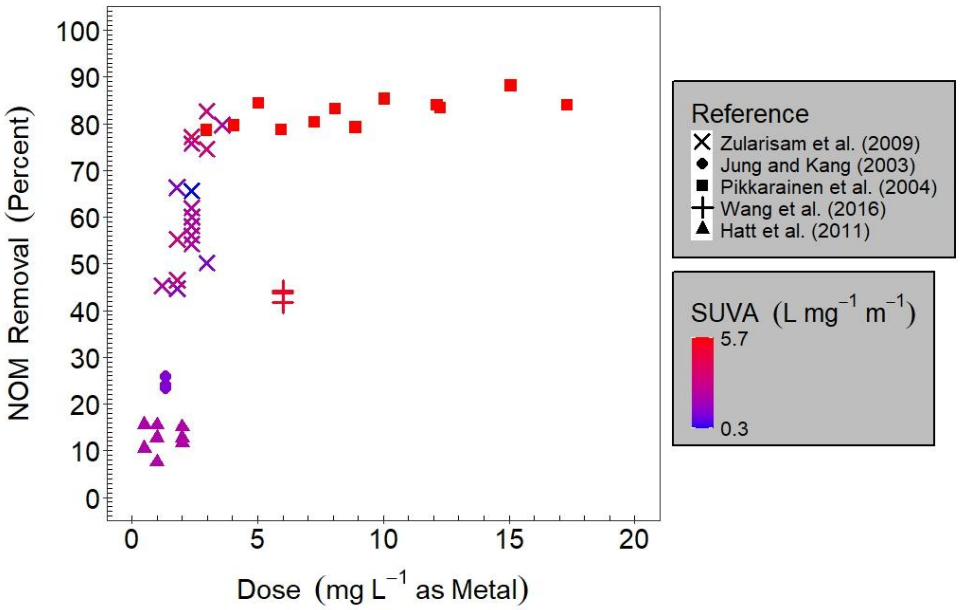


Fig. A.2. Relationship between applied coagulant dose, SUVA, and filtered removal of organics for pretreatment by Type I, Type II, and Type III C-IN. Note: References include Zularisam et al. (2009), Jung and Kang (2003), Pikkarainen et al. (2004), Wang et al. (2016), and Hatt et al. (2011)

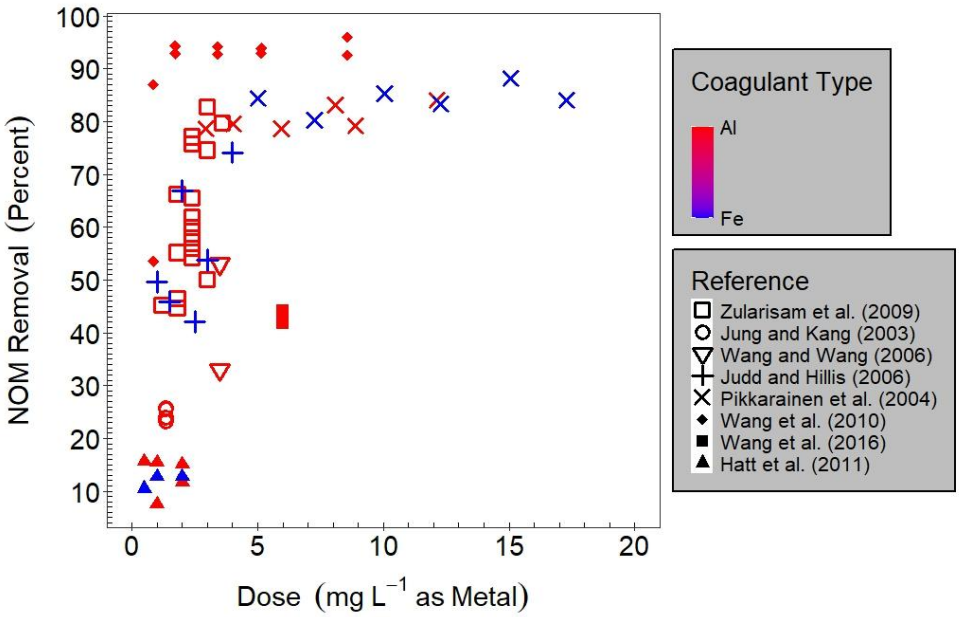


Fig. A.3. Relationship between applied coagulant dose, coagulant type, and filtered removal of organics for pretreatment by Type I, Type II, and Type III C-IN. Note: References include Zularisam et al. (2009), Jung and Kang (2003), Wang and Wang (2006), Judd and Hillis (2001), Pikkarainen et al. (2004), Wang et al. (2010), Wang et al. (2016), and Hatt et al. (2011).

A.2. References

Amjad, H., Z. Khan, and V. V. Tarabara. 2015. "Fractal structure and permeability of membrane cake layers: Effect of coagulation–flocculation and settling as pretreatment steps." *Separation and Purification Technology*, 143: 40–51. https://doi.org/10.1016/j.seppur.2015.01.020.

Chen, Y., B. Z. Dong, N. Y. Gao, and J. C. Fan. 2007. "Effect of coagulation pretreatment on fouling of an ultrafiltration membrane." *Desalination*, 204 (1-3 SPEC. ISS.): 181–188. https://doi.org/10.1016/j.desal.2006.04.029.

Chen, Y., J. Teng, B.-Q. Liao, R. Li, and H. Lin. 2020. "Molecular insights into the impacts of iron(III) ions on membrane fouling by alginate." *Chemosphere*, 242: 125232. https://doi.org/10.1016/j.chemosphere.2019.125232.

Cho, M.-H., C.-H. Lee, and S. Lee. 2006. "Effect of flocculation conditions on membrane permeability in coagulation–microfiltration." *Desalination*, 191 (1–3): 386–396. https://doi.org/10.1016/j.desal.2005.08.017.

Choi, K. Y. J., and B. A. Dempsey. 2004. "In-line coagulation with low-pressure membrane filtration." *Water Research*, 38 (19): 4271–4281. https://doi.org/10.1016/j.watres.2004.08.006.

Choi, Y. H., H. S. Kim, and J. H. Kweon. 2008. "Role of hydrophobic natural organic matter flocs on the fouling in coagulation-membrane processes." *Separation and Purification Technology*, 62 (3): 529–534. https://doi.org/10.1016/j.seppur.2008.03.001.

Feng, L., W. Wang, R. Feng, S. Zhao, H. Dong, S. Sun, B. Gao, and Q. Yue. 2015. "Coagulation performance and membrane fouling of different aluminum species during coagulation/ultrafiltration combined process." *Chemical Engineering Journal*, 262: 1161–1167. Elsevier B.V. https://doi.org/10.1016/j.cej.2014.10.078.

Hatt, J. W., E. Germain, and S. J. Judd. 2011. "Precoagulation-microfiltration for wastewater reuse." *Water Research*, 45 (19): 6471–6478. https://doi.org/10.1016/j.watres.2011.09.039.

Howe, K. J., A. Marwah, K.-P. Chiu, and S. S. Adham. 2006. "Fouling of microfiltration and ultrafiltration membranes by natural waters." *Environmental Science & Technology*, 40 (24): 7908–7913. https://doi.org/10.1021/es0616480.

Judd, S. J., and P. Hillis. 2001. "Optimisation of combined coagulation and microfiltration for water treatment." *Water Research*, 35 (12): 2895–2904. https://doi.org/10.1016/S0043-1354(00)00586-8.

Jung, C. W., and L. S. Kang. 2003. "Application of combined coagulation-ultrafiltration membrane process for water treatment." *Korean Journal of Chemical Engineering*, 20 (5): 855–861. https://doi.org/10.1007/BF02697288.

Long, Y., X. You, Y. Chen, H. Hong, B.-Q. Liao, and H. Lin. 2020. "Filtration behaviors and fouling mechanisms of ultrafiltration process with polyacrylamide flocculation for water treatment." *Science of The Total Environment*, 703: 135540. https://doi.org/10.1016/j.scitotenv.2019.135540.

Long, Y., G. Yu, L. Dong, Y. Xu, H. Lin, Y. Deng, X. You, L. Yang, and B.-Q. Liao. 2021. "Synergistic fouling behaviors and mechanisms of calcium ions and polyaluminum chloride associated with alginate solution in coagulation-ultrafiltration (UF) process." *Water Research*, 189: 116665. https://doi.org/10.1016/j.watres.2020.116665.

Ma, B., X. Wang, C. Hu, W. A. Jefferson, H. Liu, and J. Qu. 2017. "Antifouling by pre-deposited Al hydrolytic flocs on ultrafiltration membrane in the presence of humic acid and bovine

serum albumin." *Journal of Membrane Science*, 538: 34–40. https://doi.org/10.1016/j.memsci.2017.05.029.

Ma, B., W. Yu, H. Liu, and J. Qu. 2014. "Effect of low dosage of coagulant on the ultrafiltration membrane performance in feedwater treatment." *Water Research*, 51: 277–283. https://doi.org/10.1016/j.watres.2013.10.069.

Nan, J., M. Yao, Q. Li, D. Zhan, T. Chen, Z. Wang, and H. Li. 2016. "The role of shear conditions on floc characteristics and membrane fouling in coagulation/ultrafiltration hybrid process – the effect of flocculation duration and slow shear force." *RSC Advances*, 6 (1): 163–173. https://doi.org/10.1039/C5RA18328F.

Pikkarainen, A. T., S. J. Judd, J. Jokela, and L. Gillberg. 2004. "Pre-coagulation for microfiltration of an upland surface water." *Water Research*, 38 (2): 455–465. https://doi.org/10.1016/j.watres.2003.09.030.

Ren, L., C. Liu, T. Meng, and Y. Sun. 2021. "Effects of micro-flocculation pretreatment on the ultrafiltration membrane fouling caused by different dissolved organic matters in treated wastewater." *Journal of Water Reuse and Desalination*, 11 (4): 597–609. https://doi.org/10.2166/wrd.2021.051.

Teng, J., Y. Chen, G. Ma, H. Hong, T. Sun, B.-Q. Liao, and H. Lin. 2020. "Membrane fouling by alginate in polyaluminum chloride (PACl) coagulation/microfiltration process: Molecular insights." *Separation and Purification Technology*, 236: 116294. https://doi.org/10.1016/j.seppur.2019.116294.

Wang, F., B. Gao, D. Ma, Q. Yue, R. Li, and Q. Wang. 2016. "Reduction of disinfection by-product precursors in reservoir water by coagulation and ultrafiltration." *Environmental Science and Pollution Research*, 23 (22): 22914–22923. https://doi.org/10.1007/s11356-016-7496-1.

Wang, J., J. Guan, S. R. Santiwong, and T. D. Waite. 2010. "Effect of aggregate characteristics under different coagulation mechanisms on microfiltration membrane fouling." *Desalination*, 258 (1–3): 19–27. https://doi.org/10.1016/j.desal.2010.03.056.

Wang, J., S. Pan, and D. Luo. 2013. "Characterization of cake layer structure on the microfiltration membrane permeability by iron pre-coagulation." *Journal of Environmental Sciences*, 25 (2): 308–315. https://doi.org/10.1016/S1001-0742(12)60025-4.

Wang, J., and X. Wang. 2006. "Ultrafiltration with in-line coagulation for the removal of natural humic acid and membrane fouling mechanism." *Journal of Environmental Sciences*, 18 (5): 880–884. https://doi.org/10.1016/S1001-0742(06)60008-9.

Yan, M., X. Shen, B. Gao, K. Guo, and Q. Yue. 2021. "Coagulation-ultrafiltration integrated process for membrane fouling control: Influence of Al species and SUVA values of water." *Science of The Total Environment*, 793: 148517. https://doi.org/10.1016/j.scitotenv.2021.148517.

Yao, M., J. Nan, Q. Li, D. Zhan, T. Chen, Z. Wang, and H. Li. 2015. "Effect of under-dosing coagulant on coagulation–ultrafiltration process for treatment of humic-rich water with divalent calcium ion." *Journal of Membrane Science*, 495: 37–47. https://doi.org/10.1016/j.memsci.2015.08.001.

You, X., J. Zhang, L. Shen, R. Li, Y. Xu, M. Zhang, H. Hong, L. Yang, Y. Ma, and H. Lin. 2021. "Thermodynamic mechanisms of membrane fouling during filtration of alginate solution in coagulation-ultrafiltration (UF) process in presence of different ionic strength and iron(III) ion concentration." *Journal of Membrane Science*, 635: 119532. https://doi.org/10.1016/j.memsci.2021.119532.

Zularisam, A. W., A. F. Ismail, M. R. Salim, M. Sakinah, and T. Matsuura. 2009. "Application of coagulation – ultrafiltration hybrid process for drinking water treatment : Optimization of operating conditions using experimental design." 65: 193–210. https://doi.org/10.1016/j.seppur.2008.10.018.

APPENDIX B

Dissolved Air Flotation Pretreatment for Low-Pressure Membranes in Water Treatment: A Review of Fouling Mitigation and Product Water Quality

Context: The literature review presented in Chapter 2 generated a review article on coagulation/flocculation/dissolved-air-flotation (CF-DAF) pretreatment of low-pressure membranes. In the interest of completeness, this article is presented in this appendix. A version of this appendix was published as:

Ladouceur, J.D., Narbaitz, R.M., & Lan, C.Q. (2023). Dissolved air flotation pretreatment for low-pressure membranes in water treatment: A review of fouling mitigation and product water quality. *Journal of Water Process Engineering, 56, 104391.*

List of Abbreviations

AOM	Algal organic matter
CF-DAF	Coagulation/flocculation/dissolved air flotation
CF-SED	Coagulation/flocculation/sedimentation
C-IN	Inline coagulation
DBP	Disinfection by-product
DOC	Dissolved organic carbon
DWT	Drinking water treatment
G	Mean velocity gradient
HPO	Hydrophobic
LC-OCD	Liquid chromatography organic carbon detection
LPM	Low-pressure membrane
MF	Microfiltration
MWCO	Molecular weight cut-off
OPEX	Operating expense
PDO	Pressure-driven outside-in
PES	Polyethersulfone
PVDF	Polyvinylidene fluoride
SUVA	Specific ultraviolet absorbance at 254nm
SWRO	Seawater reverse osmosis
TFI	Total fouling index
TMP	Transmembrane pressure
UF	Ultrafiltration
USD	United States dollar
UV_{254}	Ultraviolet absorbance at 254nm

B.1 Abstract

Coagulation/flocculation/dissolved-air-flotation (CF-DAF) has garnered increased interest in recent years as pretreatment for low-pressure membranes (LPM) due to its ability to treat colored and algal-laden waters. These challenging water types are now more frequently encountered due to eutrophication and the effects of climate change, which necessitates pretreatment to prevent

severe LPM fouling. In this study, pertinent literature regarding CF-DAF as pretreatment for LPMs in water treatment applications is reviewed. Specifically, the paper presents a brief overview of CF-DAF, compares CF-DAF pretreatment performance with other coagulation alternatives, outlines relationships between CF-DAF treated water quality and LPM fouling, reviews the treated water quality from the integrated system (i.e., CF-DAF-LPM), and finally discusses cost considerations of CF-DAF implementation as LPM pretreatment. When comparing CF-DAF with inline coagulation and coagulation/flocculation/sedimentation as pretreatment strategies for LPM fouling mitigation, it was found that the relative performance is influenced by both the feed water quality and the membrane configuration/type. CF-DAF pretreatment improved removal of hydrophobic organics (as measured by UV_{254} and SUVA) and for the limited waters tested resulted in reduced irreversible fouling measures, which are critical to long-term economic operation. According to the knowledge gaps identified throughout the study, the manuscript concludes by outlining guidance on potential foci of future research.

B.2. Introduction

Low-pressure membranes (LPM) have become a well-established technology in drinking water treatment (DWT) applications, with rapid growth over the past two decades (Alresheedi et al. 2022; Chang et al. 2017a; Lee et al. 2023; Pearce 2018). The popularity of LPMs may be attributed to several factors including: (1) reliable operation with a superior quality product water, even in the face of changing feed water quality (Kinser 2021; Suárez et al. 2015); (2) modularity, which results in a compact process that can be operated with a high degree of automation (Peters et al. 2021; Schulz et al. 2016); (3) excellent removal of microorganisms, pathogens, and protozoa (Huang et al. 2009; Li et al. 2019; Ren et al. 2021; Wray and Andrews 2014); (4) increasingly stringent treated water quality regulations (Bermea 1999; Obotey Ezugbe and Rathilal 2020; Pearce 2011); (5) decreasing membrane costs due to economies of scale (Gao et al. 2011; Pearce 2011); and (6) the use of lower-quality freshwater sources in response to stress from climate change, industrialization, and population growth (Amjad et al. 2015). Despite the numerous advantages of LPMs compared to conventional treatment using dual-media deep bed filtration, problems associated with membrane fouling remain a crucial impediment preventing a more extensive usage of LPMs for DWT (Kimura and Kume 2020; Peiris et al. 2010; Yamamura et al. 2014; Zietzschmann et al. 2014). LPM fouling is characterized by a loss of productivity over time

resulting from the deposition of feed water constituents on the membrane surface or within the membrane pores (Peiris et al. 2010; Walker and Narbaitz 2016; Wray and Andrews 2014; Yamamura et al. 2007). For LPMs operated with a constant filtration flux, this productivity loss is manifested through greater pressure drops, which results in increased energy costs (Chang et al. 2017b; Souza and Basu 2013; Tanudjaja et al. 2022).

Natural organic matter (NOM), which is ubiquitous in natural waters, has been identified by many researchers as the consensus principal foulant of LPMs (Amy 2008; Tian et al. 2018; Zularisam et al. 2011). Besides NOM, it has also been reported that severe LPM fouling can result from the filtration of algal-laden surface waters (Schurer et al. 2013; Zhang and Fu 2018). With climate change yielding an increase in the total NOM content (Delpla et al. 2009; Evans et al. 2005; Sillanpaa 2015) and color (Anderson et al. 2021) of natural waters globally, as well as resulting in increased frequency and intensity of algal blooms (Gobler 2020; Jöhnk et al. 2008; Moore et al. 2008; Venne et al. 2020), LPM feed water pretreatment strategies are needed as climate change adaptation measures to achieve improved economy of operation. Coagulation prior to LPM filtration is the most commonly applied feed water pretreatment strategy (Wray et al. 2014, 2016) as it is reported to be an efficient and cost effective solution to simultaneously mitigate LPM fouling as well as produce a superior-quality product water (Gao et al. 2011; Huang et al. 2009). Although there has been recent interest in inline coagulation (C-IN) pretreatment (without particle separation prior to LPM filtration) due to its reduced process complexity and shorter retention times (Kamińska et al. 2020), several studies have found it unsuitable for the control of LPM fouling by water supplies with elevated NOM content (i.e., > 5 mg L^{-1}) (Braghetta et al. 1997; Choi et al. 2008), color (Ladouceur and Narbaitz 2023), or those that are algal impacted (Liang et al. 2008, 2009). Compared to conventional technologies involving coagulation/flocculation and clarification by gravity sedimentation (CF-SED), coagulation/flocculation/dissolved-air-flotation (CF-DAF) is a high-rate process with a small footprint that compliments the compactness of membrane installations well (Ladouceur and Narbaitz 2023). Furthermore, for highly colored or algal impacted waters, CF-DAF provides a superior performance compared to CF-SED due to the low densities of NOM and algae flocs, which makes them more amenable to removal by flotation (Edzwald and Haarhoff 2012; Ladouceur and Narbaitz 2022; Teixeira and Rosa 2006).

Several detailed reviews on alternative pretreatment strategies for LPMs in water treatment (Farahbakhsh et al. 2004; Gao et al. 2011; Huang et al. 2009) were presented over a decade ago.

Since this time, Malkoske et al. (2020) have offered an updated perspective on coagulation pretreatment for LPMs in a recent paper which surveys both C-IN and conventional (i.e., CF-SED) approaches. However, despite the increasing research interest and number of publications on CF-DAF pretreatment of LPMs in water treatment (Fig. B.1), none of these existing studies have reviewed this research area. Accordingly, the current work aims at reviewing pertinent literature to provide a comprehensive perspective of CF-DAF pretreatment for LPM technologies with a specific focus on DWT applications. This report will be organized into four principal sections. The first section briefly presents an overview of CF-DAF practice and discusses its integration with LPMs for application in drinking water and wastewater treatment. In the next section, the performance of CF-DAF for LPM fouling mitigation is compared with CF-SED and C-IN. Furthermore, analysis and discussion of the impacts of key coagulation, flotation, and water quality parameters on LPM fouling is provided. In the third section, the reported quality of CF-DAF-LPM product water is reviewed. The final section provides a discussion of some of the practical economic considerations associated with implementing CF-DAF for LPM pretreatment. The report concludes by summarizing critical knowledge gaps and recommending directions for future research.

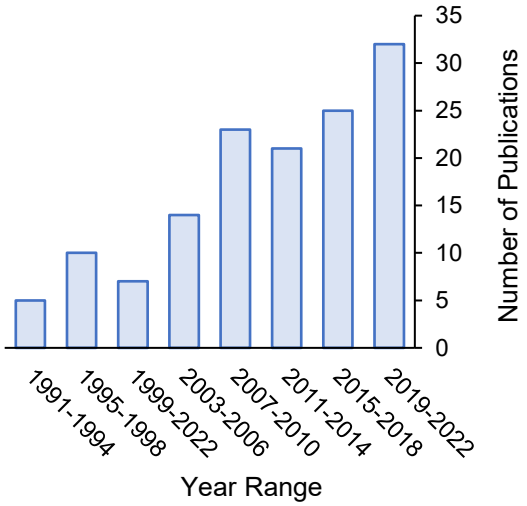


Fig. B.1. Number of publications regarding flotation pretreatment for LPMs. Note: Scopus search: ((ultrafiltration OR microfiltration) AND (flotation OR floatation OR “dissolved air flotation”) AND water); data retrieved on April 11, 2023.

B.3. Dissolved Air Flotation

In this section, a brief overview of CF-DAF is presented followed by a discussion of its application to LPM technologies. For a more comprehensive review of CF-DAF and CF-DAF modeling, the reader is directed to the reviews by Edzwald (2010), Crossley and Valade (2006), and Haarhoff and Edzwald (2004).

B.3.1. A Brief Overview

CF-DAF, which uses dissolved air flotation as an alternative to gravity sedimentation (i.e., CF-SED) for particle clarification, may be implemented in conventional treatment schemes or for LPM pretreatment (Edzwald 2010; Teixeira and Rosa 2006). CF-DAF can be sub-divided into two principle processes: (1) pretreatment, and (2) flotation (Shawwa and Smith 2000). In the CF-DAF process, pretreatment by coagulation and flocculation is required for the destabilization of particles and improvement of particle bubble attachment efficiency (Edzwald 1993a, 2011; Edzwald and Haarhoff 2012). Without coagulation pretreatment, the particles in the feed water are negatively charged so that as they approach one another, they exert a repulsive force and do not agglomerate (Edzwald 1993b, 2011). Properly conditioned feed water in CF-DAF uses pH alteration and coagulant addition to reduce the zeta potential of the particles to zero, or near zero, such that attachment is improved (Ducker et al. 1994; Edzwald 2010, 2011). Besides particle removal, coagulation as pretreatment for flotation is implemented to enhance the removal of organic matter (measured as dissolved organic carbon (DOC)), which is known to be a precursor for the formation of potentially harmful disinfection by-products (DBP) (Archer and Singer 2006; Edzwald 2011; Hua and Reckhow 2007) and is poorly removed by LPMs (Pearce 2011). In fact, it is the quality and quantity of NOM, not turbidity causing particles, that are principally responsible for controlling the coagulant dose in the CF-DAF process (Edzwald 1993b; Edzwald and Haarhoff 2012; Matilainen et al. 2010). The flocculation requirements for facilities with clarification by flotation are fundamentally different than those for conventional gravity sedimentation. In CF-DAF, the goal of flocculation is to produce a floc particle that can be removed by floating to the basin surface following attachment to microscopic air bubbles (Valade et al. 2009). In contrast, for CF-SED, flocculation seeks to produce larger sized flocs with densities greater than water and which settle at a rapid rate (Valade et al. 1996). Therefore, unlike for sedimentation which necessitates floc particles >100 μm to achieve reasonable settling velocities, the optimum size of

floc particles for CF-DAF treatment is in the range of 25-50 µm (Edzwald 2011; Edzwald et al. 1992; Edzwald and Haarhoff 2012). In fact, small sized, compact flocs which are resistant to shear are preferable to avoid breakup. Accordingly, successful CF-DAF operation has been achieved using shorter duration flocculation (only 5 to 10 min) to produce pinpoint sized flocs (Edzwald 1995, 2007).

The flotation basin is divided into two main compartments by means of a baffle (Fig. B.2). The first zone of the basin is the contact zone, which brings the air bubbles and particulates into contact. The goal of the contact zone is to provide sufficient opportunity for collisions between air bubbles and particles such that attachment may occur (Lundh et al. 2002). If the feed water has been properly conditioned prior to entering the contact zone, collisions between flocs and bubbles may yield attachment and the formation of floc-bubble aggregates. The suspension of bubbles, particulates, and floc-bubble aggregates moves from the contact zone downstream to the separation zone by means of passing over a baffle wall. In the separation zone, free bubbles and floc-bubble aggregates rise to the top of the basin where they are collected into a foam layer termed the float. The float layer concentrates over the course of operation prior to being removed either continuously or intermittently by means of a hydraulic flooding process or by a mechanical scraper (Crossley and Valade 2006; Edzwald and Haarhoff 2012; Zabel 1985). The clarified water is commonly withdrawn from the bottom of the basin using evenly distributed pipe manifolds.

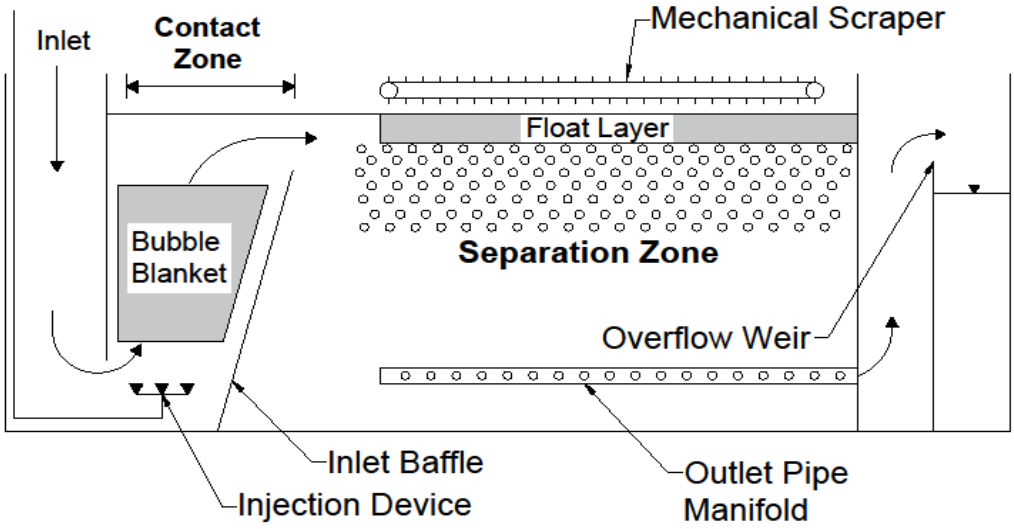


Fig. B.2. Schematic diagram of flotation basin. Adapted from Crittenden et al. (2012).

To provide air bubbles to the system, a portion of the treated CF-DAF effluent or filtered product water is recycled. In the most common configuration, the recycle flow is pumped to a packed saturator tower where air is supersaturated in the water under pressure. The pressurized recycle flow is then introduced to the contact zone by means of an injection device (typically nozzles or engineered valves) located at the floor of the contact zone (Crossley and Valade 2006; Lundh et al. 2000). The immediate release of pressure in the recycle stream to that of the hydrostatic head in the tank causes cavitation and forces the air out of solution in the form of microbubbles (Leppinen 1999; Peleka et al. 2018). The bubble nuclei formed through the release of pressure in the nozzle grow principally by coalescence, producing bubbles ranging in size from 10 to 150 μm (Edzwald and Haarhoff 2012; Rykaart and Haarhoff 1995). It has been shown that in the contact zone, the air bubble size is most commonly between 40 to 80 μm in diameter with an average size of 60 μm (Leppinen and Dalziel 2004). As the bubbles move to the separation zone, the bubble size increases slightly with sizes ranging from 50 to 150 μm and a mean size of 80 μm (Leppinen and Dalziel 2004). Regarding the bubble size, it has been shown that smaller sized bubbles yield a more efficient performance (Haarhoff and Edzwald 2004; Rajapakse et al. 2022; de Rijk et al. 1994). It is for this reason that dissolved air flotation results in a superior performance compared to dispersed air flotation, which uses bubbles of much greater size (>1 mm). A final comment is regarding the bubble volume concentration, or the amount of air delivered to the system, which is considered to be the most important CF-DAF operating variable (Edzwald 2010). The bubble volume concentration is governed by the saturation pressure and the recycle rate, and for typical values used in practice ranges between 7,000 – 9,000 ppm (Edzwald and Haarhoff 2012). A summary of typical values of key CF-DAF operating parameters is provided in Table B.1.

Table B.1. Summary of Typical CF-DAF Parameters.

Parameter	Range	Typical Value	Ref.
Recycle Ratio (%)	8-12	10	Edzwald and Haarhoff (2012)
Saturator Pressure (kPa)	400-600	500	Edzwald et al. (1992); Malley and Edzwald (1991)
Flocculation Retention Time (min)	5-20	<10	Valade et al. (2009)
Contact Zone Retention Time (min)	1-2.5	-	Edzwald (2010)

Loading Rate (m h^{-1}) [a]	5-15 (conventional)	-	Edzwald (2010); Malley and Edzwald (1991); Valade et al. (2009)
	15-40 (high-rate)[b]	-	Edzwald (2007); Edzwald (2010)
Contact Zone Bubble Size (μm)	10-100	60	Han (2002); Leppinen and Dalziel (2004); de Rijk et al. (1994)

[a] The design loading rate for CF-DAF is affected by water temperature. For cold weather conditions, water viscosity increases, decreasing the bubble rise rate and CF-DAF performance (Edzwald 2006a; Gonzalez-Galvis and Narbaitz 2022).

[b] Although not strictly required for effective performance, many conventional and high-rate CF-DAF facilities dose polymer to reduce metal coagulant dose (Bratby 2016), minimise pH variation, modify bubble surface properties (Henderson et al. 2009, 2010a), and/or improve the retention of sludge in the float (Edzwald and Haarhoff 2012).

Some of the key advantages of CF-DAF technology which have led to its growth as a treatment technology of choice include:

1. Flow patterns within the separation zone permit loading rates of 5-15 m h^{-1} for conventional CF-DAF, which is at least twice as great as those for sedimentation basins (Crittenden et al. 2012; Kawamura 2000).
2. Compared to CF-SED, CF-DAF facilities are more adept for treating waters with low-density particles or flocs, including wastewaters contaminated with oils, grease or fats and highly colored or algal impacted natural waters (Arnold et al. 1995; Edzwald 2006a). Natural organic matter and algae form low-density flocs which yield settling velocities too low to settle within reasonable period of time (Teixeira and Rosa 2007; Zabel 1985).
3. CF-DAF produces a high-quality effluent with turbidity values often less than 0.5 NTU (Crossley and Valade 2006; Edzwald 2006b; Voutchkov 2010) and has been shown to have superior removals of pathogenic organisms such as *Giardia* and *Cryptosporidium* compared to sedimentation (Edzwald et al. 2000).
4. The total cost for operating a CF-DAF facility is comparable to that of CF-SED facilities. Greater costs associated with pumping and saturating the recycle flow as well as a slightly more complicated operation are offset by the savings in plant footprint as well as the energy savings from smaller sized flocculation basins (Schofield 2001).

5. For float layer removal by mechanical scrapers, the float solids concentrate to greater than 3%, which can significantly reduce the sludge volume and the costs associated with handling and disposal (Crossley and Valade 2006).

B.3.2. Application of CF-DAF as LPM Pretreatment

B.3.2.1. Drinking Water Treatment

Owing to the low rejection of NOM afforded by LPMs (<10-20%) (Ladouceur and Narbaitz 2023; Pearce 2011), as well as the increasing frequency and severity of algal blooms, integration of CF-DAF as pretreatment for LPMs has gained increasing popularity in DWT as a promising technique to simultaneously mitigate membrane fouling as well as minimize the formation potential of DBPs. Indeed, the integrated system has been applied not only at laboratory scale, but also in numerous full-scale installations globally. The treatment scheme for a typical CF-DAF-LPM facility is shown in Fig. B.3. Here, the pretreatment and clarification sub-processes are the same as described previously in Section B.3.1. The high-quality product water (turbidity < 1 NTU and reduced DOC) collected from the flotation tank effluent is used as influent to the LPM system, delivering a reduced foulant load to the LPM compared to direct filtration. The integration of CF-DAF with LPMs also provides a multi-barrier approach for the removal of pathogenic protozoa as it has been shown that CF-DAF can achieve log removal of 2.4 for *Giardia* (Edzwald et al. 2000) and greater than 2.1 for *Cryptosporidium* (Edzwald et al. 2000; Edzwald and Kelley 1998). Several authors have demonstrated that these removals exceed those achieved by CF-SED, reported to be 0.45-1.15 log for *Giardia* (Logsdon et al. 1985) and 0.8-1.2 log for *Cryptosporidium* under a variety of conditions (varying coagulant type, dose, pH) (Edzwald and Kelley 1998; Plummer et al. 1995; Xagoraraki and Harrington 2004).

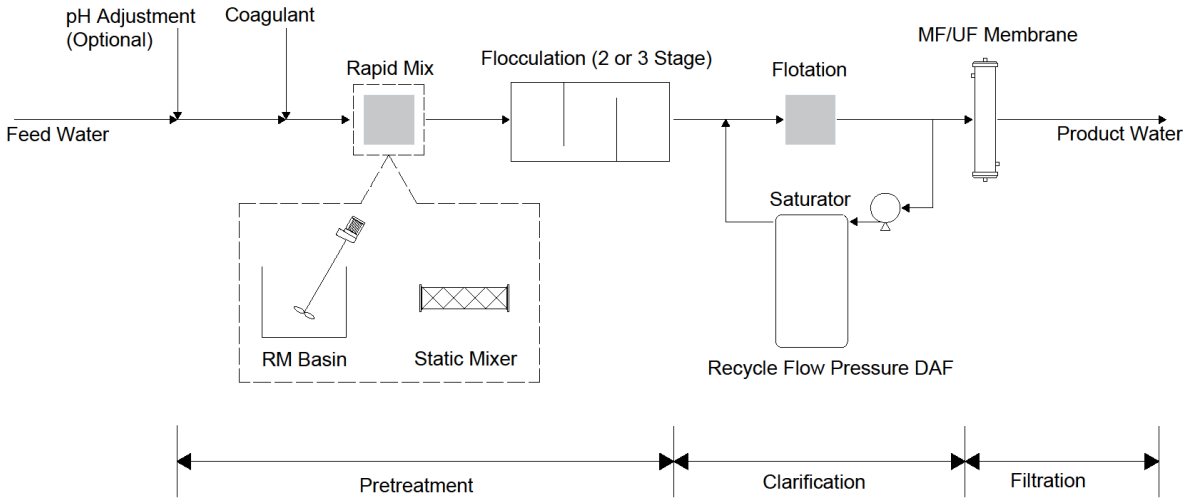


Fig. B.3. Low-pressure membrane system integrated with CF-DAF pretreatment (not to scale).

The integrated CF-DAF-LPM system has also been considered as pretreatment for seawater reverse osmosis (SWRO) systems (Amato et al. 2013; Petry et al. 2007; Salinas-Rodríguez et al. 2021). Increasing stress on fresh water resources from climate change and population growth, as well as improved social and economic status, has driven an increasingly large number of utilities in arid and semi-arid regions to resort to desalination to satisfy water demands (Deka et al. 2020; Khanzada et al. 2017). As is the case for LPMs treating freshwaters, membrane fouling (specifically biological fouling) remains one of the most significant challenges for SWRO technology, especially during red tide events or periods of heavy algal blooms (Alayande et al. 2022; Alshahri et al. 2021). In response to these challenges, the number of SWRO facilities that have incorporated CF-DAF in combination with LPM filtration as pretreatment for reverse osmosis has drastically increased since 2010 (Alayande et al. 2022). For these facilities, the typical pre-treatment scheme is essentially the same as shown in Fig. B.3. Good performance in terms of fouling mitigation has been reported by a number of authors, proposed to be a result of reduced turbidity, algae cell count, and organics (Guastalli et al. 2013; Harvey et al. 2020; Park et al. 2013).

In summary, it is anticipated that the combined use of CF-DAF and LPMs for drinking water production will continue to grow in the coming years. Increased demand for SWRO facilities, as well as increasing frequency of algae blooms and decreased natural water quality drive

designers to implement the integrated CF-DAF-LPM system, which has been proven as an effective treatment (or pretreatment for SWRO) technology for these water types.

B.3.2.2. Wastewater Treatment

For treating municipal wastewater, several studies have investigated combining the CF-DAF process with a membrane bioreactor to achieve enhanced removals of phosphorus as well as organics and suspended solids (Kim et al. 2015; Lee et al. 2016). Besides municipal sources, an emerging area of application for the CF-DAF-LPM process is in the treatment of oily wastewater, primarily due to the significant volumes produced yearly (10-15 billion m^3) (Zhao et al. 2021) and its associated health and environmental impacts (Zulkefli et al. 2021). Oily wastewaters are commonly generated as a byproduct of a number of industries including (but not limited to) food and beverage, oil and petroleum, metal processing, and textiles (An et al. 2017; Hui et al. n.d.). The large number of sources producing oily wastewater results in significant variability of its character and composition, which can pose challenges in selecting appropriate treatment strategies to meet regional discharge guidelines (which range from 10 mg L^{-1} to 42 mg L^{-1} as oil) (An et al. 2017; Tanudjaja et al. 2019; Yu et al. 2017). Previous studies have shown treatment by optimized CF-DAF to remove 90-99% of oil and grease, although, removal of emulsified oil droplets (< 20 nm size) is incomplete and flotation retention times were long (60-90 min) (Ebrahimi et al. 2010; Reed et al. 1998). Recently, LPM technologies have become an increasingly popular treatment option for oily wastewaters owing to their proven effectiveness to separate oil/water mixtures (Padaki et al. 2015) (with efficiencies as high as 97-99% (Yu et al. 2017)) including small sized droplets < 20 nm (Tanudjaja et al. 2019). As is the case for LPMs in DWT applications, membrane fouling remains the principal barrier to a more widespread implementation of these technologies for the treatment of oily wastewater (Ahmad et al. 2020; Tanudjaja et al. 2019). Several studies have shown that for dead-end filtration of oil in water emulsions, low-permeability gel layers are formed which consolidate with time due to the deformation of oil droplets under increasing pressure (Iritani et al. 2008; Lipp et al. 1988; Matsumoto et al. 1999; Tummons et al. 2016). This is especially true for low-stability emulsions, which will coalesce to form a contiguous gel layer on the membrane surface (Tummons et al. 2020). Severe decline in membrane permeability following gel layer formation is proposed to be a result of the large chemical potential energy gap that exists between the free water in solution and the bound water present in the gel layer, which

necessitates increased energy input for LPM operation at the same flux (Chen et al. 2020; Long et al. 2020, 2021; You et al. 2021). Integration of LPMs with conventional technologies (including CF-DAF) in a hybridized system configuration has shown promise for improved performance in terms of both membrane fouling mitigation and product water quality. The reported reduction in the magnitude of LPM fouling for the integrated CF-DAF-LPM system is likely due to the near complete elimination of oil from solution prior to contacting the membrane module. Alternatively, improved performance may be because CF-DAF is effective in removing the large sized oil droplets (Saththasivam et al. 2016), which are principally responsible for the initial formation of the oily gel layer on the membrane surface (Kurada and De 2018). Regarding water quality improvement, the study by Zhang et al. (2012) reported that the optimized CF-DAF-ultrafiltration (UF) system (coagulation by 0.75 mg L^{-1} polyacrylamide and 150 mg L^{-1} polyaluminum ferric chloride) could improve removals of oil and grease from a carwash wastewater by over 20%. For a produced water (from the oil industry), Subramani et al. (2011) reported highly variable oil and grease removal (25-90%) following CF-DAF treatment (1 h flotation time with coagulation by 1-3 mg L^{-1} polymer and 50-100 mg L^{-1} aluminum chlorohydrate) due to fluctuating feedwater quality and the associated challenges in optimizing coagulation pretreatment. When the CF-DAF unit was integrated with a ceramic (Al_2O_3-Zr) UF membrane, a further 25% of the remaining oil and grease content could be removed with only a 14% decline in permeability following 550 hours of operation. The degree of improvement in fouling mitigation following CF-DAF pretreatment could not be assessed, however, as filtration tests with untreated wastewater were not conducted. Based on the results of this last study, more research is required to develop real-time CF-DAF-LPM process control tools capable of adjusting optimal operation according to the characteristics of highly variable feed waters.

As noted in the introduction, the focus of the current review article will be on CF-DAF-LPM applications in DWT, specifically trends in membrane fouling and product water quality. This will be the subject of the remaining sections. For a complete review of available technologies in treating oily wastewaters, the authors direct the reader to the review papers by Yu et al. (2017) and Abuhasel et al. (2021). Furthermore, the use of CF-DAF as treatment for oily wastewater was specifically examined in the review by Saththasivam et al. (2016) , while Li et al. (2023), Tanudjaja et al. (2019), Ahmad et al. (2020), and Tummons et al. (2020) have provided perspective on the use of LPM-based treatment strategies.

B.4. Membrane Fouling in the Integrated Flotation-LPM System

In general, several researchers have reported that LPMs filtering CF-DAF pretreated water exhibit reduced fouling potential compared to when raw feed water is considered (Kang et al. 2021; Pissibanganga et al. 2016). However, other research studies have suggested that CF-DAF pretreatment for LPMs does not necessarily lead to improved fouling reduction, but may improve the quality of product waters (Amaral et al. 2013). Table B.2 presents a summary of pertinent data for select CF-DAF-LPM studies including information on the raw water quality, coagulation/flotation characteristics, and fouling metrics. Although there has been heightened research interest regarding the integration of CF-DAF with LPMs in recent years (Fig. B.1), there remains a limited number of studies which directly compare the performance of CF-DAF pretreatment for LPMs with that of other coagulation approaches, including C-IN or CF-SED. A discussion of the relative performance of CF-DAF compared to these two alternative coagulation pretreatment strategies is warranted and is provided in the next sub-sections.

Appendix B

Table B.2. Summary of Pretreatment Parameters and Fouling Behavior for Selected CF-DAF-LPM Studies[a].

Mat.-Config. NPS or MWCO	Raw Water Characteristics			Coagulation Characteristics			Flotation Parameters		Fouling Measures			Ref. (see notes)
	Water Type	DOC (mg L^{-1})	SUVA ($Lmg^{-1}m^{-1}$)	Coag. Type	Coag. Dose (mg-Me^{+} L^{-1})	Polymer Dose (mg L^{-1})	Recycle Ratio (%)	Recycle Pressure (kPa)	Permeability Decline Rate ($Lm^{-2}h^{-1}bar^{-1}d^{-1}$)	Hyd. Irrev. Fouling Rate (kPa h^{-1})	Chem. Irrev. Fouling Rate (kPa h^{-1})	
PVDF-FS 0.1 µm	River	3.8	3.41	PACl	50 (as coag.)	N/A	10	517	6088	N/A	N/A	[1]
	Lake	2.2	1.53	PACl	12 (as coag.)	N/A	10	517	8645	N/A	N/A	
	Lake	2.0	1.58	PACl	18 (as coag.)	N/A	10	517	6391	N/A	N/A	
	Lake	2.2	1.15	PACl	20 (as coag.)	N/A	10	517	9912	N/A	N/A	
PVDF-PDO 0.1 µm	Lake	2.2	1.5	PACl	Variable[b]	N/A	10	N/A	N/A	0.248	N/A	[1]
	Lake	2.0	1.3	PACl	Variable[b]	N/A	10	N/A	N/A	1.87	N/A	
PP-PDO 0.2 µm	RES	6.9 (TOC)	2.3	Alum	45 (as coag.)	N/A	N/A	N/A	N/A	0.0937	N/A	[2]
PES-PDI 100 kDa	River	8.16	3.92	Alum	3.18-3.36	0.072-0.1[c] (PAM)	N/A	N/A	N/A	1.53	0.143	[3]
		7.09	3.56	Alum	3.18-3.36	0.072-0.1[c] (PAM)	N/A	N/A	N/A	0.837	0.0375	
		7.09	3.56	Alum	3.18-3.36	0.072-0.1[c] (PAM)	N/A	N/A	N/A	1.24[d]	0.398	
		7.09	3.56	Alum	3.18-3.36	0.072-0.1[c] (PAM)	N/A	N/A	N/A	2.14[e]	0.672	
PES-PDI 100 kDa	River	6.07	4.16	Alum	2.99	0.07[c] (PAM)	N/A	N/A	N/A	1.045	0.643	[4]
PES-PDI 100 kDa	River	6.64	4.16	Alum	3.36	0.072[c] (PAM)	10	483	N/A	0.102	0.017	[5]
PVDF-PDO 100 kDa	River	6.54	4.22	Alum	3.36	0.072[c] (PAM)	10	483	N/A	0.032	0.0096	[6]
PVDF-PDO 0.01 µm	RES	3.06	N/A	PACl	3.18	N/A	N/A	N/A	N/A	N/A	0.05875	[7]
		3.06	N/A	PACl	3.18	N/A	N/A	N/A	N/A	N/A	0.02666	
		3.06	N/A	PACl	2.12	N/A	N/A	N/A	N/A	N/A	0.00708	
Al_2O_3-FS 0.2 µm	River	6.25-10.1 (TOC)	N/A	$FeCl_3$	10	0.1 (PAM)	N/A	N/A[f]	N/A	2	N/A	[8]
PAN-PDO 0.025 µm	River	3.37-6.64 (COD)	N/A	N/A	N/A	N/A	N/A	N/A	N/A	N/A	0.033	[9]

[a] COD=chemical oxygen demand; DOC = dissolved organic carbon; FS = flat sheet; N/A = not available; PACl = polyaluminum chloride; PAM = polyacrylamide; PAN = polyacrylonitrile; PDI = pressure-driven inside-out; PDO = pressure-driven outside-in; PVDF = polyvinylidene fluoride; RES = reservoir; SUVA = specific ultraviolet absorbance at 254nm; TOC = total organic carbon; WAC = aluminum polyhydroxichlorosulphate. [b]Coagulant dose was adjusted using influent feed water turbidity measurements. [c] Cationic charge. [d] Evaluated at the end of a 60 min filtration cycle instead of 30 min. [e] Evaluated 90 min filtration cycle instead of 30 min. [f] Used novel ceramic disc diffusers operated at 2 bar with a mean bubble size of 50 µm. Note, references are: [1] Van Benschoten et al. (2002); [2] Braghetta et al. (1997); [3] Xu and Narbaitz (2016); [4]Walker and Narbaitz (2016); [5] Ladouceur and Narbaitz (2022); [6] Ladouceur and Narbaitz (2023); [7]Kang et al. (2021); [8] Hög et al. (2015); [9]Shi et al. (2017)

B.4.1. Comparison with C-IN

LPM pretreatment by C-IN involves the direct addition of coagulants (as well as pH adjusting chemicals and flocculants) to the feed stream (continuously) prior to the membrane module without any clarification process. Although inherent differences exist between C-IN and CF-DAF (i.e., inclusion of particle separation), the principal objective of coagulant addition in both processes remains to agglomerate colloidal (microparticle) foulants as well as to precipitate, complex, and adsorb NOM (the principal LPM foulant) from solution (Edzwald and Van Benschoten 1990; Henderson et al. 2006; Sillanpää et al. 2018). Instinctively, CF-DAF pretreatment should result in reduced LPM fouling compared to C-IN as the flotation clarification significantly reduces the solids mass loading being delivered to the membrane. In fact, results from several studies (Braghetta et al. 1997; Hög et al. 2015; Ladouceur and Narbaitz 2023; Van Benschoten et al. 2002) have indicated increased fouling by C-IN compared to CF-DAF using both lab- and pilot-scale filtration systems, whereby elevated fouling tendencies were purported to be a result of increased membrane solids loadings. For example, Braghetta et al. (1997) compared the performance of C-IN and CF-DAF for treatment of a reservoir water ahead of a polypropylene microfiltration (MF) membrane. In that study, following CF-DAF pretreatment with the addition of 45 mg L^{-1} alum (as coagulant), the MF membrane was found to operate stably at a flux of 120 L m^{-2} h^{-1} for a period of over 30 d without reaching the terminal transmembrane pressure (TMP) for initiating chemical cleaning (155 kPa). When coagulated feed water was delivered directly to the membrane module without clarification by flotation (using same coagulation chemistry as for CF-DAF), membrane fouling was found to be exacerbated, exceeding the terminal operating TMP within a short time (~1 d). Moreover, the recovery of membrane permeability by chemical cleaning was found to be incomplete, leading to reduced filter run times for each subsequent chemical clean cycle. It should be noted that, while the coagulant dose was kept consistent for comparative purposes, the dose was selected to achieve optimal DOC removals in accordance with the legislated enhanced coagulation requirement. Based on the results, for C-IN, coagulant dosages lower than that necessary for DOC removal may be optimal in terms of fouling reduction; excessive coagulant usage likely induced an additional resistance to filtration (Kimura et al. 2008; Lerch et al. 2003; Paar et al. 2011; Wray et al. 2016). Similar observations were also reported by Hög et al. (2015) when comparing CF-DAF and C-IN as pretreatment for a process intensified flotation-LPM unit. For a river water pretreated with ferric chloride addition at a dose of 10 mg-

Fe L^{-1}, vacuum-driven ceramic MF membranes were found to reach the terminal operating TMP of -0.5 bar after only 4 h of filtration time, representing a total fouling rate of 6 kPa h^{-1}. In contrast, when CF-DAF was implemented using ferric chloride at the same dose, a stable TMP of -0.28 bar was sustained for the operating flux of 112 L m^{-2} h^{-1}, with a total fouling rate only one third of that for C-IN pretreatment (i.e., 2 kPa h^{-1}). The superiority of CF-DAF pretreatment compared to C-IN for fouling mitigation of LPMs was also reported by Ladouceur and Narbaitz (2023). In this study, which considered a pressure-driven outside-in polyvinylidene fluoride (PVDF) UF membrane filtering a colored river water, C-IN conditions optimized for removal of organics as well as a 20% reduced coagulant dose condition were unable to mitigate LPM fouling to the levels seen for CF-DAF. In fact, at the end of a three-day filtration test, the normalized TMP (TMP normalized to initial membrane clean water value) for the optimal and reduced dosages was found to be 3.3 and 6.8 times greater than for CF-DAF, respectively.

Not all studies, however, have reported reduced LPM fouling by CF-DAF compared to C-IN. In a second study by Ladouceur and Narbaitz (2022), it was reported that for the same colored river water and identical pretreatment conditions, C-IN at the optimal dose could result in a reduced normalized TMP increase compared to CF-DAF for a tubular multi-channel polyethersulfone (PES) UF membrane. Van Benschoten et al. (2002) also reported reduced fouling by C-IN pretreatment compared to CF-DAF for a hydrophobic (HPO) reservoir water (specific ultraviolet absorbance at 254 nm (SUVA) = 3.41 L mg^{-1} m^{-1}) and a flat sheet PVDF MF membrane, while for a lake water with a relatively high turbidity (67 NTU), CF-DAF and C-IN pretreatment performed equally well. The results of these studies seem to indicate a dependence of pretreatment relative performance on LPM type/configuration and feed water quality, respectively. It is possible that each specific membrane type may have a unique threshold value above which the benefits of C-IN pretreatment (i.e., porous cake formation) are offset by the increased mass loading, resulting in elevated TMPs and increased irreversible fouling compared to CF-DAF.

B.4.2. Comparison with CF-SED

There exists relatively few studies comparing the performance of CF-SED and CF-DAF pretreatment for LPMs. Using a synthetic water simulating algal impacted seawater, Deka et al. (2020) evaluated the suitability of these two alternatives as pretreatment for a bench-scale flat sheet MF (0.22 μm) membrane. Rapid mixing and flocculation durations, as well as coagulant

dose (2.5 mg-Fe L^{-1}), were identical for both CF-SED and CF-DAF, however, CF-DAF pretreated water was also oxidized by applying potassium permanganate at a dose of 1.5 mg L^{-1} prior to coagulant addition. After filtration for 120 min at a constant pressure (75 kPa), the final normalized flux for CF-DAF pretreated water was found to be nearly 30% greater than for CF-SED pretreated water. Although CF-DAF pretreated water exhibited significantly improved filtration performance compared to water pretreated by CF-SED (Deka et al. 2020), caution must be exercised in the interpretation of the results. As a result of the differences in coagulation chemistry during feed water conditioning (i.e., use of pre-oxidant for CF-DAF pretreatment), the reduced LPM fouling following pretreatment by CF-DAF in this study cannot be attributed solely to the differences in separation mechanism (i.e., sedimentation vs. flotation). Instead, the improved performance may have also resulted from the reduced foulant load delivered to the membrane, as inclusion of pre-oxidation during CF-DAF pretreatment resulted in a significantly reduced DOC (1.41 mg L^{-1} vs. 2.96 mg L^{-1}) and turbidity (2.12 NTU vs. 4.18 NTU) compared to CF-SED pretreated water. Another consideration when interpreting the results of this study is that only a single algal impacted synthetic water was evaluated. Several studies have shown that alga specific properties including the concentration of the algal-derived organic matter (AOM) as well as the AOM protein content, carbohydrate molecular weight, and charge density, all influence optimal coagulation chemistry and the properties of the formed flocs (Gonzalez-Torres et al. 2019; Henderson et al. 2010b; Lama et al. 2016). For example, Gonzalez-Torres et al. (2019) noted that for five different algal species, larger sized flocs were formed when the extracted AOM was present in higher concentration, had lower proportions of biopolymers/proteins, and increased charge densities. Changes in floc properties arising from differences in feed water algal species may alter the degree of improvement in LPM fouling reduction by CF-DAF compared to CF-SED. For certain algal species with a propensity for forming large and compact flocs, characteristics which are well suited to treatment by gravity sedimentation (Rao et al. 2023), the reported superiority of CF-DAF pretreatment compared to CF-SED may be diminished.

Walker and Narbaitz (2016) performed bench-scale experiments to evaluate the performance of CF-SED and CF-DAF as LPM pretreatment using colored water from the Ottawa River (Ottawa, Canada), which is predominated by HPO organics. This river has a large watershed (140,000 km^2), a large average flowrate (1,950 m^3/s), and a low population density. Moreover, the river is fairly pristine, the nearest secondary effluent discharge point is nearly 80 km upstream

from Ottawa, and the total phosphorus content is less than 0.03 mg-P L^{-1}, so it is not eutrophic. The pretreatment (i.e., CF-SED and CF-DAF) was performed at nearby full-scale facilities under different conditions which were optimized for the greatest removal of organics. For pretreatment by CF-SED, alum and activated silica were applied at dosages of 3.17 mg-Al L^{-1} and 0.91 mg L^{-1}, respectively, while for CF-DAF pretreated water the full-scale facility dosed 2.99 mg-Al L^{-1} alum and 0.07 mg L^{-1} cationic polyacrylamide. Following multi-day filtration tests using inside-out PES UF membranes, the TMP development for CF-SED pretreated water using alum as coagulant was found to be greater than for CF-DAF pretreated water with the same coagulant type. When ferric sulfate was investigated as coagulant for CF-SED pretreatment (dosed at 9.33 mg-Fe L^{-1} with 1 mg L^{-1} activated silica), the TMP increase was also reported to be more severe than for CF-DAF pretreatment (using alum), although it must be acknowledged that CF-SED pretreated water with ferric sulfate was produced using a pilot-plant facility which was not operating under optimized conditions. This resulted in elevated levels of CF-SED treated turbidity (4.88 NTU) and DOC (4.38 mg L^{-1}) compared to those for CF-SED (0.88 NTU and 2.45 mg L^{-1}, respectively) and CF-DAF (0.37 NTU and 2.07 mg L^{-1}, respectively) pretreatment with alum as coagulant. The significantly greater membrane solids and organics loading for CF-SED pretreatment with ferric sulfate as coagulant was thus likely responsible for the poor performance of this alternative.

Xu and Narbaitz (2016) used the same colored river water and inside-out PES UF membranes as Walker and Narbaitz (2016) to investigate the superiority of CF-DAF pretreatment compared to CF-SED during summer and winter seasons. To ensure differences in coagulation chemistry used by the full-scale facilities producing CF-DAF and CF-SED pretreated water were not responsible for observed performance differences, coagulated water from the flotation facility was also settled for a period of 24 h using a lab-scale column. Therefore, three challenge waters were investigated using two different coagulation chemistries: (1) settled water from the full-scale CF-SED facility which applied alum and activated silica at dosages of 3.17-Al mg L^{-1} and 1.85 mg L^{-1} , respectively; and (2) settled and floated water from the full-scale CF-DAF facility, which dosed 3.18 mg-Al L^{-1} alum and 0.072 mg L^{-1} cationic polyacrylamide polymer. As the settled and floated water from the CF-DAF facility were produced under identical conditions, any observed performance differences would be due to the difference in separation mechanism (i.e., flotation vs. sedimentation) and not coagulation chemistry. The comparison of CF-DAF and CF-SED performance was assessed using resistance-in-series based fouling indices (Nguyen et al. 2011;

Zupančič et al. 2014), where the total fouling index (TFI) describes the total fouling potential of the water-membrane configuration and the hydraulically irreversible fouling index (HIFI) describes the fraction of fouling which is not recoverable by hydraulic backwashing (i.e., physical cleaning methods). For both settled waters as well as the floated water, the TFI was found to mirror the performance of the TMP profiles, although, for CF-DAF pretreatment the TFI was two-three times lower than for CF-SED. Regarding the HIFI, CF-SED pretreated water was found to result in consistently higher values (at least 1.8 times greater) than CF-DAF regardless of season. This was the case for both the settled water collected from the full-scale sedimentation facility as well as that produced using coagulated water from the flotation facility. The better performance of CF-DAF compared to CF-SED (in terms of TMP development and fouling indices) may have been a result of the reduced organics load by the former. Better removal of bulk organics (measured as DOC) was also reported by Walker and Narbaitz (2016), and is likely due to the aforementioned suitability of CF-DAF for removing low-density NOM flocs (Section B.3). In addition, it was also proposed that the improved performance might have resulted from greater removal of HPO organic material by CF-DAF. For the winter season, CF-DAF pretreatment was found to remove a significantly greater amount of HPO organics (75.6%) compared to pretreatment by CF-SED, which averaged 63.3% removal for the two coagulation chemistries investigated. In fact, for all waters tested, the TFI and HIFI values during both seasons displayed strong positive linear correlations with the feed water SUVA value (a surrogate for HPO NOM material). It was postulated in this study, and in others (Braghetta et al. 1997; Edzwald 1995), that improved removal of HPO organics by CF-DAF is achieved as a result of HPO interactions at the air-bubble surface, although, to the knowledge of the authors, this has not been proven experimentally. Based on these findings, it would be of interest for future studies to employ advanced organic characterisation techniques (i.e., liquid chromatography organic carbon detection (LC-OCD)) to ascertain whether differences in the removals of key organic foulants by CF-DAF and CF-SED could be responsible for different degrees of LPM fouling mitigation.

Recent studies by Ladouceur and Narbaitz (2022, 2023) also undertook to compare the performance of CF-SED and CF-DAF pretreatment using the same colored river water as for Walker and Narbaitz (2016) and Xu and Narbaitz (2016), but with different membrane types. Like the latter two studies, CF-SED treated water was obtained from a local full-scale facility, however, due to COVID-19 access limitations, the former two studies (Ladouceur and Narbaitz 2022, 2023)

could not sample from the full-scale flotation facility and instead conducted CF-DAF pretreatment using a large bench-scale flotation unit (Gonzalez-Galvis and Narbaitz 2020, 2022). In all studies, practically identical coagulation chemistries were used for CF-SED and CF-DAF pretreatment, however, it should be noted that floated water produced by the batch unit in the studies by Ladouceur and Narbaitz (2022, 2023) used coagulant (ALS, Kemira, Varennes, QC) obtained from the chemical supplier of the full-scale treatment plant and not from the plant itself (i.e., coagulant was possibly from different lots). Although the raw river water quality was similar between the four studies and CF-DAF was reported to remove greater amounts of bulk and HPO organics (as indicated by UV_{254} and SUVA) compared to CF-SED in all cases, the two pretreatment alternatives were found to perform equally well for the outside-in PVDF and multi-channel inside-out PES UF membranes considered. It must be stressed that the nominal molecular weight cut-off (MWCO) value for all three membrane types used in these four studies was the same (100 kDa). It was also acknowledged by the authors that the difference in optimal pretreatment strategy between studies may not only have arisen from differences in the membrane type/configuration, but also from changes in how the pretreatment was conducted. Besides using bench- and full-scale systems in the production of CF-DAF pretreated water, the full-scale facility from which CF-SED pretreated water was collected had undergone upgrades to their sedimentation basins (inclusion of inclined plates) in the time between the studies. The findings of these studies suggest that the relative performance of CF-DAF and CF-SED for pretreatment of LPMs is likely dependent on a unique interaction between the feed water and the specific membrane type/configuration employed. Further discussion on the impact of membrane type/configuration is presented in Section B.4.3.2.

B.4.3. Effects of System Parameters on LPM Fouling

The nature and extent of LPM fouling are known to be strongly influenced by the feed water quality, the membrane system characteristics (membrane properties and operating conditions), and the degree of pretreatment (Fig. B.4). The effects of these system parameters on LPM fouling in the integrated CF-DAF-LPM system are considered in turn below.

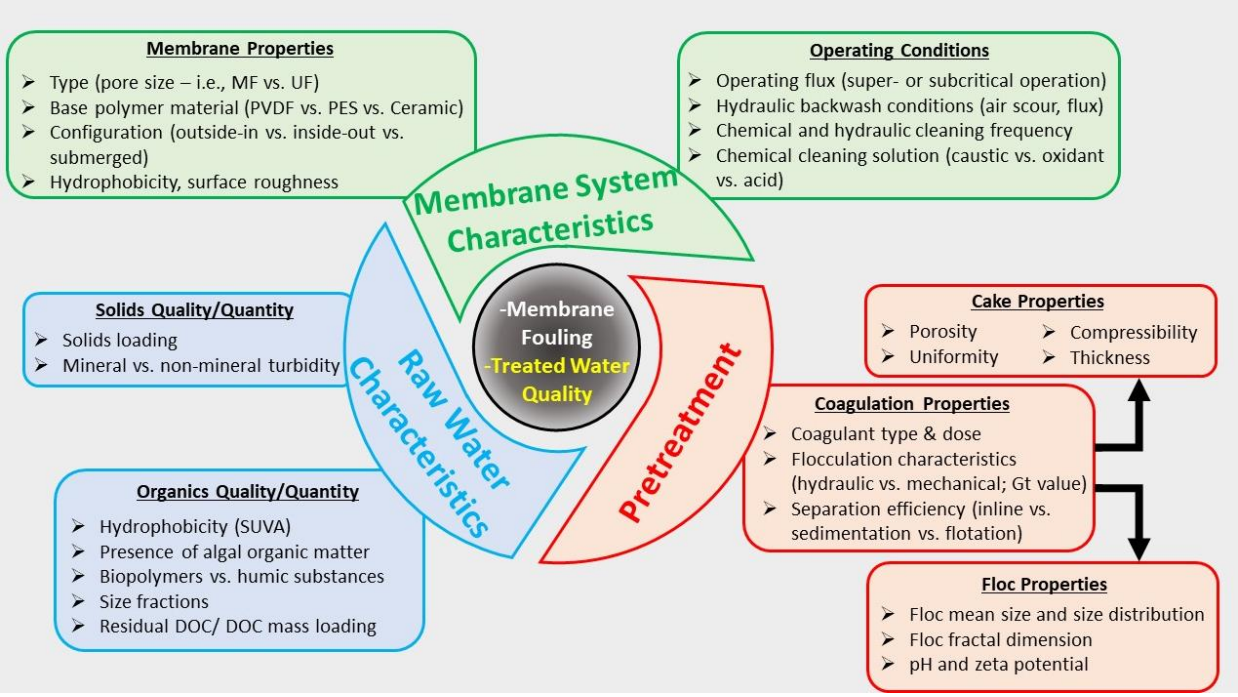


Fig. B.4. Factors influencing membrane fouling for LPMs in drinking water treatment. Note: information sourced from (Chang et al. 2002; Guo et al. 2012).

B.4.3.1. Water Quality

Relationships between measures of LPM irreversible fouling and CF-DAF treated water quality are presented in Fig. B.5. The hydraulically and chemically irreversible fouling rates are described by Eqn. (1) and Eqn. (2), respectively, which have been used previously by a number of authors to quantify LPM fouling rates for both real and synthetic challenge waters (Aly et al. 2021; Hatt et al. 2011; Resosudarmo et al. 2013):

$$FR_{hirr} = \frac{TMP_{cc,n_f} - TMP_{cc,n_i}}{t_{cc}} \quad \text{(B.1)}$$

$$FR_{cirr} = \frac{TMP_{cc,n+1_i} - TMP_{cc,n_i}}{t_{cc}} \quad \text{(B.2)}$$

where FR_{hirr} is the hydraulically irreversible fouling rate (mBar h^{-1}), TMP_{cc,n_f} is the TMP following the final hydraulic backwash of chemical clean cycle n (mBar), TMP_{cc,n_i} is the measured TMP at the beginning of chemical clean cycle n (mBar), FR_{cirr} is the chemically irreversible fouling rate (mBar h^{-1}), $TMP_{cc,n+1_i}$ is the measured TMP at the beginning of chemical clean cycle

$n+1$ (mBar), and t_{cc} is the time period between chemical cleanings (h). It must be noted that, due to the disparate character of the experimental setups used in the evaluation of CF-DAF performance, only a limited number of studies with the necessary data for calculation of fouling rates could be considered in the analysis provided by Fig. B.5. In Fig. B.5a and Fig. B.5b, relationships between the chemically irreversible fouling rate and the removal of UV_{254} as well as between the chemically irreversible fouling rate and the CF-DAF treated SUVA value are presented. Increased removal of UV_{254}, as well as lower residual SUVA values, are seen to result in reduced magnitude of chemically irreversible fouling. These findings suggest that, for the integrated CF-DAF-LPM system, chemically irreversible fouling is governed by the removal of HPO organic compounds (for which UV_{254} and SUVA are surrogate measures). It must be acknowledged that the data used for Figs. B.5a and B.5b consider only a single natural water which has been previously shown to be dominated by HPO organics and contains low concentrations of hydrophilic biopolymers (Croft 2012). It is therefore recommended that studies involving a more hydrophilic feed water be performed to confirm whether the relationships outlined in Fig. B.5 are generalizable for a variety of water types.

A relationship between the coagulated pH and the hydraulically irreversible fouling rate is presented in Fig. B.5c. As the CF-DAF treated pH value decreases from ~7.5 towards a value of 6, the rate of hydraulically irreversible fouling is seen to decrease. This is in agreement with the findings of Fu and Dempsey (1998) and Choi and Dempsey (2004), who reported that charged particles produced under coagulation conditions of reduced pH were more amenable to removal from the membrane surface following hydraulic backwashing. Direct relationships between the floc/particle charge characteristics (i.e., zeta potential) of CF-DAF pretreated water and measures of LPM fouling were not possible as many studies report only raw water characteristics or bulk water quality parameters for CF-DAF pretreated water (i.e., DOC and turbidity). It is recommended that future studies for CF-DAF pretreatment of LPMs investigate charge characteristics of coagulated and floated waters due to their potential significance for LPM fouling mitigation, which to date has not been reported on.

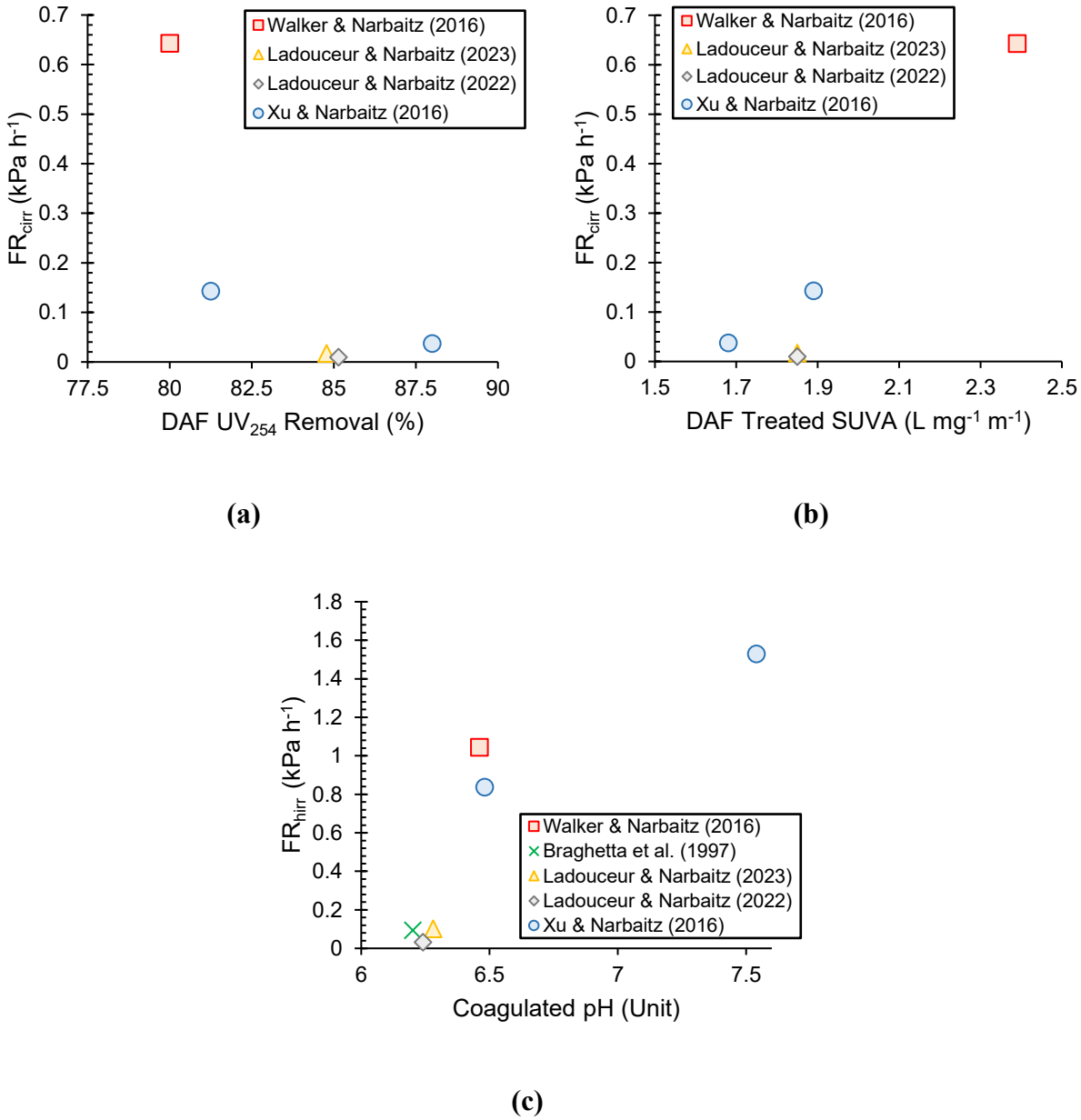


Fig. B.5. Relationships between fouling measures and source water quality parameters: **(a)** FR_{cirr} vs. CF-DAF UV_{254} Removal; **(b)** FR_{cirr} vs. CF-DAF Treated SUVA; **(c)** FR_{hirr} vs. Coagulated pH.

The impact of raw water turbidity on the performance of the integrated system is also worth discussing. Van Benschoten et al. (2002) reported raw water turbidities of 67 NTU and 37 NTU

for a reservoir water and a lake water, respectively, yet despite having the same DOC content the water with greater turbidity resulted in greater LPM permeability decline. Kang et al. (2021) considered average and maximum turbidity values as process controls for a CF-DAF-MF system. Under conditions of reduced raw water turbidity (average of 3.4 NTU) the MF module could be operated without CF-DAF pretreatment and with a weeklong interval between chemical maintenance cleanings. For elevated turbidity conditions (with average and maximum turbidity values reaching 10.1 NTU and 83 NTU, respectively), fouling mitigation could only be achieved with the implementation of optimised CF-DAF pretreatment in combination with enhanced physical backwashing and daily chemical maintenance cleaning. Therefore, for the integrated system, it is suggested that raw water turbidity (in addition to the feed water NOM) may also be critical in determining the fouling potential of a given source water. It is recommended that future CF-DAF-LPM studies distinguish between mineral and non-mineral turbidity when characterising the raw water quality. As proposed by Valade et al. (2009), CF-DAF is most effectively employed for average mineral turbidities (clays and silts) less than 10 NTU, while is recommended for average non-mineral turbidities (algae, particulate NOM) up to 100 NTU. When operated for feed waters with sustained turbidities above these levels, the CF-DAF effluent water quality may deteriorate, resulting in greater LPM fouling. Turbidity removals by CF-DAF amongst the literature surveyed in this review were found to be mostly greater than 75% and no relationships could be identified between raw water turbidity or CF-DAF treated turbidity and LPM irreversible fouling measures. It is likely, however, that the effects of turbidity on LPM fouling in the integrated system are more important for hydraulically reversible fouling, which is less critical for long-term operation, and for which sufficient data was not available.

B.4.3.2. Membrane Properties

In addition to feed water quality, membrane type and configuration have been shown to influence the performance of the integrated system. The study by Van Benschoten et al. (2002) reported somewhat conflicting results when using bench- and pilot-scale membranes with different configurations (the membrane pore size and principal polymer material were the same) to compare the performance of CF-DAF and C-IN for a lake water sampled in seasons of high and low turbidity. At bench-scale, flat sheet PVDF membranes indicated that CF-DAF provided superior performance for the high turbidity season, while C-IN and CF-DAF performed equally well for

the low turbidity season. When hollow fiber PVDF membranes were used at the pilot-scale, CF-DAF pretreatment yielded reduced LPM fouling compared to C-IN regardless of the season.

A similar dependence of LPM fouling potential on membrane configuration, but also material type, was identified by comparison of the studies using Ottawa River water reviewed in Section B.4.2. In the earlier two studies (Walker and Narbaitz 2016; Xu and Narbaitz 2016) (which used hollow fiber PES membranes with inside-out configuration), CF-DAF pretreatment resulted in final TMP values which were significantly reduced compared to pretreatment by CF-SED, while in the two recent studies (Ladouceur and Narbaitz 2022, 2023) (which considered the same water type but different membrane materials/configurations) the fouling performance of CF-DAF and CF-SED was the same. Another important observation of these last two studies was that by changing the membrane material/configuration from hollow fiber PVDF with an outside-in configuration to tubular multi-channel PES with an inside-out configuration, the optimal LPM pretreatment strategy changed from CF-DAF to C-IN. Thus, besides feed water quality, the membrane system characteristics play a key role in determining the optimal pretreatment strategy for a particular water type: this was highlighted in Fig. B.4. Considering all four studies (Ladouceur and Narbaitz 2022, 2023; Walker and Narbaitz 2016; Xu and Narbaitz 2016), the impact of membrane material type and configuration on LPM fouling could not be isolated as the membranes used were of PES and PVDF material with either inside-out or outside-in configuration and hollow fiber or tubular geometry. Accordingly, it would be of interest for future studies to examine the performance of the integrated system using a number of different water types and LPMs of consistent material but different configurations (and vice versa). Such a study could quantify the impact of both membrane type and configuration (separately) as well as determine whether these impacts are independent of the feed water character.

Besides membrane material and configuration, Minhalma and De Pinho (2001) also reported an influence of membrane MWCO on the fouling of UF membranes pretreated by CF-DAF. In this study, critical flux tests were performed using CF-DAF pretreated water and UF membranes made from cellulose acetate but with MWCO values ranging from 6 kDa to 86 kDa. As the MWCO of the UF membranes increased, the difference between the critical flux values for raw and CF-DAF pretreated waters increased (i.e., diverged at higher TMP). Furthermore, for greater MWCO values, the limiting flux value (below which the increase in pressure is linearly proportional to the flux increase) was found to decrease.

B.4.3.3. CF-DAF Parameters

The influence of CF-DAF related parameters on LPM fouling in the integrated system has not been adequately characterized. No study has systematically investigated whether the CF-DAF process parameters can influence the performance of the LPM in the integrated system. For example, in the study by Minhalma and De Pinho (2001), although attempts are made at optimising the coagulation and CF-DAF process parameters (recycle ratio and saturation pressure) in terms of organics removals, these goals were not simultaneously balanced with membrane performance. The importance of CF-DAF process parameter optimization was shown in the study by Valade et al. (1996), where changes to the coagulant type, mixing intensity (G value), and flocculation characteristics (number of stages and mixer type) resulted in treated waters with different residual particle numbers and size distributions, which may lead to different LPM fouling tendencies. Gonzalez-Galvis and Narbaitz (2022) also reported that alteration of the flocculation mean velocity gradient (G), the recycle ratio, or the saturator pressure may impact the removal of turbidity in CF-DAF, however, the degree to which differences in turbidity removal affected LPM fouling was not assessed. Concerning the removals of organics, this last study noted almost no impact by changing the flotation process conditions. Instead, the coagulation chemistry (i.e., pH and coagulant dose) was noted as the most critical factor impacting the removal of organics. Given the relationships outlined in Fig. B.5a-c, CF-DAF conditions resulting in greater removals of HPO organics at reduced pH conditions are expected to yield superior performance.

A final comment on the impact of CF-DAF parameters is regarding the use of polymer in the integrated system. As can be seen from Table B.2, more than half the studies surveyed applied low dose polyacrylamide polymer as a flotation aid. Although successful CF-DAF operation does not require polymer addition (Schofield 2001), utilities may employ low dosages to adjust the properties of the floated sludge (i.e., improve dewaterability). Alternatively, some utilities dose both cationic polymer and coagulant during rapid mixing in a strategy referred to as dual coagulation, with the aim of reducing alkalinity consumption and chemical sludge production (Edzwald and Haarhoff 2012). Although polymers have previously been reported to cause severe LPM fouling (Wang et al. 2011, 2013), studies consulted in this review did not demonstrate a propensity for increased fouling by CF-DAF pretreated waters with polymer addition. This can be seen in the study by Ladouceur and Narbaitz (2023) where CF-DAF pretreated water (which included the addition of cationic polyacrylamide) and CF-SED pretreated water (which did not

include polymer addition) resulted in practically identical TMP profiles. Moreover, the studies by Xu and Narbaitz (2016) and Walker and Narbaitz (2016) reported significantly reduced LPM fouling by CF-DAF pretreated water compared to CF-SED pretreated water, despite the conditioning of floated water by polymer. It should be noted, however, that these studies only evaluate short-term (<5 d) fouling behavior (despite simulating chemically enhanced backwashing and chemical clean-in-place) and the long-term impact of polymer use (in CF-DAF) on LPM irreversible fouling cannot be presently quantified based on these studies.

It is recommended that future studies undertake to systematically evaluate the impact of coagulation and CF-DAF parameters on the integrated system performance using a variety of water types. It is expected that, although CF-DAF is a robust clarification method, the alteration of operating conditions will result in a clarified feed water with different particle size distributions and/or different composition of organics which may influence LPM filterability.

B.4.4. Summary of CF-DAF-LPM Studies and Fouling Mechanism

While current studies have focused on validating the utility of the integrated CF-DAF-LPM process for a number of applications as well as comparing its performance with other pretreatment alternatives, they have not undertaken to establish the specific mechanism of LPM fouling mitigation. Despite this, several points may be inferred from existing results. The most critical factors governing LPM fouling mitigation by CF-DAF pretreatment appear to be the foulant mass loading delivered to the membrane and the specific feed water – membrane interactions. In Section B.4.1, several studies (Braghetta et al. 1997; Hög et al. 2015) were reviewed citing elevated solids mass loadings by C-IN as the likely reason for worsened LPM fouling compared to CF-DAF. The study by Walker and Narbaitz (2016) also reported worsened fouling by CF-SED (using iron coagulant) compared to CF-DAF (with alum), purported to be the result of the significantly greater foulant mass loading delivered to the membrane surface by the former. Based on these results, the existence of a critical threshold value was proposed, above which benefits of C-IN are offset by the elevated mass loading. From the results of the studies by Ladouceur and Narbaitz (2022, 2023), where C-IN performed best amongst pretreatment alternatives for a tubular PES membrane but worst for a hollow-fiber PVDF membrane, this threshold value is likely unique to each water-membrane combination.

The importance of water-membrane specific interactions on CF-DAF-LPM performance was also seen in Section B.4.2 when reviewing the four studies that used colored Ottawa River water. While Walker and Narbaitz (2016) and Xu and Narbaitz (2016) observed superior fouling mitigation by CF-DAF compared to CF-SED, Ladouceur and Narbaitz (2022, 2023) reported that these two pretreatment alternatives performed equally well when using LPMs of different type/configuration (but consistent coagulation chemistries). Membrane type also seemed to impact which components of the treated CF-DAF water matrix most significantly affected LPM fouling. For the inside-out PES membrane used by Xu and Narbaitz (2016) and the outside-in PVDF membrane used by Ladouceur and Narbaitz (2023), hydraulically and chemically irreversible fouling were strongly dependent on the hydrophobicity of the CF-DAF treated water, while for the tubular PES membrane used in the second study by Ladouceur and Narbaitz (2022), no such dependence was observed.

In summary, the mechanism of LPM fouling mitigation by CF-DAF remains unclear and should be further elucidated through systematic investigation of how: (1) the feed water characteristics and CF-DAF operating parameters alter the removal of specific components of the water matrix (i.e., biopolymers vs. humic substances; turbidity vs. DOC); (2) the presence of these components in the CF-DAF treated water affects the reversibility of fouling (hydraulically and chemically); and (3) the removal of specific components of the water matrix affects the fouling type (pore blocking vs. cake layer vs. pore constriction). This should be the subject of future research.

B.5. Water Quality of Integrated DAF-LPM System

Table B.3 summarizes the removals of organic and particulate water quality measures following CF-DAF pretreatment and LPM filtration for selected studies. Important CF-DAF parameters as well as bulk measures of the raw water quality are also presented for each study.

Appendix B

Table B.3. Removals of Bulk Water Quality Parameters for Selected CF-DAF-LPM Studies[a].

Coagulation/Flotation Characteristics				Raw Water Characteristics					Post CF-DAF Treatment[b]				Post LPM Filtration[b]		
Coag. Type	Coag. Dose (mg-Me^{+} L^{-1})	Recycle Pressure (kPa)	Recycle Ratio (%)	Water Type	DOC (ppm)	SUVA ($Lmg^{-1}m^{-1}$)	Turbidity (NTU)	pH	DOC Removal (%)	Turbidity Removal (%)	UV_{254} Removal (%)	pH	DOC Removal (%)	Turbidity Removal (%)	Ref. (see notes)
Alum	5	450	20	SE	9.85	2.5	3.2	8.2	N/A	N/A	N/A	N/A	10.0 (8.87)	N/A	[1]
CHIT	200 (as coag.)	600	19	CWW	3.35 (TOC)	N/A	N/A	4.9	12	N/A	N/A	3.0	Variable[c]	N/A	[2]
Alum	3.43	400	10	Lake	4.87	1.44	5.32	N/A	37.8 (3.03)	60.9 (2.08)	57.1 (0.03)	N/A	52.2 (2.33)	92 (0.43)	[3]
$FeCl_3$	10	200	N/A	River	6.25-10.1 (TOC)	N/A	>10	6.8-7.4	N/A	N/A	N/A	N/A	34	90	[4]
PACl	50 (as coag.)	517	10	River	3.8	3.41	2.3	7.0	N/A	78.3 (0.50)	69.9 (0.039)	N/A	59.2 (1.55)	97.8 (0.05)	[5]
PACl	12 (as coag.)	517	10	Lake	2.2	1.53	1.65	8.1	N/A	77.6 (0.37)	48.8 (0.017)	N/A	19.5 (1.77)	97.0 (0.05)	
PACl	18 (as coag.)	517	10	Lake	2.0	1.58	37	8.0	11.0 (1.79)	87.5 (4.61)	43.0 (0.018)	N/A	11.0 (1.78)	99.9 (0.04)	
PACl	20 (as coag.)	517	10	Lake	2.2	1.15	66	8.1	N/A	96.0 (2.7)	37.1 (0.016)	N/A	21.4 (1.73)	99.9 (0.04)	
PACl	Variable[d]	N/A	10	Lake	2.2	1.50	1.4	8.1	N/A	N/A	N/A	N/A	17.0 (1.83)	N/A	
PACl	Variable[d]	N/A	10	Lake	2.0	1.30	15	8.0	N/A	N/A	N/A	N/A	N/A	N/A	
PACl	2	400	N/A	SYN	N/A	N/A	110-125	5.5	N/A	72	N/A	N/A	N/A	N/A	[6]
PACl	2	400	N/A	SYN	N/A	N/A	110-125	5.5	N/A	72	N/A	N/A	N/A	N/A	
PACl	2	400	N/A	SYN	N/A	N/A	110-125	5.5	N/A	72	N/A	N/A	N/A	N/A	
PACl	2	400	N/A	SYN	N/A	N/A	50-70	5.0	N/A	29	N/A	N/A	N/A	N/A	
PACl	2	400	N/A	SYN	N/A	N/A	50-70	5.0	N/A	29	N/A	N/A	N/A	N/A	
PACl	2	400	N/A	SYN	N/A	N/A	50-70	5.0	N/A	29	N/A	N/A	N/A	N/A	
Alum	45 (as coag.)	N/A	N/A	RES	6.9 (TOC)	2.3	2.7	7.3	(3.5-5.3)	(0.3-1.0)	43.8 (0.09)	6.2	2.6-11.1[e]	(<0.03)	[7]
Alum	3.18-3.36	N/A	N/A	River	8.16	3.92	3.56	7.7	62.4 (3.07)	85.4 (0.52)	81.3 (0.06)	7.54	73.7	N/A	[8]
Alum	3.18-3.36	N/A	N/A	River	7.09	3.56	1.63	6.77	72.4 (1.96)	82.2 (0.29)	88.0 (0.03)	6.48	N/A	N/A	
Alum	2.99	N/A	N/A	River	6.07	4.16	1.52	6.97	65.9 (2.07)	75.7 (0.37)	80.0 (0.05)	6.46	69 (1.88)	N/A	[9]
PACl	3.16	N/A	N/A	RES	3.06	N/A	8.3	N/A	41.2 (1.8)	(<1)	N/A	N/A	N/A	N/A	[10]
Alum	3.36	483	10	River	6.64	4.16	4.88	7.52	65.8 (2.27)	87.9 (0.59)	85.1 (0.041)	6.28	71.5 (1.89)	99 (0.052)	[11]
Alum	3.36	483	10	River	6.54	4.22	4.92	7.76	65.9 (2.23)	88.8 (0.55)	84.8 (0.042)	6.24	67 (2.16)	99 (0.056)	[12]

[a] CHIT = chitosan; CWW = cork processing wastewater; DOC = dissolved organic carbon; N/A = not available; PACl = polyaluminum chloride; RES = reservoir; SE = secondary effluent; SUVA = specific ultraviolet absorbance at 254nm; SW= seawater; SYN = synthetic water; TOC = total organic carbon. [b] Residual values in brackets. [c] Performed critical flux testing with five membrane types reporting 15-99% rejection. [d] Coagulant dose was adjusted using influent feed water turbidity measurements. [e] Removal by MF membrane only. Note, references given by: [1] Goh et al. (2010); [2] Minhalma and De Pinho (2001); [3] Amaral et al. (2013); [4] Hög et al. (2015); [5] Van Benschoten et al. (2002); [6] Pissibanganga et al. (2016); [7] Braghetta et al. (1997); [8]Xu and Narbaitz (2016); [9] Walker and Narbaitz (2016); [10] Kang et al. (2021); [11] Ladouceur and Narbaitz (2022); [12]Ladouceur and Narbaitz (2023)

The analysis of integrated system product water quality will be made by considering the performance in terms of organics, particulate, and algae removals. It can be seen from Table B.3 that the removal of organics (measured as DOC) by LPMs following CF-DAF pretreatment varies between 0-14.4% (calculated by subtracting the post CF-DAF DOC from the post LPM filtration DOC). Although this is within the range of removals (5-20%) suggested by Pearce (2011), it has been proposed that the removal of organics by the LPM following CF-DAF pretreatment will be lower than what is typical for LPMs without pretreatment or even with alternative coagulation pretreatment strategies (i.e., CF-SED) (Guastalli et al. 2013; Minhalma and De Pinho 2001; Shi et al. 2017). The propensity of CF-DAF pretreatment for removing HPO organic materials results in a membrane feed water with a more hydrophilic character and greater proportions of low-molecular weight (LMW) organics, which are poorly retained by LPMs. This was observed in the study by Shi et al. (2017), where the UF membranes reduced the organics (measured as chemical oxygen demand (COD)) by only 6.4%, as well as in the study by Guastalli et al. (2013) where only 6% of LMW organics (measured by LC-OCD) were retained by the UF membrane.

The integrated system has been shown to effectively reduce turbidity in treated water, with a number of studies reporting finished water qualities < 0.06 NTU (Braghetta et al. 1997; Ladouceur and Narbaitz 2022, 2023; Van Benschoten et al. 2002). The integrated system has also proven to effectively manage variable feed water quality. For example, Braghetta et al. (1997) reported that, despite a variable average feed water turbidity ranging between 2 and 5 NTU, CF-DAF pretreatment was able to produce a LPM feed water with a consistent quality (turbidities < 0.5 NTU). Kang et al. (2021) also reported that for an average CF-DAF feed water turbidity of 10.1 NTU but variable conditions reaching a maximum value of 83 NTU the integrated system could produce an effluent with a consistent quality.

A few authors have monitored the removal of algal cells throughout the various stages of the integrated system. Amaral et al. (2013) reported that for a freshwater lagoon source known to contain high densities of microalgae (cyanobacterial density of 39,000 cells mL^{-1}), CF-DAF pretreatment could remove 71% of organisms, while CF-DAF integrated with MF consistently achieved complete cyanobacterial removal. This finding was corroborated by Goh et al. (2010) who reported negligible Chlorophyll-a concentration following CF-DAF-MF of a secondary effluent spiked with *M. aeruginosa*. Regarding the removal of algae, it would be of interest to evaluate the seasonality of the CF-DAF performance and its effect on LPM fouling. Many studies

have indicated that their source water is subject to seasonal algal blooms, yet only report average values for bulk parameters and do not adequately discuss any observed performance differences (in terms of fouling and water quality) between conditions of normal and algal impacted water quality. It would also be of interest to investigate whether the integrated process requires continuous optimization using a water quality measure as a process control tool or whether the CF-DAF process is robust enough to satisfy fouling and water quality objectives during all water quality events.

B.6. Economic Considerations

A detailed cost-benefit analysis of the integrated CF-DAF-LPM system is beyond the scope of this review, however, cost considerations associated with the implementation of CF-DAF pretreatment merit discussion. Table B.4 presents a survey of the operating and maintenance costs (OPEX) for LPM and CF-DAF facilities. All costs have been adjusted to May 2023 values in United States Dollars (USD) using the US consumer price index, for which historical information was obtained from the U.S. Bureau of Labor Statistics (2023). A number of cost analyses for LPM installations have been previously undertaken with results indicating a wide range of OPEX values (Table B.4), the magnitude of which are highly dependent on the assumptions of the authors. For example, using data collected from a limited number of full-scale facilities, Guo et al. (2014) developed a cost model indicating an OPEX of 0.322 USD/m^3 for a 20 MLD UF facility. Brehant et al. (2015) reported that, including expenses for power consumption, cleaning chemicals, labor for maintenance, and the cost of membrane replacement, OPEX for full-scale facilities with capacities of 91 MLD and 61 MLD were 0.021 USD/m^3 and 0.028 USD/m^3, respectively. Pearce (2008) noted an OPEX of 0.039 USD/m^3 for a 20 MLD UF facility including the cost of pretreatment by inline coagulation and either clarification or flotation, but not the cost of labor or maintenance. Pretreatment and labor costs, however, represent the most significant and variable component of the OPEX for an LMP facility (Gere 1997). For C-IN pretreatment, Guo et al. (2014) reported the OPEX of a coagulation/flocculation process train to be 0.072 USD/m^3. This last estimate assumed a coagulant and caustic dose of 56.5 mg L^{-1} and 2.5 mg L^{-1}, respectively; it must be noted that the cost of coagulation will be site-specific and is highly dependent on the raw water quality, the destabilization mechanism employed (i.e., sweep floc vs. charge neutralization), and the coagulant type. Concerning pretreatment by CF-DAF, McGivney and Kawamura (2008) estimated an OPEX

of 0.105 USD/m^3 (including labor, power, chemical and maintenance costs), while Cromphout et al. (2013) demonstrated the OPEX of a full-scale CF-DAF facility to be 0.116 USD/m^3 (excluding labor costs). These represent additional costs of up to ~7 times the OPEX for standalone LPM filtration (0.016 – 0.322 USD/m^3) based on the values obtained from the survey of available literature (Table B.4). The dependence of CF-DAF OPEX on raw water quality should also be mentioned. As CF-DAF requires conditioning by coagulation for effective particle-bubble attachment, and the coagulation chemistry is sensitive to the influent water quality, the coagulation/flocculation process is also expected to introduce some degree of variability in the OPEX of CF-DAF. The study by Cromphout et al. (2013) provides some insight into the importance of coagulation conditions, reporting that over 95% of the OPEX value (excluding labor) was associated with the cost of chemicals for coagulation and their waste disposal. The uncertainty should be primarily a function of the degree of variability in raw water quality. It is well known that CF-DAF systems are not well suited for waters with mean mineral turbidities exceeding 10 NTU (Valade et al. 2009). Based on this, CF-DAF systems are not incorporated in the design of water treatment facilities for source waters with high turbidity feeds: CF-SED or ballasted sedimentation are recommended instead (Valade et al. 2009). Thus, based on the lower feed turbidities typical of CF-DAF systems, one would expect less variability in raw water quality and a corresponding lower uncertainty in the OPEX associated with coagulation chemistry.

Labor is an often-overlooked component of the cost estimate, which has resulted in significant underestimation of OPEX in previous studies. In a recent study by Judd and Carra (2021), it has been shown that over 50% of the total labor costs for a LPM facility are associated with reactive labor for the remedy of membrane pinning and clogging events. These events necessitate operator intervention and can negatively impact key contributors to facility OPEX including labor effort, chemical and energy consumption, membrane lifespan, and waste disposal, leading to increased costs. Due to its excellent separation efficiency (Edzwald 1995), pretreatment of LPM feed water by CF-DAF is expected to reduce the incidence of process upsets due to membrane pinning and clogging events. This could result in a cost savings (as a proportion of capital costs) of at least 20% (over the plant life) for facilities with flow rates of 160 MLD and a greater percentage for plants with smaller capacities (Judd and Carra 2021). The potential savings in OPEX associated with elimination of the reactive labor costs of LPM operation should be compared with the capital and operating costs for CF-DAF to assess whether the investment in

pretreatment is acceptable based on the risk reduction for process upset events. Such an analysis should also examine the potential reduction in LPM capital cost following CF-DAF pretreatment, which may be realized due to prolonged membrane lifespan or reduced membrane area arising from operation at higher flux values. Finally, the quality of the treated water must also be considered, as additional unit processes may be required to meet applicable treatment standards (i.e., DBP formation potential, enhanced coagulation under the Stage 1 DBP Rule) should pretreatment not be included or if alternative pretreatment strategies do not produce the same quality of treated water.

Appendix B

Table B.4. Survey of Operating Expenditure (OPEX) costs for Low-Pressure-Membrane and Dissolved Air Flotation Facilities.

Reference	Capacity (MLD)	OPEX (USD/m^3)	May 2023 OPEX (USD/m^3)	Qualifications
Costs for Standalone Low-Pressure Membrane Filtration				
Pearce (2008)	20	0.0275	0.039	- Monthly CIP Cleaning. - Excludes cost of labor, maintenance costs. - Includes cost for pretreatment by coagulation and either clarification or flotation.
American Water Works Association (2016)	0.1	0.054	0.068	- High flux condition.[a]
	1	0.033	0.042	- Monthly CIP cleaning.
	10	0.025	0.032	- Excludes cost of labor, pretreatment processes, and equipment maintenance.
	20	0.024	0.030	- Includes cost of membrane replacement.
	100	0.02	0.025	
	0.1	0.042	0.053	- Medium flux condition.
	1	0.026	0.033	- Monthly CIP cleaning.
	10	0.02	0.025	- Excludes cost of labor, pretreatment processes, and equipment maintenance.
	20	0.018	0.023	- Includes cost of membrane replacement.
	100	0.016	0.02	
	0.1	0.034	0.043	- Low flux condition.[b]
	1	0.021	0.027	- Monthly CIP cleaning.
	10	0.016	0.02	- Excludes cost of labor, pretreatment processes, and equipment maintenance.
	20	0.015	0.019	- Includes cost of membrane replacement.
	100	0.013	0.016	
Guo et al. (2014)	20	0.243	0.322	- Based on OPEX cost model developed using data obtained from full-scale installations. -Model developed using only 6 data points. - Includes cost for power, membrane replacement, cleaning chemicals, replacement parts, and maintenance labor.
Adham et al. (1996)	20 (MF)	0.022	0.044	- Developed using data obtained from a survey of 20 MF and 10 UF full-scale facilities. - Includes costs for cleaning chemicals, residuals disposal, energy, membrane replacement costs, labor, and equipment maintenance.
	20 (UF)	0.09	0.180	
Gere (1997)	20	0.082	0.164	- Includes costs for membrane replacement, residuals disposal, cleaning chemicals, replacement parts, power, and labor.
Bergman (2012)		0.066	0.089	N/A
Brehant et al. (2015)	91	0.016	0.021	- Data obtained from full-scale installation which pretreats water by alum coagulation and settling. - Cost based on 6-month CIP interval. - Includes costs for power, cleaning chemicals, labor for maintenance, and membrane replacement. -Excludes costs for pretreatment processes.
	61	0.022	0.028	- Data obtained from full-scale installation which pretreats water by PACl coagulation and flotation. - Cost based on 1-month CIP interval. - Includes costs for power, cleaning chemicals, labor for maintenance, and membrane replacement. -Excludes costs for pretreatment processes.
Campinas et al. (2021)	100	0.059	0.066	- Includes costs for power, membrane replacement, labor, replacement parts.

				-Includes cost cleaning chemicals.
Costs of Coagulation and Flocculation				
Guo et al. (2014)	20	0.054	0.072	- Based on assumption of neutral pH, 56.5 mg L^{-1} alum or ferric coagulant, and 2.5 mg L^{-1} caustic dose. - Includes cost for chemicals, power, replacement parts, and maintenance labor.
Costs of Dissolved Air Flotation				
McGivney and Kawamura (2008)	20	0.072	0.105	- Includes costs of power, chemicals, labor, and replacement parts.
Cromphout et al. (2013)	20	0.089	0.116	- Developed using data obtained from a full-scale CF-DAF facility. - Includes costs of power, chemicals, sludge disposal.

[a] High flux condition suitable for high quality water source with low total organic carbon and/or turbidity. [b] Low flux condition suitable for low quality feed water with high and/or variable total organic carbon and turbidity.

B.7. Conclusions and Future Research

This review compiled the results of studies investigating the performance of CF-DAF as pretreatment for LPMs in water treatment. Based on the literature surveyed, the findings of the study are as follows:

(1) CF-DAF is an excellent option for LPM fouling mitigation, particularly for highly colored waters or those with elevated DOC contents above 5 mg L^{-1}. For these water types, CF-DAF pretreatment has been shown to lead to significantly less fouling than for direct LPM filtration.

(2) While CF-DAF resulted in slightly lower DOC levels than CF-SED, better removals of organics did not necessarily imply improved fouling mitigation. In most cases, CF-DAF did result in improved performance compared to CF-SED, however, for several studies CF-SED and CF-DAF were found to perform similarly.

(3) In general, C-IN yielded reduced LPM fouling mitigation compared to CF-DAF, likely due to the higher mass loading delivered to the membrane surface. However, for a particular river water, changing the membrane type resulted in better LPM performance after pretreatment by C-IN than CF-DAF. Therefore, fouling mitigation appears to be dependent on unique interactions between the feed water quality and the membrane system characteristics (material and configuration). Accordingly, identifying the optimal pretreatment strategy for a particular water and membrane type will likely require bench- or pilot-scale testing.

(4) The majority of CF-DAF-LPM studies were conducted using limited water types (low alkalinity, colored, high NOM content, low biopolymer content). Relationships between the CF-DAF treated water quality and measures of LPM fouling indicate that improved removals of HPO organics (measured as UV_{254} and SUVA) as well as lower pH values result in reduced magnitude hydraulically and chemically irreversible fouling.

(5) The integrated system can effectively remove particulate matter as well as algal cells from feed water. Moreover, it has been shown that the CF-DAF-LPM system can provide robust treatment during periods of variable water quality.

(6) Integration of CF-DAF as LPM pretreatment represents a significant increase in OPEX compared to that of standalone LPM filtration. Detailed cost analysis should consider the economic benefits arising from CF-DAF pretreatment including the potential elimination or reduction of reactive labor and prolonged membrane lifespan. Furthermore, the possible elimination of downstream unit processes needed to meet DBP requirements should also be considered.

Based on the findings of this study, it is recommended that future research be undertaken to determine the performance of the CF-DAF-LPM system for waters with different organic character so that the universality of the relationships in Fig. B.5 can be confirmed for waters not dominated by HPO organics. Moreover, studies should attempt to separate the impact of membrane type and configuration on LPM fouling, which have been shown to be influential for the relative performance of CF-DAF compared to other coagulation pretreatment alternatives. Finally, longitudinal studies with emphasis on the characterisation of performance across seasons and during times of algal blooms (as opposed to average conditions) should be performed to identify process control tools and to assess the superiority of CF-DAF as LPM pretreatment in these conditions.

B.8. Acknowledgements

This work was supported by the Natural Sciences and Engineering Research Council of Canada (NSERC) under grant RGPIN 2018-06571 as well as the NSERC Postgraduate Scholarship-Doctoral program (ID 579943-2023).

B.9. References

Abuhasel, K., M. Kchaou, M. Alquraish, Y. Munusamy, and Y. T. Jeng. 2021. "Oily Wastewater Treatment: Overview of Conventional and Modern Methods, Challenges, and Future Opportunities." *Water*, 13 (7): 980. https://doi.org/10.3390/w13070980.

Adham, S. S., J. G. Jacangelo, and J.-M. Laîné. 1996. "Characteristics and costs of MF and UF plants." *Journal AWWA*, 88 (5): 22–31. https://doi.org/10.1002/j.1551-8833.1996.tb06551.x.

Ahmad, T., C. Guria, and A. Mandal. 2020. "A review of oily wastewater treatment using ultrafiltration membrane: A parametric study to enhance the membrane performance." *Journal of Water Process Engineering*, 36: 101289. https://doi.org/10.1016/j.jwpe.2020.101289.

Alayande, A. B., J. Lim, J. Kim, S. Hong, A. S. Al-Amoudi, and B. Park. 2022. "Fouling control in SWRO desalination during harmful algal blooms: A historical review and future developments." *Desalination*, 543: 116094. https://doi.org/10.1016/j.desal.2022.116094.

Alresheedi, M. T., S. L. D. Kenari, B. Barbeau, and O. D. Basu. 2022. "Flux modulation: A novel approach for ultrafiltration fouling control." *Journal of Water Process Engineering*, 46: 102551. https://doi.org/10.1016/j.jwpe.2021.102551.

Alshahri, A. H., L. Fortunato, N. Zaouri, N. Ghaffour, and T. Leiknes. 2021. "Role of dissolved air flotation (DAF) and liquid ferrate on mitigation of algal organic matter (AOM) during algal bloom events in RO desalination." *Separation and Purification Technology*, 256: 117795. https://doi.org/10.1016/j.seppur.2020.117795.

Aly, S. A., W. B. Anderson, and P. M. Huck. 2021. "In-line coagulation assessment for ultrafiltration fouling reduction to treat secondary effluent for water reuse." *Water Science and Technology*, 83 (2): 284–296. https://doi.org/10.2166/wst.2020.571.

Amaral, P. A. P. do, L. A. Coral, M. E. Nagel-Hassemer, T. J. Belli, and F. R. Lapolli. 2013. "Association of dissolved air flotation (DAF) with microfiltration for cyanobacterial removal in water supply." *Desalination and Water Treatment*, 51 (7–9): 1664–1671. https://doi.org/10.1080/19443994.2012.715128.

Amato, T., K.-S. Park, W. Yim, and T. Kim. 2013. "SWRO pre-treatment design using high-rate dissolved air flotation including preliminary pilot-scale results." *Desalination and Water Treatment*, 51 (7–9): 1804–1816. https://doi.org/10.1080/19443994.2012.694231.

American Water Works Association. 2016. *Manual of water supply practices - M53, Microfiltration and ultrafiltration membranes for drinking water*. 2nd ed. Denver, CO.

Amjad, H., Z. Khan, and V. V. Tarabara. 2015. "Fractal structure and permeability of membrane cake layers: Effect of coagulation–flocculation and settling as pretreatment steps." *Separation and Purification Technology*, 143: 40–51. https://doi.org/10.1016/j.seppur.2015.01.020.

Amy, G. 2008. "Fundamental understanding of organic matter fouling of membranes." *Desalination*, 231 (1–3): 44–51. https://doi.org/10.1016/j.desal.2007.11.037.

An, C., G. Huang, Y. Yao, and S. Zhao. 2017. "Emerging usage of electrocoagulation technology for oil removal from wastewater: A review." *Science of The Total Environment*, 579: 537–556. https://doi.org/10.1016/j.scitotenv.2016.11.062.

Anderson, L. E., B. F. Trueman, D. W. Dunnington, and G. A. Gagnon. 2021. "Relative importance of organic- and iron-based colloids in six Nova Scotian lakes." *npj Clean Water*, 4 (26): 10.

Archer, A. D., and P. C. Singer. 2006. "Effect of SUVA and enhanced coagulation on removal of TOX precursors." *Journal AWWA*, 98 (8): 11.

Arnold, S. R., T. P. Grubb, and P. J. Harvey. 1995. "Recent applications of dissolved air flotation pilot studies and full scale design." *Water Science and Technology*, 31 (3–4). https://doi.org/10.1016/0273-1223(95)00227-E.

Bergman, R. A. 2012. "Cost of membrane treatment - current costs and trends." Glendale, AZ.

Bermea, E. A. 1999. "Dual-membrane treatment of the Rio Grande: Meeting El Paso's future water demands." M.Sc, University of Texas at El Paso.

Braghetta, A., J. G. Jacangelo, S. Chellam, B. A. Utne, and M. L. Hotaling. 1997. "DAF pretreatment: its effect on MF performance." *Journal AWWA*, 89 (10): 90–101.

Bratby, J. 2016. *Coagulation and Flocculation in Water and Wastewater Treatment*. 3rd ed. London, UK: IWA Publishing.

Brehant, A., A. Fabre, and R. Bonnard. 2015. "What is the total cost of ownership for a low-pressure membrane plant for drinking water production? The comparison of three membrane materials: PVDF, PES, and CTA." Orlando, FL.

Campinas, M., R. M. C. Viegas, C. Silva, H. Lucas, and M. J. Rosa. 2021. "Operational performance and cost analysis of PAC/ceramic MF for drinking water production: Exploring treatment capacity as a new indicator for performance assessment and optimization." *Separation and Purification Technology*, 255: 117443. https://doi.org/10.1016/j.seppur.2020.117443.

Chang, H., H. Liang, F. Qu, B. Liu, H. Yu, X. Du, G. Li, and S. A. Snyder. 2017a. "Hydraulic backwashing for low-pressure membranes in drinking water treatment: A review." *Journal of Membrane Science*, 540 (May): 362–380. Elsevier B.V. https://doi.org/10.1016/j.memsci.2017.06.077.

Chang, H., B. Liu, H. Liang, H. Yu, S. Shao, and G. Li. 2017b. "Effect of filtration mode and backwash water on hydraulically irreversible fouling of ultrafiltration membrane." *Chemosphere*, 179 (2): 254–264. https://doi.org/10.1016/j.chemosphere.2017.03.122.

Chang, I.-S., P. Le Clech, B. Jefferson, and S. Judd. 2002. "Membrane Fouling in Membrane Bioreactors for Wastewater Treatment." *Journal of Environmental Engineering*, 128 (11): 1018–1029. https://doi.org/10.1061/(ASCE)0733-9372(2002)128:11(1018).

Chen, Y., J. Teng, B.-Q. Liao, R. Li, and H. Lin. 2020. "Molecular insights into the impacts of iron(III) ions on membrane fouling by alginate." *Chemosphere*, 242: 125232. https://doi.org/10.1016/j.chemosphere.2019.125232.

Choi, K. Y. J., and B. A. Dempsey. 2004. "In-line coagulation with low-pressure membrane filtration." *Water Research*, 38 (19): 4271–4281. https://doi.org/10.1016/j.watres.2004.08.006.

Choi, Y. H., H. S. Kim, and J. H. Kweon. 2008. "Role of hydrophobic natural organic matter flocs on the fouling in coagulation-membrane processes." *Separation and Purification Technology*, 62 (3): 529–534. https://doi.org/10.1016/j.seppur.2008.03.001.

Crittenden, J. C., R. R. Trussell, D. W. Hand, K. J. Howe, and G. Tchobanoglous. 2012. *Water treatment: Principles and design*. 3rd ed. New York, NY: McGraw-Hill.

Croft, J. 2012. "Natural Organic Matter Characterization of Different Source and Treated Waters; Implications for Membrane Fouling Control." M.A.S.c Thesis, University of Waterloo.

Cromphout, J., H. Lagast, G. Peleman, and L. Verdickt. 2013. "Flotation outperforms sedimentation and ultrafiltration for turbidity and NOM removal at the drinking water

treatment plant of Kluizen." *Water Supply*, 13 (2): 302–308. https://doi.org/10.2166/ws.2013.023.

Crossley, I. A., and M. T. Valade. 2006. "A review of the technological developments of dissolved air flotation." *Journal of Water Supply: Research and Technology - AQUA*, 55 (7–8): 479–491. https://doi.org/10.2166/aqua.2006.057.

Deka, B. J., J. Guo, S. Jeong, M. Kumar, and A. K. An. 2020. "Control of membrane fouling by dissolved algal organic matter using pre-oxidation with coagulation as seawater pretreatment." *Environmental Science: Water Research and Technology*, 6 (4): 935–944. Royal Society of Chemistry. https://doi.org/10.1039/c9ew00955h.

Delpla, I., A.-V. Jung, E. Baures, M. Clement, and O. Thomas. 2009. "Impacts of climate change on surface water quality in relation to drinking water production." *Environment International*, 35 (8): 1225–1233. https://doi.org/10.1016/j.envint.2009.07.001.

Ducker, W. A., Z. Xu, and J. N. Israelachvili. 1994. "Measurements of Hydrophobic and DLVO Forces in Bubble-Surface Interactions in Aqueous Solutions." *Langmuir*, 10 (9): 3279–3289. https://doi.org/10.1021/la00021a061.

Ebrahimi, M., D. Willershausen, K. S. Ashaghi, L. Engel, L. Placido, P. Mund, P. Bolduan, and P. Czermak. 2010. "Investigations on the use of different ceramic membranes for efficient oil-field produced water treatment." *Desalination*, 250 (3): 991–996. https://doi.org/10.1016/j.desal.2009.09.088.

Edzwald, J. K. 1993a. "Algae, bubbles, coagulants, and dissolved air flotation." *Water Science and Technology*, 27 (10): 67–81. https://doi.org/10.2166/wst.1993.0207.

Edzwald, J. K. 1993b. "Coagulation in drinking water treatment: Particles, organics and coagulants." *Water Science and Technology*, 27 (11): 21–35. https://doi.org/10.2166/wst.1993.0261.

Edzwald, J. K. 1995. "Principles and applications of dissolved air flotation." *Water Science and Technology*, 31 (3–4): 1–23. International Association on Water Quality. https://doi.org/10.1016/0273-1223(95)00200-7.

Edzwald, J. K. 2006a. "Dissolved air flotation in drinking water treatment." *Interface Science and Technology*, edited by G. Newcombe and D. Dixon, 89–107. Amsterdam, Netherlands: Elsevier.

Edzwald, J. K. 2006b. "Dissolved air flotation in drinking water treatment." *Interface Science in Drinking Water Treatment: Theory and Application*, edited by G. Newcombe and D. Dixon. London, UK: Academic Press.

Edzwald, J. K. 2007. "Developments of high rate dissolved air flotation for drinking water treatment." *Journal of Water Supply: Research and Technology-Aqua*, 56 (6–7): 399–409. https://doi.org/10.2166/aqua.2007.013.

Edzwald, J. K. 2010. "Dissolved air flotation and me." *Water Research*, 44 (7): 2077–2106. Elsevier Ltd. https://doi.org/10.1016/j.watres.2009.12.040.

Edzwald, J. K., ed. 2011. *Water quality & treatment: A handbook on drinking water*. 6th ed. Denver, CO: American Water Works Association.

Edzwald, J. K., and J. Haarhoff. 2012. *Dissolved Air Flotation for Water Clarification*. New York, NY: McGraw-Hill.

Edzwald, J. K., and M. B. Kelley. 1998. "Control of From reservoirs to clarifiers to filters." *Water Science and Technology*, 37 (2). https://doi.org/10.1016/S0273-1223(98)00004-3.

Edzwald, J. K., J. E. Tobiason, L. M. Parento, M. B. Kelley, G. S. Kaminski, H. J. Dunn, and P. B. Galant. 2000. "Giardia and Cryptosporidium Removals by clarification and filtration

under challenge conditions." *Journal AWWA*, 92 (12): 70–84. https://doi.org/10.1002/j.1551-8833.2000.tb09072.x.

Edzwald, J. K., and J. E. Van Benschoten. 1990. "Aluminum coagulation of natural organic matter." *Chemical Water and Wastewater Treatment*, edited by H. H. Hahn and R. Klute, 341–359. Berlin, Heidelberg: Springer Berlin Heidelberg.

Edzwald, J. K., J. P. Walsh, G. S. Kaminski, and H. J. Dunn. 1992. "Flocculation and air requirements for dissolved air flotation." *Journal AWWA*, 84 (3): 92–100. https://doi.org/10.1002/j.1551-8833.1992.tb07325.x.

Evans, C. D., D. T. Monteith, and D. M. Cooper. 2005. "Long-term increases in surface water dissolved organic carbon: Observations, possible causes and environmental impacts." *Environmental Pollution*, 137 (1): 55–71. https://doi.org/10.1016/j.envpol.2004.12.031.

Farahbakhsh, K., C. Svrcek, R. K. Guest, and D. W. Smith. 2004. "A review of the impact of chemical pretreatment on low-pressure water treatment membranes." *Journal of Environmental Engineering and Science*, 3 (4): 237–253. https://doi.org/10.1139/S03-078.

Fred Fu, L., and B. A. Dempsey. 1998. "Modeling the effect of particle size and charge on the structure of the filter cake in ultrafiltration." *Journal of Membrane Science*, 149 (2): 221–240. https://doi.org/10.1016/S0376-7388(98)00169-0.

Gao, W., H. Liang, J. Ma, M. Han, Z. Chen, Z. Han, and G. Li. 2011. "Membrane fouling control in ultrafiltration technology for drinking water production: A review." *Desalination*, 272 (1–3): 1–8. Elsevier B.V. https://doi.org/10.1016/j.desal.2011.01.051.

Gere, A. R. 1997. "Microfiltration operating costs." *Journal AWWA*, 89 (10): 40–49. https://doi.org/10.1002/j.1551-8833.1997.tb08304.x.

Gobler, C. J. 2020. "Climate Change and Harmful Algal Blooms: Insights and perspective." *Harmful Algae*, 91: 101731. https://doi.org/10.1016/j.hal.2019.101731.

Goh, Y. T., J. L. Harris, and F. A. Roddick. 2010. "Reducing the effect of cyanobacteria in the microfiltration of secondary effluent." *Water Science and Technology*, 62 (7): 1682–1688. https://doi.org/10.2166/wst.2010.482.

Gonzalez-Galvis, J. P., and R. M. Narbaitz. 2020. "Large batch bench-scale dissolved air flotation system (LB-DAF) for drinking water treatability tests." *Environmental Science: Water Research and Technology*, 6 (4): 1004–1017. Royal Society of Chemistry. https://doi.org/10.1039/c9ew00935c.

Gonzalez-Galvis, J. P., and R. M. Narbaitz. 2022. "Large batch bench-scale dissolved air flotation system for simulating full-scale turbidity removal." *Environmental Technology*, 43 (12): 1791–1804. https://doi.org/10.1080/09593330.2020.1852317.

Gonzalez-Torres, A., M. Pivokonsky, and R. K. Henderson. 2019. "The impact of cell morphology and algal organic matter on algal floc properties." *Water Research*, 163: 114887. https://doi.org/10.1016/j.watres.2019.114887.

Guastalli, A. R., F. X. Simon, Y. Penru, A. de Kerchove, J. Llorens, and S. Baig. 2013. "Comparison of DMF and UF pre-treatments for particulate material and dissolved organic matter removal in SWRO desalination." *Desalination*, 322: 144–150. Elsevier B.V. https://doi.org/10.1016/j.desal.2013.05.005.

Guo, T., J. Englehardt, and T. Wu. 2014. "Review of cost versus scale: water and wastewater treatment and reuse processes." *Water Science and Technology*, 69 (2): 223–234. https://doi.org/10.2166/wst.2013.734.

Guo, W., H.-H. Ngo, and J. Li. 2012. "A mini-review on membrane fouling." *Bioresource Technology*, 122: 27–34. https://doi.org/10.1016/j.biortech.2012.04.089.

Haarhoff, J., and J. K. Edzwald. 2004. "Dissolved air flotation modelling: insights and shortcomings." *Journal of Water Supply: Research and Technology-Aqua*, 53 (3): 127–150. https://doi.org/10.2166/aqua.2004.0012.

Han, M. Y. 2002. "Modeling of DAF: The effect of particle and bubble characteristics." *Journal of Water Supply: Research and Technology - AQUA*, 51 (1): 27–34. https://doi.org/10.2166/aqua.2002.0003.

Harvey, N. J., Z. ur Rehman, T. O. Leiknes, N. Ghaffour, H. Urakawa, and T. M. Missimer. 2020. "Organic compounds and microbial assessment of a seawater reverse osmosis facility at Tampa Bay Water, USA." *Desalination*, 496 (August): 114735–114735. Elsevier. https://doi.org/10.1016/j.desal.2020.114735.

Hatt, J. W., E. Germain, and S. J. Judd. 2011. "Precoagulation-microfiltration for wastewater reuse." *Water Research*, 45 (19): 6471–6478. https://doi.org/10.1016/j.watres.2011.09.039.

Henderson, R. K., S. A. Parsons, and B. Jefferson. 2009. "The Potential for Using Bubble Modification Chemicals in Dissolved Air Flotation for Algae Removal." *Separation Science and Technology*, 44 (9): 1923–1940. https://doi.org/10.1080/01496390902955628.

Henderson, R. K., S. A. Parsons, and B. Jefferson. 2010a. "Polymers as bubble surface modifiers in the flotation of algae." *Environmental Technology*, 31 (7): 781–790. https://doi.org/10.1080/09593331003663302.

Henderson, R. K., S. A. Parsons, and B. Jefferson. 2010b. "The impact of differing cell and algogenic organic matter (AOM) characteristics on the coagulation and flotation of algae." *Water Research*, 44 (12): 3617–3624. https://doi.org/10.1016/j.watres.2010.04.016.

Henderson, R., E. Sharp, P. Jarvis, S. Parsons, and B. Jefferson. 2006. "Identifying the linkage between particle characteristics and understanding coagulation performance." *Water Supply*, 6 (1): 31–38. https://doi.org/10.2166/ws.2006.005.

Hög, A., J. Ludwig, and M. Beery. 2015. "The use of integrated flotation and ceramic membrane filtration for surface water treatment with high loads of suspended and dissolved organic matter." *Journal of Water Process Engineering*, 6: 129–135. Elsevier Ltd. https://doi.org/10.1016/j.jwpe.2015.03.010.

Hua, G., and D. A. Reckhow. 2007. "Characterization of disinfection byproduct precursors based on hydrophobicity and molecular size." *Environmental Science & Technology*, 41 (9): 3309–3315. https://doi.org/10.1021/es062178c.

Huang, H., K. Schwab, and J. G. Jacangelo. 2009. "Pretreatment for low pressure membranes in water treatment: A review." *Environmental Science and Technology*, 43 (9): 3011–3019. https://doi.org/10.1021/es802473r.

Hui, L., W. Yan, W. Juan, and L. Zhongming. n.d. "A Review: Recent Advances in Oily Wastewater Treatment."

Iritani, E., S. Matsumoto, and N. Katagiri. 2008. "Formation and consolidation of filter cake in microfiltration of emulsion–slurry." *Journal of Membrane Science*, 318 (1–2): 56–64. https://doi.org/10.1016/j.memsci.2008.02.009.

Jöhnk, K. D., J. Huisman, J. Sharples, B. Sommeijer, P. M. Visser, and J. M. Stroom. 2008. "Summer heatwaves promote blooms of harmful cyanobacteria: HEATWAVES PROMOTE HARMFUL CYANOBACTERIA." *Global Change Biology*, 14 (3): 495–512. https://doi.org/10.1111/j.1365-2486.2007.01510.x.

Judd, S. J., and I. Carra. 2021. "Low-pressure membrane technology for potable water filtration: true costs." *Water Research*, 191: 116826. https://doi.org/10.1016/j.watres.2021.116826.

Kamińska, G., W. Pronk, and J. Traber. 2020. "Effect of coagulant dose and backflush pressure on NOM membrane fouling in inline coagulation-ultrafiltration." *Desalination and Water Treatment*, 199: 188–197. https://doi.org/10.5004/dwt.2020.25657.

Kang, J., J. Seong, J. Yoo, P. Kim, K. Park, J. Lee, J. Cheon, H. Kim, and S. Lee. 2021. "Applicability of a combined DAF-MF process to respond to changes in reservoir water quality through a two-year pilot plant operation." *Membranes*, 11 (12): 964. https://doi.org/10.3390/membranes11120964.

Kawamura, S. 2000. *Integrated Design and Operation of Water Treatment Facilities*. New York, NY: John Wiley & Sons.

Khanzada, N. K., S. J. Khan, and P. A. Davies. 2017. "Performance evaluation of reverse osmosis (RO) pre-treatment technologies for in-land brackish water treatment." *Desalination*, 406: 44–50. https://doi.org/10.1016/j.desal.2016.06.030.

Kim, Y., D. Choi, M. Cui, J. Lee, B. Kim, K. Park, H. Jung, and B. Lee. 2015. "Dissolved air flotation separation for pretreatment of membrane bioreactor in domestic wastewater treatment." *Journal of Water Supply: Research and Technology-Aqua*, 64 (2): 186–193. https://doi.org/10.2166/aqua.2014.003.

Kimura, K., and K. Kume. 2020. "Irreversible fouling in hollow-fiber PVDF MF / UF membranes filtering surface water: Effects of precoagulation and identification of the foulant." *Journal of Membrane Science*, 602 (February): 117975–117975. Elsevier B.V. https://doi.org/10.1016/j.memsci.2020.117975.

Kimura, K., T. Maeda, H. Yamamura, and Y. Watanabe. 2008. "Irreversible membrane fouling in microfiltration membranes filtering coagulated surface water." *Journal of Membrane Science*, 320 (1–2): 356–362. https://doi.org/10.1016/j.memsci.2008.04.018.

Kinser, K. 2021. "Membrane Filtration: Past, Present, and Future." *Journal AWWA*, 113 (8): 72–75. https://doi.org/10.1002/awwa.1791.

Kurada, K. V., and S. De. 2018. "Polyaniline doped ultrafiltration membranes: Mechanism of membrane formation and pH response characteristics." *Polymer*, 153: 201–213. https://doi.org/10.1016/j.polymer.2018.08.032.

Ladouceur, J. D., and R. M. Narbaitz. 2022. "Reduced low–pressure membrane fouling by inline coagulation pretreatment for a colored river water." *Membranes*, 12 (11): 1028. https://doi.org/10.3390/membranes12111028.

Ladouceur, J. D., and R. M. Narbaitz. 2023. "Comparing sedimentation, flotation, and inline pre-treatment for low-pressure membrane fouling reduction." *Journal of Environmental Engineering (United States)*, 149 (4).

Lama, S., K. Muylaert, T. B. Karki, I. Foubert, R. K. Henderson, and D. Vandamme. 2016. "Flocculation properties of several microalgae and a cyanobacterium species during ferric chloride, chitosan and alkaline flocculation." *Bioresource Technology*, 220: 464–470. https://doi.org/10.1016/j.biortech.2016.08.080.

Lee, E.-J., H.-S. Kim, and A. Jang. 2016. "Application of dissolved air flotation (DAF) with coagulation process for treatment of phosphorus within permeate of membrane bioreactor (MBR)." *Desalination and Water Treatment*, 57 (19): 9043–9050. https://doi.org/10.1080/19443994.2015.1057034.

Lee, Y.-G., J. Shin, S. J. Kim, K. H. Cho, P. Westerhoff, H. Rho, and K. Chon. 2023. "An autopsy study of hollow fiber and multibore ultrafiltration membranes from a pilot-scale ultra high-recovery filtration system for surface water treatment." *Science of The Total Environment*, 866: 161311. https://doi.org/10.1016/j.scitotenv.2022.161311.

Leppinen, D. M. 1999. "Trajectory analysis and collision efficiency during microbubble flotation." *Journal of Colloid and Interface Science*, 212 (2): 431–442. https://doi.org/10.1006/jcis.1998.6075.

Leppinen, D. M., and S. B. Dalziel. 2004. "Bubble size distribution in dissolved air flotation tanks." *Journal of Water Supply: Research and Technology - AQUA*, 53 (8): 531–543. https://doi.org/10.2166/aqua.2004.0042.

Lerch, A., G. Hagmeyer, R. Gimbel, and J. Fehn. 2003. "A comparison of laboratory and pilot plant experiments on the combination of flocculation/ultrafiltration for direct potable water treatment of river water." *Water Supply*, 3 (5–6): 345–352. https://doi.org/10.2166/ws.2003.0187.

Li, B., B. Qi, Z. Guo, D. Wang, and T. Jiao. 2023. "Recent developments in the application of membrane separation technology and its challenges in oil-water separation: A review." *Chemosphere*, 327: 138528. https://doi.org/10.1016/j.chemosphere.2023.138528.

Li, K., G. Wen, S. Li, H. Chang, S. Shao, T. Huang, G. Li, and H. Liang. 2019. "Effect of pre-oxidation on low pressure membrane (LPM) for water and wastewater treatment: A review." *Chemosphere*, 231: 287–300. https://doi.org/10.1016/j.chemosphere.2019.05.081.

Liang, H., W. Gong, and G. Li. 2008. "Performance evaluation of water treatment ultrafiltration pilot plants treating algae-rich reservoir water." *Desalination*, 221 (1–3): 345–350. https://doi.org/10.1016/j.desal.2007.01.093.

Liang, H., W.-J. Gong, Z.-L. Chen, J.-Y. Tian, L. Qi, and G.-B. Li. 2009. "Effect of chemical preoxidation coupled with in-line coagulation as a pretreatment to ultrafiltration for algae fouling control." *Desalination and Water Treatment*, 9 (1–3): 241–245. https://doi.org/10.5004/dwt.2009.809.

Lipp, P., C. H. Lee, A. G. Fane, and C. J. D. Fell. 1988. "A fundamental study of the ultrafiltration of oil-water emulsions." *Journal of Membrane Science*, 36: 161–177. https://doi.org/10.1016/0376-7388(88)80014-0.

Logsdon, G. S., V. C. Thurman, E. S. Frindt, and J. G. Stoecker. 1985. "Evaluating Sedimentation and Various Filter Media for Removal of Giardia Cysts." *Journal AWWA*, 77 (2): 61–66. https://doi.org/10.1002/j.1551-8833.1985.tb05493.x.

Long, Y., X. You, Y. Chen, H. Hong, B.-Q. Liao, and H. Lin. 2020. "Filtration behaviors and fouling mechanisms of ultrafiltration process with polyacrylamide flocculation for water treatment." *Science of The Total Environment*, 703: 135540. https://doi.org/10.1016/j.scitotenv.2019.135540.

Long, Y., G. Yu, L. Dong, Y. Xu, H. Lin, Y. Deng, X. You, L. Yang, and B.-Q. Liao. 2021. "Synergistic fouling behaviors and mechanisms of calcium ions and polyaluminum chloride associated with alginate solution in coagulation-ultrafiltration (UF) process." *Water Research*, 189: 116665. https://doi.org/10.1016/j.watres.2020.116665.

Lundh, M., L. Jönsson, and J. Dahlquist. 2000. "Experimental studies of the fluid dynamics in the separation zone in dissolved air flotation." *Water Research*, 34 (1): 21–30. https://doi.org/10.1016/S0043-1354(99)00136-0.

Lundh, M., L. Jönsson, and J. Dahlquist. 2002. "The influence of contact zone configuration on the flow structure in a dissolved air flotation pilot plant." *Water Research*, 36 (6): 1585–1595. https://doi.org/10.1016/S0043-1354(01)00357-8.

Malkoske, T. A., P. R. Bérubé, and R. C. Andrews. 2020. "Coagulation/flocculation prior to low pressure membranes in drinking water treatment: A review." *Environmental Science:*

Water Research and Technology, 6 (11): 2993–3023. Royal Society of Chemistry. https://doi.org/10.1039/d0ew00461h.

Malley, J. P., and J. K. Edzwald. 1991. "Laboratory Comparison of DAF With Conventional Treatment." *Journal AWWA*, 83 (9): 56–61. https://doi.org/10.1002/j.1551-8833.1991.tb07214.x.

Matilainen, A., M. Vepsäläinen, and M. Sillanpää. 2010. "Natural organic matter removal by coagulation during drinking water treatment: A review." *Advances in Colloid and Interface Science*, 159 (2): 189–197. https://doi.org/10.1016/j.cis.2010.06.007.

Matsumoto, Y., T. Kawakatsu, M. Nakajima, and Y. Kikuchi. 1999. "Visualization of filtration phenomena of a suspended solution including O/W emulsion or solid particle and membrane separation properties of the solution." *Water Research*, 33 (4): 929–936. https://doi.org/10.1016/S0043-1354(98)00303-0.

McGivney, W., and S. Kawamura. 2008. *Cost Estimating Manual for Water Treatment Facilities*. 1st ed. Hoboken, NJ: John Wiley & Sons.

Minhalma, M., and M. N. De Pinho. 2001. "Flocculation/flotation/ultrafiltration integrated process for the treatment of cork processing wastewaters." *Environmental Science and Technology*, 35 (24): 4916–4921. https://doi.org/10.1021/es010119n.

Moore, S. K., V. L. Trainer, N. J. Mantua, M. S. Parker, E. A. Laws, L. C. Backer, and L. E. Fleming. 2008. "Impacts of climate variability and future climate change on harmful algal blooms and human health." *Environmental Health*, 7 (Suppl 2): S4. https://doi.org/10.1186/1476-069X-7-S2-S4.

Nguyen, A. H., J. E. Tobiason, and K. J. Howe. 2011. "Fouling indices for low pressure hollow fiber membrane performance assessment." *Water Research*, 45 (8): 2627–2637. Elsevier Ltd. https://doi.org/10.1016/j.watres.2011.02.020.

Obotey Ezugbe, E., and S. Rathilal. 2020. "Membrane technologies in wastewater treatment: A review." *Membranes*, 10 (5): 89. https://doi.org/10.3390/membranes10050089.

Paar, H., J. Benecke, M. Ernst, and M. Jekel. 2011. "Pre-coagulation and ultrafiltration of effluent impaired surface water for phosphorus removal and fouling control." *Water Supply*, 11 (2): 211–218. https://doi.org/10.2166/ws.2011.037.

Padaki, M., R. Surya Murali, M. S. Abdullah, N. Misdan, A. Moslehyani, M. A. Kassim, N. Hilal, and A. F. Ismail. 2015. "Membrane technology enhancement in oil–water separation. A review." *Desalination*, 357: 197–207. https://doi.org/10.1016/j.desal.2014.11.023.

Park, K. S., S. S. Mitra, W. K. Yim, and S. W. Lim. 2013. "Algal bloom—critical to designing SWRO pretreatment and pretreatment as built in Shuwaikh, Kuwait SWRO by Doosan." *Desalination and Water Treatment*, 51 (31–33): 6317–6328. https://doi.org/10.1080/19443994.2013.780992.

Pearce, G. K. 2008. "A cost optimization study of flux and fouling rate for UF in the water industry." *Water Supply*, 8 (1): 113–120. https://doi.org/10.2166/ws.2008.004.

Pearce, G. K. 2011. *UF/MF membrane water treatment: Principles and design*. 387. 1st ed. Bangkok: Water Treatment Academy.

Pearce, G. K. 2018. "Is the Water Membrane Market in a State of Flux?" *Water World*.

Peiris, R. H., H. Budman, C. Moresoli, and R. L. Legge. 2010. "Understanding fouling behaviour of ultrafiltration membrane processes and natural water using principal component analysis of fluorescence excitation-emission matrices." *Journal of Membrane Science*, 357 (1–2): 62–72. Elsevier B.V. https://doi.org/10.1016/j.memsci.2010.03.047.

Peleka, E. N., G. P. Gallios, and K. A. Matis. 2018. "A perspective on flotation: a review." *Journal of Chemical Technology & Biotechnology*, 93 (3): 615–623. https://doi.org/10.1002/jctb.5486.

Peters, C. D., T. Rantissi, V. Gitis, and N. P. Hankins. 2021. "Retention of natural organic matter by ultrafiltration and the mitigation of membrane fouling through pre-treatment, membrane enhancement, and cleaning - A review." *Journal of Water Process Engineering*, 44: 102374. https://doi.org/10.1016/j.jwpe.2021.102374.

Petry, M., M. A. Sanz, C. Langlais, V. Bonnelye, J.-P. Durand, D. Guevara, W. M. Nardes, and C. H. Saemi. 2007. "The El Coloso (Chile) reverse osmosis plant." *Desalination*, 203 (1–3): 141–152. https://doi.org/10.1016/j.desal.2006.05.007.

Pissibanganga, O. G. M., J. Jung, Y. Choi, S. Lee, J. Sohn, and N. Cho. 2016. "Influence of microbial floatation on membrane fouling due to particles and organic matters in submerged microfiltration." *Desalination and Water Treatment*, 57 (51): 24557–24565. Taylor & Francis. https://doi.org/10.1080/19443994.2016.1152645.

Plummer, J. D., J. K. Edzwald, and M. B. Kelley. 1995. "Removing Cryptosporidium by dissolved-air flotation." *Journal - American Water Works Association*, 87 (9): 85–95. https://doi.org/10.1002/j.1551-8833.1995.tb06425.x.

Rajapakse, N., M. Zargar, T. Sen, and M. Khiadani. 2022. "Effects of influent physicochemical characteristics on air dissolution, bubble size and rise velocity in dissolved air flotation: A review." *Separation and Purification Technology*, 289: 120772. https://doi.org/10.1016/j.seppur.2022.120772.

Rao, N. R. H., A. Gonzalez-Torres, B. Tamburic, Y. W. Wong, I. Foubert, K. Muylaert, R. K. Henderson, and D. Vandamme. 2023. "The influence of physical floc properties on the separation of marine microalgae via alkaline flocculation followed by dissolved air flotation." *Algal Research*, 71: 103024. https://doi.org/10.1016/j.algal.2023.103024.

Reed, B. E., P. Carriere, W. Lin, G. Roark, and R. Viadero. 1998. "Oily Wastewater Treatment by Ultrafiltration: Pilot-Scale Results and Full-Scale Design." *Practice Periodical of Hazardous, Toxic, and Radioactive Waste Management*, 2 (3): 100–107. https://doi.org/10.1061/(ASCE)1090-025X(1998)2:3(100).

Ren, L., C. Liu, T. Meng, and Y. Sun. 2021. "Effects of micro-flocculation pretreatment on the ultrafiltration membrane fouling caused by different dissolved organic matters in treated wastewater." *Journal of Water Reuse and Desalination*, 11 (4): 597–609. https://doi.org/10.2166/wrd.2021.051.

Resosudarmo, A., Y. Ye, P. Le-Clech, and V. Chen. 2013. "Analysis of UF membrane fouling mechanisms caused by organic interactions in seawater." *Water Research*, 47 (2): 911–921. https://doi.org/10.1016/j.watres.2012.11.024.

de Rijk, S. E., G. Jaap H.J.M. aivan der, and J. G. den Blanken. 1994. "Bubble size in flotation thickening." *Water Research*, 28 (2): 465–473. https://doi.org/10.1016/0043-1354(94)90284-4.

Rykaart, E. M., and J. Haarhoff. 1995. "Behaviour of air injection nozzles in dissolved air flotation." *Water Science and Technology*, 31 (3–4): 25–35. International Association on Water Quality. https://doi.org/10.1016/0273-1223(95)00201-W.

Salinas-Rodríguez, S. G., J. C. Schippers, G. L. Amy, I. S. Kim, and M. D. Kennedy. 2021. *Seawater Reverse Osmosis Desalination: Assessment and Pre-treatment of Fouling and Scaling*. 1st ed. London, UK: IWA Publishing.

Saththasivam, J., K. Loganathan, and S. Sarp. 2016. "An overview of oil–water separation using gas flotation systems." *Chemosphere*, 144: 671–680. https://doi.org/10.1016/j.chemosphere.2015.08.087.

Schofield, T. 2001. "Dissolved air flotation in drinking water production." *Water Science and Technology*, 43 (8): 9–18. https://doi.org/10.2166/wst.2001.0453.

Schulz, M., A. Soltani, X. Zheng, and M. Ernst. 2016. "Effect of inorganic colloidal water constituents on combined low-pressure membrane fouling with natural organic matter (NOM)." *Journal of Membrane Science*, 507: 154–164. Elsevier. https://doi.org/10.1016/j.memsci.2016.02.008.

Schurer, R., A. Tabatabai, L. Villacorte, J. C. Schippers, and M. D. Kennedy. 2013. "Three years operational experience with ultrafiltration as SWRO pre-treatment during algal bloom." *Desalination and Water Treatment*, 51 (4–6): 1034–1042. https://doi.org/10.1080/19443994.2012.713739.

Shawwa, A. R., and D. W. Smith. 2000. "Dissolved air flotation model for drinking water treatment." *Canadian Journal of Civil Engineering*, 27 (2): 373–382. https://doi.org/10.1139/l99-071.

Shi, Y., J. Ma, D. Wu, and Q. Pan. 2017. "Dessolved air flotation in combination with ultrafiltration membrane modules in surface water treatment." *Journal of Harbin Institute of Technology*, 24 (3).

Sillanpaa, M. 2015. *Natural Organic Matter in Water*. 1st ed. Oxford, UK: Butterworth-Heinemann.

Sillanpää, M., M. C. Ncibi, A. Matilainen, and M. Vepsäläinen. 2018. "Removal of natural organic matter in drinking water treatment by coagulation: A comprehensive review." *Chemosphere*, 190: 54–71. https://doi.org/10.1016/j.chemosphere.2017.09.113.

Souza, N. P. D., and O. D. Basu. 2013. "Comparative analysis of physical cleaning operations for fouling control of hollow fiber membranes in drinking water treatment." *Journal of Membrane Science*, 436: 28–35. Elsevier. https://doi.org/10.1016/j.memsci.2013.02.014.

Suárez, J., B. Salgado, A. Casañas, J. C. González, and J. Pordomingo. 2015. "One-year operational experience with ultrafiltration as pretreatment of seawater reverse osmosis desalination system (Maspalomas-I Plant)." *Desalination and Water Treatment*, 55 (10): 2813–2821. https://doi.org/10.1080/19443994.2014.959742.

Subramani, A., R. Schlicher, J. Long, J. Yu, S. Lehman, and J. G. Jacangelo. 2011. "Recovery optimization of membrane processes for treatment of produced water with high silica content." *Desalination and Water Treatment*, 36 (1–3): 297–309. https://doi.org/10.5004/dwt.2011.2604.

Tanudjaja, H. J., A. Anantharaman, A. Q. Q. Ng, Y. Ma, M. B. Tanis-Kanbur, A. L. Zydney, and J. W. Chew. 2022. "A review of membrane fouling by proteins in ultrafiltration and microfiltration." *Journal of Water Process Engineering*, 50: 103294. https://doi.org/10.1016/j.jwpe.2022.103294.

Tanudjaja, H. J., C. A. Hejase, V. V. Tarabara, A. G. Fane, and J. W. Chew. 2019. "Membrane-based separation for oily wastewater: A practical perspective." *Water Research*, 156: 347–365. https://doi.org/10.1016/j.watres.2019.03.021.

Teixeira, M. R., and M. J. Rosa. 2006. "Comparing dissolved air flotation and conventional sedimentation to remove cyanobacterial cells of Microcystis aeruginosa. Part I: The key operating conditions." *Separation and Purification Technology*, 52 (1): 84–94. https://doi.org/10.1016/j.seppur.2006.03.017.

Teixeira, M., and M. Rosa. 2007. "Comparing dissolved air flotation and conventional sedimentation to remove cyanobacterial cells of Microcystis aeruginosaPart II. The effect of water background organics." *Separation and Purification Technology*, 53 (1): 126–134. https://doi.org/10.1016/j.seppur.2006.07.001.

Tian, J., C. Wu, H. Yu, S. Gao, G. Li, F. Cui, and F. Qu. 2018. "Applying ultraviolet/persulfate (UV/PS) pre-oxidation for controlling ultrafiltration membrane fouling by natural organic matter (NOM) in surface water." *Water Research*, 132: 190–199. https://doi.org/10.1016/j.watres.2018.01.005.

Tummons, E., Q. Han, H. J. Tanudjaja, C. A. Hejase, J. W. Chew, and V. V. Tarabara. 2020. "Membrane fouling by emulsified oil: A review." *Separation and Purification Technology*, 248: 116919. https://doi.org/10.1016/j.seppur.2020.116919.

Tummons, E. N., V. V. Tarabara, J. W. Chew, and A. G. Fane. 2016. "Behavior of oil droplets at the membrane surface during crossflow microfiltration of oil–water emulsions." *Journal of Membrane Science*, 500: 211–224. https://doi.org/10.1016/j.memsci.2015.11.005.

U.S. Bureau of Labor Statistics. 2023. "Historical Cnsumer Price Index for All Urban Consumers (CPI-U)." *Consumer Price Index*. Accessed June 26, 2023. https://www.bls.gov/cpi/tables/supplemental-files/home.htm.

Valade, M. T., W. C. Becker, and J. K. Edzwald. 2009. "Treatment selection guidelines for particle and NOM removal." *Journal of Water Supply: Research and Technology - AQUA*, 58 (6): 424–432. https://doi.org/10.2166/aqua.2009.201.

Valade, M. T., J. K. Edzwald, J. E. Tobiason, J. Dahlquist, T. Hedberg, and T. Amato. 1996. "Particle removal by flotation and filtration: Pretreatment effects." *Journal AWWA*, 88 (12): 35–47. https://doi.org/10.1002/j.1551-8833.1996.tb06660.x.

Van Benschoten, J. E., C. Martin, J. Schaefer, L. Xu, and S. Franceschini. 2002. "Evaluation of dissolved air flotation and membrane filtration for drinking water treatment." Niagara Falls: ASCE.

Venne, S., O. D. Basu, and B. Barbeau. 2020. "Ozone Chemically Enhanced Backwash for Ceramic Membrane Fouling Control in Cyanobacteria-Laden Water." *Membranes*, 10 (9): 213. https://doi.org/10.3390/membranes10090213.

Voutchkov, N. 2010. "Considerations for selection of seawater filtration pretreatment system." *Desalination*, 261 (3): 354–364. https://doi.org/10.1016/j.desal.2010.07.002.

Walker, S., and R. M. Narbaitz. 2016. "Hollow fiber ultrafiltration of Ottawa River water: Floatation versus sedimentation pre-treatment." *Chemical Engineering Journal*, 288: 228–237. Elsevier B.V. https://doi.org/10.1016/j.cej.2015.11.064.

Wang, S., C. Liu, and Q. Li. 2011. "Fouling of microfiltration membranes by organic polymer coagulants and flocculants: Controlling factors and mechanisms." *Water Research*, 45 (1): 357–365. https://doi.org/10.1016/j.watres.2010.08.009.

Wang, S., C. Liu, and Q. Li. 2013. "Impact of polymer flocculants on coagulation-microfiltration of surface water." *Water Research*, 47 (13): 4538–4546. https://doi.org/10.1016/j.watres.2013.04.040.

Wray, H. E., and R. C. Andrews. 2014. "Optimization of coagulant dose for biopolymer removal: Impact on ultrafiltration fouling and retention of organic micropollutants." *Journal of Water Process Engineering*, 1: 74–83. https://doi.org/10.1016/j.jwpe.2014.03.007.

Wray, H. E., R. C. Andrews, and P. R. Bérubé. 2014. "Ultrafiltration organic fouling control: Comparison of air-sparging and coagulation." *Journal - American Water Works Association*, 106 (2): E76–E85. https://doi.org/10.5942/jawwa.2014.106.0018.

Wray, H. E., R. C. Andrews, and P. R. Bérubé. 2016. "Coagulation optimization for DOC removal: pilot-scale analysis of UF fouling and disinfection byproduct formation potential." *Water Supply*, 16 (2): 473–480. https://doi.org/10.2166/ws.2015.157.

Xagoraraki, I., and G. W. Harrington. 2004. "Zeta Potential, Dissolved Organic Carbon, and Removal of Cryptosporidium Oocysts by Coagulation and Sedimentation." *Journal of Environmental Engineering*, 130 (12): 1424–1432. https://doi.org/10.1061/(ASCE)0733-9372(2004)130:12(1424).

Xu, B., and R. M. Narbaitz. 2016. "Improved membrane pretreatment of high hydrophobic natural organic matter (NOM) waters by floatation." *Journal of Membrane Science*, 518: 120–130. Elsevier. https://doi.org/10.1016/j.memsci.2016.02.056.

Yamamura, H., K. Okimoto, K. Kimura, and Y. Watanabe. 2007. "Influence of calcium on the evolution of irreversible fouling in microfiltration/ultrafiltration membranes." *Journal of Water Supply: Research and Technology-Aqua*, 56 (6–7): 425–434. https://doi.org/10.2166/aqua.2007.018.

Yamamura, H., K. Okimoto, K. Kimura, and Y. Watanabe. 2014. "Hydrophilic fraction of natural organic matter causing irreversible fouling of microfiltration and ultrafiltration membranes." *Water Research*, 54: 123–136. Elsevier Ltd. https://doi.org/10.1016/j.watres.2014.01.024.

You, X., J. Zhang, L. Shen, R. Li, Y. Xu, M. Zhang, H. Hong, L. Yang, Y. Ma, and H. Lin. 2021. "Thermodynamic mechanisms of membrane fouling during filtration of alginate solution in coagulation-ultrafiltration (UF) process in presence of different ionic strength and iron(III) ion concentration." *Journal of Membrane Science*, 635: 119532. https://doi.org/10.1016/j.memsci.2021.119532.

Yu, L., M. Han, and F. He. 2017. "A review of treating oily wastewater." *Arabian Journal of Chemistry*, 10: S1913–S1922. https://doi.org/10.1016/j.arabjc.2013.07.020.

Zabel, T. 1985. "Advantages of Dissolved-Air Flotation for Water Treatment." *Journal / American Water Works Association*, 77 (5): 42–46. https://doi.org/10.1002/j.1551-8833.1985.tb05537.x.

Zhang, J. K., Y. B. Yang, H. Y. Wang, and Z. B. Dong. 2012. "CFU Combined Process for the Treatment of Oily Car Washing Wastewater." *Applied Mechanics and Materials*, 253–255: 999–1004. https://doi.org/10.4028/www.scientific.net/AMM.253-255.999.

Zhang, Y., and Q. Fu. 2018. "Algal fouling of microfiltration and ultrafiltration membranes and control strategies: A review." *Separation and Purification Technology*, 203: 193–208. https://doi.org/10.1016/j.seppur.2018.04.040.

Zhao, C., J. Zhou, Y. Yan, L. Yang, G. Xing, H. Li, P. Wu, M. Wang, and H. Zheng. 2021. "Application of coagulation/flocculation in oily wastewater treatment: A review." *Science of The Total Environment*, 765: 142795. https://doi.org/10.1016/j.scitotenv.2020.142795.

Zietzschmann, F., M. Ernst, M. Godehardt, H. Paar, X. Zheng, and M. Jekel. 2014. "Linking UF reversible and irreversible fouling to the water quality of surface water and treated municipal wastewater." *Desalination and Water Treatment*, 52 (40–42): 7598–7608. https://doi.org/10.1080/19443994.2013.834271.

Zularisam, A. W., A. Ahmad, M. Sakinah, A. F. Ismail, and T. Matsuura. 2011. "Role of natural organic matter (NOM), colloidal particles, and solution chemistry on ultrafiltration performance." *Separation and Purification Technology*, 78 (2): 189–200. Elsevier B.V. https://doi.org/10.1016/j.seppur.2011.02.001.

Zulkefli, N. F., N. H. Alias, N. S. Jamaluddin, N. Abdullah, S. F. Abdul Manaf, N. H. Othman, F. Marpani, M. S. Mat-Shayuti, and T. D. Kusworo. 2021. "Recent Mitigation Strategies on Membrane Fouling for Oily Wastewater Treatment." *Membranes*, 12 (1): 26. https://doi.org/10.3390/membranes12010026.

Zupančič, M., D. Novak, J. Diaci, and I. Golobič. 2014. "An evaluation of industrial ultrafiltration systems for surface water using fouling indices as a performance indicator." *Desalination*, 344: 321–328. https://doi.org/10.1016/j.desal.2014.04.002.

APPENDIX C

Phased-Inline Coagulation for Low-Pressure Membranes in Water and Wastewater Treatment: A Review of Fouling Mitigation, Process Control, and Water Quality

Context: The literature review presented in Chapter 2 generated a review article on phased-inline coagulation (C-IN-P) pretreatment of low-pressure membranes. In the interest of completeness, this article is presented in this appendix. A version of this appendix was published as:

Ladouceur, J.D., Narbaitz, R.M., & Lan, C.Q. (2024). Phased-inline coagulation for low-pressure membranes in water and wastewater treatment: A review of fouling mitigation, process control, and water quality. *Environmental Technology Reviews, 13:1, 305-324*.

List of Abbreviations

CEB	Chemically enhanced backwash
C-IDX	Coating index
C-IN	Inline coagulation
C-IN-P	Phased-inline coagulation
C-IN-S	Stepped-inline coagulation
CIP	Clean-in-place
COD	Chemical oxygen demand
DBP	Disinfection by-product
DOC	Dissolved organic carbon
DWT	Drinking water treatment
MF	Microfiltration
NOM	Natural organic matter
OPEX	Operating expense
PACl	Polyaluminum chloride
PES	Polyethersulfone
PFAS	Per- and polyfluoroalkyl substances
RO	Reverse osmosis
SE	Secondary effluent
SUVA	Specific ultraviolet absorbance at 254nm
UF	Ultrafiltration
UV_{254}	Ultraviolet absorbance at 254nm

C.1. Abstract

Low-pressure membranes (LPM) are increasingly popular in water treatment due to their effective removal of microorganisms, pathogens, and protozoa. A more widespread implementation of LPMs in water treatment is prevented due to membrane fouling, which increases operating and maintenance costs. Coagulation pretreatment of the LPM feed water by continuous inline coagulation (C-IN), which involves coagulant addition without particle separation prior to LPM filtration, is a commonly applied approach for fouling mitigation. Phased-inline coagulation (C-IN-P), a variant of C-IN where the coagulant is dosed inline for the initial portion of the filtration

cycle, is the subject of increased interest due to the potential for significant cost savings through reduced coagulant usage. In this chapter, existing knowledge from pertinent publications regarding C-IN-P pretreatment of LPM feed waters is critically reviewed. Specifically, the C-IN-P approach is reviewed with emphasis placed on understanding fouling behavior, process control, and the removal of organics. Available studies suggest that intermittent coagulant addition by C-IN-P pretreatment can achieve comparable fouling mitigation to C-IN, where coagulant is injected continuously. It has also been shown that C-IN-P can achieve comparable removal of bulk organics measures to C-IN pretreatment for different water types, while also offering significant cost savings on coagulant. According to the knowledge gaps identified throughout the study, the manuscript concludes by outlining guidance on potential foci of future research.

C.2. Introduction

Ultrafiltration (UF) and microfiltration (MF) membranes have seen rapid growth in their installed capacity for drinking water treatment (DWT) applications since the late 1990s (Anis et al. 2019; Li et al. 2019; Xu et al. 2022). In North America, this steady increase in the number of low-pressure membrane (LPM) installations has largely been driven by the April 1993 Cryptosporidium outbreak in Milwaukee (WI, USA) (Crittenden et al. 2012; Pearce 2011), which demonstrated that conventional treatment processes could be inadequate for complete removal of protozoans in the face of variable feed water quality (Fox and Lytle 1996). In response to the outbreak in Milwaukee, the United States enacted more stringent regulatory guidelines (i.e., Interim Enhanced Surface Water Treatment Rule), which had the goal of reducing filtered turbidity and enhancing the removal of disinfectant-tolerant pathogens such as *Giardia* and *Cryptosporidium* (American Water Works Association 2016; Emelko et al. 2005; Regli et al. 1999). Since most commercially available UF and MF membranes have nominal pore sizes in the range of 0.02 μm to 0.04 μm, near complete removal of *Giardia* and *Cryptosporidium* can be achieved by LPM filtration (Edzwald 2011; Jacangelo et al. 1991; Pearce 2011). Other drivers for the growth of LPM facilities include smaller plant footprint (Mecha et al. 2023; Xue et al. 2020), effective removal of particulates (Álvarez-Arroyo et al. 2023; Wray and Andrews 2014), degrading global water quality (Boretti and Rosa 2019; Patwardhan et al. 2023), increased water demand in stressed areas due to social and economic growth (Amjad et al. 2015), and a shift

towards water/wastewater reuse (Tang et al. 2018; Tow et al. 2022). Moreover, LPMs can provide superior quality product water with a more consistent performance in the face of variable feed water quality when compared to deep bed filters (Crittenden et al. 2012). As a result of these factors, the global cumulative installed capacity of LPMs surpassed 80,000 MLD in 2018, with an established long-term annual growth rate of 10,000 MLD based on data between 2011-2018 (Pearce 2018).

Although the number and size of LPM facilities continues to grow globally, membrane fouling persists as a major obstacle to a more widespread application of this technology (Chen et al. 2022; Hao et al. 2011; Kimura and Kume 2020). Fouling can be defined as the continual loss of performance (or productivity) of a membrane due to deposition on its surface or within its pores (AlSawaftah et al. 2021; Guo et al. 2012; Koros et al. 1996; Schäfer et al. 2021). While physical cleaning methods such as routine hydraulic backwashing can recover some degree of productivity loss, irreversible membrane fouling will develop over long periods of operation, leading to increased operating and maintenance costs as well as shortened membrane lifespan (Kimura and Kume 2020; Shi et al. 2014; Yamamura et al. 2007). Dissolved organics, particulate organic and inorganic materials, as well as microorganisms have all been recognized as important foulants of LPMs, with synergistic fouling between these components being reported in the literature (Cui and Choo 2014; Gao et al. 2011; Guo et al. 2012; Hilal et al. 2005; Jermann et al. 2008b; a; Liu et al. 2019; Schulz et al. 2016; Tian et al. 2013). For most UF/MF applications, however, natural organic matter (NOM) has been identified as the consensus principal foulant (AWWA 2005; Kim et al. 2006; Lee et al. 2008; Peters et al. 2021; Porcelli and Judd 2010; Zularisam et al. 2007, 2011). To control LPM fouling by NOM, strategies such as chemical cleaning (Arnal et al. 2009; Bogati et al. 2015; Ding et al. 2020; Shi et al. 2014), feed water pretreatment (Cheng et al. 2016; Huang et al. 2019; Liang et al. 2008; Lin et al. 1999), membrane surface modification (Baghbanzadeh et al. 2016; Mosqueda-Jimenez et al. 2004; Nguyen et al. 2007; Pezeshk and Narbaitz 2012; Rana and Matsuura 2010; Xie et al. 2016), and alteration of operating conditions (Alresheedi et al. 2022; Crozes et al. 1997; Kim et al. 2015; Li et al. 2014; Souza and Basu 2013) have all been investigated.

Concerning feed water pretreatment, coagulation prior to LPM filtration has become the most common method for fouling reduction due to its simple implementation, relatively low cost, and familiarity with plant operators (Gao et al. 2011; Huang et al. 2009). Since coagulation was first proposed as a means of mitigating LPM fouling (Wiesner et al. 1989), it has evolved

significantly, including hybridization with other particle separation processes (i.e., dissolved-air-flotation or sedimentation) and the development of novel operating strategies. These include two-stage coagulation, where coagulant is added during rapid mixing as well as part way through the flocculation stage (Liu et al. 2011; Park et al. 2015). A summary of the development and trends of coagulation pretreatment for LPMs is presented in Fig. C.1.

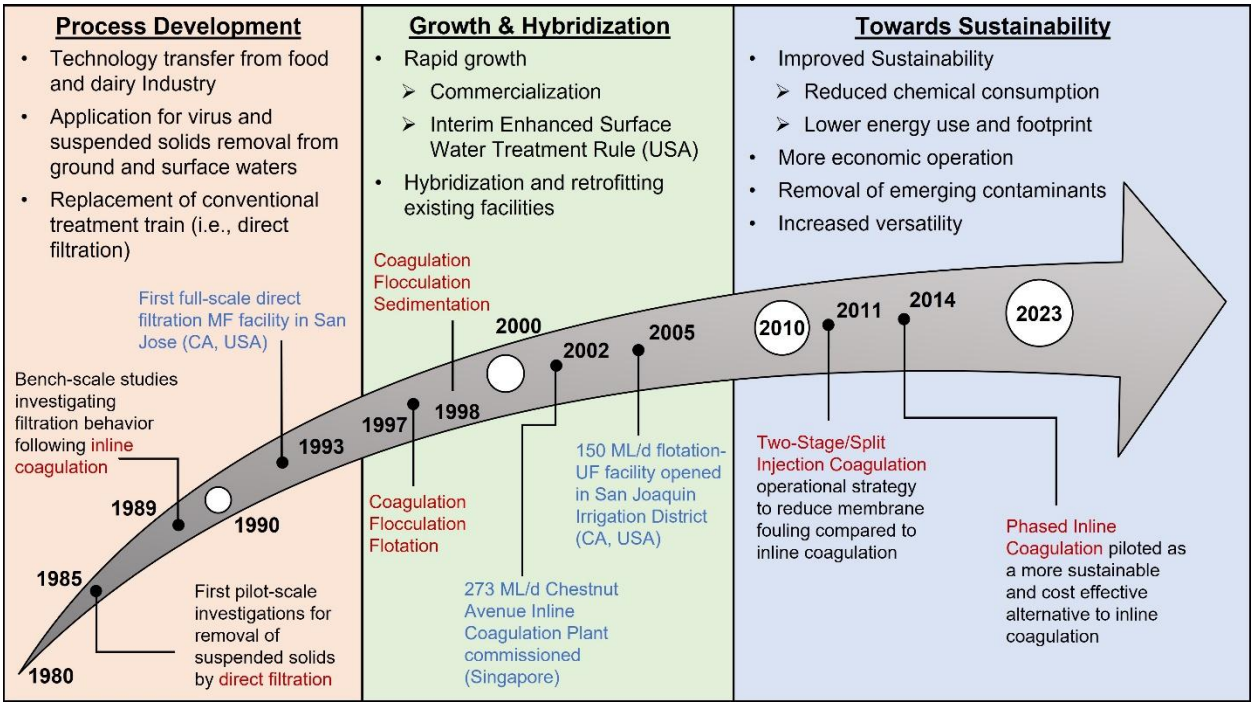


Fig. C.1. Development and trends in coagulation pretreatment for LPMs. Note. information sourced from: (American Water Works Association 2016; Braghetta et al. 1997; Edzwald and Haarhoff 2012; Fiessinger et al. 1985; Lebeau et al. 1998; Liu et al. 2011; Naim et al. 2014; Wiesner et al. 1989; Yoo et al. 1995).

Continuous inline-coagulation (C-IN) pretreatment involves the use of coagulants but, unlike conventional treatment processes that involve particle separation by sedimentation or dissolved-air-flotation, delivers the coagulated solids directly to the membrane surface (Aly et al. 2021; Choi and Dempsey 2004; Koyuncu et al. 2015). As shown in Fig. C.2a, for C-IN pretreatment, coagulant is added continuously to the feed at a prescribed dosage for the entirety of each filtration cycle. A significant number of published studies have investigated C-IN pretreatment for LPM applications owing to its shorter flocculation time (since settleable flocs are not required) and reduced process

complexity compared to conventional water treatment (Kamińska et al. 2020; Keucken et al. 2017; Konieczny et al. 2009; Sillanpaa 2015). Phased-inline coagulation (C-IN-P) is a variation of C-IN pretreatment where, instead of continuous coagulant addition, the coagulant is dosed only for the initial portion (i.e., fraction) of the filtration cycle that immediately follows hydraulic backwashing (Fig. C.2b). Once the coagulant has been added for the prescribed duration to produce an initial cake layer, the addition is ceased, and filtration proceeds for the remainder of the cycle with untreated (raw) water. Recently, there has been an increased interest in C-IN-P pretreatment of LPM feed waters as it has not only been reported to successfully mitigate fouling by NOM but also significantly reduce coagulant demand (Malkoske et al. 2020; Naim et al. 2014). Successful implementation of C-IN-P has the potential to greatly reduce the cost associated with LPM pretreatment through lower chemical consumption and sludge processing/disposal costs when compared with C-IN (Lok et al. 2017).

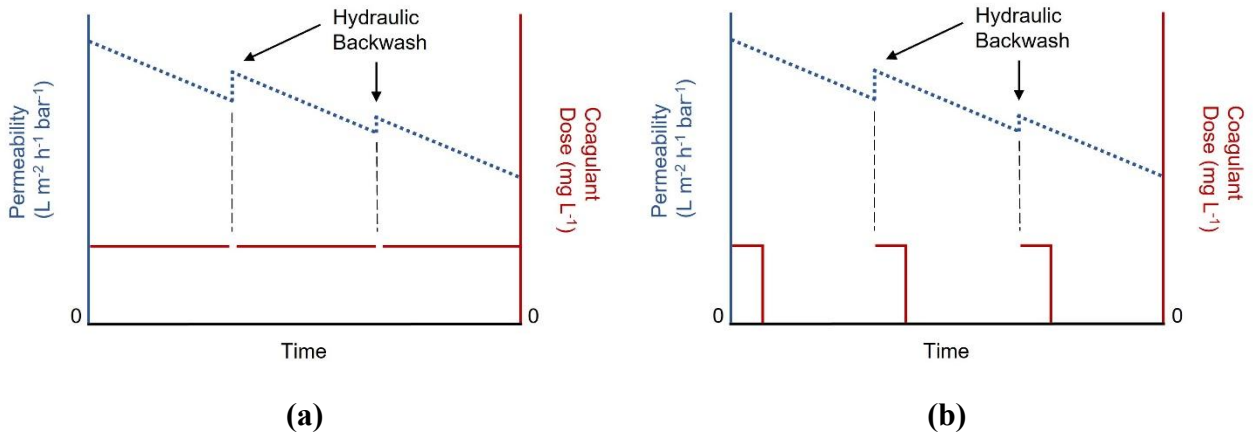


Fig. C.2. Idealized permeability profiles for three filtration cycles with: **(a)** continuous coagulant addition (C-IN); **(b)** phased coagulant addition (C-IN-P).

A few detailed reviews on pretreatment approaches for LPMs in water treatment (Arhin et al. 2016; Gao et al. 2011; Huang et al. 2009), as well as on chemical pretreatment for LPMs (Farahbakhsh et al. 2004), were presented over a decade ago. More recently, Malkoske et al. (2020) presented a comprehensive review on coagulation pretreatment for LPMs in DWT which considered inline and conventional coagulation (i.e., with particle separation by sedimentation). This review did not, however, present an exhaustive discussion of C-IN-P pretreatment. To date, there has not been any review on C-IN-P pretreatment of LPMs, specifically with respect to the

role of coagulation conditions on fouling mitigation and finished water quality. Accordingly, in the current review, we strive to provide a comprehensive perspective of C-IN-P pretreatment for LPM technologies in drinking water and wastewater treatment. This report will be organized into three principal sections. The first section presents an overview of C-IN-P process configuration as well as a summary of the key experimental conditions most frequently used in C-IN-P practice. In the second section, a comprehensive analysis and discussion of C-IN-P fouling mitigation and process control is presented. Furthermore, the reported quality of C-IN-P product water is discussed and compared with that of C-IN pretreated water. In the final section, critical knowledge gaps are summarized and directions for future research are outlined.

C.3. Phased-Inline Coagulation Process Configuration

Studies investigating C-IN-P have most commonly been performed at pilot-scale without a dedicated flocculation stage (i.e., no flocculation basin is used) (Buchta et al. 2019; Lok et al. 2017; Naim et al. 2014). For example, in the pilot-scale study by Naim et al. (2014), a rapid mix basin with a retention time between 10 and 21 s was used for coagulant mixing, while for the bench-scale investigation by Park et al. (2002) the velocity gradients that exist in the peristaltic feed pump (Formato et al. 2019; Palmada et al. 2022) were used to provide the necessary turbulence for blending of coagulant (added to the suction side) with the feed water. Buchta et al. (2019) and Lok et al. (2017) reported injecting the coagulant directly inline in their pilot-scale investigations such that the coagulant was blended using only the turbulence of the pipe system. Inline static mixers are a third possible option for blending of coagulant/pH adjustment chemicals with the feed water, although their use has not been specifically investigated in C-IN-P studies. Based on studies considering feed water pretreatment by C-IN without flocculation, suitable mixing times for systems with static mixers range from instantaneous mixing (Judd and Hillis 2001) to 60 s (Galjaard et al. 2001; Wang and Wang 2006). It is recommended that future C-IN-P studies investigate the effects that different mixing types (i.e., mechanical vs. incidental) have on the properties of the formed cake layer and the subsequent impacts this may have on membrane fouling. No C-IN-P studies available in the literature systematically evaluate the impact of the coagulation mixing type (i.e., static mixer, rapid mix tank, etc.) or their operating conditions (i.e., mean velocity gradient, contact time) on pretreatment performance. This is despite the fact that C-

IN studies have demonstrated altered floc and cake structure (and hence membrane fouling) resulting from differing mixing conditions (Amjad et al. 2015; Nan et al. 2016). Fig. C.3 below presents a schematic diagram of the C-IN-P-LPM system.

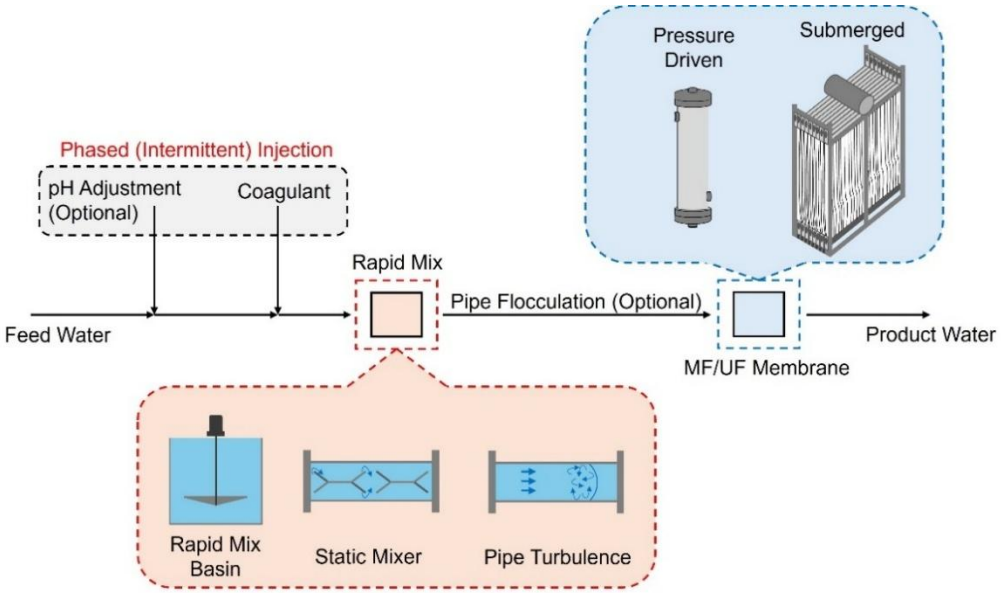


Fig. C.3. Schematic diagram of a LPM system with C-IN-P pretreatment.

C.4. Performance of Phased-Inline Coagulation as Pretreatment for LPMs

Studies involving C-IN-P pretreatment have, in general, considered the effects of the coagulant dose and the length of its addition (i.e., dosing time) on membrane fouling behaviour. These two variables, as well as the membrane flux, can be encompassed within the membrane coating index (C-IDX), a coagulation parameter first defined by Schweiger et al. (2018b) with potential application in C-IN-P process control. The C-IDX is calculated using Eqn. (C.1) below.

$$C - IDX = J \times Q \times T \times \left(\frac{1}{60}\right) \quad \text{(C.1)}$$

where $C - IDX$ is the coating index in mg m^{-2}, J is the membrane flux in L m^{-2} h^{-1}, Q is the coagulant dose (as metal) in mg L^{-1}, and T is the duration of coagulant addition in min. For a LPM facility with a constant flux (as is typical in DWT applications), lower values of the C-IDX suggest either a lower coagulant dose and/or a lower dosing time. While a reduction in either of these factors is expected to lower the operating expense (OPEX) of a facility due to decreased coagulant consumption, membrane fouling may become exacerbated, sacrificing the stability of operation

and resulting in higher energy and chemical cleaning demand (Schweiger et al. 2018b). In contrast, a higher C-IDX for a constant flux facility suggests higher coagulant dosages and/or longer dosing times, which may lead to higher coagulant consumption without necessarily achieving any significant improvement in fouling reduction. More on the suitability of the C-IDX as a tool for controlling C-IN-P process performance will be discussed in Section C.4.2.

In Table C.1, pertinent data regarding raw water quality, coagulation characteristics, and fouling measures are presented for selected C-IN-P studies. Some of the most salient points that can be drawn from an analysis of the data contained within Table C.1 are as follows. First, only a limited number of published studies have been reported regarding C-IN-P pretreatment for LPM technologies in DWT. For this reason, studies examining secondary effluent (SE) as source water (which account for 50% of reported studies) will be analyzed together in this report with those that consider natural surface waters as LPM feed. It has to be acknowledged that the different water types have different characteristics which may markedly impact the performance of the integrated C-IN-P-LPM system. For example, biologically treated SEs are majority composed of soluble microbial products having low specific ultraviolet absorbance at 254 nm (SUVA) values and a hydrophilic character (Jarusutthirak and Amy 2007) while river waters are dominated by humic substances (Filella et al. 2005). Second, half of the studies presented in Table C.1 used tubular multi-channel polyethersulfone (PES) membranes with an inside-out pressure-driven configuration in the evaluation of C-IN-P performance, while only a single study evaluated an outside-in submerged membrane. Finally, owing to the disparate methods used in the literature for quantifying and reporting fouling development, several measures of LPM fouling are presented in Table C.1, including fouling resistances (using resistance-in-series based models) and permeability decline rates. For this reason, a direct comparison of results between studies is not always possible.

Appendix C

Table C.1. C-IN-P Fouling Measures and Coagulation Characteristics.

Material Config. NPS or MWCO	Raw Water Characteristics			Coagulation Characteristics						Fouling Measures			Ref. (see Notes)
	Water Type	DOC (ppm)	SUVA ($Lmg^{-1}m^{-1}$)	Coag. Type	Mixing Type	Coag. Dose (mg/L as metal)	Dose Duration (min)	Fraction of Cycle (%)	Coating Index (mg/m^2)	Permeability Decline Rate ($Lm^{-2}h^{-1}bar^{-1}d^{-1}$)	Irrev. Resistance ($\times 10^{11}$ 1/m)	Total Resistance ($\times 10^{11}$ 1/m)	
PVDF SUB 0.02 µm	Lake	3.9	0.73	PACl	INC	4 (as PACl)	10	8.3	N/A	N/A	0.5-2.72	N/A	[1]
	Lake	3.8	0.71	PACl	INC	4 (as PACl)	60	50	N/A	N/A	0.5-1.6	N/A	
	Lake	3.9	0.73	PACl	INC	4 (as PACl)	120	100	N/A	N/A	0.3-1.5	N/A	
PES PDI 50 kDa	SE	13.5	2.04	$FeCl_3$	RMCB [a]	20	15	50	300	1.34	N/A	N/A	[2]
	SE	13.5	2.04	$FeCl_3$	RMCB	20	5	17	100	2.4	N/A	N/A	
	SE	13.5	2.04	$FeCl_3$	RMCB	20	2.5	8.3	50	24	N/A	N/A	
	SE	13.5	2.04	$FeCl_3$	RMCB	1	2.5	8.3	2.5	26.4	N/A	N/A	
PES PDI 0.02 µm	SE	N/A	N/A	PACl	INC	5	40	100	233	2.88	N/A	N/A	[3,4]
	SE	N/A	N/A	PACl	INC	2	40	100	93	0	N/A	N/A	
	SE	N/A	N/A	PACl	INC	5	4	10	23	38.4	N/A	N/A	
	SE	N/A	N/A	PACl	INC	2	10	25	23	21.5	N/A	N/A	
PS PDI 0.01 µm	River	2.3-2.9	1.27	PACl	N/A	0.53 [b]	1	5	N/A	181.67	N/A	N/A	[5]
	River	2.3-2.9	1.27	PACl	N/A	1.06	1	5	N/A	251.22	N/A	N/A	
	River	2.3-2.9	1.27	PACl	N/A	2.17	1	5	N/A	268.7	N/A	N/A	
PES PDI 100 kDa	Lake	3.909	N/A	$FeCl_3$	N/A	2.0/1.0 [c]	30	50	N/A	N/A	N/A	5.3-10.4	[6]

Note: INC = incidental; MWCO = molecular weight cut-off; NPS = nominal pore size; PACl = polyaluminum chloride; PDI = pressure driven inside-out; PES = polyether sulfone; PVDF = polyvinylidene fluoride; RMCB = rapid mix contact basin; SUB = vacuum submerged; SE = secondary effluent. [a] 10-21 s contact time. [b] dose reported as that which would deliver an equivalent mass for continuous coagulant addition. [c] 2 mg/L first cycle and 1 mg/L subsequent cycles, dosed for half the cycle duration. Refs: [1] Lok et al. (2017); [2] Naim et al. (2014); [3]Buchta et al. (2019); [4] Schweiger et al. (2018b);[5] Park et al. (2002); [6] Pronk et al. (2016)

C.4.1. Fouling Mitigation

C.4.1.1. Effects of the Coagulation Process

Available studies in the literature exclusively compare the performance of C-IN-P pretreatment for LPM fouling mitigation to that of C-IN pretreatment (Buchta et al. 2019; Lok et al. 2017; Naim et al. 2014; Schweiger et al. 2018b). Lok et al. (2017) compared the irreversible fouling resistance (derived from the resistance-in-series model) of a submerged hollow-fiber UF membrane filtering a hydrophilic (as measured by the SUVA value) lake water following pretreatment by either C-IN or C-IN-P. For both C-IN and C-IN-P pretreatment alternatives, the filtration cycle duration was fixed at 120 min, while for C-IN-P the duration of coagulant addition was set to either 10 min or 60 min. This last study established that dosing coagulant for only the initial portion (fraction) of the filtration cycle did not result in a higher steady-state hydraulically irreversible fouling resistance compared to continuous coagulant addition. Furthermore, while the hydraulically irreversible fouling resistance increased rapidly initially, minimal increase was observed for both the 10 min and 60 min injection conditions after 10-20 h of operation, likely due to the establishment of a protective cake layer on the membrane surface. These findings were corroborated by Pronk et al. (2016), who found that phased addition of ferric chloride for only the initial 50% of the filtration cycle did not result in greater total membrane fouling resistance when compared to continuous coagulant injection. Moreover, the total fouling resistance for C-IN-P pretreated water stabilized (plateaued) after only five filtration cycles (Pronk et al. 2016).

Buchta et al. (2019) compared C-IN and C-IN-P pretreatment of two different SE samples using a tubular monolithic UF membrane made from hydrophilized PES material and operated inside-out. For both SE samples, polyaluminum chloride (PACl) was added at either 2 mg-Al L^{-1} or 5 mg-Al L^{-1} continuously, or for only the initial portion of the filtration cycle to a fixed C-IDX value of 23 mg m^{-2}. They reported that C-IN-P pretreatment resulted in a higher degree of permeability variation between chemical cleanings compared to continuous inline dosing, although the permeability following chemically enhanced backwashing (CEB) was identical for the two conditions. These findings suggest that: a) the change in coagulant addition technique did not alter the fraction of foulants that were chemically irreversible; and b) that the phased addition of coagulant throughout the filtration cycle led to a reduced hydraulic backwash efficiency, which promoted a greater permeability decline.

Naim et al. (2014) also investigated the performance of C-IN-P for pretreatment of SE using the same tubular monolithic membrane (although with a different nominal molecular weight cut-off) as Buchta et al. (2019). A single membrane module was employed for all tests, however, CEB cleaning performed following each experiment (which used different C-IDX values) was reported to eliminate any signs of cumulative irreversible fouling. This suggests that the observed performance for each tested C-IDX value was not due to poorly removed protective cake layers formed during earlier experiments. Results of the study indicate that, for a fixed ferric chloride dose of 20 mg-Fe L^{-1}, the permeability following CEB did not change significantly when the time of dosing was reduced from 15 min (out of a 30 min cycle) to 2.5 min (corresponding to a C-IDX reduction from 300 to 50 mg m^{-2}). When the time of dosing was fixed at 2.5 min and the coagulant dose was reduced from 20 mg-Fe L^{-1} to 1 mg-Fe L^{-1} (corresponding to a C-IDX decrease from 50 mg m^{-2} to 2.5 mg m^{-2}), the rate of permeability decline increased only slightly from 24 to 26.4 L m^{-2} h^{-1} bar^{-1} d^{-1}. Thus, significant savings in chemical coagulant are possible without greatly impacting the rate of membrane permeability decline.

In addition to details surrounding how the coagulant is added to the feed during C-IN-P (i.e., dosing time, dose, and C-IDX), the coagulant type is another parameter of the coagulation process whose impact on process performance merits discussion. All studies surveyed in this review considered PACl and ferric chloride as coagulants. Importantly, no author has directly compared the effects of these two coagulants (or others) on fouling mitigation using the same membrane type, operating conditions, and water source despite the fact that coagulant type has been shown to exert an influence on LPM fouling in C-IN pretreatment (Aly et al. 2021; Arhin et al. 2016; Hatt et al. 2011). Therefore, based on the limited data available, it is difficult to arrive at any conclusion regarding the impact of coagulant type on fouling mitigation for C-IN-P. This should be the subject of future research, as later described in Section C.5.

C.4.1.2. Effects of Cake Properties

For both the studies by Buchta et al. (2019) and Naim et al. (2014), properties of the cake layer including its thickness, roughness, and coverage of the fiber appear to be critical aspects governing LPM fouling (permeability decline and reversibility) in the C-IN-P-LPM process. In the study by Buchta et al. (2019), the reduced hydraulic backwash efficiency observed for pretreatment by C-IN-P compared to C-IN was postulated to be a result of incomplete coverage of the membrane

fiber surface by the cake layer or due to the reduced thickness of the cake layer (Buchta et al. 2019) (Fig. C.4a). Complete coverage of the membrane fiber by the cake layer formed during the initial fraction of the filtration cycle (i.e., with coagulant addition) (Fig. C.4b) may more effectively prevent membrane-foulant interactions (and promote foulant-foulant interactions) leading to improved hydraulic reversibility (De Angelis and de Cortalezzi 2013; Dong et al. 2007; Ye et al. 2011). An assessment of how modified operational strategies or altered C-IDXs affect coverage of the membrane fiber during C-IN-P pretreatment is thus warranted.

As the morphological properties of the cake could not be assessed for the tubular membranes used in their C-IN-P tests, Naim et al. (2014) collected atomic force microscopy micrographs for C-IN tests (using a flat-sheet membrane of identical polymer-dope solution and pore size as the tubular PES membrane) to help elucidate how properties of the cake layer impact fouling behavior in C-IN-P. When the coagulant dose was increased from 1 mg-Fe L^{-1} to 15 mg-Fe L^{-1}, the measured surface roughness of the fouled (but not cleaned) membranes decreased from 40 nm to 19 nm. This was postulated to be the result of a thicker and smoother cake layer formed at higher dosages, which led to reduced membrane fouling. Increased cake layer thickness at elevated coagulant dosages have also been reported by a number of other authors (Gu et al. 2018). While this result considered continuous coagulant addition, it may suggest that C-IN-P conditions (i.e., C-IDX values) resulting in a more uniform and smooth cake layer could help to alleviate membrane fouling (Fig. C.4c). It has been proposed by numerous authors that surface roughness (Fig. C.4d) exerts an important influence on fouling phenomena (Buisson et al. 2004; Tsuyuhara et al. 2010; Van Der Bruggen et al. 2003).

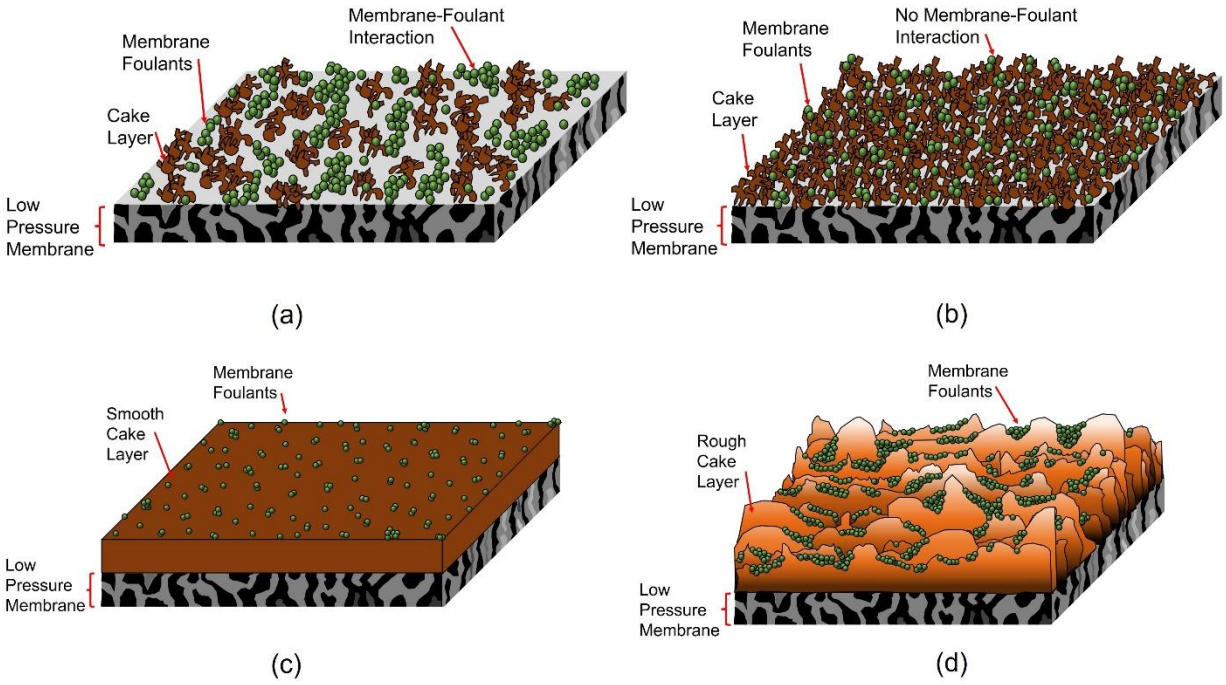


Fig. C.4. Visualization of the effect of cake layer properties on C-IN-P fouling: **(a)** incomplete coverage of membrane fiber by the cake layer; **(b)** complete coverage of membrane fiber by the cake layer; **(c)** uniform and smooth cake layer; **(d)** rough cake layer.

Despite these studies demonstrating the importance of cake layer properties in governing LPM fouling mitigation following pretreatment by C-IN-P, there has been no investigation which explicitly studies how variable C-IDX values may impact the cake layer thickness, roughness, and coverage of the fiber. Moreover, while it was reported that reduced cake thickness led to greater foulant-membrane interaction and increased fouling (Naim et al. 2014), other studies investigating C-IN pretreatment have found that thicker cakes can result in reduced porosity and hydraulic permeability (Ma et al. 2020; Yu et al. 2013). This can lead to the surface cake presenting its own significant resistance to filtration. A final consideration regarding cake thickness is that its value is likely to be different for different C-IDXs and for different source water qualities (i.e., high vs. low SUVA, high vs. low turbidity), even when these waters are treated using the same C-IDX. Regarding the coverage of the membrane fiber by the cake layer, the packing density of the membrane module is expected to be a critical factor for membranes operated with an outside-in flow configuration, as higher densities may impair the ability to cover the entire fiber surface (Günther et al. 2012; Salinas-Rodriguez et al. 2016).

C.4.1.3. Effect of Other Parameters

A final word on fouling mitigation by C-IN-P is regarding the impact of several other process conditions, including membrane type/configuration and feed water type. The studies by Lok et al. (2017) and Pronk et al. (2016) both used resistance-in-series-based fouling measures to report that C-IN-P did not result in greater fouling (total and hydraulically irreversible) compared to C-IN and that the resistances stabilized after only a short period of time. The similar performance was despite the fact that the two studies considered membranes with disparate characteristics (submerged polyvinylidene fluoride vs. pressure-driven inside-out PES), although, definitive conclusions regarding the impact of membrane configuration/type cannot be made owing to the differences in other operating conditions (coagulant type, dose, and duration of dosing). Moreover, comparison with studies using tubular multi-channeled membranes was not possible due to the different measures used for performance assessment. Regarding feed water quality, besides SE sources, only natural waters with relatively low dissolved organic carbon (DOC) concentrations (< 3.9 mg L^{-1}) and hydrophilic character (based on low SUVA values < 1.27 L mg^{-1} m^{-1}) have been investigated. While fouling mitigation by C-IN-P and C-IN exhibit similar performance for these water types, this has not been confirmed for waters with a greater hydrophobicity (> 3 L mg^{-1} m^{-1}) and DOC content (> 5 mg L^{-1}), which are present in many regions globally (Westerhoff et al. 1999; White et al. 1997).

C.4.2. Process Control: The Coating Index

Due to the limited data available for C-IN-P, data for studies investigating C-IN is first consulted with a focus on the impact of coagulant dose, a parameter encompassed by the C-IDX (Eqn. C.1). A number of studies considering C-IN pretreatment of LPM feed waters have previously reported that an increase in coagulant dose can actually worsen membrane fouling, likely due to the formation of a thick filtration cake (Paar et al. 2011; Wang et al. 2013; Wray et al. 2016). This is shown in Fig. C.5 where, although there is some degree of dispersion in the data, C-IN membrane fouling (measured as the rate of normalized flux decline) appears to initially decrease with increasing coagulant dose up to about 0.05-0.1 mmol L^{-1} (as metal), before worsening upon a further increase in dose. It should be noted that the line in the figure was fit by regressing a quadratic model using minimization of the sum of least square errors criterion and that the rate of

normalized flux decline was determined according to Eqn. (C.2) below (Chen et al. 2015; Li et al. 2007):

$$RNFD = \frac{\left(\frac{J_{t_i}}{J_0}\right) - \left(\frac{J_{t_f}}{J_0}\right)}{\Delta t} \quad \text{(C.2)}$$

where $RNFD$ is the rate of normalized flux decline in h^{-1}, J_{t_i} is the membrane flux at time t_i in L m^{-2} h^{-1}, J_{t_f} is the membrane flux at time t_f in L m^{-2} h^{-1}, J_0 is the initial clean water flux in L m^{-2} h^{-1}, and Δt is the difference in time between t_i and t_f in h (where $t_f > t_i$). Based on the C-IN data analyzed, for C-IN-P it is possible that an excessively large increase in the C-IDX could not only greatly increase the facility's OPEX, but also worsen membrane fouling compared to when lower C-IDXs are used. It should be mentioned that, to date, worsening performance at high C-IDX values has not been reported for C-IN-P (Fig. C.6a). Future research should investigate different water and membrane types than previously studied to identify whether conditions of high C-IDX can lead to worsened membrane fouling. Such a study should also examine whether increasing C-IDX values only impact cake thickness, or whether other properties such as cake density/porosity are also altered.

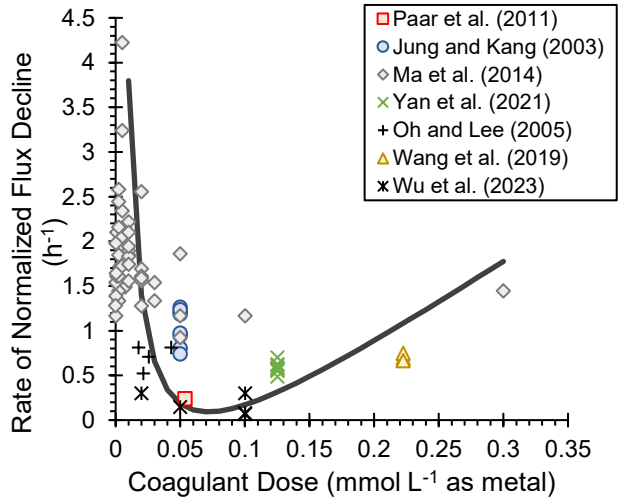


Fig. C.5. Rate of normalized flux decline with increasing coagulant dosage for C-IN-LPM system. Note: plotted data obtained from articles (Jung and Kang 2003; Ma et al. 2014; Oh and Lee 2005; Paar et al. 2011; Wang et al. 2019; Wu et al. 2023; Yan et al. 2021).

The reported trade-off between OPEX (i.e., as represented by the C-IDX) and membrane fouling is exhibited in Fig. C.6a below where the rate of permeability decline reported from available literature follows a near asymptotic relationship. At high values of C-IDX (i.e., greater than 93 mg m^{-2}), the rate of permeability decline was found to be low (less than 2.88 L m^{-2} h^{-1} bar^{-1} d^{-1}), although as pointed out by Buchta et al. (2019), operation at such high C-IDX values leads to increased OPEX due to higher chemical coagulant consumption. In contrast, at low values of C-IDX the rate of permeability decline is exacerbated, exceeding 21.5 L m^{-2} h^{-1} bar^{-1} d^{-1} in all cases. While Schweiger et al. (2018a) proposed that, in terms of stable operational performance and lowest OPEX, the optimal C-IDX lies within the range of 20 – 25 mg m^{-2}, the analysis in Fig. C.6a seems to suggest that C-IDX values between 50 - 100 mg m^{-2} may be required for optimal performance. In fact, the range of C-IDXs evaluated by Naim et al. (2014) seem to suggest the possible existence of a threshold C-IDX value (which is likely dependent on the specific feed water, membrane type, and metal salt used) below which the thickness of the cake layer is insufficient and fouling becomes exacerbated. Given that the literature presents limited data for the various waters tested, there is a need to investigate to what C-IDX values the permeability decline rate remains low. This should be pursued for different membrane configuration/types, different raw water types, as well as different coagulant types to ascertain the variability of this apparent exponential drop in permeability decline rate with C-IDX values.

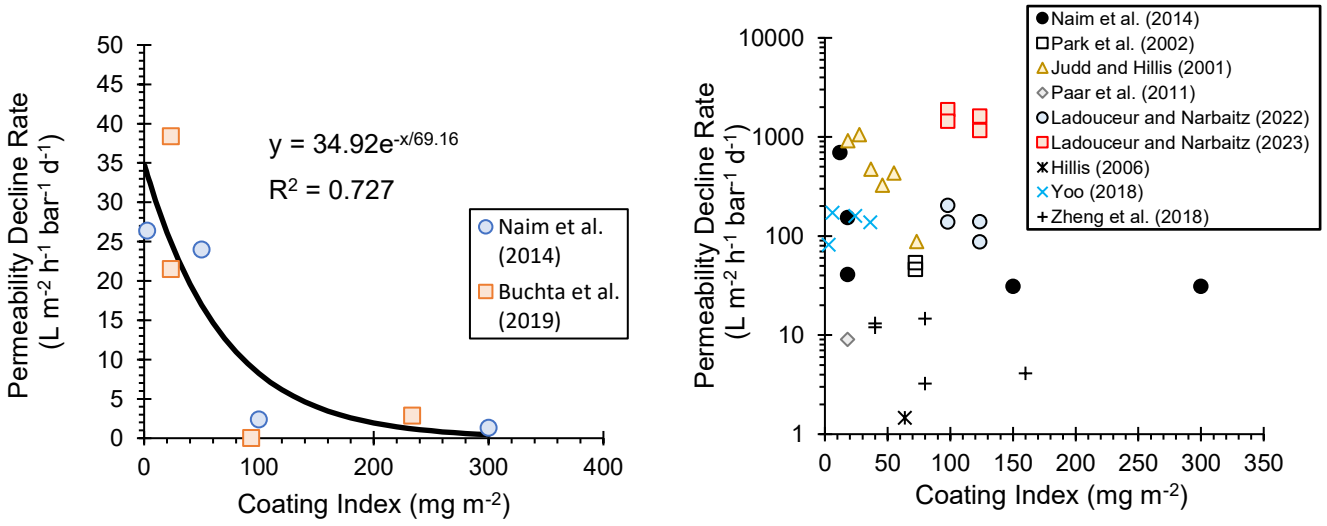


Fig. C.6. Relationship between C-IDX and membrane permeability decline rate for: **(a)** C-IN-P; **(b)** C-IN. Note: plotted data obtained from articles by Hillis (2006); Judd and Hillis (2001); Ladouceur and Narbaitz (2022, 2023); Naim et al. (2014); Paar et al. (2011); Park et al. (2002); Yoo (2018); Zheng et al. (2017).

From a physical sense, the C-IDX represents the actual mass of coagulant coating the membrane per square meter of filtration area. Therefore, although the C-IDX was developed for C-IN-P process control, the model given by Eqn. C.1 can also be applied to studies considering C-IN pretreatment to help elucidate LPM behavior for different C-IDX values. Unlike for the limited studies involving C-IN-P (Fig. C.6a), no trend could be observed in the relationship between permeability decline rate and C-IDX for C-IN pretreatment (Fig. C.6b). The observed differences between Fig. C.6a and Fig. C.6b highlight some of the limitations of using the current form of the C-IDX for process control, which should be acknowledged. First, the C-IDX does not account for variable coagulant types, despite significant differences in the molecular weights of inorganic aluminum or iron species. For comparative reasons, it may be more appropriate in future to develop the C-IDX using a molar basis for the coagulant dose. Second, the current form of the C-IDX does not account for differences in membrane type (i.e., pore size, material, or configuration) nor does it consider the fact that facilities/studies employ filtration cycles with different durations. Variations in these last two may have led to the significant discrepancies in permeability decline rate observed for the same C-IDX value in Fig. C.6b. A final limitation of the current C-IDX model worth noting is that it does not follow the principle of the single variable, making comparisons between studies difficult. The same C-IDX value may be arrived at by a number of facilities operating with different combinations of fluxes, coagulant dosages, and durations of coagulant addition. Therefore, future research should investigate the sensitivity of the C-IDX when different dosing time/coagulant dose combinations are used for the same C-IDX value, which to date has not been assessed.

Finally, a discussion of the considerations involved in defining a zone of optimal operation for C-IN-P pretreatment is warranted. Optimal operation of the integrated C-IN-P-LPM system must appropriately balance considerations of: (a) coagulant usage, as LPM pretreatment significantly effects the overall treatment costs (Schäfer et al. 2001); (b) membrane fouling reduction, which will impact the energy consumption as well as chemical cleaning frequency; and

(c) finished water quality, as the product water must meet applicable regulatory guidelines. By considering Fig. C.6a, both coagulant usage and fouling reduction could theoretically be optimized within the region of lowest C-IDX and lowest permeability decline rate. However, owing to the dearth of experimental studies available in the literature, the boundaries for the optimal operating zone cannot be well defined. Moreover, the zone of optimal operation for the C-IN-P-LPM system is likely dependent on several factors, including the source water and its chemistry, the specific membrane type, as well as the criteria for chemical cleaning frequency. For example, in selecting the coagulant dose (as a component of the C-IDX), the removal of NOM is often the governing criterion (Edzwald and Van Benschoten 1990; O'Melia et al. 1999). Depending on pH, it is reported that the stoichiometric requirement for coagulation is 0.5 – 1.0 mg (as metal) per mg DOC for a variety of natural waters (Edzwald 1993; Edzwald and Van Benschoten 1990). For an average North American surface water with a DOC reported to be less than 10 mg L^{-1} (Edzwald and Van Benschoten 1990; Moore and Nagpal 1998; Toming et al. 2020), the inorganic coagulant dose most commonly employed in DWT facilities is thus expected to be less than 5-10 mg L^{-1} (as metal), and often is much lower, although it is highly dependent on the nature of the challenge water. In contrast, treatment of SEs have reported using higher coagulant dosages in the range of 15 to 30 mg L^{-1} (as metal) (Citulski et al. 2009; Nir et al. 2009; Water Environment Federation and American Society of Civil Engineers n.d.), which would lead to higher C-IDX values and an alteration of the optimal zone boundaries compared to natural waters. Concerning chemical cleaning, the optimal rate of permeability decline should be defined according to the target chemical clean-in-place (CIP) frequency, which is in turn dependent on the membrane permeability and flux values recommended by the manufacturer for initiating a chemical clean. A more complete understanding of the impact of water type, coagulant dose, and duration of coagulant addition (or C-IDX as the combined parameter) on LPM fouling is necessary to better define the suitable operating conditions for the C-IN-P configuration.

C.4.3. Removal of Natural Organic Matter

The removal of organic matter by LPMs with C-IN-P pretreatment must also be assessed as an important parameter in the integrated design process of drinking water and wastewater facilities. Several studies have reported similar removals of bulk organics measures by LPM systems with C-IN-P and C-IN pretreatment for both natural waters and SEs. Lok et al. (2017) reported that

when PACl was dosed for 50% of the filtration cycle (i.e., 60 min out of 120 min) the DOC and SUVA removal rates in the permeate were 13.2% and 7%, respectively, for a low SUVA (0.73 L mg^{-1} m^{-1}) lake water. When the dosing time was reduced from 60 min to 10 min for the same water, the DOC and SUVA removals decreased to 7.7% and 6.8%, respectively. Surprisingly, for both C-IN-P conditions, the SUVA removals exceeded those obtained using C-IN pretreatment, while dosing for 50% of the cycle was sufficient to achieve greater bulk DOC removal. Thus, the removal of organics achieved by the C-IN-P-LPM system did not appear to be negatively impacted by the reduced coagulant mass delivered for C-IN-P compared to C-IN. Park et al. (2002) considered the low SUVA (1.27 L mg^{-1} m^{-1}) Han River (Seoul, Korea) as the source water for their study and reported the removal of UV_{254} absorbance (UVA_{254}) to be 44.1% following C-IN pretreatment with a PACl dose of 2.17 mg-Al L^{-1}. When C-IN-P pretreatment was investigated using coagulant dosages equivalent to continuous addition of 0.53, 1.06, and 2.17 mg-Al L^{-1}, the corresponding UVA_{254} removals were found to be 27.3%, 38.8%, and 49.6%. Therefore, compared to C-IN pretreatment, C-IN-P with an equivalent mass loading of coagulant improved UVA_{254} removals by 5.5% and could achieve comparable removals with half the coagulant dose. In the study by Buchta et al. (2019), the two SE sources considered had different levels of bulk organics, as displayed by chemical oxygen demand (COD) values of 17.6 mg L^{-1} and 35 mg L^{-1}. When comparing the removals of organics by continuous and phased coagulant addition, different tendencies were reported depending on the source water. For the first SE (with a COD of 17.6 mg L^{-1}), continuous and phased coagulant addition resulted in nearly identical COD removals of 43% and 41%, respectively. In contrast, for the second SE (with a COD of 35 mg L^{-1}), continuous coagulant addition resulted in a 10% greater (30% vs. 20%) removal of COD than C-IN-P.

In summary, similar removals of bulk organics can be achieved by C-IN-P and C-IN pretreatment of LPM feed waters, although the removals appear to be dependent on a unique interaction between the membrane type, the source water quality, as well as the dose and fraction of cycle it is applied (i.e., coating index). For some waters, the removals of organics by C-IN or C-IN-P were found to be similar, however, the water types and organic loadings for which this is true have not been properly elucidated. Future studies should consider advanced characterization/fractionation techniques of organics for natural waters or synthetic waters with a controlled composition to identify which water quality indicators govern the removals of organics in the C-IN-P scheme. Results from Lok et al. (2017) suggest that a reduction in the C-IDX (by

reducing the dosing time from 60 min to 10 min) had minimal effect on the removal of hydrophobic organic materials (as measured by SUVA). This fact may be critical to the applicability of C-IN-P for LPM pretreatment in DWT facilities as these organics have been suggested as the main precursor to trihalomethanes and haloacetic acids (Hua and Reckhow 2007; Jung and Kang 2003), which are regulated in North America and Europe.

C.5. Outlook and Future Direction

C.5.1. Research Needs for C-IN-P

The immediate future development of C-IN-P as a LPM pretreatment strategy for DWT or the treatment of SE must be focused on a more complete assessment of its performance for a variety of previously untested conditions. Owing to the relative novelty of the C-IN-P approach and the lack of scientific studies investigating its application, there remains a number of important gaps in our understanding of the effects of (1) membrane configuration, (2) varying operational conditions, and (3) feed water quality. Regarding the first two research gaps, the performance of C-IN-P pretreatment needs to be evaluated in terms of both fouling reduction and organics removals using different membrane types/configurations (which have been shown to influence fouling behavior (Ladouceur and Narbaitz 2022)), a range of C-IDXs (especially in the range of 20 – 100 mg m^{-2} which has limited data), and different coagulant types (i.e., ferric coagulants). The impact of rapid mixing type and intensity (i.e., mean velocity gradient, contact time) on C-IN-P performance, which is expected to alter the characteristics of the protective cake layer (e.g., porosity) formed during the initial portion of the cycle, should also be evaluated.

In terms of feed water quality, it would be of interest to investigate C-IN-P performance using challenge waters with greater SUVA values (i.e., > 3 L mg^{-1} m^{-1}) and bulk organics content (DOC > 5 mg L^{-1}). Previous studies reported comparable DOC and SUVA reduction by both C-IN and C-IN-P pretreatment, however, these used raw waters with low DOC and low SUVA (see Table C.1), for which the organics reduction may not be so critical (based on United States Environmental Protection Agency Enhanced Coagulation Requirements) (United States Environmental Protection Agency 1999). Besides C-IN-P, the development of the novel stepped-inline coagulation (C-IN-S), introduced in the next subsection, is a direction that is expected to be successful in achieving acceptable performance for these high SUVA and high DOC water types.

Finally, the performance of C-IN-P pretreatment should also be compared with that of other treatment schemes involving coagulation (i.e., coagulation/flocculation/sedimentation or coagulation/flocculation/flotation), which has not been studied up to now. Previous studies have shown that the selection of coagulation pretreatment strategy is dependent on a unique interaction between the feedwater quality as well as the membrane material/configuration (Ladouceur et al. 2023; Ladouceur and Narbaitz 2023). Conditions for which C-IN-P may present improved performance compared to coagulation strategies involving particle separation should thus be identified.

C.5.2. Development of Novel C-IN-P Strategies

The typical permeability profile for C-IN-S, a novel variation of the C-IN-P operational scheme, is shown in Fig. C.7. The concept of C-IN-S addition is similar to that of C-IN-P (Fig. C.2b), however, instead of setting the coagulant dose to zero for the latter portion of the filtration cycle, the dose is reduced to a lower (non-zero) value.

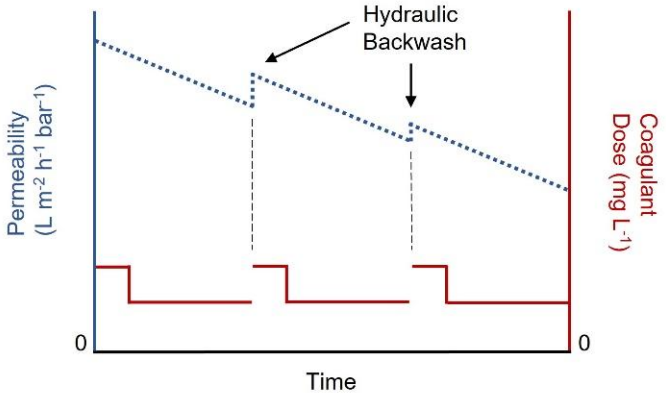


Fig. C.7. Idealized permeability profiles for three filtration cycles with stepped coagulant addition (C-IN-S).

C-IN-S has not been included in any previous studies, although, due to the formation of a protective coating and the continuous addition of low levels of coagulant it may better manage the treatment goals of fouling reduction and product water quality (in terms of filtrate NOM content) compared to C-IN-P pretreatment. Other authors studying C-IN have noted that continuous low-level addition of coagulant (which is employed in the latter portion of the C-IN-S filtration cycle) can improve the removals of organics compared to direct filtration of raw water (Alizadeh

Tabatabai et al. 2014; Aly et al. 2021; Wray et al. 2014; Zheng et al. 2012). It should be noted, however, that the potentially higher product water NOM content for C-IN-S pretreatment compared to pretreatment by C-IN (due to higher NOM:coagulant ratios) or conventional treatment approaches (i.e., coagulation/flocculation coupled with sedimentation or flotation) may be critical for some DWT plants with disinfection by-product (DBP) challenges (Best et al. 2001; Jung and Kang 2003; Vickers et al. 1995; Wang et al. 2016) or for wastewater applications with stringent SE quality restrictions. The suitability of C-IN-P and C-IN-S for reducing DBP formation potential in the hybrid process for high DOC and high SUVA waters (which necessitate higher coagulant dosages (Shin et al. 2008)) must be assessed and is critical to establishing the limitations of these approaches as coagulation pretreatment strategies for LPMs.

A final note regarding C-IN-S is the impact of coagulation mixing conditions. While it was noted in Section C5.1 that the impact of rapid mixing type should be studied for C-IN-P, for C-IN-S it is also recommended to investigate the impact of a dedicated flocculation stage on LPM fouling. The inclusion of a flocculation stage for C-IN-S is logical compared to C-IN-P as coagulant is added (although at different dosages) throughout the entire cycle duration. To date, the impact of flocculation has only been assessed in studies considering C-IN pretreatment where pipe flocculation (Judd and Hillis 2001; Kamińska et al. 2020) and spiral flocculators (Paar et al. 2011) have been implemented with different mixing durations (determined according to the flocculator pipe length). Regarding spiral flocculators, it has been shown by De Oliveira and Teixeira (2017), as well as Cahyana et al. (2021) that the system flowrate, pipe length, pipe diameter, and helical diameter all influence the mean velocity gradient and subsequently the properties (size, fractal dimension) of the formed flocs. Therefore, the implementation of a flocculation stage as well as alteration of its operating conditions is expected to influence the structure of the resulting membrane surface cake formed during C-IN-S pretreatment and the character of the corresponding fouling (Amjad et al. 2015; Hlavacek and Remy 1995).

C.5.3. Regulatory Aspects Driving Technology Development

Regulatory pressures are also expected to drive the development of both C-IN-P and C-IN-S in the coming years. For example, the new national drinking water standard on per- and polyfluoroalkyl substances (PFAS) in the United States is expected to require between 50-60 billion dollars in investment in new drinking water infrastructure, including reverse osmosis (RO) facilities (Black

& Veatch 2023). LPMs represent a compact process which can achieve strict particle removal for RO pretreatment. Furthermore, C-IN-P and C-IN-S are especially well suited for pretreatment of LPMs in this application as not only can they improve organics removals (and reduce fouling of RO membranes) but also the intermittent (or stepped) addition of coagulant could lead to reduced residual dissolved metal concentrations, which exert important impacts on scaling of high-pressure membranes by minerals (Gabelich et al. 2006; Kim et al. 2009).

C.6. Conclusions

Currently, studies evaluating C-IN-P performance only investigate a limited number of operating conditions. Based on the literature consulted in this review, the following conclusions can be made:

1. In general, measures of LPM fouling were found to be similar whether C-IN or C-IN-P pretreatment was applied. It seems that regulation of the cake layer thickness, roughness and coverage of the membrane fiber surface may be critical to the success of C-IN-P for fouling mitigation.
2. The membrane C-IDX may be a suitable tool for C-IN-P process control, with existing studies suggesting fouling becomes exacerbated at low C-IDXs. Optimal operation, which must balance considerations of fouling mitigation, operating expenditure, and product water quality, is likely dependent on the membrane type and the source water characteristics. The current version of the C-IDX has a number of limitations; thus, a modified C-IDX model may be required to adequately describe the performance of the hybrid C-IN-P-LPM system under different conditions.
3. For two different natural waters, as well as a SE source, the removal of bulk organics measured by C-IN-P was found to be similar to, or better than, that by C-IN pretreatment. This suggests that for some water types, reductions in feed water organic concentrations achieved by C-IN pretreatment are not compromised by the reduced coagulant mass delivered by the C-IN-P approach.

C.7. Acknowledgements

This work was supported by the Natural Sciences and Engineering Research Council of Canada under grant RGPIN 2018-06571 and the Canada Graduate Scholarship-Doctoral (CGS-D) program (ID 579943-2023).

C.8. References

Alizadeh Tabatabai, S. A., J. C. Schippers, and M. D. Kennedy. 2014. "Effect of coagulation on fouling potential and removal of algal organic matter in ultrafiltration pretreatment to seawater reverse osmosis." *Water Research*, 59: 283–294. https://doi.org/10.1016/j.watres.2014.04.001.

Alresheedi, M. T., S. L. D. Kenari, B. Barbeau, and O. D. Basu. 2022. "Flux modulation: A novel approach for ultrafiltration fouling control." *Journal of Water Process Engineering*, 46: 102551. https://doi.org/10.1016/j.jwpe.2021.102551.

AlSawaftah, N., W. Abuwatfa, N. Darwish, and G. Husseini. 2021. "A comprehensive review on membrane fouling: Mathematical modelling, prediction, diagnosis, and mitigation." *Water*, 13 (9): 1327. https://doi.org/10.3390/w13091327.

Álvarez-Arroyo, R., J. I. Pérez, L. M. Ruiz, and M. Á. Gómez. 2023. "Analysis of the evolution of ultra-filtered water quality in a drinking water distribution system by particle size distribution: Influence of pre-ozonation." *Water Environment Research*, 95 (2). https://doi.org/10.1002/wer.10840.

Aly, S. A., W. B. Anderson, and P. M. Huck. 2021. "In-line coagulation assessment for ultrafiltration fouling reduction to treat secondary effluent for water reuse." *Water Science and Technology*, 83 (2): 284–296. https://doi.org/10.2166/wst.2020.571.

American Water Works Association. 2016. *Manual of water supply practices - M53, Microfiltration and ultrafiltration membranes for drinking water*. 2nd ed. Denver, CO.

Amjad, H., Z. Khan, and V. V. Tarabara. 2015. "Fractal structure and permeability of membrane cake layers: Effect of coagulation–flocculation and settling as pretreatment steps." *Separation and Purification Technology*, 143: 40–51. https://doi.org/10.1016/j.seppur.2015.01.020.

Anis, S. F., R. Hashaikeh, and N. Hilal. 2019. "Microfiltration membrane processes: A review of research trends over the past decade." *Journal of Water Process Engineering*, 32: 100941. https://doi.org/10.1016/j.jwpe.2019.100941.

Arhin, S. G., N. Banadda, A. J. Komakech, I. Kabenge, and J. Wanyama. 2016. "Membrane fouling control in low pressure membranes: A review on pretreatment techniques for fouling abatement." *Environmental Engineering Research*, 21 (2): 109–120. https://doi.org/10.4491/eer.2016.017.

Arnal, J. M., B. Garcia-Fayos, M. Sancho, and G. Verdu. 2009. "Ultrafiltration membrane cleaning with different chemical solutions after treating surface water." *Desalination and Water Treatment*, 7 (1–3): 198–205. https://doi.org/10.5004/dwt.2009.709.

AWWA. 2005. "Committee Report: Recent advances and research needs in membrane fouling." *Journal AWWA*, 97 (8): 79–89. https://doi.org/10.1002/j.1551-8833.2005.tb07452.x.

Baghbanzadeh, M., D. Rana, C. Q. Lan, and T. Matsuura. 2016. "Effects of inorganic nano-additives on properties and performance of polymeric membranes in water treatment." *Separation & Purification Reviews*, 45 (2): 141–167. https://doi.org/10.1080/15422119.2015.1068806.

Best, G., M. Singh, D. Mourato, and Y. J. Chang. 2001. "Application of immersed ultrafiltration membranes for organic removal and disinfection by-product reduction." *Water Supply*, 1 (5–6): 221–231. https://doi.org/10.2166/ws.2001.0118.

Black & Veatch. 2023. *PFAS National Cost Model Report*. Memorandum. American Water Works Association.

Bogati, R., C. Goodwin, K. Marshall, K. T. Leung, and B. Q. Liao. 2015. "Optimization of chemical cleaning for improvement of membrane performance and fouling control in drinking water treatment." *Separation Science and Technology (Philadelphia)*, 50 (12): 1835–1845. Taylor & Francis. https://doi.org/10.1080/01496395.2015.1009116.

Boretti, A., and L. Rosa. 2019. "Reassessing the projections of the World Water Development Report." *npj Clean Water*, 2 (1): 15. https://doi.org/10.1038/s41545-019-0039-9.

Braghetta, A., J. G. Jacangelo, S. Chellam, B. A. Utne, and M. L. Hotaling. 1997. "DAF pretreatment: its effect on MF performance." *Journal AWWA*, 89 (10): 90–101.

Buchta, P., P. Berg, A. Schweiger, and D. Vial. 2019. "In-line coagulation upstream ultrafiltration - comparison of continuous vs. intermittent addition." 8. New Orleans, LA: American Water Works Association.

Buisson, H., N. Lee, G. Amy, and J. Croue. 2004. "Identification and understanding of fouling in low-pressure membrane (MF / UF) filtration by natural organic." *Water Research*, 38: 4511–4523. https://doi.org/10.1016/j.watres.2004.08.013.

Cahyana, G. H., P. Suwandhi, and T. Mulyani. 2021. "Novel helical or coiled flocculator for turbidity reduction in drinking water treatment: a performance study." *IOP Conference Series: Earth and Environmental Science*, 623 (1): 012009. https://doi.org/10.1088/1755-1315/623/1/012009.

Chen, M., J. Nan, X. Ji, F. Wu, X. Ye, and Z. Ge. 2022. "Effect of adsorption and coagulation pretreatment sequence on ultrafiltration membrane fouling: Process study and targeted prediction." *Desalination*, 540: 115967. https://doi.org/10.1016/j.desal.2022.115967.

Chen, S. C., C. F. Wan, and T.-S. Chung. 2015. "Enhanced fouling by inorganic and organic foulants on pressure retarded osmosis (PRO) hollow fiber membranes under high pressures." *Journal of Membrane Science*, 479: 190–203. https://doi.org/10.1016/j.memsci.2015.01.037.

Cheng, X., H. Liang, A. Ding, F. Qu, S. Shao, B. Liu, H. Wang, D. Wu, and G. Li. 2016. "Effects of pre-ozonation on the ultrafiltration of different natural organic matter (NOM) fractions: Membrane fouling mitigation, prediction and mechanism." *Journal of Membrane Science*, 505: 15–25. Elsevier. https://doi.org/10.1016/j.memsci.2016.01.022.

Choi, K. Y. J., and B. A. Dempsey. 2004. "In-line coagulation with low-pressure membrane filtration." *Water Research*, 38 (19): 4271–4281. https://doi.org/10.1016/j.watres.2004.08.006.

Citulski, J., K. Farahbakhsh, and F. Kent. 2009. "Optimization of phosphorus removal in secondary effluent using immersed ultrafiltration membranes with in-line coagulant pretreatment - implications for advanced water treatment and reuse applications." *Canadian Journal of Civil Engineering*, 36 (7): 1272–1283. https://doi.org/10.1139/L09-062.

Crittenden, J. C., R. R. Trussell, D. W. Hand, K. J. Howe, and G. Tchobanoglous. 2012. *Water treatment: Principles and design*. 3rd ed. New York, NY: McGraw-Hill.

Crozes, G. F., J. G. Jacangelo, C. Anselme, and J. M. Laîné. 1997. "Impact of ultrafiltration operating conditions on membrane irreversible fouling." *Journal of Membrane Science*, 124 (1): 63–76. https://doi.org/10.1016/S0376-7388(96)00244-X.

Cui, X., and K. H. Choo. 2014. "Natural organic matter removal and fouling control in low-pressure membrane filtration for water treatment." *Environmental Engineering Research*, 19 (1): 1–8. https://doi.org/10.4491/eer.2014.19.1.001.

De Angelis, L., and M. M. F. de Cortalezzi. 2013. "Ceramic membrane filtration of organic compounds: Effect of concentration, pH, and mixtures interactions on fouling." *Separation and Purification Technology*, 118: 762–775. https://doi.org/10.1016/j.seppur.2013.08.016.

De Oliveira, D. S., and E. C. Teixeira. 2017. "Experimental evaluation of helically coiled tube flocculators for turbidity removal in drinking water treatment units." *Water SA*, 43 (3): 378. https://doi.org/10.4314/wsa.v43i3.02.

Ding, Q., K. Ochiai, and H. Yamamura. 2020. "In situ and online monitoring of the chemical cleaning efficiency by solid-phase fluorescence excitation–emission matrix spectroscopy (SPF-EEM)." *Journal of Membrane Science*, 611: 118296. https://doi.org/10.1016/j.memsci.2020.118296.

Dong, B., Y. Chen, N. Gao, and J. Fan. 2007. "Effect of coagulation pretreatment on the fouling of ultrafiltration membrane." *Journal of Environmental Sciences*, 19 (3): 278–283. https://doi.org/10.1016/S1001-0742(07)60045-X.

Edzwald, J. K. 1993. "Coagulation in drinking water treatment: Particles, organics and coagulants." *Water Science and Technology*, 27 (11): 21–35. https://doi.org/10.2166/wst.1993.0261.

Edzwald, J. K., ed. 2011. *Water quality & treatment: A handbook on drinking water*. 6th ed. Denver, CO: American Water Works Association.

Edzwald, J. K., and J. Haarhoff. 2012. *Dissolved Air Flotation for Water Clarification*. New York, NY: McGraw-Hill.

Edzwald, J. K., and J. E. Van Benschoten. 1990. "Aluminum coagulation of natural organic matter." *Chemical Water and Wastewater Treatment*, edited by H. H. Hahn and R. Klute, 341–359. Berlin, Heidelberg: Springer Berlin Heidelberg.

Emelko, M. B., P. M. Huck, and B. M. Coffey. 2005. "A review of Cryptosporidium removal by granular media filtration." *Journal AWWA*, 97 (12): 101–115. https://doi.org/10.1002/j.1551-8833.2005.tb07544.x.

Farahbakhsh, K., C. Svrcek, R. K. Guest, and D. W. Smith. 2004. "A review of the impact of chemical pretreatment on low-pressure water treatment membranes." *Journal of Environmental Engineering and Science*, 3 (4): 237–253. https://doi.org/10.1139/S03-078.

Fiessinger, F., J. Mallevialle, A. Leprince, and M. R. Wiesner. 1985. "Megatrends in water treatment technologies." 4 (1): 9–12.

Filella, M., J. Buffle, and N. Parthasarathy. 2005. "HUMIC AND FULVIC COMPOUNDS." *Encyclopedia of Analytical Science*.

Formato, G., R. Romano, A. Formato, J. Sorvari, T. Koiranen, A. Pellegrino, and F. Villecco. 2019. "Fluid–structure interaction modeling applied to peristaltic pump flow simulations." *Machines*, 7 (3): 50. https://doi.org/10.3390/machines7030050.

Fox, K. R., and D. A. Lytle. 1996. "Milkwaukee's crypto outbreak: Investigation and recommendations." *Journal AWWA*, 88 (9): 87–94. https://doi.org/10.1002/j.1551-8833.1996.tb06615.x.

Gabelich, C. J., K. P. Ishida, F. W. Gerringer, R. Evangelista, M. Kalyan, and I. H. "Mel" Suffet. 2006. "Control of residual aluminum from conventional treatment to improve reverse osmosis performance." *Desalination*, 190 (1–3): 147–160. https://doi.org/10.1016/j.desal.2005.09.002.

Galjaard, G., J. van Paassen, P. Buijs, and F. Schoonenberg. 2001. "Enhanced pre-coat engineering (EPCE) for micro- and ultrafiltration: the solution for fouling?" *Water Supply*, 1 (5–6): 151–156. https://doi.org/10.2166/ws.2001.0109.

Gao, W., H. Liang, J. Ma, M. Han, Z. Chen, Z. Han, and G. Li. 2011. "Membrane fouling control in ultrafiltration technology for drinking water production: A review." *Desalination*, 272 (1–3): 1–8. Elsevier B.V. https://doi.org/10.1016/j.desal.2011.01.051.

Gu, H., A. Rahardianto, L. X. Gao, X. P. Caro, J. Giralt, R. Rallo, P. D. Christofides, and Y. Cohen. 2018. "Fouling indicators for field monitoring the effectiveness of operational strategies of ultrafiltration as pretreatment for seawater desalination." *Desalination*, 431: 86–99. https://doi.org/10.1016/j.desal.2017.11.038.

Günther, J., D. Hobbs, C. Albasi, C. Lafforgue, A. Cockx, and P. Schmitz. 2012. "Modeling the effect of packing density on filtration performances in hollow fiber microfiltration module: A spatial study of cake growth." *Journal of Membrane Science*, 389: 126–136. https://doi.org/10.1016/j.memsci.2011.10.055.

Guo, W., H.-H. Ngo, and J. Li. 2012. "A mini-review on membrane fouling." *Bioresource Technology*, 122: 27–34. https://doi.org/10.1016/j.biortech.2012.04.089.

Hao, Y., A. Moriya, T. Maruyama, Y. Ohmukai, and H. Matsuyama. 2011. "Effect of metal ions on humic acid fouling of hollow fiber ultrafiltration membrane." *Journal of Membrane Science*, 376 (1–2): 247–253. https://doi.org/10.1016/j.memsci.2011.04.035.

Hatt, J. W., E. Germain, and S. J. Judd. 2011. "Precoagulation-microfiltration for wastewater reuse." *Water Research*, 45 (19): 6471–6478. https://doi.org/10.1016/j.watres.2011.09.039.

Hilal, N., O. O. Ogunbiyi, N. J. Miles, and R. Nigmatullin. 2005. "Methods employed for control of fouling in MF and UF membranes: A comprehensive review." *Separation Science and Technology*, 40 (10): 1957–2005. https://doi.org/10.1081/SS-200068409.

Hillis, P. 2006. "Enhanced coagulation, flocculation and immersed ultrafiltration for treatment of low alkalinity and highly coloured upland water." *Journal of Water Supply: Research and Technology-Aqua*, 55 (7–8): 549–558. https://doi.org/10.2166/aqua.2006.043.

Hlavacek, M., and J. F. Remy. 1995. "Simple relationships among zeta potential, particle size distribution, and cake specific resistance for colloid suspensions coagulated with ferric chloride." *Separation Science and Technology*, 30 (4): 549–563. https://doi.org/10.1080/01496399508225609.

Hua, G., and D. A. Reckhow. 2007. "Characterization of disinfection byproduct precursors based on hydrophobicity and molecular size." *Environmental Science & Technology*, 41 (9): 3309–3315. https://doi.org/10.1021/es062178c.

Huang, H., K. Schwab, and J. G. Jacangelo. 2009. "Pretreatment for low pressure membranes in water treatment: A review." *Environmental Science and Technology*, 43 (9): 3011–3019. https://doi.org/10.1021/es802473r.

Huang, W., W. Lv, W. Zhou, M. Hu, and B. Dong. 2019. "Investigation of the fouling behaviors correlating to water characteristics during the ultrafiltration with ozone treatment." *Science of the Total Environment*, 676: 53–61. Elsevier B.V. https://doi.org/10.1016/j.scitotenv.2019.04.271.

Jacangelo, J. G., J. M. Laine, J. Mallevialle, K. E. Carns, and E. W. Cummings. 1991. "Low-pressure membrane filtration for removing giardia and microbial indicators." *Journal AWWA*, 83 (9): 97–106.

Jarusutthirak, C., and G. Amy. 2007. "Understanding soluble microbial products (SMP) as a component of effluent organic matter (EfOM)." *Water Research*, 41 (12): 2787–2793. https://doi.org/10.1016/j.watres.2007.03.005.

Jermann, D., W. Pronk, and M. Boller. 2008a. "Mutual influences between natural organic matter and inorganic particles and their combined effect on ultrafiltration membrane fouling." *Environmental Science & Technology*, 42 (24): 9129–9136. https://doi.org/10.1021/es800654p.

Jermann, D., W. Pronk, R. Ka, M. Halbeisen, and M. Boller. 2008b. "Influence of interactions between NOM and particles on UF fouling mechanisms." *Water Research*, 42: 3870–3878. https://doi.org/10.1016/j.watres.2008.05.013.

Judd, S. J., and P. Hillis. 2001. "Optimisation of combined coagulation and microfiltration for water treatment." *Water Research*, 35 (12): 2895–2904. https://doi.org/10.1016/S0043-1354(00)00586-8.

Jung, C. W., and L. S. Kang. 2003. "Application of combined coagulation-ultrafiltration membrane process for water treatment." *Korean Journal of Chemical Engineering*, 20 (5): 855–861. https://doi.org/10.1007/BF02697288.

Kamińska, G., W. Pronk, and J. Traber. 2020. "Effect of coagulant dose and backflush pressure on NOM membrane fouling in inline coagulation-ultrafiltration." *Desalination and Water Treatment*, 199: 188–197. https://doi.org/10.5004/dwt.2020.25657.

Keucken, A., G. Heinicke, K. M. Persson, and S. J. Köhler. 2017. "Combined coagulation and ultrafiltration process to counteract increasing NOM in brown surface water." *Water*, 9 (9): 697. Multidisciplinary Digital Publishing Institute. https://doi.org/10.3390/w9090697.

Kim, H.-C., J.-H. Hong, and S. Lee. 2006. "Fouling of microfiltration membranes by natural organic matter after coagulation treatment: A comparison of different initial mixing conditions." *Journal of Membrane Science*, 283 (1–2): 266–272. https://doi.org/10.1016/j.memsci.2006.06.041.

Kim, M., J. Au, A. Rahardianto, J. Glater, Y. Cohen, F. W. Gerringer, and C. J. Gabelich. 2009. "Impact of conventional water treatment coagulants on mineral scaling in RO desalting of brackish water." *Industrial & Engineering Chemistry Research*, 48 (6): 3126–3135. https://doi.org/10.1021/ie800937c.

Kim, Y.-J., J.-W. Jung, and S. Lee. 2015. "Comparison of fouling rates for pressurized and submerged ultrafiltration membranes." *Desalination and Water Treatment*, 54 (13): 3610–3615. https://doi.org/10.1080/19443994.2014.923208.

Kimura, K., and K. Kume. 2020. "Irreversible fouling in hollow-fiber PVDF MF / UF membranes filtering surface water: Effects of precoagulation and identification of the foulant." *Journal of Membrane Science*, 602 (February): 117975–117975. Elsevier B.V. https://doi.org/10.1016/j.memsci.2020.117975.

Konieczny, K., D. Sąkol, J. Płonka, M. Rajca, and M. Bodzek. 2009. "Coagulation—ultrafiltration system for river water treatment." *Desalination*, 240 (1–3): 151–159. https://doi.org/10.1016/j.desal.2007.11.072.

Koros, W. J., Y. H. Ma, and T. Shimidzu. 1996. "Terminology for membranes and membrane processes (IUPAC Recommendations 1996)." *Pure and Applied Chemistry*, 68 (7): 1479–1489. https://doi.org/10.1351/pac199668071479.

Koyuncu, I., R. Sengur, T. Turken, S. Guclu, and M. E. Pasaoglu. 2015. "Advances in water treatment by microfiltration, ultrafiltration, and nanofiltration." *Advances in Membrane Technologies for Water Treatment*, 83–128. Elsevier.

Ladouceur, J. D., and R. M. Narbaitz. 2022. "Reduced low–pressure membrane fouling by inline coagulation pretreatment for a colored river water." *Membranes*, 12 (11): 1028. https://doi.org/10.3390/membranes12111028.

Ladouceur, J. D., and R. M. Narbaitz. 2023. "Comparing sedimentation, flotation, and inline pre-treatment for low-pressure membrane fouling reduction." *Journal of Environmental Engineering (United States)*, 149 (4).

Ladouceur, J. D., R. M. Narbaitz, and C. Q. Lan. 2023. "Dissolved air flotation pretreatment for low-pressure membranes in water treatment: A review of fouling mitigation and product water quality." *Journal of Water Process Engineering*, 56: 104391. https://doi.org/10.1016/j.jwpe.2023.104391.

Lebeau, T., C. Lelièvre, H. Buisson, D. Cléret, L. W. Van de Venter, and P. Côté. 1998. "Immersed membrane filtration for the production of drinking water: combination with PAC for NOM and SOCs removal." *Desalination*, 117 (1–3): 219–231. https://doi.org/10.1016/S0011-9164(98)00101-5.

Lee, E. K., V. Chen, and A. G. Fane. 2008. "Natural organic matter (NOM) fouling in low pressure membrane filtration — effect of membranes and operation modes." *Desalination*, 218 (September 2006): 257–270. https://doi.org/10.1016/j.desal.2007.02.021.

Li, K., G. Wen, S. Li, H. Chang, S. Shao, T. Huang, G. Li, and H. Liang. 2019. "Effect of pre-oxidation on low pressure membrane (LPM) for water and wastewater treatment: A review." *Chemosphere*, 231: 287–300. https://doi.org/10.1016/j.chemosphere.2019.05.081.

Li, L., H. E. Wray, R. C. Andrews, P. R. Bérubé, L. Li, H. E. Wray, R. C. Andrews, P. R. Bérubé, L. Li, H. E. Wray, R. C. Andrews, and P. R. Bérubé. 2014. "Ultrafiltration fouling: Impact of backwash frequency and air sparging." *Separation Science and Technology*, 49 (18): 2814–2823. Taylor & Francis. https://doi.org/10.1080/01496395.2014.948964.

Li, Q., Z. Xu, and I. Pinnau. 2007. "Fouling of reverse osmosis membranes by biopolymers in wastewater secondary effluent: Role of membrane surface properties and initial permeate flux." *Journal of Membrane Science*, 290 (1–2): 173–181. https://doi.org/10.1016/j.memsci.2006.12.027.

Liang, H., W. Gong, and G. Li. 2008. "Performance evaluation of water treatment ultrafiltration pilot plants treating algae-rich reservoir water." *Desalination*, 221 (1–3): 345–350. https://doi.org/10.1016/j.desal.2007.01.093.

Lin, C. F., Y. J. Huang, and O. J. Hao. 1999. "Ultrafiltration processes for removing humic substances: Effect of molecular weight fractions and PAC treatment." *Water Research*, 33 (5): 1252–1264. https://doi.org/10.1016/S0043-1354(98)00322-4.

Liu, L., X.-B. Luo, L. Ding, and S.-L. Luo. 2019. "Application of nanotechnology in the removal of heavy metals from water." *Nanomaterials for the Removal of Pollutants and Resource Reutilization*, 83–147. Elsevier.

Liu, T., Z. Chen, W. Yu, J. Shen, and J. Gregory. 2011. "Effect of two-stage coagulant addition on coagulation-ultrafiltration process for treatment of humic-rich water." *Water Research*, 45 (14): 4260–4268. https://doi.org/10.1016/j.watres.2011.05.037.

Lok, A., H. Wray, P. Bérubé, and R. C. Andrews. 2017. "Optimization of air sparging and in-line coagulation for ultrafiltration fouling control." *Separation and Purification Technology*, 188: 60–66. https://doi.org/10.1016/j.seppur.2017.06.064.

Ma, B., W. Xue, Y. Bai, R. Liu, W. Chen, H. Liu, and J. Qu. 2020. "Enhanced alleviation of ultrafiltration membrane fouling by regulating cake layer thickness with pre-coagulation during drinking water treatment." *Journal of Membrane Science*, 596 (November 2019): 117732–117732. Elsevier B.V. https://doi.org/10.1016/j.memsci.2019.117732.

Ma, B., W. Yu, H. Liu, and J. Qu. 2014. "Effect of low dosage of coagulant on the ultrafiltration membrane performance in feedwater treatment." *Water Research*, 51: 277–283. https://doi.org/10.1016/j.watres.2013.10.069.

Malkoske, T. A., P. R. Bérubé, and R. C. Andrews. 2020. "Coagulation/flocculation prior to low pressure membranes in drinking water treatment: A review." *Environmental Science: Water Research and Technology*, 6 (11): 2993–3023. Royal Society of Chemistry. https://doi.org/10.1039/d0ew00461h.

Mecha, A. C., M. N. Chollom, B. F. Babatunde, E. K. Tetteh, and S. Rathilal. 2023. "Versatile silver-nanoparticle-impregnated membranes for water treatment: A review." *Membranes*, 13 (4): 432. https://doi.org/10.3390/membranes13040432.

Moore, D. R. J., and N. K. Nagpal. 1998. *Ambient water quality guidelines for organic carbon in British Columbia: a report*. Victoria, B.C.: Environment and Resource Management Dept., Ministry of Environment, Lands and Parks.

Mosqueda-Jimenez, D. B., R. M. Narbaitz, and T. Matsuura. 2004. "Manufacturing conditions of surface-modified membranes: Effects on ultrafiltration performance." *Separation and Purification Technology*, 37 (1): 51–67. https://doi.org/10.1016/j.seppur.2003.07.003.

Naim, R., R. Epsztein, A. Felder, M. Heyer, M. Heijnen, and V. Gitis. 2014. "Rethinking the role of in-line coagulation in tertiary membrane filtration of municipal effluents." *Separation and Purification Technology*, 125: 11–20. Elsevier B.V. https://doi.org/10.1016/j.seppur.2014.01.036.

Nan, J., M. Yao, Q. Li, D. Zhan, T. Chen, Z. Wang, and H. Li. 2016. "The role of shear conditions on floc characteristics and membrane fouling in coagulation/ultrafiltration hybrid process – the effect of flocculation duration and slow shear force." *RSC Advances*, 6 (1): 163–173. https://doi.org/10.1039/C5RA18328F.

Nguyen, A. H., R. M. Narbaitz, and T. Matsuura. 2007. "Impacts of hydrophilic membrane additives on the ultrafiltration of river water." *Journal of Environmental Engineering*, 133 (5): 515–522. https://doi.org/10.1061/(asce)0733-9372(2007)133:5(515).

Nir, T., E. Arkhangelsky, I. Levitsky, and V. Gitis. 2009. "Removal of phosphorus from secondary effluents by coagulation and ultrafiltration." *Desalination and Water Treatment*, 8 (1–3): 24–30. https://doi.org/10.5004/dwt.2009.686.

Oh, J., and S. Lee. 2005. "Influence of streaming potential on flux decline of microfiltration with in-line rapid pre-coagulation process for drinking water production." *Journal of Membrane Science*, 254 (1–2): 39–47. https://doi.org/10.1016/j.memsci.2004.12.030.

O'Melia, C. R., W. C. Becker, and K.-K. Au. 1999. "Removal of humic substances by coagulation." *Water Science and Technology*, 40 (9): 47–54. https://doi.org/10.2166/wst.1999.0440.

Paar, H., J. Benecke, M. Ernst, and M. Jekel. 2011. "Pre-coagulation and ultrafiltration of effluent impaired surface water for phosphorus removal and fouling control." *Water Supply*, 11 (2): 211–218. https://doi.org/10.2166/ws.2011.037.

Palmada, N., J. E. Cater, L. K. Cheng, and V. Suresh. 2022. "Experimental and computational studies of peristaltic flow in a duodenal model." *Fluids*, 7 (1): 40. https://doi.org/10.3390/fluids7010040.

Park, J., H.-Y. Kim, and P.-K. Park. 2015. "Split injection of coagulant to enhance the water permeability of a cake layer in a coagulation–microfiltration process." *Journal of Industrial and Engineering Chemistry*, 21: 363–368. https://doi.org/10.1016/j.jiec.2014.02.046.

Park, P. K., C. H. Lee, S. J. Choi, K. H. Choo, S. H. Kim, and C. H. Yoon. 2002. "Effect of the removal of DOMs on the performance of a coagulation-UF membrane system for drinking water production." *Desalination*, 145 (1–3): 237–245. https://doi.org/10.1016/S0011-9164(02)00418-6.

Patwardhan, S., S. Palekar, N. S. Wagh, and J. Lakkakula. 2023. "Extended investigation processes in advanced wastewater treatment for water reuse." *Membrane and membrane-based processes for wastewater treatment*, 129–152. 1st ed. Boca Raton, FL: CRC Press.

Pearce, G. K. 2011. *UF/MF membrane water treatment: Principles and design*. 387. 1st ed. Bangkok: Water Treatment Academy.

Pearce, G. K. 2018. "Is the Water Membrane Market in a State of Flux?" *Water World*.

Peters, C. D., T. Rantissi, V. Gitis, and N. P. Hankins. 2021. "Retention of natural organic matter by ultrafiltration and the mitigation of membrane fouling through pre-treatment, membrane enhancement, and cleaning - A review." *Journal of Water Process Engineering*, 44: 102374. https://doi.org/10.1016/j.jwpe.2021.102374.

Pezeshk, N., and R. M. Narbaitz. 2012. "More fouling resistant modified PVDF ultrafiltration membranes for water treatment." *Desalination*, 287: 247–254. https://doi.org/10.1016/j.desal.2011.11.048.

Porcelli, N., and S. Judd. 2010. "Chemical cleaning of potable water membranes: A review." *Separation and Purification Technology*, 71 (2): 137–143. https://doi.org/10.1016/j.seppur.2009.12.007.

Pronk, W., J. Traber, and G. Kamińska. 2016. "Optimization of process parameters of the coagulation/ultrafiltration process for the reduction of membrane fouling." In: *Adv. Part. Sci. Sep. Meet. Tomorrows Chall.*, 198–205. Oslo, Norway: International Water Association.

Rana, D., and T. Matsuura. 2010. "Surface modifications for antifouling membranes." *Chemical Reviews*, 110 (4): 2448–2471. https://doi.org/10.1021/cr800208y.

Regli, S., R. Odom, J. Cromwell, M. Lustic, and V. Blank. 1999. "Benefits and costs of the IESWTR." *Journal AWWA*, 91 (4): 148–158. https://doi.org/10.1002/j.1551-8833.1999.tb08621.x.

Salinas-Rodriguez, S. G., A. Prabowo, A. Abushaban, F. Battes, J. C. Schippers, and M. D. Kennedy. 2016. "Pre-coating of outside-inside capillary UF membranes with iron hydroxide particles to limit non-backwashable fouling during seawater algal blooms." *Desalination and Water Treatment*, 57 (55): 26730–26740. https://doi.org/10.1080/19443994.2016.1190111.

Schäfer, A. I., N. Andritsos, A. J. Karabelas, E. M. V. Hoek, R. Schneider, and M. Nyström. 2021. "Fouling in nanofiltration." *Nanofiltration: Principles, applications, and new materials*, edited by A. I. Schäefer and A. G. Fane, 273–379. 2nd ed. Wiley-VCH GmbH.

Schäfer, A. I., A. G. Fane, and T. D. Waite. 2001. "Cost factors and chemical pretreatment effects in the membrane filtration of waters containing natural organic matter." *Water Research*, 35 (6): 1509–1517. https://doi.org/10.1016/S0043-1354(00)00418-8.

Schulz, M., A. Soltani, X. Zheng, and M. Ernst. 2016. "Effect of inorganic colloidal water constituents on combined low-pressure membrane fouling with natural organic matter (NOM)." *Journal of Membrane Science*, 507: 154–164. Elsevier. https://doi.org/10.1016/j.memsci.2016.02.008.

Schweiger, A., P. Buchta, D. Vial, and P. Berg. 2018a. "Coating of ultrafiltration membranes - the solution to improve the efficiency of the pre-treatment." In: *Desalination Environ. - Clean Water Energy*. Athens.

Schweiger, A., C. Starke, D. Vial, P. Buchta, and P. Berg. 2018b. "Coating - a dramatic change in ultrafiltration treatment of secondary effluent." Valencia, Spain.

Shi, X., G. Tal, N. P. Hankins, and V. Gitis. 2014. "Fouling and cleaning of ultrafiltration membranes: A review." *Journal of Water Process Engineering*, 1: 121–138. Elsevier Ltd. https://doi.org/10.1016/j.jwpe.2014.04.003.

Shin, J. Y., R. F. Spinette, and C. R. O'Melia. 2008. "Stoichiometry of coagulation revisited." *Environmental Science and Technology*, 42 (7): 2582–2589. https://doi.org/10.1021/es071536o.

Sillanpaa, M. 2015. *Natural Organic Matter in Water*. 1st ed. Oxford, UK: Butterworth-Heinemann.

Souza, N. P. D., and O. D. Basu. 2013. "Comparative analysis of physical cleaning operations for fouling control of hollow fiber membranes in drinking water treatment." *Journal of Membrane Science*, 436: 28–35. Elsevier. https://doi.org/10.1016/j.memsci.2013.02.014.

Tang, C. Y., Z. Yang, H. Guo, J. J. Wen, L. D. Nghiem, and E. Cornelissen. 2018. "Potable water reuse through advanced membrane technology." *Environmental Science & Technology*, 52 (18): 10215–10223. https://doi.org/10.1021/acs.est.8b00562.

Tian, J., M. Ernst, F. Cui, and M. Jekel. 2013. "Effect of particle size and concentration on the synergistic UF membrane fouling by particles and NOM fractions." *Journal of Membrane Science*, 446: 1–9. https://doi.org/10.1016/j.memsci.2013.06.016.

Toming, K., J. Kotta, E. Uuemaa, S. Sobek, T. Kutser, and L. J. Tranvik. 2020. "Predicting lake dissolved organic carbon at a global scale." *Scientific Reports*, 10 (1): 8471. https://doi.org/10.1038/s41598-020-65010-3.

Tow, E. W., B. Rad, and R. Kostecki. 2022. "Biofouling of filtration membranes in wastewater reuse: In situ visualization with confocal laser scanning microscopy." *Journal of Membrane Science*, 644: 120019. https://doi.org/10.1016/j.memsci.2021.120019.

Tsuyuhara, T., Y. Hanamoto, T. Miyoshi, K. Kimura, and Y. Watanabe. 2010. "Influence of membrane properties on physically reversible and irreversible fouling in membrane bioreactors." *Water Science and Technology*, 61 (9): 2235–2240. https://doi.org/10.2166/wst.2010.122.

United States Environmental Protection Agency. 1999. "Enhanced Coagulation and Enhanced Precipitative Softening Guidance Manual."

Van Der Bruggen, B., C. Vandecasteele, T. Van Gestel, W. Doyen, and R. Leysen. 2003. "A review of pressure-driven membrane processes in wastewater treatment and drinking water production." *Environmental Progress*, 22 (1): 46–56. https://doi.org/10.1002/ep.670220116.

Vickers, J. C., M. A. Thompson, and U. G. Kelkar. 1995. "The use of membrane filtration in conjunction with coagulation processes for improved NOM removal." *Desalination*, 102 (1–3): 57–61. https://doi.org/10.1016/0011-9164(95)00041-Y.

Wang, F., B. Gao, D. Ma, Q. Yue, R. Li, and Q. Wang. 2016. "Reduction of disinfection by-product precursors in reservoir water by coagulation and ultrafiltration." *Environmental Science and Pollution Research*, 23 (22): 22914–22923. https://doi.org/10.1007/s11356-016-7496-1.

Wang, J., and X. Wang. 2006. "Ultrafiltration with in-line coagulation for the removal of natural humic acid and membrane fouling mechanism." *Journal of Environmental Sciences*, 18 (5): 880–884. https://doi.org/10.1016/S1001-0742(06)60008-9.

Wang, L., R. Miao, X. Wang, Y. Lv, X. Meng, Y. Yang, D. Huang, L. Feng, Z. Liu, and K. Ju. 2013. "Fouling behavior of typical organic foulants in polyvinylidene fluoride ultrafiltration membranes: Characterization from microforces." *Environmental Science and Technology*, 47 (8): 3708–3714. https://doi.org/10.1021/es4004119.

Wang, W., Q. Yue, K. Guo, F. Bu, X. Shen, and B. Gao. 2019. "Application of Al species in coagulation/ultrafiltration process: Influence of cake layer on membrane fouling." *Journal of Membrane Science*, 572 (September 2018): 161–170. Elsevier B.V. https://doi.org/10.1016/j.memsci.2018.11.014.

Water Environment Federation, and American Society of Civil Engineers. n.d. *Design of Water Resource Recovery Facilities*. 6th ed. New York, NY: McGraw-Hill.

Westerhoff, P., G. Aiken, G. Amy, and J. Debroux. 1999. "Relationships between the structure of natural organic matter and its reactivity towards molecular ozone and hydroxyl radicals." *Water Research*, 33 (10): 2265–2276. https://doi.org/10.1016/S0043-1354(98)00447-3.

White, M. C., J. D. Thompson, G. W. Harrington, and P. C. Singer. 1997. "Evaluating criteria for enhanced coagulation compliance." *Journal (American Water Works Association)*, 89 (5): 64–77. American Water Works Association.

Wiesner, B. M. R., M. M. Clark, A. Members, and J. Mallevialle. 1989. "Membrane filtration o f coagulated suspensions." 115 (1): 20–40.

Wray, H. E., and R. C. Andrews. 2014. "Optimization of coagulant dose for biopolymer removal: Impact on ultrafiltration fouling and retention of organic micropollutants." *Journal of Water Process Engineering*, 1: 74–83. https://doi.org/10.1016/j.jwpe.2014.03.007.

Wray, H. E., R. C. Andrews, and P. R. Bérubé. 2014. "Ultrafiltration organic fouling control: Comparison of air-sparging and coagulation." *Journal - American Water Works Association*, 106 (2): E76–E85. https://doi.org/10.5942/jawwa.2014.106.0018.

Wray, H. E., R. C. Andrews, and P. R. Bérubé. 2016. "Coagulation optimization for DOC removal: pilot-scale analysis of UF fouling and disinfection byproduct formation potential." *Water Supply*, 16 (2): 473–480. https://doi.org/10.2166/ws.2015.157.

Wu, S., B. Ma, C. Hu, X. Hua, H. Fan, M. Ulbricht, and J. Qu. 2023. "Cake layer 3D structure regulation to optimize water channels during Al-based coagulation-ultrafiltration process." *Water Research*, 236: 119941. https://doi.org/10.1016/j.watres.2023.119941.

Xie, Y., B. Ma, X. Zhang, H. Liu, and J. Qu. 2016. "Modification of ultrafiltration membrane with iron/aluminum mixed hydrolyzed precipitate layer for humic acid fouling reduction." *Desalination and Water Treatment*, 57 (54): 26022–26030. https://doi.org/10.1080/19443994.2016.1159991.

Xu, X., Y. Yang, T. Liu, and B. Chu. 2022. "Cost-effective polymer-based membranes for drinking water purification." *Giant*, 10: 100099. https://doi.org/10.1016/j.giant.2022.100099.

Xue, W., M. Jian, T. Lin, B. Ma, R. Wu, and X. Li. 2020. "A novel strategy to alleviate ultrafiltration membrane fouling by rotating membrane module." *Chemosphere*, 260: 127535. https://doi.org/10.1016/j.chemosphere.2020.127535.

Yamamura, H., K. Kimura, and Y. Watanabe. 2007. "Mechanism involved in the evolution of physically irreversible fouling in microfiltration and ultrafiltration membranes used for drinking water treatment." *Environmental Science and Technology*, 41 (19): 6789–6794. https://doi.org/10.1021/es0629054.

Yan, M., X. Shen, B. Gao, K. Guo, and Q. Yue. 2021. "Coagulation-ultrafiltration integrated process for membrane fouling control: Influence of Al species and SUVA values of water." *Science of The Total Environment*, 793: 148517. https://doi.org/10.1016/j.scitotenv.2021.148517.

Ye, Y., V. Chen, and P. Le-Clech. 2011. "Evolution of fouling deposition and removal on hollow fibre membrane during filtration with periodical backwash." *Desalination*, 283: 198–205. Elsevier B.V. https://doi.org/10.1016/j.desal.2011.03.087.

Yoo, R. S., D. R. Brown, R. J. Pardini, and G. D. Bentson. 1995. "Microfiltration: a case study." *Journal - American Water Works Association*, 87 (3): 38–49. https://doi.org/10.1002/j.1551-8833.1995.tb06330.x.

Yoo, S. S. 2018. "Operating cost reduction of in-line coagulation/ultrafiltration membrane process attributed to coagulation condition optimization for irreversible fouling control." *Water (Switzerland)*, 10 (8). https://doi.org/10.3390/w10081076.

Yu, W. zheng, N. Graham, H. juan Liu, and J. hui Qu. 2013. "Comparison of FeCl3 and alum pre-treatment on UF membrane fouling." *Chemical Engineering Journal*, 234: 158–165. Elsevier B.V. https://doi.org/10.1016/j.cej.2013.08.105.

Zheng, X., S. Plume, M. Ernst, J. P. Croué, and M. Jekel. 2012. "In-line coagulation prior to UF of treated domestic wastewater - foulants removal, fouling control and phosphorus removal." *Journal of Membrane Science*, 403–404: 129–139. Elsevier B.V. https://doi.org/10.1016/j.memsci.2012.02.051.

Zheng, X., F. Zietzschmann, S. Plume, H. Paar, M. Ernst, Z. Wang, and M. Jekel. 2017. "Understanding and control of biopolymer fouling in ultrafiltration of different water types." *Water (Switzerland)*, 9 (4). https://doi.org/10.3390/w9040298.

Zularisam, A. W., A. Ahmad, M. Sakinah, A. F. Ismail, and T. Matsuura. 2011. "Role of natural organic matter (NOM), colloidal particles, and solution chemistry on ultrafiltration performance." *Separation and Purification Technology*, 78 (2): 189–200. Elsevier B.V. https://doi.org/10.1016/j.seppur.2011.02.001.

Zularisam, A. W., A. F. Ismail, M. R. Salim, M. Sakinah, and H. Ozaki. 2007. "The effects of natural organic matter (NOM) fractions on fouling characteristics and flux recovery of ultrafiltration membranes." *Desalination*, 212 (1–3): 191–208. https://doi.org/10.1016/j.desal.2006.10.010.

APPENDIX D

Supplemental Information for Chapter 3

Context: This appendix presents supporting information associated with Chapter 3 of this thesis *Comparing Sedimentation, Flotation, and Inline Pretreatment for Low-Pressure Membrane Fouling Reduction.*

List of Abbreviations

CEB	Chemically enhanced backwash
CIFI	Chemically irreversible fouling index
C-IN	Inline coagulation
DI	Deionised water
FI	Fouling index
HIFI	Hydraulically irreversible fouling index
HRFI	Hydraulically reversible fouling index
MWCO	Molecular weight cut-off
TFI	Total fouling index
UF	Ultrafiltration

D.1. Multi-Day Filtration Tests

A summary of the operating conditions used during the multi-day filtration tests conducted as part of the work in Chapter 3 is presented in Table D.1. below.

Table D.1. Summary of Multi-day Testing Parameters

Characteristic	Value
Pore Size, µm	0.02[a]
Permeability, $L/m^2/h/Bar$	5000 [a]
Fiber Material	PVDF [a]
Contact Angle	45 [a]
Operation	Pressure driven outside-in
Filtration Flux, $L/m^2/h$	80
Backwash Flux, $L/m^2/h$	200
Filtration Cycle Duration, min	30
Backwash Cycle Duration, min	2
CEB Interval, day	1
CEB Chemicals	100ppm Cl^-
CIP Interval, day	3
CIP Chemicals	0.1N NaOH + 200ppm Cl^-

[a] Obtained from Kuraray Co. Ltd.

D.2. Molecular Weight Fractionation

D.2.1. Background

Membrane filtration is one of many techniques that can be employed for the analysis and fractionation of aquatic natural organic matter (NOM). Many researchers have employed membrane filtration as a fractionation technique previously and have highlighted several advantages and disadvantages (Amy et al. 1987; Cai 1999; Dang 2009; Logan and Jiang 1990; Mosqueda-Jimenez 2003; Nilson and DiGiano 1996). It has been observed that the success of this type of NOM fractionation is dependent on the degree of concentration polarization and NOM-membrane interactions. Concentration polarization can induce a resistance to filtration that, in the case of ultrafiltration (UF) membranes, can be severe due to the high flux and low mass transfer coefficients of macromolecular solutes (Mulder 1996). Furthermore, adsorptive interactions leading to pore constriction of the membrane can lead to changes in membrane permeability and retention (Sillanpaa 2015). Another limitation of membrane fractionation is that the membranes themselves inherently possess a distribution of pore sizes: the reported molecular weight cutoff (MWCO) value corresponds only to the ability of the membrane to retain 90% of compounds with this molecular weight and is not an absolute cutoff. The driving force for UF membranes is a chemical potential gradient, which is governed by pressure and concentration gradient for low pressure membranes. This means that as the filtration proceeds, the concentration gradient will increase across the membrane as solutes are rejected, potentially affecting rejection (Aiken et al. 1985).

D.2.2. Procedures

The following steps were taken for the preparation of the stirred filtration cell and UF membrane discs:

1. All components of the stirred filtration cells (Model 8400, Amicon, Darmstadt) were soaked for a period not less than several hours in a mild laboratory detergent (Contrex AL Liquid Detergent, Decon Labs, King of Prussia, PA) bath. Following this, the cells were thoroughly rinsed with deionized water (DI) (Barnstead, MicroPure, ThermoFisher Scientific, Waltham, MA) and were stored in a sealed container to prevent contamination.

2. The membrane filtration discs were prepared in accordance with the manufacturer recommended practice. As per manufacturer recommendations (EMD Millipore Corporation 2019) and Mosqueda-Jimenez (2003) the membrane discs were soaked skin-side face down in DI for a period of 90 minutes, changing the water three-times during that period in order to remove the protective glycerine coating. Additionally, the discs were placed in the cell, glossy side up, and rinsed using DI for a minimum of 5 min at a pressure of 55 psi.

The operation of the stirred filtration cells was according to a cascade, or serial, filtration method, as in the work by Dang (2009), which involved sequential passage of sample through membrane filter discs with decreasing molecular weight cutoff values. A flow chart of the filtration protocol is shown in Fig. D.1:

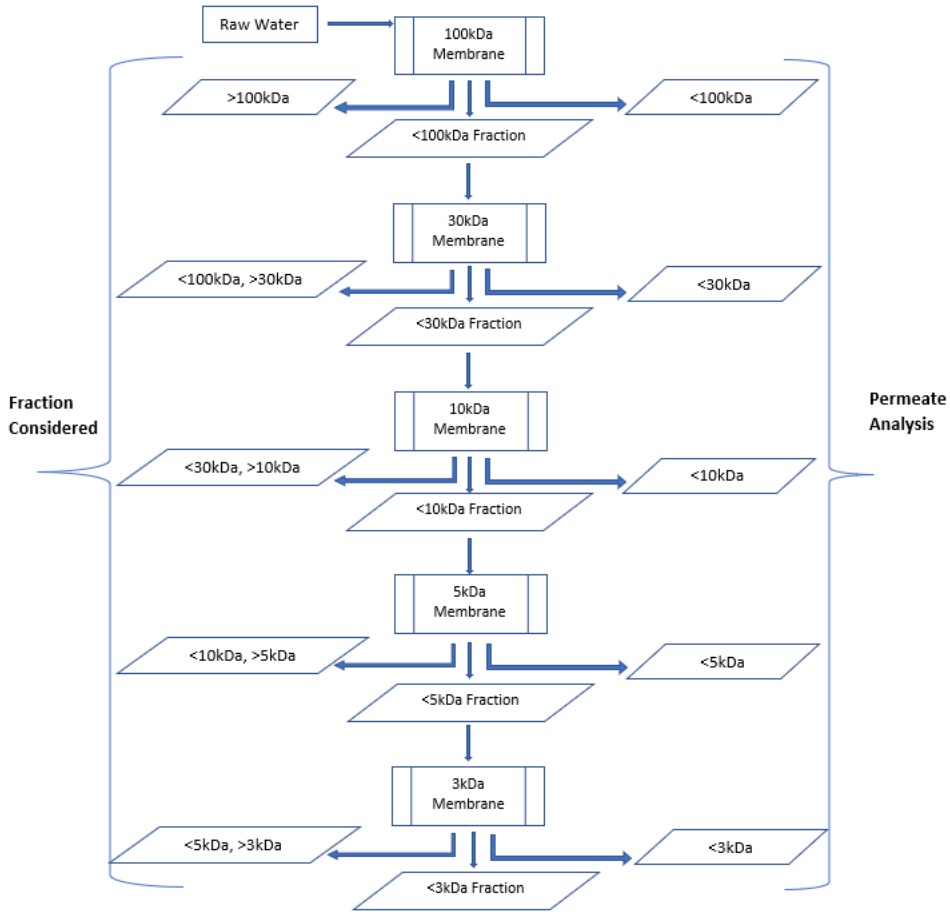


Fig. D.1. Serial filtration procedure

The proposed fractionation protocol is adapted from the methods used by Mosqueda-Jimenez (2003), Dang (2009), Nilson and DiGiano (1996), and Aiken et al. (1985):

3a) The challenge water was initially filtered through a 0.45 µm filter (GN-6 Metrical, Cytiva, Wilmington, DE) to remove particulate material.

3b) The Amicon cell was then assembled. The UF disc was placed glossy side up on the permeate collector, and an O-ring is placed between the membrane and the body. The base plate was then screwed into the body to seal the apparatus. DI followed by 0.45 µm filtered sample water was used to rinse the assembled cell.

3c) 350 mL of the pre-filtered sample water was placed in the UF cell body, with the first cell containing the 100 kDa membrane (PBHK07610, Millipore Sigma, Oakville). The lid of the cell was put in place with the O-Ring providing a tight seal, and the entire assembly placed inside the cell holder prior to pressurization. The magnetic stirrer was engaged (VWR Advance Stirrer, VWR, Mississauga, ON, Canada) and the manifold was used to set the filtration pressure at a constant level of 10 psi for the 100 kDa membrane and 30 psi for UF membranes with lower MWCO values. The first 5 mL of filtrate was wasted before filtering and collecting 80% of the sample volume. A 40 mL sample of permeate was set aside in a headspace free vial for DOC analysis.

3d) The remaining balance of the permeate was from the first cell was then placed in a second stirred UF cell which contains a 30 kDa membrane disc (PLTK07610, Millipore Sigma, Oakville) that was preconditioned according to step 2.

3e) The filtration procedure was then carried out according to steps 3b)-3d). This is repeated for UF membranes with MWCO values of 10 kDa (PLGC07610, Millipore Sigma, Oakville), 5 kDa (PLCC07610, Millipore Sigma, Oakville), and 3 kDa (PLBC07610, Millipore Sigma, Oakville).

D.3. Fouling Indices

The mathematical formulation of the fouling index (FI) model was provided in Chapter 3. Fig. D.2 below presents a graphical representation of the various FIs. The FI that is computed will depend on the operational cycles that are considered during the analysis. For the total fouling index (TFI), the data between hydraulic backwashes is used, while the hydraulically irreversible fouling index

(HIFI) is calculated by regressing the data between chemically enhanced backwashes. The chemically irreversible fouling index (CIFI) is determined by considering the slope of the line connecting the initial normalized specific flux value to that after the chemical clean-in-place.

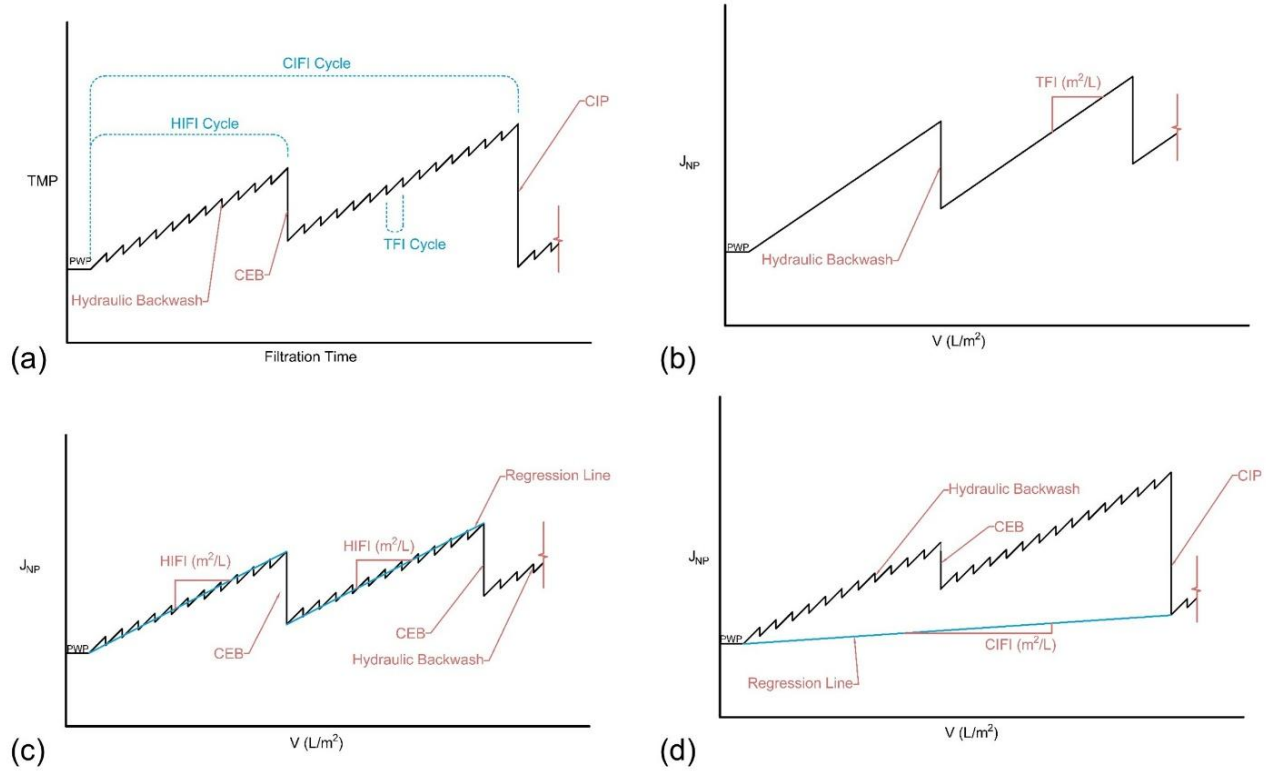


Fig. D.2. Visual description of fouling index cycles: **(a)** FI cycle classification; **(b)** Method of TFI analysis; **(c)** Method of HIFI analysis; **(d)** Method of CIFI analysis.

Table D.2 presents a summary of the FIs observed for all test conditions using water collected during the summer and winter season.

Table D.2. Three-day Average Fouling Indices

	Winter					Summer	
				C-IN		C-IN	
	Raw	**CF-DAF**	**CF-SED**	**27 mg L^{-1}**	**34 mg L^{-1}**	**27 mg L^{-1}**	**34 mg L^{-1}**
TFIx10^{-4} (m^2 L^{-1})	516.53 ± 34.55	34.26 ± 1.00	40.04 ± 1.43	638.64 ± 52.78	249.67 ± 17.72	153.47	84.46
HIFIx10^{-4} (m^2 L^{-1})	41.55 ± 19.53	1.67 ± 0.29	1.54 ± 0.36	20.52 ± 6.86	10.07 ± 1.99	9.71	3.98
HRFIx10^{-4} (m^2 L^{-1})	474.98	32.59	38.5	618.12	239.6	143.76	80.48
CIFIx10^{-4} (m^2 L^{-1})	7.02 ± 3.90[a]	0.58	0.66	2.69 ± 1.05	1.06 ± 0.36	0.87	0.92
HRFI/TFI	0.920	0.951	0.962	0.968	0.960	0.937	0.953
HIFI/TFI	0.080	0.049	0.038	0.032	0.040	0.063	0.047
CIFI/TFI	0.014	0.017	0.016	0.004	0.004	0.006	0.011
CIFI/HIFI	0.169	0.347	0.429	0.131	0.105	0.095	0.231

Note: CIFI based on CIP cycle

[a]μ ± 95% Confidence Interval

D.4. Performance of Chemically Enhanced Backwash

Fig. D.3 below visualizes the removal of the foulant cake from the membrane surface over the course of the 20 min-long chemically enhanced backwash (CEB) cycle.

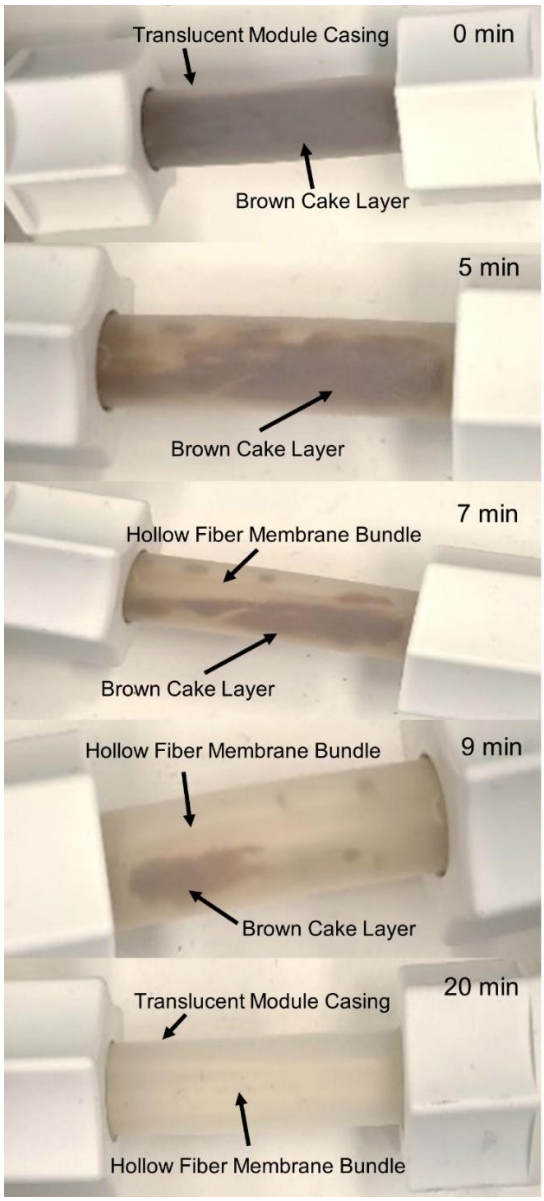


Fig. D.3. Surface cake removal at various stages of chemically enhanced backwash. View of white membrane fibers through translucent module casing. At time t = 0 min the CEB commences and a brown, gel-like cake layer is present on fiber surface. At time t = 20 min, the RO flush has visually removed the cake layer.

D.5. References

Aiken, G. R., D. M. McKnight, R. L. Wershaw, and P. MacCarthy. 1985. *Humic Substances in Soil, Sediment, and Water: Geochemistry, Isolation, and Characterization*. 1st ed. Toronto: John Wiley & Sons.

Amy, G. L., M. R. Collins, C. J. Kuo, and P. H. King. 1987. "Comparing Gel Permeation Chromatography and Ultrafiltration for the Molecular Weight Characterization of Aquatic Organic Matter." *Journal AWWA*, 79 (1): 43–49. https://doi.org/10.1002/j.1551-8833.1987.tb02782.x.

Cai, Y. 1999. "Size distribution measurements of dissolved organic carbon in natural waters using ultrafiltration technique." *Water Research*, 33 (13): 3056–3060. https://doi.org/10.1016/S0043-1354(99)00012-3.

Dang, H. T. 2009. "Surface Modifying Macromolecules (SMM) - Incorporated Ultrafiltration Membranes for Natural Organic Matter (NOM) Removal: Characterization and Cleaning." Doctoral Dissertation, University of Ottawa.

EMD Millipore Corporation. 2019. "Ultrafiltration Membranes." User Guide.

Logan, B. E., and Q. Jiang. 1990. "Molecular Size Distributions of Dissolved Organic Matter." *Journal of Environmental Engineering*, 116 (6): 1046–1062.

Mosqueda-Jimenez, D. B. 2003. "Impact of manufacturing conditions of polyethersulfone membranes on final characteristics and fouling reduction." Doctoral Dissertation, University of Ottawa.

Mulder, M. 1996. *Basic Principles of Membrane Technology*. 2nd ed. Dordrecht, The Netherlands: Kluwer Academic Publisher.

Nilson, J. A., and F. A. DiGiano. 1996. "Influence of NOM composition on nanofiltration." *Journal AWWA*, 88 (5): 53–66. https://doi.org/10.1002/j.1551-8833.1996.tb06555.x.

Sillanpaa, M. 2015. *Natural Organic Matter in Water*. 1st ed. Oxford, UK: Butterworth-Heinemann.

APPENDIX E

Supplemental Information for Chapter 4

Context: This appendix presents supporting information associated with Chapter 4 of this thesis *Reduced Low-Pressure Membrane fouling by Inline Coagulation Pretreatment for a Colored River Water*

List of Abbreviations

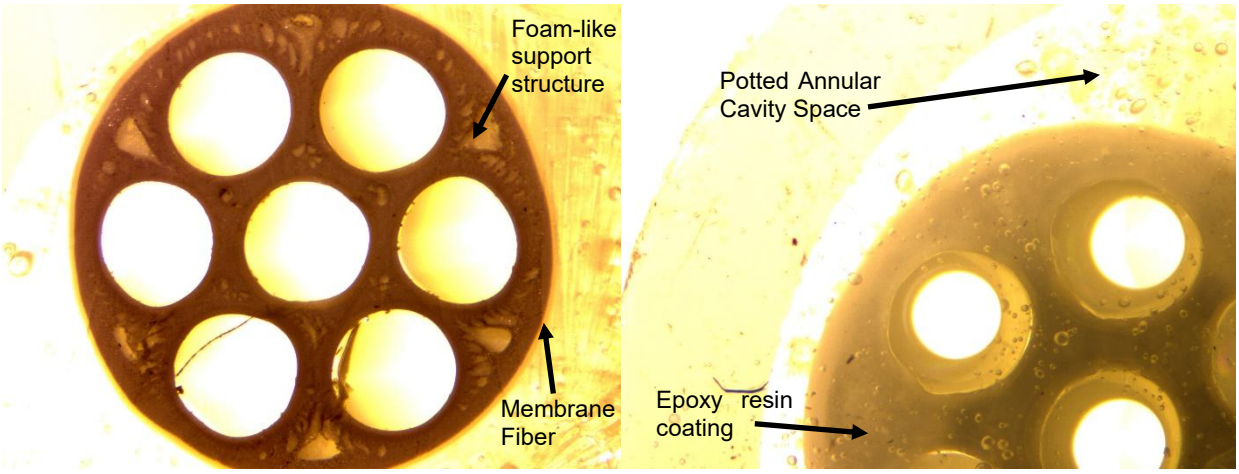
ANOVA	Analysis of variance
CF-DAF	Coagulation/flocculation/dissolved air flotation
CF-SED	Coagulation/flocculation/sedimentation
FR_{hr}	Hydraulically reversible fouling rate
FR_{hirr}	Hydraulically irreversible fouling rate
FR_{CEB}	Irreversible fouling rate over one CEB cycle
FR_{CIP}	Irreversible fouling rate over one CIP cycle
ORW	Ottawa River water
SUVA	Specific ultraviolet absorbance at 254nm
TMC	Tubular multichannel
TMP	Transmembrane pressure

E.1. Validation of Tubular Multichannel Membrane Potting Procedure

The tubular multichannel (TMC) membranes (Multibore 0.9, Dupont, Wilmington, DE) used in this study had a total diameter of approximately 4 mm and contained seven concentrically positioned lumen, each with a diameter of 0.9 mm. Between each capillary is a ~ 300 μm thick high porosity foam-like support structure with a pore size in the range of 10 μm, representing a 500 fold increase compared to the pore size of the membrane separation skin (Heijnen et al. 2012).

As the lab-scale modules were made in-house from virgin fibers, there was a need to seal the foam-like support structure to ensure that the feed water does not enter this highly porous (and low resistance) structure but instead enter the fiber lumen and cross the separation skin. To accomplish this, the fiber end was potted using a high-strength epoxy resin (Slow-Cure, BSI Inc, Pasco Robles, CA). Compressed air was supplied through the capillaries using a 21- gauge needle during curing to ensure that the epoxy sealed only the support structure and did not obstruct the capillary inlets. Once the epoxy had set at the feed water inlet, approximately 1 cm of fiber was trimmed at the opposite end (to eliminate the possibility for any fiber damage arising from needle insertion during compressed air delivery) and the fiber was potted shut. Fig. E.1a shows an image (Stemi 355, Zeiss, Oberkochen, Germany) of the TMC membrane potted in the module casing. Here, the face had been prepared (to be flat) using an ultrasharp razor blade. In Fig. E.1b, it can be seen that the foam-like support structure is sealed by the high-strength epoxy, while the fiber lumen

remain open and only marginally reduced in diameter.



(a) **(b)**

Fig. E.1. Potted tubular multichannel membrane fiber: **(a)** Prior to sealing foam-like support structure; **(b)** After sealing support structure.

E.2. Preliminary Work

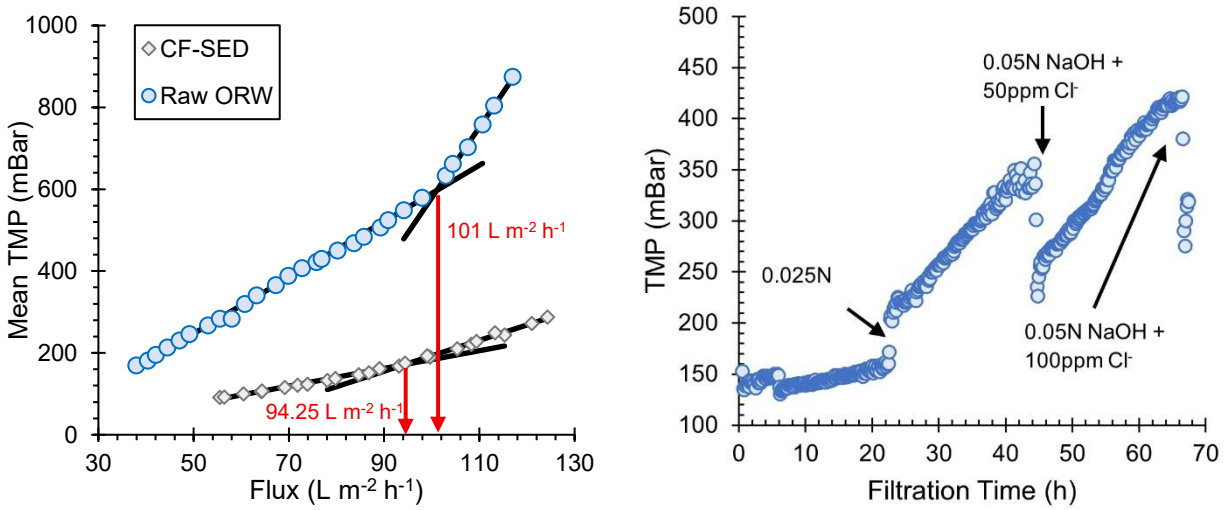
Preliminary critical flux testing was performed following the approach of Le Clech et al. (2003). Briefly, the flux was increased by 3 L m^{-2} h^{-1} (i.e., the step height) every 15 min (i.e., the step length). The values for the step height and length were selected based on guidance provided by a number of studies to impart the minimal impact on the final critical flux value (Bacchin et al. 2006; Beier and Jonsson 2010; Field et al. 1995; Howell 1995).

Critical flux values were determined using the approach proposed by Choi and Dempsey (2005), which has been shown to be simpler and more reproducible than alternative methods. In this analysis, the mean transmembrane pressure (TMP) is plotted against the mean permeate flux for each flux step. Two distinct linear regions are typically observed: a lower-flux region characterized by a relatively shallow slope and a higher-flux region exhibiting a steeper slope. The intersection of these two regressions is defined as the critical flux value. Based on prior experience with the bench-scale LPM system, mean TMP and flux values for each step were calculated using data from the final minute of the step to ensure that the filtration pump voltage had stabilized.

The subcritical and supercritical regions were fitted using Excel's Data Analysis toolpack, and the significance of each regression was evaluated using the analysis of variance (ANOVA) *p*-value. A summary of the fitted models and goodness-of-fit statistics is provided in Table E.1. The

critical flux values were determined to be 94.25 L m^{-2} h^{-1} for the CF-SED pretreated water and approximately 101 L m^{-2} h^{-1} for raw Ottawa River water (ORW). Although pretreatment would generally be expected to increase critical flux relative to direct filtration, the CF-SED water exhibited a slightly lower critical flux than the raw ORW. To avoid operation within the supercritical regime and minimize unrealistic fouling development, an operating flux of 80 L m^{-2} h^{-1} was selected for all experiments.

A preliminary cleaning study was also performed using raw ORW to identify the most effective cleaning chemistry for the membrane-water combination employed in this work. The results are presented in Fig. E.2b. Membrane operation followed the procedure described in Section 4.3.4, however, the cleaning chemical and/or its concentration were varied between tests to evaluate permeability recovery. Because organic matter was identified as the primary foulant, caustic (NaOH) and oxidizing (sodium hypochlorite) cleaning agents were investigated. Among the tested conditions, a combined solution of 0.05 N NaOH + 50 mg-Cl^- L^{-1} achieved the highest permeability recovery. Accordingly, this cleaning protocol was adopted for all experiments.



(a) **(b)**

Fig. E.2. Preliminary testing: **(a)** Critical flux determination; **(b)** Chemically enhanced backwash optimization.

Table E.1. Fitted Models from Critical Flux Testing

Model	Slope (mBar m^2 h L^{-1})	Intercept (mBar)	R^2	*p*-Value
	Raw ORW			
Sub-Critical	6.85	-95.36	0.9969	<.0001
Super-Critical	17.15	-1135.06	0.9953	0.0001
	CF-SED			
Sub-Critical	2.17	-33.00	0.9889	<.0001
Super-Critical	3.77	-183.65	0.9818	<.0001

E.3. Membrane Fouling Rate Calculation

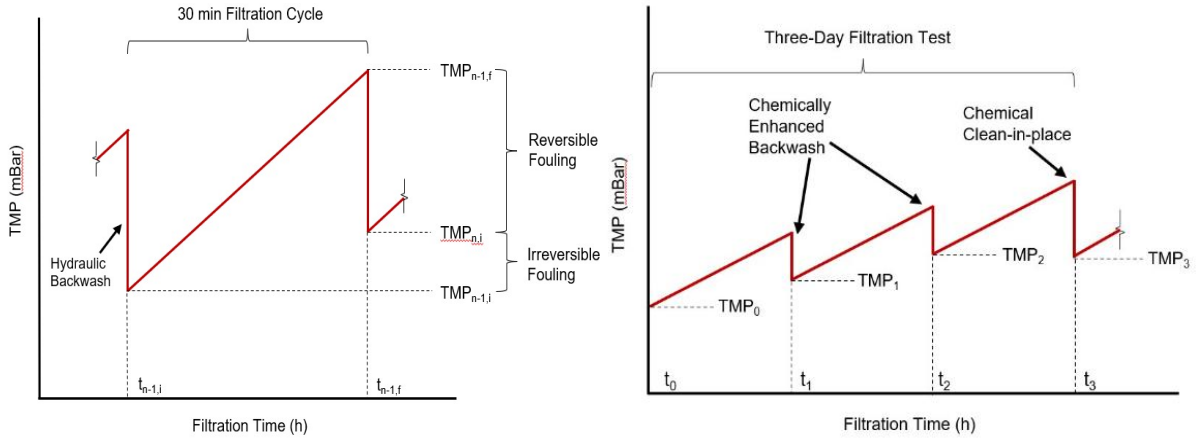
Fig. E.3. below provides a graphical overview of the calculation of the various fouling rates used in this study. The corresponding equations for each fouling rate are presented at the top of the figure. Definition of the variables used to calculate the hydraulically reversible and hydraulically irreversible fouling rates (i.e., FR_{hr} FR_{hirr}, respectively) are provided in Fig. E.3a while the variables and methodologies used for calculating chemically irreversible fouling rates (i.e., FR_{CEB} and FR_{CIP}) are illustrated in Fig. E.3b.

$$FR_{hr} = \frac{TMP_{n-1,f} - TMP_{n,i}}{t_{n-1,f} - t_{n-1,i}}$$

$$FR_{hirr} = \frac{TMP_{n,i} - TMP_{n-1,i}}{t_{n-1,f} - t_{n-1,i}}$$

$$FR_{CEB} = \frac{TMP_k - TMP_{k-1}}{t_k - t_{k-1}}$$

$$FR_{CIP} = \frac{TMP_3 - TMP_0}{t_3}$$



(**a**) (**b**)

Fig. E.3. Fouling rate computation: **(a)** Individual filtration cycle reversible and irreversible fouling rate; **(b)** Chemically irreversible fouling rates.

E.4. Supplemental Fouling Data

In Fig. E.4 the relationship between the specific ultraviolet absorbance at 254 nm (SUVA) and the hydraulically irreversible fouling rate (FR_{hirr}) is shown. As can be seen from this figure, there is no observable correlation between the SUVA and FR_{hirr}. This is in contrast to the findings of our previous study (see Chapter 3) which used identical test conditions and pretreated waters, but a different membrane type, highlighting the impact of membrane material/configuration on LPM performance.

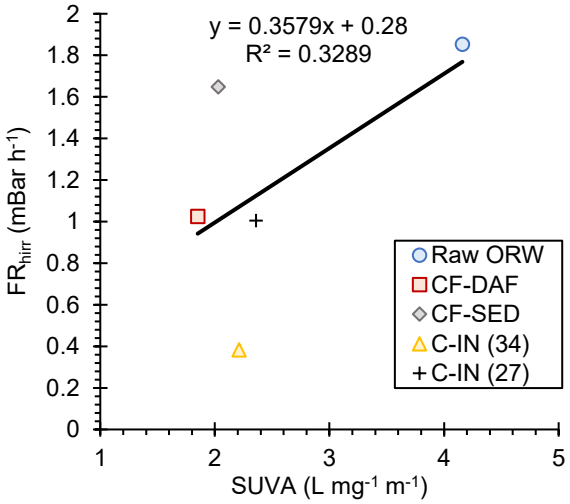


Fig. E.4. Relationship between FR_{hirr} and SUVA for winter season

Table E.2 below presents the total, hydraulically reversible, hydraulically irreversible, and chemically irreversible fouling rates for the TMC membranes and all pre-treated waters. It should be noted the data in this table is the average data for the replicated filtration tests.

Table E.2. TMC Membrane Fouling Rates.

Parameter	Raw ORW	CF-DAF	CF-SED	C-IN (34 mg L^{-1})		C-IN (27 mg L^{-1})	
	Winter	Winter	Winter	Winter	Summer	Winter	Summer
FR_{hr} (mBar h^{-1})	35.1 ± 1.12	9.77 ± 0.50	8.50 ± 0.44	12.5 ± 1.0	11.7 ± 0.51	9.23 ± 0.53	16.8 ± 0.82
FR_{hirr} (mBar h^{-1})	1.85 ± 0.51	1.03 ± 0.38	1.65 ± 0.43	0.46 ± 0.27	0.28 ± 0.43	1.0 ± 0.59	0.25 ± 0.41
FR_{TOT} (mBar h^{-1})	37 ± 1.15	10.8 ± 0.61	10.2 ± 0.55	13 ± 1.02	11.9 ± 0.56	10.2 ± 0.71	17.1 ± 0.84
FR_{CEB} (mBar h^{-1})	0.474	0.615	0.481	0.014	0.256	0.516	0.132
FR_{CIP} (mBar h^{-1})	0.880	0.815	0.420	0.027	0.190	0.683	0.119

Note: ± represents the 95% confidence interval calculated using the students t-test as $\mu \pm t_{0.025,n}\frac{s}{\sqrt{n}}$

E.5. References

Bacchin, P., P. Aimar, and R. W. Field. 2006. "Critical and sustainable fluxes: Theory, experiments and applications." *Journal of Membrane Science*, 281 (1–2): 42–69. https://doi.org/10.1016/j.memsci.2006.04.014.

Beier, S. P., and G. Jonsson. 2010. "Critical Flux Determination by Flux-Stepping." *AIChE Journal*, 56 (7): 1739–1747.

Choi, K. Y. J., and B. A. Dempsey. 2005. "Bench-scale evaluation of critical flux and TMP in low-pressure membrane filtration." *Journal AWWA*, 97 (7): 134–143.

Field, R. W., D. Wu, J. A. Howell, and B. B. Gupta. 1995. "Critical flux concept for microfiltration fouling." *Journal of Membrane Science*, 100 (3): 259–272. https://doi.org/10.1016/0376-7388(94)00265-Z.

Heijnen, M., R. Winkler, and P. Berg. 2012. "Optimisation of the geometry of a polymeric Multibore® ultrafiltration membrane and its operational advantages over standard single bore fibres." *Desalination and Water Treatment*, 42 (1–3): 24–29. https://doi.org/10.1080/19443994.2012.682968.

Howell, J. A. 1995. "Sub-critical flux operation of microfiltration." *Journal of Membrane Science*, 107 (1–2): 165–171. https://doi.org/10.1016/0376-7388(95)00114-R.

Le Clech, P., B. Jefferson, I. S. Chang, and S. J. Judd. 2003. "Critical flux determination by the flux-step method in a submerged membrane bioreactor." *Journal of Membrane Science*, 227 (1–2): 81–93. https://doi.org/10.1016/j.memsci.2003.07.021.

APPENDIX F

Supplemental Information for Chapter 5

Context: This appendix presents supporting information associated with Chapter 5 of this thesis, *Characterizing the Impact of Geometry on the Performance of Inline-Coagulation Pretreatment Systems with Helical Flocculators*.

List of Abbreviations

BSA	Bovine serum albumin
DI	Deionised water
DOC	Dissolved organic carbon
DW	Distilled water
ECD	Equivalent circular diameter
FFD	Full-factorial design
G	Mean velocity gradient
HA	Humic acid
HCTF	Helically coiled tube flocculator
HRT	Hydraulic retention time
PSE	Pseudo-standard error
SA	Sodium alginate
SUVA	Specific ultraviolet absorbance at 254nm

List of Variables

Variable	Description
τ	HCTF torsion (mm^{-1})
β_0	HCTF torsion parameter (dimensionless)
γ	Dimensionless helical coil pitch
δ_{nd}	Dimensionless curvature of HCTF
ΔP	Pressure differential across mixer (Pa)
ϑ	Theoretical hydraulic detention time (s)
λ	HCTF torsion/curvature ratio (dimensionless)
μ	Dynamic viscosity of the solution ($\frac{kg}{m \cdot s}$)
τ	HCTF torsion (mm^{-1})
τ_{nd}	Dimensionless HCTF torsion
b_{ps}	HCTF helical pitch slope ($mm\ rad^{-1}$)
c_R	HCTF curvature ratio (dimensionless)
D_p	Perimeter-based fractal dimension (dimensionless)

H_0	Null hypothesis
H_1	Alternate hypothesis
h_L	Mixer headloss (m)
L	HCTF pipe length (mm)
p	HCTF coil pitch (mm)
r_c	HCTF helical coil radius (mm)
r_p	HCTF pipe radius (mm)
S^2_{Center}	Sample variance of factorial design center points
S^2_{Corner}	Sample variance of factorial design corner points
t_0	Test statistic for Student's t-test
$\overline{y_{Center}}$	Mean response of tests conducted at the center point of the factorial design (varies)
$\overline{y_{Corner}}$	Mean response of tests conducted at the factorial design corner points (varies)

F.1. Additional Methodological Details

F.1.1. Preparation of Stock Model Organics

Bovine Serum Albumin (BSA) was found to be readily dissolvable in deionised water (DI) (ZenoPure Quatra 90LC, Zenon Environmental Inc., Burlington, ON). Accordingly, 0.5 g BSA was transferred to a half-full volumetric flask using a glass weighing scoop (SL000922, StonyLab, Nesconset, NY), the flask was swirled to dissolve the BSA and then brought to volume using DI. The stock solution of humic acid (HA) was prepared by initially dissolving 0.5 g of HA in 100 mL of 0.025 M NaOH using a 250 mL Erlenmeyer flask (Pyrex Conical Flask, Corning, NY) with vigorous mixing by magnetic stir bar as recommended by others (Maeng et al. 2017; Yang et al. 2021). Following several hours of stirring, the solution (and rinsate) was transferred to a 1 L volumetric flask (Lifetime-Red 5660 Class-A, Corning, NY) and brought to volume using DI. The sodium alginate (SA) solution was prepared by dissolving 0.5 g of the model organic initially into 250 mL of DI in a 400 mL griffin beaker (1000400, Corning, NY). As SA is difficult to completely dissolve, a variable speed mixer (OS-200D-C-SYS, Cole Parmer, Quebec, QC) set to 1,100 rpm was used to induce a vortex in the beaker prior to the addition of the powdered SA at a point near the impeller shaft. After vigorous mixing for at least 2 h, the solution (and rinsate) was transferred

to a 1 L volumetric flask (Lifetime-Red 5660 Class-A, Corning, NY) and brought to volume. All stock solutions were magnetically stirred for a period of 24 h (VWR Advance Stirrer, VWR, Mississauga, ON, Canada) prior to being filtered through a 0.45 µm membrane (Supor 47 mm, 60043, Pall, NY) to remove residual insoluble matter. Filtered solutions were placed in sterilized (SR-24B, Consolidated Sterilizer Systems, Billerica, MA) glass 1 L volumetric flasks and stored in the dark at 4 °C prior to use. Stock solutions were stirred and brought to room temperature prior to the preparation of all working solutions.

F.1.2. Preparation of Synthetic Water

Synthetic water was prepared using the large baffled completely mixed reactor developed by Gonzalez-Galvis and Narbaitz (2020, 2022). Initially, the reactor, its baffle insert, and the impeller were rinsed thoroughly with distilled water (DW). The baffle insert and the impeller (10 cm x 10 cm stainless steel) were placed inside the reactor and the assembly placed on a high-resolution industrial balance (Model 3807MP8-1, Sartorius Gottingen, Germany). Then, the reactor was filled with a measured amount of DW which has been passed through a five-stage commercial reverse osmosis-activated carbon system (TGI-525 NO. 92821, TGI Pure Water Systems, Brea, CA). Pre-calculated volumes of stock model organic compounds were measured using mechanical pipettors (High Performance Pipettor, VWR, Mississauga, ON, Canada) and/or volumetric flasks (Class A, Corning, New York, NY) and added to the reactor. Next, the inorganic background components including kaolin clay (~5 mg L^{-1}, corresponding to a turbidity of 5.5 NTU, Laboratory Grade 75185, Fisher Scientific, Hampton, NH), calcium chloride (0.6mM, Dried Powder 97%, Thermo Scientific, Hampton, NH), and sodium bicarbonate (0.9 mM, Certified ACS, Fisher Scientific, Hampton, NH) were added to the reactor and it was brought to the desired volume. The reactor was then inserted into its frame and the motor (Stir-Pak high torque, low-speed mixer 50007-12, Cole Parmer, Quebec, QC, Canada) put in place. The motor was set to its top speed (setting 10 on the speed controller, which is approximately a G value of 296 s^{-1}) to provide intense mixing of the contents of the reactor. The batches of synthetic water were thoroughly mixed in this system for a period of more than 2 h.

F.1.3. HRT Determination of Tested Helically Coiled Tube Flocculators (HCTFs)

The flowrate used in the majority of this study was 5 mL min^{-1}, which was selected to simulate conditions typical of bench-scale low-pressure membrane tests. A sample calculation estimating the mean hydraulic residence time (HRT) of the 1000 mm length HCTF with 3.175 mm pipe diameter is provided below.

$$holdup\ vol. = \pi L {r_p}^2$$

Where: L is the HCTF pipe length, cm

r_p is the HCTF pipe diameter, cm

$$holdup\ vol. = \pi(100\ cm)(0.15875\ cm)^2 = 7.92\ cm^3$$

$$Residence\ Time = \frac{holdup\ vol.}{Flowrate}$$

$$Residence\ Time = \frac{7.92\ cm^3}{\frac{5\ mL}{min} \times \frac{cm^3}{mL}} \cong 1.6\ min$$

HRT values for other HCTF configurations operated at 5 mL min^{-1} are computed similarly and are presented in Table F.1 below. Note for the full factorial design, only pipes of 3.175 mm were considered, while for the preliminary screening study pipe diameters of 4.7625 mm and 6.35 mm were also investigated.

Table F.1. HRT Values for Different HCTF Geometries.

HRT (min)	Pipe Length (mm)		
Pipe Diameter (mm)	1000	1500	2000
3.175	1.60	2.4	3.2
4.7625	3.56	5.34	7.12
6.35	6.33	9.5	12.66

F.1.4. Jar Test Results for Challenge Water

To select a coagulant type for the synthetic water used in this study, preliminary jar testing was conducted using both aluminum- and iron-based coagulants. The tested coagulants were provided

courtesy of Kemira Water Solutions Canada Inc. and include alum (ALS), polyaluminum chloride (PAX-XL8), ferric sulfate (PIX-312), aluminum chlorohydrate (PAX-XL1900), and alufer (ALS-3330). The ALS-3330 product contains a blend of ferric and aluminum sulfates at a mass ratio of 25% ferric to 75% aluminum. A summary of the principal characteristics of the different coagulants tested is provided in Table F.2 below.

Table F.2. Coagulant Technical Data

Product Name	Specific Gravity	Aluminum or Iron (%)	Basicity (%)
ALS	1.32	4.3	N/A
ALS-3330 (Alufer)	1.38	3-3.5 (Al) 2.4-3.6 (Fe)	N/A
PAX-XL8 (PACl)	1.2-1.28	5.2-5.8	65-75
PAX-XL1900 (ACH)	1.32-1.35	12.1-12.7	82.4-84.2
PIX-312 (Ferric Sulfate)	1.51-1.58	12-12.7	N/A

Several studies have noted that pre-coagulation using conditions that yield circumneutral zeta potential values is an effective strategy to reduce membrane fouling (Maeng et al. 2017; Wang et al. 2013). Accordingly, in this jar test study, the efficiency of each coagulant type with this synthetic water was assessed in terms of the zeta potential reduction. Samples of coagulated water were collected immediately following rapid mixing and analyzed for zeta potential using a zetasizer nano particle analyzer (Nano ZS Series Model ZEN 3600, Malvern Instruments Ltd., Worcestershire, UK) with a folded capillary cell (DTS1060/1070, Malvern Instruments Ltd., Worcestershire, UK). The variation in zeta potential as a function of applied coagulant dose (reported as metal) is shown in Fig. F.1.

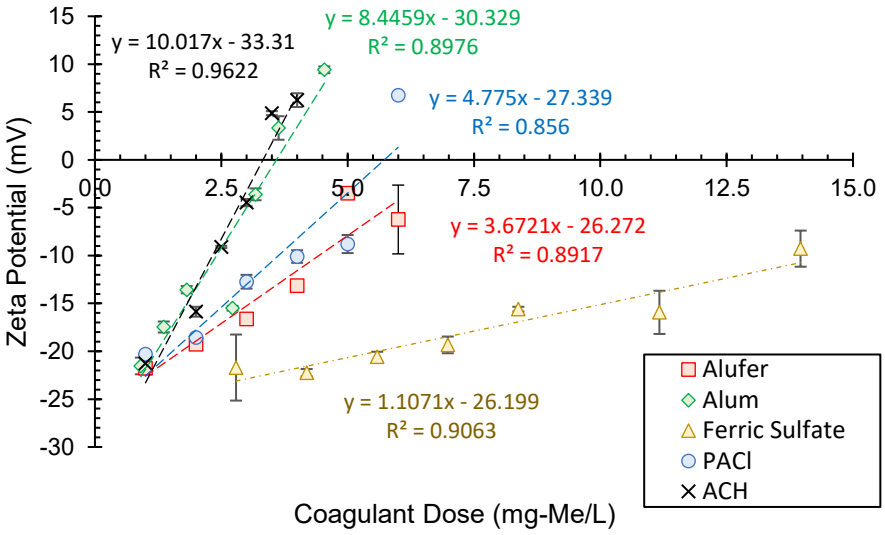


Fig. F.1. Efficiency of alum compared to alternative coagulant types for synthetic challenge water.

As alum, which is a lower-cost coagulant, performed similarly to the pre-polymerized ACH coagulant, it was selected for further investigation. Additional jar testing was performed to identify the optimal conditions, in terms of dissolved organic carbon (DOC) removal, to use in the preliminary screening study. Fig. F.2 below presents the removal of DOC as a function of the alum dose and coagulated pH, where it can be seen that the removals are maximized near a dose of 3 mg-Al L^{-1} and a pH of 6. The DOC removals were consistently high and exceeded that which would be expected for a natural water with a similar specific UV absorbance at 254 nm (SUVA) value (Edzwald and Tobiason 1999), indicating that this synthetic water is not fully representative of the behaviour of natural waters. This observation is consistent with the findings Kim and Dempsey (2013), who reported important differences in the chemical composition and molecular weight distribution between natural waters and their surrogate organic compounds, which resulted in altered membrane fouling behaviour.

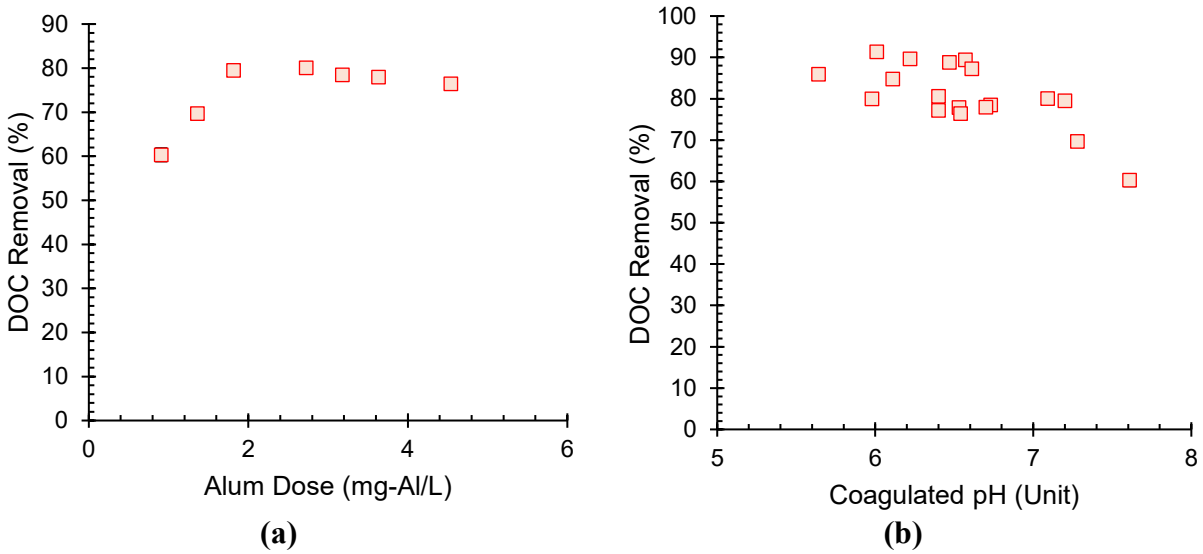


Fig. F.2. Removal of DOC by alum coagulant with varying: **(a)** Dose as aluminum; **(b)** Coagulated pH.

F.2. Preliminary Screening Study

As part of a sequential experimentation strategy, an unreplicated fractional factorial design of resolution IV was initially performed to screen among six different coagulation chemistry and HCTF geometry factors to identify which (if any) had the largest effects on the response variables, namely the floc equivalent circular diameter (ECD), floc concentration, and floc fractal dimension. The selection of a resolution IV design permits efficient estimation of the main effects of the six individual factors (using only 16 tests) as they are only confounded with three-factor or higher interactions, which are almost always negligible in magnitude. Those factors which had the greatest effect were subsequently investigated more thoroughly in the 2^3 full-factorial design.

F.2.1. Factorial Design and Alias Structure

A one quarter fraction of the general 2^k design, denoted as 2^{k-2}, can be constructed by first writing down the basic full-factorial design for $k-2$ factors and then adding two additional columns based on generators chosen from interactions involving the first $k-2$ factors (Myers et al. 2016). The generators (words) for the one quarter fraction 2_{IV}^{6-2} screening design are $x_5 = x_1x_2x_3$ and $x_6 = x_2x_3x_4$. The defining relation for the design is the set of all columns which is equal to the identity matrix and can be determined using the generators:

$$x_5 \cdot x_5 = x_1x_2x_3 \cdot x_5$$

$$I = x_1x_2x_3x_5$$

Similarly, $I = x_2x_3x_4x_6$. From the product of the two generators, we also have the following:

$$I = x_1x_2x_3x_5 \cdot x_2x_3x_4x_6$$

$$I = x_1x_4x_5x_6$$

$$\therefore I = x_1x_4x_5x_6 = x_1x_2x_3x_5 = x_2x_3x_4x_6$$

It can be noted here that the resolution of the design (i.e., IV) is equal to the number of letters in the shortest word. As aforementioned, the design is constructed by first writing out the basic design for a full 2^4 two-level factorial design with 16 runs. The columns x_5 and x_6 are added in what is termed the calculation matrix by multiplying the coded factor settings (i.e., high- and

low-level factor settings) from the generator term. A sample calculation is provided below for the first row of x_5 in Table F.3:

$$x_5 = x_1 x_2 x_3$$

$$x_5 = (-1)(-1)(-1) = (-1)$$

Table F.3. Treatment Combinations for 2_{IV}^{6-2} Screening Design.

x_0	x_1	x_2	x_3	x_4	$x_5 = x_1x_2x_3$	$x_6 = x_2x_3x_4$	Treatment
(+1)	(–1)	(–1)	(–1)	(–1)	(–1)	(–1)	
(+1)	(+1)	(–1)	(–1)	(–1)	(+1)	(–1)	x_1x_5
(+1)	(–1)	(+1)	(–1)	(–1)	(+1)	(+1)	$x_2x_5x_6$
(+1)	(+1)	(+1)	(–1)	(–1)	(–1)	(+1)	$x_1x_2x_6$
(+1)	(–1)	(–1)	(+1)	(–1)	(+1)	(+1)	$x_2x_5x_6$
(+1)	(+1)	(–1)	(+1)	(–1)	(–1)	(+1)	$x_1x_3x_6$
(+1)	(–1)	(+1)	(+1)	(–1)	(–1)	(–1)	x_2x_3
(+1)	(+1)	(+1)	(+1)	(–1)	(+1)	(–1)	$x_1x_2x_3x_5$
(+1)	(–1)	(–1)	(–1)	(+1)	(–1)	(+1)	x_4x_6
(+1)	(+1)	(–1)	(–1)	(+1)	(+1)	(+1)	$x_1x_4x_5x_6$
(+1)	(–1)	(+1)	(–1)	(+1)	(+1)	(–1)	$x_2x_4x_5$
(+1)	(+1)	(+1)	(–1)	(+1)	(–1)	(–1)	$x_1x_2x_4$
(+1)	(–1)	(–1)	(+1)	(+1)	(+1)	(–1)	$x_3x_4x_5$
(+1)	(+1)	(–1)	(+1)	(+1)	(–1)	(–1)	$x_1x_3x_4$
(+1)	(–1)	(+1)	(+1)	(+1)	(–1)	(+1)	$x_2x_3x_4x_6$
(+1)	(+1)	(+1)	(+1)	(+1)	(+1)	(+1)	$x_1x_2x_3x_4x_5x_6$

It should be noted that the treatment combinations presented in Table F.3 are in standard order, which differs from the randomized order that the experiments were conducted to eliminate the possibility for interferences by unknown systematic or happenstance errors.

The alias or confounding pattern of the design can be obtained by multiplying the effects by each word of the defining relation. A sample calculation is shown below for first, second, and third order effects while a summary of all the aliasing relationships is presented in Table F.4.

For the Main Effect x_1:

$$I = x_1x_2x_3x_5 = x_2x_3x_4x_6 = x_1x_4x_5x_6$$

$$x_1 \cdot I = x_1 \cdot x_1x_2x_3x_5 = x_1 \cdot x_2x_3x_4x_6 = x_1 \cdot x_1x_4x_5x_6$$

$$x_1 = x_2x_3x_5 = x_1x_2x_3x_4x_6 = x_4x_5x_6$$

For the Interaction Effect x_1x_2:

$$I = x_1x_2x_3x_5 = x_2x_3x_4x_6 = x_1x_4x_5x_6$$

$$x_1x_2 \cdot I = x_1x_2 \cdot x_1x_2x_3x_5 = x_1x_2 \cdot x_2x_3x_4x_6 = x_1x_2 \cdot x_1x_4x_5x_6$$

$$x_1x_2 = x_3x_5 = x_1x_3x_4x_6 = x_2x_4x_5x_6$$

For the Interaction Effect $x_1x_2x_3$:

$$I = x_1x_2x_3x_5 = x_2x_3x_4x_6 = x_1x_4x_5x_6$$

$$x_1x_2x_3 \cdot I = x_1x_2x_3 \cdot x_1x_2x_3x_5 = x_1x_2x_3 \cdot x_2x_3x_4x_6 = x_1x_2x_3 \cdot x_1x_4x_5x_6$$

$$x_1x_2x_3 = x_5 = x_1x_4x_6 = x_2x_3x_4x_5x_6$$

Table F.4. Alias Structure for Screening Design

Main Effects	Two Factor Interactions
$x_1 = x_2x_3x_5 = x_1x_2x_3x_4x_6 = x_4x_5x_6$	$x_1x_2 = x_3x_5 = x_1x_3x_4x_6 = x_2x_4x_5x_6$
$x_2 = x_1x_3x_5 = x_3x_4x_6 = x_1x_2x_4x_5x_6$	$x_1x_3 = x_2x_5 = x_1x_2x_4x_6 = x_3x_4x_5x_6$
$x_3 = x_1x_2x_5 = x_2x_4x_6 = x_1x_3x_4x_5x_6$	$x_1x_4 = x_5x_6 = x_2x_3x_4x_5 = x_1x_2x_3x_6$
$x_4 = x_2x_3x_6 = x_1x_5x_6 = x_1x_2x_3x_4x_5$	$x_1x_5 = x_2x_3 = x_4x_6 = x_1x_2x_3x_4x_5x_6$
$x_5 = x_1x_2x_3 = x_1x_4x_6 = x_2x_3x_4x_5x_6$	$x_1x_6 = x_4x_5 = x_2x_3x_5x_6 = x_1x_2x_3x_4$
$x_6 = x_2x_3x_4 = x_1x_4x_5 = x_1x_2x_3x_5x_6$	$x_2x_4 = x_3x_6 = x_1x_3x_4x_5 = x_1x_2x_5x_6$
	$x_2x_6 = x_3x_4 = x_1x_3x_5x_6 = x_1x_2x_4x_5$
Three Factor Interactions	
$x_1x_2x_4 = x_3x_4x_5 = x_1x_3x_6 = x_2x_5x_6$	$x_1x_3x_4 = x_2x_4x_5 = x_1x_2x_6 = x_3x_5x_6$

F.2.2. Experimental Factors for Screening Design

The selection of factor settings for the HCTF geometrical parameters was already described in the manuscript. Measures of coagulation chemistry, including the coagulant dose (x_1) and coagulated pH (x_6), were also considered as factors due to the strong influence they are known to exert on properties of the formed flocs (Li et al. 2006; Tambo 1979). The high factor setting of the coagulant dose was set to the optimum for DOC removal based on the results of preliminary jar testing (see Section F.1.4), while the low factor setting was specified as a 20% reduced dose, which has been

reported by some authors to lead to the lowest permeability decline in inline coagulation pretreatment systems (Konieczny et al. 2009). The high and low factor settings for coagulation pH were selected based on the aluminum coagulation domain presented by Amirtharajah and Mills (1982) as well as the humic and fulvic acid removal domains presented by Edwards and Amirtharajah (1985) and Hundt and O'Melia (1988), respectively. A summary of the factor settings for the preliminary screening study is presented in Table F.5.

Table F.5. Controlled Factor Level Settings for Preliminary Screening Design

		Levels	
Factors	**Unit**	**(-1)**	**(+1)**
x_1: Coagulant Dose	mg-Al L^{-1}	2.4	3
x_2: Coil Pitch	(mm)	15	45
x_3: Pipe Length	(mm)	1000	2000
x_4: Coil Diameter	(mm)	50	100
x_5: Pipe Diameter	(mm)	3.175 (1/8")	6.35 (1/4")
x_6: Coagulation pH	Unit	6	7

F.2.3. Results of Preliminary Screening Study

Table F.6 - Table F.8 below present the results of the screening study. Statistical analysis was performed using JMP® Pro 18 software (SAS Institute Inc., Cary, NC). Because the screening study is an unreplicated design, the software uses the method proposed by Lenth (1989) where the t-statistic for the Students *t*-test is calculated by dividing the parameter estimate by the Lenth pseudo-standard error (PSE). A Students *t*-test is then performed to determine the "pseudo" *p*-value for the parameter effect, with a threshold *p*-value ~0.2-0.25 considered for factor screening. The calculation of the Lenth PSE was performed according to Montgomery (2020). From Table F.6 below, no effects were significant according to the criteria set out by JMP (i.e., $p > 0.25$), however, the coagulant dose and pH were found to have the greatest effect on ECD as they had the smallest *p*-values.

Table F.6. Factor Screening Results for ECD

Parameter	**Estimate**	**Pseudo t-Ratio**	***p*-Value**
Intercept	44.4869	14.7014	<.0001
x_1: Dose	3.3692	1.1134	0.3162

x_2: Pitch	1.8138	0.5994	0.575
x_3: Length	-2.001	-0.6612	0.5377
x_4: Coil Diameter	2.2043	0.7284	0.499
x_5: Pipe Diameter	-2.0959	-0.6926	0.5194
x_6: pH	-3.5957	-1.1882	0.2881
Dose*Pitch	-0.8378	-0.2769	0.793
Dose*Length	1.8887	0.6242	0.5599
Dose*Coil Diameter	2.0174	0.6667	0.5345
Dose*Pipe Diameter	-2.9306	-0.9685	0.3773
Dose*pH	-1.3507	-0.4464	0.674
Pitch*Coil Diameter	-3.1201	-1.0311	0.3498
Pitch*pH	2.1401	0.7072	0.511
Dose*Pitch*Coil Diameter	-1.9266	-0.6367	0.5523
Dose*Length*Coil Diameter	-0.9266	-0.3062	0.7718

In Table F.7, the pipe length and the interaction between the coagulant dose and coil pitch were found to have the most significant effects on the floc D_p, (i.e., $p < 0.2$).

Table F.7. Factor Screening Results for D_p

Parameter	Estimate	Pseudo t-Ratio	*p*-Value
Intercept	1.6139	361.9101	<.0001
x_1: Dose	-0.00332	-0.7453	0.4896
x_2: Pitch	-0.00122	-0.273	0.7958
x_3: Length	0.00741	1.6614	0.1575
x_4: Coil Diameter	0.00564	1.2658	0.2614
x_5: Pipe Diameter	0.00086	0.1926	0.8548
x_6: pH	0.00265	0.5932	0.5789
Dose*Pitch	0.00724	1.6243	0.1652
Dose*Length	-0.00297	-0.6667	0.5345
Dose*Coil Diameter	0.00623	1.3976	0.2211
Dose*Pipe Diameter	-0.0026	-0.5836	0.5848
Dose*pH	0.0016	0.3584	0.7347
Pitch*Coil Diameter	0.00356	0.7981	0.461
Pitch*pH	-0.00537	-1.2033	0.2827
Dose*Pitch*Coil Diameter	0.00059	0.1327	0.8996
Dose*Length*Coil Diameter	-0.00244	-0.5464	0.6083

From Table F.8, the effects of the coil pitch, the pH, as well as the interaction between the coagulant dose and coil diameter were found to have the greatest significance on the floc concentration (i.e., $p < 0.25$).

Table F.8. Factor Screening Results for Floc Concentration

Parameter	Estimate	Pseudo t-Ratio	*p*-Value
Intercept	16451.7	10.6645	0.0001
x_1: Dose	153.7	0.0997	0.9245
x_2: Pitch	-2221.2	-1.4398	0.2095
x_3: Length	-773.2	-0.5012	0.6375
x_4: Coil Diameter	1049.6	0.6804	0.5265
x_5: Pipe Diameter	1588.7	1.0298	0.3503
x_6: pH	-3189.4	-2.0675	0.0935
Dose*Pitch	161.6	0.1048	0.9206
Dose*Length	-783.6	-0.5079	0.6331
Dose*Coil Diameter	-2153.8	-1.3961	0.2215
Dose*Pipe Diameter	588.3	0.3814	0.7186
Dose*pH	1177.3	0.7632	0.4798
Pitch*Coil Diameter	1028.4	0.6667	0.5345
Pitch*pH	1412.8	0.9158	0.4018
Dose*Pitch*Coil Diameter	546.6	0.3543	0.7376
Dose*Length*Coil Diameter	-105.4	-0.0683	0.9482

F.3. Estimation of Mean Velocity Gradient for Inline Static Mixer (ISM)

Due to privacy concerns related to product competitiveness, the manufacturer of the ISM does not make any data or formulas for calculating mixing quality/efficiency openly available. As a result, the mean velocity gradient (G) was estimated using Eqn. F.1 below (Crittenden et al. 2012):

$$G = \sqrt{\frac{\rho g h_L}{\mu \vartheta}} \tag{F.1}$$

where G is the mean velocity gradient (s^{-1}), h_L is the measured headloss across the mixer (m), μ is the dynamic viscosity of the solution, which for dilute streams at 20 °C is approximately $1.002 \times 10^{-3} \frac{kg}{m \cdot s}$, and ϑ is the hydraulic detention time (s). The headloss across the mixer can be expressed in terms of the pressure differential, which simplifies the expression to:

$$G = \sqrt{\frac{\Delta P}{\mu \vartheta}} \tag{F.2}$$

Where ΔP is the measured pressure differential across the mixer (Pa) and all other terms have already been defined. In this study, the pressure differential across the mixer was evaluated by fitting a pair of pressure transducers (PX309-030AV, Omega Sensing Solution, St. Eustache, QC) to the mixer inlet and outlet in the bench-scale system. A LabView program (National Instruments,

Austin, TX) was developed to automatically log the pressure readings from each location and calculate the differential pressure value. For the flowrate of 5 mL min^{-1}, the average pressure differential across the ISM was found to be 103.42 Pa and the HRT was estimated to be 2.58 min. The HRT estimation was based on a gravimetric approach: the ISM was filled with DI, the mass of which was subsequently measured using an analytical balance (AJ150, Mettler Toledo, Columbus, OH). Using the temperature corrected density, the volume of DI was determined, and the mean HRT was calculated by dividing the storage volume by the system flowrate. Therefore:

$$G = \sqrt{\frac{103.42\ \frac{kg}{m \cdot s^2}}{1.002 \times 10^{-3} \frac{kg}{m \cdot s} \times 2.58\ min \times 60 s/min}}$$

$$G = 25.8\ s^{-1}$$

F.4. Additional Data for Full Factorial Design (FFD)

F.4.1. Randomized Run Order

To mitigate the risk of systematic bias or time-dependent trends in the results, the experiments for the full factorial design were carried out in a randomized order defined by Table F.9.

Table F.9. Randomized Run Order for 2^3 Full-Factorial Design

Pattern	Coil Diameter (mm)	Pipe Length (mm)	Coil Pitch (mm)
+ − +	75	1000	45
− + +	50	2000	45
+ + −	75	2000	15
0 0 0	62.5	1500	30
− − +	50	1000	45
− + −	50	2000	15
+ − −	75	1000	15
0 0 0	62.5	1500	30
+ + −	75	2000	15
+ − +	75	1000	45
− + +	50	2000	45
− − +	50	1000	45
+ + +	75	2000	45
0 0 0	62.5	1500	30
0 0 0	62.5	1500	30
− + −	50	2000	15
+ − −	75	1000	15
− − −	50	1000	15
0 0 0	62.5	1500	30
0 0 0	62.5	1500	30
+ + +	75	2000	45
− − −	50	1000	15

F.4.2. FFD Model Fitting and Adequacy Check

For a simple linear regression model, the errors at each value of the predictor should be normally distributed. Fig. F.3 shows the normal quantile plot of residuals, which plots the observed residual quantiles against a theoretical normal quantile distribution. If the variable is normally distributed, the normal quantile plot approximates a diagonal straight line. The graphs in Fig. F.3 show that the three response variables were normally distributed.

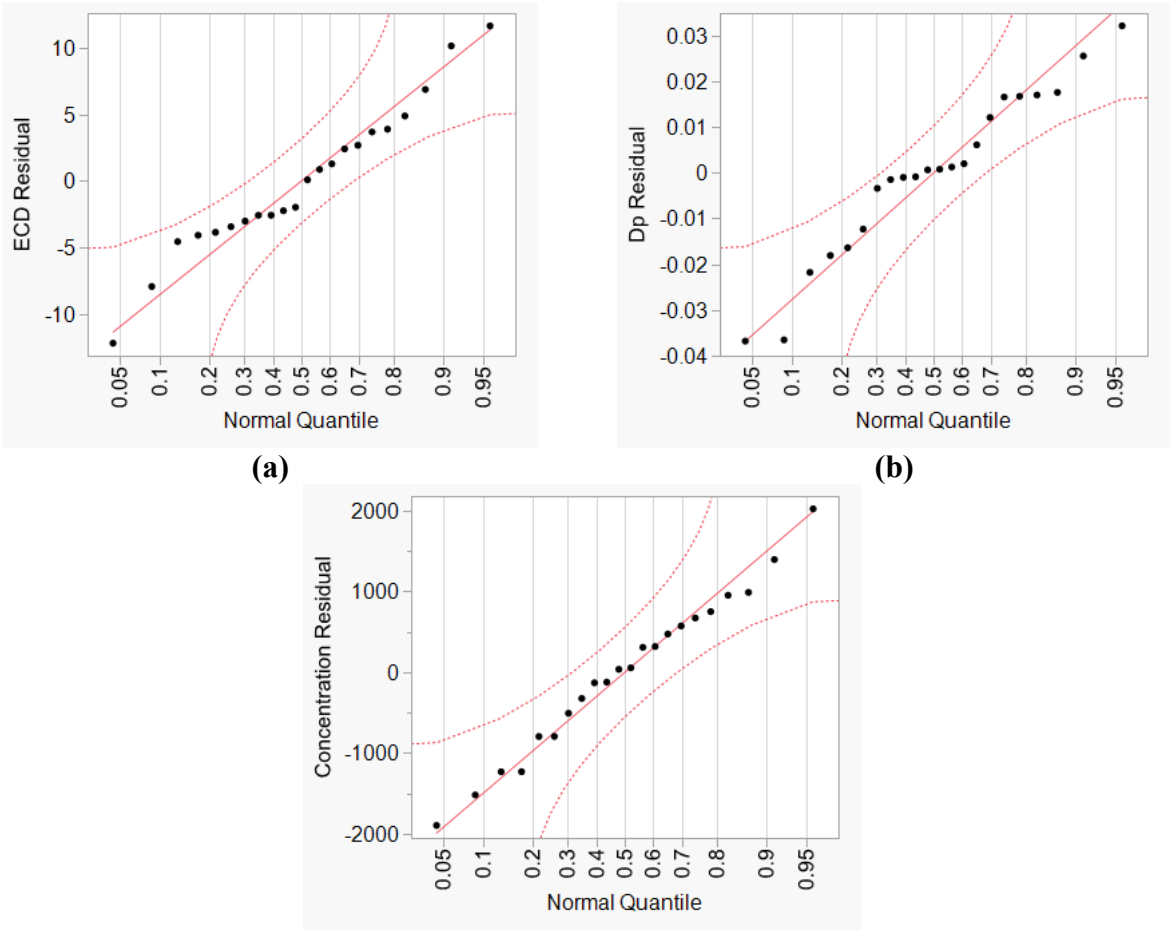


Fig. F.3. QQ plots for model residuals: **(a)** ECD; **(b)** D_p; **(c)** Concentration

F.4.3 Test for Model Curvature in FFD

To test for curvature, a *t*-test (assuming unequal variances) was performed comparing the mean of the replicated center points to the mean of the replicated corner points as proposed by Montgomery (2020).

The hypotheses are given by:

$$H_0: \mu_{Center} = \mu_{Corner}$$

$$H_1: \mu_{Center} \neq \mu_{Corner}$$

And the test statistic is given by:

$$t_0 = \frac{\overline{y_{Center}} - \overline{y_{Corner}}}{\sqrt{\frac{S^2_{Center}}{n_{center}} + \frac{S^2_{Corner}}{n_{corner}}}}$$

Using this approach, the test statistic and corresponding *p*-values can be computed for the three response variables considered in this study, namely, the ECD, D_p, and the floc concentration.

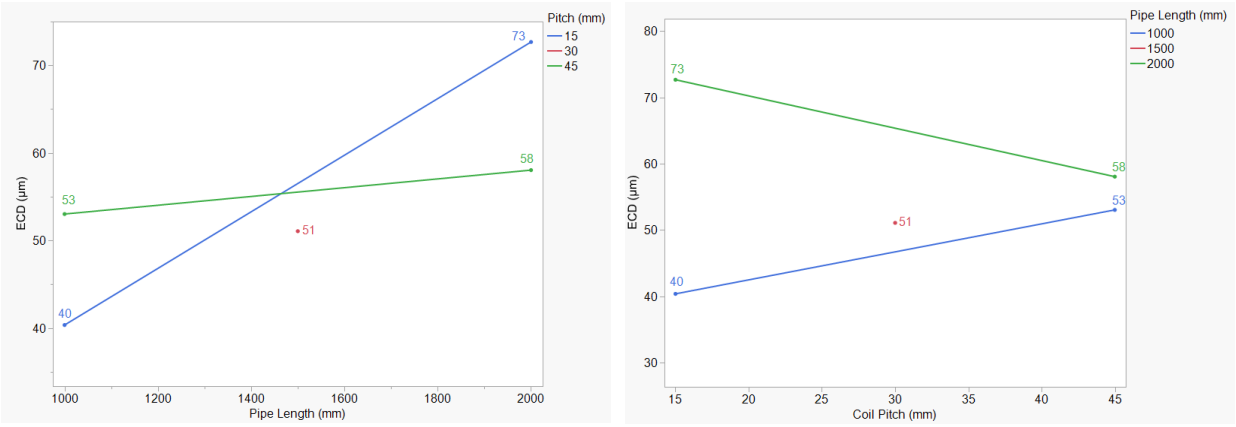
Table F.10. Students *t*-Test for Assessment of Response Function Curvature

Response Variable	$\overline{y_{Center}} - \overline{y_{Corner}}$	t_0	*p*-value
ECD	4.956	1.175886	0.2548
D_p	-0.01831	-1.5938	0.1284
Concentration	-1278.8	-1.4440	0.1659

Therefore, based on a significance level α=0.05, there is insufficient evidence ($p > 0.05$) to reject the null hypothesis for all three response variables. This finding suggests that the assumption of linearity by the factorial design holds and the first-order interaction model is adequate for modeling the factor effects.

F.4.4. Interaction Diagrams

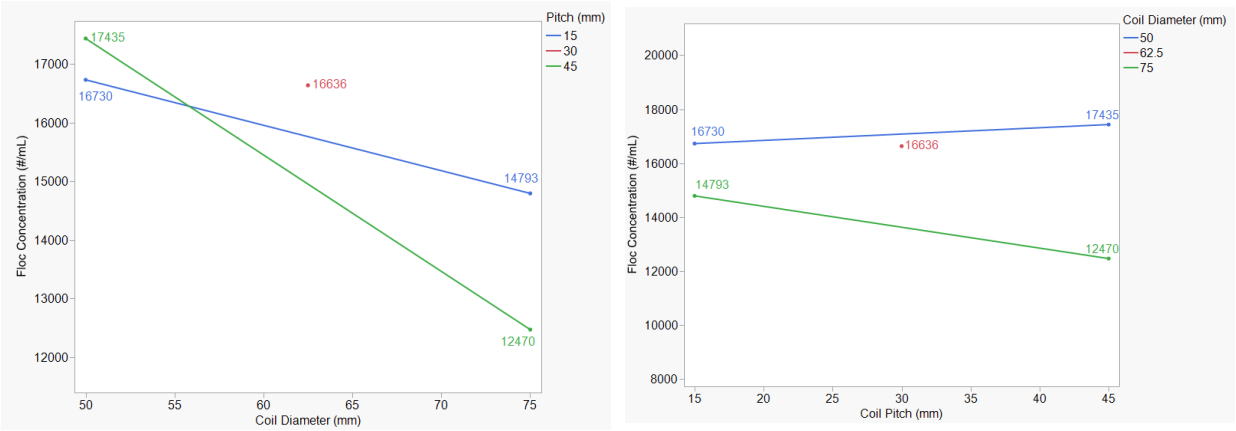
As part of the analysis of the full factorial design results, this section provides the interaction diagrams for select parameters and response variables. From Fig. F.4 below, the effect of coil pitch on ECD is seen to change depending on the setting of pipe length. For the short length HCTF, increasing coil pitch led to larger sized flocs whereas for the longer HCTF the floc size decreased with increasing coil pitch.



(a) **(b)**

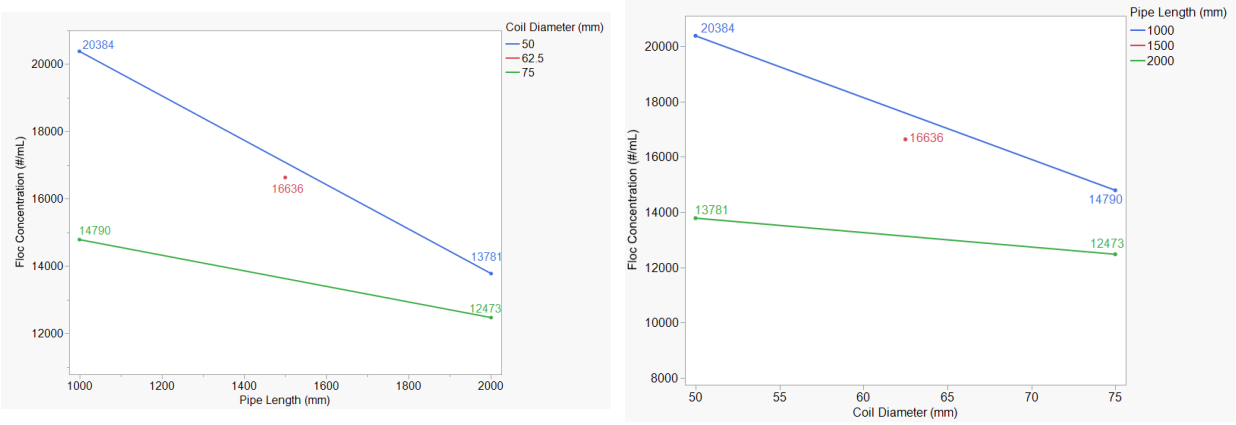
Fig. F.4. Interaction diagrams between pipe length and coil pitch for floc ECD: **(a)** Effect of pipe length at high and low factor setting of coil pitch; **(b)** Effect of coil pitch at high and low factor settings of pipe length

At the high factor setting for coil pitch, the effect of increasing coil diameter leads to a more rapid decline in floc concentration compared to at the low factor setting (Fig. F.5a). From Fig. F.5b, the effect of coil pitch is changed depending on the setting of coil diameter. For HCTFs with large diameter, increasing the coil pitch reduced the floc concentration while for small diameter HCTFs the floc concentration increased slightly with increasing coil pitch. From Fig. F.6 below, the effect of pipe length on floc concentration is greater at the low setting of coil diameter than for the large diameter HCTF. The effect of coil diameter on concentration is also seen to be greater for the short length HCTF compared to for the 2000 mm length flocculator.



(a) **(b)**

Fig. F.5. Interaction diagrams between coil diameter and coil pitch for floc concentration: **(a)** Effect of coil diameter at high and low factor setting of coil pitch; **(b)** Effect of coil pitch at high and low factor settings of coil diameter



(a) **(b)**

Fig. F.6. Interaction diagrams between coil diameter and pipe length for floc concentration: **(a)** Effect of pipe length at high and low factor setting of coil diameter; **(b)** Effect of coil diameter at high and low settings of pipe length

F.5. Correlation Analysis

This section presents the complete results of the multivariate correlation analysis between the three response variables (floc ECD, D_p, and floc concentration) and measures of floc curvature and torsion. Here, Eqn. (F.3) and Eqn. (F.4) were considered in addition to Eqns. (5.2) – (5.8), which were already presented in Chapter 5.

$$\tau_{nd} = \frac{r_p b_{ps}}{{b_{ps}}^2 + r_c^2} \tag{F.3}$$

$$\tau = \frac{p}{(r_c^2 + p^2)} \tag{F.4}$$

Where τ_{nd} is the dimensionless torsion, τ is the torsion (mm^{-1}), b_{ps} is the pitch slope (mm rad^{-1}), p is the coil pitch (mm), r_p is the pipe radius (mm), and r_c is the coil radius (mm). Tables F.11 and F.12 below present the regression results separated according to the factor setting for the pipe length. Below the diagonal the Pearson Correlation Coefficient values are presented while above the diagonal, shaded in grey, the p-values for the correlation are provided. Those shown to be significant with greater than 95% confidence are highlighted in red text.

Table F.11. Multivariate Correlation Analysis Between Floc Response Variables and Measures of Torsion and Curvature for 1000 mm Pipe Length

L=1000	ECD (µm)	D_p	Conc. (#/mL)	De	δ_{nd}	τ_{nd}	λ	β_0	c	τ	γ
ECD (µm)		0.0203	0.7229	0.6630	0.6557	0.3157	0.1570	0.0922	0.7965	0.9240	0.1570
D_p	-0.9797		0.8508	0.7772	0.7682	0.2353	0.1230	0.0894	0.9158	0.8775	0.1230
Conc. (#/mL)	-0.2771	0.1492		0.0051	0.0064	0.4890	0.7267	0.8859	0.0046	0.1568	0.7267
De	-0.3370	0.2228	0.9949		<.0001	0.5472	0.7810	0.9352	0.0098	0.1482	0.7810
δ_{nd}	-0.3443	0.2318	0.9936	0.9999		0.5548	0.7879	0.9414	0.0112	0.1477	0.7879
τ_{nd}	0.6843	-0.7647	0.5110	0.4528	0.4452		0.0394	0.1030	0.4272	0.2961	0.0394
λ	0.8430	-0.877	0.2733	0.2190	0.2121	0.9606		0.0155	0.6497	0.4163	
β_0	0.9078	-0.9106	0.1141	0.0648	0.0586	0.8970	0.9845		0.8023	0.5128	0.0155
c	-0.2035	0.0842	0.9954	0.9902	0.9888	0.5728	0.3503	0.1977		0.1107	0.6497
τ	0.0760	-0.1225	0.8432	0.8518	0.8523	0.7039	0.5837	0.4872	0.8893		0.4163
γ	0.8430	-0.8770	0.2733	0.2190	0.2121	0.9606		0.9845	0.3503	0.5837	

Note: *p*-values are shown above the diagonal in shaded grey while Pearson correlation coefficients are shown below the diagonal in white; Correlations with significance at greater than 95% confidence are highlighted in red text.

Table F.12. Multivariate Correlation Analysis Between Floc Response Variables and Measures of Torsion and Curvature for 2000 mm Pipe Length

L=2000	ECD (µm)	D_p	Conc. (#/mL)	De	δ_{nd}	τ_{nd}	λ	β_0	c	τ	γ
ECD (µm)		0.4827	0.8030	0.7150	0.7239	0.0193	0.0255	0.0694	0.5837	0.4467	0.0255
D_p	-0.5173		0.6814	0.0362	0.0379	0.3325	0.5300	0.6717	0.0101	0.0627	0.5300
Conc. (#/mL)	-0.1970	0.3186		0.6139	0.6226	0.8123	0.9728	0.8354	0.6062	0.9803	0.9728
De	-0.2850	0.9638	0.3861		<.0001	0.5472	0.7810	0.9352	0.0098	0.1483	0.7810
δ_{nd}	-0.2761	0.9621	0.3774	0.9999		0.5548	0.7879	0.9414	0.0112	0.1477	0.7879
τ_{nd}	-0.9807	0.6675	0.1877	0.4528	0.4452		0.0394	0.1030	0.4272	0.2961	0.0394
λ	-0.9745	0.4700	-0.0272	0.2190	0.2121	0.9606		0.0155	0.6497	0.4163	
β_0	-0.9306	0.3284	-0.1646	0.0648	0.0586	0.8970	0.9845		0.8023	0.5128	0.0155
c	-0.4163	0.9899	0.3938	0.9902	0.9888	0.5728	0.3503	0.1977		0.1107	0.6497
τ	-0.5533	0.9373	-0.0197	0.8518	0.8523	0.7039	0.5837	0.4872	0.8893		0.4163
γ	-0.9745	0.4700	-0.0272	0.2190	0.2121	0.9606		0.9845	0.3503	0.5837	

Note: *p*-values are shown above the diagonal in shaded grey while Pearson correlation coefficients are shown below the diagonal in white; Correlations with significance at greater than 95% confidence are highlighted in red text.

F.6. Batch Mixing Data

To prevent flocs from settling, the batch reactor mixing strategy involved continuous mixing at G-values higher than those used in conventional flocculation practice. Accordingly, to verify whether this caused a time-dependent effect on floc properties, samples of flocs were collected over the course of 3 hours after the addition of coagulant. The sample ECD and floc concentration are summarized in Fig. F.7 below.

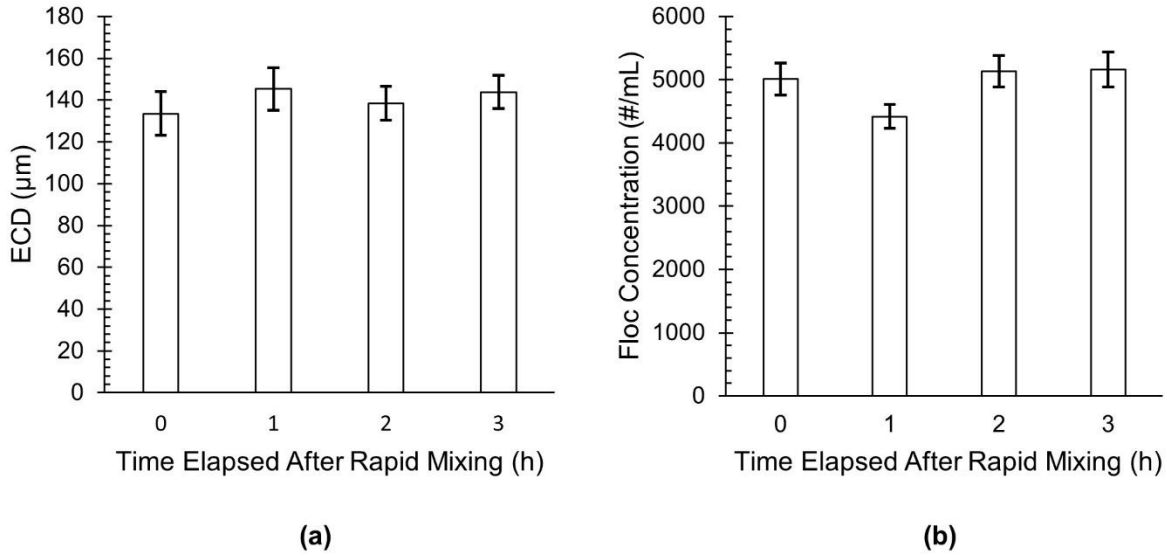


Fig. F.7. Kinetic assessment of floc properties in batch reactor system with continuous-stirring at G=200 s^{-1}: **(a)** ECD; **(b)** Floc Concentration.

F.7. References

Amirtharajah, A., and K. M. Mills. 1982. "Rapid-mix design for mechanisms of alum coagulation." *Journal AWWA*, 74 (4): 210–216. https://doi.org/10.1002/j.1551-8833.1982.tb04890.x.

Crittenden, J. C., R. R. Trussell, D. W. Hand, K. J. Howe, and G. Tchobanoglous. 2012. *Water treatment: Principles and design*. 3rd ed. New York, NY: McGraw-Hill.

Edwards, G. A., and A. Amirtharajah. 1985. "Removing color caused by humic acids." *Journal AWWA*, 77 (3): 50–57. https://doi.org/10.1002/j.1551-8833.1985.tb05508.x.

Edzwald, J. K., and J. E. Tobiason. 1999. "Enhanced coagulation: US requirements and a broader view." *Water Science & Technology*, 40 (9): 63–70. https://doi.org/10.1016/S0273-1223(99)00641-1.

Gonzalez-Galvis, J. P., and R. M. Narbaitz. 2020. "Large batch bench-scale dissolved air flotation system (LB-DAF) for drinking water treatability tests." *Environmental Science: Water Research and Technology*, 6 (4): 1004–1017. Royal Society of Chemistry. https://doi.org/10.1039/c9ew00935c.

Gonzalez-Galvis, J. P., and R. M. Narbaitz. 2022. "Large batch bench-scale dissolved air flotation system for simulating full-scale turbidity removal." *Environmental Technology*, 43 (12): 1791–1804. https://doi.org/10.1080/09593330.2020.1852317.

Hundt, T. R., and C. R. O'Melia. 1988. "Aluminum-fulvic acid interactions: mechanisms and applications." *Journal AWWA*, 80 (4): 176–186. https://doi.org/10.1002/j.1551-8833.1988.tb03023.x.

Kim, H.-C., and B. A. Dempsey. 2013. "Membrane fouling due to alginate, SMP, EfOM, humic acid, and NOM." *Journal of Membrane Science*, 428: 190–197. https://doi.org/10.1016/j.memsci.2012.11.004.

Konieczny, K., D. Sąkol, J. Płonka, M. Rajca, and M. Bodzek. 2009. "Coagulation—ultrafiltration system for river water treatment." *Desalination*, 240 (1–3): 151–159. https://doi.org/10.1016/j.desal.2007.11.072.

Lenth, R. V. 1989. "Quick and easy analysis of unreplicated factorials." *Technometrics*, 31 (4): 469–473.

Li, T., Z. Zhu, D. Wang, C. Yao, and H. Tang. 2006. "Characterization of floc size, strength and structure under various coagulation mechanisms." *Powder Technology*, 168 (2): 104–110. https://doi.org/10.1016/j.powtec.2006.07.003.

Maeng, S. K., T. C. Timmes, and H.-C. Kim. 2017. "Characteristics of flocs formed by polymer-only coagulation in water treatment and their impacts on the performance of downstream membrane separation." *Environmental Technology*, 38 (20): 2601–2610. https://doi.org/10.1080/09593330.2016.1271460.

Montgomery, D. C. 2020. *Design and Analysis of Experiments*. 10th ed. Hoboken, NJ, USA: Wiley.

Myers, R. H., D. C. Montgomery, and C. M. Anderson-Cook. 2016. *Response Surface Methodology: Process and Product Optimization Using Designed Experiments*. 4th ed. Hoboken, NJ, USA: Wiley.

Tambo, N. 1979. "Physical characteristics of flocs—I. The floc density function and aluminium floc." *Water Research*, 13 (5): 409–419. https://doi.org/10.1016/0043-1354(79)90033-2.

Wang, J., S. Pan, and D. Luo. 2013. "Characterization of cake layer structure on the microfiltration membrane permeability by iron pre-coagulation." *Journal of Environmental Sciences*, 25 (2): 308–315. https://doi.org/10.1016/S1001-0742(12)60025-4.

Yang, H., N. J. D. Graham, W. Wang, M. Liu, and W. Yu. 2021. "Evaluating and improving the reliability of the UV-persulfate method for the determination of TOC/DOC in surface waters." *Water Research*, 196: 116918. https://doi.org/10.1016/j.watres.2021.116918.

APPENDIX G

Supplemental Information for Chapter 6

Context: This appendix presents supporting information associated with Chapter 6 of this thesis, *Impact of Flocculator Type on Continuous Inline Coagulation for Low-Pressure Membrane Pretreatment in Drinking Water Production*.

List of Abbreviations

ANOVA	Analysis of variance
CDF	Cumulative distribution function
C-IN	Inline coagulation
CFSTR	Continuous flow stirred tank reactor
DI	Deionised water
ECD	Equivalent circular diameter
FLOCC	Flocculation only
FR_{hr}	Hydraulically reversible fouling rate
FR_{hirr}	Hydraulically irreversible fouling rate
HCTF	Helically coiled tube flocculator
HIFI	Hydraulically irreversible fouling index
HRT	Hydraulic retention time
ISM	Inline static mixer
MFI	Micro-flow imaging
PDF	Probability density function
PFR	Plug flow reactor
RM	Rapid mixing
RM+FLOCC	Rapid mixing and flocculation
TFI	Total fouling index
TMP	Transmembrane pressure
UV_{254}	Ultraviolet absorbance at 254nm
WQI	Water quality indicators

List of Variables

α_{CR}	Specific cake resistance (m kg^{-1})
ϑ	Theoretical hydraulic detention time (s)
ε_c	Cake layer porosity (dimensionless)
ϵ_{ij}	Random error component of means model
μ_{MM}	Overall mean of the *i* samples for the *j* treatments in means model
$\tau_{MM,i}$	Effect of the i^{th} treatment in means model

ψ	Sphericity of particles that form the cake layer (dimensionless)
D	diffusion coefficient ($m^2\ s^{-1}$)
d_{eq}	Equivalent spherical diameter (m)
$E(t)$	Exit age distribution for tracer study
F_0	F-ratio test statistic for F-test
FI	Fouling index ($m^2\ L^{-1}$)
$F(t)$	Cumulative age distribution for tracer study
H_0	Null hypothesis
H_1	Alternate hypothesis
K	Kozeny constant (dimensionless)
L	Characteristic length of pipe (m)
n_1^2	Sample number of population 1
n_2^2	Sample number of population 2
s_1^2	Sample variance of population 1
s_2^2	Sample variance of population 2
S_A	Specific surface area of the cake ($\frac{m^2}{m^3}$)
${s_p}^2$	Pooled sample variance
SS_E	Sum of squares due to error
$SS_{treatments}$	Sum of squares due to treatments
$\bar{t}$	Mean HRT estimated from tracer studies (min)
t_0	Test statistic for Student's t-test
V_s	specific volume ($L\ m^{-2}$)
u	axial velocity of the fluid ($m\ s^{-1}$)
y_{ij}	The j^{th} observation for the i^{th} treatment with a variance of σ^2 in means model (varies)
$\bar{y}_{i\cdot}$	Average of the observations for the i^{th} treatment (varies)
$\bar{y}_{\cdot\cdot}$	Grand average of all observations across the *i* different treatments (varies)

G.1. Additional Methodological Details

G.1.1. Critical Flux Test

The critical flux, defined as the theoretical flux value below which low-pressure membrane fouling is not observed (Bacchin et al. 2006; Field et al. 1995; Howell 1995), was assessed for this membrane and water combination using the flux-stepping method adapted from Le Clech et al. (2003). Briefly, the pure water permeability of the membrane fiber was measured by filtering deionised water (DI) (ZenoPure Quatra 90LC, Zenon Environmental Inc., Burlington, ON) at a flux of 60 L m^{-2} h^{-1} for a period of 1 h. Following this, the flux rate was increased by 3 L m^{-2} h^{-1} (i.e., the step height) every 15 minutes (i.e., the step length) of operation for a total of 25 steps where it was deemed that the critical flux point had been surpassed. The step height and step length, which are known to have an important impact on the rate of transmembrane pressure (TMP) increase, and therefore the measured critical flux value, were selected based on the guidance provided in the studies by Le Clech et al. (2003), Choi and Dempsey (2005), as well as Beier and Jonsson (2010). Analysis of the data was performed by plotting the mean TMP recorded for every flux step against the mean permeate flux. In this approach, which Choi and Dempsey (2005) argued provides greater reproducibility, linear regression is used to fit the initial shallow slope and the second, more steeply sloped, region. The intersection of these two fitted lines is defined as the critical flux value. Based on previous experience with our filtration system, the mean flux and TMP values were calculated using the data collected from the final minute of the 15-minute flux step, as the system had reached stable operation (i.e., the pump voltage has stabilized). The critical flux test data as well as the two fitted models are shown in Fig. G.1 below.

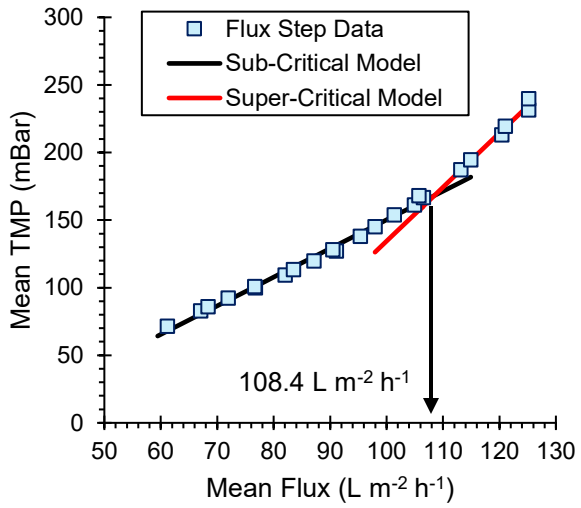


Fig. G.1. Flux-stepping test data and fitted models for critical flux determination

A summary of the fit of the two models is provided in Table G.1 below and, by equation of the two models, the critical flux value was determined to be 108.4 L m^{-2} h^{-1}. Note that the regression analysis was performed using Excel's built-in *Data Analysis* tool pack and the significance of the fit was determined by the *p*-value calculated from the analysis of variance (ANOVA). Based on this result, a flux of 80 L m^{-2} h^{-1} was selected for all filtration experiments so that the membrane was operated in the sub-critical flux zone (to prevent unrealistic fouling development). Moreover, this flux value permitted comparison (on an equivalent flux basis) with our previous studies (if warranted) and necessitated reasonable volumes of synthetic water, which was an important consideration due to the cost and significant amount of time required for its preparation.

Table G.1. Fitted Models from Critical Flux Testing

Model	Slope (mBar m^2 h L^{-1})	Intercept (mBar)	R^2	*p*-Value
Sub-Critical	2.12	-61.80	0.9932	<.0001
Super-Critical	3.99	-264.88	0.9773	.0002

G.1.2. Inline Rapid Mixer

The bench-scale continuous-flow inline rapid mixer was created by modifying a cylindrical inline strainer housing (GY-29595-05, Cole Parmer, Montreal, QC). A hole was drilled through the top

of the housing to permit passage of a 3.175 mm diameter stainless steel pipe (SS-T2-S-065-20, Swagelok, Solon, OH), which was connected to the syringe pump for coagulant injection. A two-way plug valve (SS-2P4T, Swagelok, Solon, OH) was added to be able to isolate the coagulant feed line from the remainder of the pressurized system. As the feed water enters the rapid mixer, an inlet baffle directs the flow towards the bottom of the housing, where the coagulant is added just above a magnetic stir bar that was driven by a disc stirrer (3907500, IKA, Wilmington, NC). The stirrer was set to its high-speed setting to ensure high intensity mixing. A schematic of the inline rapid mixer is provided in Fig. G.2 below.

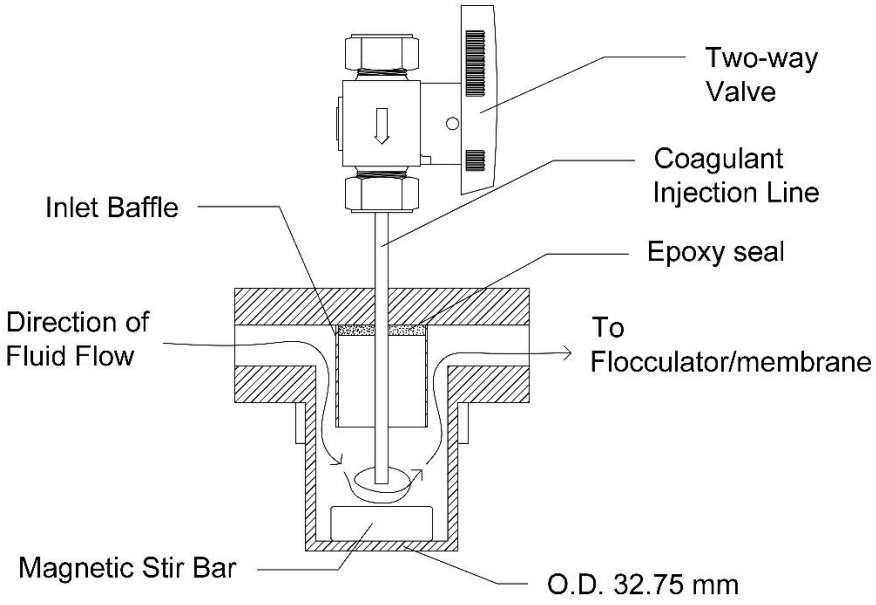


Fig. G.2. Schematic of inline rapid mixer

G.1.3. Tracer Studies

To determine the mean residence time of the inline rapid mixer as well as the various flocculators used in this study, preliminary tracer tests were performed using a precision metering pump (Optos 3HM, Eldex, Napa, CA) operated at the same flowrate as the bench-scale filtration system (~ 5 mL min^{-1}). A 2% salt solution was prepared by dissolving NaCl (Certified ACS, Fisher Scientific, Hampton, NH) in DI (ZenoPure Quatra 90LC, Zenon Environmental Inc., Burlington, ON),

resulting in a conductivity of approximately 28.8 mS cm^{-1}. The tracer test was conducted using a step input approach: the system was initially pumping DI before the feed was instantaneously switched to the NaCl solution with operation continuing until the effluent concentration from the mixer was the same as the feed concentration. Conductivity was the basis of measurement for the tracer study and was analyzed in one-minute intervals (limited by the low throughput volume) using a benchtop conductivity meter (Orion Star 3, Thermo Scientific, St. Louis, MO).

The analysis of the tracer data was performed according to the method outlined by Benjamin and Lawler (2013). Considering that the mean hydraulic retention time (HRT) is the first moment of the probability density function (PDF) divided by the zeroth moment we have:

$$\bar{t} = \frac{\int_0^\infty tE(t)\mathrm{d}t}{\int_0^\infty E(t)\mathrm{d}t} \tag{G.1}$$

where $\bar{t}$ is the mean HRT (min) and $E(t)$ is the exit age distribution, or PDF (min^{-1}). Remembering that the cumulative distribution function (CDF) is the integral of the PDF we have:

$$\bar{t} = \frac{\int_0^\infty t(\frac{\mathrm{d}F(t)}{\mathrm{d}t})\mathrm{d}t}{\int_0^\infty (\frac{\mathrm{d}F(t)}{\mathrm{d}t})\mathrm{d}t} \tag{G.2}$$

Where $F(t)$ is the CDF. This can be simplified further as:

$$\bar{t} = \int_0^1 t\ \mathrm{d}F(t) \tag{G.3}$$

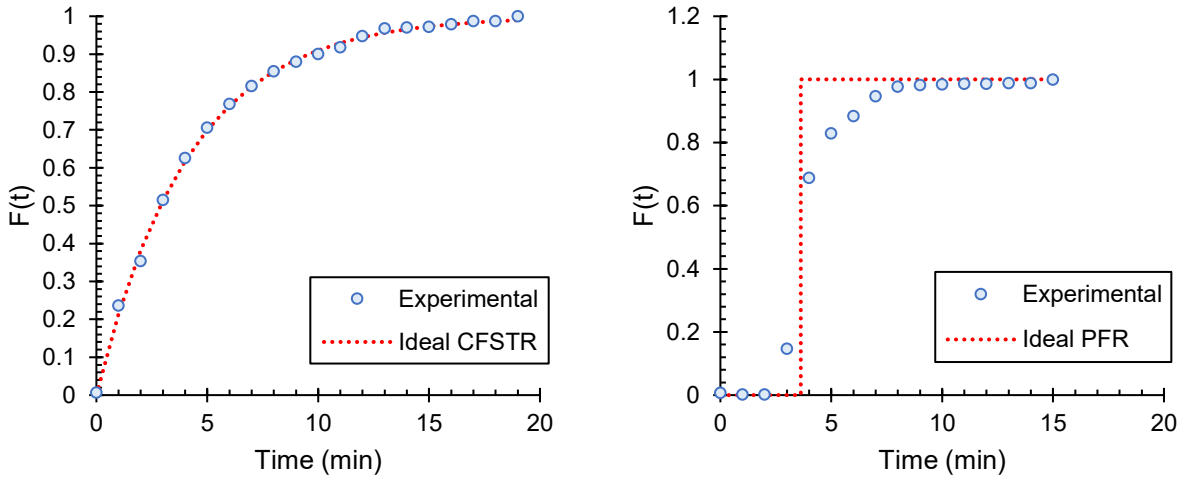
For a discrete data set collected from a tracer study, we can then simplify the expression to:

$$\bar{t} = \sum_{all\ i} \left(\frac{t_i + t_{i-1}}{2}\right)(F_i(t) - F_{i-1}(t)) \tag{G.4}$$

It should also be noted that, for an ideal continuous-flow stirred tank reactor (CFSTR), the theoretical CDF is given by:

$$F(t) = 1 - e^{-t/\vartheta} \tag{G.5}$$

where ϑ is the theoretical HRT given by V/Q. Fig. G.3 below presents two tracer curves obtained for the inline rapid mixer (representative of a CFSTR) and the HF-2000-⅛ flocculator (modeled as a plug-flow reactor (PFR)). Note that in Fig. G.3a and G.3b, the theoretical CDFs for an ideal CFSTR and PFR, respectively, are also shown as a dotted lines.



(a) **(b)**

Fig. G.3. Cumulative distribution function curves derived from tracer studies for: **(a)** Rapid mixer; **(b)** HF-2000-⅛

Table G.2 below summarizes the mean HRT values for each flocculator type used in this study. The $\vartheta_{Experimental}$ column reports the HRT value calculated from the tracer study while $\vartheta_{Theoretical}$ was determined using a gravimetric approach. Here, the flocculator was filled with DI and then the mass of DI contained within the mixer was measured using an analytical balance (AJ150, Mettler Toledo, Columbus, OH). Using the temperature corrected density, the volume was determined and the mean HRT was calculated by dividing the holdup volume by the system flowrate.

The tracer response for the rapid mixer (Fig. G.3a) demonstrated that the unit strongly matches the expected performance of an ideal CFSTR. However, from Table G.2, the $\vartheta_{Experimental}/\vartheta_{Theoretical}$ is only 0.57 indicating the presence of substantial dead volume within the reactor. Since a portion of the dead volume is likely located in the region behind the inlet baffle, it is recommended that future versions of this rapid mixer fill this zone (with epoxy, for example) to reduce the dead volume. Additional modifications are discussed in Section G.2.1.3. For the inline static mixer (ISM), $\vartheta_{Experimental}/\vartheta_{Theoretical}$ was 0.88, meaning that its behavior was not exactly that

of an ideal PFR. This is not entirely surprising, however, as low-flow rates within these mixers have been reported to cause a widening of the range of retention times and significant deviation from ideal PFR behavior (Albertazzi et al. 2021). For the control and all helically coiled tube flocculators (HCTFs) investigated, the behavior was very similar to a PFR (see Fig. G.3b). However, for the HF-1000-⅛ and HF-2000-⅛ reactors $\vartheta_{Experimental}/\vartheta_{Theoretical}$ was greater than unity, which is not theoretically possible. Accordingly, this result must be due to pure experimental error. If we consider then that the experimental error is in the order of ~6% (based on the $\vartheta_{Experimental}/\vartheta_{Theoretical}$ for the HF-2000-⅛), then this would account for the observed deviation of the other HCTFs and control from the ideal PFR behavior.

Table G.2. Summary of Mixer Properties and Hydraulic Retention Times

Mixer Type	Description	Tube O.D. (mm/in.)	Tube I.D. (mm/in.)	Pipe Length (mm)	$\vartheta_{Theoretical}$ (min)	$\vartheta_{Experimental}$ (min)	$\frac{\vartheta_{Experimental}}{\vartheta_{Theoretical}}$
Rapid Mixer	Modified inline screen housing used to provide high intensity mixing at coagulant injection point	N/A	N/A	N/A	7.16 [a]	4.08 [b]	0.57
Inline Static Mixer	Commercial mixer from Koflo Corp. with 21 helical elements (Part No. 3/8-21)	9.525 (⅜")	6.35 (¼")	286 (11")	2.58	2.29	0.88
Control-¼	System control made from ¼" I.D. 316 stainless steel tubing (SS-T6-S-065-20, Swagelok, Solon, OH)	9.525 (⅜")	6.35 (¼")	286 (11")	2.82	2.74	0.97
HF-1000-⅛	HCTF with pitch = 15 mm; coil diameter = 50 mm; pipe O.D. = 6.35 mm; pipe length = 1000 mm	6.35 (¼")	3.175 (⅛")	1000 (39 ⅜")	1.92	2.00	1.04
HF-2000-⅛	HCTF with pitch = 15 mm; coil diameter = 50 mm; pipe O.D. = 6.35 mm; pipe length = 2000 mm	6.35 (¼")	3.175 (⅛")	2000 (78 ¾")	3.77	4.00	1.06
HF-1000-¼	HCTF with pitch = 15 mm; coil diameter = 50 mm; pipe O.D. = 9.525 mm; pipe length = 1000 mm	9.525 (⅜")	6.35 (¼")	1000 (39 ⅜")	6.31	6.15	0.97
HF-2000-¼	HCTF with pitch = 15 mm; coil diameter = 50 mm; pipe O.D. = 9.525 mm; pipe length = 2000 mm	9.525 (⅜")	6.35 (¼")	2000 (78 ¾")	13.48	12.75	0.95
HF-3000-⅛	HCTF with pitch = 15 mm; coil diameter = 50 mm; pipe O.D. = 6.35 mm; pipe length = 3000 mm	6.35 (¼")	3.175 (⅛")	3000 (118 7⁄64")	5.23	5.24	1.00

Note. [a] $\tau_{Theor.}$ is calculated by determining the holdup volume gravimetrically and dividing by the system flowrate; [b] determined from tracer test

G.1.4. Micro-Flow Imaging (MFI) Technologies

As an alternative to microscopic analysis of flocs with manual image processing and analysis, micro-flow imaging (MFI) techniques have been employed by a number of previous studies (e.g., Kollu and Örmeci 2012, 2015). MFI offers several advantages including automated image acquisition and analysis, the ability to process large numbers of particles, and reduced reliance on manual image processing. However, several considerations associated with MFI led to the selection of manual microscopy for floc characterisation in the present study. The following limitations are discussed with specific reference to the DPA 4100 (Brightwell Technologies, Ottawa, ON), which was the MFI system accessible to the authors.

- **Limited Size Range**: The optical resolution of the MFI device can limit the size range of flocs that can be reliably characterized. For example, the high-resolution flow cell (BP-4100-FC-100-U) of the DPA 4100 has a limit of detection of 0.75 μm, which is more than twice the resolution of the optical microscope used in the present study. Particles near or below the instrument's reliable detection limit may therefore be measured with reduced accuracy and can potentially bias the resulting particle size distribution towards smaller sizes. This phenomenon was visible in the study by Gonzalez-Galvis and Narbaitz (2020), where the floc size for alum coagulation of a colored water via sweep flocculation mechanism (dosage > 6 mg-Al/L) was exponentially distributed with the highest number concentrations in the lowest size ranges.
- **Limited Sample Volume:** The volumes of sample analyzed by the MFI system is very small, raising doubts as to whether it is representative of the in-situ conditions, particularly for heterogenous floc suspensions. For example, the DPA 4100 uses a low flowrate of 0.1 mL/min when analyzing particles under its high magnification setting, resulting in sample volumes of < 0.25 mL in some instances (Sharma et al. 2010).
- **Sample Disturbance:** Although automated sample handling is an important advantage of MFI in terms of analysis speed and reproducibility, the transport of flocs through the measurement device may alter their structure. In the DPA 4100, the sample is maintained in a vessel with continuous magnetic stirring and is subsequently transported through relatively narrow tubing and the flow cell. These conditions may subject flocs to hydrodynamic shear that could result in breakage, compaction, or restructuring of fragile aggregates. The dimensions of the tubing and flow cell may also constrain the maximum

size of flocs that can be analyzed. Consequently, the aggregates observed by the MFI system may not fully represent their structure under the original sampling conditions.

- **System Cleanliness and Image Overlap:** MFI measurements can be sensitive to the cleanliness of the flow path and the presence of residual particles within the system. For the DPA 4100, the manufacturer's guidelines recommend flushing the microfluidic flow cell with HPLC-grade reagent water and a specialty detergent between analyses. Thorough cleaning is particularly important because relatively large flocs may become lodged within the flow cell. Residual aggregates adhering to the flow-cell walls may not be completely removed through background subtraction and could therefore be detected repeatedly during subsequent analyses, potentially leading to overestimation of particle abundance. In addition, particles transported through the flow cell may overlap with aggregates adhered to the cell wall, making their boundaries difficult to resolve and introducing uncertainty into the measured particle characteristics. Similar image-overlap issues may arise at elevated particle concentrations, where multiple flocs can simultaneously occupy the imaging field.
- **Sensitivity to Imaging Conditions:** Accurate MFI characterization depends on appropriate illumination, focus, magnification, and image-processing parameters. In particular, the thresholding algorithm used to distinguish particles from the background can substantially influence the measured particle size and morphology. This may be especially important for relatively transparent or low-contrast flocs, such as the alum flocs examined in the present study. Small changes in thresholding can alter the apparent boundaries of individual aggregates and, consequently, affect calculated parameters such as particle size, projected area, and shape.

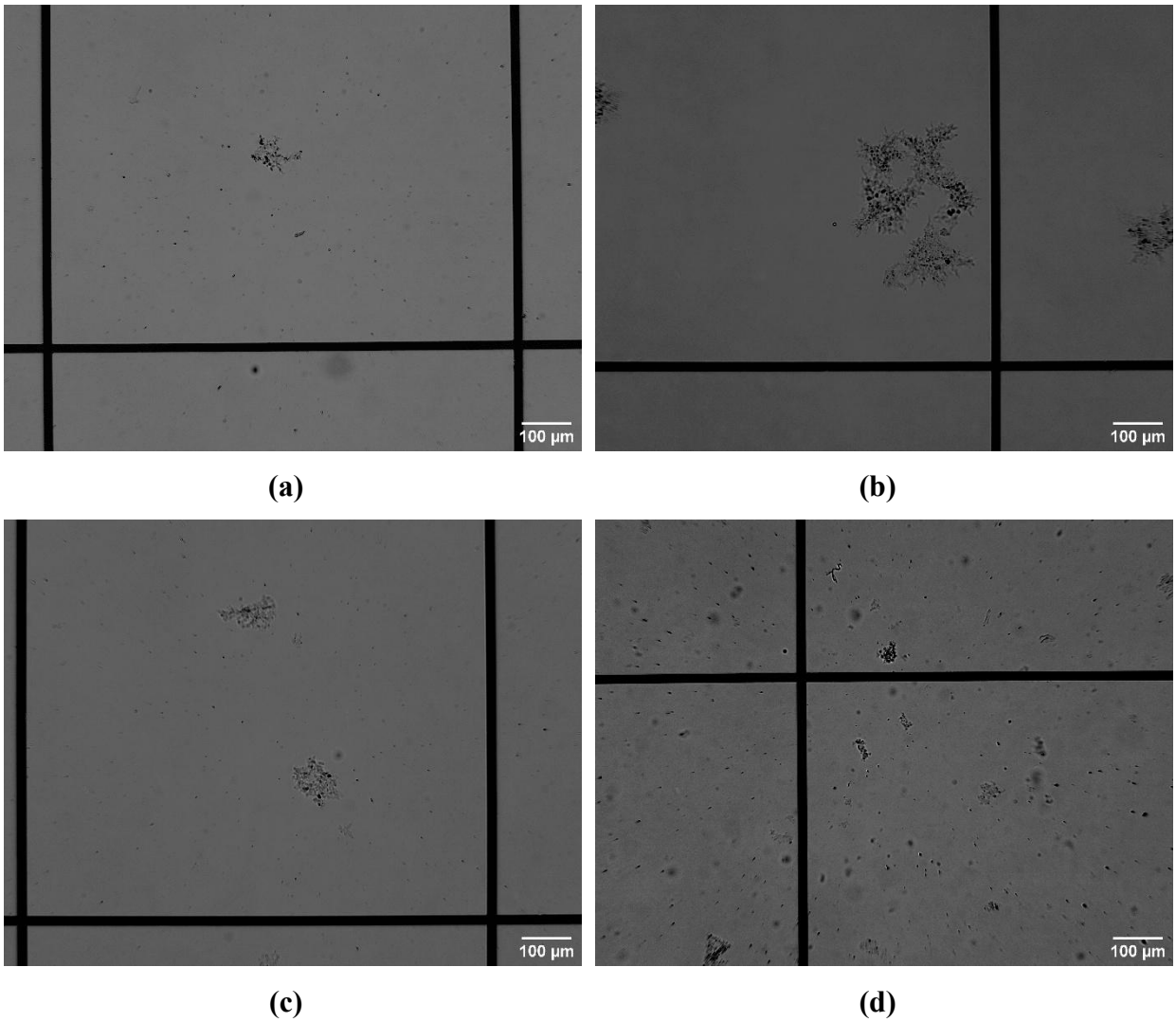
G.2. Supplemental Results

G.2.1. Evaluation of Small-Scale Inline Rapid Mixer

G.2.1.1. Floc Assessment and Imaging

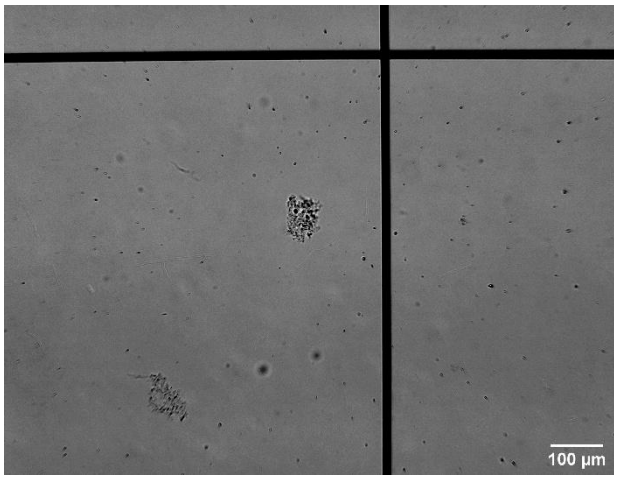
As noted in the manuscript, floc imaging was performed for all flocculator types, both with and without the small-scale rapid mixer (RM). Fig. G.4 presents representative floc images acquired under each tested condition. Visual comparison of the images indicates that the inclusion of the RM resulted in substantially larger flocs than those observed with the flocculation only (FLOCC)

configuration across all flocculator types investigated. The images also illustrate the highly transparent nature of the floc aggregates, which presented considerable challenges during image processing and limited the number of images that could be practically analyzed.

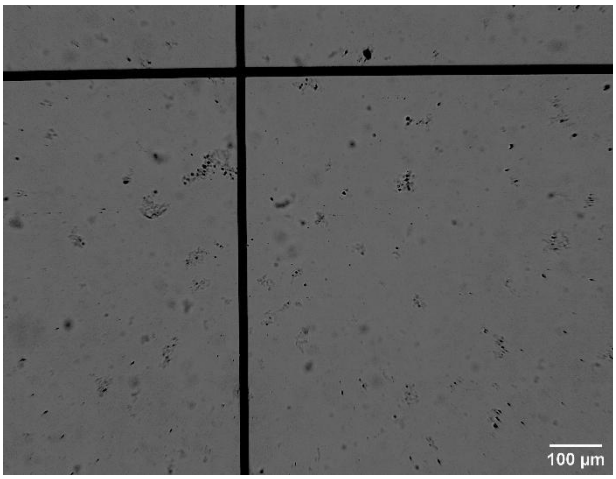


(a) **(b)**

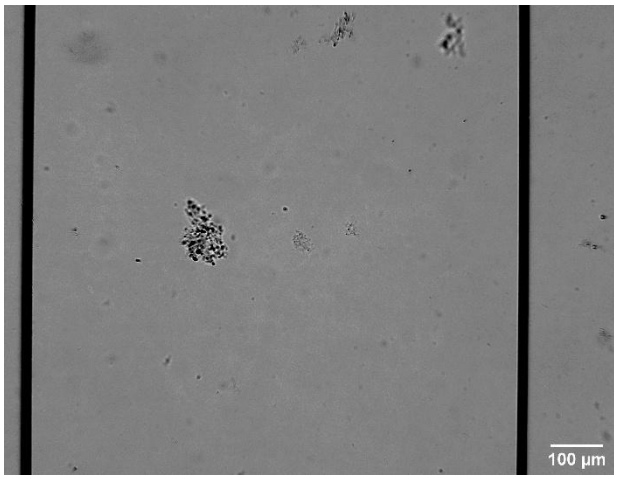
(c) **(d)**



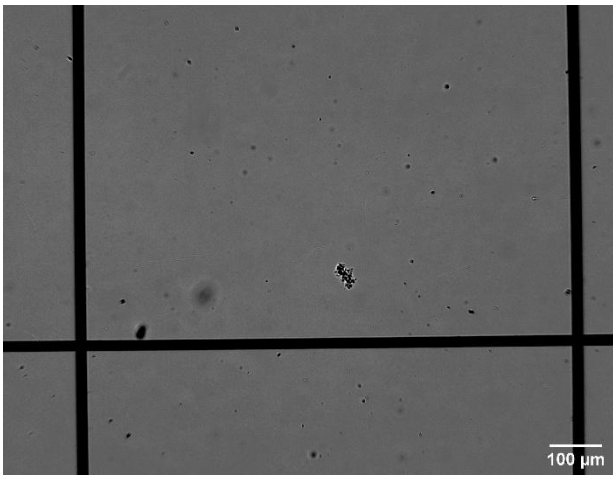
(e)



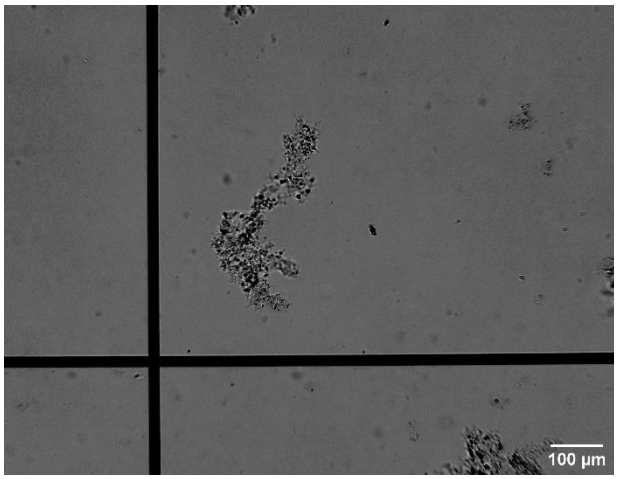
(f)



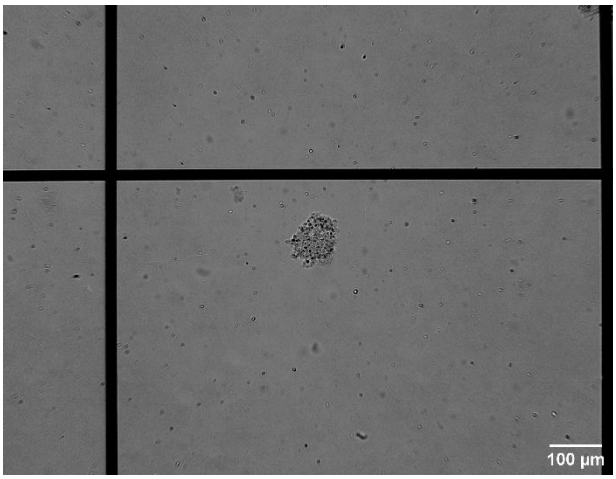
(g)



(h)



(i)



(j)

Fig. G.4. Representative microscopic images of flocs produced by: **(a)** RM Only; **(b)** Batch; **(c)** RM+Control; **(d)** Control; **(e)** RM+ISM; **(f)** ISM; **(g)** RM+HF-1000-⅛; **(h)** HF-1000-⅛; **(i)** RM+HF-2000-⅛; **(j)** HF-2000-⅛.

The percentage change in floc equivalent circular diameter (ECD) for rapid mixing + flocculation (RM+FLOCC) compared to FLOCC was plotted against the corresponding change in floc concentration in Fig. G.5 below. Using Excel's built-in regression feature, it was noted that the increase in floc size is nearly 2.99 times greater than for the decrease in floc concentration (Table G.3). If the floc growth was due to improved agglomeration of the same primary particle pool, the floc ECD would have been expected to increase by the same amount as the decrease in floc concentration (i.e., 1:1 slope). This suggests that the inclusion of RM produces a greater number of primary particles that, when incorporated within the floc structure, lead to larger ECD for RM+FLOCC compared to FLOCC only.

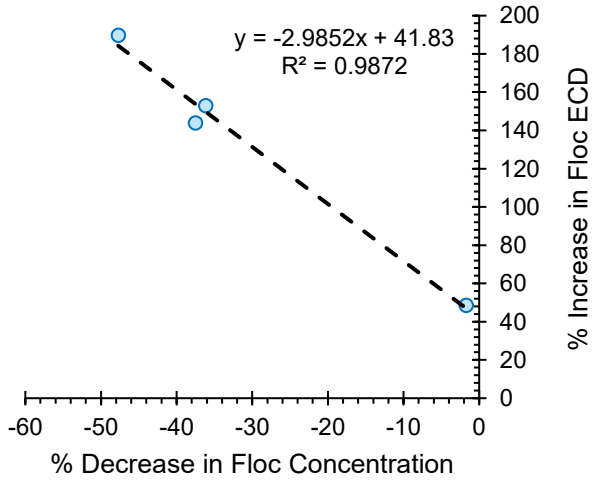


Fig. G.5. Relationship between percentage change in floc ECD and floc concentration for the addition of rapid mixing

Table G.3. Summary of Fitted Model Relating Percentage Change in Floc ECD and Concentration

Model	Slope (%/%)	Intercept (%)	R^2	*p*-Value
ECD-Conc.	-2.99	41.83	0.9872	.006

G.2.1.2. Peclet Number for Hypothesized Mixing Mechanism

The Peclet number is a dimensionless number defined as the ratio between the advective transport rate and the diffusive transport rate. The Peclet number is given by:

$$P_e = \frac{Lv}{D} \tag{G.6}$$

Where L is the characteristic length (pipe diameter) (m), v is the axial velocity of the fluid (m s^{-1}), and D is the diffusion coefficient (m^2 s^{-1}) which the aquo-metal aluminum ion is $0.559 \times 10^{-9} \frac{m^2}{s}$. For the Control in the current study, $L = \frac{6.35}{1000} m$ and $v = \frac{Q}{A} = \frac{5.5 cm^3}{min} \times \frac{min}{60\ s} \times \frac{m^3}{100^3 cm^3} \times \frac{4}{\pi\left(\frac{6.35}{1000} m\right)^2} = 0.00289 \frac{m}{s}$. Therefore:

$$P_e = \frac{Lv}{D} = \frac{(\frac{6.35}{1000} m\ ) \times 0.00289 \frac{m}{s}}{0.559 \times 10^{-9} \frac{m^2}{s}} = 32{,}880$$

Based on the large Peclet number (>> 1), advective mass transport is the governing transport phenomenon for the mixing of the hydrated aquo-metal aluminum ions in solution.

G.2.1.3. Revised Rapid Mixer Design

It was noted in Section G.1.3. that the ratio of $\tau_{Experimental}/\tau_{Theoretical}$ for the RM indicated the presence of a dead-zone, likely in the region behind the inlet baffle. Moreover, this study recommended to evaluate the performance of the RM using reduced HRTs more representative of the conditions typically employed in practice at full-scale facilities. Based on these, a modified RM design was developed and is presented in Fig. G.6. Here, the region behind the inlet baffle has been filled in using an epoxy seal to eliminate the possible formation of a dead zone. Additionally, the active mixing area has been reduced using epoxy to provide for a minimum retention time. As noted in the manuscript, it may be possible to leverage 3-D printing technologies to manufacture custom RM geometries with built-in baffles that conform to the design guidelines for cylindrical mixing basins (Crittenden et al. 2012).

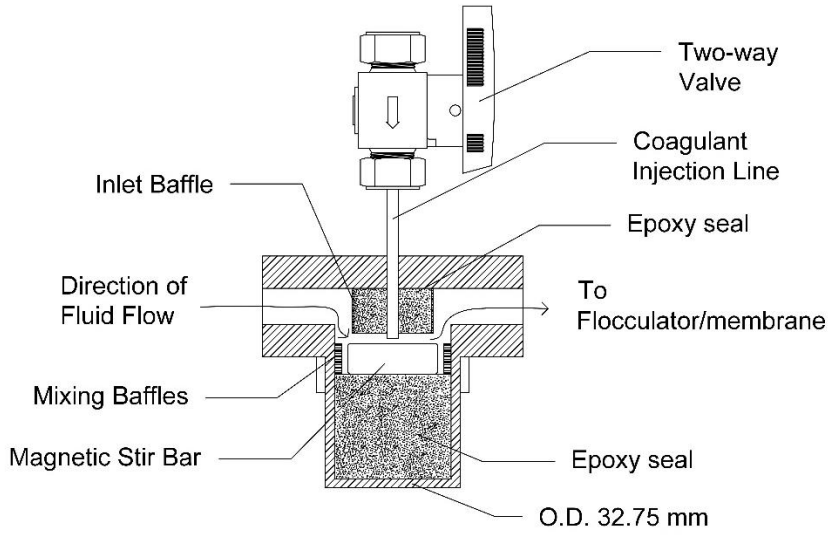


Fig. G.6. Schematic of modified RM.

G.2.2. Membrane Fouling Index

Nguyen et al. (2011) developed a modified fouling index model which, unlike the unified membrane fouling index model proposed by Huang et al. (2008), has the advantage of not requiring the assumption of a particular fouling mechanism. The general format of this model is given by:

$$\frac{1}{J_s'} = 1 + (FI)V_s \tag{G.7}$$

Where $\frac{1}{J_s'}$ is the inverse normalized specific flux, V_s is the specific volume of permeate (L m^{-2}), and FI is the fouling index (m^2 L^{-1}). Therefore, the fouling index is the slope of the linear regression between the inverse normalized specific flux and the specific volume. Depending on the operational cycles that are considered within the data, different indices can be defined. For the data of a single filtration cycle between hydraulic backwashes, the total fouling index (TFI) is computed. For numerous hydraulic backwash cycles, without chemical cleaning, the hydraulically irreversible fouling index (HIFI) is determined.

Fig. G.7 below gives a summary of the HIFI values for the direct filtration of raw water as well as for inline coagulation (C-IN) pretreatment across mixer configurations. From this figure it can be seen that, although the mean values of this metric are somewhat larger than the FR_{hirr}, the 95% confidence intervals (based on students *t*-test) are wide and often include zero within their

range. Despite the overlapping 95% confidence intervals, the mean HIFI values for continuous-flow coagulation with RM+FLOCC were substantially lower (>56%) than for FLOCC only. This highlights the potential beneficial impact of using combined rapid mix and flocculation for irreversible fouling mitigation with C-IN pretreatment.

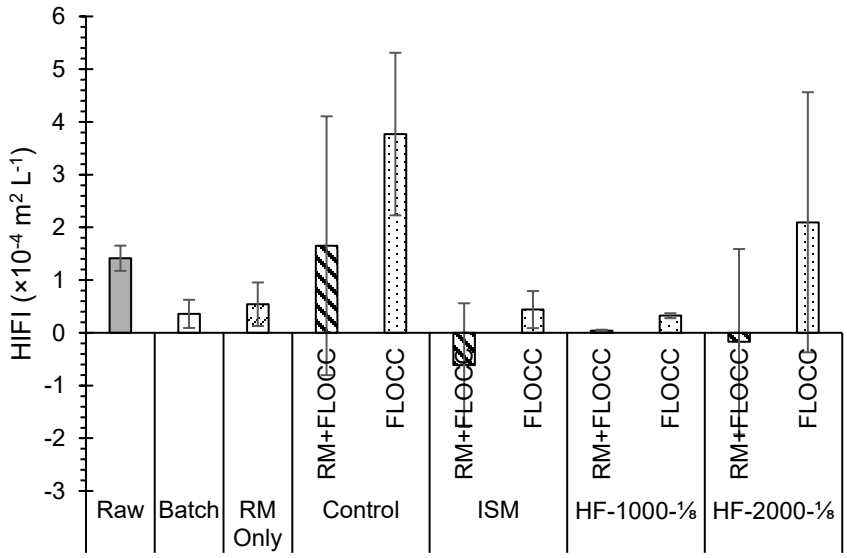


Fig. G.7. Mean HIFI for direct filtration and C-IN pretreatment

G.2.3. Evolution of LPM Fouling with Alternative Mixing Configurations

In Table G.4 below a summary of the mean hydraulically reversible (FR_{hr}) and irreversible (FR_{hirr}) fouling rates is provided for each mixing configuration investigated. It should be noted that the values reported represent the mean of the replicated tests. Furthermore, the cycle-by-cycle data obtained from each test was screened for outliers using a boxplot method with outliers defined as a deviation of more than 3 interquartile ranges from the first and third quartiles (Bonakdari et al. 2023).

Table G.4. Summary of Hydraulically Reversible and Irreversible Fouling Rates Across Mixing Configurations

Flocculator Type	Treatment	FR_{hr} (mBar h^{-1})	FR_{hirr} (mBar h^{-1})	FR_{hr} (% of Total)
Raw	-	110.20 ± 1.51	0.77 ± 0.84	99.30

Batch	-	7.88 ± 0.51	0.17 ± 0.49	97.85
RM Only	-	35.73 ± 5.98	0.68 ± 4.36	98.13
Control	RM+FLOCC	26.20 ± 4.24	-0.02 ± 2.95	100.08
	FLOCC	70.75 ± 11.38	2.86 ± 7.40	96.12
ISM	RM+FLOCC	25.11 ± 3.32	0.30 ± 2.83	98.81
	FLOCC	29.76 ± 2.64	0.52 ± 1.74	98.29
HF-1000-⅛	RM+FLOCC	22.57 ± 2.11	-0.05 ± 1.19	100.22
	FLOCC	49.20 ± 8.25	2.68 ± 4.66	94.83
HF-2000-⅛	RM+FLOCC	14.43 ± 1.26	0.06 ± 0.49	99.56
	FLOCC	34.13 ± 5.83	0.40 ± 3.46	98.83

Note: ± represents the 95% confidence interval calculated using the students t-test as $\mu \pm t_{0.025,n}\frac{s}{\sqrt{n}}$ where $n = 72$ for replicated day-long filtration tests.

To evaluate the effect of alternative mixing configurations, the pooled *t*-test on the difference in means was used with the assumption of unknown but equal variances. Briefly, the test hypotheses are given by Montgomery and Runger (2014):

$$H_0: \mu_1 - \mu_2 = \Delta_0$$

$$H_1: \mu_1 - \mu_2 \neq \Delta_0$$

And the corresponding test statistic is:

$$t_0 = \frac{\bar{x}_1 - \bar{x}_2 - \Delta_0}{s_p\sqrt{\frac{1}{n_1} + \frac{1}{n_2}}} \tag{G.8}$$

Where:

$$s_p{}^2 = \frac{(n_1 - 1)s_1^2 + (n_2 - 1)s_2^2}{n_1 + n_2 - 2} \tag{G.9}$$

And the rejection criteria is defined by $t_0 > t_{\alpha/2,n_1+n_2-2}$ or $t_0 < -t_{\alpha/2,n_1+n_2-2}$. In the above expressions n_i is the number of observations from sample *i*, and $\bar{x}_i$ and s_i^2 are the sample means and variances, respectively. Table G.5 below presents the pairwise comparison of FR_{hr} between direct filtration of raw water and pretreatment by C-IN with all mixer configurations. For all configurations, FR_{hr} for direct filtration was found to be significantly (> 95%) greater than for pre-treatment by C-IN.

Table G.5. Results of Pooled *t*-test on Difference in Mean FR_{hr} Between Direct Filtration and Alternative C-IN Strategies

Configuration	Configuration	Difference (mBar h^{-1})	St. Error Diff. (mBar h^{-1})	Lower 95% Limit	Upper 95% Limit	*p*-Value
Raw	Batch	102.32	0.81	100.72	103.92	<.0001
Raw	RM Only	74.25	3.04	68.25	80.25	<.0001
Raw	Control	39.45	5.68	28.22	50.68	<.0001
Raw	ISM	80.44	1.48	77.50	83.37	<.0001
Raw	HF-1000-⅛	61.00	4.13	52.85	69.16	<.0001
Raw	HF-2000-⅛	75.67	2.95	69.85	81.50	<.0001
Raw	RM+Control	84.00	2.21	79.63	88.37	<.0001
Raw	RM+ISM	85.09	1.80	81.53	88.64	<.0001
Raw	RM+HF-1000-⅛	87.63	1.29	85.07	90.18	<.0001
Raw	RM+HF-2000-⅛	95.77	1.00	93.80	97.74	<.0001

Table G.6 presents the results of the pooled *t*-test for the comparison of FR_{hr} for batch coagulation with C-IN by continuous flow strategies both with and without the inline rapid mixer. In all cases, batch coagulation was found to have significantly (p <.0001) lower FR_{hr} than continuous-flow strategies.

Table G.6. Results of Pooled *t*-test on Difference in Mean FR_{hr} Between Batch Coagulation and Alternative Continuous-Flow Coagulation Strategies

Configuration	Configuration	Difference (mBar h^{-1})	St. Error Diff. (mBar h^{-1})	Lower 95% Limit	Upper 95% Limit	*p*-Value
Batch	RM Only	27.84	2.99	21.94	33.75	<.0001
Batch	Control	62.86	5.71	51.57	74.16	<.0001
Batch	ISM	21.88	1.29	19.32	24.43	<.0001
Batch	HF-1000-⅛	41.31	4.12	33.17	49.45	<.0001
Batch	HF-2000-⅛	26.25	2.89	20.53	31.97	<.0001
Batch	RM+Control	18.31	2.11	14.14	22.49	<.0001
Batch	RM+ISM	17.23	1.66	13.94	20.51	<.0001
Batch	RM+ HF-1000-⅛	14.69	1.07	12.57	16.80	<.0001
Batch	RM+ HF-2000-⅛	6.55	0.67	5.23	7.86	<.0001

Table G.7 presents the results of the pooled *t*-test for the comparison between the four flocculator types with and without the inclusion of the inline rapid mixer. For all flocculator types, the FR_{hr} was found to be significantly (p <.0317) lower for combined rapid mixing+flocculation compared to flocculation alone.

Table G.7. Results of Pooled *t*-test on Difference in Mean FR_{hr} Between FLOCC and RM+FLOCC Across Four Flocculator Type

Configuration	Configuration	Difference (mBar h^{-1})	St. Error Diff. (mBar h^{-1})	Lower 95% Limit	Upper 95% Limit	*p*-Value
Control	RM+Control	44.55	6.16	32.38	56.72	<.0001
ISM	RM+ISM	4.65	2.14	0.41	8.88	.0317
HF-1000-⅛	RM+ HF-1000-⅛	26.62	4.33	18.07	35.18	<.0001
HF-2000-⅛	RM+ HF-2000-⅛	19.70	3.03	13.71	25.69	<.0001

Table G.8 uses the pooled *t*-test to evaluate the difference in means between RM only and RM+FLOCC with all four flocculator types. The addition of flocculation led to significantly (p <.0107) lower FR_{hr} compared to rapid mixing only, regardless of the flocculator type.

Table G.8. Results of Pooled *t*-test on Difference in Mean FR_{hr} Between RM and RM+FLOCC Across Four Flocculator Types

Configuration	Configuration	Difference (mBar h^{-1})	St. Error Diff. (mBar h^{-1})	Lower 95% Limit	Upper 95% Limit	*p*-Value
RM Only	RM+Control	9.53	3.68	2.24	16.81	.0107
RM Only	RM+ISM	10.61	3.44	3.81	17.42	.0025
RM Only	RM+ HF-1000-⅛	13.15	3.21	6.80	19.50	<.0001
RM Only	RM+ HF-2000-⅛	21.30	3.12	15.12	27.47	<.0001

G.2.4. Carman-Kozeny Equation

The Carman-Kozeny equation can be used to model the specific hydraulic resistance of the membrane cake according to Mulder (1996):

$$\alpha_{CR} = K\frac{{S_A}^2}{{\varepsilon_c}^3} \tag{G.10}$$

Where K is the Kozeny constant, S_A is the specific surface area of the cake ($\frac{m^2}{m^3}$), and ε_c is the cake porosity. This expression can also be written with the dependence of the specific surface area on the particle properties made explicit (Amjad et al. 2015):

$$\alpha_{CR} = K \frac{1}{{\varepsilon_c}^3} \left[\frac{6(1-\varepsilon_c)}{\psi d_{eq}} \right]^2 \quad \text{(G.11)}$$

Where ψ is the sphericity of the particles that form the cake layer and d_{eq} is equivalent spherical diameter. The sphericity of the particles is determined by first finding the area of a sphere with an equivalent volume to the particles comprising the cake layer. This value is then normalized to the measured intrinsic area of the particles to determine the sphericity, with $\psi = 1$ for a perfect sphere. The equivalent spherical diameter is the diameter of a sphere with an equivalent volume as the particles.

G.2.5. Treated Water Quality Indicators

The removal of several commonly used water quality indicators (WQI) was tracked for the filtration of raw synthetic water as well as for all C-IN pretreatment strategies (with various combinations of rapid mixing and flocculation) considered in this study. The turbidity, which was determined in accordance with Standard Method 2130B using a benchtop turbidimeter (2100AN, Hach, Loveland, CO) (American Public Health Association et al. 2012), was used to measure the removal of suspended particulates and colloidal materials. The apparent and true color, as well as the UV_{254}, were used as measures of the organic quality of the raw and treated synthetic water. The apparent and true color were measured in accordance with Hach Method 8025 on raw and filtered (GN-6 Metrical, Cytiva, Wilmington, DE) samples, respectively, using a benchtop spectrophotometer (DR6000, Hach, Loveland, CO). The UV absorbance at 254 nm of 0.45 µm filtered (GN-6 Metricel, Cytiva, Wilmington, DE) samples was measured in accordance with Standard Methods 5910B using a benchtop spectrophotometer (DR6000, Hach, Loveland, CO) (American Public Health Association et al. 2012). Table G.9 below presents a summary of the average removal for each WQI across all mixing configurations.

Table G.9. Removal of Key Water Quality Indicators by C-IN-LPM with Various Mixing Configurations

Flocculator Type	Treatment	Turbidity (%)	True Color (%)	App. Color (%)	UV_{254} (%)
Raw	-	97.30 ± 0.15	53.44 ± 1.33	75.30 ± 0.42	44.28 ± 0.01
Batch	-	98.46 ± 0.04	98.55 ± 0.72	99.25 ± 0.37	97.14 ± 0.50
RM Only	-	97.79 ± 0.30	99.43 ± 0.87	99.42 ± 0.45	97.37 ± 1.01
Control	RM+FLOCC	97.85 ± 0.16	99.38 ± 0.97	99.25 ± 0.37	97.00 ± 1.13
	FLOCC	98.12 ± 0.23	98.46 ± 0.77	98.95 ± 0.36	96.78 ± 2.24
ISM	RM+FLOCC	98.21 ± 0.14	99.08 ± 1.01	99.70 ± 0.46	96.79 ± 1.99
	FLOCC	98.08 ± 0.10	99.07 ± 1.01	99.40 ± 0.47	96.45 ± 0.29
HF-1000-⅛	RM+FLOCC	98.19 ± 0.38	98.79 ± 0.94	99.25 ± 0.37	96.46 ± 1.17
	FLOCC	98.27 ± 0.07	98.81 ± 0.92	99.25 ± 0.37	96.72 ± 0.10
HF-2000-⅛	RM+FLOCC	97.99 ± 0.04	99.39 ± 0.94	99.40 ± 0.46	97.24 ± 0.70
	FLOCC	97.74 ± 0.23	99.39 ± 0.95	99.25 ± 0.37	95.60 ± 4.78

Note: ± represents the 95% confidence interval calculated using the students t-test as $\mu \pm t_{0.025,n}\frac{s}{\sqrt{n}}$ where $n = 6$ for replicated measures made in triplicate.

The ANOVA was used to evaluate whether the means for each WQI differed statistically from one another. We can represent the experimental observations using the means model (Montgomery 2020):

$$y_{ij} = \mu_{MM} + \tau_{MM,i} + \epsilon_{ij} \tag{G.12}$$

Where μ_{MM} is the overall mean, $\tau_{MM,i}$is the effect of the i^{th} treatment, ϵ_{ij} is the random error component, and y_{ij} is the j^{th} observation for the i^{th} treatment with a variance of σ^2. The one-way ANOVA tests the null hypothesis that the treatment effects are zero against the alternative hypothesis that at least one effect is different from zero:

$$H_0: \tau_1 = \tau_2 = \cdots \tau_a = 0$$
$$H_1: \tau_i \neq 0 \text{ for at least one } i$$

The test statistic is given by the ratio (Montgomery 2020):

$$F_0 = \frac{SS_{treatments}/(a-1)}{SS_E/(N-a)} = \frac{MS_{Treatments}}{MS_E} \tag{G.13}$$

Which has an *F* distribution with $a-1$ and $N-a$ degrees of freedom. Note that a is the number of treatment levels and N is the total number of observations. The variability between treatments is given by the sum of squares due to treatments, while the variability within treatments is the sum of squares due to error and represents the pure random experimental error (Berthouex and Brown 2002). These are defined mathematically by Montgomery and Runger (2014):

$$SS_{Treatments} = n\sum_{i=1}^{a}(\bar{y}_{i\,.} - \bar{y}_{..})^2 \tag{G.14}$$

$$SS_{Error} = \sum_{i=1}^{a}\sum_{j=1}^{n}\left(y_{ij} - \bar{y}_{i\,.}\right)^2 \tag{G.15}$$

Where n is the number of observations for the i^{th} treatment, $\bar{y}_{i\,.}$ is the average of the observations for the i^{th} treatment, $\bar{y}_{..}$ is the grand average of all observations across the i different treatments, and all other parameters have been previously defined. The null hypothesis should be rejected, with 95% confidence, if the following condition is met:

$$F_0 > F_{0.05,a-1,N-a}$$

Alternatively, using JMP® Student 19 (SAS Institute Inc., Cary, NC) the *p*-value that corresponds to the *F* statistic can be computed and used to compare the means at any level of confidence.

Table G.10 presents the ANOVA analysis comparing the mean WQI removals for direct filtration (i.e., raw water filtration) and C-IN. Here, it can be seen that the *p*-values are all below 0.05. Therefore, there is evidence that the null hypothesis should be rejected and that the mean removals are not the same. Practically, this confirms that pre-treatment by C-IN, regardless of the mixer type, improves the removal of WQIs compared to direct filtration.

Table G.10. One-way ANOVA Test for Removal of WQIs by Direct Filtration and C-IN Pretreatment

Source of Variation	Sum of Squares (SS)	Degrees of Freedom (DF)	Mean Square (MS)	F_0	*p*-Value
Turbidity Removal					
Flocculator	2.016	10	0.202	3.315	0.031
Error	0.669	11	0.061		
Total	2.686	21			
True Color Removal					
Flocculator	3782.78	10	378.28	1545.14	<.0001

Error	2.693	11	0.245		
Total	3785.48	21			
Apparent Color Removal					
Flocculator	1048.82	10	104.88	2564.79	<.0001
Error	0.450	11	0.04		
Total	1049.27	21			
UV_{254} Removal					
Flocculator	5011.18	10	501.12	1403.11	<.0001
Error	3.929	11	0.357		
Total	5015.11	21			

Table G.11 presents the results of the *F*-test for the four WQIs with different C-IN strategies. In all cases, the *p*-value was greater than 0.05 indicating that there is insufficient evidence to reject the null hypothesis, and the mean removal values are statistically similar for all C-IN strategies.

Table G.11. One-way ANOVA Test for Removal of WQIs Across Different C-IN Mixing Configurations

Source of Variation	**Sum of Squares (SS)**	**Degrees of Freedom (DF)**	**Mean Square (MS)**	F_0	***p*-Value**
Turbidity Removal					
Flocculator	0.937	9	0.104	1.592	0.239
Error	0.654	10	0.065		
Total	1.592	19			
True Color Removal					
Flocculator	2.434	9	0.270	1.849	0.176
Error	1.463	10	0.146		
Total	3.898	19			
Apparent Color Removal					
Flocculator	0.655	9	0.073	2.701	0.069
Error	0.269	10	0.049		
Total	0.924	19			
UV_{254} Removal					
Flocculator	4.675	9	0.519	1.322	0.333
Error	3.929	10	0.393		
Total	8.60	19			

The WQIs were also assessed for the three HCTFs with varying HRT values to see whether HRT had an impact on their removal. From Table G.12 below the *p*-values are all greater than 0.05 indicating that there is insufficient evidence to reject the null hypothesis. Therefore, the flocculation HRT in HCTF systems did not have a significant impact on the removal of turbidity, true and apparent color, and UV_{254} for this synthetic water.

Table G.12. One-way ANOVA Test for Removal of WQIs by HCTFs With Varying HRT

Source of Variation	Sum of Squares (SS)	Degrees of Freedom (DF)	Mean Square (MS)	F_0	*p*-Value
Turbidity Removal					
HRT	0.042	2	0.021	0.256	0.789
Error	0.249	3	0.083		
Total	0.292	5			
True Color Removal					
HRT	0.530	2	0.265	1.044	0.453
Error	0.762	3	0.254		
Total	1.29	5			
Apparent Color Removal					
HRT	0.680	2	0.340	1.282	0.396
Error	0.796	3	0.265		
Total	1.476	5			
UV_{254} Removal					
HRT	0.785	2	0.393	4.896	0.114
Error	0.241	3	0.080		
Total	1.026	5			

G.3. References

Albertazzi, J., F. Florit, V. Busini, and R. Rota. 2021. "Mixing Efficiency and Residence Time Distributions of a Side-Injection Tubular Reactor Equipped with Static Mixers." *Industrial & Engineering Chemistry Research*, 60 (29): 10595–10602. https://doi.org/10.1021/acs.iecr.1c00575.

American Public Health Association, Water Environment Foundation, and American Water Works Association. 2012. *Standard Methods for the Examination of Water and Wastewater*. 1496. Edited by L. Clesceri, A. Greenberg, and A. Eaton. 22nd Editi. Washington: APHA Press.

Amjad, H., Z. Khan, and V. V. Tarabara. 2015. "Fractal structure and permeability of membrane cake layers: Effect of coagulation–flocculation and settling as pretreatment steps." *Separation and Purification Technology*, 143: 40–51. https://doi.org/10.1016/j.seppur.2015.01.020.

Bacchin, P., P. Aimar, and R. W. Field. 2006. "Critical and sustainable fluxes: Theory, experiments and applications." *Journal of Membrane Science*, 281 (1–2): 42–69. https://doi.org/10.1016/j.memsci.2006.04.014.

Beier, S. P., and G. Jonsson. 2010. "Critical Flux Determination by Flux-Stepping." *AIChE Journal*, 56 (7): 1739–1747.

Benjamin, M. M., and D. Lawler. 2013. *Water Quality Engineering: Physical/Chemical Treatment Processes*. 1st ed. Hoboken, NJ, USA: John Wiley & Sons.

Berthouex, P. M., and L. C. Brown. 2002. *Statistics for Environmental Engineers*. 2nd ed. Boca Raton, FL: Lewis Publishers.

Bonakdari, H., I. Ebtehaj, and J. D. Ladouceur. 2023. *Machine Learning in Earth, Environmental and Planetary Sciences: Theoretical and Practical Applications*. 1st ed. Amsterdam, Netherlands: Elsevier.

Choi, K. Y. J., and B. A. Dempsey. 2005. "Bench-scale evaluation of critical flux and TMP in low-pressure membrane filtration." *Journal AWWA*, 97 (7): 134–143.

Crittenden, J. C., R. R. Trussell, D. W. Hand, K. J. Howe, and G. Tchobanoglous. 2012. *Water Treatment: Principles and Design*. 3rd ed. New York, NY: McGraw-Hill.

Field, R. W., D. Wu, J. A. Howell, and B. B. Gupta. 1995. "Critical flux concept for microfiltration fouling." *Journal of Membrane Science*, 100 (3): 259–272. https://doi.org/10.1016/0376-7388(94)00265-Z.

Gonzalez-Galvis, J. P., and R. M. Narbaitz. 2020. "Large batch bench-scale dissolved air flotation system (LB-DAF) for drinking water treatability tests." *Environmental Science: Water Research and Technology*, 6 (4): 1004–1017. Royal Society of Chemistry. https://doi.org/10.1039/c9ew00935c.

Howell, J. A. 1995. "Sub-critical flux operation of microfiltration." *Journal of Membrane Science*, 107 (1–2): 165–171. https://doi.org/10.1016/0376-7388(95)00114-R.

Huang, H., T. Young, and J. G. Jacangelo. 2008. "Unified Membrane Fouling Index for Low Pressure Membrane Filtration of Natural Waters : Principles and Methodology." 42 (3): 714–720. https://doi.org/10.1021/es071043j.

Kollu, K., and B. Örmeci. 2012. "Effect of particles and bioflocculation on ultraviolet disinfection of Escherichia coli." *Water Research*, 46 (3): 750–760. https://doi.org/10.1016/j.watres.2011.11.046.

Kollu, K., and B. Örmeci. 2015. "Monitoring Simulated Bioflocculation: Application of Micro-Flow Imaging Technology." *Water, Air, & Soil Pollution*, 226 (3): 79. https://doi.org/10.1007/s11270-015-2299-4.

Le Clech, P., B. Jefferson, I. S. Chang, and S. J. Judd. 2003. "Critical flux determination by the flux-step method in a submerged membrane bioreactor." *Journal of Membrane Science*, 227 (1–2): 81–93. https://doi.org/10.1016/j.memsci.2003.07.021.

Montgomery, D. C. 2020. *Design and Analysis of Experiments*. 10th ed. Hoboken, NJ, USA: Wiley.

Montgomery, D. C., and G. C. Runger. 2014. *Applied Statistics and Probability for Engineers*. 6th ed. Hoboken, NJ: John Wiley & Sons.

Mulder, M. 1996. *Basic Principles of Membrane Technology*. 2nd ed. Dordrecht, The Netherlands: Kluwer Academic Publisher.

Nguyen, A. H., J. E. Tobiason, and K. J. Howe. 2011. "Fouling indices for low pressure hollow fiber membrane performance assessment." *Water Research*, 45 (8): 2627–2637. Elsevier Ltd. https://doi.org/10.1016/j.watres.2011.02.020.

Sharma, D. K., D. King, P. Oma, and C. Merchant. 2010. "Micro-Flow Imaging: Flow Microscopy Applied to Sub-visible Particulate Analysis in Protein Formulations." *The AAPS Journal*, 12 (3): 455–464. https://doi.org/10.1208/s12248-010-9205-1.

APPENDIX H

Supplemental Information for Chapter 7

Context: This appendix presents supporting information associated with Chapter 7 of this thesis, *Phased-Inline-Coagulation Pretreatment for Low-Pressure Membrane Fouling Reduction*.

List of Abbreviations

ACH	Aluminum chlorohydrate
ANOVA	Analysis of variance
BSA	Bovine serum albumin
BSA^*	FEEM-derived DOC concentration of bovine serum albumin
BWE	Hydraulic backwash efficiency
CFSTR	Continuous flow stirred tank reactor
C-IDX	Coating index
C-IN-P	Phased-inline coagulation
DI	Deionised water
DOC	Dissolved organic carbon
DOM	Dissolved organic matter
DW	Distilled water
DW-RO	Distilled water passed through 5-stage reverse osmosis unit
FEEM	Fluorescence excitation-emission matrices
FR_{hr}	Hydraulically reversible fouling rate
FR_{hirr}	Hydraulically irreversible fouling rate
G	Mean velocity gradient
HA	Humic acid
HA^*	FEEM-derived DOC concentration of humic acid
HRT	Hydraulic retention time
H-SUVA	High SUVA synthetic water
KHP	Potassium hydrogen phthalate
L-SUVA	Low SUVA synthetic water
MAE	Mean absolute error
MAPE	Mean absolute percent error
MSE	Mean square error
M-SUVA	Medium hydrophobicity synthetic water
PARAFAC	Parallel factor analysis
PDF	Probability density function
PFR	Plug flow reactor

R^2	Coefficient of determination
RMSE	Root mean square error
SA	Sodium alginate
SA^*	FEEM-derived DOC concentration of sodium alginate
SSE	Sum of squared errors
SUVA	Specific ultraviolet absorbance at 254nm
TMC	Tubular multichannel
UV_{254}	Ultraviolet absorbance at 254nm
ZP	Zeta potential

List of Variables

Variable	Description
ϑ	Theoretical hydraulic detention time (s)
ϵ_{ij}	Random error of the *i* samples for the *j* treatments in means model
μ_{MM}	Overall mean of the *i* samples for the *j* treatments in means model
$\tau_{MM,i}$	Effect of the i^{th} treatment in means model
a,b,c	Model fitting parameters
A_i	Actual value for the i^{th} sample
BWE	Hydraulic backwash efficiency (%)
c_{in}	Influent tracer concentration (µS cm^{-1})
$c_s(t)$	Effluent tracer concentration (µS cm^{-1})
E_i	Estimated value for the i^{th} sample
$E(t)$	Exit age distribution for tracer study
F_0	F-ratio test statistic for F-test
$F(t)$	Cumulative age distribution for tracer study
$H_\vartheta(t)$	Heaviside function for tracer studies
H_0	Null hypothesis
H_1	Alternate hypothesis
MAE	Mean absolute error
$MAPE$	Mean absolute percent error (%)

MS_E	Mean squared error
$MS_{Treatments}$	Mean squared error due to treatments
P_d	Coagulant dosing time as a percent of the cycle length (%)
R^2	Coefficient of determination
$RMSE$	Root mean square error
s_1^2	Sample variance of population 1
s_2^2	Sample variance of population 2
SS_E	Sum of squares due to error
${s_p}^2$	Pooled sample variance
$SS_{treatments}$	Sum of squares due to treatments
$\bar{t}$	Mean HRT estimated from tracer studies (min)
$TMP_{n-1,f}$	TMP at the end of cycle *n-1* (mBar)
$TMP_{n,i}$	TMP at the beginning of cycle *n* (mBar)
$TMP_{n-1,i}$	TMP at the beginning of cycle *n-1* (mBar)
y_{ij}	The j^{th} observation for the i^{th} treatment with a variance of σ^2 in means model (varies)
$\bar{y}_{i\,.}$	Average of the observations for the i^{th} treatment (varies)
$\bar{y}_{..}$	Grand average of all observations across the *i* different treatments (varies)

H.1. Supplemental Methodological Details

H.1.1. Survey of Natural Water Quality

In designing the composition of the synthetic challenge waters, a survey was performed to identify the typical range of organic and inorganic water quality indicators (WQIs) from available literature that had natural (e.g., lake or river) waters as their source. Fig. H.1 presents the results for dissolved organic carbon (DOC), turbidity, alkalinity, and pH in the form of a box plot. It should be noted that the mean, median, and population number for each parameter are summarized above the boxplot. Furthermore, not every literature study presented values for all the WQIs, resulting in varying numbers of samples for each boxplot.

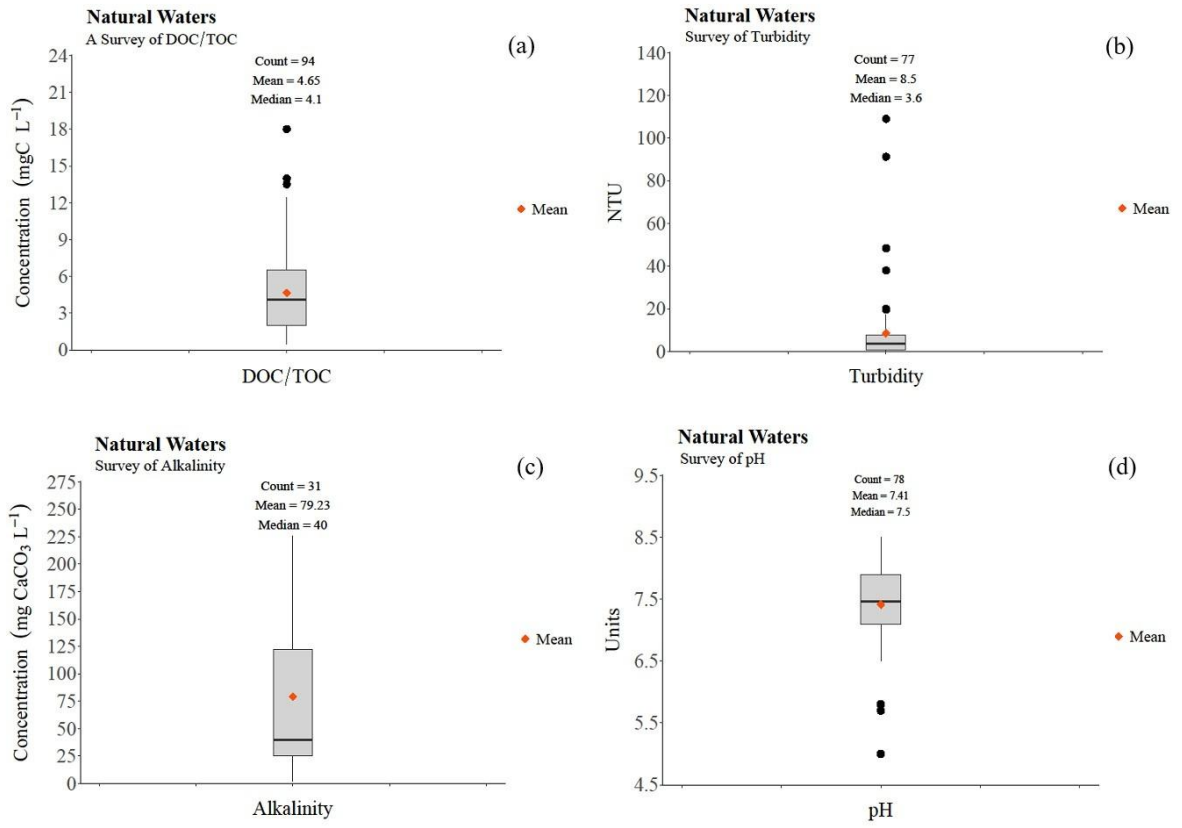


Fig. H.1. Survey of WQIs from natural water sources reported in literature: **(a)** DOC; **(b)** Turbidity; **(c)** Alkalinity; **(d)** pH. Note: Data obtained from literature studies (Arhin et al. 2018, 2019; Best et al. 2001; Brinkman and Hozalski 2011; Chen et al. 2007; Choi et al. 2008; Croft 2012; Dang et al. 2010; Dixon et al. 2013; Farahbakhsh and Smith 2002; Hillis 2006; Howe et al. 2006; Huck et al. 2011; Judd and Hillis 2001; Jung and Kang 2003; Kamińska et al. 2020; Keucken et al. 2017; Kim et al. 2006; Kimura et al. 2014, 2015, 2018; Kimura and Kume 2020; Lee et al. 2000; Mosqueda-Jimenez et al. 2004; Nguyen et al. 2007; Oh and Lee 2005; Paar et al. 2011; Park et al. 2015, 2002; Peiris et al. 2010; Peldszus et al. 2011; Peleato et al. 2017; Pernitsky and Edzwald 2006; Peter-Varbanets et al. 2011; Pezeshk and Narbaitz 2012; Rahman et al. 2014; Ratajczak et al. 2012; Siddiqui et al. 2000; Siembida-Lösch et al. 2016; Su et al. 2017; Walker and Narbaitz 2016; Walsh et al. 2009; Wang et al. 2015; Waterman 2008; Wray et al. 2014, 2016; Wu et al. 2022; Xiangli et al. 2008; Xu and Narbaitz 2016; Yamamura et al. 2007; Yan et al. 2007; Yang et al. 2010; Zevenhuizen et al. 2015; Zhao et al. 2015).

Based on the results, a DOC concentration of 5 mg-C L^{-1} was selected for the current study, as it closely approximates the mean value reported across 94 natural water sources. The turbidity and pH were set to 5 NTU and 7.5, respectively, as intermediate values between the corresponding mean and median values reported in the literature. Alkalinity was fixed at 50 mg $CaCO_3$ L^{-1}, which similarly falls within this range of values and also closely matches the conditions used by several previous authors (Alresheedi et al. 2019; Cheng et al. 2016; Katsoufidou et al. 2010; Tian et al. 2013; Zhang et al. 2018).

H.1.2. Preparation of Stock Model Organic Compounds and Synthetic Water

Stock solutions of bovine serum albumin (BSA), humic acid (HA), and sodium alginate (SA) were prepared in deionised water (DI) (ZenoPure Quatra 90LC, Zenon Environmental Inc., Burlington, ON). As BSA was found to be readily soluble in DI, 0.5 g BSA was transferred to a half-full volumetric flask using a glass weighing scoop (SL000922, StonyLab, Nesconset, NY) and dissolved by swirling before being brought to volume with DI. The HA stock solution was prepared using a two-step procedure. First, 0.5 g of HA was dissolved in 100 mL of 0.025 M NaOH using a 250 mL Erlenmeyer flask (Pyrex Conical Flask, Corning, NY) and vigorous mixing by magnetic stir bar as recommended by others (Maeng et al. 2017; Yang et al. 2021). After several hours, the solution (and rinsate) was transferred to a 1 L volumetric flask (Lifetime-Red 5660 Class-A, Corning, NY) and brought to volume using DI. SA was found to be difficult to completely dissolve in DI as, due to its high hydrophilicity, it hydrates rapidly and forms a gel. To ensure complete dissolution of SA and the homogenization of the solution, a variable speed mixer (OS-200D-C-SYS, Cole Parmer, Quebec, QC) set to 1,100 rpm was used to induce a vortex prior to gradual addition of 0.5 g of SA powder at a point near the impeller shaft. After vigorous mixing for at least 2 h, the solution (and rinsate) was transferred to a 1 L volumetric flask (Lifetime-Red 5660 Class-A, Corning, NY) and brought to volume. All stock solutions were magnetically stirred for a period of 24 h (VWR Advance Stirrer, VWR, Mississauga, ON, Canada) prior to being filtered through a 0.45 μm membrane (GN-6 Metricel, Cytiva, Marlborough, MA) to remove residual insoluble matter. Filtered solutions were placed in sterilized (SR-24B, Consolidated Sterilizer Systems, Billerica, MA) glass 1 L volumetric flasks and stored in the dark at 4 °C prior to use. Stock

solutions were stirred and brought to room temperature prior to the preparation of all working solutions.

The synthetic challenge waters were prepared using the large baffled completely mixed reactor developed by Gonzalez-Galvis and Narbaitz (2020, 2022) as a mixer. Prior to use, the reactor, the baffle insert, and the impeller were thoroughly rinsed with distilled water (DW). The baffle insert and the impeller (10 cm x 10 cm stainless steel) were placed inside the reactor and the assembly placed on a high-resolution industrial balance (Model 3807MP8-1, Sartorius Gottingen, Germany). The reactor was then filled with a measured amount of DW which has been passed through a five-stage commercial reverse osmosis-activated carbon system (TGI-525 NO. 92821, TGI Pure Water Systems, Brea, CA), abbreviated as DW-RO water. Pre-determined volumes of stock model organic compounds were measured using mechanical pipettors (High Performance Pipettor, VWR, Mississauga, ON, Canada) and/or volumetric flasks (Class A, Corning, New York, NY) and added to the reactor. Next, the inorganic background components including kaolin clay (~5 mg L^{-1}, corresponding to a turbidity of 5.5 NTU; Laboratory Grade 75185, Fisher Scientific, Hampton, NH), calcium chloride (0.6mM; Dried Powder 97%, Thermo Scientific, Hampton, NH), and sodium bicarbonate (0.9 mM; Certified ACS, Fisher Scientific, Hampton, NH) were added to the reactor and it was brought to the desired final volume. The reactor was then mounted into its frame and mixed using a high-torque, low-speed motor (Stir-Pak 50007-12, Cole Parmer, Quebec, QC, Canada) operated at its maximum speed (setting 10 on the speed controller, which is approximately a G value of 296 s^{-1}). The batches of synthetic water were thoroughly mixed in this system for a period of more than 2 h to ensure dissolution of the inorganic background and homogeneity of the solution.

H.1.3. Standard Curves for Model Organic Compounds

As part of the preliminary work to determine the suitable combinations of model organic compounds for each water type (based on the DOC and specific ultraviolet absorbance at 254 nm (SUVA) values), standard curves relating the mass concentration and DOC were generated for HA, BSA, and SA. These relationships are presented in Fig. H.2. The analysis of DOC was performed using a wet-chemical oxidation analyzer (Phoenix 8000, Tekmar-Dohrmann, Cincinnati, OH) with oxidation by UV-Persulfate in accordance with Standard Methods 5310C. Additional details regarding the methodology for DOC quantification is provided in Section H.1.7.

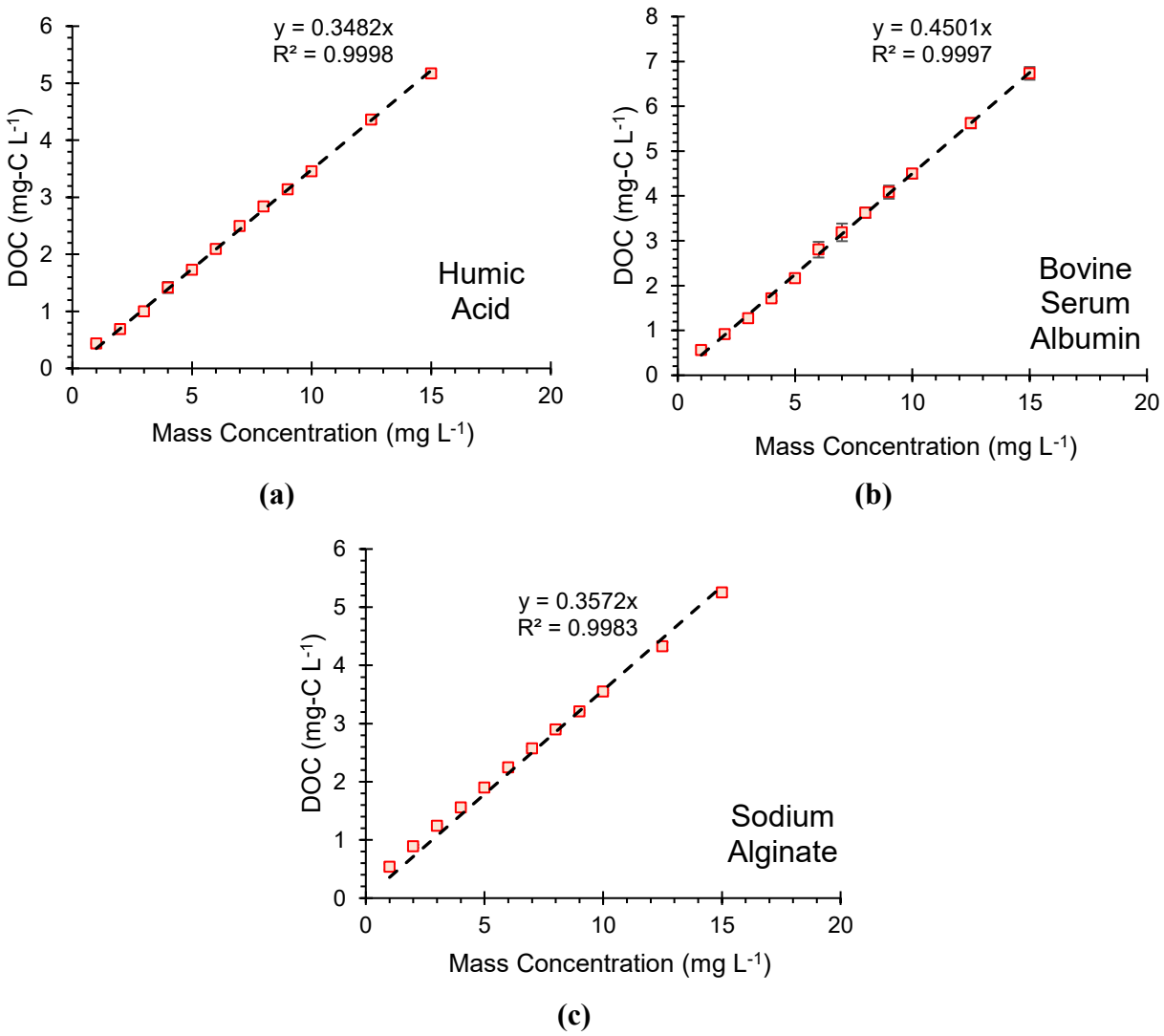


Fig. H.2. Standard curve relating mass concentration to DOC for: **(a)** HA; **(b)** BSA; **(c)** SA.

Linear regression analysis was performed using Excel's built-in *Data Analysis* tool-pack for each model organic compound to determine the relationship between mass concentration and DOC. As the DOC of the background DI is accounted for by the DOC analyzer during instrument calibration, the regression was set to pass through the origin. Table H.1 below summarizes the slope value for each model compound as well as the goodness-of-fit in terms of the coefficient of determination and the *p*-value, determined by the analysis of variance (ANOVA). In all cases, the linear models were found to be statistically significant (i.e., $p < 0.05$) and described the variation in the data well, with $R^2 > 0.9983$.

Table H.1. Regression Analysis of Standard Curves for Model Organics Measured by DOC Analyzer

Organic Type	Slope (mg-C mg-TOT^{-1})	R^2	*p*-Value
HA	0.3482 ± 0.0033	0.9998	<.0001
BSA	0.4501 ±0.0058	0.9997	<.0001
SA	0.3572 ± 0.0066	0.9983	<.0001

Note. ± represents the 95% confidence interval on the model parameters

The repeatability of the analysis was also assessed by preparing and analyzing (in triplicate) a second set of the same standards for each model organic. Following regression analysis, the 95% confidence intervals (CIs) on the slope values were found to be overlapping for all three organic compounds (Fig. H.3).

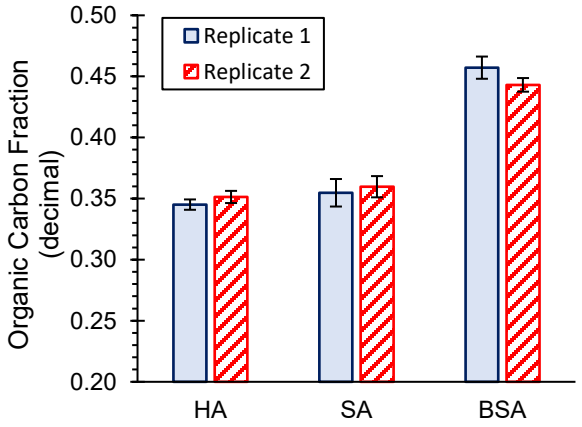


Fig. H.3. Assessment of the reproducibility of mass-concentration:DOC relationships for HA, BSA, and SA. Note: error bars represent the 95% CIs on the regressed slope value.

H.1.4. Preliminary Jar Testing

Preliminary jar testing was conducted to determine the optimum coagulation chemistry for the various combinations of water and coagulant types. Alum (ALS, Kemira Water Solutions, Varennes, QC) and aluminum chlorohydrate (ACH) (PAX-XL1900, Kemira Water Solutions, Varennes, QC) were the two coagulant types investigated. Alum was chosen to match our previous work (see Chapter 3 and Chapter 4) while ACH was selected as several studies have noted that it

has improved sludge properties (Bratby 2016), is effective over a broad range of pH values (Papineau et al. 2019), and has improved floc strength under low-temperature conditions (Omar and Aziz 2021). A summary of the main properties of the two coagulants is given in Table H.2.

Table H.2. Summary of Technical Properties for Alum and ACH

Product Name	Specific Gravity	Percent Aluminum	Basicity (%)
ALS (Alum)	1.32	4.3	N/A
PAX-XL 1900 (ACH)	1.32-1.35	12.1-12.7	82.4-84.2

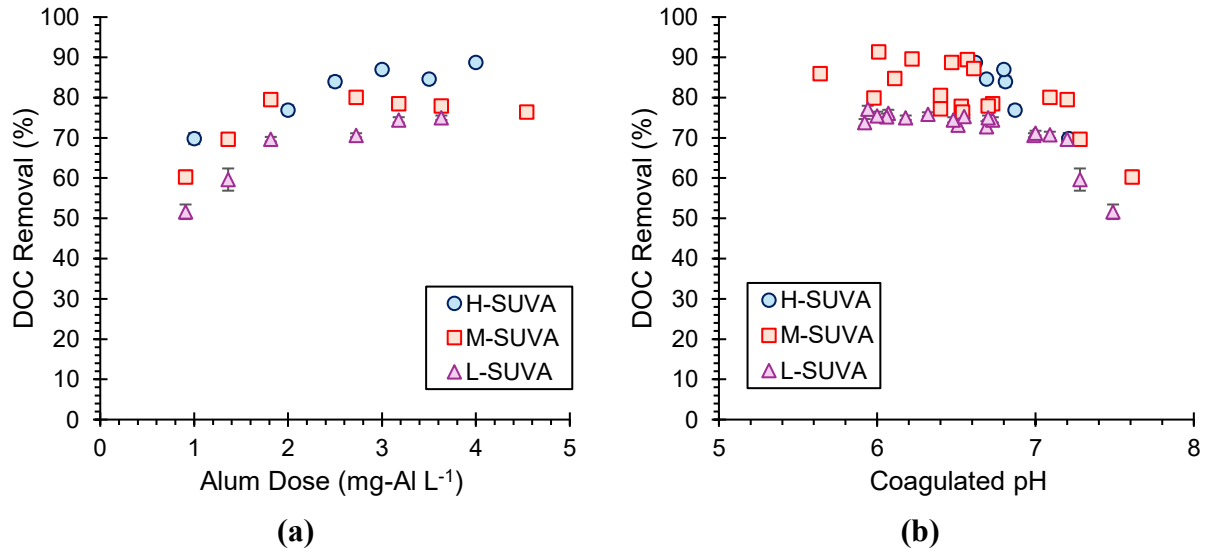
Jar testing was conducted using a Phipps and Bird Model 7790-400 (Richmond, VA) with 2 L gator jars (BKER, Phipps and Bird, Richmond, VA) and an illumination table. The synthetic waters were prepared according to the procedure outlined in Section H.1.2. The gator jars were individually placed on a high-resolution industrial balance (Model 3807MP8-1, Sartorius Gottingen, Germany) and filled to 2000 g (dilute solutions assumption is employed). These jars were then placed on the illumination table, the location of the stirrer paddle (slightly off-centre with sufficient distance between the jar walls) was verified, and the stirrer set to a speed of 120 rpm ($G \sim 196\ s^{-1}$). Pre-calculated volumes of coagulant solution were pipetted into disposable plastic cups and then brought to a volume of 5 mL with DI. At the same instant, the coagulant was added to all four jars from the disposable plastic cups. The cups were then rinsed with DI into the gator jar to ensure all the coagulant is delivered to the jar. Rapid mixing was performed for a total duration of 60 s at 120 rpm before the stirrer was slowed to 30 rpm ($G \sim 24.6\ s^{-1}$) for a period of 15 min. After the flocculation period, the stirrer was turned off, the paddles were withdrawn from the jar, and the jar was left to settle under quiescent conditions for a total of 30 min. Mixing speeds, durations, settling times, and procedures were selected in consultation with a number of sources including Bratby (2016), Kawamura (2000), ASTM D2035-13 (D19 Committee n.d.), and Pivokonský et al. (2022).

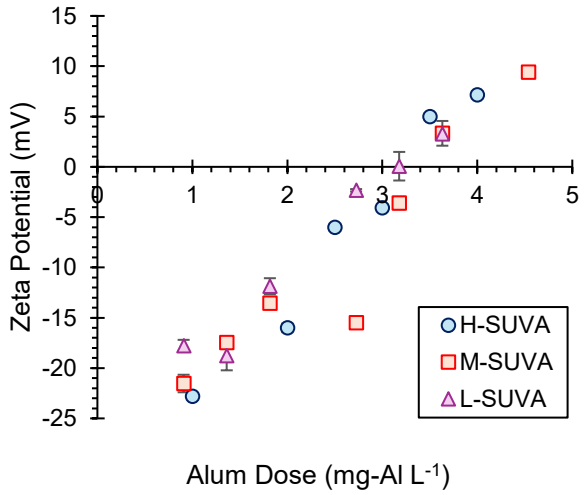
For pH and zeta potential (ZP) measurement, the samples were collected following the rapid mixing stage and analyzed immediately. The pH was measured using a portable meter (HQ30d, Hach, London, ON, Canada) and electrode (Red Rod Intellical PHC80501, Hach, London, ON, Canada), which was calibrated prior to each use by a three-point method, using standard buffer solutions of pH 4, 7, and 10 (BDH5024/ BDH5046/ BDH5072, VWR,

Mississauga, ON, Canada). ZP was measured using a zetasizer nano particle analyzer (Nano ZS Series Model ZEN 3600, Malvern Instruments Ltd., Worcestershire, UK) and a folded capillary cell (DTS1060/1070, Malvern Instruments Ltd., Worcestershire, UK). For each test condition, two samples were collected and measured for ZP in triplicate (each replicate with up to 100 sub-runs) to help reduce the amount of noise in the response.

Following the 30-min settling period, samples of coagulated/flocculated/settled water were collected from sampling ports located at one-third depth of the jar for analysis. Samples for DOC were filtered using 0.45 µm membrane filters (GN-6 Metricel, Cytiva, Marlborough, MA) and analyzed using a UV-Persulfate analyzer (Phoenix 8000, Tekmar-Dohrmann, Cincinnati, OH). Further details regarding the DOC analysis are provided in Section H.1.7.

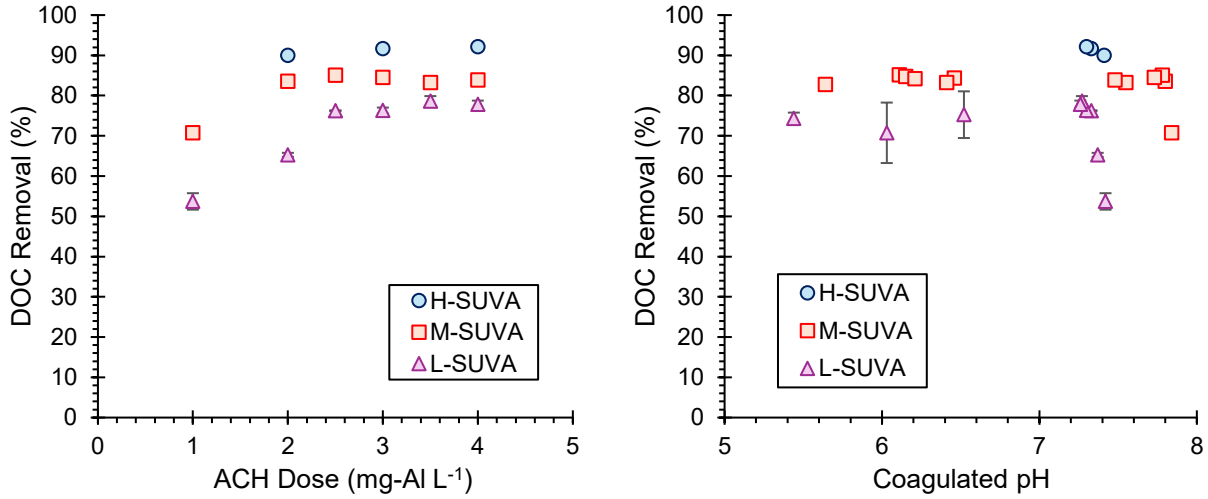
The DOC removal, coagulated pH, and coagulated ZP values for alum and ACH coagulant types are presented in Fig. H.4 and Fig. H.5, respectively. For both coagulant types and all three water types, the DOC removal was seen to reach a plateau ~ 2.5 mg-Al L^{-1}. For alum, the ZP was found to be circumneutral for all three water types at a coagulant dose ~ 3.0-3.2 mg-Al L^{-1}, while for ACH ~ 3.3-4.0 mg-Al L^{-1} was required. According to these results, a coagulant dose of 3 mg-Al L^{-1} was selected for use throughout the study.



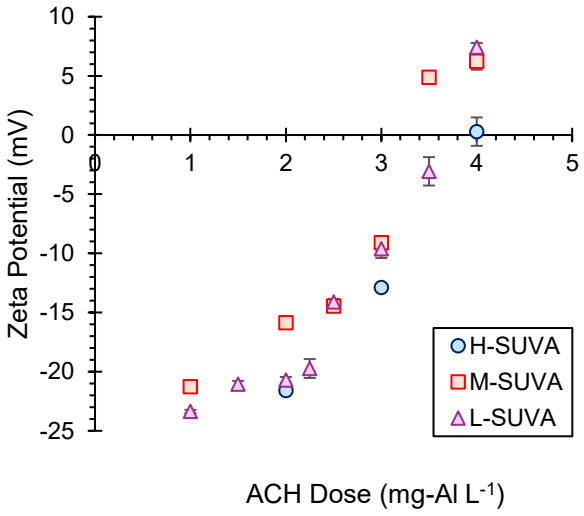


(c)

Fig. H.4. Preliminary jar test data for three synthetic challenge waters with alum: **(a)** DOC removal vs. alum dose; **(b)** DOC removal vs. coagulated pH; **(c)** Coagulated ZP vs. alum dose. Note: additional tests were performed for various dose conditions with pH adjustment by sulfuric acid.



(a) **(b)**



(c)

Fig. H.5. Preliminary jar test data for three synthetic challenge waters with ACH: **(a)** DOC removal vs. alum dose; **(b)** DOC removal vs. coagulated pH; **(c)** Coagulated ZP vs. alum dose.

H.1.5. Tracer Study for Hydraulic Residence Time Assessment

To determine the hydraulic residence time (HRT) of the small-scale inline rapid mixer and helical flocculator preliminary tracer studies were performed using a precision metering pump (Optos 3HM, Eldex, Napa, CA) at the same flowrate as for the bench-scale filtration tests (~5.6 mL min^{-1}). A 2% salt solution was used as the tracer and was prepared by dissolving NaCl (Certified ACS, Fisher Scientific, Hampton, NH) into DI (ZenoPure Quatra 90LC, Zenon Environmental Inc., Burlington, ON), resulting in a conductivity of approximately 28.8 mS cm^{-1}. The test was performed using a step-input approach: the system was initially pumping DI at the specified flowrate prior to the feed stream being instantaneously switched to the NaCl solution. Conductivity was the basis of analysis, with samples analyzed every minute of operation (limited by the volume required for analysis) using a benchtop conductivity meter (Orion Star 3, Thermo Scientific, St. Louis, MO).

Data analysis was performed according to the method outlined by Benjamin and Lawler (2013). For a step-input tracer test, the cumulative age distribution, $F(t)$, can be determined by normalizing the time-variant effluent concentration by the influent concentration according to Eqn. H.1 below:

$$F(t) = \frac{c_s(t)}{c_{in}} \tag{H.1}$$

Where $c_s(t)$ is the effluent tracer concentration, and c_{in} is the influent tracer concentration. The mean HRT value is defined as the ratio of the first to zeroth moment of the probability density function (PDF) of residence times. The PDF is given by the exit age distribution, $E(t)$, which is the derivative of the cumulative age distribution, therefore:

$$\bar{t} = \frac{\int_0^\infty tE(t)\mathrm{d}t}{\int_0^\infty E(t)\mathrm{d}t} = \frac{\int_0^\infty t[\mathrm{d}F(t)/\mathrm{d}t]\mathrm{d}t}{\int_0^\infty [\mathrm{d}F(t)/\mathrm{d}t]\mathrm{d}t} = \frac{\int_{F(0)}^{F(\infty)} t\mathrm{d}F(t)}{\int_{F(0)}^{F(\infty)} \mathrm{d}F(t)} = \frac{\int_{F(0)}^{F(\infty)} t\mathrm{d}F(t)}{F(\infty) - F(0)} \tag{H.2}$$

As the probability that a tracer particle will remain in the reactor for less than some time, t=∞, is equal to one, and the probability that tracer particles have left the reactor at time, t=0, is zero, we have $F(\infty) = 1$ and $F(0) = 0$. Thus, Eqn. H.2 can be simplified to:

$$\bar{t} = \int_0^1 t\mathrm{d}F(t) \tag{H.3}$$

For discrete data collected from the step-tracer test the integral form of the expression shown in Eqn. H.3, which was derived for a continuous data set, can be represented as follows:

$$\bar{t} = \sum_{all\ i} \left(\frac{t_i + t_{i-1}}{2}\right)(F_i(t) - F_{i-1}(t)) \tag{H.4}$$

Where t_i and t_{i-1} represent the i^{th} and $i-1^{th}$ time step of the tracer study.

In the present study, the small-scale rapid mixer was modeled as a continuous-flow stirred tank reactor (CFSTR), while the helical flocculator was represented as a plug-flow reactor (PFR). For an ideal CFSTR, the cumulative age distribution, $F(t)$, can be determined by performing a simple mass balance around the reactor and isolating for the effluent concentration. The expression that results is (Benjamin and Lawler 2013; Droste 1996):

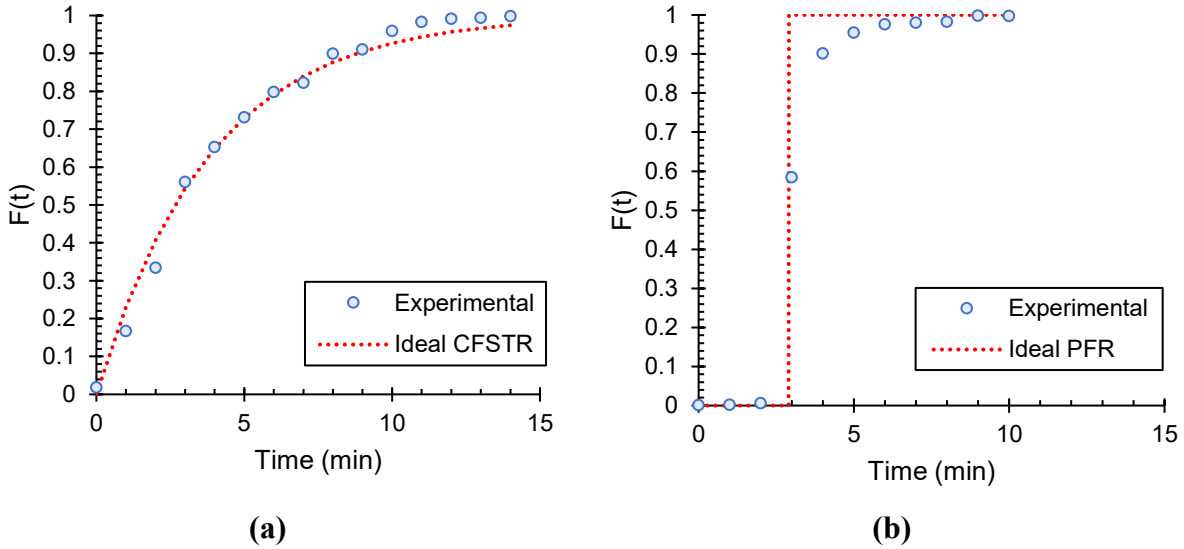
$$F(t) = 1 - e^{-t/\vartheta} \tag{H.5}$$

Where ϑ is the theoretical detention time (min), given by the ratio of the reactor volume to system flowrate (i.e., $\vartheta = {}^{V}/_{Q}$), and t is the elapsed time since the beginning of the tracer test (min). For

the ideal PFR, $F(t)$ is modeled by the Heaviside function (Eqn. H.6), where $F(t) = 0$ for $t < \vartheta$ and $F(t) = 1$ for $t \geq \vartheta$

$$F(t) = H_{\vartheta}(t) = \begin{cases} 0, t < \vartheta \\ 1, t \geq \vartheta \end{cases} \quad \text{(H.6)}$$

Fig. H.6a and H.6b present the results of the tracer study as well as the theoretical $F(t)$ values for the ideal CFSTR and PFR, respectively, which are plotted using dotted lines. To obtain an estimate for the experimental error, the tracer tests were replicated three times for each mixer, the results of which are summarized in Table H.3.



(a) **(b)**

Fig. H.6. Cumulative age distribution curves for preliminary tracer study tests conducted at 100 L m^{-2} h^{-1} equivalent flowrate: **(a)** Rapid mixer; **(b)** Helical flocculator.

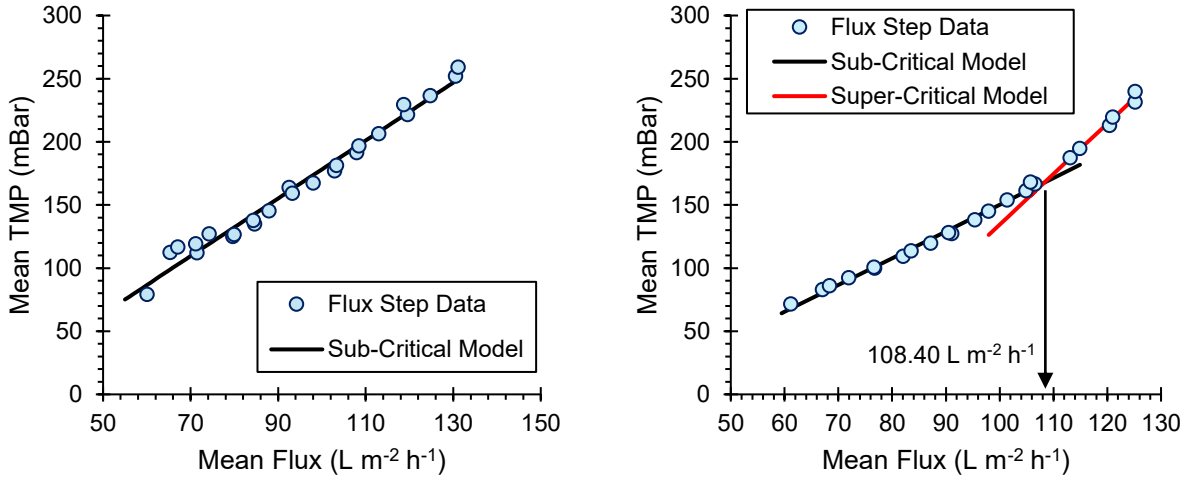
Table H.3. Summary of Preliminary Tracer Study Data for Rapid Mixer and Helical Flocculator

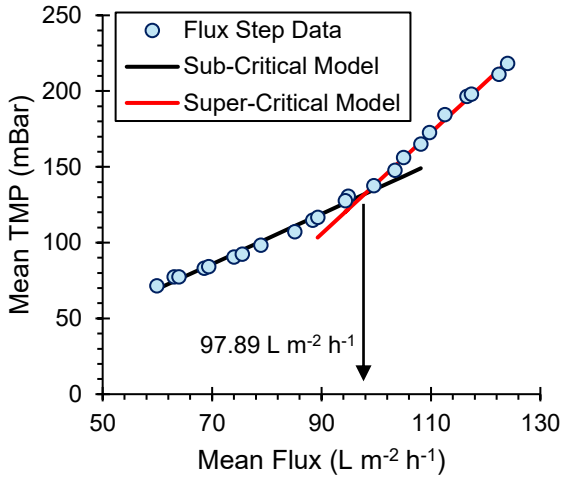
Mixer	Small-Scale Rapid Mixer	Helical Flocculator
$\bar{t}$ (min)	3.66	3.11
$t_{0.05,n}\frac{\sigma}{\sqrt{n}}$ (min)	0.09	0.06

H.1.6. Critical Flux Assessment

The critical flux was determined using the flux-stepping method adapted from Le Clech et al. (2003). Briefly, the pure water permeability (PWP) of the clean membrane was initially assessed

at a flux of 60 L m^{-2} h^{-1} for a period of 1 h. After this, for each synthetic challenge water, the flux was increased by 3 L m^{-2} h^{-1} (the step height) every 15 min (the step length). The step height and step length were chosen based on the guidance provided by Beier and Jonsson (2010), Choi and Dempsey (2005), and Le Clech et al. (2003) to minimize the impacts of system variables on the measured critical flux value. Data analysis was performed by plotting the mean permeate flux against the mean transmembrane pressure (TMP) for each flux step. It should be noted that, based on experience with our bench-scale filtration apparatus, the mean flux and TMP values were determined in the final minute of the 15 min step in order to ensure that the peristaltic feed pump had reached steady state operation (i.e., constant pump voltage). In this approach, two distinct regions can be identified, the first with a shallow slope and the second (being after the critical flux value) with a steeper slope. Linear regression was used to identify lines of best fit for both the shallow and steep sloped portions of the data, and the intersection of the lines was considered the point of critical flux. Choi and Dempsey (2005) argued that this approach provides the best practice for analysis of the flux-step data to determine the critical flux. Through a series of replicate tests, they found that the shape of the diagram is more consistent across a range of experimental conditions, and that the data manipulation is simpler than finding the numerical derivative of the TMP-flux data. The flux step data for the three synthetic waters considered in the current study is presented in Fig. H.7 as well as the regressed sub- and super-critical models.





(c)

Fig. H.7. Flux stepping data from critical flux testing for: **(a)** L-SUVA; **(b)** M-SUVA; **(c)** H-SUVA

Table H.4 below identifies the critical flux value for each of the three waters while also summarizing the coefficients and adequacy of the fitted sub- and super-critical models. Linear regression was performed using Excel's built-in *Data Analysis* tool and the significance of the fit was assessed using the *p*-value calculated from the ANOVA *F*-test.

Table H.4. Fitted Models from Critical Flux Testing

Water	Critical Flux ($L\ m^{-2}\ h^{-1}$)	Model	Slope ($mBar\ m^2\ h\ L^{-1}$)	Intercept (mBar)	R^2	*p*-Value
L-SUVA	> 131	Sub-Critical	2.29	-50.76	0.98	<.0001
M-SUVA	108.40	Sub-Critical	2.12	-61.80	0.99	<.0001
		Super-Critical	3.99	-264.88	0.98	<.0001
H-SUVA	97.89	Sub-Critical	1.66	-29.96	0.99	<.0001
		Super-Critical	3.34	-194.60	0.99	<.0001

In general, all models had a good fit ($R^2 > 0.98$) and were found to be significant (i.e., $p < 0.05$). For the high SUVA (H-SUVA) and medium SUVA (M-SUVA) waters, the critical flux values were 97.89 L m^{-2} h^{-1} and 108.40 L m^{-2} h^{-1}, respectively. For the low SUVA (L-SUVA) water, however, the mean TMP was found to increase linearly with the mean flux value for the entire range of flux values investigated, indicating that the critical flux value was not contained within

the range $60 \leq J \leq 130$ (L m^{-2} h^{-1}). Accordingly, for this tubular multichannel membrane (TMC) and the L-SUVA water it can be said that the critical flux value is greater than 130 L m^{-2} h^{-1}. In our previous study (see Chapter 6), which used the M-SUVA water and same TMC membrane, a flux of 80 L m^{-2} h^{-1} was selected to operate within the sub-critical flux zone in order to prevent unrealistic fouling development. However, the irreversible fouling rates for all test conditions, including the direct filtration of raw water, were found to include zero within their 95% confidence range, meaning that they were not statistically significant. Therefore, in an attempt to increase the irreversible fouling rate in the current study, the flux was increased to 100 L m^{-2} h^{-1}. Although it was desirable to set the flux in the super-critical region for all three-water types, limitations on the mass of permeate that can be retained and measured by the system analytical balance during overnight operation prevented the use of higher flux values. Future work may consider using the self-discharging permeate collection apparatus developed by Qi and Ladner (2023) which would likely permit unsupervised operation at higher flux values without the limitations associated with the produced permeate volume.

H.1.7. Method of DOC Quantification

DOC analysis by wet-chemical oxidation was carried out according to Standard Methods 5310C, the Persulfate-Ultraviolet Method (American Public Health Association et al. 2012), using a Phoenix 8000 analyzer (Tekmar-Dohrmann, Cincinnati, OH). According to the results of the study presented by Yang et al. (2021), the settings of the analyzer were adjusted and are summarized in Table H.5 below. Note that the modified settings used in the current work are presented as well as the default values recommended by the manufacturer. 0.5 mL of 21 % phosphoric acid solution (85% ACS grade, VWR Chemicals BDH, Mississauga, ON) was used to acidify samples prior to sparging by high purity N_2 (99.999 %) gas for inorganic carbon removal. A 10 % persulfate / 5% phosphoric acid solution along with UV irradiation was used for sample oxidation. The volume of persulfate ($Na_2S_2O_8$, 98%+, Thermo Scientific Chemicals, St. Louis, MO) solution added was set to 2.5 mL, which was recommended by Yang et al. (2021) for improved oxidation performance. Since, in the current study, all samples were designed to have low-level DOC (i.e., < 20 mg L^{-1}), the sample injection volume could be safely increased to 5 mL to improve instrument precision (while still being within the linear range of the non-dispersive infrared detector). Finally, the

integration time was automatically determined by the analysis software (TOC Talk 3.2, Tekmar-Dohrmann, Cincinnati, OH), with a maximum integral time set to 8 min to prevent secondary oxidation reactions from impacting results.

Table H.5. Method Setup for DOC Analysis by Tekmar-Dohrmann Phoenix 8000

Parameter	Recommended Setting[a]	Modified Procedure
Max Integration Time (min)	4.0	8.0
Acid Volume (mL)	0.5 (0.5-0.8)	0.5
Persulfate Volume (mL)	0.5 (0.5-1.0)	2.50
Injection Volume (mL)	4.0 (< 100 µg-C to NDIR)	5.0
No. of Injections	N/A	3
Sparge Time (s)		120
NDIR Threshold Value (mV)	< 5% of Peak Height	1.0

[a]manufacturer guidance from Tekmar-Dohrmann (1997). Note. NDIR = non-dispersive infrared detector

Prior to each set of analyses, the instrument was cleaned 5 times. Calibration was performed using potassium hydrogen phthalate (KHP) (ACS grade, VWR Chemicals BDH, Mississauga, ON) standard solutions at concentrations of 1, 2, 4, 8, and 10 mg-C L^{-1} prior to every set of tests. Regularly, the inorganic carbon sparger and UV reactor were removed from the instrument and soaked overnight in an alkaline detergent solution (Contrex AL Alkaline liquid detergent, Cat # 5301, Decon Labs Inc., King of Prussia, PA) to remove interference by organic contaminants, followed by overnight cleaning in 0.1 % HCl solution.

H.2. Supplemental Results

H.2.1. Fouling Studies with C-IN-P

Table H.6 below presents a summary of the fouling data across all water types and coating index (C-IDX) values for phased-inline-coagulation (C-IN-P).

Table H.6. Summary of Fouling Data for C-IN-P Pretreatment with Varying C-IDX and Water Type

C-IDX (mg m^{-2})	Dosing Time (min)	FR_{hr} (mBar h^{-1})	FR_{hirr} (mBar h^{-1})	BWE (%)
		L-SUVA		
0	0	274.83 ± 5.40	3.67 ± 2.28	98.51 ± 0.84
30	6	649.27 ± 50.73	0.10 ± 7.15	100.45 ± 1.37
75	15	144.48 ± 4.08	1.36 ± 1.43	99.58 ± 1.19
112.5	22.5	109.34 ± 12.39	3.63 ± 10.46	95.56 ± 7.83
150	30	66.11 ± 8.46	3.21 ± 3.46	91.73 ± 6.01
		M-SUVA		
0	0	216.72 ± 8.66	13.81 ± 2.13	93.92 ± 0.93
30	6	212.84 ± 9.75	6.06 ± 3.55	97.52 ± 1.68
75	15	154.25 ± 7.27	2.76 ± 4.58	98.57 ± 8.19
112.5	22.5	34.49 ± 6.15	3.99 ± 6.02	88.06 ± 15.52
150	30	58.65 ± 9.56	2.76 ± 3.88	88.16 ± 11.00
		H-SUVA		
0	0	146.02 ± 4.66	9.37 ± 2.04	94.12 ± 1.10
30	6	273.60 ± 10.00	1.49 ± 6.35	98.76 ± 2.14
50	10	48.34 ± 5.43	1.25 ± 1.67	97.27 ± 4.66
75	15	26.85 ± 3.55	4.33 ± 3.11	84.37 ± 9.23
112.5	22.5	20.14 ± 1.49	1.13 ± 1.06	97.01 ± 5.67
150	30	25.88 ± 1.71	0.34 ± 0.99	99.06 ± 4.35

Fig. H.8 below presents the hydraulic backwash efficiency (BWE) for each treatment condition evaluated in this study. The BWE was calculated following the approach presented by Chellam et al. (1998) and is presented in Eqn. H.7 below:

$$BWE\ (\%) = \frac{TMP_{n-1,f} - TMP_{n,i}}{TMP_{n-1,f} - TMP_{n-1,i}} \times 100 \qquad \text{(H.7)}$$

Where $TMP_{n,i}$ is the measured TMP at the beginning of cycle *n* (mBar), $TMP_{n-1,f}$ is the measured TMP at the end of cycle *n-1* (mBar), and $TMP_{n-1,i}$ is the measured TMP at the beginning of cycle *n-1* (mBar).

From Fig. H.8 it can be seen that the BWEs across C-IDX and water type were all quite similar and, in many cases, had overlapping 95% CIs. The M-SUVA and L-SUVA waters demonstrated similar patterns, with slightly lower mean BWEs as the C-IDX increased beyond 75 mg m^{-2}, potentially indicating that for these two water types the coagulant also becomes an important foulant for high dosages/dosing times. The most salient finding from this analysis is that the BWE for C-IN-P was not significantly lower than for continuous C-IN. This is in contrast to

the findings of Buchta et al. (2019) who proposed that the thinner cake layer generated by C-IN-P pretreatment promoted greater membrane–foulant interactions, thereby reducing the BWE relative to C-IN.

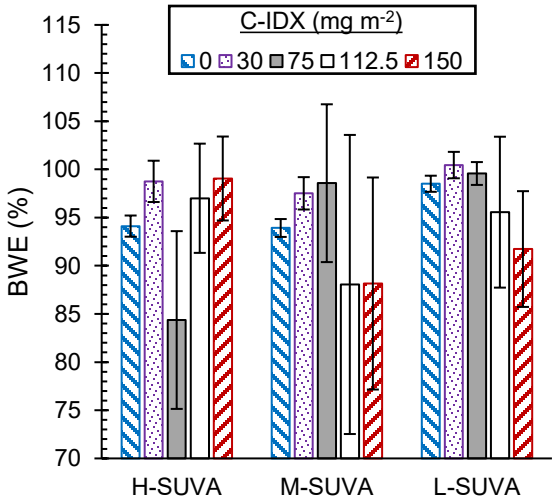


Fig. H.8. Variation in BWE across C-IDX values and water type.

Fig. H.9 below presents the cycle-by-cycle development of the hydraulically reversible fouling rate (FR_{hr}) for the three water types with coagulant addition for 20% of the cycle length. Here, the evolution for the first 4 h of operation is shown in blue circles, whereas the data for the remainder of the test is represented as red squares. From this figure, it can be seen that the FR_{hr} value increased rapidly for all water types during the first 4 h of operation, after which it plateaued and did not increase for the remainder of the test duration. This pattern generally repeated itself for the waters tested and at different C-IDX values. Accordingly, the FR_{hr} values reported in this paper were based on the data between the 9^{th} to 45^{th} cycles of operation.

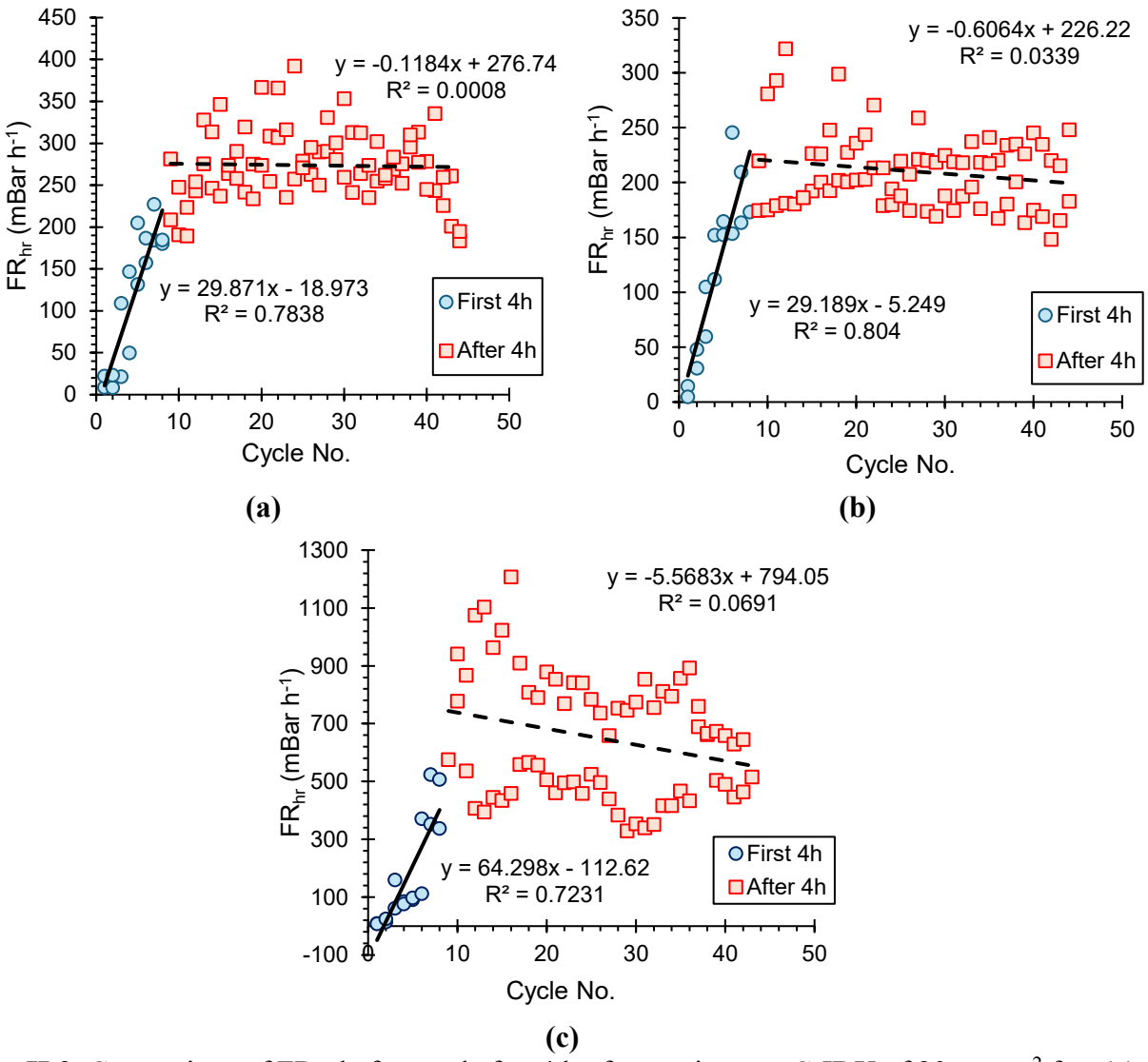


Fig. H.9. Comparison of FR_{hr} before and after 4 h of operation at a C-IDX of 20 mg m^{-2} for: **(a)** H-SUVA; **(b)** M-SUVA; **(c)** L-SUVA

Table H.7 below presents the results of a pooled *t*-test on the difference in means between the FR_{hr} values for the three water types, with the assumption of unknown but equal variances, evaluated for each C-IDX value. The null and alternate hypotheses for the test are given by:

$$H_0: \mu_1 - \mu_2 = \Delta_0$$

$$H_1: \mu_1 - \mu_2 \neq \Delta_0$$

And the corresponding test statistic is calculated using Eqn. H.8 (Montgomery and Runger 2014):

$$t_0 = \frac{\bar{x}_1 - \bar{x}_2 - \Delta_0}{s_p\sqrt{\frac{1}{n_1} + \frac{1}{n_2}}} \tag{H.8}$$

Where:

$$s_p{}^2 = \frac{(n_1 - 1)s_1^2 + (n_2 - 1)s_2^2}{n_1 + n_2 - 2} \tag{H.9}$$

And the rejection criteria are defined by $t_0 > t\alpha_{/2,n_1+n_2-2}$ or $t_0 < -t\alpha_{/2,n_1+n_2-2}$. In the above expressions n_i is the number of observations from sample i, $\bar{x}_i$ and $s_i^2$are the sample means and variances, respectively, and $s_p{}^2$is the pooled sample variance. Except for L-SUVA vs. M-SUVA at C-IDX=150 mg m^{-2}, all differences in means were statistically significant (i.e., p <0.05), highlighting the impact of water type on the observed fouling potential.

Table H.7. Results of Pooled *t*-test on Difference in Mean FR_{hr} Between Water Types Across C-IDX Values of 30-150 mg m^{-2}

Water Type	Water Type	Mean FR_{hr} Difference (mBar h^{-1})	St. Error Diff. (mBar h^{-1})	Lower 95% Limit	Upper 95% Limit	*p*-Value
		C-IDX= 150 mg m^{-2}				
H-SUVA	M-SUVA	-32.00	4.83	-41.54	-22.45	<.0001
H-SUVA	L-SUVA	-39.46	4.24	-47.85	-31.07	<.0001
L-SUVA	M-SUVA	7.47	6.41	-5.22	20.15	0.2463
		C-IDX = 112.5 mg m^{-2}				
H-SUVA	M-SUVA	-14.35	3.19	-20.66	-8.04	<.0001
H-SUVA	L-SUVA	-89.20	6.17	-101.40	-77.00	<.0001
L-SUVA	M-SUVA	74.85	6.85	61.30	88.39	<.0001
		C-IDX = 75 mg m^{-2}				
H-SUVA	M-SUVA	-127.40	4.04	-135.39	-119.42	<.0001
H-SUVA	L-SUVA	-117.64	2.71	-122.99	-112.29	<.0001
L-SUVA	M-SUVA	-9.76	4.21	-18.08	-1.44	0.0219
		C-IDX = 30 mg m^{-2}				
H-SUVA	M-SUVA	63.56	6.47	50.77	76.36	<.0001
H-SUVA	L-SUVA	-375.67	25.23	-425.57	-325.77	<.0001
L-SUVA	M-SUVA	439.24	25.22	389.36	489.11	<.0001

H.2.2. Modeling FR_{hr}

The FR_{hr} was modeled using an exponential model of the form:

$$FR_{hr} = ae^{P_d/b} + c \tag{H.10}$$

Where FR_{hr} is the hydraulically reversible fouling rate (mBar h^{-1}), P_d is the coagulant dosing time as a percent of the cycle length (%), and a, b, and c are adjustable model parameters. It should be noted that models with the same form could also be fitted in terms of the C-IDX value. The model parameters were determined using Excel's built-in *Solver* tool and a minimization of the sum of square errors criterion. The performance of the model was validated against other model types using a number of dimensional and non-dimensional statistical indicators including the coefficient of determination (R^2), the sum of squared error (SSE), the mean square error (MSE), the root mean square error (RMSE), the mean absolute error (MAE), and the mean absolute percent error (MAPE). The mathematical definitions of these statistical indices are presented below as defined by Bonakdari et al. (2023).

$$R^2 = \left[\frac{\sum_{i=1}^{N}(A_i - \bar{A})\sum_{i=1}^{N}(E_i - \bar{E})}{\sqrt{\sum_{i=1}^{N}(A_i - \bar{A})^2 \sum_{i=1}^{N}(E_i - \bar{E})^2}}\right]^2 \tag{H.11}$$

$$SSE = \sum_{i=1}^{N}(A_i - E_i)^2 \tag{H.12}$$

$$MSE = \frac{1}{N}\sum_{i=1}^{N}(A_i - E_i)^2 \tag{H.13}$$

$$RMSE = \sqrt{\frac{1}{N}\sum_{i=1}^{N}(A_i - E_i)^2} \tag{H.14}$$

$$MAE = \frac{1}{N}\sum_{i=1}^{N}|A_i - E_i| \tag{H.15}$$

$$MAPE = \frac{100}{N}\sum_{i=1}^{N}\left|\frac{A_i - E_i}{A_i}\right| \tag{H.16}$$

where A_i and E_i are the i^{th} samples of the actual and estimated values (respectively), $\bar{A}$ and $\bar{E}$ are the mean of the actual and estimated samples (respectively), and N is the number of samples. Table H.8 summarizes the fitted model parameters and the statistical indices of the models developed for each water type.

Table H.8. Fitted Model Adequacy Data for Relationship Between FR_{hr} and Coagulant Dosing Time

a	*b*	*c*	R^2	SSE	MSE	RMSE	MAE	MAPE
				L-SUVA				
2316.18	14.38	77.97	0.88	61429.20	7678.65	87.63	52.91	0.18
				M-SUVA				
325.26	50.99	0	0.86	5797.96	724.75	26.92	23.03	0.42
				H-SUVA				
8195.20	5.73	24.02	0.99	440.40	44.40	6.64	5.25	0.13

H.2.3. Organics Removals by C-IN-P and Model Development

Table H.9 summarizes the mean removals of bulk organics measures across all water types and C-IDX values. Briefly, apparent color was measured using a spectrophotometer (DR6000, Hach, Loveland, CO) and Hach Method 8025. For UV_{254} and true color analysis, the samples were filtered using a 0.45 µm membrane filter disc (GN-6 Metricel, Cytiva, Marlborough, MA). True color was measured using the same procedure as for apparent color, while UV_{254} was measured in accordance with Standard Method 5910B (American Public Health Association et al. 2012).

Table H.9. Summary of Organics Removals for C-IN-P Pretreatment with Varying C-IDX and Water Type

C-IDX (mg m^{-2})	Dosing Time (min)	DOC (%)	UV_{254} (%)	SUVA (%)	True Color (%)	App. Color (%)
			L-SUVA			
0	0	32.11	32.20	0.13	39.97	85.23
30	6	56.29 ± 3.59	45.28 ± 6.72	-25.63 ± 6.68	60.91 ± 1.73	85.85 ± 1.59
75	15	67.13 ± 1.69	75.53 ± 5.97	25.23 ± 8.25	84.58 ± 2.17	94.22 ± 1.01
112.5	22.5	75.32 ± 2.17	88.44 ± 4.31	53.20 ± 0.82	98.61 ± 2.15	98.17 ± 0.72
150	30	84.37 ± 0.97	95.59 ± 0.47	71.63 ± 2.41	98.48 ± 2.34	99.55 ± 0.70
			M-SUVA			
0	0	35.18	46.74	17.84	60.24	76.83
30	6	52.73 ± 1.28	60.33 ± 6.87	15.95 ± 5.83	80.31 ± 0.95	88.92 ± 1.10
75	15	78.83 ± 0.92	94.56 ± 3.44	74.34 ± 3.67	98.15 ± 1.65	98.55 ± 0.73
112.5	22.5	86.76 ± 0.27	96.64 ± 0.67	74.63 ± 1.16	99.43 ± 0.87	99.42 ± 0.45
150	30	89.18 ± 2.86	97.64 ± 0.03	77.83 ± 3.20	99.04 ± 1.05	99.41 ± 0.46
			H-SUVA			
0	0	32.29	45.60	19.65	59.05	71.46
30	6	55.82 ± 1.38	79.88 ±4.01	54.37 ± 3.62	88.00 ± 1.02	91.57 ± 0.77
50	10	67.78 ± 3.81	89.70 ± 9.02	67.78 ± 3.81	95.61 ± 0.96	96.71 ± 1.04
75	15	76.13 ± 1.51	92.75 ± 9.66	78.25 ± 0.64	97.66 ± 1.06	98.72 ± 0.45
112.5	22.5	89.28 ± 1.38	97.15 ± 1.93	73.55 ± 1.29	97.15 ± 1.93	99.45 ± 0.01
150	30	92.04 ± 0.17	97.81 ± 0.99	72.49 ± 3.25	99.71 ± 0.65	99.55 ± 0.22

Note: ± represents the 95% CI calculated using the Students *t*-test as $\mu \pm t_{0.025,n}\frac{s}{\sqrt{n}}$

The removal of bulk WQIs across different lengths of coagulant addition (or C-IDX) was seen to exhibit a saturation-like behavior, increasing towards a maximum of 100% removal as C-IDX increased. Accordingly, the relationship between the percent removal of each WQI and the coagulant dosing time expressed as a percentage of the cycle length was modeled using the Sips model (Aguareles et al. 2023):

$$Removal\ (\%) = \frac{aP_d{}^{1/c}}{1 + bP_d{}^{1/c}} \tag{H.17}$$

Where P_d is the coagulant dosing time expressed as a percentage of the filtration cycle length (%), and a, b, and c are adjustable model parameters. The parameter values were determined using Excel's built-in *Solver* tool and a minimization of the sum of squared errors criterion. The Sips model was selected as the best model amongst a number of alternatives based on comparison of a number of dimensional and non-dimensional performance indicators.

The fitted model parameters for the relationships between the coagulant dosing time and DOC, true color, and UV_{254} removal are presented in Table H.10 - Table H.12. For all water types and WQIs, the developed models were found to have a good fit, with $R^2 > 0.941$ and the mean absolute percent error (MAPE) < 3.24% in all cases. Among the three challenge waters, the models developed for the M-SUVA water seemed to have the best fit compared to the H-SUVA and L-SUVA water types.

Table H.10. Fitted Model Adequacy Data for DOC Across Water Type

a	***b***	***c***	**R^2**	**SSE**	**MSE**	**RMSE**	**MAE**	**MAPE**
				L-SUVA				
25.724	0	3.956	0.941	52.443	6.555	2.560	2.197	3.240
				M-SUVA				
1.516	0.016	0.691	0.995	7.670	0.959	0.979	0.878	1.211
				H-SUVA				
10.952	0.081	1.390	0.973	50.159	5.016	2.240	1.876	2.542

Table H.11. Fitted Model Adequacy Data for True Color Across Water Type

a	***b***	***c***	**R^2**	**SSE**	**MSE**	**RMSE**	**MAE**	**MAPE**
				L-SUVA				
4.973	0.043	0.926	0.980	38.305	4.788	2.188	1.898	2.109
				M-SUVA				
0.010	1.03×10^{-4}	0.282	0.995	2.679	0.335	0.578	0.442	0.454

				H-SUVA				
0.040	4×10^{-4}	0.304	0.961	7.669	0.767	0.876	0.674	0.709

Table H.12. Fitted Model Adequacy Data for UV_{254} Across Water Type

a	***b***	***c***	**R^2**	**SSE**	**MSE**	**RMSE**	**MAE**	**MAPE**
				L-SUVA				
2.733	0.022	0.920	0.996	11.087	1.386	1.177	1.025	1.645
				M-SUVA				
0.020	2.03×10^{-4}	0.334	0.997	6.746	0.843	0.918	0.682	0.958
				H-SUVA				
0.256	0.003	0.400	0.953	25.547	2.555	1.598	1.326	1.447

H.2.4. FEEM Model Development

H.2.4.1. Background

Recently, fluorescence spectroscopy has garnered increased attention for analysis and characterization of dissolved organic matter (DOM) matrices as it possess a number of distinct advantages including a fast measurement time, high sensitivity and selectivity, requires little to no pre-treatment, and has a reduced sensitivity to interferences as compared to UV-absorbance (Peleato 2013; Wang et al. 2025; Xu et al. 2022).

The most common fluorescence technique for water sample analysis is the collection of fluorescence excitation-emission matrices (FEEM), which are acquired by scanning the fluorescence intensity at various excitation-emission pairs (Peleato 2013). The response at a specific wavelength pair is related to the concentration of the optically active DOM within the sample. The fluorescence values for specific excitation-emission pairs can be used to help identify the composition of different water samples as several classes of organics are known to have unique fluorescent signatures that allow them to be distinguished from one another (Locquet et al. 2018). Using FEEMs, humic acids, fulvic acids, and aromatic proteins are typically identifiable (Peleato 2013) with some evidence suggesting that the source of the humic acids (terrestrial or anthropogenic) may also be resolved (McKnight et al. 2001). Based on a survey of the literature, Table H.13 below highlights some of the DOM regions that can be discriminated using FEEM analysis.

Appendix H

Table H.13. Summary of Reported FEEM Peaks and their Corresponding DOM Classification from Select Studies

DOM Class	Fluorophore Name	Ex/Em Range (nm)	Ex/Em Wavelength (nm)	Description
Protein-Like	B-peak[b]	225-280 (Ex)	225-237/309-321[b]	Tyrosine-like, protein-like[b,K, M]
	γ-peak[K]	280-380 (Em)	275/310[b]	Amino acids, protein-bound[c]
			270/306[c]	
			<300/280-380[f]	
			275/345[h]	
			270-280/300-320[K]	
			240-250/330-380[L]	
			270-280/305-310[M]	
			275/304[N]	
	T-peak[b]	220-280 (Ex)	275/340[b,d,g,N]	Tryptophan-like, protein-like[b,d,K, M,O]
	δ-peak[K]	280-350 (Em)	280/330[I]	Protein-like substances[I]
			220-275/300-350[J,O]	
			270-280/320-350[K]	
			240-250/280-330[L]	
			270-280/340[M]	
Humic-Like	A-peak[b]	237-290 (Ex)	260/380-460[b]	Humic-like[b,d,K,P]
	α'-peak[K]	380-500 (Em)	260/480[c]	Terrestrial humic substances[c,e]
			250/410[c]	Terrestrial/anthropogenic HS[c]
			260/380-460[d]	Terrestrial-derived humic-like[f]
			260/490[e]	Terrestrial or autochthonous[M]
			<290/340-500[f]	
			260/450[g]	
			265/525[h]	
			230-260/420-450[J]	
			250-260/380-480[K]	
			237-260/400-500[M]	
			260/460[N]	
			270-540[P]	
	C-peak[b]	320-370 (Ex)	320-360/420-460[d]	Humic-like[d,K,O]
	α-peak[K]	420-525 (Em)	340/428-440[g,O]	Humic-like; terrestrial or anthropogenic; Agriculture[M]
			360/525[h]	
			320/415[I]	
			330-350/420-480[K]	
			300-370/400-500[M]	
			340/440[N]	
	M-peak[b]	<312 (Ex)	312/380-420	Marine humic-like[b,d,K]
	β-peak[K]	340-420 (Em)	290-310/370-410[d]	Marine/terrestrial humic materials[e]
			315/418[e]	Anthropogenic; wastewater and agriculture[M]
			<260/340-420[f]	
			300/390[g]	
			320/425[h]	
			310-320/380-420[K]	
			290-312/370-420[M]	
			300/390[N]	

Note. [a](Peiris et al. 2010); [b](Coble 1996); [c](Baghoth et al. 2011); [d](Stedmon et al. 2003); [e](Murphy et al. 2008);[f](Shutova et al. 2014);[g](Hansen et al. 2016);[h](Sierra et al. 2005);[I](Peiris et al. 2010);[J](Persson and Wedborg 2001);[K](Parlanti and Wo 2000);[L](Locquet et al. 2018);[M](Omanović et al. 2023); [N](Hansen et al. 2018);[O](Wells et al. 2022);[P](Mealio et al. 2024)

One challenge in the analysis of complex DOM mixtures is that multiple chromophores exist and the yield of the fluorescent spectra is highly dependent on the structure, molecular weight, and functional groups associated with the individual compounds (Baghoth et al. 2011). As a result of the overlapping structural and chemical features of NOM chromophores, many FEEM spectra display broad peak regions (Gilmore 2011; Persson and Wedborg 2001). To address this issue, multivariate analysis techniques have been employed to help reduce the dimensionality of the collected datasets by modelling variance between samples (Peleato 2013). Recently, parallel factor analysis (PARAFAC) has been used to process FEEMs collected from aquatic environments. PARAFAC is a multi-way statistical approach that is used to detect underlying structures in complex data sets and distill these response signatures into a number of distinct fluorescent components (fluorophores) (Hansen et al. 2018). The number of components, as well as the positioning and intensity of the components have been linked to changes in concentration and character of DOM (Shutova et al. 2014).

H.2.4.2. Experimental Approach

Samples of the three synthetic challenge waters were prepared using the methods outlined in Section H.1.2. To aid the PARAFAC model development, 5 single-solute samples were prepared for the optically active model organic components (i.e., HA, BSA) to provide the model with a second order advantage. The concentration of these samples matched those used in the synthetic water mixtures and also included samples with higher concentrations ranging up to 20 mg L^{-1} (on a mass basis). A summary of the samples used for the model development is presented in Table H.14.

Table H.14. Synthetic Water Samples Tested for PARAFAC Model Calibration

Sample Code	HA (mg L^{-1})	BSA (mg L^{-1})	SA (mg L^{-1})
H-SUVA	10	4	2
M-SUVA	5	4	4
L-SUVA	2	4	7
2-HA	2	0	0
5-HA	5	0	0
7-HA	7	0	0

10-HA	10	0	0
20-HA	20	0	0
2-BSA	0	2	0
4-BSA	0	4	0
7-BSA	0	7	0
10-BSA	0	10	0
20-BSA	0	20	0

All samples were analyzed using a fluorescence spectrophotometer (Aqualog, HORIBA Instruments Inc, Piscataway, NJ). After equilibration to 20°C, 3.5 mL of 0.45 µm filtered sample was pipetted into a 1 cm pathlength quartz cuvette (Starna Spectrosil 3-Q-10, Atascadero, CA) for measurement in duplicate. To prevent cross-contamination between samples during analysis, the quartz cuvette was rinsed five times using DI and flushed with sample water before being filled. The fluorescence excitation range was set between 250-600 nm, while the fluorescence emission was measured over a range of 250-800 nm. Both excitation and emission spectra were measured using a 5 nm band pass, an increment of 5 nm, and an integration time of 1.1 s. The sample integration time was determined through preliminary testing in accordance with the manufacturer's recommended procedures (Horiba Scientific 2021). The CCD settings were medium gain and 8-pixel binning (4.64 nm/pixel). All FEEM spectra were subsequently corrected for first- and second-order Rayleigh masking (10 nm sum of slit widths) and inner filter effects (i.e., diminished excitation intensity due to absorption effects within the sample (Horiba Scientific n.d.)). The model masking parameters included first-order Rayleigh scattering (16 nm), second-order Rayleigh scattering (32 nm), and Raman scattering (10 nm). Data was normalized using water Raman scattering units (Madhav and Gilmore 2024). Reference blank correction was conducted using a permanently fused, capped, quartz cuvette with ultra-high purity water (Starna RM-H20, Atascadero, CA, USA).

Following analysis, the FEEM data was imported into SOLO software (Eigenvector Research Inc., Mason, WA, USA), which was used to develop the PARAFAC model. The SOLO software allows users to quickly and conveniently adjust the number of components included in the model. Accordingly, PARAFAC models with either two or three components were evaluated and compared on the basis of percent variance captured, core consistency, model residuals, and split-half validation results. These metrics were previously recommended for comparing

PARAFAC model performance on FEEM data by Stedmon and Bro (2008). Higher values of the core consistency metric (tending towards 100) are desirable and can help to diagnose the appropriate number of components to include in the PARAFAC model (Wells et al. 2022). The number of components is selected to be the number in the largest model that still possesses a high core consistency value (i.e., > 90, which indicates a high tri-linearity of the data (Bro and Kiers 2003)). The split-half validation divides the data set into two halves with the model considered validated if the models developed for each half are sufficiently similar (Murphy et al. 2018; Stedmon and Bro 2008).

H.2.4.3. FEEM Model Validation

Both the 2- and 3-component PARAFAC models were found to have a high percent variance captured, although the 3-component model performed slightly better (99.355% vs. 97.565%). The core consistency value was introduced by Bro and Kiers (2003) as a method for evaluating the appropriateness of a PARAFAC model for fitting trilinear data. Briefly, the PARAFAC model can be expressed in terms of the parameter matrices (i.e., scores, emission, excitation loadings) and a three-way binary core array, which has zeros in all places except for the superdiagonal. In fitting the PARAFAC model to the data, the core array is determined using simple regression. In determining the core consistency value, the regressed core array derived during the model fitting is compared against the idealized binary core array: the regressed array should resemble the binary core array. If the data is poorly represented by the trilinear model, or if there is too many model components, then significant deviations are expected (Bro 1998). A sample of the core consistency evaluation output by the SOLO software is provided in Fig. H.10 for the 2-component model. Here, the red circles represent the elements of the fitted superdiagonal while the green crosses represent the off-superdiagonal elements of the array. In this case, the superdiagonal elements were all close to one, while the off-superdiagonal elements were all close to zero, indicating that the model is not overfitting. For the data in this study, both the 2- and 3- component models were found to perform similarly and had high core consistency values of 99.

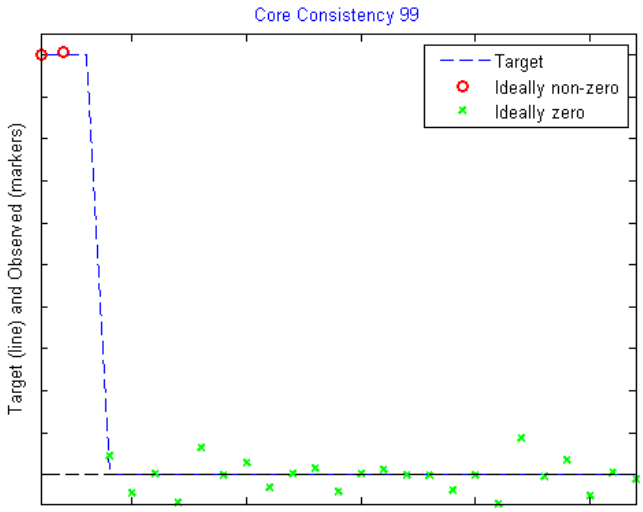
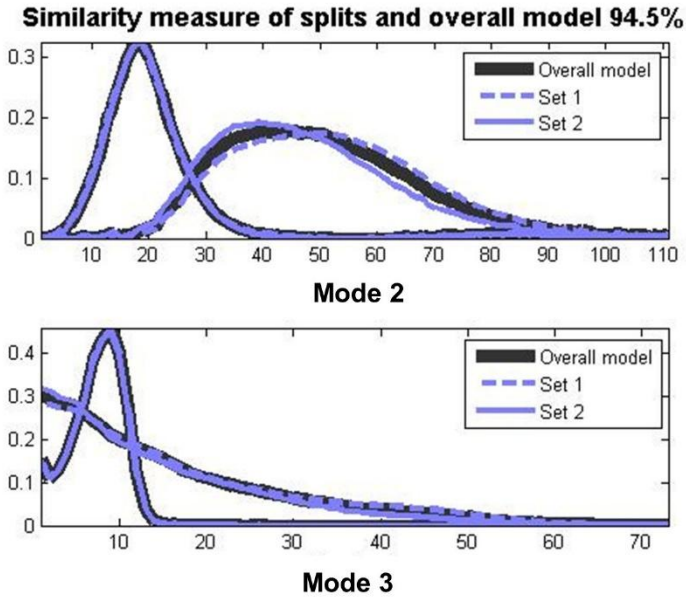


Fig. H.10. Core consistency graph for 2-Component model.

Recall, in addition to the three synthetic challenge waters, single solute solutions of HA and BSA were also used during model development to provide a second order advantage to the model. During the split-half validation process, the data is divided into two sub-sets and the similarity of the models developed on each subset of data compared to the model developed using the overall data. In order to prevent one sub-set from containing only single solute samples, which would in essence force the software to fit a model developed on (for example) HA data to a BSA profile, the data was re-organized using the SOLO software's built-in shuffle feature prior to performing validation. Fig. H.11. Shows the results of the split-half validation where, although both models were considered adequate and had similarity results greater than 90%, the 3-component model demonstrated a superior internal consistency with a similarity of 100%.

(a)



(b)

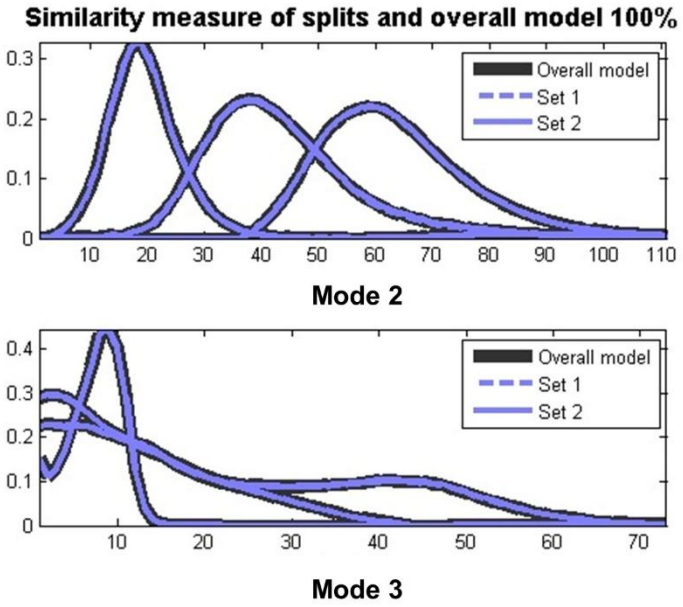
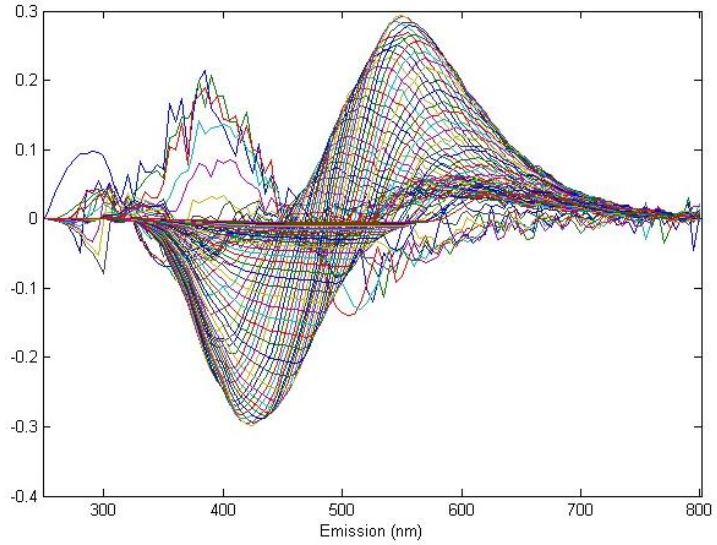


Fig. H.11. Split-half evaluation for: **(a)** 2-component model; **(b)** 3-component model. Note. Mode 2 refers to the emission loadings and Mode 3 refers to excitation loadings.

Finally, to further evaluate the adequacy of the two PARAFAC models the residual plots, which are plots of the difference between the experimental data and the model, were evaluated. The residual plots for the 2- and 3- component model applied to a sample of H-SUVA challenge water are presented in Fig. H.12. Here it can be seen that the amplitude of the residuals is about

twice as great for the 2-component model as for the 3-component model. Moreover, a good fitting model should have residuals that are randomly distributed, and positively/negatively balanced, around zero (Murphy et al. 2013). However, for the 2-component model there is positive residuals that are not offset by negative residuals.

(a)



(b)

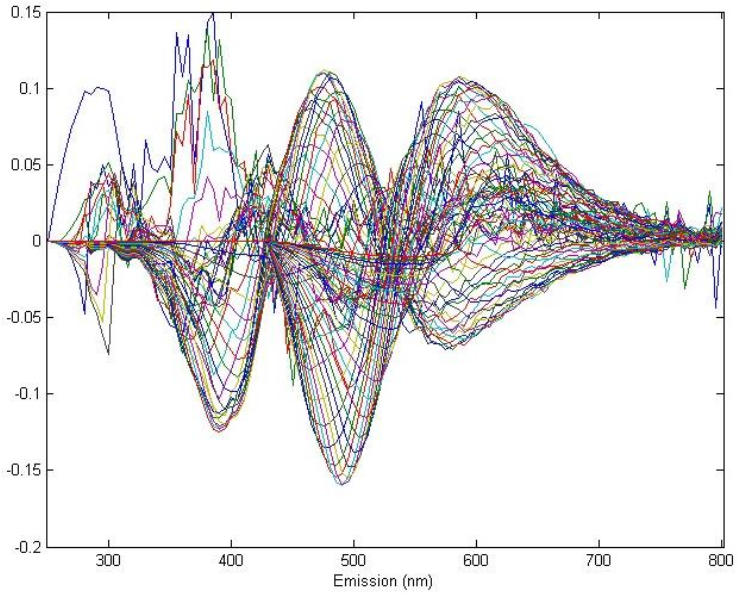
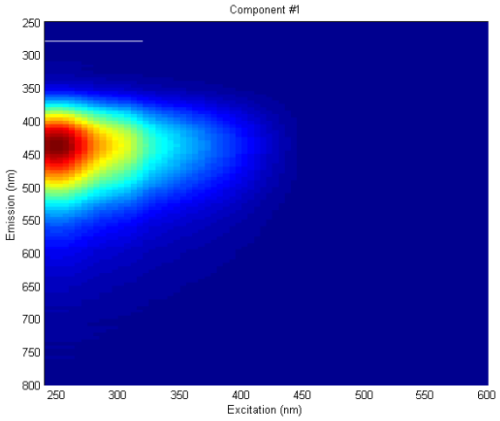
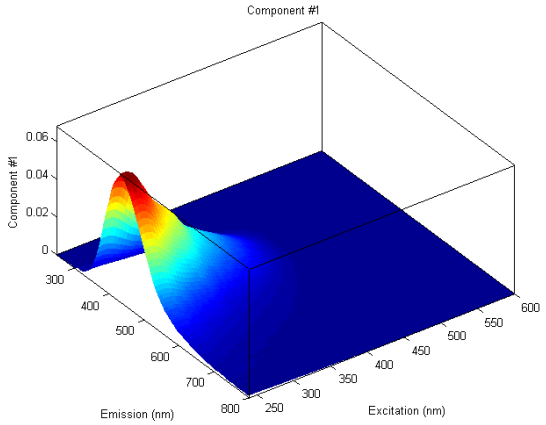


Fig. H.12. Comparison of PARAFAC model residuals for: **(a)** 2-component model; **(b)** 3-component model

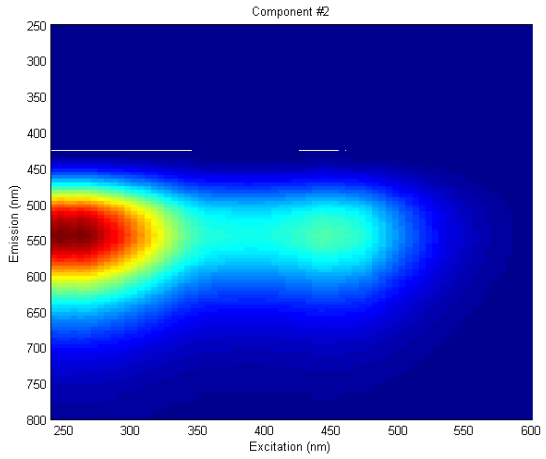
Taken together, the results of the split-half validation, residuals analysis, and percent variance captured indicated that the 3-component model was best fitted to the data. The three components contributing to the organic matter in this dataset are shown in Fig. H.13.



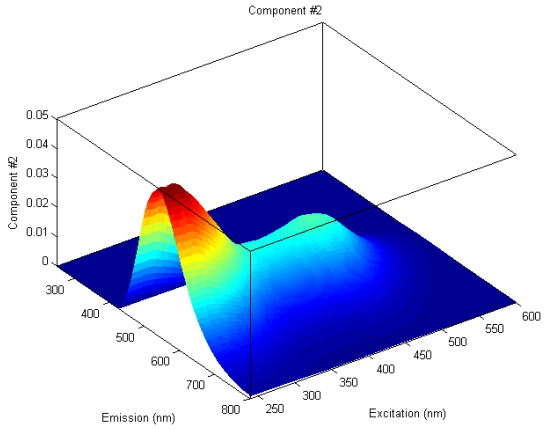
(a)



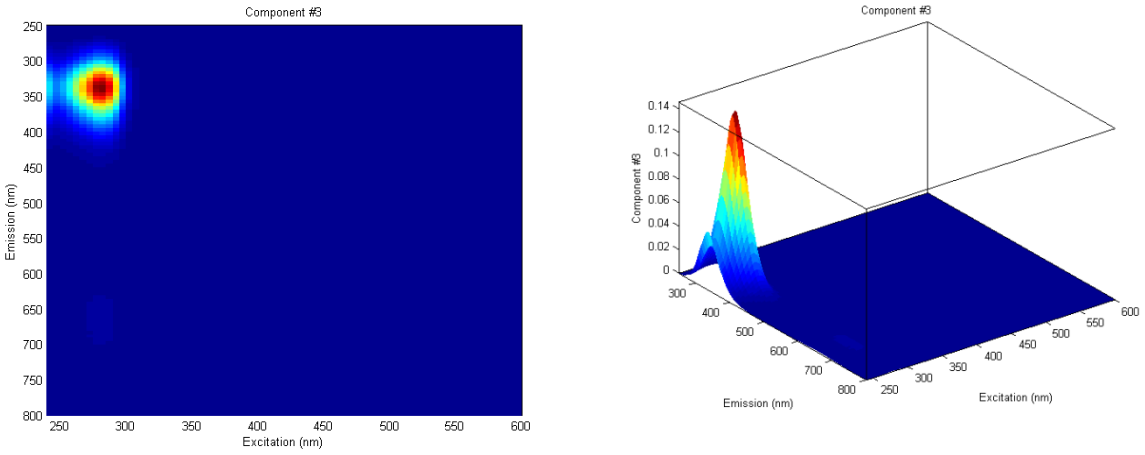
(b)



(c)



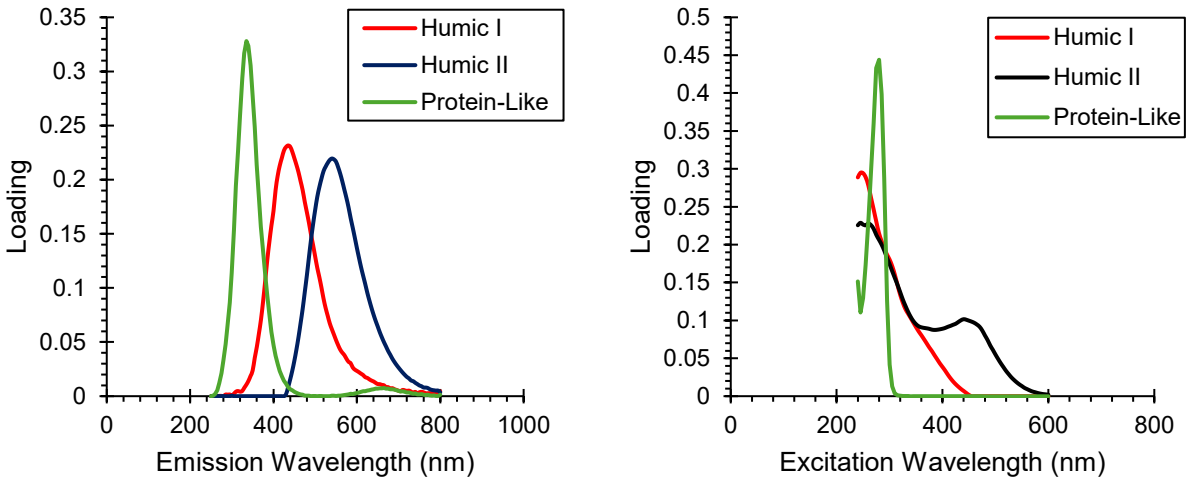
(d)



(e) **(f)**

Fig. H.13. FEEM PARAFAC model components: **(a)-(c)-(e)** 2-D Excitation-Emission spectra for component 1, 2, and 3, respectively; **(b)-(d)-(f)** 3-D Excitation-Emission spectra for component 1, 2, and 3, respectively.

The peak values for each component were identified from the loading diagrams for the emission and excitation spectra, shown in Fig. H.14, while classification was made by comparing the spectral features of each component with ranges reported by previous studies (Table H.13). In order of increasing emission wavelength the three components could be identified as protein-like/tryptophan-like substances (Ex/Em=280/335), humic-like I (Ex/Em=245/435), and humic-like II (Ex/Em=260/540). The most significant proportion of variance captured in the model was explained as humic-like I component (45.46%), followed by humic-like II (32.19%), and protein-like (22.35%) components.

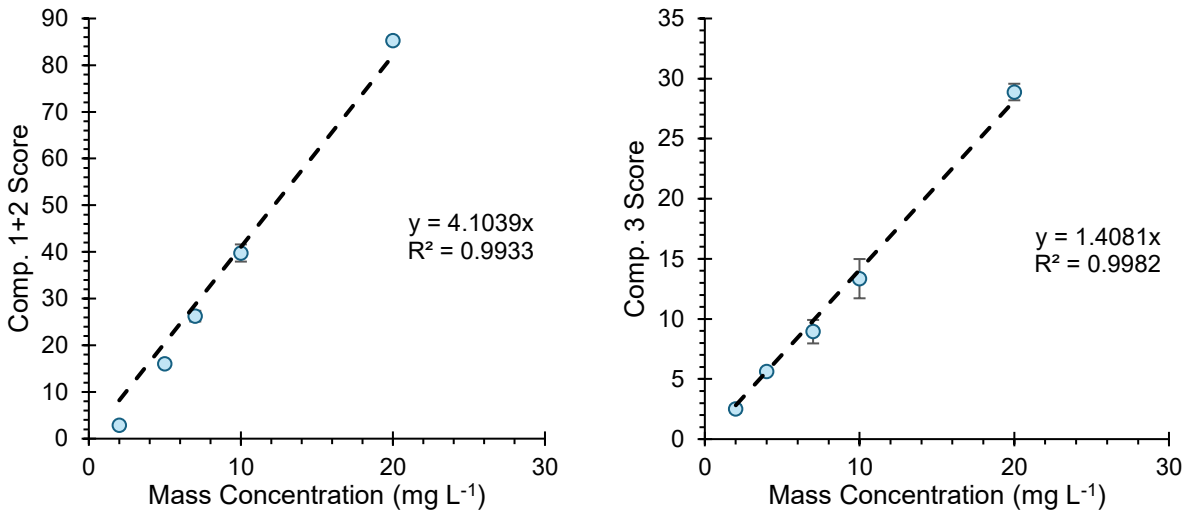


(a) **(b)**

Fig. H.14. (a) Emission; **(b)** Excitation loading diagrams for three component FEEM model

H.2.4.4. DOC Quantification from FEEM Data

In fluorescence analysis, the fluorescence quantum efficiency defines the ratio of the number of photons emitted to the number of photons absorbed. Within the linear Beer-Lambert concentration range, the inner-filter effect corrected fluorescent yields should be linear (Gilmore and Schober 2025). In this study, the spectrofluorometer measurement settings (i.e., gain, integration time) were adjusted to maintain all samples within the linear region of the detector. Using HA and BSA standards that exceeded the range of concentrations used in the preparation of the three synthetic waters, the linearity of the fluorescent response was confirmed (Fig. H.15).



(a) **(b)**

Fig. H.15. Linearity assessment of component scores for: **(a)** HA; **(b)** BSA

Table H.15 presents a summary of the linear fit for the HA and BSA, where the ANOVA indicates that both models are statistically significant.

Table H.15. Linearity Assessment of EEM Scores for Model Organics

Organic Type	Slope	R^2	*p*-Value
HA	4.104± 0.47	0.9933	.0001
BSA	1.408 ±0.082	0.9982	<.0001

If there is more than one fluorophore in the sample and Beer-Lambert law is assumed valid (both of which are true in the current study), then the measured FEEM is the sum of the contributions of all *F* fluorophores, each weighted by their respective concentration (Stedmon and Bro 2008). If it is reasonably assumed that the change in analyte concentration results in a change in only the fluorescence intensity and not the shape of the excitation and emission spectra, then a single point calibration relating the known concentration of an analyte to its FEEM score can be used for quantification. Madhav and Gilmore (2024) previously followed a similar approach calibrating the FEEM scores of benzene, toluene, ethylbenzene, xylene, and naphthalene against known standard concentrations. Calibration was performed using the maximum concentration of HA and BSA used in the synthetic challenge waters (i.e., 10 mg-HA L^{-1} and 4 mg-BSA L^{-1}) which

corresponded to DOC concentrations of 2.94±0.10 mg-C L^{-1} and 1.61±0.04 mg-C L^{-1}, respectively. The mean score for the sum of the humic-like components for the HA standard was found to be 39.77±1.15 and the score for the protein-like components and BSA was 5.61±0.12. The ratio of measured DOC to component score was used to estimate the organic carbon concentration of each component within the measured samples. As SA does not exhibit any inherent fluorescent properties (Mohammadi et al. 2025), its concentration was determined by subtracting the estimated concentrations of HA and BSA from the bulk DOC measurement. As within the manuscript, FEEM-derived DOC concentrations of each component will be differentiated from references to the model organic compounds using an asterisk.

H.2.5. Relationships Between FR_{hr} and Removal Rates of HA and SA

The FR_{hr} values for the three challenge waters under all C-IDX conditions were regressed against the removal of HA^*, SA^*, and combined HA^*+SA^* using exponential models of the same format as presented in Eqn. H.10. The best fitting models for each water type are shown in Fig. H.16 while the fitted model parameters and associated statistical performance metrics (which were calculated as shown previously in Section H.2.2.) are summarized in Table H.16. For the L-SUVA water, FR_{hr} was best described in terms of the removal of SA^* (Fig. H.16c). The FR_{hr} results of the M-SUVA water could also be somewhat better modeled using SA^* compared to combined HA^*+SA^* removal (Fig. H.16b). These results support the importance of SA^* in governing membrane FR_{hr}, consistent with a large number of previous studies that have identified hydrophilic biopolymers as the primary foulant of LPMs (Chen et al. 2014; Kimura et al. 2018; Kimura and Ando 2016; Kimura and Kume 2020; Wray and Andrews 2014; Yamamura et al. 2014; Zheng et al. 2021). In contrast, the FR_{hr} results for the H-SUVA water were best simulated in terms of the HA^* removal. Although this contradicts the prevailing consensus in the literature that biopolymers are the principal foulant, it is consistent with experience from our research group for a high SUVA water (Walker and Narbaitz 2016; Xu and Narbaitz 2016; Chapter 3; Chapter 4).

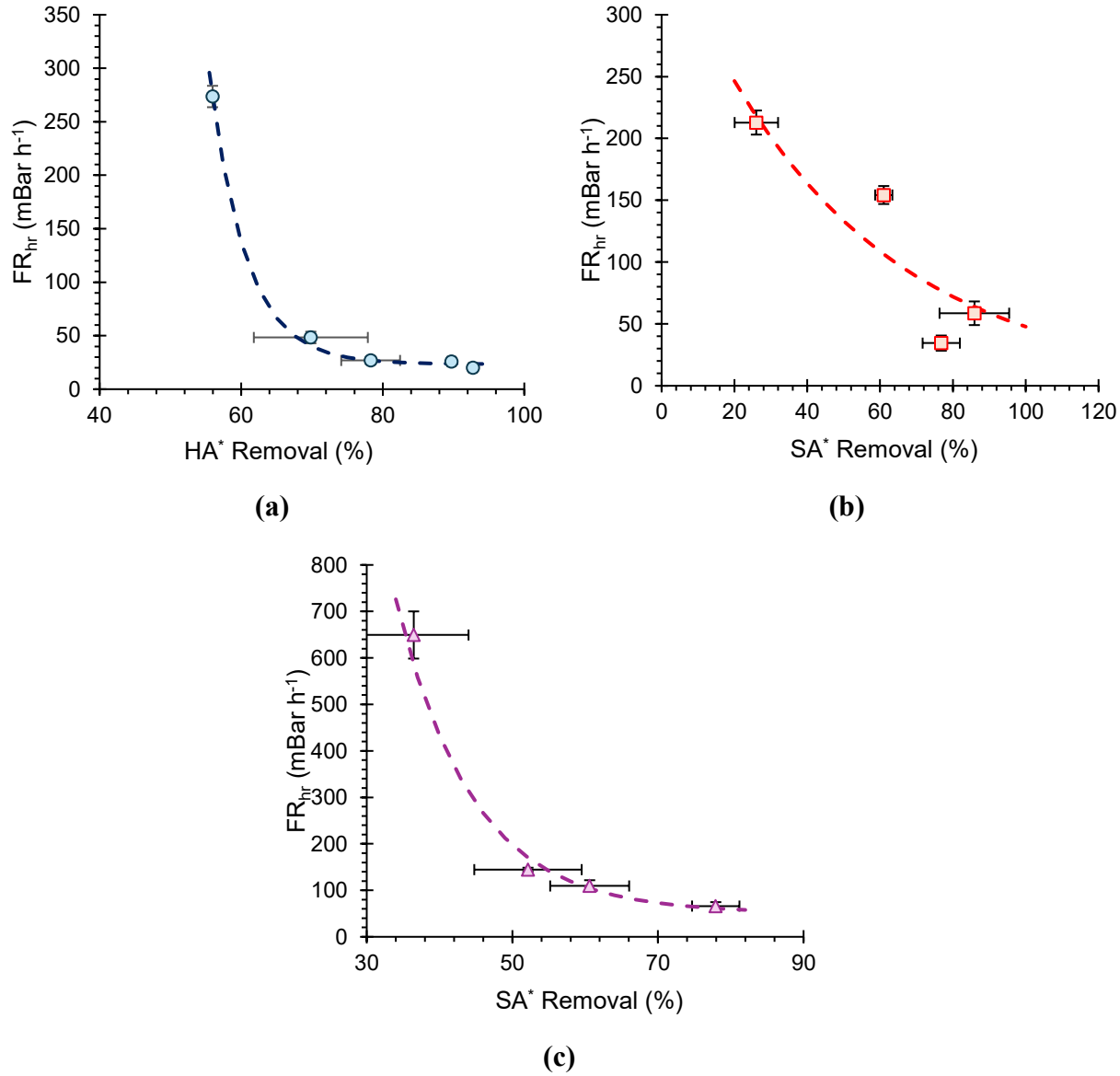


Fig. H.16. Relationships between the removal of HA* or SA* and FR_{hr} for: **(a)** H-SUVA; **(b)** M-SUVA; **(c)** L-SUVA waters.

Table H.16. Fitted Model Adequacy Data for Relationship Between FR_{hr} and Percent HA* or SA* Removal

a	*b*	*c*	R^2	SSE	MSE	RMSE	MAE	MAPE
				L-SUVA[1]				
17,268.57	10.49	50.89	0.975	13,014.74	1,626.84	40.33	29.83	18.06
				M-SUVA[1]				
371.36	48.78	0	0.786	8,963.98	1,120.50	33.47	27.56	44.49
				H-SUVA[2]				
1.307×10^7	5.15	23.45	0.998	169.02	16.90	4.11	3.72	10.40

Note: [1]Regression based on percent SA^* removal; [2]Regression based on percent HA^* removal.

From a practical perspective, however, the development of a single predictive framework (which has a minimum acceptable level of performance) across all water types is preferable. Based on our modeling results, the best simulations across the three water types were obtained using the combined removal of HA^*+SA^*. Models based on HA^*+SA^* removal yielded lower combined SEE and MSE values across the three water types than models based on HA^* or SA^* removal individually. Furthermore, the coefficients of determination for the models developed using HA^*+SA^* decreased only slightly relative to the optimal water specific models for the H-SUVA (0.970 vs. 0.998) and L-SUVA waters (0.967 vs. 0.975). The fitted model parameters for the FR_{hr} versus HA^*+SA^* removal are summarized in Table H.17 below.

Table H.17. Fitted Model Adequacy Data for Relationship Between FR_{hr} and Percent HA^*+SA^* Removal

a	*b*	*c*	R^2	SSE	MSE	RMSE	MAE	MAPE
				L-SUVA				
11,852.88	13.03	0	0.967	19,173.27	2,396.66	48.96	37.41	33.12
				M-SUVA				
316.48	61.44	0	0.675	13,554.25	1,694.28	41.16	36.52	55.92
				H-SUVA				
4.32×10^5	7.04	18.25	0.970	2,804.01	280.40	16.75	11.81	18.59

H.2.6. Fouling Data for Sensitivity Assessment of C-IDX for C-IN-P Operational Control

H.2.6.1. Differences in FR_{hr}

To evaluate the impact of coagulant type as well as coagulant dose/dosing time on the performance of C-IN-P at a fixed C-IDX and for the H-SUVA water type, a pooled *t*-test on the difference in means was used with the assumption of unknown but equal variances. Table H.18 below presents the pairwise comparison of FR_{hr} for the different combinations of dose/dosing time using both alum and ACH. For a fixed coagulant type, altering the combination of dose/dosing time resulted in statistically significant ($p < 0.05$) differences in FR_{hr}. When the coagulant dose was fixed at either 3 mg-Al L^{-1} or 45 mg-Al L^{-1} (for a constant C-IDX of 75 mg m^{-2}), changing coagulant type also yielded statistically significant differences in FR_{hr}.

Table H.18. Results of Pooled *t*-test on Sensitivity of FR_{hr} to Coagulant Dose/Dosing Time and Coagulant Type

Configuration	Configuration	Mean FR_{hr} Difference (mBar h^{-1})	St. Error Diff. (mBar h^{-1})	Lower 95% Limit	Upper 95% Limit	*p*-Value
Impact of Coagulant Dose/Dosing Time						
ALS-1.5	ALS-3	81.48	8.23	65.22	97.74	<.0001
ALS-45	ALS-1.5	74.93	11.82	51.57	98.29	<.0001
ALS-45	ALS-3	156.41	8.86	138.88	173.93	<.0001
PAX-3	PAX-45	39.31	8.06	23.37	55.25	<.0001
Impact of Coagulant Type						
PAX-3	ALS-3	77.39	7.62	62.32	92.46	<.0001
ALS-45	PAX-45	113.23	9.26	94.93	131.54	<.0001

H.2.6.2. Differences in FR_{hirr} and BWE

The ANOVA was used to evaluate whether the mean FR_{hirr} and BWE differed statistically from one another. The experimental observations can be expressed using the means model (Montgomery 2020):

$$y_{ij} = \mu_{MM} + \tau_{MM,i} + \epsilon_{ij} \tag{H.18}$$

Where and y_{ij} is the j^{th} observation for the i^{th} treatment with a variance of σ^2, μ_{MM} is the overall mean, $\tau_{MM,i}$ is the effect of the i^{th} treatment, and ϵ_{ij} is the random error component. The one-way ANOVA tests the null hypothesis that the treatment effects are zero against the alternative hypothesis that at least one effect is different from zero:

$$H_0: \tau_{MM,1} = \tau_{MM,2} = \cdots \tau_{MM,a} = 0$$

$$H_1: \tau_{MM,i} \neq 0 \text{ for at least one } i$$

The test statistic, F_0, is given by the *F*-ratio according to Eqn. H.19 (Montgomery 2020):

$$F_0 = \frac{SS_{treatments}/(a-1)}{SS_E/(N-a)} = \frac{MS_{Treatments}}{MS_E} \tag{H.19}$$

Which has an *F* distribution with $a-1$ and $N-a$ degrees of freedom where a is the number of treatment levels and N is the total number of observations. The variability between treatments is given by the sum of squares due to treatments ($SS_{treatments}$), while the variability within treatments is the sum of squares due to error (SS_E) and represents the pure random experimental

error (Berthouex and Brown 2002). These are defined mathematically by Eqn. H.20 and Eqn. H.21, respectively (Montgomery and Runger 2014):

$$SS_{Treatments} = n\sum_{i=1}^{a}(\bar{y}_{i\,.} - \bar{y}_{..})^2 \tag{H.20}$$

$$SS_{Error} = \sum_{i=1}^{a}\sum_{j=1}^{n}\left(y_{ij} - \bar{y}_{i\,.}\right)^2 \tag{H.21}$$

Where n is the number of observations for the i^{th} treatment, $\bar{y}_{i\,.}$ is the average of the observations for the i^{th} treatment, $\bar{y}_{..}$ is the grand average of all observations across the i different treatments, and all other parameters have been previously defined. By dividing the $SS_{Treatments}$ by its number of degrees of freedom, $a-1$, the mean squared error due to treatments ($MS_{Treatments}$) is obtained. The mean squared error (MS_E) is obtained by a similar procedure. The *p*-value for the test is given by $P(F_{a-1,N-a} > F_0)$ and can be used to determine the observed significance level of the findings.

In Table H.19 below, an *F*-Test was used to demonstrate that the FR_{hirr} and BWE were unaffected by changing combinations of coagulant dose/dosing time and coagulant type. In both cases, the *p*-values were greater than *p*=0.05, indicating that the there was insufficient evidence to reject the null hypothesis that the treatment effect is zero.

Table H.19. One-way ANOVA Test for FR_{hirr} and BWE for Sensitivity Evaluation of C-IDX

Source of Variation	Sum of Squares (SS)	Degrees of Freedom (DF)	Mean Square (MS)	F_0	*p*-Value
		FR_{hirr}			
Dosing Method	2,210.45	4	552.61	0.970	0.424
Error	201,673.01	354	569.70		
Total	203,883.46	358			
		BWE			
Dosing Method	6,664.05	4	1666.01	1.720	0.145
Error	337,948.55	349	968.33		
Total	344,612.6	353			

H.2.7. Organic Removal Data for Sensitivity Assessment of C-IDX for C-IN-P Operational Control

The removal of several WQIs including turbidity, true and apparent color, UV_{254}, DOC, and SUVA were evaluated as part of the sensitivity assessment of the C-IDX for C-IN-P operational control. Turbidity was measured using a benchtop turbidimeter (2100AN, Hach, Loveland, CO) according to Standard Method 2130B (American Public Health Association et al. 2012) and the measurement of all other WQIs has been already described. Table H.20 below presents the average removal values for organic WQIs across both replicates for each treatment.

Table H.20. Removal of Organic WQIs for H-SUVA Water with C-IN-P Pretreatment at 75 mg m^{-2} During C-IDX Sensitivity Assessment

Coag. Dose (mg-Al L^{-1})	Dosing Time (min)	DOC (%)	UV_{254} (%)	SUVA (%)	True Color (%)	App. Color (%)
			Alum			
1.5	30	79.38 ± 4.01	93.92 ± 3.79	79.38 ± 4.01	98.15 ± 0.63	98.63 ± 0.29
3.0	15	76.13 ± 1.51	92.75 ± 9.66	78.25 ± 0.64	97.66 ± 1.06	98.72 ± 0.45
45	1	77.27 ± 3.98	89.87 ± 3.50	77.27 ± 3.98	97.30 ± 0.34	98.18 ± 0.28
			ACH			
3.0	30	79.42 ± 5.32	90.63 ± 7.02	79.42 ± 5.32	97.88 ± 1.17	98.19 ± 0.65
45	1	79.24 ± 0.67	92.88 ± 1.78	79.24 ± 0.67	98.45 ± 0.35	98.73 ± 0.28

Note: ± represents the 95% confidence interval calculated using the students t-test as $\mu \pm t_{0.025,n}\frac{s}{\sqrt{n}}$

Table H.21 presents the results of the *F*-test for the removal of WQIs during the C-IDX sensitivity analysis across both coagulant types and all combinations of dose/dosing length. Based on the results, the *p*-values were found to be all equal to, or greater, than 0.05 indicating that at the 95% confidence level there is insufficient evidence to reject the null hypothesis. Therefore, changing the combination of dose/dosing time, or the coagulant type, for a fixed C-IDX value did not have a statistically significant impact on the removal of turbidity, true and apparent color, UV_{254}, DOC, or SUVA for the H-SUVA water considered in this analysis.

Table H.21. One-way ANOVA Test for Removal of WQIs During C-IDX Sensitivity Analysis

Source of Variation	Sum of Squares (SS)	Degrees of Freedom (DF)	Mean Square (MS)	F_0	*p*-Value
Turbidity Removal					
Treatment	0.58	4	0.14	5.21	0.05
Error	0.14	5	0.03		
Total	0.72	9			
True Color Removal					
Treatment	1.55	4	0.39	0.75	0.60
Error	2.59	5	0.52		
Total	4.13	9			
Apparent Color Removal					
Treatment	0.64	4	0.16	0.91	0.52
Error	0.87	5	0.17		
Total	1.51	9			
UV_{254} Removal					
Treatment	35.86	4	8.97	5.21	0.05
Error	8.60	5	1.72		
Total	44.46	9			
DOC Removal					
Treatment	19.71	4	4.93	0.43	0.78
Error	57.22	5	11.44		
Total	76.93	9			
SUVA Removal					
Treatment	834.88	4	208.72	4.39	0.07
Error	237.75	5	47.55		
Total	1072.63	9			

H.3. References

Aguareles, M., E. Barrabés, T. Myers, and A. Valverde. 2023. "Mathematical analysis of a Sips-based model for column adsorption." *Physica D: Nonlinear Phenomena*, 448: 133690. https://doi.org/10.1016/j.physd.2023.133690.

Alresheedi, M. T., O. D. Basu, and B. Barbeau. 2019. "Chemosphere Chemical cleaning of ceramic ultra fi ltration membranes e Ozone versus conventional cleaning chemicals." *Chemosphere*, 226: 668–677. Elsevier Ltd. https://doi.org/10.1016/j.chemosphere.2019.03.188.

American Public Health Association, Water Environment Foundation, and American Water Works Association. 2012. *Standard Methods for the Examination of Water and Wastewater*. 1496. Edited by L. Clesceri, A. Greenberg, and A. Eaton. 22nd Editi. Washington: APHA Press.

Arhin, S. G., N. Banadda, A. J. Komakech, W. Pronk, and S. J. Marks. 2018. "Optimization of hybrid coagulation-ultrafiltration process for potable water treatment using response surface methodology." *Water Supply*, 18 (3): 862–874. https://doi.org/10.2166/ws.2017.159.

Arhin, S. G., N. Banadda, A. J. Komakech, W. Pronk, and S. J. Marks. 2019. "Application of hybrid coagulation–ultrafiltration for decentralized drinking water treatment: impact on flux, water quality and costs." *Water Supply*, 19 (7): 2163–2171. https://doi.org/10.2166/ws.2019.097.

Baghoth, S. A., S. K. Sharma, and G. L. Amy. 2011. "Tracking natural organic matter (NOM) in a drinking water treatment plant using fluorescence excitation-emission matrices and PARAFAC." *Water Research*, 45 (2): 797–809. Elsevier Ltd. https://doi.org/10.1016/j.watres.2010.09.005.

Beier, S. P., and G. Jonsson. 2010. "Critical Flux Determination by Flux-Stepping." *AIChE Journal*, 56 (7): 1739–1747.

Benjamin, M. M., and D. Lawler. 2013. *Water Quality Engineering: Physical/Chemical Treatment Processes*. 1st ed. Hoboken, NJ, USA: John Wiley & Sons.

Berthouex, P. M., and L. C. Brown. 2002. *Statistics for Environmental Engineers*. 2nd ed. Boca Raton, FL: Lewis Publishers.

Best, G., M. Singh, D. Mourato, and Y. J. Chang. 2001. "Application of immersed ultrafiltration membranes for organic removal and disinfection by-product reduction." *Water Supply*, 1 (5–6): 221–231. https://doi.org/10.2166/ws.2001.0118.

Bonakdari, H., I. Ebtehaj, and J. D. Ladouceur. 2023. *Machine Learning in Earth, Environmental and Planetary Sciences: Theoretical and Practical Applications*. 1st ed. Amsterdam, Netherlands: Elsevier.

Bratby, J. 2016. *Coagulation and Flocculation in Water and Wastewater Treatment*. 3rd ed. London, UK: IWA Publishing.

Brinkman, B. M., and R. M. Hozalski. 2011. "Temporal variation of NOM and its effects on membrane treatment." *Journal AWWA*, 103 (2): 98–106. https://doi.org/10.1002/j.1551-8833.2011.tb11405.x.

Bro, R. 1998. "Multi-way analysis in the food industry: models, algorithms, and applications." Universiteit van Amsterdam.

Bro, R., and H. A. L. Kiers. 2003. "A new efficient method for determining the number of components in PARAFAC models." *Journal of Chemometrics*, 17 (5): 274–286. https://doi.org/10.1002/cem.801.

Buchta, P., P. Berg, A. Schweiger, and D. Vial. 2019. "In-line coagulation upstream ultrafiltration - comparison of continuous vs. intermittent addition." 8. New Orleans, LA: American Water Works Association.

Chellam, S., J. G. Jacangelo, and T. P. Bonacquisti. 1998. "Modeling and Experimental Verification of Pilot-Scale Hollow Fiber, Direct Flow Microfiltration with Periodic Backwashing." *Environmental Science & Technology*, 32 (1): 75–81. https://doi.org/10.1021/es9610040.

Chen, F., S. Peldszus, R. H. Peiris, A. S. Ruhl, R. Mehrez, M. Jekel, R. L. Legge, and P. M. Huck. 2014. "Pilot-scale investigation of drinking water ultrafiltration membrane fouling rates using advanced data analysis techniques." *Water Research*, 48 (1): 508–518. https://doi.org/10.1016/j.watres.2013.10.007.

Chen, Y., B. Z. Dong, N. Y. Gao, and J. C. Fan. 2007. "Effect of coagulation pretreatment on fouling of an ultrafiltration membrane." *Desalination*, 204 (1-3 SPEC. ISS.): 181–188. https://doi.org/10.1016/j.desal.2006.04.029.

Cheng, X., H. Liang, A. Ding, F. Qu, S. Shao, B. Liu, H. Wang, D. Wu, and G. Li. 2016. "Effects of pre-ozonation on the ultrafiltration of different natural organic matter (NOM) fractions: Membrane fouling mitigation, prediction and mechanism." *Journal of Membrane Science*, 505: 15–25. Elsevier. https://doi.org/10.1016/j.memsci.2016.01.022.

Choi, K. Y. J., and B. A. Dempsey. 2005. "Bench-scale evaluation of critical flux and TMP in low-pressure membrane filtration." *Journal AWWA*, 97 (7): 134–143.

Choi, Y. H., H. S. Kim, and J. H. Kweon. 2008. "Role of hydrophobic natural organic matter flocs on the fouling in coagulation-membrane processes." *Separation and Purification Technology*, 62 (3): 529–534. https://doi.org/10.1016/j.seppur.2008.03.001.

Coble, P. G. 1996. "Characterization of marine and terrestrial DOM in seawater using excitation-emission matrix spectroscopy." *Marine Chemistry*, 51 (4): 325–346. https://doi.org/10.1016/0304-4203(95)00062-3.

Croft, J. 2012. "Natural Organic Matter Characterization of Different Source and Treated Waters; Implications for Membrane Fouling Control." M.A.S.c Thesis, University of Waterloo.

D19 Committee. n.d. *Practice for Coagulation-Flocculation Jar Test of Water*. ASTM International.

Dang, H. T., R. M. Narbaitz, and T. Matsuura. 2010. "Evaluation of apparatus for membrane cleaning tests." *Journal of Environmental Engineering*, 136 (10): 1161–1170. https://doi.org/10.1061/(ASCE)EE.1943-7870.0000254.

Dixon, M., C. Staaks, R. Fabris, V. Vimonses, C. W. K. Chow, S. Panglisch, J. A. van Leeuwen, and M. Drikas. 2013. "The impact of optimised coagulation on membrane fouling for coagulation/ultrafiltration process." *Desalination and Water Treatment*, 51 (13–15): 2718–2725. https://doi.org/10.1080/19443994.2012.749367.

Droste, R. L. 1996. *Theory and Practice of Water and Wastewater Treatment*. 1st ed. Hoboken, NJ, USA: Wiley.

Farahbakhsh, K., and D. W. Smith. 2002. "Performance comparison and pretreatment evaluation of three water treatment membrane pilot plants treating low turbidity water." *Journal of Environmental Engineering and Science*, 1 (2): 113–122. https://doi.org/10.1139/S02-006.

Gilmore, A. M. 2011. "Water Quality Measurements with HORIBA Jobin Yvon Fluorescence Instrumentation." *Horiba Technical Reports*, 38.

Gilmore, A., and D. Schober. 2025. "Simultaneous Absorbance and Fluorescence Instrument Measuring and Analysis Principles for Quantitative Analysis." *Practical Quantitative Vibrational and Electronic Spectroscopy*, edited by D. A. Peru, 207–229. 1st ed. Wiley.

Gonzalez-Galvis, J. P., and R. M. Narbaitz. 2020. "Large batch bench-scale dissolved air flotation system (LB-DAF) for drinking water treatability tests." *Environmental Science: Water Research and Technology*, 6 (4): 1004–1017. Royal Society of Chemistry. https://doi.org/10.1039/c9ew00935c.

Gonzalez-Galvis, J. P., and R. M. Narbaitz. 2022. "Large batch bench-scale dissolved air flotation system for simulating full-scale turbidity removal." *Environmental Technology*, 43 (12): 1791–1804. https://doi.org/10.1080/09593330.2020.1852317.

Hansen, A. M., J. A. Fleck, T. E. C. Kraus, B. D. Downing, T. von Dessonneck, and B. A. Bergamaschi. 2018. *Procedures for Using the Horiba Aqualog Fluorometer to Measure Absorbance and Fluorescence from DOM*. Open-File Report. Open-File Report. U.S. Geological Survey.

Hansen, A. M., T. E. C. Kraus, B. A. Pellerin, J. A. Fleck, B. D. Downing, and B. A. Bergamaschi. 2016. "Optical properties of dissolved organic matter (DOM): Effects of biological and photolytic degradation." *Limnology and Oceanography*, 61 (3): 1015–1032. https://doi.org/10.1002/lno.10270.

Hillis, P. 2006. "Enhanced coagulation, flocculation and immersed ultrafiltration for treatment of low alkalinity and highly coloured upland water." *Journal of Water Supply: Research and Technology-Aqua*, 55 (7–8): 549–558. https://doi.org/10.2166/aqua.2006.043.

Horiba Scientific. 2021. "Aqualog Operation Manual."

Horiba Scientific. n.d. "What is an Excitation Emission Matrix (EEM)?" Accessed May 5, 2026. https://www.horiba.com/int/scientific/technologies/fluorescence-spectroscopy/what-is-an-excitation-emission-matrix-eem/.

Howe, K. J., A. Marwah, K.-P. Chiu, and S. S. Adham. 2006. "Fouling of microfiltration and ultrafiltration membranes by natural waters." *Environmental Science & Technology*, 40 (24): 7908–7913. https://doi.org/10.1021/es0616480.

Huck, P. M., S. Peldszus, C. Hallé, H. Ruiz, X. Jin, M. Van Dyke, G. Amy, W. Uhl, M. Theodoulou, and D. B. Mosqueda-Jimenez. 2011. "Pilot scale evaluation of biofiltration as an innovative pre-treatment for ultrafiltration membranes for drinking water treatment." *Water Supply*, 11 (1): 23–29. https://doi.org/10.2166/ws.2011.004.

Judd, S. J., and P. Hillis. 2001. "Optimisation of combined coagulation and microfiltration for water treatment." *Water Research*, 35 (12): 2895–2904. https://doi.org/10.1016/S0043-1354(00)00586-8.

Jung, C. W., and L. S. Kang. 2003. "Application of combined coagulation-ultrafiltration membrane process for water treatment." *Korean Journal of Chemical Engineering*, 20 (5): 855–861. https://doi.org/10.1007/BF02697288.

Kamińska, G., W. Pronk, and J. Traber. 2020. "Effect of coagulant dose and backflush pressure on NOM membrane fouling in inline coagulation-ultrafiltration." *Desalination and Water Treatment*, 199: 188–197. https://doi.org/10.5004/dwt.2020.25657.

Katsoufidou, K. S., D. C. Sioutopoulos, S. G. Yiantsios, and A. J. Karabelas. 2010. "UF membrane fouling by mixtures of humic acids and sodium alginate: Fouling mechanisms and reversibility." *Desalination*, 264 (3): 220–227. https://doi.org/10.1016/j.desal.2010.08.017.

Kawamura, S. 2000. *Integrated Design and Operation of Water Treatment Facilities*. New York, NY: John Wiley & Sons.

Keucken, A., G. Heinicke, K. M. Persson, and S. J. Köhler. 2017. "Combined coagulation and ultrafiltration process to counteract increasing NOM in brown surface water." *Water*, 9 (9): 697. Multidisciplinary Digital Publishing Institute. https://doi.org/10.3390/w9090697.

Kim, H.-C., J.-H. Hong, and S. Lee. 2006. "Fouling of microfiltration membranes by natural organic matter after coagulation treatment: A comparison of different initial mixing conditions." *Journal of Membrane Science*, 283 (1–2): 266–272. https://doi.org/10.1016/j.memsci.2006.06.041.

Kimura, K., and N. Ando. 2016. "Maximizing biopolymer removal by coagulation for mitigation of fouling in the following membrane process." *Separation and Purification Technology*, 163: 8–14. Elsevier B.V. https://doi.org/10.1016/j.seppur.2016.02.013.

Kimura, K., and K. Kume. 2020. "Irreversible fouling in hollow-fiber PVDF MF / UF membranes filtering surface water: Effects of precoagulation and identification of the foulant." *Journal of Membrane Science*, 602 (February): 117975–117975. Elsevier B.V. https://doi.org/10.1016/j.memsci.2020.117975.

Kimura, K., K. Shikato, Y. Oki, K. Kume, and S. A. Huber. 2018. "Surface water biopolymer fractionation for fouling mitigation in low-pressure membranes." *Journal of Membrane Science*, 554 (February): 83–89. Elsevier B.V. https://doi.org/10.1016/j.memsci.2018.02.024.

Kimura, K., K. Tanaka, and Y. Watanabe. 2014. "Microfiltration of different surface waters with/without coagulation: Clear correlations between membrane fouling and hydrophilic biopolymers." *Water Research*, 49: 434–443. https://doi.org/10.1016/j.watres.2013.10.030.

Kimura, K., K. Tanaka, and Y. Watanabe. 2015. "Confirmation of the correlation between membrane fouling in microfiltration and biopolymer concentrations in various Japanese surface waters." *Water Science and Technology: Water Supply*, 15 (2): 288–293. https://doi.org/10.2166/ws.2014.112.

Le Clech, P., B. Jefferson, I. S. Chang, and S. J. Judd. 2003. "Critical flux determination by the flux-step method in a submerged membrane bioreactor." *Journal of Membrane Science*, 227 (1–2): 81–93. https://doi.org/10.1016/j.memsci.2003.07.021.

Lee, J. D., S. H. Lee, M. H. Jo, P. K. Park, C. H. Lee, and J. W. Kwak. 2000. "Effect of coagulation conditions on membrane filtration characteristics in coagulation - Microfiltration process for water treatment." *Environmental Science and Technology*, 34 (17): 3780–3788. https://doi.org/10.1021/es9907461.

Locquet, N., A. Aït-Kaddour, and C. B. Y. Cordella. 2018. "3D Fluorescence Spectroscopy and Its Applications." *Encyclopedia of Analytical Chemistry*, edited by R. A. Meyers, 1–39. 1st ed. Wiley.

Madhav, H., and A. Gilmore. 2024. "Identification of oil contamination in process water using fluorescence excitation emission matrix (FEEM) and parallel factor analysis (PARAFAC)." *Water Science & Technology*, 90 (3): 908–919. https://doi.org/10.2166/wst.2024.223.

Maeng, S. K., T. C. Timmes, and H.-C. Kim. 2017. "Characteristics of flocs formed by polymer-only coagulation in water treatment and their impacts on the performance of downstream membrane separation." *Environmental Technology*, 38 (20): 2601–2610. https://doi.org/10.1080/09593330.2016.1271460.

McKnight, D. M., E. W. Boyer, P. K. Westerhoff, P. T. Doran, T. Kulbe, and D. T. Andersen. 2001. "Spectrofluorometric characterization of dissolved organic matter for indication of

precursor organic material and aromaticity." *Limnology and Oceanography*, 46 (1): 38–48. https://doi.org/10.4319/lo.2001.46.1.0038.

Mealio, K. N., M. J. M. Wells, K. Y. Bell, D. Wolgemuth, and H. A. Stretz. 2024. "Fluorescent EEM-PARAFAC considerations of Aldrich humic acid salt as an aquatic or terrestrial organic matter surrogate." *Journal of Environmental Chemical Engineering*, 12 (5): 113864. https://doi.org/10.1016/j.jece.2024.113864.

Mohammadi, S., C. Sandoval-Pauker, Z. N. Dorado, T. P. Senftle, R. Pankow, and H. Sharifan. 2025. "Fluorescent Sodium Alginate Hydrogel–Carbon Dots Sensor for Detecting Perfluorooctanoic Acid in Potable Water." *Analytical Chemistry*, 97 (18): 10075–10084. https://doi.org/10.1021/acs.analchem.5c01991.

Montgomery, D. C. 2020. *Design and Analysis of Experiments*. 10th ed. Hoboken, NJ, USA: Wiley.

Montgomery, D. C., and G. C. Runger. 2014. *Applied Statistics and Probability for Engineers*. 6th ed. Hoboken, NJ: John Wiley & Sons.

Mosqueda-Jimenez, D. B., R. M. Narbaitz, and T. Matsuura. 2004. "Manufacturing conditions of surface-modified membranes: Effects on ultrafiltration performance." *Separation and Purification Technology*, 37 (1): 51–67. https://doi.org/10.1016/j.seppur.2003.07.003.

Murphy, K. R., C. A. Stedmon, D. Graeber, and R. Bro. 2013. "Fluorescence spectroscopy and multi-way techniques. PARAFAC." *Analytical Methods*, 5 (23): 6557. https://doi.org/10.1039/c3ay41160e.

Murphy, K. R., C. A. Stedmon, T. D. Waite, and G. M. Ruiz. 2008. "Distinguishing between terrestrial and autochthonous organic matter sources in marine environments using fluorescence spectroscopy." *Marine Chemistry*, 108 (1–2): 40–58. https://doi.org/10.1016/j.marchem.2007.10.003.

Murphy, K. R., S. A. Timko, M. Gonsior, L. C. Powers, U. J. Wünsch, and C. A. Stedmon. 2018. "Photochemistry Illuminates Ubiquitous Organic Matter Fluorescence Spectra." *Environmental Science & Technology*, 52 (19): 11243–11250. https://doi.org/10.1021/acs.est.8b02648.

Nguyen, A. H., R. M. Narbaitz, and T. Matsuura. 2007. "Impacts of hydrophilic membrane additives on the ultrafiltration of river water." *Journal of Environmental Engineering*, 133 (5): 515–522. https://doi.org/10.1061/(asce)0733-9372(2007)133:5(515).

Oh, J., and S. Lee. 2005. "Influence of streaming potential on flux decline of microfiltration with in-line rapid pre-coagulation process for drinking water production." *Journal of Membrane Science*, 254 (1–2): 39–47. https://doi.org/10.1016/j.memsci.2004.12.030.

Omanović, D., S. Marcinek, and C. Santinelli. 2023. "TreatEEM—A Software Tool for the Interpretation of Fluorescence Excitation-Emission Matrices (EEMs) of Dissolved Organic Matter in Natural Waters." *Water*, 15 (12): 2214. https://doi.org/10.3390/w15122214.

Omar, I. A., and S. Q. Aziz. 2021. "Optimization of ACH Coagulant, Settling Time and Powdered Activated Carbon as Coagulant Aid with Economic Analysis." *Global NEST Journal*, 23 (3). https://doi.org/10.30955/gnj.003797.

Paar, H., J. Benecke, M. Ernst, and M. Jekel. 2011. "Pre-coagulation and ultrafiltration of effluent impaired surface water for phosphorus removal and fouling control." *Water Supply*, 11 (2): 211–218. https://doi.org/10.2166/ws.2011.037.

Papineau, I., M. Lapointe, N. M. Peleato, S. Peldszus, and B. Barbeau. 2019. "Selecting the best coagulant for NOM removal: Conventional monometric hydroxide vs. polynuclear Al-species."

Park, J., H.-Y. Kim, and P.-K. Park. 2015. "Split injection of coagulant to enhance the water permeability of a cake layer in a coagulation–microfiltration process." *Journal of Industrial and Engineering Chemistry*, 21: 363–368. https://doi.org/10.1016/j.jiec.2014.02.046.

Park, P. K., C. H. Lee, S. J. Choi, K. H. Choo, S. H. Kim, and C. H. Yoon. 2002. "Effect of the removal of DOMs on the performance of a coagulation-UF membrane system for drinking water production." *Desalination*, 145 (1–3): 237–245. https://doi.org/10.1016/S0011-9164(02)00418-6.

Parlanti, E., and K. Wo. 2000. "Dissolved organic matter Fluorescence spectroscopy as a tool to estimate biological activity in a coastal zone submitted to anthropogenic inputs." *Organic Geochemistry*, 31: 1765–1781.

Peiris, R. H., H. Budman, C. Moresoli, and R. L. Legge. 2010. "Understanding fouling behaviour of ultrafiltration membrane processes and natural water using principal component analysis of fluorescence excitation-emission matrices." *Journal of Membrane Science*, 357 (1–2): 62–72. Elsevier B.V. https://doi.org/10.1016/j.memsci.2010.03.047.

Peldszus, S., C. Hallé, R. H. Peiris, M. Hamouda, X. Jin, R. L. Legge, H. Budman, C. Moresoli, and P. M. Huck. 2011. "Reversible and irreversible low-pressure membrane foulants in drinking water treatment: Identification by principal component analysis of fluorescence EEM and mitigation by biofiltration pretreatment." *Water Research*, 45 (16): 5161–5170. https://doi.org/10.1016/j.watres.2011.07.022.

Peleato, N. M. 2013. "Applications of Principal Component Analysis of Fluorescence Excitation-Emission Matrices for Characterization of Natural Organic Matter in Water Treatment." University of Toronto.

Peleato, N. M., R. L. Legge, and R. C. Andrews. 2017. "Characterization of UF foulants and fouling mechanisms when applying low in-line coagulant pre-treatment." *Water Research*, 126: 1–11. https://doi.org/10.1016/j.watres.2017.08.064.

Pernitsky, D. J., and J. K. Edzwald. 2006. "Selection of alum and polyaluminum coagulants: principles and applications." *Journal of Water Supply: Research and Technology - Aqua*, 55 (2): 121–141. https://doi.org/10.2166/aqua.2006.062.

Persson, T., and M. Wedborg. 2001. "Multivariate evaluation of the fluorescence of aquatic organic matter." *Analytica Chimica Acta*, 434 (2): 179–192. https://doi.org/10.1016/S0003-2670(01)00812-1.

Peter-Varbanets, M., J. Margot, J. Traber, and W. Pronk. 2011. "Mechanisms of membrane fouling during ultra-low pressure ultrafiltration." *Journal of Membrane Science*, 377 (1–2): 42–53. Elsevier B.V. https://doi.org/10.1016/j.memsci.2011.03.029.

Pezeshk, N., and R. M. Narbaitz. 2012. "More fouling resistant modified PVDF ultrafiltration membranes for water treatment." *Desalination*, 287: 247–254. https://doi.org/10.1016/j.desal.2011.11.048.

Pivokonský, M., K. Novotná, L. Čermáková, and R. Petříček. 2022. *Jar Tests for Water Treatment Optimisation: How to Perform Jar Tests – a handbook*. IWA Publishing.

Qi, W., and D. A. Ladner. 2023. "Automated Testing Apparatus for Ceramic Membrane Filtration of High-Strength Industrial Wastewater." *Journal of Environmental Engineering*, 149 (10): 04023063. https://doi.org/10.1061/JOEEDU.EEENG-7337.

Rahman, I., S. Ndiongue, X. Jin, M. I. Van Dyke, W. B. Anderson, and P. M. Huck. 2014. "Fouling of low-pressure membranes during drinking water treatment: effect of NOM components and biofiltration pretreatment." *Water Supply*, 14 (3): 453–460. https://doi.org/10.2166/ws.2013.221.

Ratajczak, M. J., K. N. Exall, and P. M. Huck. 2012. "Factors affecting coagulation as a pretreatment to ultrafiltration membranes." *Water Quality Research Journal*, 47 (2): 103–116. https://doi.org/10.2166/wqrjc.2012.010.

Shutova, Y., A. Baker, J. Bridgeman, and R. K. Henderson. 2014. "Spectroscopic characterisation of dissolved organic matter changes in drinking water treatment: From PARAFAC analysis to online monitoring wavelengths." *Water Research*, 54: 159–169. https://doi.org/10.1016/j.watres.2014.01.053.

Siddiqui, M., G. Amy, J. Ryan, and W. Odem. 2000. "Membranes for the control of natural organic matter from surface waters." *Water Research*, 34 (13).

Siembida-Lösch, B., W. B. Anderson, J. Bonsteel, and P. M. Huck. 2016. "Biopolymer removal in full-scale conventional and advanced drinking water treatment trains at two large adjacent plants." *Desalination and Water Treatment*, 57 (47): 22277–22289. https://doi.org/10.1080/19443994.2016.1140595.

Sierra, M. M. D., M. Giovanela, E. Parlanti, and E. J. Soriano-Sierra. 2005. "Fluorescence fingerprint of fulvic and humic acids from varied origins as viewed by single-scan and excitation/emission matrix techniques." *Chemosphere*, 58 (6): 715–733. https://doi.org/10.1016/j.chemosphere.2004.09.038.

Stedmon, C. A., and R. Bro. 2008. "Characterizing dissolved organic matter fluorescence with parallel factor analysis: a tutorial." *Limnology and Oceanography: Methods*, 6 (11): 572–579. https://doi.org/10.4319/lom.2008.6.572.

Stedmon, C. A., S. Markager, and R. Bro. 2003. "Tracing dissolved organic matter in aquatic environments using a new approach to fluorescence spectroscopy." *Marine Chemistry*, 82 (3–4): 239–254. https://doi.org/10.1016/S0304-4203(03)00072-0.

Su, Z., T. Liu, W. Yu, X. Li, and N. J. D. Graham. 2017. "Coagulation of surface water: Observations on the significance of biopolymers." *Water Research*, 126: 144–152. Elsevier Ltd. https://doi.org/10.1016/j.watres.2017.09.022.

Tekmar-Dohrmann. 1997. "Phoenix 8000 User Manual." Cincinnati.

Tian, J. yu, M. Ernst, F. Cui, and M. Jekel. 2013. "Correlations of relevant membrane foulants with UF membrane fouling in different waters." *Water Research*, 47 (3): 1218–1228. Elsevier Ltd. https://doi.org/10.1016/j.watres.2012.11.043.

Walker, S., and R. M. Narbaitz. 2016. "Hollow fiber ultrafiltration of Ottawa River water: Floatation versus sedimentation pre-treatment." *Chemical Engineering Journal*, 288: 228–237. Elsevier B.V. https://doi.org/10.1016/j.cej.2015.11.064.

Walsh, M. E., N. Zhao, S. L. Gora, and G. A. Gagnon. 2009. "Effect of coagulation and flocculation conditions on water quality in an immersed ultrafiltration process." *Environmental Technology*, 30 (9): 927–938. https://doi.org/10.1080/09593330902971287.

Wang, J., S. Yang, W. Guo, H.-H. Ngo, H. Jia, J. Yang, H. Zhang, and X. Zhang. 2015. "Characterization of fouling layers for in-line coagulation membrane fouling by apparent zeta potential." *RSC Advances*, 5 (128): 106087–106093. https://doi.org/10.1039/C5RA18826A.

Wang, W., F. Wang, Z. Wang, X. Shi, and C. Xu. 2025. "Robust S3Former deep learning model for the direct diagnosis and prediction of natural organic matter (NOM) from three-dimensional excitation-emission-matrix (3D-EEM) data." *Water Research*, 284: 123994. https://doi.org/10.1016/j.watres.2025.123994.

Waterman, D. 2008. "Bench Scale Analysis of Ultrafiltration Membranes for Investigation of Fouling by Natural Organic Matter in Surface Waters." *Analysis*. M.A.S.c Thesis, University of Ottawa.

Wells, M. J. M., J. Hooper, G. A. Mullins, and K. Y. Bell. 2022. "Development of a fluorescence EEM-PARAFAC model for potable water reuse monitoring: Implications for inter-component protein–fulvic–humic interactions." *Science of The Total Environment*, 820: 153070. https://doi.org/10.1016/j.scitotenv.2022.153070.

Wray, H. E., and R. C. Andrews. 2014. "Optimization of coagulant dose for biopolymer removal: Impact on ultrafiltration fouling and retention of organic micropollutants." *Journal of Water Process Engineering*, 1: 74–83. https://doi.org/10.1016/j.jwpe.2014.03.007.

Wray, H. E., R. C. Andrews, and P. R. Bérubé. 2014. "Ultrafiltration organic fouling control: Comparison of air-sparging and coagulation." *Journal - American Water Works Association*, 106 (2): E76–E85. https://doi.org/10.5942/jawwa.2014.106.0018.

Wray, H. E., R. C. Andrews, and P. R. Bérubé. 2016. "Coagulation optimization for DOC removal: pilot-scale analysis of UF fouling and disinfection byproduct formation potential." *Water Supply*, 16 (2): 473–480. https://doi.org/10.2166/ws.2015.157.

Wu, S., C. Lu, B. Ma, R. Liu, C. Hu, M. Ulbricht, and J. Qu. 2022. "Long-term direct ultrafiltration without chemical cleaning for purification of micro-polluted water in rural regions: Feasibility and application prospects." *Chemical Engineering Journal*, 443: 136531. https://doi.org/10.1016/j.cej.2022.136531.

Xiangli, Q., Z. Zhenjia, W. Nongcun, V. Wee, M. Low, C. S. Loh, and N. Teck Hing. 2008. "Coagulation pretreatment for a large-scale ultrafiltration process treating water from the Taihu River." *Desalination*, 230 (1–3): 305–313. https://doi.org/10.1016/j.desal.2007.11.032.

Xu, B., and R. M. Narbaitz. 2016. "Improved membrane pretreatment of high hydrophobic natural organic matter (NOM) waters by floatation." *Journal of Membrane Science*, 518: 120–130. Elsevier. https://doi.org/10.1016/j.memsci.2016.02.056.

Xu, R.-Z., J.-S. Cao, G. Feng, J.-Y. Luo, Q. Feng, B.-J. Ni, and F. Fang. 2022. "Fast identification of fluorescent components in three-dimensional excitation-emission matrix fluorescence spectra via deep learning." *Chemical Engineering Journal*, 430: 132893. https://doi.org/10.1016/j.cej.2021.132893.

Yamamura, H., S. Chae, K. Kimura, and Y. Watanabe. 2007. "Transition in fouling mechanism in microfiltration of a surface water." *Water Research*, 41 (17): 3812–3822. https://doi.org/10.1016/j.watres.2007.05.060.

Yamamura, H., K. Okimoto, K. Kimura, and Y. Watanabe. 2014. "Hydrophilic fraction of natural organic matter causing irreversible fouling of microfiltration and ultrafiltration membranes." *Water Research*, 54: 123–136. Elsevier Ltd. https://doi.org/10.1016/j.watres.2014.01.024.

Yan, M., D. Wang, J. Qu, W. He, and C. W. K. Chow. 2007. "Relative importance of hydrolyzed Al(III) species (Ala, Alb, and Alc) during coagulation with polyaluminum chloride: A case study with the typical micro-polluted source waters." *Journal of Colloid and Interface Science*, 316 (2): 482–489. https://doi.org/10.1016/j.jcis.2007.08.036.

Yang, H., N. J. D. Graham, W. Wang, M. Liu, and W. Yu. 2021. "Evaluating and improving the reliability of the UV-persulfate method for the determination of TOC/DOC in surface waters." *Water Research*, 196: 116918. https://doi.org/10.1016/j.watres.2021.116918.

Yang, J. S., D. X. Yuan, and T. P. Weng. 2010. "Pilot study of drinking water treatment with GAC, O3/BAC and membrane processes in Kinmen Island, Taiwan." *Desalination*, 263 (1–3): 271–278. Elsevier B.V. https://doi.org/10.1016/j.desal.2010.06.069.

Zevenhuizen, E., V. A. Reed, M. S. Rahman, and G. A. Gagnon. 2015. "In-line coagulation to reduce high-pressure membrane fouling in an integrated membrane system: a case study." *Desalination and Water Treatment*, 56 (8): 1987–1998. https://doi.org/10.1080/19443994.2014.958106.

Zhang, S., Y. Yang, S. Takizawa, and L. Hou. 2018. "Removal of dissolved organic matter and control of membrane fouling by a hybrid ferrihydrite-ultrafiltration membrane system." *Science of The Total Environment*, 631–632: 560–569. https://doi.org/10.1016/j.scitotenv.2018.03.045.

Zhao, S., B. Gao, S. Sun, Q. Yue, H. Dong, and W. Song. 2015. "Coagulation efficiency, floc properties and membrane fouling of polyaluminum chloride in coagulation–ultrafiltration system: The role of magnesium." *Colloids and Surfaces A: Physicochemical and Engineering Aspects*, 469: 235–241. https://doi.org/10.1016/j.colsurfa.2015.01.036.

Zheng, X., M. T. Khan, X. Cao, and J. P. Croue. 2021. "Importance of origin and characteristics of biopolymers in reversible and irreversible fouling of ultrafiltration membranes." *Science of the Total Environment*, 784: 147157–147157. Elsevier B.V. https://doi.org/10.1016/j.scitotenv.2021.147157.